CONF-960836--

BNL - 52523
Formal Report

NSF-ITP-96-154I

RECEIVED
APR 10 1997
OSTI

NEW MODES OF PARTICLE ACCELERATIONS TECHNIQUES AND SOURCES

August 19 - 23, 1996

Edited / Compiled

by

Zohreh Parsa

INSTITUTE FOR THEORETICAL PHYSICS
UC, SANTA BARBARA, CALIFORNIA,
93106-4030 USA

&

BROOKHAVEN NATIONAL LABORATORY
UPTON, NY 11973 - 5000 USA

BNL-52523
NSF-ITP-96-154i

NEW MODES OF PARTICLE ACCELERATIONS TECHNIQUES AND SOURCES

August 19 - 23, 1996

Edited/ Compiled

by

Zohreh Parsa

INSTITUTE FOR THEORETICAL PHYSICS
UC, SANTA BARBARA, CALIFORNIA,
93106-4030 USA

Support for this symposium was provided by
NSF-PHY-94-07194, and also
under the auspices of the Department of Energy,
under Contract No. DE-AC02-76CH00016 (USA)

FORWARD

This Report includes copies of transparencies and notes from the presentations made at the Symposium on New Modes of Particle Accelerations - Techniques and Sources, August 19 - 23, 1996 at the Institute for Theoretical Physics, University of California, Santa Barbara California, that was made available by the authors. Editing, reduction and changes to the authors contributions were made only to fulfill the printing and publication requirements.

We would like to take this opportunity and thank the speakers for their informative presentations and for providing copies of their transparencies and notes for inclusion in this Report.

We also would like to thank ITP staff for their assistance, with our special thanks to Ms. Deborah Storm for her continuous efforts and help with the meeting, announcements and processing of this Report.

Zohreh Parsa
Symposium Chairperson
Institute for Theoretical Physics
UC, Santa Barbara California, USA.

INSTITUTE FOR THEORETICAL PHYSICS

UNIVERSITY OF CALIFORNIA
SANTA BARBARA, CALIFORNIA 93106-4030
http://www.itp.ucsb.edu

CONFERENCES/VISAS: (805) 893-3178
OFFICE FAX: (805) 893-2431
CREDIT CARD FAX: (805) 893-3486

ITP Conference on

NEW MODES OF PARTICLE ACCELERATIONS TECHNIQUES AND SOURCES

August 19-23, 1996

Coordinator: : Z. Parsa

SCHEDULE

Monday, August 19, 1996:

Convener: Z. Parsa

Time	Speaker	Title
:00 am	Registration	ITP Lobby
:40	J. Hartle, ITP Director	Welcoming Remarks
	Z. Parsa, BNL	Introduction to Program

Defining Perspective Presentation:

:10	R. Siemann, SLAC	Status and Future Direction of Advanced Accelerator Research
0:10	Refreshment Break	ITP Front Patio

onvener: A Sessler

ower Sources - Status, Advances and Limitations:

0:30	R. Phillips, SLAC	RF Sources
1:15	G. Mourou, U. Michigan	Laser as a Power Source
2:00 pm	Lunch Break	ITP Front Patio

onvener: A. Skrinsky

:30	M. Gunderson, USC	Pulsed Power Sources -- Physics Issues Underlying Power Conditioning for Accelerators

dvanced Accelerator Schemes:

:15	W.B. Mori, UCLA	Laser Acceleration
:00	Refreshment Break	ITP Front Patio

20	S. Yu, LBL	Two Beam Accelerator
)5	C. Pellegrini, UCLA	Advances in Inverse Free Electron lasers and an Update on Free Electron Lasers
50	W. Kimura, STI Optronics	New Advances in Inverse Cerenkov Accelerator
30	Wine & Cheese	ITP Front Patio
00	Buffet Dinner	ITP Front Patio

esday, August 20, 1996

ıvener: C. Pellegrini

v Modes of Acceleration & Applications:

ne	Speaker	Title
) am	T. Katsouleas, USC	Plasma Beat Wave Accelerator (PBWA) and Overview of Plasma Acceleration
5	A. Skrinsky, BINP	Plasma Wafefield Accelerator (PWFA) and System Designs
30	Refreshment Break	ITP Front Patio
50	C. Joshi, UCLA	Progress in Laser Plasma Experiments
35	R. Pantel, Stanford Univ.	Open Waveguide Structure for Laser Acceleration
15 pm	Lunch	ITP Front Patio

vener: R. Siemann

ittance Issues of Acceleration Methods:

5	E. Esarey, Naval Res. Lab.	Laser Plasma Physics Issues
)	N. Andreev, RAS	Self-Modulation of Intense Laser Pulses in Homogeneous Plasma and Plasma Channels
5	Refreshment Break	ITP Front Patio
5	B. Breizman, Univ. Texas	Beam Dynamic Issues in Plasma Wakefield Accelerators
)	T. Katsouleas, USC	Beam Dynamic Issues in Laser Plasma Accelerators
5	**end of session**	

ednesday, August 21, 1996

nvener: W. B. Mori

me	Speaker	Title
0 am	C. Barty, UCSD	Production of Ultra Short Laser Pulses
5	D. Umstadter, U. Michigan	Short Bunch Injection, Synchronization, and Acceleration in Laser Wakefields
30	Refreshment Break	ITP Front Patio
50	A. Skrinsky, BINP	Beam Cooling Techniques
35	A. Sessler, LBL	Laser Cooling
15 pm	Lunch	ITP Front Patio

ivener: E. Esarey

5	P. Chen, SLAC	Crystal Accelerator (Plasma wake in conduction electron and channeling
0	A. Skrinsky, Z. Parsa, N. Andreev, B. Breizman C. Joshi, W.B. Mori G. Stupakov, T. Katsouleas V. Gorev, D. Umstadter, and others	**Reports*** on New Advances in Lasers, Plasma based Acceleration Techniques **and Panel Discussions** [*= to be announced]
0	Refreshment Break	ITP Front Patio
0	G. Stupakov	Beam Emittance in PWFA
0	T. Marshall, Columbia	Microwave Inverse Cerenkov and FEL Accelerators: "Tabletop" Systems for Applications at 10 -20 MeV.
0	V. Telnov, BINP	Requirements of Beam Emittances in Photon--Photon Colliders and Methods of Realization
0	**end of session**	

ursday, August 22, 1996

vener: D. Rule

ne	**Speaker**	**Title**
0 am	A. Shchagin, KIPT	Parametric X-ray radiation as Source of Short pulses of X-ray beam
0	A. Zholents, LBNL	Generation of Femto-Second X-Ray Pulses at Synchrotron Sources
5	Refreshment Break	ITP Front Patio
vener : K. von Bibber		
5	D. Cline, UCLA	Advanced Linear Accelerator Development for Linac Ring Colliders
wmass 96		
00	J. Wurtele, LBL	Summary of Accelerator Issues
m Sources - Status, Advances, and Limitations:		
0	K. Leung , LBL	High Current Short Pulse Ion Sources
0 pm	Lunch	ITP Front Patio
vener: B. Zotter		
	R. Macek, LANL	High Intensity Neutron Spallation Sources
ort on New Advances:		
	W. Molzon, UCI	High Intensity Muon Source
	C. Bula, Princeton Univ.	Observation of Nonlinear QED Effects in Electron-Laser Collisions
	Refreshment Break	ITP Front Patio
	M. Ottinger, Univ. Texas	SYN2 - A New Model for Tracking Space Charge Perturbed Snychrotron Beams
	Z. Parsa, C. Pellegrini, A. Sessler, R. Siemann, J. Wurtele, V. Telnov, T .Marshall V. Gorev, R. Macek, K. Leung, D. Cline, A. Skrinsky and others.	Reports* on New Advances and Round Table Discussion on Basic Issues
	TBA	
	Beer and Chips	ITP Front Patio
	Fiesta Barbeque	ITP Front Patio

iday, August 23, 1996

nvener: N. Andreev

ne	Speaker	Title
orts on New Advances (continues):		
0 am	J. Allen, UCSB	Photon Assisted Transport in Semiconductor Quantum Structures with the UCSB FEL's.
5	J. Wells, Harvard Univ.	Superintense Laser - Atom Interactions:
15	Refreshment Break	ITP Front Patio
35	W. Lee, Princeton Univ.	Perturbative Particle Simulation of Space Charge Efects for a K-V Beam
05	M. Pato, Univ. Sao Paulo	TBA
15 pm	Lunch	ITP Front Patio
5		Reports* (continues)
	Z. Parsa	Summary and Closing Talk

\	To Be Announced
	To Be Confirmed
L	Brookhaven National Laboratory
	Lawrence Berkeley National Laboratory
NL	Los Alamos National Laboratory
IP	Budker Institute of Nuclear Physics, Novosibirsk
S	Russian Acacdemy of Science
T	Kharkov Institute of Physics and Technology, Ukraine
AC	Stanford Linear Accelerator Center

NEW MODES OF PARTICLE ACCELERATIONS TECHNIQUES AND SOURCES

INTRODUCTION

Z. Parsa, BNL/ITP

New Methods of Particle Accelerations
Techniques and Sources
August 19 - 23, 1996

Zohreh Parsa
Brookhaven National Lab/ ITP

This is the first Symposium we are holding at the Institute for Theoretical Physics (ITP) as part of our 5 month program on "New Ideas for Particle Accelerators" (sponsored by the ITP).

To put this symposium in context; this program started in July 22, 1996 and has hosted 12 - 15 residence Physicists who study variety of problems related to particle accelerator physics. The primary objective of this program is an indepth study of the underlying principles and problems in particle acceleration . Topics of discussion will include:

- Advanced Accelerator Concepts, Novel Modes of Acceleration using Plsdms, Lsdrtd, Particle beams, microwaves, collective modes etc., Power sources and their limitations;
- High Intensity Muon Source
- short wave FEL - 4th Generation Light Sources
- Parametric X-ray, as an alternate to Synchrotron source
- Laser-Plasma-wake Accelerator schemes
- Limitaions of existing accelerator Technology
- Collider Physics and New types of Particle colliders such as muon-antimuon and photon-photon.
- Theoretical advances and formalism for studying nonlinear dynamics and beam stability.

In addition to this symposium, we will be hosting :

2nd symposium on "Future High Energy Colliders" October 21-25, 1996. The purpose of this symposium will be to discuss the future direction of high energy physics by bringing together leaders from the theoretical, experimental and accelerator physics communities. They will provide perspectives on the physics objectives and the technology demands of future high energy colliders. To collectively form a vision for where the field should be heading and how it might best reach its objectives and how the U.S. High Energy Physics community should best marshal its national scientific resources while continuing a high level of international collaboration.

3rd Symposium on "Beam Stability and Nonlinear Dynamics" Dec 3 - 5, 1996. Which would deal with some of the fundamental thoereticla problems associated with accelerator physics (see Program)

Some of the topics of our studies during the 5 month workshop and this symposium on Nonlinear Dynamics include:

- Single particle orbit theory

1. Symplectic geometry
2. Hamiltonian system
3. Bifurcation theory
4. Long-term prediction
5. Symplectic integrators
6. Long-term stability of orbits
7. Long-term stability estimates
8. Symbolic methods
9. Truncated power series and truncated poisson series algebra
10.Lie methods
11.Transformation methods
12.normal forms
13.Computation, manipulation and analysis of maps
14.Iteration of maps.
15............. ....

16.Many particle effects
17.Galaxy formation and galactic dynamics
18.Globular clusters
19.Laser cooled penning traps
20.Crystal Beams
21.Generation and transport of intense space-charge dominated beams
22.Beam-beam effects
23.Wake-field effects
24.etc., ...

I would like to take this opportunity to thank ITP and its supporting agency National Science Foundation (NSF) for hosting our program and providing such a nice setting for the Symposium.

Following are the program and conference information.

After Dec 20, 1996 , My e-mail address is: parsa@bnl.gov
Tel: 516-344-2085

INSTITUTE FOR THEORETICAL PHYSICS

UNIVERSITY OF CALIFORNIA
SANTA BARBARA, CALIFORNIA 93106-4030
http://www.itp.ucsb.edu

CONFERENCES/VISAS: (805) 893-
OFFICE FAX: (805) 893-
CREDIT CARD FAX: (805) 893-

ITP Conference on
NEW MODES OF PARTICLE ACCELERATIONS TECHNIQUES AND SOURCES

August 19-23, 1996

Coordinator : Z. Parsa

SCHEDULE

Monday, August 19, 1996:

Convener: Z. Parsa

Time	Speaker	Title
8:00 am	Registration	ITP Lobby
8:40	J. Hartle, ITP Director	Welcoming Remarks
	Z. Parsa, BNL	Introduction to Program

Defining Perspective Presentation:

9:10	R. Siemann, SLAC	Status and Future Direction of Advanced Accelerator Research
10:10	Refreshment Break	ITP Front Patio

Convener: A Sessler

Power Sources - Status, Advances and Limitations:

10:30	R. Phillips, SLAC	RF Sources
11:15	G. Mourou, U. Michigan	Laser as a Power Source
12:00 pm	Lunch Break	ITP Front Patio

Convener: A. Skrinsky

1:30	M. Gunderson, USC	Pulsed Power Sources -- Physics Issues Underlying Power Conditioning for Accelerators

Advanced Accelerator Schemes:

2:15	W.B. Mori, UCLA	Laser Acceleration
3:00	Refreshment Break	ITP Front Patio

3:20	S. Yu, LBL	Two Beam Accelerator
4:05	C. Pellegrini, UCLA	Advances in Inverse Free Electron lasers and an Update on Free Electron Lasers
4:50	W. Kimura, STI Optronics	New Advances in Inverse Cerenkov Accelerator
5:30	Wine & Cheese	ITP Front Patio
6:00	Buffet Dinner	ITP Front Patio

Tuesday, August 20, 1996

Convener: C. Pellegrini

Time	Speaker	Title
New Modes of Acceleration & Applications:		
9:00 am	T. Katsouleas, USC	Plasma Beat Wave Accelerator (PBWA) and Overview of Plasma Acceleration
9:45	A. Skrinsky, BINP	Plasma Wafefield Accelerator (PWFA) and System Designs
10:30	Refreshment Break	ITP Front Patio
10:50	C. Joshi, UCLA	Progress in Laser Plasma Experiments
11:35	R. Pantel, Stanford Univ.	Open Waveguide Structure for Laser Acceleration
12:15 pm	Lunch	ITP Front Patio

Convener: R. Siemann

Emittance Issues of Acceleration Methods:		
1:45	E. Esarey, Naval Res. Lab.	Laser Plasma Physics Issues
2:30	N. Andreev, RAS	Self-Modulation of Intense Laser Pulses in Homogeneous Plasma and Plasma Channels
3:15	Refreshment Break	ITP Front Patio
3:35	B. Breizman, Univ. Texas	Beam Dynamic Issues in Plasma Wakefield Accelerators
4:20	T. Katsouleas, USC	Beam Dynamic Issues in Laser Plasma Accelerators
5:15	end of session	

Wednesday, August 21, 1996

Convener: W. B. Mori

Time	Speaker	Title
9:00 am	C. Barty, UCSD	Production of Ultra Short Laser Pulses
9:45	D. Umstadter, U. Michigan	Short Bunch Injection, Synchronization, and Acceleration in Laser Wakefields
10:30	Refreshment Break	ITP Front Patio
10:50	A. Skrinsky, BINP	Beam Cooling Techniques
11:35	A. Sessler, LBL	Laser Cooling
12:15 pm	Lunch	ITP Front Patio

Convener: E. Esarey

1:45	P. Chen, SLAC	Crystal Accelerator (Plasma wake in conduction electron and channeling
2:20	A. Skrinsky, Z. Parsa, N. Andreev, B. Breizman C. Joshi, W.B. Mori G. Stupakov, T. Katsouleas V. Gorev, D. Umstadter, and others	Reports* on New Advances in Lasers, Plasma based Acceleration Techniques and Panel Discussions [*= to be announced]
3:20	Refreshment Break	ITP Front Patio
3:40	G. Stupakov	Beam Emittance in PWFA
4:10	T. Marshall, Columbia	Microwave Inverse Cerenkov and FEL Accelerators: "Tabletop" Systems for Applications at 10 -20 MeV.
4:50	V. Telnov, BINP	Requirements of Beam Emittances in Photon--Photon Colliders and Methods of Realization
5:30	end of session	

Thursday, August 22, 1996

Convener: D. Rule

Time	Speaker	Title
9:00 am	A. Shchagin, KIPT	Parametric X-ray radiation as Source of Short pulses of X-ray beam
9:30	A. Zholents, LBNL	Generation of Femto-Second X-Ray Pulses at Synchrotron Sources
10:05	Refreshment Break	ITP Front Patio

Convener : K. von Bibber

Time	Speaker	Title
10:25	D. Cline, UCLA	Advanced Linear Accelerator Development for Linac Ring Colliders

Snowmass 96

Time	Speaker	Title
11: 00	J. Wurtele, LBL	Summary of Accelerator Issues

Beam Sources - Status, Advances, and Limitations:

Time	Speaker	Title
11:40	K. Leung , LBL	High Current Short Pulse Ion Sources
12:20 pm	Lunch	ITP Front Patio

Convener: B. Zotter

Time	Speaker	Title
1:45	R. Macek, LANL	High Intensity Neutron Spallation Sources

Report on New Advances:

Time	Speaker	Title
2:25	W. Molzon, UCI	High Intensity Muon Source
3:05	C. Bula, Princeton Univ.	Observation of Nonlinear QED Effects in Electron-Laser Collisions
3:35	Refreshment Break	ITP Front Patio
4:00	M. Ottinger, Univ. Texas	SYN2 - A New Model for Tracking Space Charge Perturbed Snychrotron Beams
4:20	Z. Parsa, C. Pellegrini, A. Sessler, R. Siemann, J. Wurtele, V. Telnov, T .Marshall V. Gorev, R. Macek, K. Leung, D. Cline, A. Skrinsky and others.	Reports* on New Advances and Round Table Discussion on Basic Issues
	TBA	
5:45	Beer and Chips	ITP Front Patio
6:15	Fiesta Barbeque	ITP Front Patio

Friday, August 23, 1996

Convener: N. Andreev

Time	Speaker	Title
Reports on New Advances (continues):		
9:00 am	J. Allen, UCSB	Photon Assisted Transport in Semiconductor Quantum Structures with the UCSB FEL's.
9:45	J. Wells, Harvard Univ.	Superintense Laser - Atom Interactions:
10:15	Refreshment Break	ITP Front Patio
10:35	W. Lee, Princeton Univ.	Perturbative Particle Simulation of Space Charge Efects for a K-V Beam
11:05	M. Pato, Univ. Sao Paulo	TBA
11:35	TBA	TBA
12:15 pm	Lunch	ITP Front Patio
1:45	TBA	Reports* (continues)
	Z. Parsa	Summary and Closing Talk

TBA	To Be Announced
*	To Be Confirmed
BNL	Brookhaven National Laboratory
LBL	Lawrence Berkeley National Laboratory
LANL	Los Alamos National Laboratory
BINP	Budker Institute of Nuclear Physics, Novosibirsk
RAS	Russian Acacdemy of Science
KIPT	Kharkov Institute of Physics and Technology, Ukraine
SLAC	Stanford Linear Accelerator Center

NEW MODES OF PARTICLE ACCELERATIONS
TECHNIQUES AND SOURCES
AUGUST 19 - 23, 1996
ZOHREH PARSA

PROGRAM — Revisions to the program will be posted on the board and Program copies will be available at the Regist desk (see Dorene)

MESSAGES ---- Messages will be posted on the board in the Lobby -- and on the board outside on the Patio

BREAKS --- There are 2 Breaks daily. Refreshments will be served outside of the Conference Room (ITP Front Patio) * Coffee and Tea will be available through the day

LUNCHES -- Lunch will be provided and served outside the Conference Room, on the ITP Front Patio (see Program for exact lunch Break times)

DINNERS -- Two special event Dinners will be provided and Served on Monday (8/19/96) and Thursday (8/22/96) evenings (ITP Front Patio):

Monday:	5:30	Wine & Cheese
	6:00	Buffet Dinner
Thursday	5:45	Beer and Chips
	6:15	Fiesta Barbecue

[For info on restaurants and local dining see Dorene]

TRANSPORTATION A Van to transport the participants to and from the conference will be available [for the participants staying at some of the local hotel/Motels. For details and schedule see Dorene at Regist Desk]

REGISTRATION: See Dorene

TRANSPARENCIES: Please Leave a copy of your transparencies at the Regist Desk

PROCEEDINGS: Please Leave Two copies of your write up at the Regist Desk (any problem or question see me during the Breaks. All Registered participants will receive a copy of the proceedings. Please leave your mailing address at which you wish to receive a copy.

▪ Welcome ▪

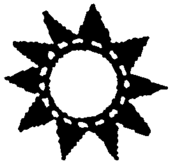

The ITP Conference on

New Modes of Particle Acceleration Techniques and Sources

invites you to attend the

Opening Buffet Dinner

All conference registrants are welcome.
Guest tickets are available from
your conference assistant for $35 each.
Children under 12 are free.

Monday night, August 19th

5:30 pm - Wine and Cheese (ITP front patio)
6:00 pm - Buffet Dinner (ITP front patio)

This gourmet dinner will be presented by the UCSB Special Events Catering.
There will be vegetarian dishes available.

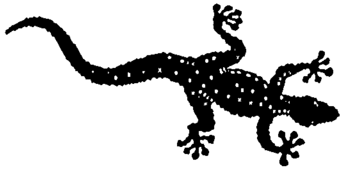

IT'S *!FIESTA!* TIME

The ITP conference on
New Modes in Particle Acceleration, Techniques and Sources

is presenting a *!FIESTA!* dinner

__Thursday evening, August 22, 1996__

5:45 pm	Chips, Salsa & Beer	(ITP Front Patio)
6:15 pm	*!FIESTA!* dinner	(vegetarian options available)

All conference registrants are welcome. Guests are $25. Children under 12 free. Tickets available from your Conference staff.

STATUS AND FUTURE DIRECTION OF ADVANCED ACCELERATOR RESEARCH

R. Siemann, SLAC

STATUS & FUTURE DIRECTIONS FOR ADVANCED ACCELERATOR RESEARCH
- A PERSONAL PERSPECTIVE -

BOB SIEMANN, SLAC
AUGUST 19, 1996
INSTITUTE FOR THEORETICAL PHYSICS
U.C.S.B

I. INTRODUCTORY REMARKS
II. HADRON COLLIDERS
III. MUON COLLIDERS
IV. LINEAR COLLIDERS
V. CONCLUDING REMARKS

I. INTRODUCTION

- FOCUS IS EXCLUSIVELY HEP
- THE MASS SCALE OF INTEREST IS

$$m \sim 0.5 - 2 \text{ TEV} \cdot \longrightarrow \infty$$

HIGGS & EW SYM. BREAKING ??

- THERE IS ONLY ONE TECHNICALLY PROVEN WAY TO REACH THESE MASS SCALES HADRON STORAGE RING COLLIDER..
- HADRON COLLIDERS ARE BASED ON SEVERAL GREAT PRINCIPLES OF ACCEL. PHYSICS & TECHNOLOGY
  - PHASE STABILITY
  - STRONG FOCUSING
  - COLLIDING BEAMS
  - SUPERCONDUCTING MAGNETS

  PLUS OTHER SUBSTANTIAL ACCOMPLISI MENTS
  - NON-LINEAR DYNAMICS
  - COLLECTIVE EFFECTS
  - BEAM DIAGNOSTICS
  - • • •

  PLUS YEARS OF EXPERIENCE WITH OPERATING COLLIDERS.
- HOWEVER, THERE ARE PROBLEMS
  - COST, SIZE
  - NATURE OF COLLISIONS & EXPERIME
- THIS HAS LED TO INTENSE INTEREST IN OTHER COLLIDERS
  - $\ell^+\ell^-$ LINEAR COLLIDER
  - μ COLLIDER

- THREE ASPECTS OF LINEAR COLLIDERS
  - SLC HAS OPERATED FOR EXTENDED PERIODS WITH

    $$\mathcal{L} \sim 5-8\times10^{29}\ cm^{-2}\ sec^{-1}$$

  - PROVIDED BASIS FOR NLC, JLC, TESLA DESIGNS WHICH AIM FOR

    $$\mathcal{L} \sim 5-10\times10^{34}\ cm^{-2}\ sec^{-1}$$

    $$E_{cm} \sim .5-1.5\ TeV$$

  - HAS RECEIVED ALMOST ALL THE ATTENTION FROM THE ADVANCED ACCELERATOR COMMUNITY (LOOK AT THE PROGRAM FOR THIS SYMPOSIUM)
- THIS FOCUS IS TOO NARROW. ADVANCED ACCELERATOR RESEARCH SHOULD ENCOMPASS
  - HADRON COLLIDERS WHERE THE PRESENT GOAL IS TO REDUCE "COSTS"
  - ADVANCED LINEAR COLLIDERS THAT TAKE ADVANTAGE OF LASERS, PLASMAS, HIGH FREQ. RF, WAKEFIELDS;–
  - ALTERNATE COLLIDER CONCEPTS OF WHICH μ-COLLIDER IS AN EXAMPLE

WHERE IS HEP GOING?

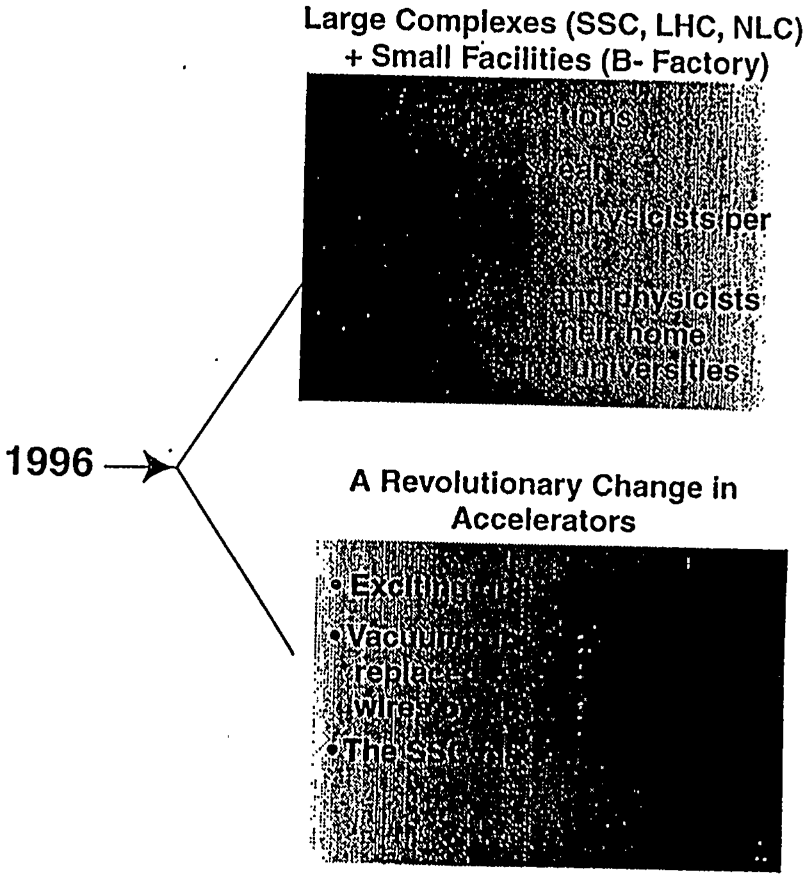

"Double-C" Twin Bore Transmission Line Magnet

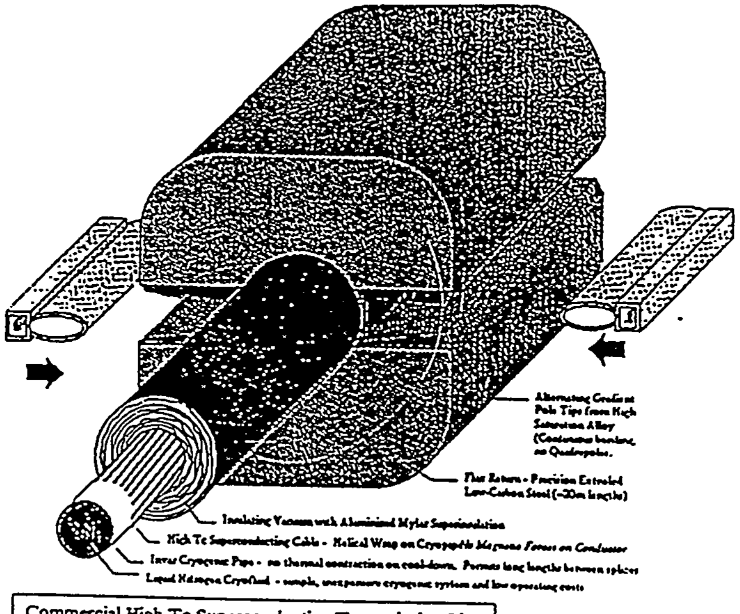

Commercial High-Tc Superconducting Transmission Line
~500m Lengths

R.R. Wilson et al, Snowmass, '82

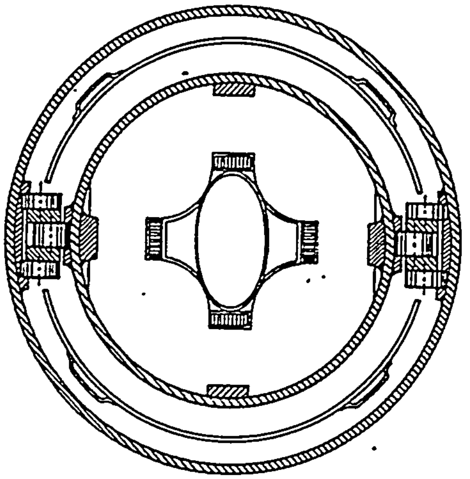

Fig. 3. 2.5 Tesla superferric magnets. (b) 100 T/m quadrupole magnet.

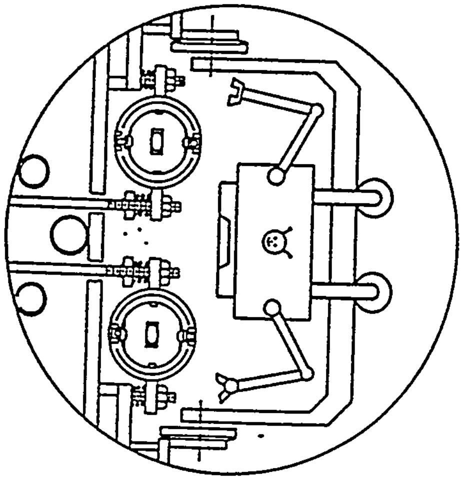

(c) Cross section of the 3-foot "tunnel" and magnets with an artist's conception of a robot.

II. HADRON COLLIDERS

- FOCUS IS ON IMPROVING PERFORM. / COST RATIO
- TWO BASIC IDEAS – LOW (~2T) & HIGH (~10–15 T) MAGNETIC FIELDS
- THE HIGH FIELD APPROACH
  - SYNCH. RADIATION AFFECTS DYNAMICS
  - REQUIRES SC MAGNET DEVELOPMENT
  - EVOLUTIONARY NOT REVOLUTIONARY
- THE LOW FIELD APPROACH
  - THIS IS REVOLUTIONARY: USE OF A SIMPLE MAGNET STRUCTURE & ADVANCED TUNNELING TO REDUCE COSTS.
- THE LOW FIELD COLLIDER IS AN OLD IDEA
  - SNOWMASS, 1982 ⟹ SSC, 1986
  - WHY? AN IDEA BASED ON LOW COST, INNOVATIVE TECHNOLOGIES IS ONE GOOD WAY TO START. BUT, BEAM DYNAMICS, PERFORMANCE, OPERABILITY, ... DO BECOME AS ISSUE.
  - IT IS DIFFICULT, BUT IMPORTANT, TO KEEP OVERALL REQUIREMENTS IN MIND
  - HOW SHOULD IDEAS BE JUDGED? THIS MUST BE FACED WHEN THERE ARE \$ LIMITS.

"SNOWMASS" PARAMETER LIST

Gerry Dugan and Mike Syphers developed a representative parameter list for both options based on 50 TeV/beam, 10^{34} cm-^{2}sec-^{1}, and 3 TeV injection energy.

Parameter	LHC	High/50	Low/50	
Energy (c-m)	14	100	100	TeV
Luminosity	1	0.35	1	10^{34}cm^{-2}sec^{-1}
Bunch spacing	25	17	17	nsec
Int./crossing	19	7.5	21	
Circumference	27	105	541	km
Dipole field	9	12.5	2	Tesla
Protons/bunch	9	0.4	1	10^{10}
Emittance (rms, normal.)	4	1	1	π mm-mr
Stored energy	377	655	8980	MJ
Radiated Power/Ring	4	137	63	kW
Power/length/Ring	0.2	1.6	0.1	W/meter
Damping time (transverse)	51	2.7	79	hours
Beam-beam tune shift (total)	.010	.006	.011	

IV. LINEAR COLLIDERS

- LINEAR COLLIDERS AS A WAY TO REACH ULTRAHIGH ENERGIES
- POSSIBLE ACCELERATION MECHANISMS
  - SHORT λ RF
  - LASER SWITCHED PULSE POWER
  - LASER DRIVEN STRUCTURES
  - LASER DRIVEN PLASMAS
  - BEAM DRIVEN STRUCTURES & PLASMAS
  - • • •
- BASIC EQUATIONS

$$\mathcal{L} = \frac{1}{4\pi} \frac{N^2 n_b f_p}{\sigma_x \sigma_y}$$

N = PART./BUNCH
n_b = BUNCHES/PULSE.
f_p = PULSE FREQ.
σ_x, σ_y = RMS BEAM SIZES.

$$P_B = N \gamma mc^2 n_b f_p$$

γ = BEAM ENERGY.

MEASURES OF BEAM-BEAM INTERACTION

$$n_\gamma \approx \frac{2\alpha r_e N}{\sigma_x}$$

n_γ = # OF BEAMSTRAHLUNG γ's PER INCIDENT PARTICLE.

$$\Upsilon = \gamma \frac{B}{B_c} \sim \frac{\gamma N}{\sigma_z(\sigma_x + \sigma_y)}$$

$B_c \cong 4.4 \times 10^{13}$ G.
= SCHWINGER CRITICAL FIELD

$$\delta(\Upsilon) = \frac{\text{AVERAGE PARTICLE ENERGY LOSS}}{\text{BEAM PARTICLE ENERGY}}$$

$$\mathcal{L} \cong \frac{1}{8\pi\alpha r_e mc^2} \frac{P_B n_\gamma}{\gamma \sigma_y}$$

$$\mathcal{L} \cong \frac{1}{8\pi\alpha r_e mc^2} \frac{P_B n_\gamma}{\gamma \sigma_y}$$

- WELL KNOWN RELATION OF $\mathcal{L}$, ENERGY, BEAM POWER P_B, BEAM SIZE σ_y, & BACKGROUNDS n_γ.

GRADIENT

- IRRELEVANT FOR ACHIEVING HIGH $\mathcal{L}$. (LOO AT TESLA IDEA FOR $E_{cm} = 0.5$ TEV)
- HOWEVER, IT IS CRITICAL. THE GOAL OF ADVANCED ACCELERATOR RESEARCH SHOULD BE TO EXPLORE REVOLUTIONAR CHANGES IN ACCELERATORS.
  - GRADIENTS MUST BE SIGNIFICANTLY GREATER THAN THOSE POSSIBLE TODAY IN OPERATING ACCELERATORS (~ 100MV/
  - WORTHWHILE GOALS
    - A MULTI TEV COLLIDER ON THE FERMILAB OR SLAC SITES
    - 5×10^8 PARTICLES ACCELERATED TO 1 GEV IN 1 m.
  - LOWER GRADIENTS ARE NOT INTERES UNLESS THEY ARE A STEP ALON THE WAY TO HIGH GRADIENTS.

EXPERIMENTATION

- n_γ, Υ, δ IMPOSE CONSTRAINTS FROM BACKGROUND & ENERGY SPREAD
- MODES OF EXPERIMENTATION AS WELL AS METHODS OF ACCELERATION MUST BE REVOLUTIONIZED THE BUBBLE CHAMBER, THE 4π DETECTOR, PIERRE AUGER.

III. MUON COLLIDERS

- TWO PREMISES
  1. LEPTON COLLISIONS ARE NECESSARY AT HIGH ENERGIES BECAUSE RADIATION DAMAGE AT HADRON COLLIDERS IS UNACCEPTABLE
  2. BEAM-BEAM EFFECTS ARE A CRITICAL FLAW OF LINEAR COLLIDERS.

  MUON COLLIDER IS RESULT

- IT IS RELATIVELY EASY TO RAISE TECHNICAL ISSUES AND TO FIND FAULT IN ASPECTS OF PRESENTATIONS ABOUT IT. PUT THIS ASIDE.

- THE MUON COLLIDER IS A COMPLETE CONCEPT FROM SOURCE TO COLLISION POINT. CLARIFIES ISSUES & INTERACTIONS BETWEEN SYSTEMS.

- A COMMENT & A QUESTION
  - THIS COMPLETE CONCEPT HAS HIGH VALUE. THERE IS LITTLE COMPARABLE WITH MOST LINEAR COLLIDER BASED ADVANCED ACCELERATOR IDEAS
  - HOW DOES ONE EVALUATE SUCH CONCEPTS WHEN MONEY & HUMAN RESOURCES ARE LIMITED?

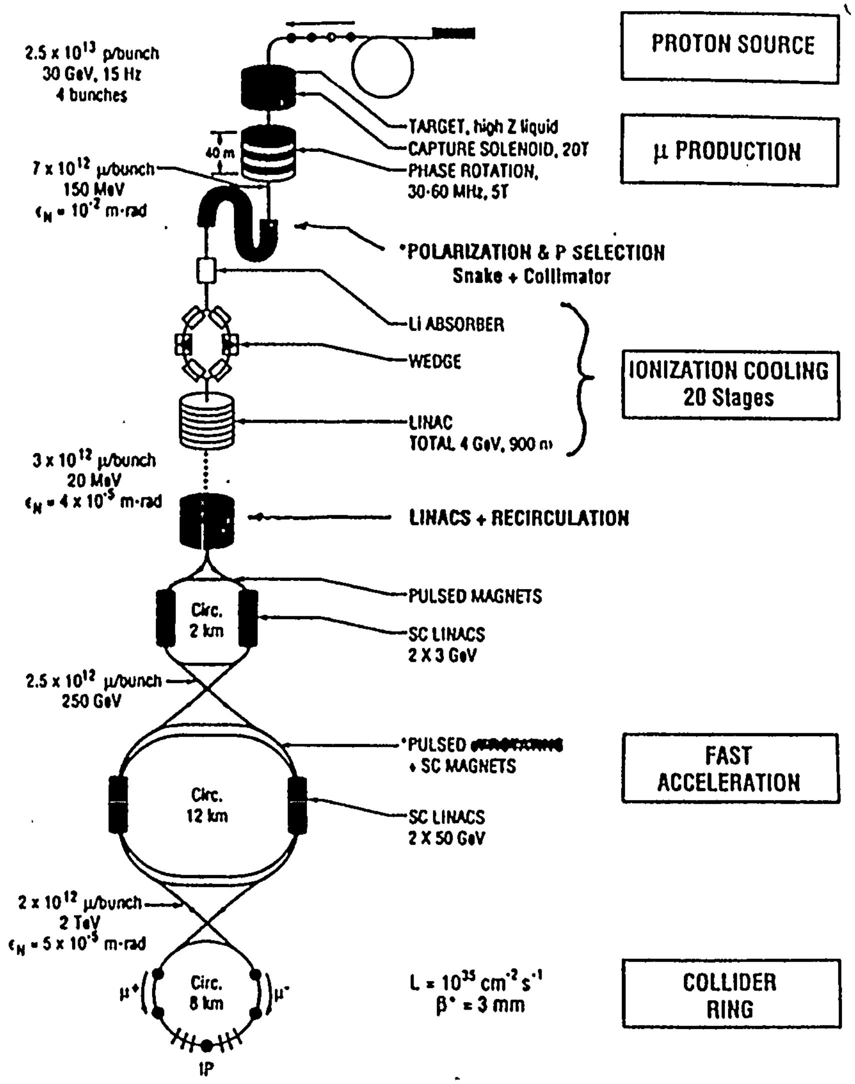

- SMALL ENERGY SPREAD & LOW BACKGROUND HAVE BEEN POWERFUL ASPECTS OF e^+e^- COLLISIONS: DISCOVERY OF THE J/ψ, STUDIES OF c-, b- QUARKS, Z's
- BUT IT MAY NOT BE POSSIBLE AT HIGHER ENERGIES. THIS NEEDS TO BE LOOKED AT CRITICALLY
- IF THE CONSTRAINTS FROM THE BEAM-BEAM INTERACTION CANNOT BE AVOIDED, γγ AND COMPENSATED COLLISIONS

MAY OFFER SOLUTIONS.

FINAL FOCUS

- IN THE NLC EACH LINAC IS ~ 10 km LONG AND 1/2 THE FINAL FOCUS IS ~ 5 km LONG (FF INTENDED FOR 1.5 TeV)
- THIS LENGTH IS WHAT IS REQUIRED FOR BACKGROUND CONTROL & CORRECTION OF OPTICAL ABERRATIONS AT THE FINAL FOCUS.
- BACKGROUND CONTROL ⇔ EXPERIMENTATION
OPTICAL CORRECTION ⇔ [illegible]
- HIGH ACCELERATION GRADIENTS MUST BE ACCOMPANIED BY EQUALLY CREATIVE SOLUTIONS FOR FINAL FOCUS SYSTEMS

EFFICIENCY

- $\mathcal{L} \propto P_B$; THIS PUTS A PREMIUM ON HIGH EFFICIENCY AC POWER → RF, LASER → BEAM
- NEEDS TO BE A CONTINUING THEME FOR BOTH POWER SOURCES & STRUCTURES.

POWER SOURCES

- PEAK POWER & EFFICIENCY ARE BOTH ISSUES

RF SOURCES

- EFFICIENCY
  - SIMULATIONS & ACTUAL PERFORMANCE AGRE WELL. RF SOURCES CAN BE DESIGNE WITH CONFIDENCE
  - PERMANENT MAGNET FOCUSING
- PEAK POWER
  - RF PULSE COMPRESSION IS THE TECHNIQU FOR INCREASING PEAK POWER
- PUSH IS TOWARDS HIGHER FREQUENCY. NE DEVICES SUCH AS SHEET BEAM KLYSTRON UBATRON,... WILL BE NEEDED.

LASERS

- THE POTENTIAL OF THE LASER AS A ACCELERATOR POWER SOURCE HAS BEEN A MAJOR STIMULUS TO THE STUDY OF ADVANCED ACCELERATORS.
- TERAWATT LASER HAS MADE ENORMOU PEAK POWER AVAILABLE ECONOMICALLY
- REP. RATE & EFFICIENCY ARE IMPROVI RAPIDLY WITH MANY MOTIVATIONS IN ADDITION TO PARTICLE ACCELERATION.

NEW IDEAS

- POTENTIAL HIGH FREQUENCY SOURCES BASED ON LASER SWITCHED SEMI-CONDUCTOR DEVICES

STRUCTURES & WAKEFIELDS

- FOR EFFICIENCY THERE MUST BE STRONG COUPLING OF ACCELERATION FIELD TO BEAM
  - CONCRETE EXAMPLE

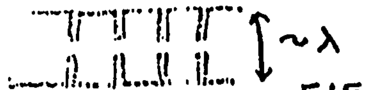

FIELD $\propto G$

STORED ENERGY $\propto G^2\lambda^2 L$;

ENERGY GAIN $= GL$;

$$\text{EFFICIENCY} \sim \frac{1}{G\lambda^2}$$

∴ LONGITUDINAL WAKEFIELD $\sim 1/\sigma_z^2 \sim 1/\lambda$

TRANSVERSE WAKEFIELD $\sim 1/\lambda^3$

→ ENERGY SPREAD & INTENSITY LIMIT

→ EMITTANCE BLOW-UP

- PLASMAS
  - IMPRESSIVE GRADIENTS
  - ISSUES ARE MACROSCOPIC ENERGY GAIN, STAGING, BEAM CURRENT & QUALITY (CRITICAL IMPORTANCE FOR APPLICATION!)

- LASER DRIVEN STRUCTURES
  - ~ GV/m GRADIENTS ARE PROPOSED
  - EXPERIMENTAL DEMONSTRATIONS ARE PLANNED
  - STRUCTURES WITH FEATURES ~ λ WILL HAVE SEVERE WAKEFIELD PROBLEMS.

  THOSE WITH LARGER FEATURES ARE ATTRACTIVE FOR WAKEFIELDS

- RF STRUCTURES
  - HIGH GRADIENT ⇒ SHORT λ. 30 GHz AT CERN & BEGINNING AT SLAC, 100 GHz AT ARGONNE, BERLIN, SLAC.
  - ISSUES AT 100 GHz

  FABRICATION – CUTTING → FORMING

  PULSED HEATING – LIKE LASER MIRROR DAMAGE

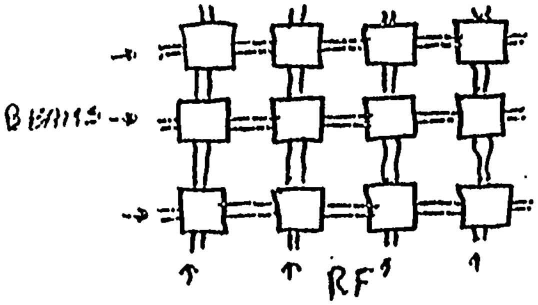

WAKEFIELDS – STRONG COUPLING TO BEAM ⇒ BIG SIGNALS ⇒ FEEDBACK TO MINIMIZE WAKEFIELDS. NOW DEMONSTRAT AT 11.4 GHz.

V. Concluding Remarks

This was a personal perspective of the Status and Future Directions of Advanced Accelerator Research.

Summary of Key Points

From the Introduction

- A revolutionary change in accelerators is needed for the long term future of particle physics.
- Advanced Accelerator research is focused too narrowly on e^+e^- linear colliders.

From Hadron Collider Section

- The “low field” collider is a revolutionary idea, but it is an old, failed one. What has changed?

From Muon Collider Section

- A complete concept has been developed and is valuable for clarifying issues.
- How should concepts such as the muon collider be evaluated when there is limited money and resources?

From the Linear Collider Section

- Power sources, structures, wakefield control are areas with substantial activity and progress.
- The following are critical for linear colliders to give revolutionary change in accelerator physics.
  - High gradients
  - New methods of experimentation, $\gamma\gamma$, and/or compensated collisions
  - New final focus concepts
  - Power source and acceleration efficiency

RF SOURCES

R. Phillips, SLAC

RF SOURCES FOR FUTURE COLLIDERS

1.0 INTRODUCTION

As we push particle colliders to 1-TeV center-of-mass collision energy and beyond, we require much more from our RF energy sources, both in terms of the RF performance and the number required for a given machine. In order to conserve real estate, the operating frequency of future colliders is apt to be higher than the S-band used for the SLAC SLC. It is this inevitable trend toward higher frequencies which presents the source designer with the greatest challenge. This paper is about that challenge. For reasons which will become clear, as we go to frequencies substantially above X-band, we will require sources other than klystrons, probably of the type referred to as "fast-wave devices," such as FEL or gyro-based amplifiers or two-beam accelerators. Because these are discussed elsewhere in this conference, I will stick to the klystron as my model in describing the challenges to be overcome, as well as the criteria which must be met by alternative sources for new accelerators.

2.0 THE CHALLENGE TO THE KLYSTRON

SLAC's design for the NLC, operating at 1 TeV, requires approximately 10,000, 75-MW, X-band klystrons, with a pulse length of 1.2 µs and a rep rate of 120 Hz. First, let's consider what properties the source, whatever it is, is required to have. Keep in mind we are talking about 10,000 units. These include:

3.1. **Klystron-like RF Performance:** For phase control purposes, an amplifier rather than an oscillator is required. High gain, preferably more than 50 dB is desirable, or the cost just gets pushed down to the driver level. About 1% bandwidth is required for pulse compression.

3.2 **Reliability/availability:** One wants every tube to turn on and operate whenever required. When a tube does misbehave, the accelerator has to be designed to go on without it.

3.3. **Long Life:** Our S-band klystrons have a meantime-to-failure of 50,000 hours, which is considered extraordinary by microwave tube standards. It is impressive by almost any standard. For instance, an automobile with 50,000 hours life averaging 40 MPH would provide 2 million miles of useful transportation.

However, with 10,000 tubes we have to do about this well. Even at this level we will be replacing 1,200 tubes per year. That's 100 per month or 3 1/2 change outs per day. Obviously, the change out procedure has to be straightforward and require little time. We might be able to live with double this rate of change outs, but 25,000 hours meantime-to-failure is pretty much the minimum acceptable.

3.4 **High Efficiency:** The efficiency of the source directly impacts wall plug power. Our S-band klystrons operate at about 42% efficiency and this is not good enough for a 10,000 tube machine. We have set a goal of 60% efficiency for the X-band sources. This is further complicated by the requirement for a beam-focusing solenoid which, in the case of the X-band tube, consumes about half as much power as the klystron itself. We found a way of completely eliminating the beam-focusing power by using permanent magnets which will be described later.

3.5 **Low Cost:** If the source has high production cost designed into it, it simply won't fly. At SLAC we have begun a major effort to cost-reduce our X-band klystrons with a goal of $30,000 per klystron in production quantities. This effort includes the detailed design of the required factory.

3.0 MATCHING THE KLYSTRON TO THE ACCELERATOR

Figure 1 illustrates the RF pulse the physicist requires for the accelerator, 300-MW peak power with about 0.3 µs pulse length. Also shown is a pulse, which is far more compatible with the output of a practical klystron, a 75-MW pulse with a maximum pulse length of 1.5 µs. This combination, in fact, is what we will use in the test accelerator for the NLC. The transformation is achieved using a pulse compressor which is basically a long, low-loss waveguide that is hooked up in a hybrid feed fashion so that it is first filled by the klystron and then made to empty when the phase of the klystron is reversed, giving a short, high amplitude output pulse. The energy difference between the two pulses is lost because the filling and emptying process is not perfect.

I have been asked, "Why not avoid the pulse compression losses by simply designing a klystron which produces 300 MW of power?" This is probably doable, but in the real world it too would be inefficient and not very practical. The beam voltage would need to increase from about 500 kV to about 850 kV, which makes for a very difficult modulator design problem. Figure 2 shows why one does not really gain in efficiency. It is a cartoon of a typical modulator pulse with a 1.5 µs flattop which has a 0.25 µs second rise time and a 0.5 µs fall time. At the higher voltage with the shorter flattop condition, it still has at least a 0.25 µs rise time and a 0.50 µs fall time, which now represents a significantly larger portion of the total energy, hence the inefficiency.

All would be well if, instead of a line-type modulator, one could use a DC voltage supply and a low-voltage, high-impedance control electrode like a non-intercepting grid, in which case the beam could be turned on and off with little wasted energy. A DC supply of 850 kV would be frightening to behold. When it arcs, the problem of crowbaring the stored energy would be difficult indeed. Furthermore, I am not sure one could design an electron gun for an X-band size beam which would hold off 850 kV DC, at least not one which would be cost effective.

4.0 KLYSTRON DESIGN AND OPERATING PARAMETERS

At SLAC we faced the problem of going from 60 MW at S-band to 75 MW at X-band. How did we modify our klystron design and operating parameters to achieve this? We knew that we faced a formidable increase in gradients, about 4 to 1, both RF and DC, and in beam power density as the structure and beam size decreased in going to four times higher frequency. First, let's consider what would happen if we did a direct scaling of the klystron from S-band to X-band, maintaining voltages and currents. As Table 1 shows, the results are rather startling. Cathode current density goes from a comfortable 6.25 A/cm^2 to 100 A/cm^2. Any value over 10 A/cm^2 will greatly shorten tube life. In fact, no one knows how to get 100 A/cm^2 reliably. The maximum gun gradient goes from 175 kV/cm to 700 kV/cm. Anything over 350 kV/cm is known to cause unacceptable gun arcing. Magnetic focusing field increases from 1500 gauss to 6000 gauss, which rules out any low-cost, permanent magnet solution. The problems continue. Although not shown in the table, an increase by a factor of four in RF gradient in the penultimate and output cavities will ensure unacceptable RF pulse shortening while the four times increase in the RF window gradient will guarantee its failure.

How does one produce a reliable X-band tube at the 75 MW level? Starting with the electron gun, we did it by raising rather than lowering the beam voltage. This allowed us to decrease the beam current with a disproportionate decrease in the microperveance, $Io/Vo^{3/2}$, of the electron gun. The next column in the table shows what happens to the operating parameters when we go from 350 kV and 414 A to 490 kV and 257 A. Electron gun microperveance goes from 2.0 to 0.75 while the required solenoid focusing field is approximately cut in half.

We now select a cathode diameter which ensures acceptable cathode current density. We chose 7.5 A/cm^2, compared with the 6.25 A/cm^2 for the S-band tube. This requires an extraordinary increase in the area convergence of the electron gun, from 25 to 1 to about 125 to 1. But this is OK. Although a high area convergence is not achievable with a high microperveance like 2.0, it is relatively straightforward to achieve at a microperveance as low as 0.75 using today's gun design programs. Figure 3 shows a typical gun run for the 125 to 1 area convergence gun.

What happens to the performance of the tube? The power went from the 60 MW of the S-band tube, to 75 MW for the X-band tube, while efficiency went from a measured value of 41% for the S-band tube to a measured value of 60% for the X-band tube. This improvement in efficiency was predictable. The expression shown here (Eff = 74 - 16 microperv), though empirical, fits a wide range of klystrons which have been developed over the last quarter century. Note that even the gradient goes from an unacceptable 700 kV/cm to a very acceptable 229 kV/cm. The large increase in the cathode area increases the cathode/anode spacing. This is one of those rare instances where nature is kind. Increasing the voltage frees up the design, allowing a wide range of problems to be addressed.

We are not done with our design yet. We still have breakdown in the buncher cavities, the output cavity and the window, plus a still unacceptable solenoid power. Figure 4 is a cross-section of one of our X-band klystrons which will illustrate the design modifications which we used to solve the remaining problems. To begin with, beam focusing was achieved using a periodic reversal of washer-shaped, high-energy rare earth magnets, which are split and attached to the tube after it is baked out. It is necessary only that the RMS value of this periodic magnetic field be made equal to the solenoidal value which is required to focus the same beam. This type of focusing is used on virtually all traveling-wave tubes. The difference between what we do and what is done on the traveling-wave tube, is that we use a magnet period which is very short compared to a plasma wavelength. This luxury is not available to the traveling-wave tube designer because of the unfavorable form factor of the TWT. We have 10 reversals of the field for every plasma wavelength. The plasma wavelength is, in a sense, a measure of the reaction distance of the electron beam to a perturbation. Hence, as long as perturbations are random, such

distance of the electron beam to a perturbation. Hence, as long as perturbations are random, such
as would be caused by the unavoidable tolerances and internal variations of commercial grade magnets, the effects are washed out in the big picture.

The short magnet period also ensures a very low stop-band voltage, that voltage below which no current is transmitted. This velocity filter characteristic is basic to all PPM-focused electron beams. We operate with a stop-band voltage of 3% of the operating voltage. This ensures that the small amount of current which is dropped out in the rise and fall of the beam pulse results in a negligible amount of heating of the klystron body. Finally, the use of a very short magnet period gives us a focusing field which is significantly lower on the axis than it is at the wall, hence the beam is trapped in a deep potential well. As it bunches, it is less inclined to expand into the wall causing heating problems. To further reduce the chance of beam interception, we profile the field as shown in Figure 5, making it higher where bunching is greatest. The success of the conversion from solenoid to PPM-focusing is attested to by the results: More than 99.9% beam transmission to the collector with no RF, less than 1% beam power intercepted with full RF output.

Progressing down the tube, we solved the problem of the penultimate cavity gradient by replacing the single penultimate cavity with three cavities which share the voltage required to provide the final bunching of the beam. We used a similar trick in the design of the output circuit in which the single output cavity was replaced by a five-cell, disc-loaded, traveling-wave output circuit. The cartoon of Figure 6 shows the last of the three buncher cavities along with the disc-loaded output circuit and the tailpipe which leads to the collector.

The principle involved in reducing the output cavity gradient is the following: The voltage across the cavity has to be comparable with the beam voltage in order for the beam to be slowed down sufficiently to get good efficiency. A voltage of 490 kV across a single X-band cavity produces a maximum surface gradient well in excess of the breakdown value, which turns out to be around 1 MeV/cm. If, instead, one designs an output circuit having a number of cells, with the cells operating at approximately equal voltage, one can reduce the maximum gradient by a factor of at least two or three. To achieve the equal voltage per cell requires that the impedance from cell to cell be properly tapered. This is achieved by increasing the disc diameter from cell to cell. In order to obtain the best possible efficiency, there is also a taper in the phase velocity of the circuit from end to end so that the wave stays in synchronism with the slowing electron bunches.

The output window breakdown problem was solved by changing from the TE_{11} mode for the round disc window to the TE_{01} mode. Figure 7 illustrates the field lines for these modes. The TE_{01} mode, which is the well-known, low-loss mode, has the distinct advantage that there are no field lines terminating on the wall. Our TE_{11} window failures were all related to the field terminating on the wall, as evidenced by the fact that failed windows always showed a crack emanating along the ceramic, originating where the field terminates, never at 90° to that plane. The use of the TE_{01} mode was made practical by the development at SLAC of the flower petal TE_{10} to TE_{01} mode converter, which performs with over 99% efficiency and requires very little space. From the standpoint of the accelerator, use of a TE_{01} window in the klystron is a natural in that the pulse compressor also operates in the TE_{01} mode.

We gained a further advantage in the window power handling capability by converting from a resonant half wave window to a traveling quarter-wave window. Figure 8 illustrates the field in the region of the window for the standing-wave case and the traveling-wave case. In the former, the standing wave is in the ceramic and there is a traveling wave on each side. This results in a maximum of the electric field at the surface of the window. In the latter, irises of appropriate dimensions are used to ensure that a match is achieved at the window, which results in a traveling wave passing through the window with standing waves on each side of the ceramic. In the latter case, the surface field is less than half of what it is for the standing-wave case. Assuming that the damage done in window breakdown is caused by surface field, the traveling-wave window is capable of supporting four times the power of the standing-wave window.

In practice, we often had failures in the TE_{11} standing-wave windows at as little as 20-MW RF power, while the TE_{01} mode traveling-wave window is good up to 100 MW. At this level we have had two failures in long-term testing in a X-band resonant ring. Each failure occurred at the point where electric field was highest. A puncture having the appearance of a volcano occurred in each case, suggesting that failure is initiated by a small occlusion of some sort in the ceramic. Our current efforts are in the direction of raising the margin by using improved hot, isostatic-pressed ceramics. We have never lost a hot, isostatic-pressed window in the resonant ring, but they are very difficult to metalize.

The design tricks which we used to "scale" the 60-MW S-band klystron, four times in frequency to high X-band, made it possible to keep the design and operating parameters within what are considered to be safe limits for long life and high reliability. Unfortunately, there is no way to get another factor of four in operating frequency from the klystron while meeting these same design and performance criteria. For instance, scaling the X-band klystron to 45 GHz, without increasing cathode current density, would require developing a reliable, long-life electron gun, having a beam area convergence of about 2000 to 1. Furthermore, the trick used for reducing the surface gradients in the buncher and output cavities would require 12 buncher cavities and a 20-cavity, traveling-wave output circuit, both of which appear to be impractical and not at all consistent with low cost. In fact, it is hard to imagine a 45 GHz, 75-MW peak-power amplifier of any known type, based on a low-cost design, which would provide long life.

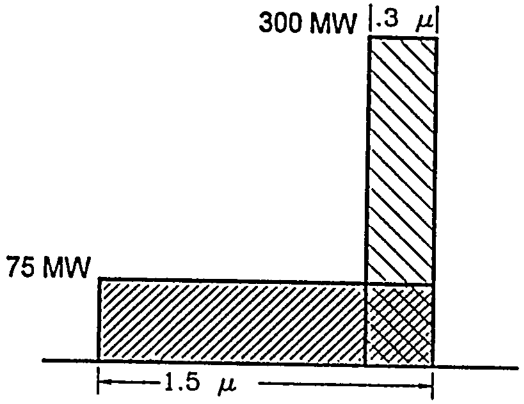

Fig 1 Matching Klystron Output to Accelerator Need

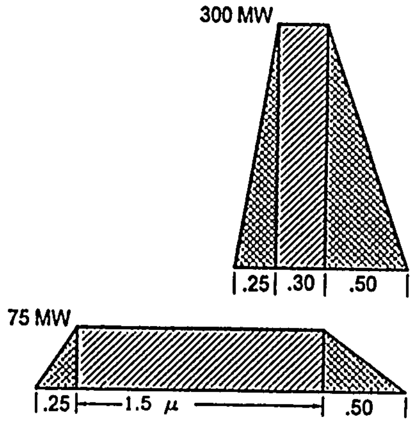

Fig. 2 Short Pulse Reduces Modulator Efficiency

TABLE 1

SCALING OF KLYSTRON
S-BAND TO X-BAND

Frequency	S-Band	Direct Scale X-Band	Modified Scale X-Band
Vo (Kv)	350	350	490
Io (A)	414	414	257
μ perv ($Io/Vo^{3/2}$)	2.0	2.0	0.75
Cathode Current Density (A/cm^2)	6.25	100	7.5
Cathode Area Convergence	25	25	125
Maximum Gun Gradient	175	700	229
Focusing Field (Gauss)	1500	6000	3120
RF Power Out (MW)	60	60	75
*Efficiency %	41	41	60

*Eff ≈ 74 - 16x μ perv

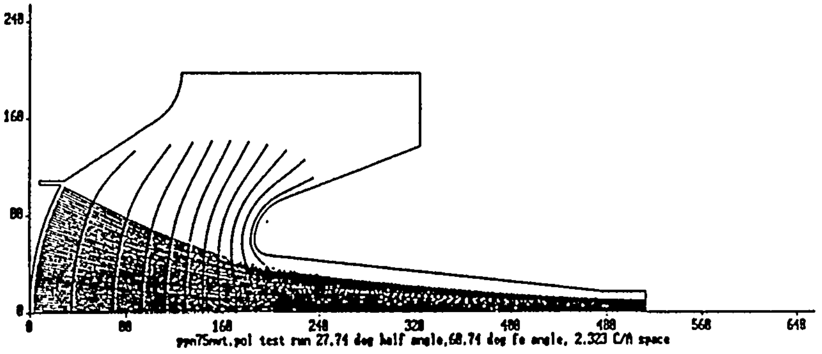

Fig. 3 Simulation of .75 E Gun with 125/1 beam area convergence.

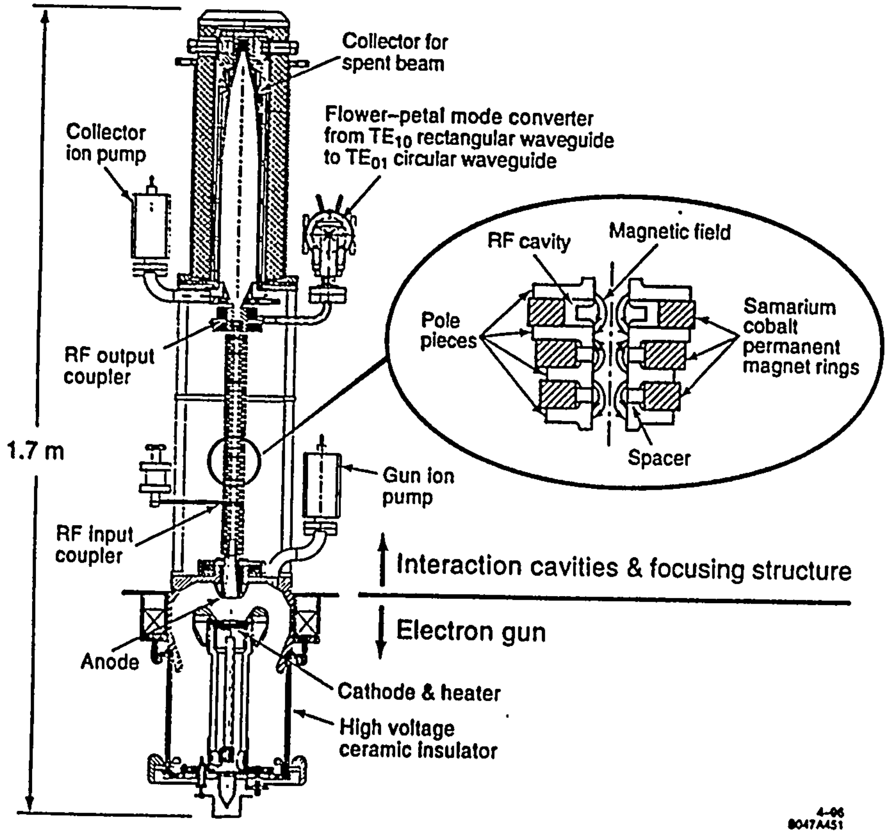

Fig. 4 Cross Section of PPM-Focused 75 MW X-Band Klystron.

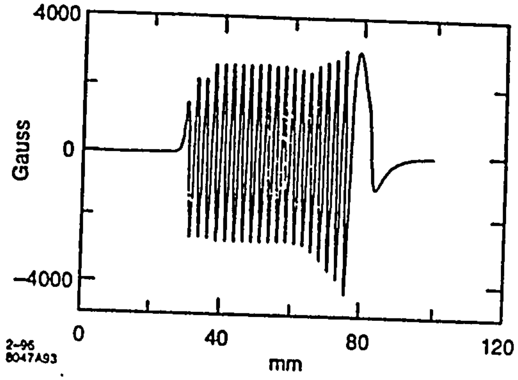

Fig. 5 Magnetic Field Profile for Best Efficiency Without Beam Interception.

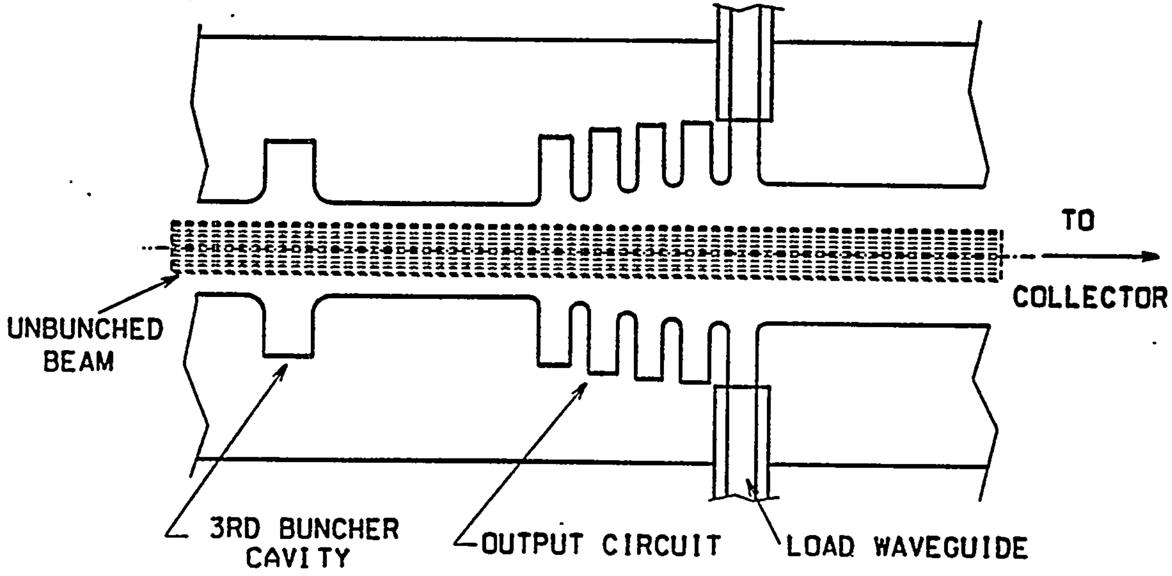

Fig. 6 Cartoon of Final Buncher Cavity and 5-Cell Disc-Loaded Output Circuit.

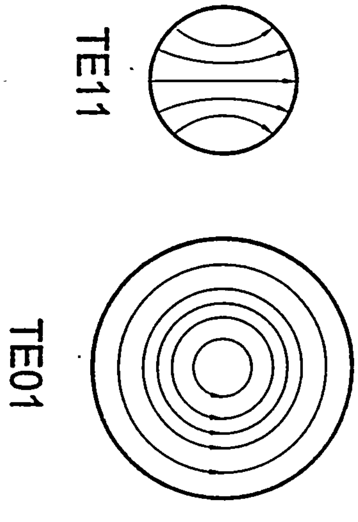

Fig. 7 Comparison of Two Window Modes

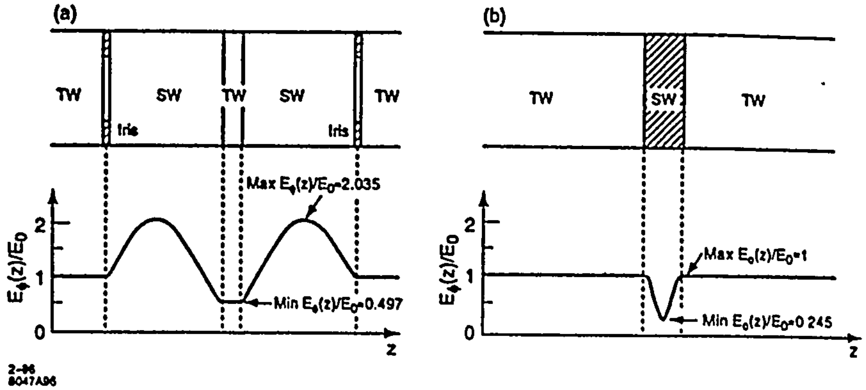

Fig. 8 Comparison of the Reduced-Field TW Window (a) with a Half-Wave Resonant SW Window (b), both Operating in the TE_{01} Circular Mode. In Addition to the TW Version having Substantially Lower RF Electric Field at the Window Surface, the Integrated Dielectric Power Losses are only 23% those of the Half-Wave Resonant Window. The Horizontal Scale is Expanded for Clarity.

LASER AS A POWER SOURCE

G. Mourou, U. Michigan

- Wake Fied acceleration and laser requirements
- How far is the laser from these requirements?

Laser as
a Power Source

G. MOUROU

NSF-Center for Ultrafast Optical
Science. U of Michigan

- Why Should we consider the Laser as a source for Acceleration?

- Over the past year impressive results have been obtained with Laser Wake Field by <u>UCLA/Rutherfo</u> and <u>U of Michigan</u>. They showed that electrons could be accelerated over <u>100 MeV</u> over a distance of <u>1mm.</u> ~~leading~~ Suggesting gradients

$$\boxed{E > 100 \text{ GeV/m.}}$$

- <u>Laser Wake Field is a reality</u>

Laser Wake Field Acceleration

(Tajima and Dawson)

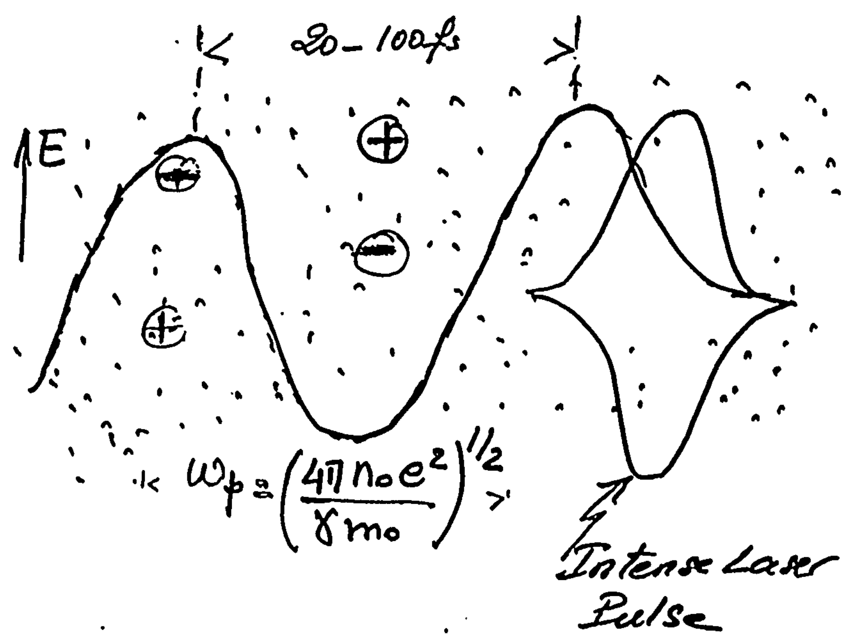

- $E \sim 100\,GV/m$ $\quad I \sim 10^{18}\,W/cm$
- Low Emittance because Large Gradient
- Problem ; Very short Acceleration bucket (20-100fs)
  Insurmountable injection problem!!!
  (See D. Umstadter talk)

PIC Simulation: Single Pump Pulse ($a_0 = 1$) without Injection Pulse (D. Umstadter)

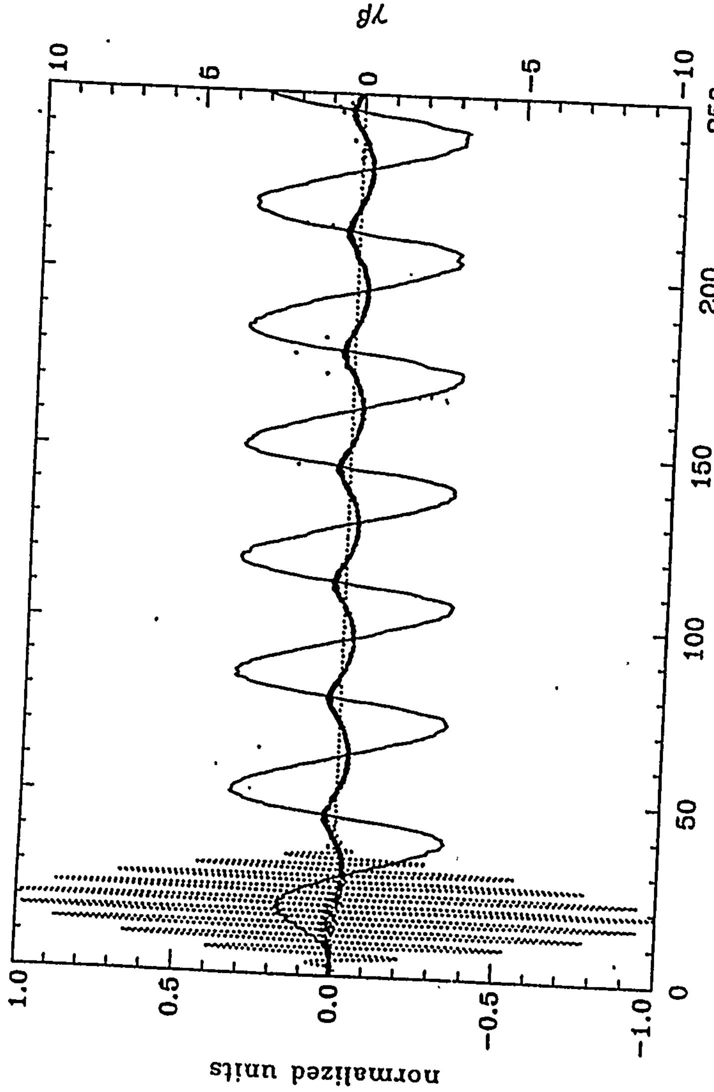

Standing wave field (no instability) Laser Injected [illegible] Accele

Schematic Diagram of Lilac D. Umstadter et Al.

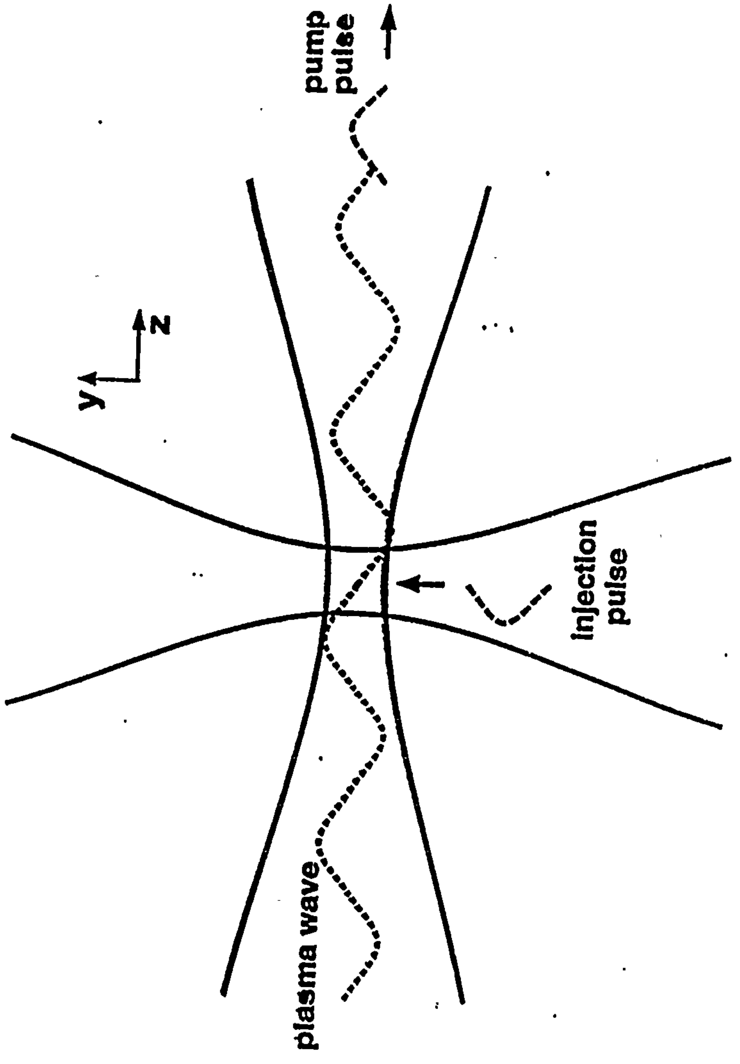

- Com bined with LWFA, the ponderomotive pressure can be used to produce burst of fs. electron at GeV. (D. Umstadter
- At the U of Michigan we are building an All Optical Accelera which will produce fs-electron at GeV level.

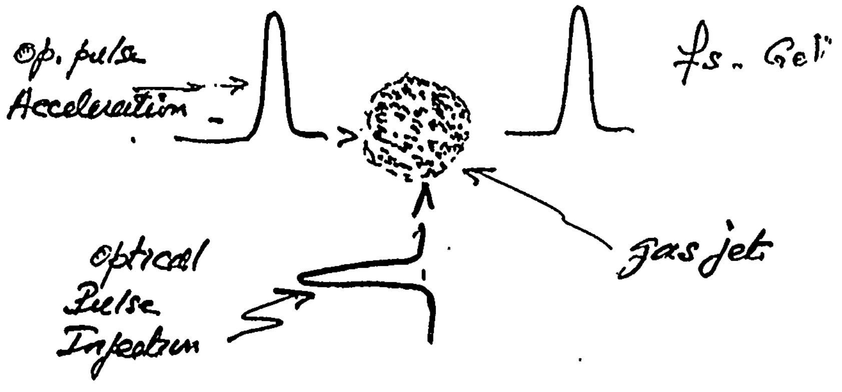

Power of Table Top Laser Systems

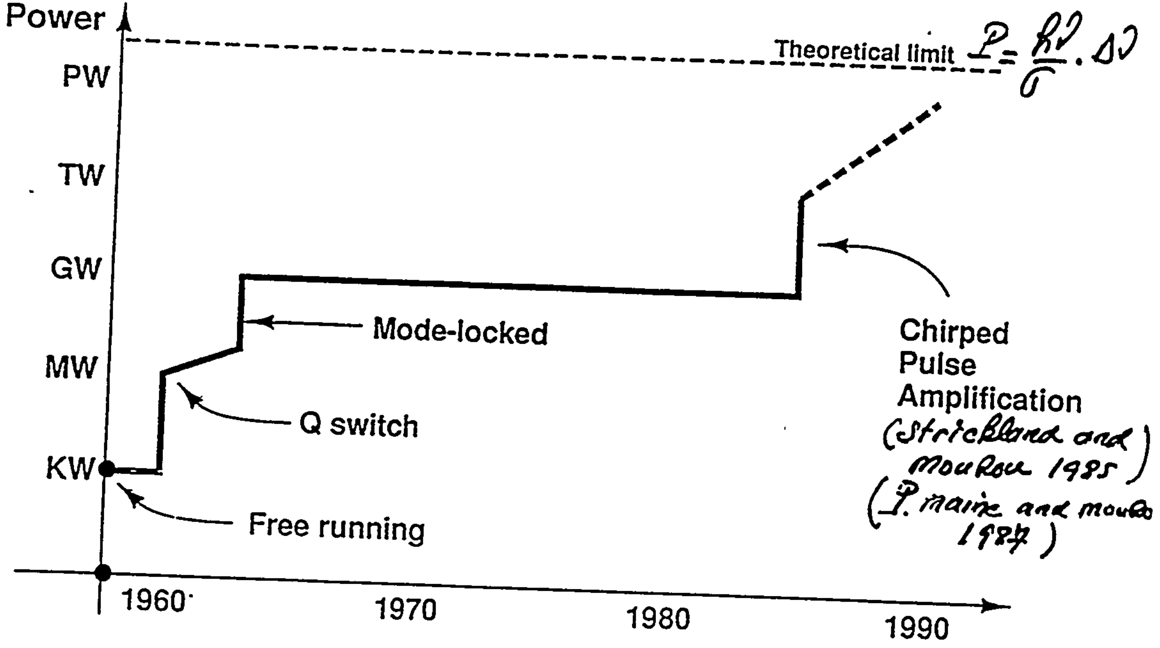

Intensity Laser vs. Years

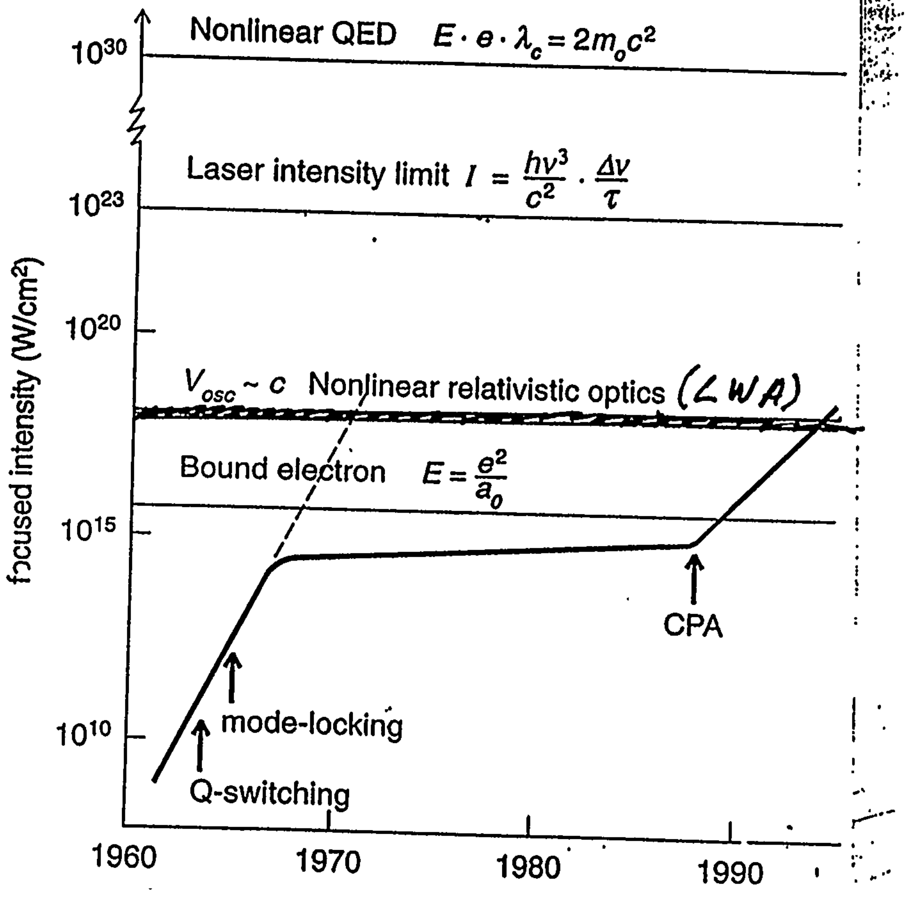

Laser Requirements for Wake Field Acceleration.

1) Peak Power in the TW
2) Adjustable Pulse Duration. (10-50
3) Pulse Shaping.
4) Average Power. (kW – MW)
5) Efficiency. (> 10%)
6) Cost

This technique is pushed to the kJ/ps Petawatt/ [illegible]

upto 600J

~~upto 30J~~
< 1ps
(Lumeil/mich, Livermore'
@ [illegible]J/30fs
. WSU
. Stanford
- Michigan
- ENSTA.
- Berkeley
- UCSD

Chirped Pulse Amplification

D. Strickland and G. Mourou Opt. Comm. 56, 219 (1985)

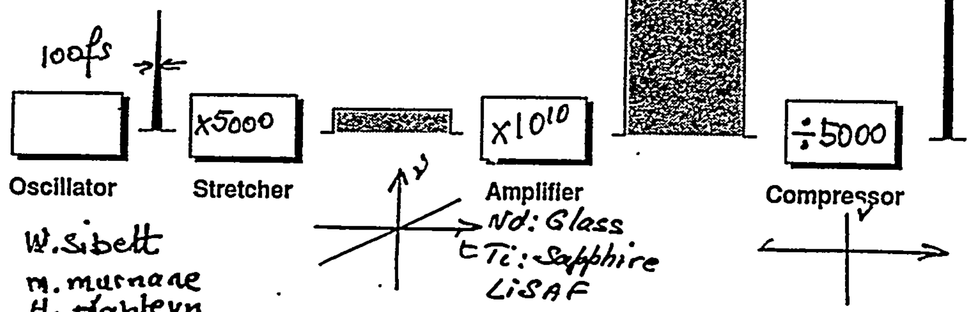

W. Sibett
M. Murnane
H. Kapteyn

Towards More Compact CPA Laser Systems

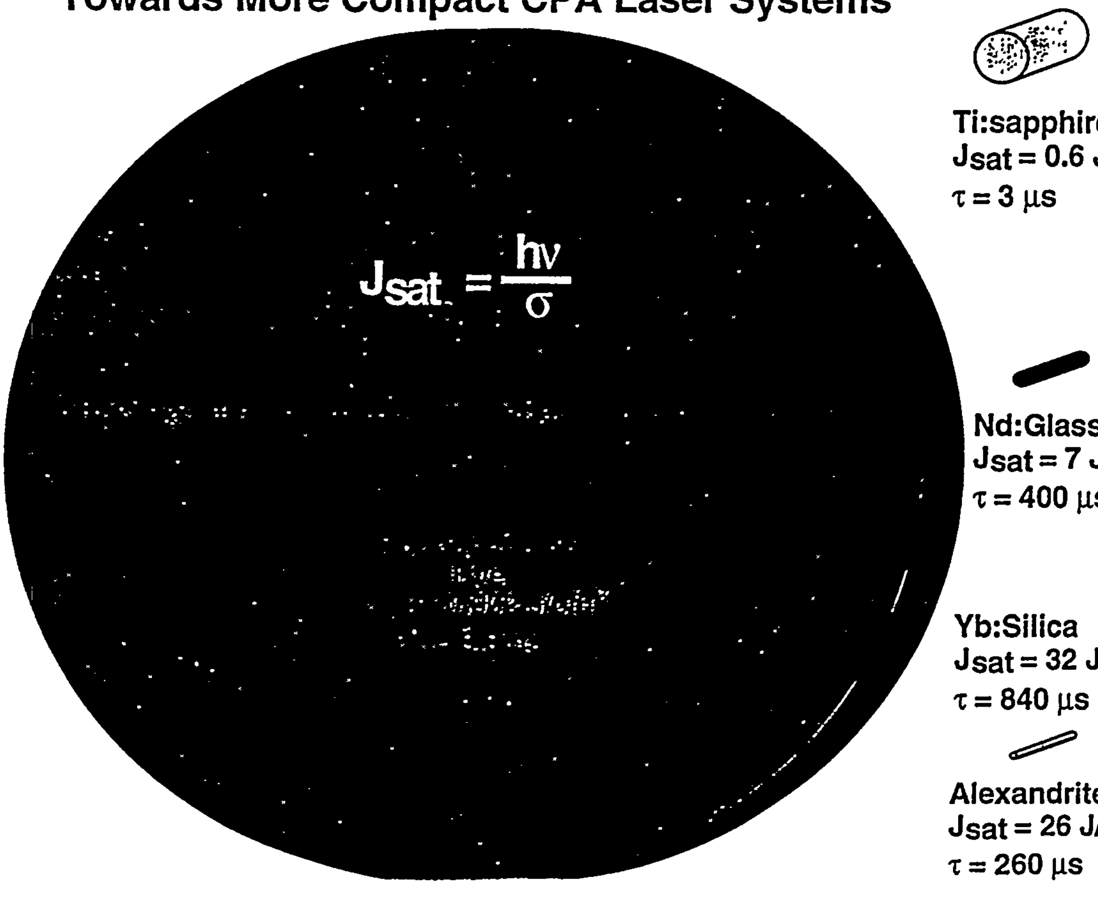

$$J_{sat} = \frac{h\nu}{\sigma}$$

Ti:sapphire
Jsat = 0.6 J/cm^2
τ = 3 µs

Nd:Glass
Jsat = 7 J/cm^2
τ = 400 µs

Yb:Silica
Jsat = 32 J/cm^2
τ = 840 µs

Alexandrite
Jsat = 26 J/cm^2
τ = 260 µs

Limits of fiber stretcher systems

In this simulation, a 100-fs pulse was stretched to 250 ps in fiber and compressed with a 600 line/mm grating pair

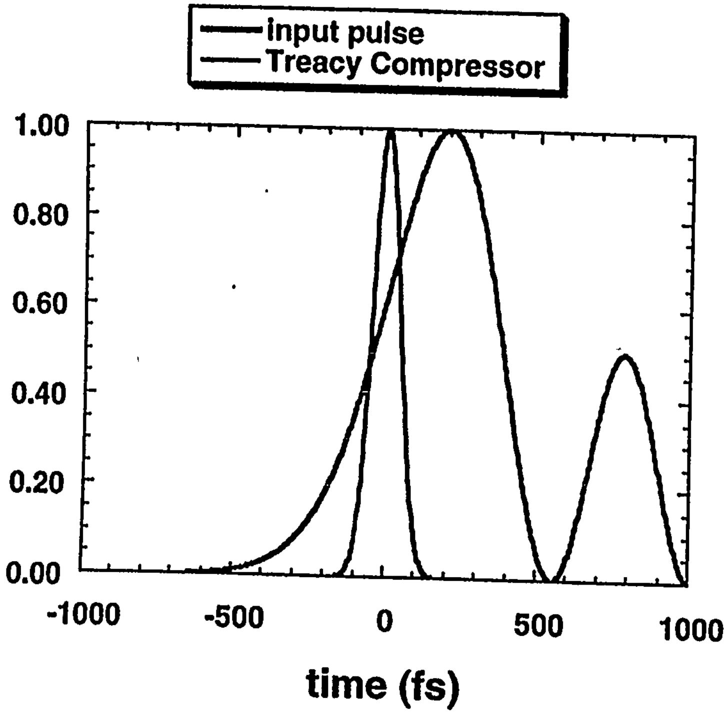

Bolan' Treacy. ('1969), Dispersion de vitesse de groupe.

Pulse Stretching / Compression.

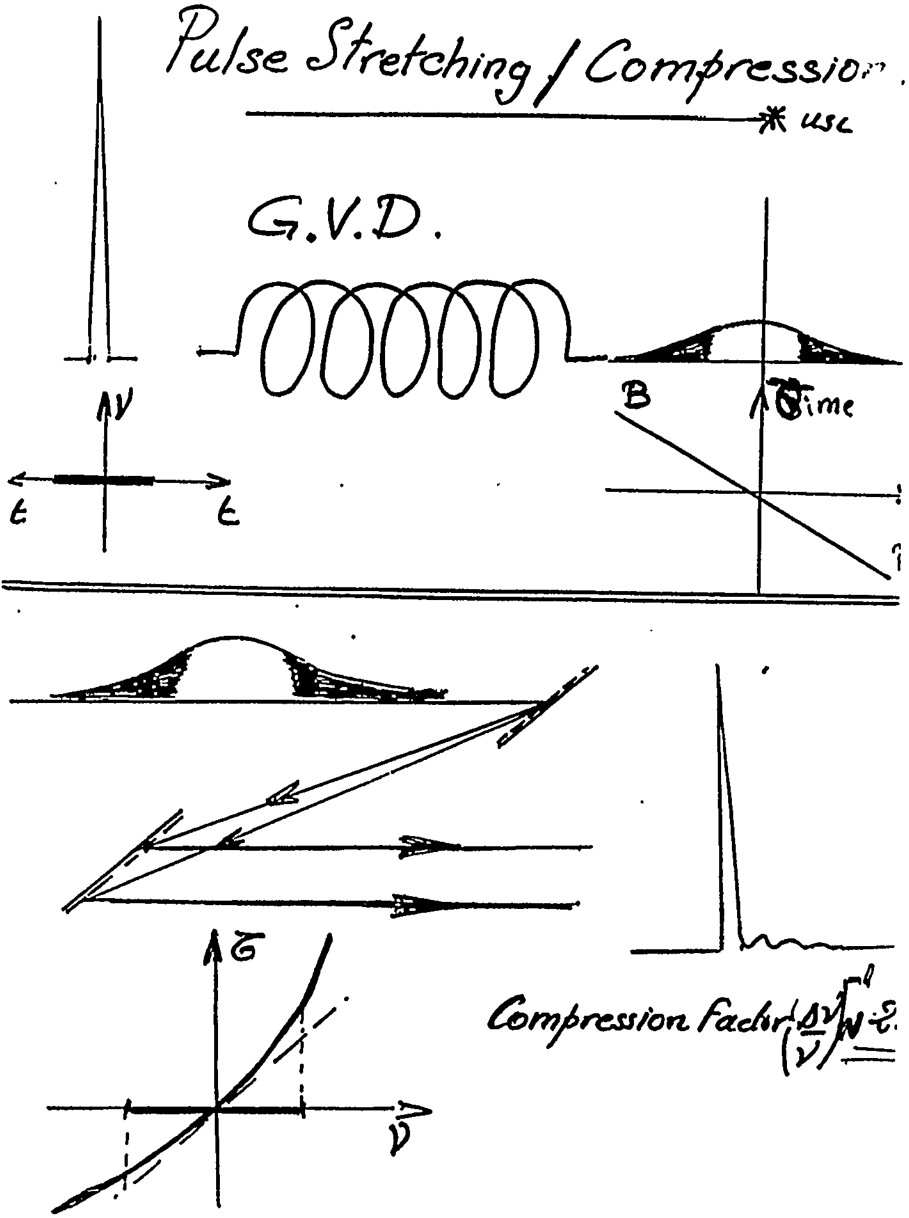

1000x Expansion/Compression of Optical Pulses

- M. Pessot and G. Mourou 1987
- O.E. Martinez IEEE QE. 23, 59 (1987.)

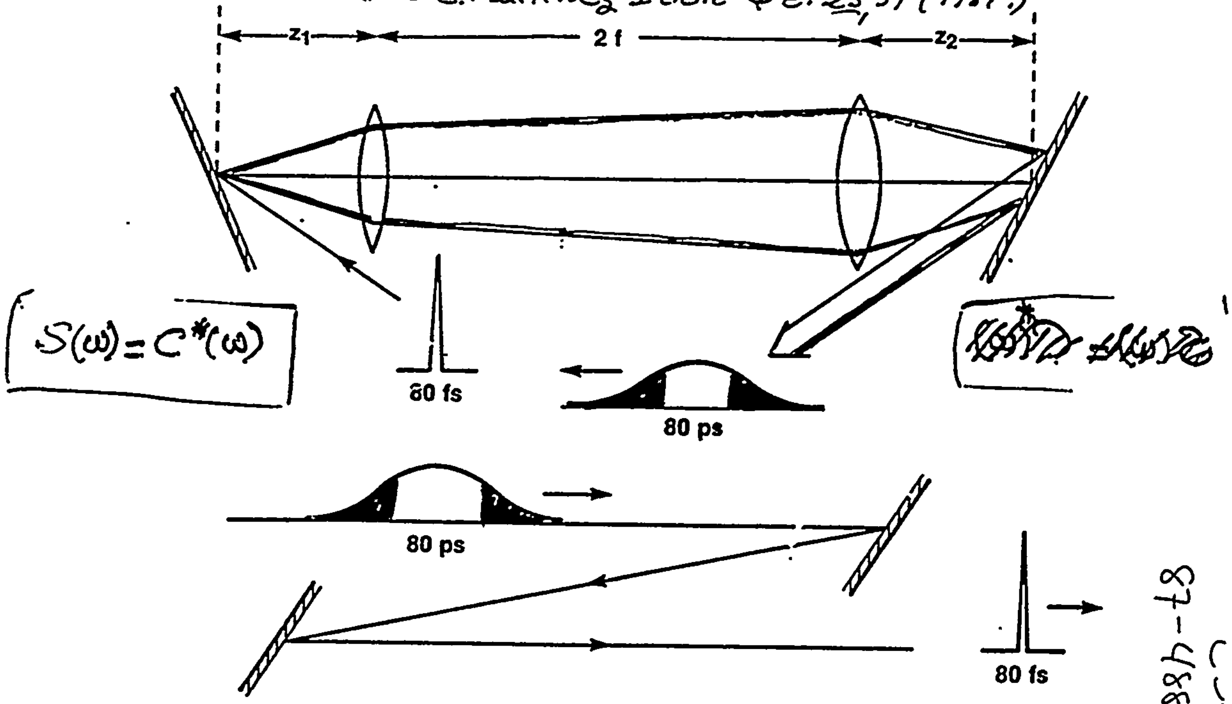

$S(\omega)=C^*(\omega)$

Z303

87-4885-2

Input Pulse and Recompressed Pulse

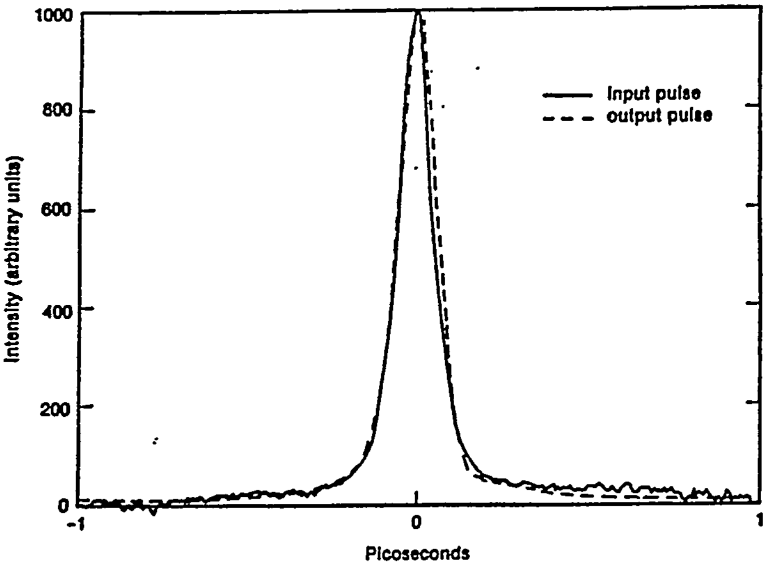

Z187

Chirped Pulse Amplification (1.06 μm)

Y. Baudouin, S. Coe, C.Y. Chien, J.L. Tapie.

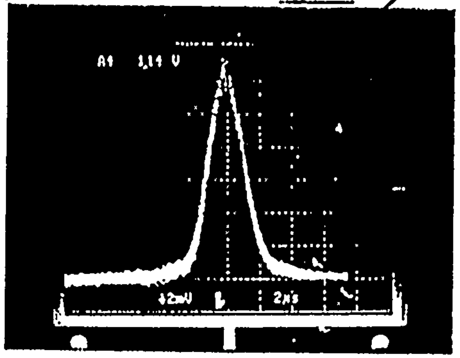

$\tau_p = 180fs$

Energy ~ 3nJ

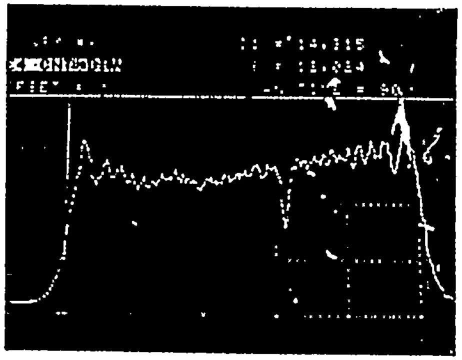

Pulse stretched

X 5000

$\tau \sim 1ns$

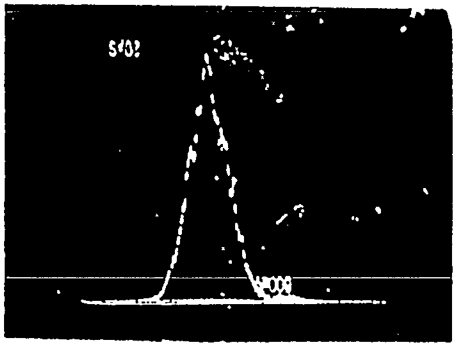

Pulse Amplified and compressed

$\tau_p \sim 400fs$

Energy ~ 2 J

$P \sim 5TW$

Y Baudouin - S. Coe. C. Yang. J.L. Tapie

Large Stretching/compression Ratio X 10^5

Chirped Pulse Amplification

D. Strickland and G. Mourou (*Opt. Commun.* 1985)

$$e^{i\varphi_s(\omega)} \cdot e^{i\varphi_A(\omega)} = e^{-i\varphi_c(\omega)}$$

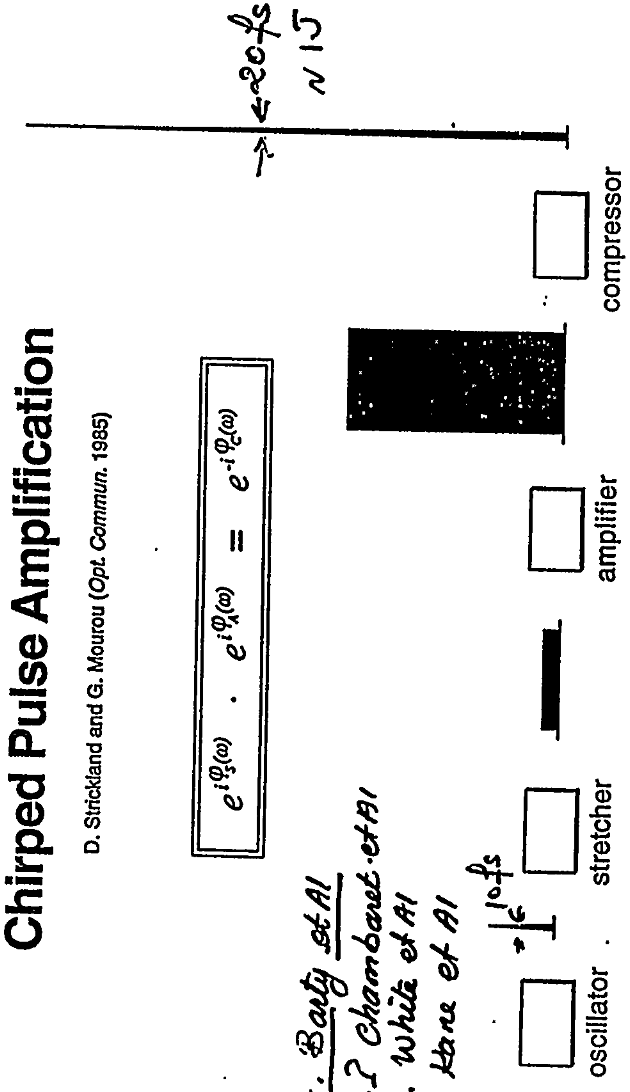

- C. Barty et Al
- J.P Chambaret et Al
- B. White et Al
- S. Kane et Al

Amplifier System : 3TW, 25fs

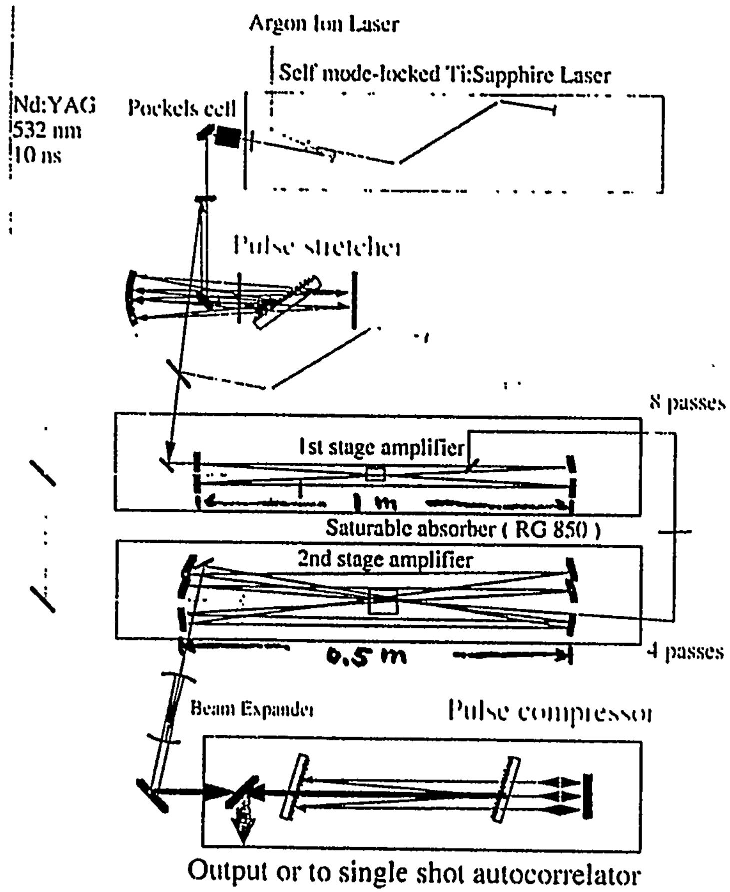

H. Kapteyn et al.
Opt. Lett. 20, 64 (1995)

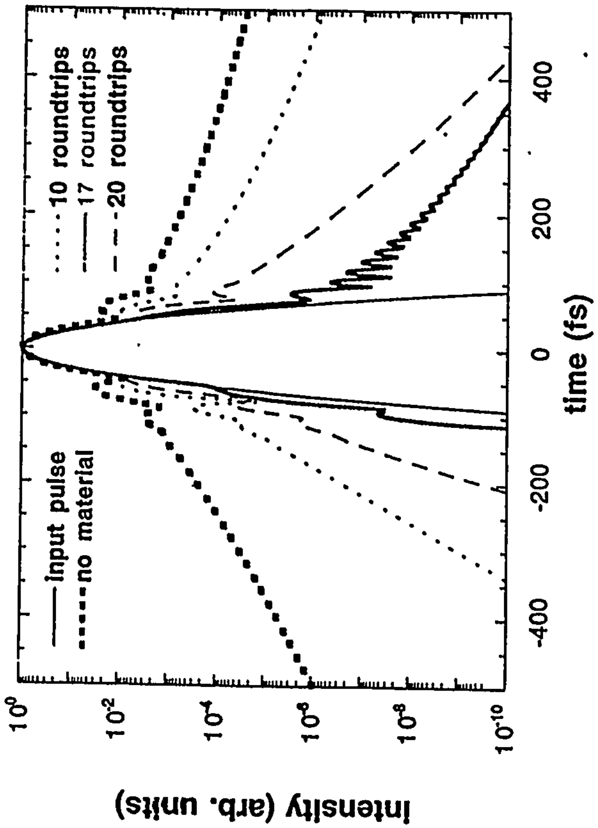

20 fs stretched to 400 ps and recompressed.
(S. Kane, J. Squier and G. Mourou)

Further mismatching the stretcher and compressor

[illegible]

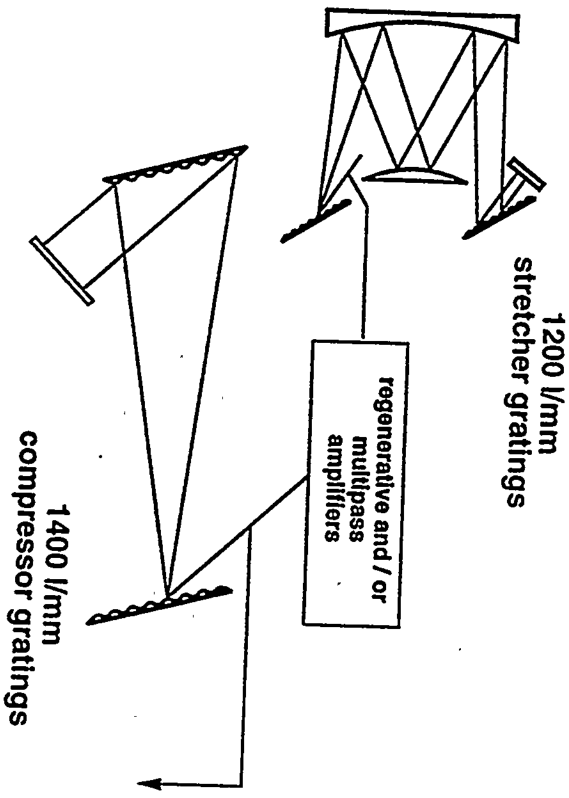

Mismatching the gratings themselves gives us fourth-order-compensated CPA

Refs → [illegible] – S. Kane and J. Squier

Rabi period. ·Hp.: perturbation Hamiltonian of the signal. ·Δω: random perturbation caused by dephasing/phonon

Theoretical Peak Power Limit.-

Chirped Pulse Amplification

$$\boxed{P_{Th} = \frac{h\nu}{\sigma} \times \Delta\nu}$$

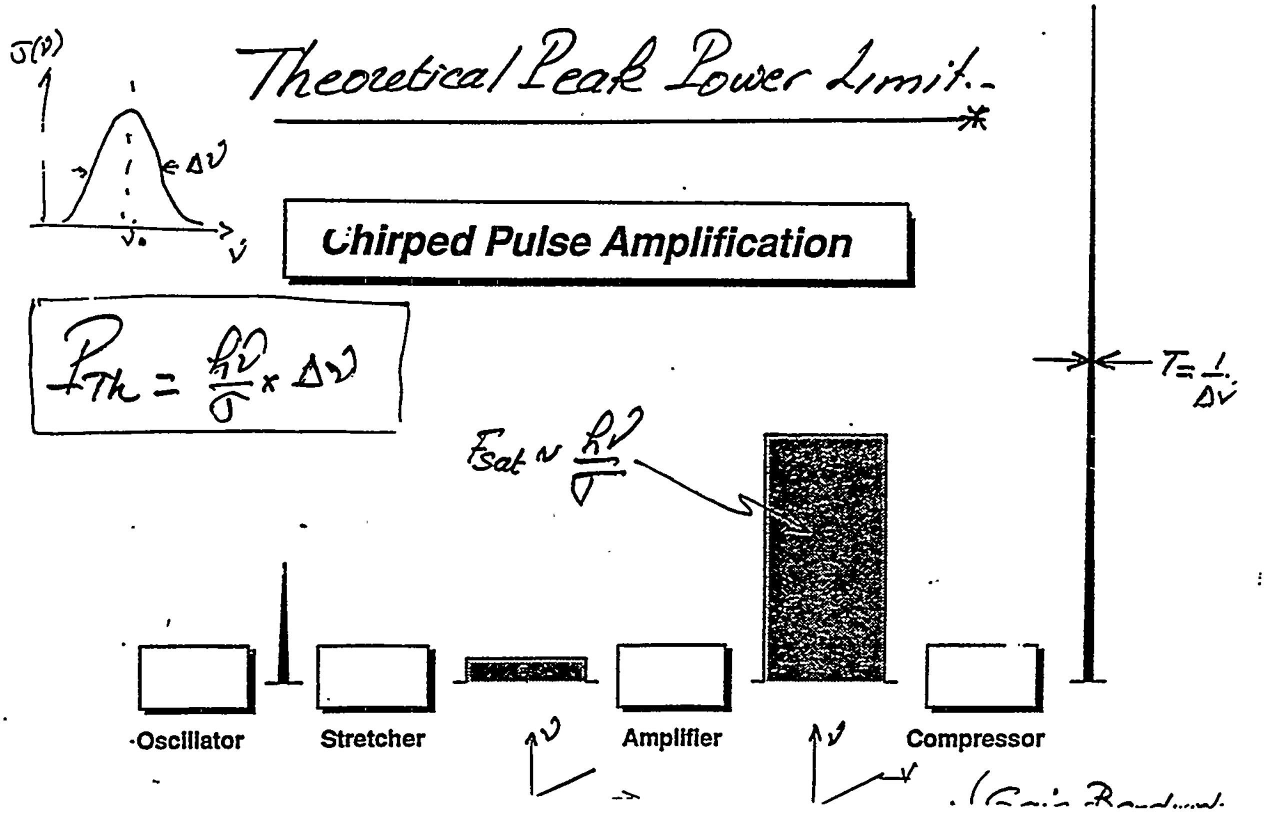

Theoretical Peak Power (cm^2 of beam)

	Pulse Duration (fs)	Peak Power (TW)
Nd: phosphate	80	60
silicate	60	100
combination	30	400
Yb: Silica	20	1000 (PW)
Alexandrite	10	2000 (2 PW)
Cr:LiSAF	15	300
Ti:sapphire	6	120

Yb: Glass : Material of Choice for LWA.

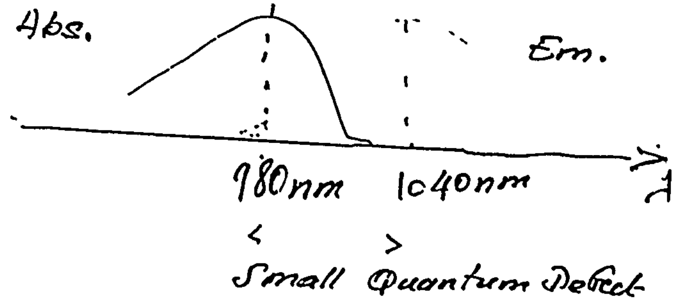

- The material can amplify upto 20fs pulse.
- Diode pumpable (Ideal)
  1) Right wavelength
  2) Long strage time. (2ms)
- Small Quantum Defect
- High efficiency ~ 10%
- Cheap.
- Ultra Compact

Pulse Shaping

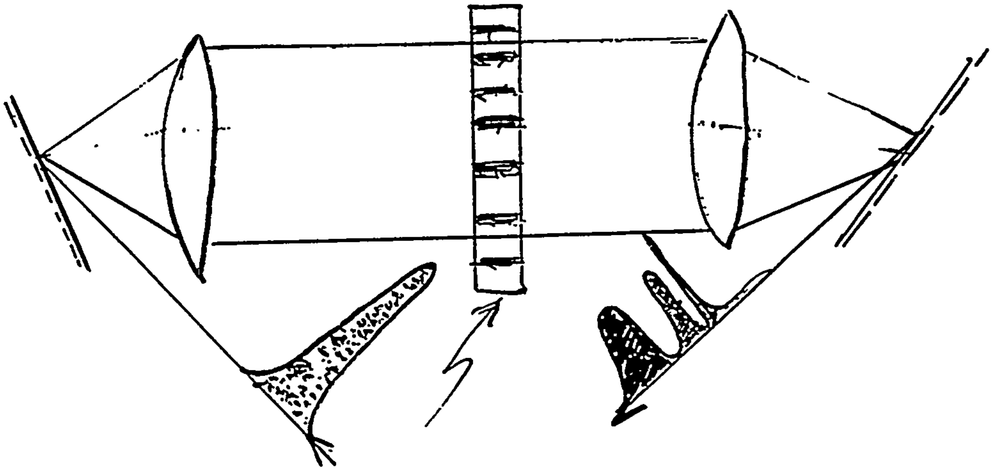

Amplitute and φ mask

The Three Types of Laser-Plasma Accelerators Differ in the Temporal Characteristics of their Driver Pulses

$$\boxed{L = c/\nu_p = c\,(\gamma m/n_e)^{1/2}}$$

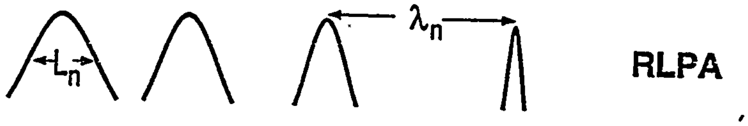

Phase shaping

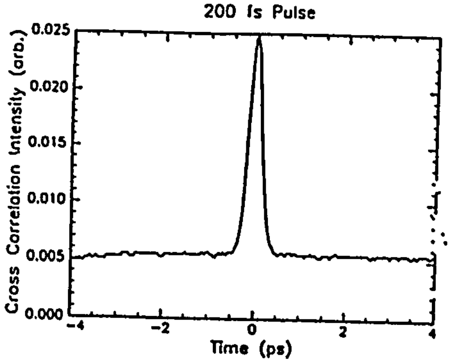

200 fs input pulse

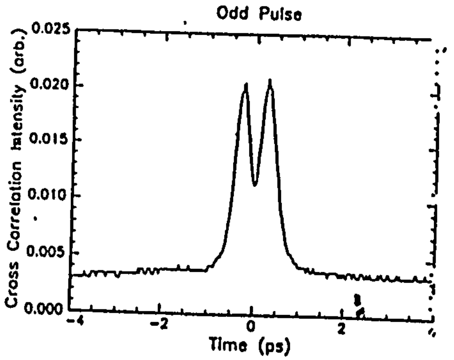

An "odd" pulse created by flipping the components shifted up with respect to the carrier frequency π radians out of phase with those frequency components shifted below the carrier frequency.

Chamberlain JAEKI IBAKIKEN

AVERAGE POWER OF AMPLIFIED PULSES

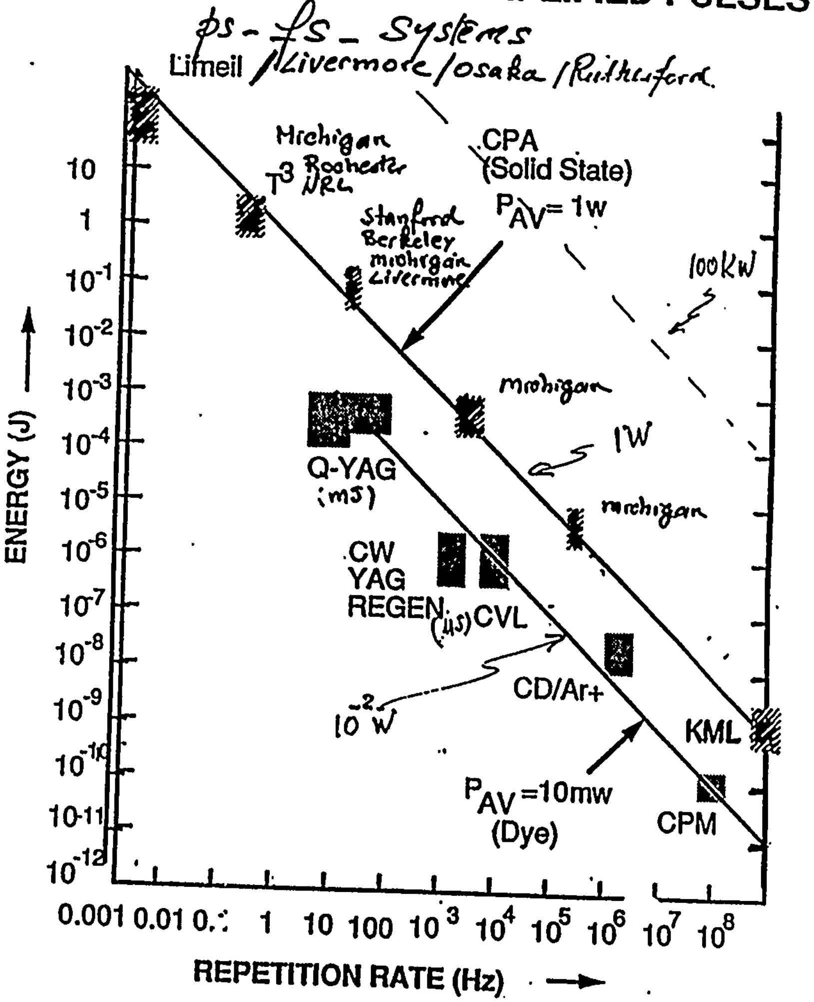

Conclusions

1) Chirped Pulse Amplification Laser matches all the requirements for Laser Wake Field Accelerations

- TW Pulses
- 10-100fs Synchronizable.
- Pulse shaping (~~RCPA~~. (RCPA).
- Average Power kW-MW should be possible
- Efficient (Yb: glass / diode pump,
- Low Cost
- Ultra compact

rce 108

CPA + CWA

⇓

All Optical GeV, fs electron Accelerator.

PULSED POWER SOURCES -- PHYSICS ISSUES UNDERLYING POWER CONDITIONING FOR ACCELERATORS

M. Gunderson, USC

Compact GeV, 10fs, All Optical Wake Field Acc.

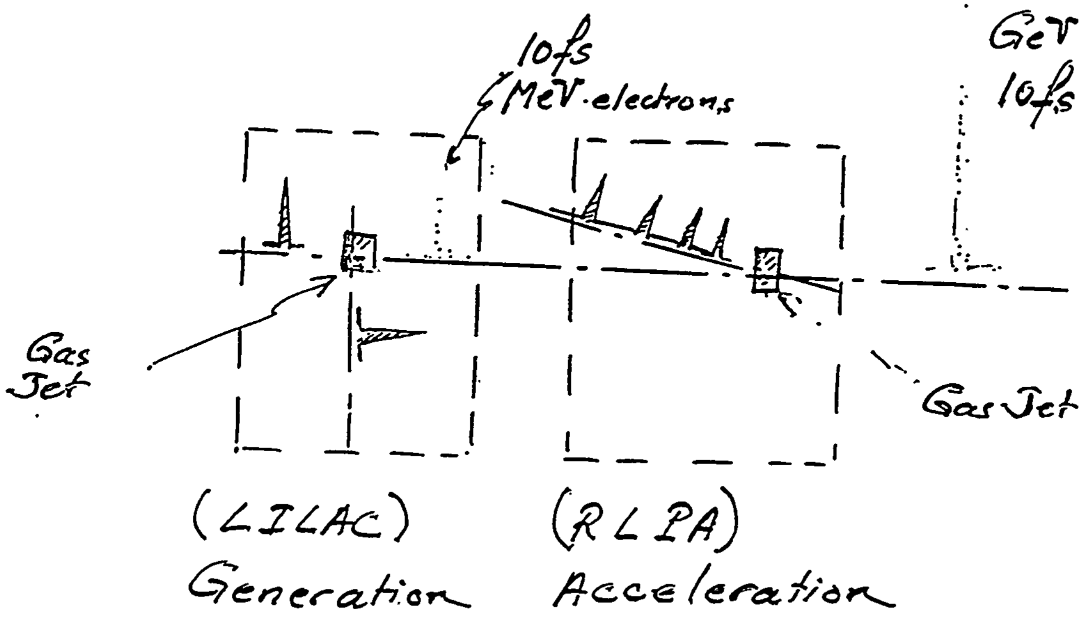

LASER ACCELERATION

W.B. Mori, UCLA

Laser Acceleration

W.B.Mori

University of California at Los Angeles

Collaborators:

K-C.Tzeng UCLA, R. Hemker UCLA
C.Joshi UCLA, J.M. Dawson UCLA
C.E.Clayton UCLA
T. Katsouleas USC and Students

High-intensity lasers have large electric fields

$$I=cE_L{}^2/8\pi$$

$$\boxed{\mathbf{eE_L \cong 30\sqrt{I(10^{18}\,W/cm^2)}}\ \mathit{GeV/cm}}$$

For example:

25TW $\lambda=1\mu m\ w_0=20\mu m$	1PW $\lambda=1\mu m\ w_0=20\mu m$
$I=5\times10^{18}\ W/cm^2$	$I=1.6\times10^{20}\ W/cm^2$
$eE_L=7\ TeV/m$	$eE_L=40\ TeV/m$

Conventional Rf technology: 100 MeV/m

Motion of a free electron in an electromagnetic wave

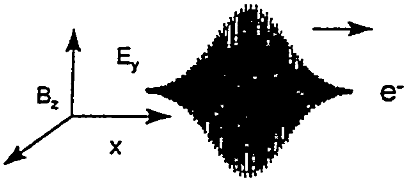

Equations of the motion

$\bar{y}$ $$\frac{d}{dt}p_y = q(E_y - v_x B_z / c)$$

$\bar{x}$ $$\frac{d}{dt}p_x = q(v_y B_z / c)$$

energy $$\frac{d}{dt}\gamma = q(v_y E_y / c)$$

Leads to two constants of the motion

$$\gamma mc - p_x = C_1$$

$$p_y + qA_y / c = C_2$$

Consider an electron starting at rest in front of the pulse

$C_1 = mc$ *and* $C_2 = 0$

Therefore

$$p_y = eA_y / c \Rightarrow p_y / mc = a$$

$$\gamma = (1 + [(p_y / mc)^2 / 2]) = (1 + (a^2 / 2))$$

$$p_x = (p_y / mc)^2 / 2 = a^2 / 2$$

Consider an electron injected with a large γ

[illegible] and $C_2 = 0$

Therefore

[illegible]

How can these large fields be utilized?

Laser acceleration schemes

I. Laser acceleration in vacuum
II. Laser acceleration in gases
III. Laser acceleration in plasmas

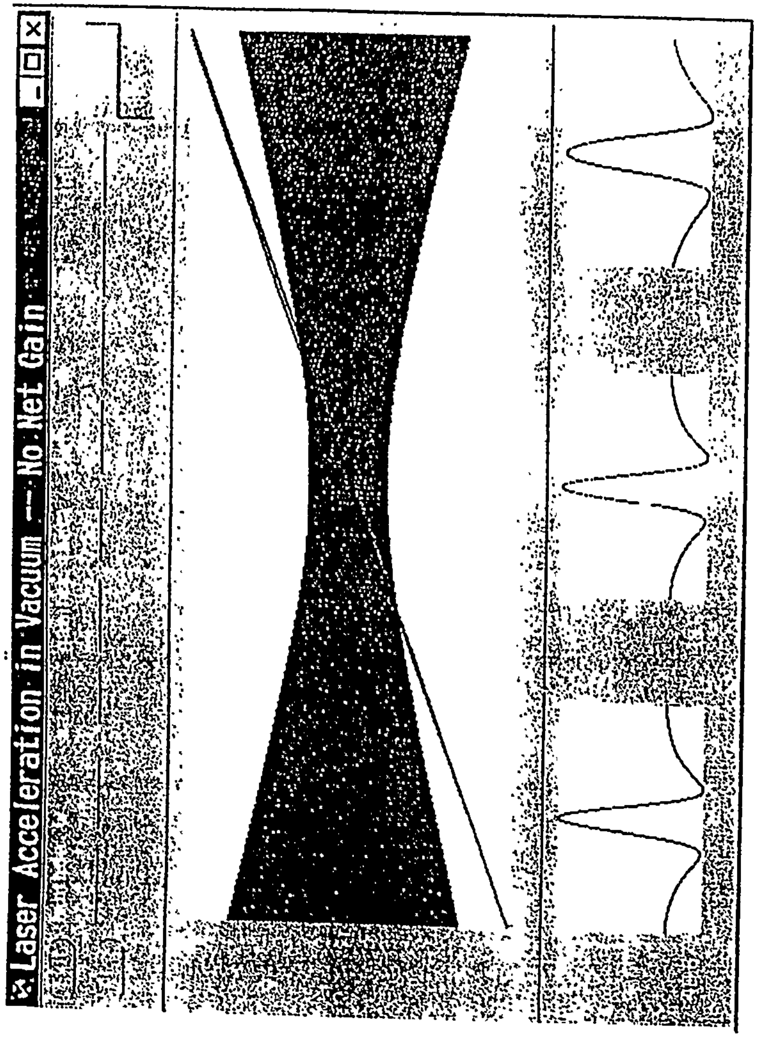

LIMITATIONS

Maximum Energy Gain

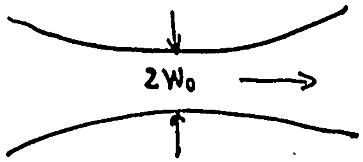

$$\mathcal{E} = -e\int d\vec{r}\cdot\vec{E}$$

$$\mathcal{E} = eE_\perp \Delta X_\perp \cong \sqrt{\pi}\, W_0 E_\perp e$$

$$\mathcal{E}\,(\text{MeV}) \cong 35\sqrt{P(\text{TW})} \qquad 10^{15}\,\text{W} \rightarrow 1\,\text{GeV}$$

Energy Gradient (Energy Gain in a Rayleigh Length)

$$\frac{d\mathcal{E}}{dt} = eE_\perp V_\perp = eE_\perp \frac{p_\perp}{\gamma} = \frac{e^2E_\perp^2}{m\gamma\omega}$$

$$\frac{d\mathcal{E}}{dx} \cong \frac{1}{c}\frac{d\mathcal{E}}{dt} = \frac{e^2E_\perp^2}{mc\gamma\omega}$$

can be integrated

$$\Delta(\gamma mc^2)^2 = \pi e^2 W_0^2 E_{\perp 0}^2$$

for $\gamma_f << \gamma_i$

$$\Delta\gamma mc^2 = e\sqrt{\pi}\, W_0 E_\perp \left[\underbrace{\frac{eE_\perp W_0\sqrt{\pi}}{\pi\gamma_i mc^2}}_{<<1}\right]$$

USC
UNIVERSITY
OF SOUTHERN
CALIFORNIA

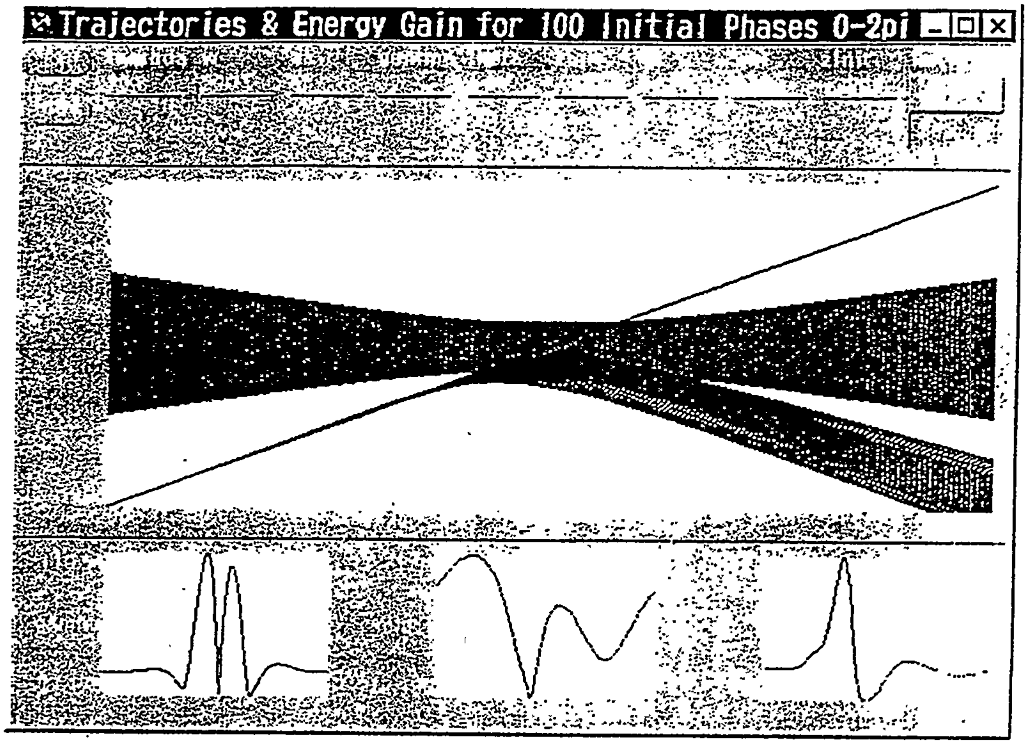

Trajectories & Energy Gain for 100 Initial Phases 0-2pi

USC
UNIVERSITY
OF SOUTHERN
CALIFORNIA

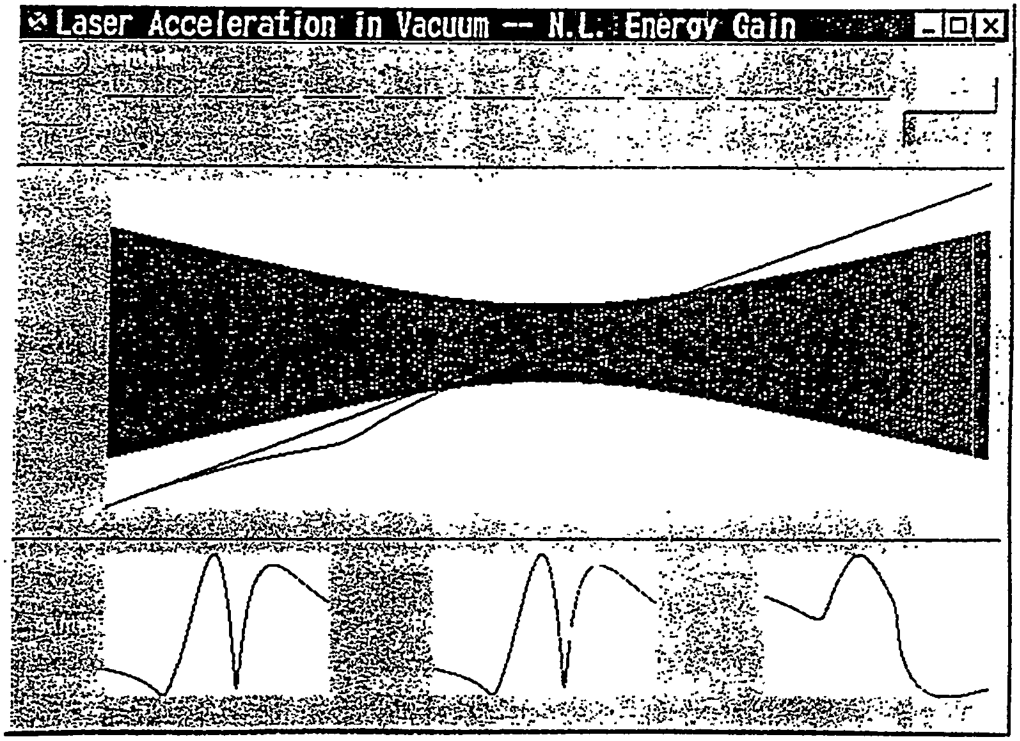

Laser Acceleration in Vacuum -- N.L. Energy Gain

Critical issues for vacuum acceleration

Laser Plasma Group

- Termination of fields (at either end)
  - Specifics
  - Damage of terminator
  - Energy losses to particles as they pass through the aperture
- Beam quality
  - um size bunches
  - off axis fields
  - reflected fields
  - synchrotron radiation

Santa Barbara, 1996

AXICON GEOMETRY Steinhauer et al.

Can increase Energy Gradient for High Injection Energies

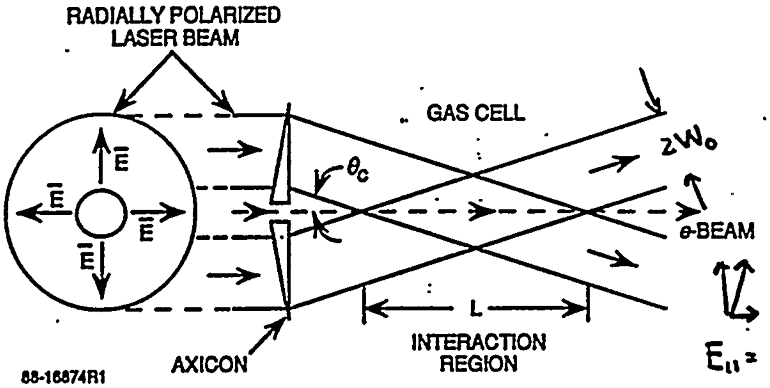

$E_{\parallel} = E_{\perp} \sin\theta_c$

$$L = \frac{2W_o}{\sin\theta_c}$$

$$\mathcal{E} = eE_{\parallel}L = \underbrace{2eE_{\perp}W_o}_{\text{same as before}}$$

Figure 1

Dephasing is a problem if

$(V_{wave} - V_{particle})\,\Delta X \cong \frac{\lambda}{2}$ $\Delta X = \lambda/(\theta_c^2 + \frac{1}{\gamma_i^2}) < L$

→ ICA Fontana & Pantell

BREAKDOWN INITIAL PLASMAS

Properties of the relativistic electron plasma wave

e^-

- The wave amplitude ε is defined as $\delta n_e / n_e$
- Acceleration gradient given by $E_{accel} \approx \varepsilon \sqrt{n_e}$ eV/cm.
- Phase velocity of wave is $\gamma_{\phi} \approx \omega_0 / \omega_{pe} >> 1$

$\varepsilon = 1$ $n = 10^{16}$
30 GeV/m

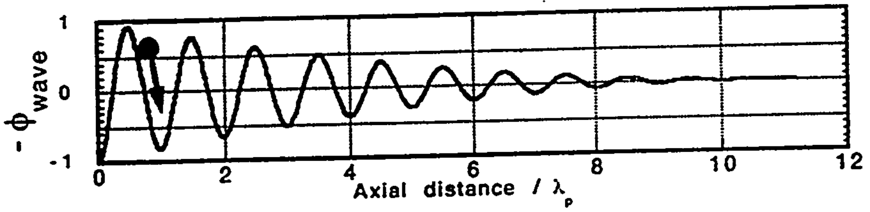

- Maximum energy gain is smaller of...

$$\gamma_{\text{final}} \approx 2\varepsilon\gamma_{\text{ph}}^2 \quad \underline{\text{or}} \quad \gamma_{final} \approx \frac{E_{accel} L_{accel}}{mc^2} \quad (\gamma_{final} >> \gamma_0)$$

(dephasing limit)

(finite interaction length limit)

Laser Channeling – Next talk

Three basic laser-plasma accelerator schemes: proposed by Tajima and Dawson in 1979

UCL
Laser Plasma Group

- A single short-pulse (LWFA)

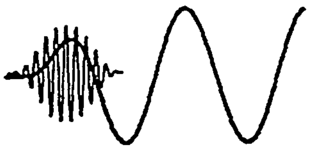

France
Texas
Japan

- Two-frequencies, i.e., a train of pulses (PBWA)

(Could vary spacing and duration of pulses)
: Umstadter et al.

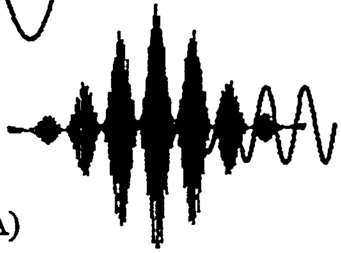

UCLA
France
Japan

- Raman forward scattering instability (SMLWFA)

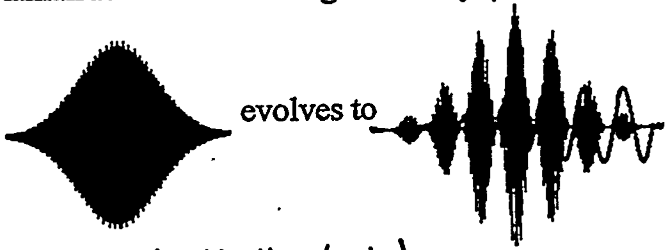

several recent experiments
LLNL *
RAL *
Japan
U of M
NRL

(SMLWFA: Krall et al.
Andreev et al.)
No wavebreaking

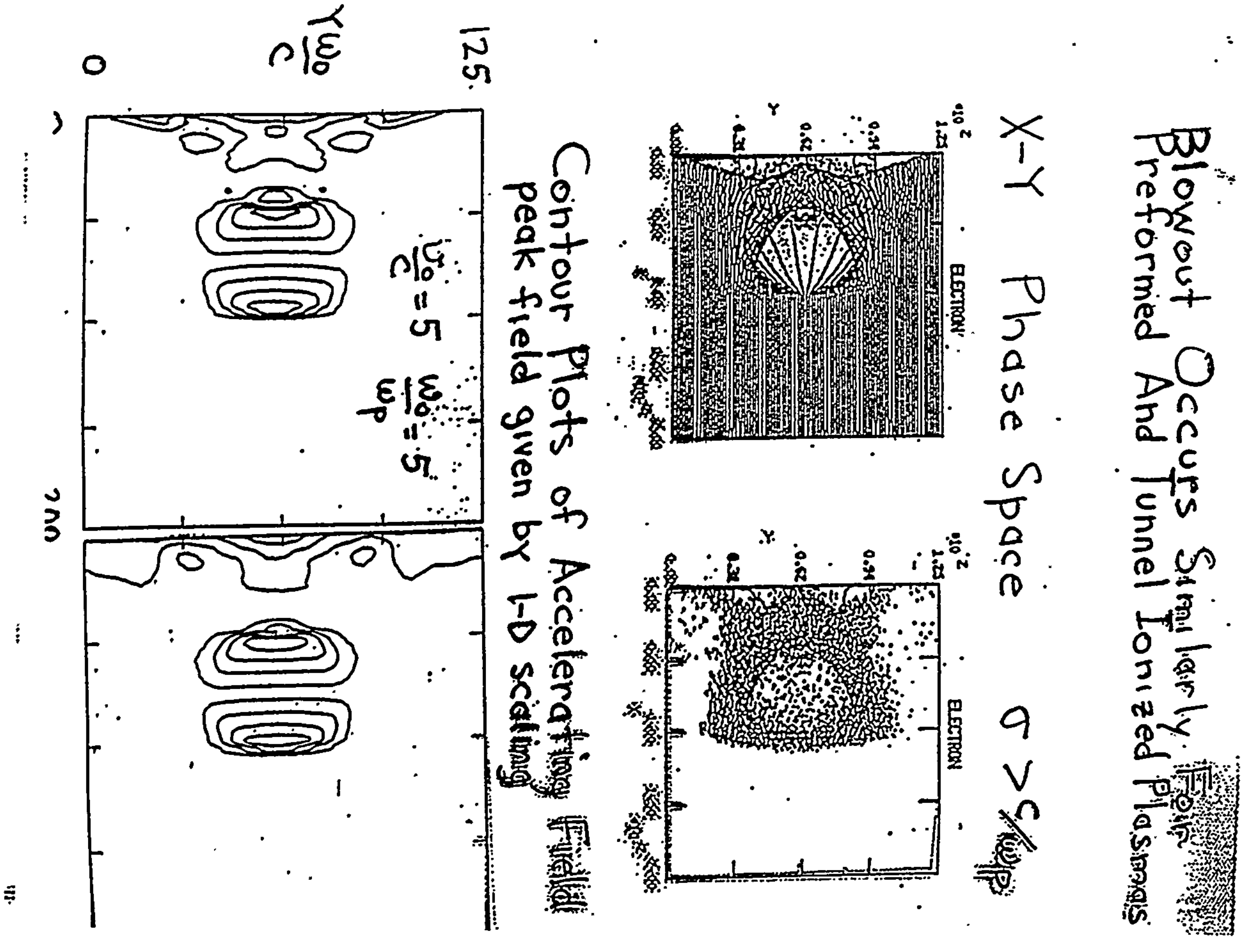

Blowout Occurs Similarly For Preformed And Tunnel Ionized Plasmas

X-Y Phase Space $\sigma > c/\omega_p$

Contour Plots of Accelerating Field
peak field given by 1-D scaling

Recent LWF excitation experiments

- University of Texas Siders et al.(1996)
- LULI (France) Marques et al.(1996)

Appeared together in PRL-similar parameters

$I = 3\times10^{17} W/cm^2$, $\lambda = .8\mu m$, $w_0 = 5\mu m$,
$\tau_L = 100 fs$, $n_p \approx 3\times10^{17} cm^{-3}$, and $k_p w_0 = .5$

Wakes were diagnosed using optical pump probe techniques--experiments worked because density flucuations are large for narrow wakes

LLNL/UCLA 1111

We observe the first and second anti-Stokes modes in the near-forward spectrum

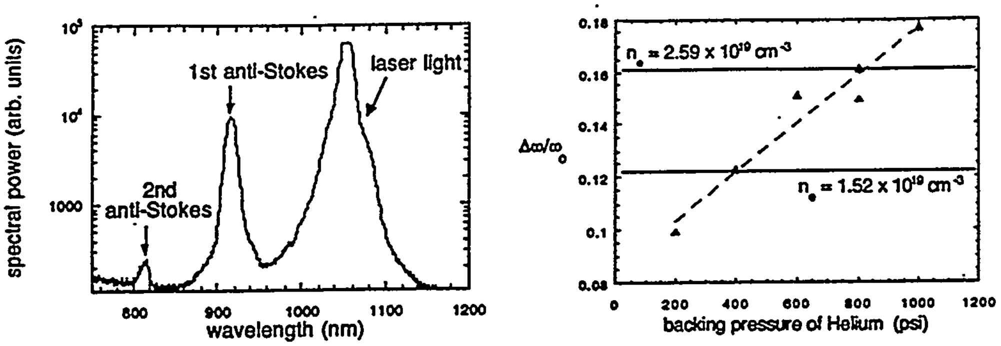

The spacing of these modes is
- not constant in λ (varies with the order),
- consistent for a density of 2.23×10^{19} cm^{-3}.

The anti-stokes signal was correlated with the detection of 2 MeV electrons

---

Some Recent Short-Pulse Electron Acceleration Experiments

Laser Plasma Group

- ✓ C. Coverdale *et al.*, PRL 74, 4659 (1995), *LLNL/UCLA.*
- ✓ A. Modena *et al.*, Nature (London), 377, 606 (1995), *RAL/UCLA/LLNL/LULI.*
- Nakajima *et al.*, PRL 74, 4428 (1995).
- D. Umstadter *et al.*, to appear in Science.

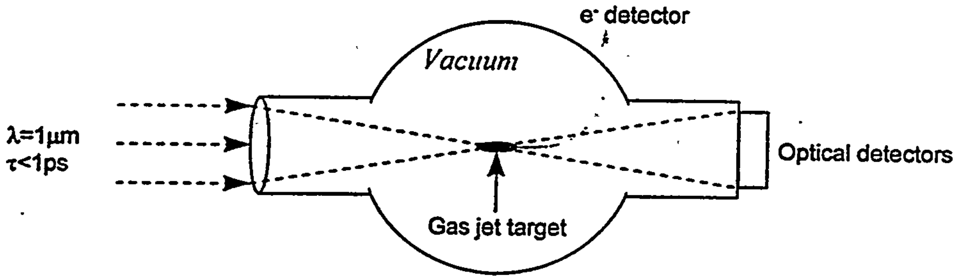

by K.-C. Tzeng

There is a correlation between the anti-Stokes mode and the energetic electrons – First Unambiguous correlation

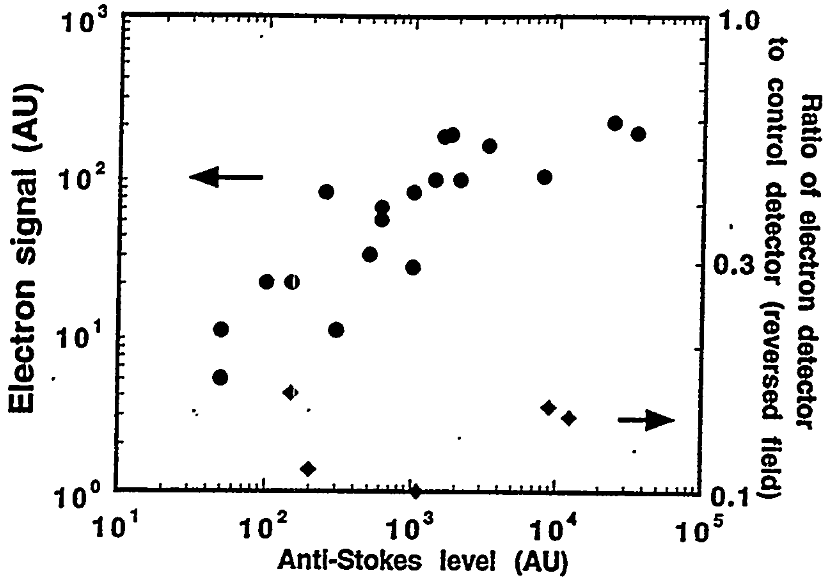

$n_e = 1.8 \times 10^{19}$ cm^{-3}

$v_{osc}/c = 0.55$

$I = 3.9 \times 10^{17}$ W/cm^2

spot size:
16 μm × 24 μm

A correlation between the anti-Stokes amplitude and the level of transmitted light was observed

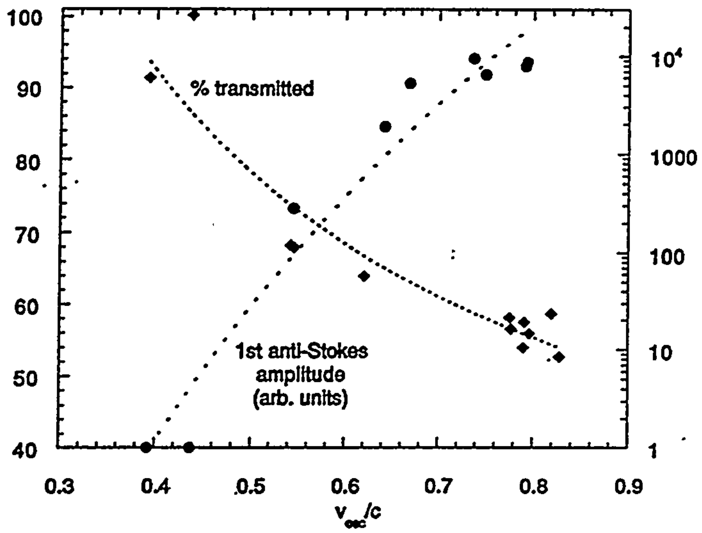

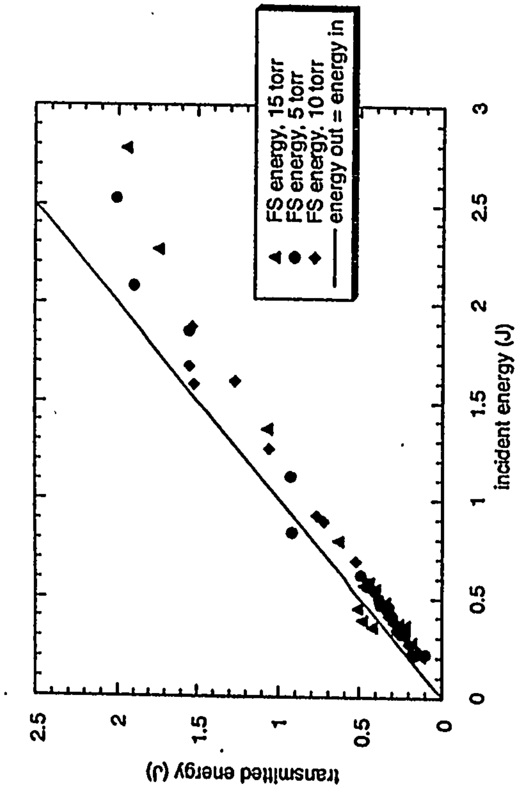

KAL Experiment $I = 5\times10^{18}$ W/cm² $n = 1.4\times10^{19}$ cm⁻³

Evidence for wavebreaking

As density is raised linearly,
electron flux rises dramatically.

$\sim 10^9$ electrons above 9MeV in f/60 cone

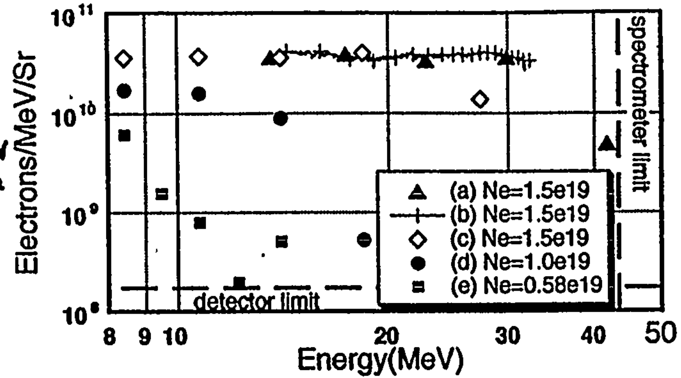

Maximum energy was spectrometer-limited, > 10 × above the noise level, and close to the dephasing limit of 70 MeV for ε ≈ 1 (the expected warm-plasma wavebreaking limit).

The once-narrow spectrum simultaneously broadens to $\Delta\omega \approx 0.5\ \omega_p$ suggesting loss of wave coherence.

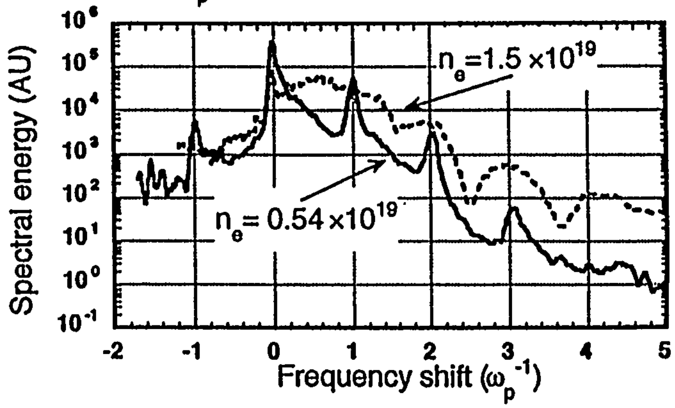

Contours of Laser Intensity and Accelerating Electric Fields

Laser Plasma Group

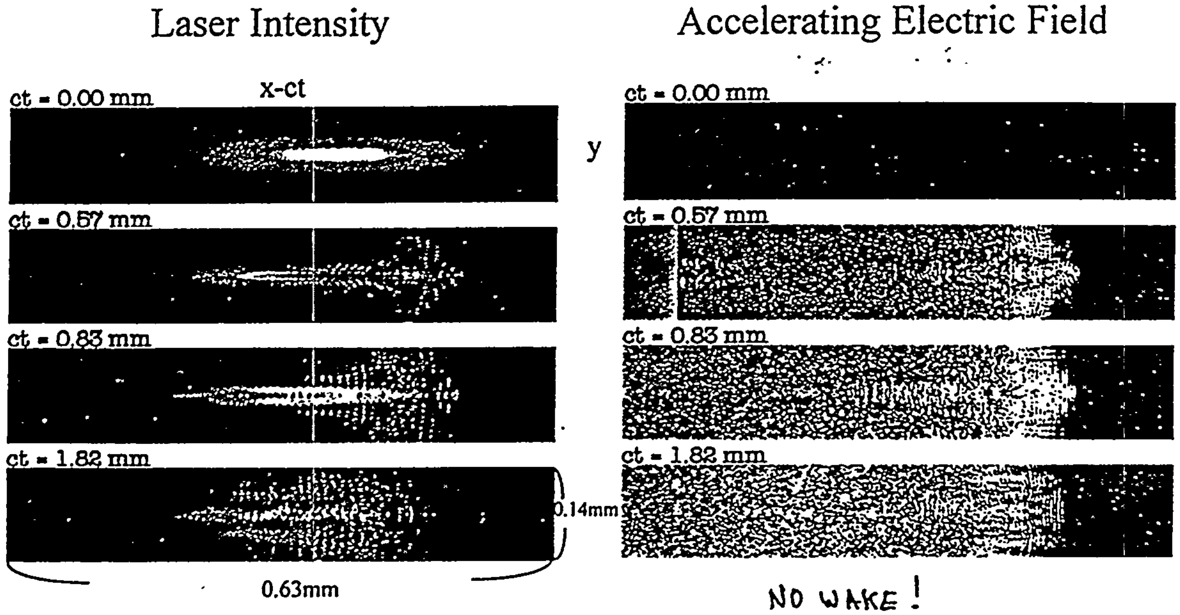

NO WAKE!

$I = 5 \times 10^{18} \frac{W}{cm^2}$ $W_0 = 18 \mu m$ $\tau_L = 800 fs$ $n_e = 1.4 \times 10^{19}$

Distribution Function vs. k-spectrum

-- a Simulation for RAL experiment

Laser Plasma Group

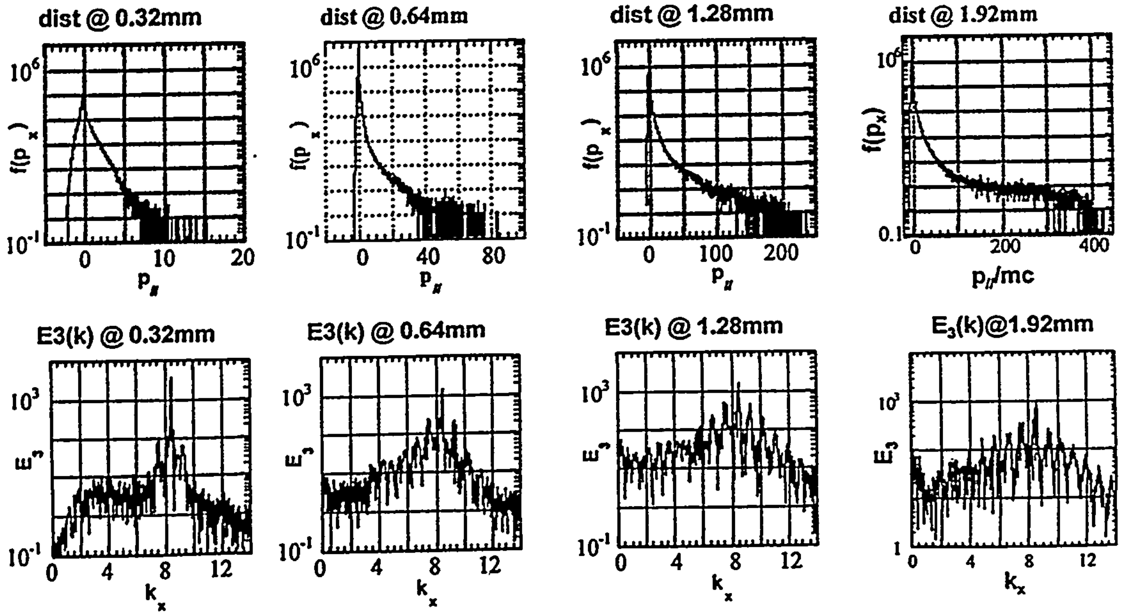

CANCELLATION OF WAKE BY LOAD BEAM

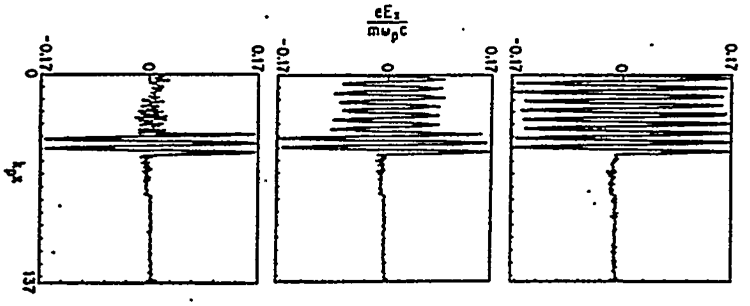

FIG. 2.4 Total axial electric field in a 1-D simulation loaded with short bunches of (a) N=0, (b) $N = 0.5N_0$, and (c) $N = N_0$ (positively charged) particles on the third peak of an accelerating wave at time $t = 40\omega_p^{-1}$. The simulation consisted of 14,000 particles on 1024 grids; system length $= 170c/\omega_p$. The bunch length was roughly one particle in size, or $\simeq 0.11c/\omega_p$, and the plasma wave amplitude was $n_1 \approx 0.16n_0$ (produced by PWFA mechanism). The energy of the beams are $\gamma_{beam} = \gamma_{wave} = 60$.

Beam Loading (Katsouleas et al.) in linear plasma waves

How much current?

Laser Plasma Group

- Estimate number of self-trapped electrons by superimposing their own wake onto the RFS excited wake and assuming complete cancellation--beam loading(assumes no phase slippage). Or we can use energy balance:

  $$ALE_x{}^2/8\pi = N_0 eE_x L/2$$

  $$N_0 = n_1 Ac/\omega_p = 5x10^5\,(n_1/n_0)\,(n_0\,cm^{-3})^{1/2}A$$

- The maximum possible density of self-trapped electrons in one plasma wave bucket is therefore (no surprise):

  $$N_0 / (Ac/\omega_p) = n_1$$

- The peak current is then

  $$I_p = ecn_1 A = 5x10^{-9}\,n_1 A \text{ Amps}$$

- If spread over ten buckets then current is

  $$I = 5x10^{-8}\,n_1 A \text{ Amps}$$

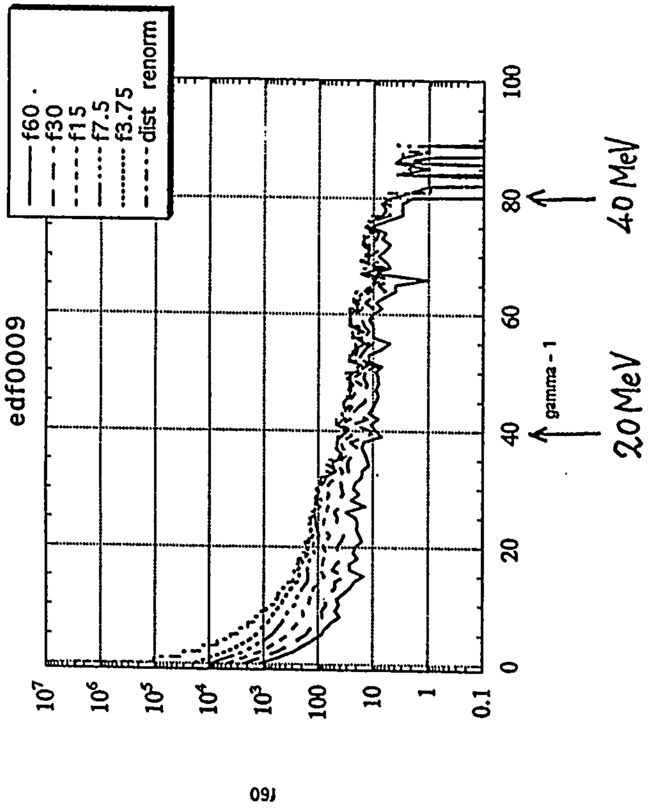

ACCELERATEC ·LECTRONS ARE BUNCHED IN SPACE

Phase space of electrons leaving the plasma

p1

Transverse spot size is ~ 5 μm.

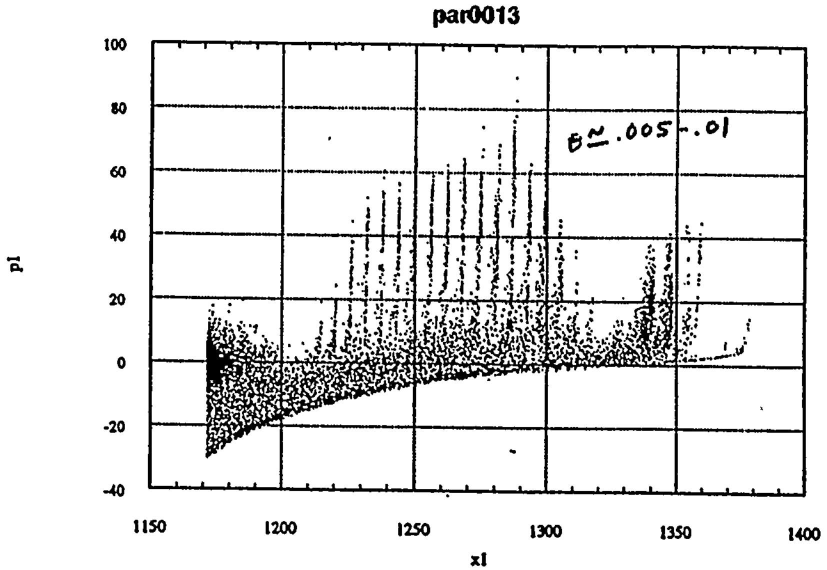

~ 10^{9}~10^{10} electrons are accelerated
consistent with simple beam loading arguments

Peak current is ~ 3 kA

Peak density is ~ 5×10^{18} cm^{-3}

Different Pulse Lengths Cause Different Pulse Evolutions

Laser Plasma Group

Laser Field Profile for L_1_0.8

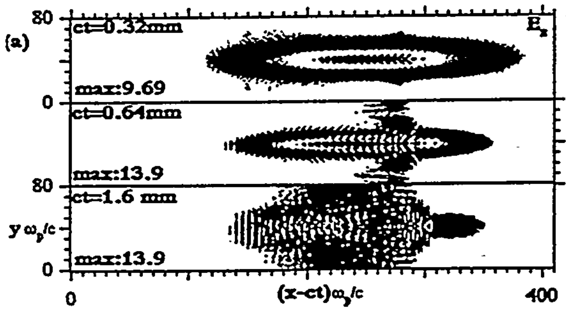

Plasma Response for L_1_0.8

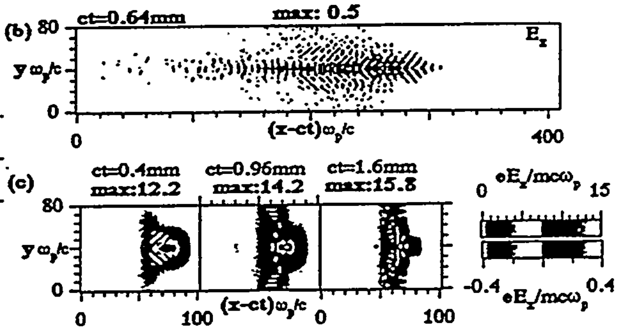

Laser Field Profile for S_1_0.8

---

rh_ave_0012_x vs. (row, col)

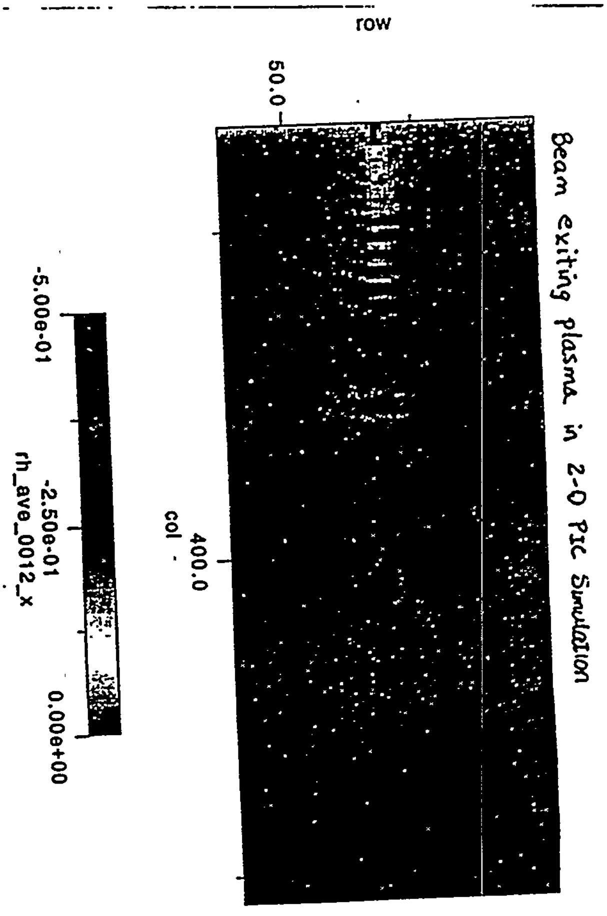

Beam exiting plasma in 2-D PIC simulation

Peak density in a bunch is

~ $.25 n_0$ ~ $4\times10^{18}/cm^3$!

Number ~ 4×10^{8}/bucket

$\epsilon_N = \frac{5\times10^{9}}{\sqrt{n}} (W\frac{\omega_p}{c})$ π mm mr

Particle-Wave Dephasing

- **Electron outruns wave when it slips half a wavelength. This occurs in a distance**

  $\square (c-v_{\phi})L_{dp} = \lambda_p/2$

  $\square L_{dp} = \gamma_{\phi}^2 \lambda_p$, where $\gamma_{\phi} = (1- v_{\phi}^2)^{-1/2}$

- **For waves generated via RFS (an instability) the phase velocity is not well defined and the electrons which constitute the wave are also the ones being accelerated. We use PIC simulations to self-consistently measure the evolution of their energy distribution**

K-C. Tzeng and W.B. Mori

The Plasma Wave Excited by a 100fs Laser with Spot Size 20 μm

PIC Simulation Example of Wake in SMLWFA

Knall et al.
Andreev et al.
Antonsen and Mora
Fluid Simulations

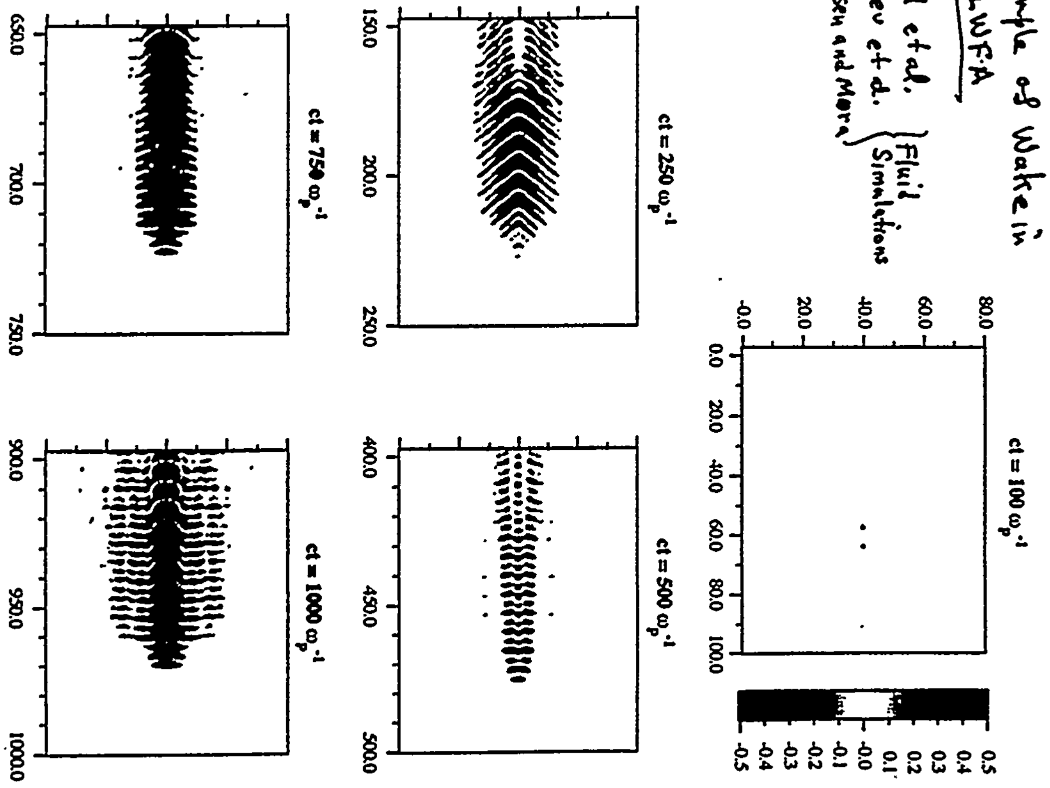

2D Phase Space

Vo = ~~8.0~~ 10.0 $\omega/\omega_p = 5.0$

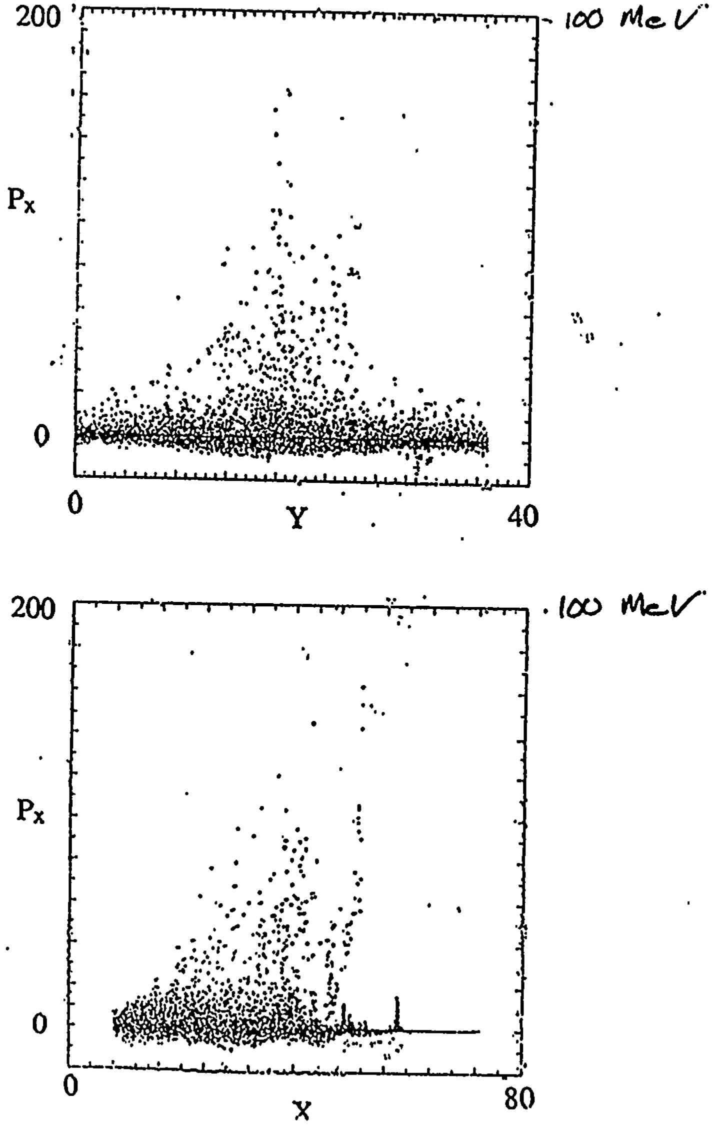

1D Simulation

$I = 10^{20}$ W/cm^2 $n = 4\text{x}10^{19}$ cm^{-3} 120 fs

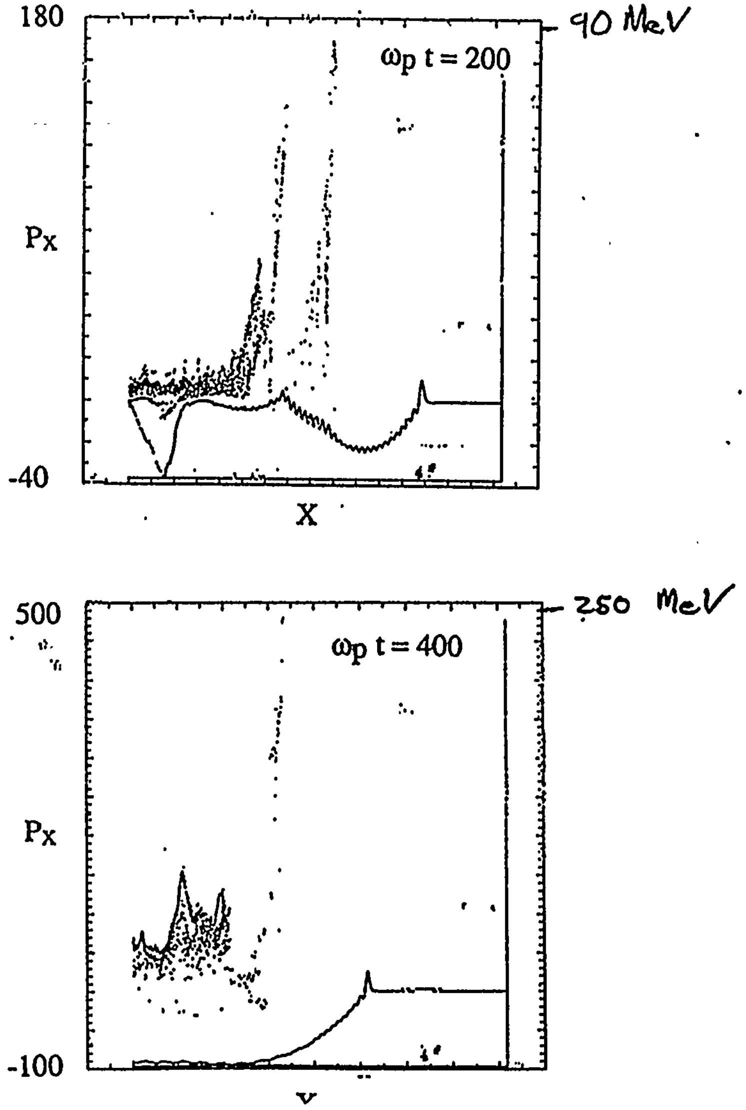

Cumulative electron energy spectrum with Mars laser

- Data acquired over many laser shots
- Spectrum falls rapidly on both sides of injection energy
- Electrons observed out to 30 MeV

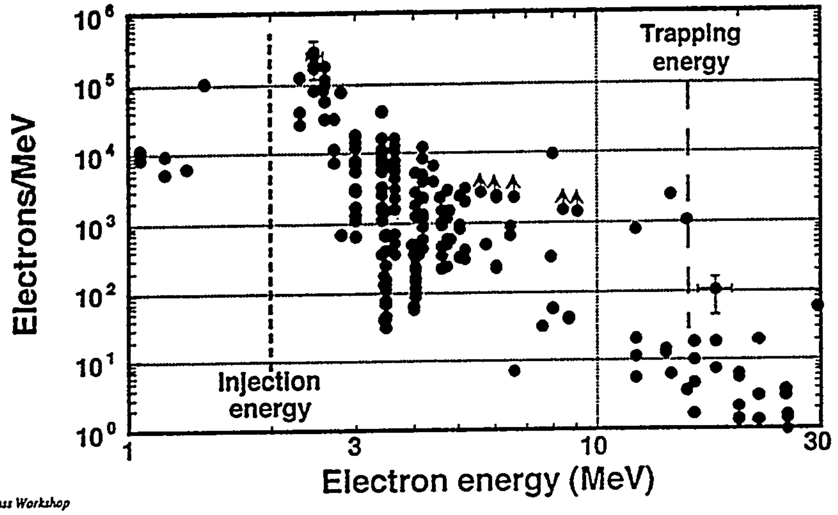

---

e⁻ Detailed view of experimental setup

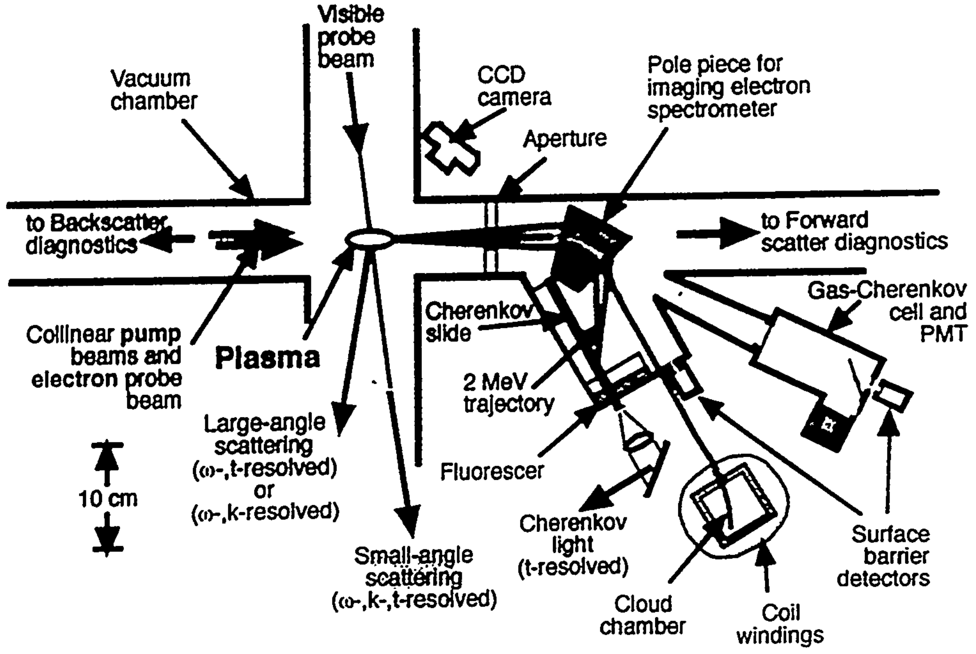

PBWA: Evolution of Laser Intensity and Accelerating Field

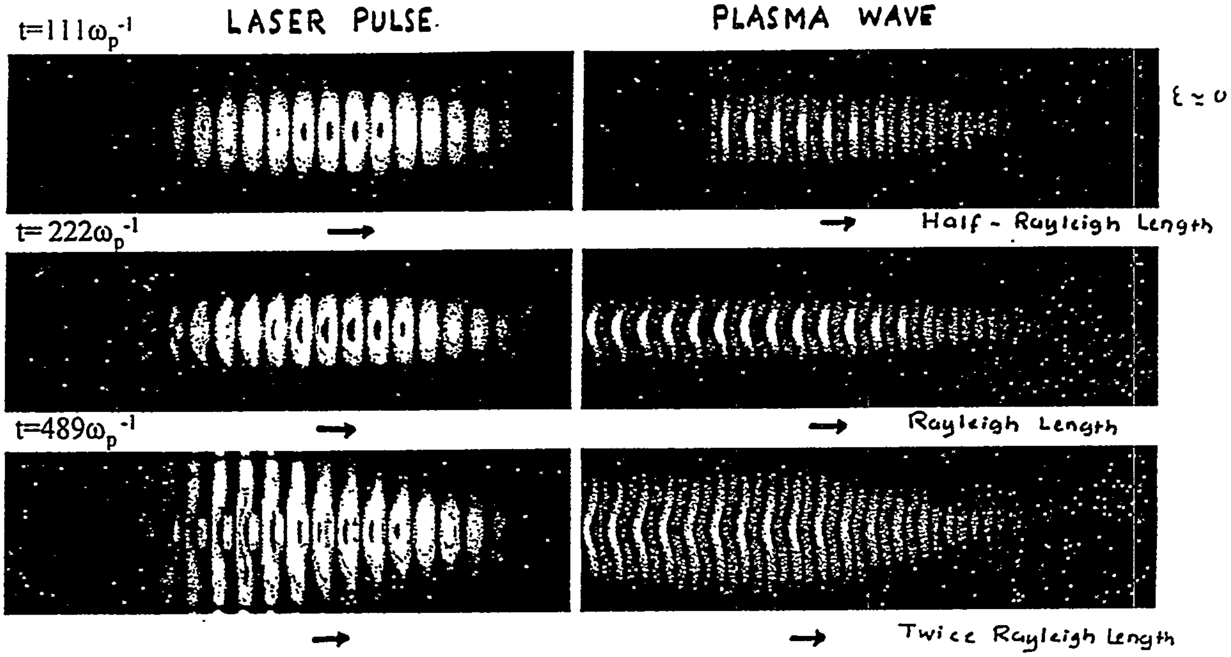

$\omega_0 - \omega_p = \omega_1$

Short-Pulse 100 MeV **PBWA**

☐ Parameters:

- ○ $\omega_{1,2}/\omega_p$=14, 15, $w_0 = 6\ c/\omega_p$ =14 μm
- ○ $N_x = 8192$, $N_y = 256$, 6 particles/cell
- ○ $n/n_{cr} = 0.5\%$, $c/\omega_p = 2.4$ μm
- ○ $a_{1,2} = 0.22, 0.22$,
- ○ $x_{max} = 144\ c/\omega_p$, $y_{max} = 41\ c/\omega_p$
- ○ $\tau_{fwhm} = 340$ fs, $p_{rise} = p_{fall} = 60\ c/\omega_p$

One GeV in a single stage

Laser Plasma Group

Laser wavelengths	1.05 and 1.06 μm
Plasma density	10^{17} cm^{-3}
Plasma source	Multiphoton ionization
Laser pulse length	4 ps (2 ps)
Laser power	14 TW (22TW)
Laser spot size (2σ)	200 μm
Raleigh range ($2Z_o$)	6.2 cm
Plasma homogeneity	few %
Peak plasma wave amplitude	$E/E_{max} \approx 0.5$
Peak accelerating gradient	160 MeV/cm
Final energy	1 GeV

$\frac{V_0}{c} = .23$

1996 Snowmass Workshop

PBWA: Phase Space Plots

Laser Plasma Group

@after 2 L_R

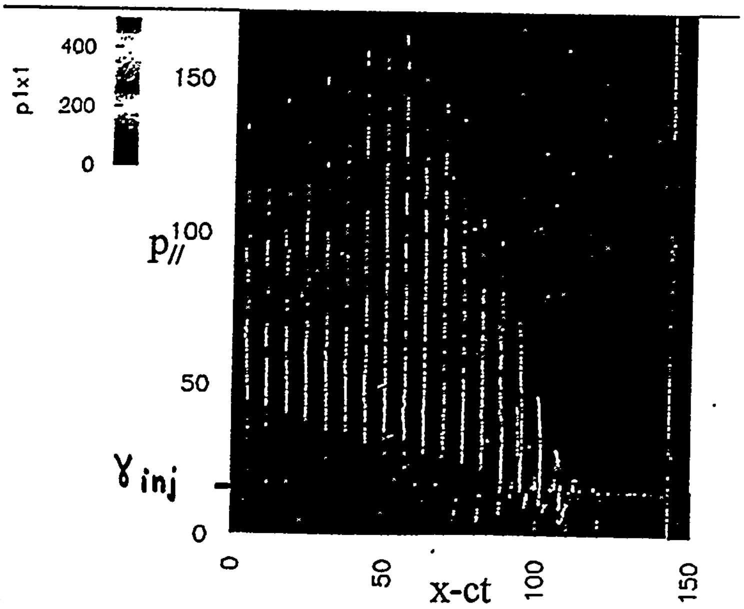

Δγ eventually reached 185

DOE Review 1996 by K-C Tzeng

Summary

Laser Plasma Group

- Laser acceleration in vacuum
    - no experiments
    - small scale experiments can address critical issues
- Laser acceleration in gases
    - no new experiments since 1994
    - need to show optical guiding (Sprangle et al.)
- Laser acceleration in plasmas
    - LWFA
        - experimental demonstration of plasma wave excitation of narrow waves(UT,LULI)
        - no acceleration
    - PBWA
        - no new results since 1994(acceleration of injected electrons)
        - new lab under construction at UCLA
    - "SMLWFA"/single frequency
        - many exciting new results in self-trapped RFS regime(LLNL,Osaka,RAL,UM)
        - upto 100MeV at 300 GeV/m
        - no SMLWFA demonstration to date
    - Tremendous progress in computer modeling and theoretical sophistication

---

Other applications for lasers

Laser Plasma Group

- Optical injectors Umstadter et al.
- Optical bunchers [illegible] et al.
- just the beginning

TWO BEAM ACCELERATOR

S. Yu, LBL

UPDATE ON FEL &IFEL

C. PELLEGRINI, UCLA

FREE ELECTRON LASERS & IFEL

C. PELLEGRINI, UCLA

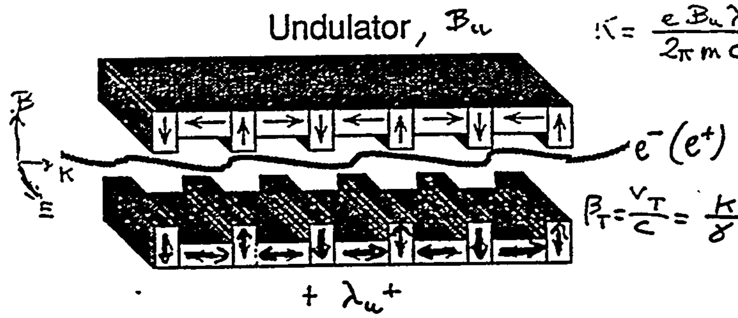

$K = \frac{e B_u \lambda_u}{2\pi m c^2}$

$\beta_T = \frac{v_T}{c} = \frac{K}{\gamma} \sin(2\pi z/\lambda_u)$

$mc^2 \frac{d\gamma}{dt} = e v_T E - P_R \Rightarrow \dot{\gamma} = \frac{eKE}{mc\gamma} \sin\psi - \frac{P_R}{mc^2}$ eq. for energy

$\psi = \left(\frac{2\pi}{\lambda_u} + \frac{2\pi}{\lambda}\right) z - \omega t \Rightarrow$ eq. for phase $\dot{\psi} = \frac{2\pi c}{\lambda_u}\left(1 - \frac{\lambda_u}{\lambda} \frac{1+K^2}{2\gamma^2}\right)$

$\Rightarrow \dot{\psi} = 0 \Rightarrow \boxed{\lambda = \frac{\lambda_u (1+K^2)}{2\gamma^2}}$

$\frac{P_R}{mc^2} = \frac{2}{3} r_e \left(\frac{2\pi}{\lambda_u} \gamma K\right)^2$

FOR IFEL define "RESONANT PARTICLE" $\Rightarrow \dot{\psi}_R = 0$, $\dot{\gamma}_R = \frac{eKE}{mc\gamma} \sin\psi_R$

Study motion around "REFERENCE" $\delta\dot{\gamma} = \frac{eKE_0}{mc\gamma}(\sin\psi - \sin\psi_R) - P_R/mc^2$

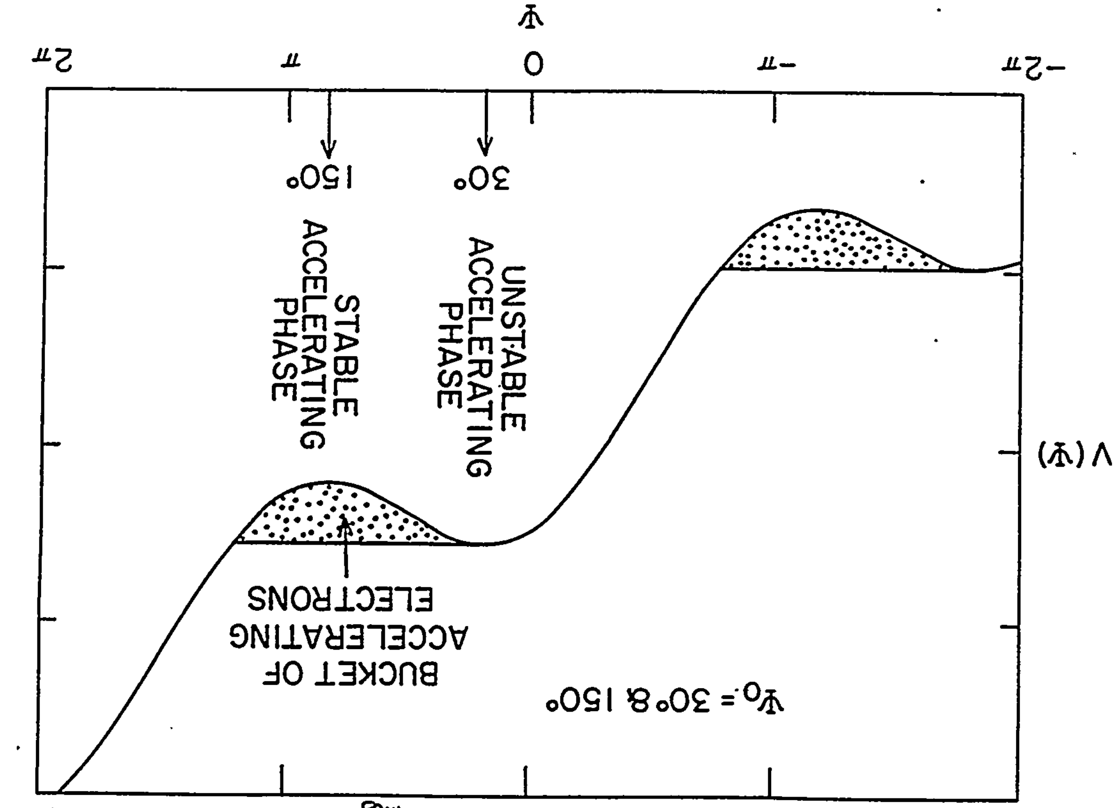

~~Feb.~~ Nov A/AT2334/5) 55%

For "Max Rate" $\Lambda_w \approx \gamma_R^{8/5}/E^{2/5}$

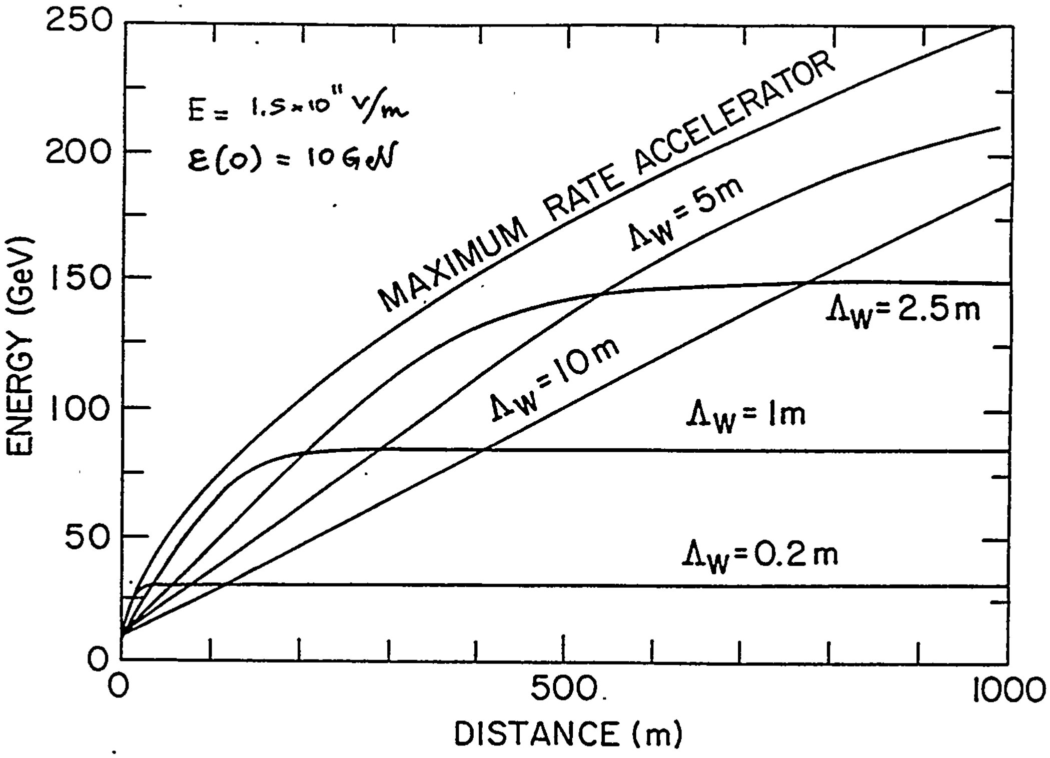

NOV
Tok. U/AT2334/2/2501.

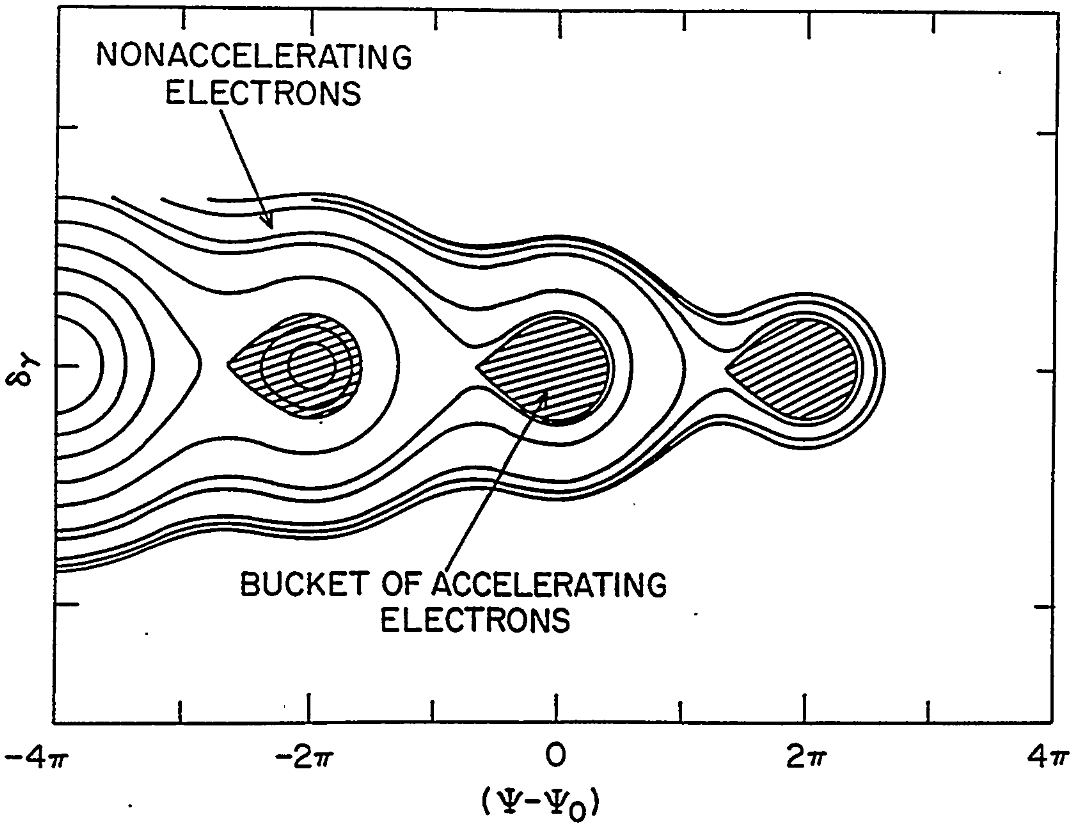

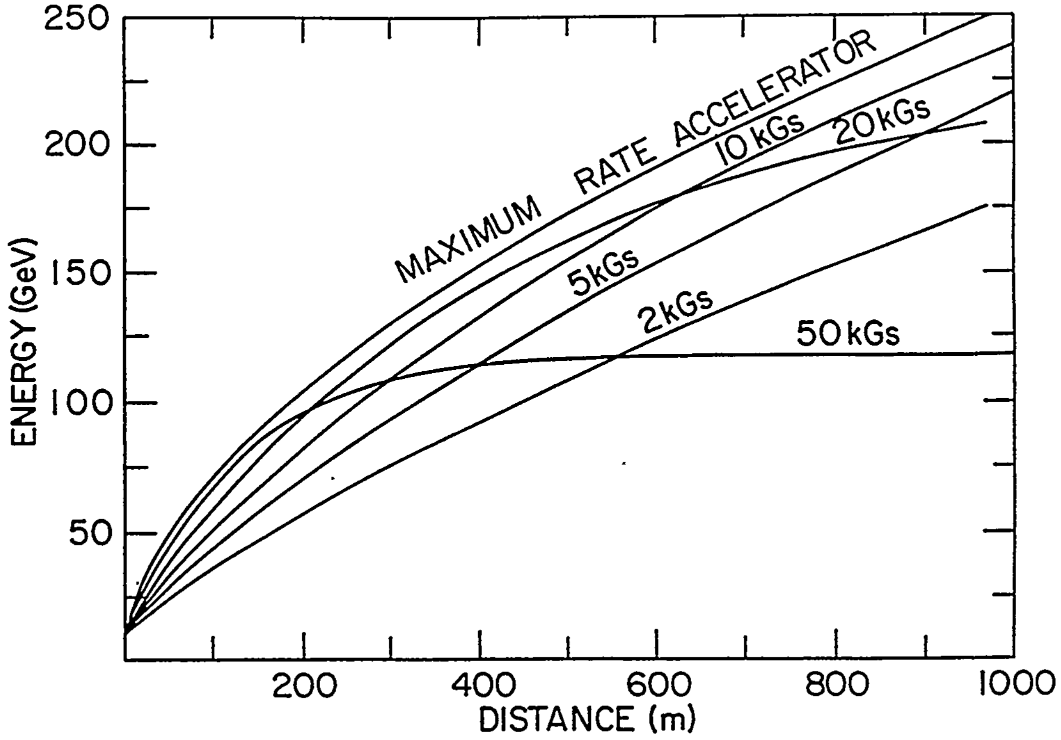

Nov
~~Feb.~~ A/AT2334/3/35%

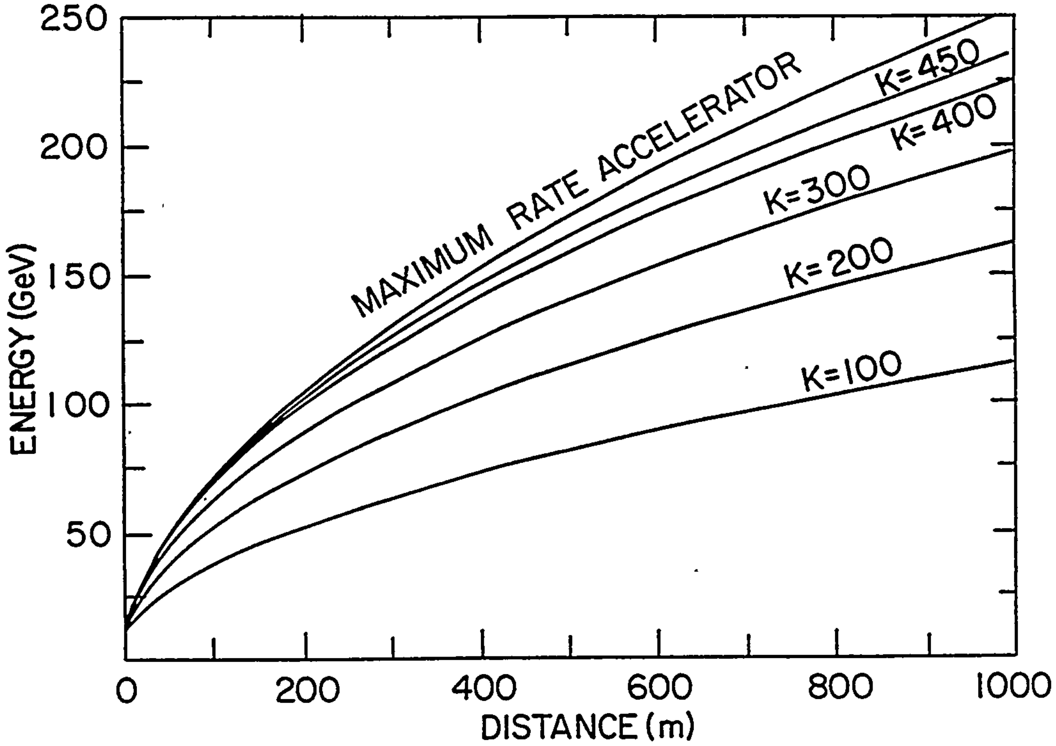

Nov

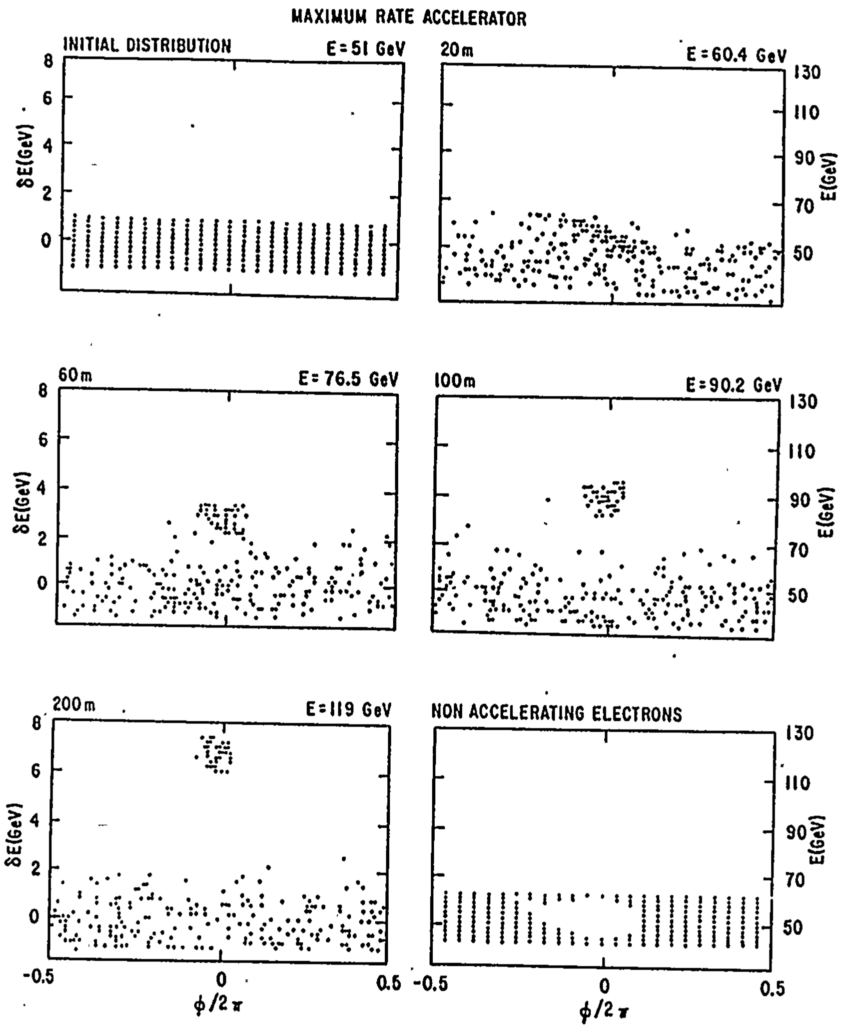

Nov
~~Feb~~A|AT2334/9/85%

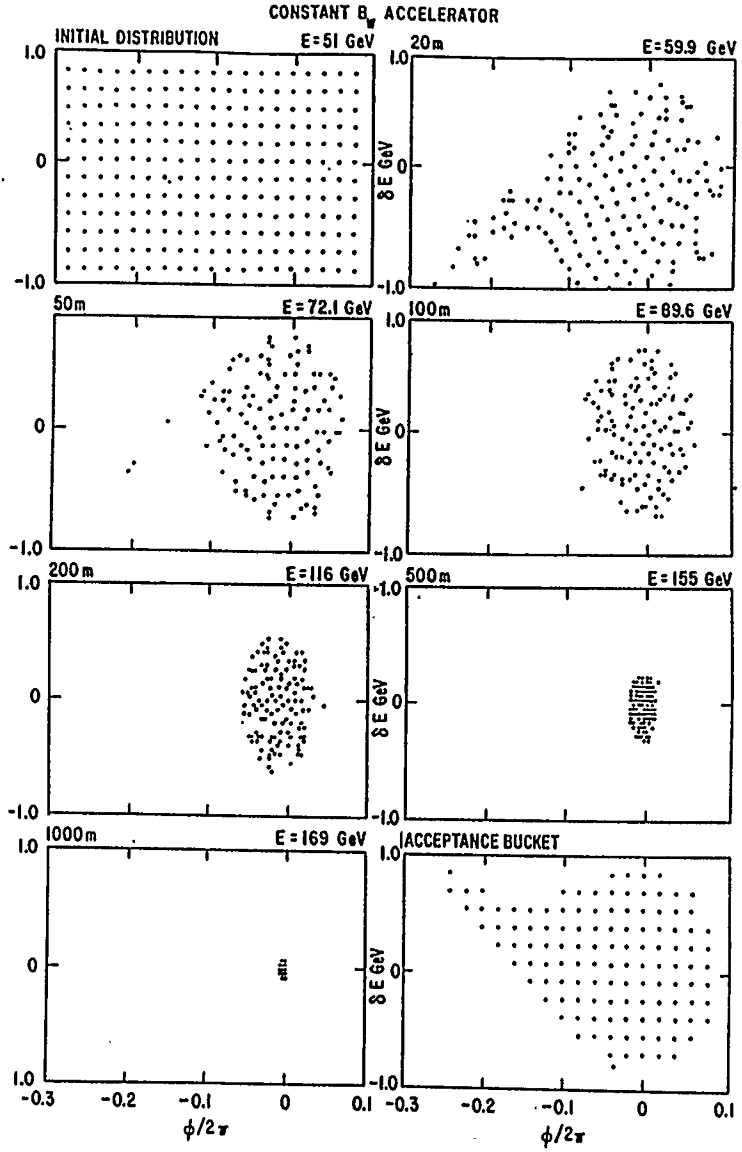

Nov
~~Feb~~A|AT2334/8/45%.

IFEL e^- Accelerator , Experimental Results:

		Yerevan[i]	Columbia[ii]	BNL/ATF[iii]
e^- beam				
Injection Energy	[MeV]	12	0.75	40
Energy Gain	[MeV]	0.02	0.25	0.9
Wiggler				
Length	[cm]	20	38	47
λ_w	[cm]	0.95	1.8 - 2.25	2.89 - 3.14
B_w	[kG]	10	0.4	10
CO_2 Laser* or FEL**				
Power, W_l	[GW]	0.02*	0.005**	1.0*
Wave length, λ	[μm]	10.	1.6 10^3	10.6

i) A.Amatuny,M.Petrosian,B.Petrosian, et.al., Proc.XIII Int.Conf. HE Accelerators, 1987

ii) I.Wernick, T.Marshall, Physical Review A, Vol.46, No.6, 1992

iii) A.van Steenbergen,J.Gallardo,J.Sandweiss,et.al.,BNL/ATF Users Meeting, Dec.,1995

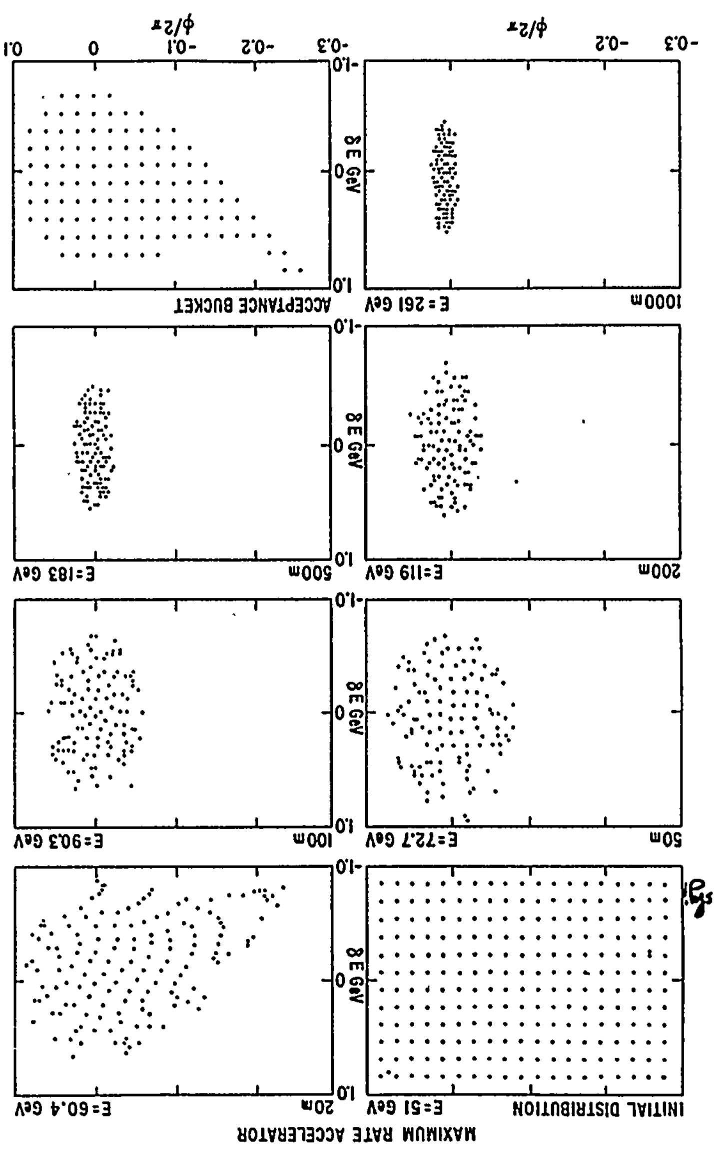

Nov

E L
celerates
+ e⁻
multaneously
be used
s a
buncher.

IFEL Accelerator Experiment

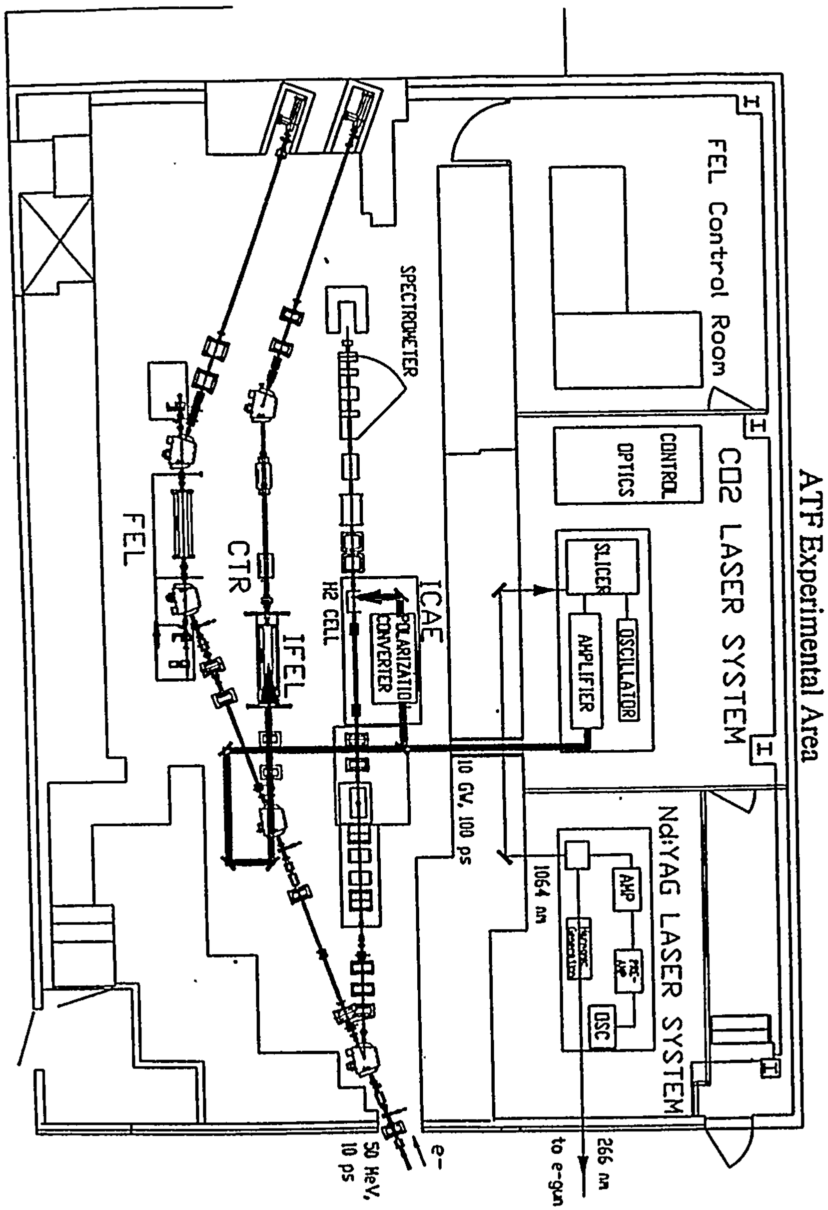

ATF Experimental Area

To be published in Physical Review Letters

Observation of Energy Gain at the BNL Inverse Free Electron Laser Accelerator

A. van Steenbergen[1*], J. Gallardo[1†], J. Sandweiss[2], J-M Fang[3]

[1]*Brookhaven National Laboratory, Upton NY 11973*

[2]*Physics Department, Yale University, New Haven CT 06511*

[3]*Department of Applied Physics, Columbia University, New York NY 10027*

(July 17, 1996)

Abstract

A 40 MeV electron beam, using the inverse free-electron laser interaction, has been accelerated by $\frac{\Delta E}{E} = 2.5\%$ over a distance of 0.47 m. The electrons interact with a 1 – 2 GW CO_2 laser beam bounded by a 2.8 mm ID sapphire circular waveguide in the presence of a tapered wiggler with $B_{max} \approx 1\,T$, and a period 2.89 cm $\leq \lambda_w \leq$ 3.14 cm. The experimental results of $\frac{\Delta E}{E}$ as a function of electron energy E, peak magnetic field B_w and laser power W_l compare well with analytical and 1-D numerical simulations and permit scaling to higher laser power and electron energy.

29.17.+w, 41.75.Ht, 41.60.Cr, 52.75.Ms, 42.62.Hk

Typeset using REVTEX

---

[*] National Synchrotron Light Source

[†] Physics Department, 901-A. To whom correspondence should be addressed. E-mail: gallardo@bnl.gov

IFEL ACCELERATOR EXPERIMENT, FIRST PHASE

Electron Beam			
	Injection energy	40.0	MeV
	Exit energy	42.3	MeV
	Mean accel.field	4.9	MV/m
	Current, nominal	5	mA
	N(bunch)	10^9	e^-
	I(max)	30	A
	$\Delta E/E$ (one σ)	$\pm 3\ 10^{-3}$	
	Emittanc(one σ)	$7\ 10^{-8}$	m.rad
	Beam radius	0.3	mm
Wiggler param.			
	Wiggler length	0.47*	m
	Section length	0.6	m
	Period length	2.89 - 3.14	cm
	Gap	4	mm
	Field max.	1.0 - 1.024	T
	Beam oscill.,$a_{1/2}$	0.16 - 0.19	mm
Laser Parameters			
	Power, P(laser)	10^9	Watts
	Wave length, λ	10.6	μm
	Max.field, E_o	$0.78\ 10^3$	MV/m
	Guide loss, α	0.05	m^{-1}
	Field attenuation	0.26	dB/section
	Pulse , (fwhm)	200 - 300	psec
	A_o	$1.53\ 10^3$	
	$r_o(L_w/2)$	1.0	mm

$E_L = E_o = [\pi W Z_o]^{1/2}/R_o$ $\quad Z_o = 377\ \Omega$ $\quad$ (R_0 = guide radius)

$\pi r_o^2(\text{min})(\tau = 0.5) = \lambda R(\text{ray})$ $\quad A = eE / m_o c^2$ $\quad *(L_w/2)_{\text{effect.}}$ ifel07.doc

IFEL e^- Acceleration

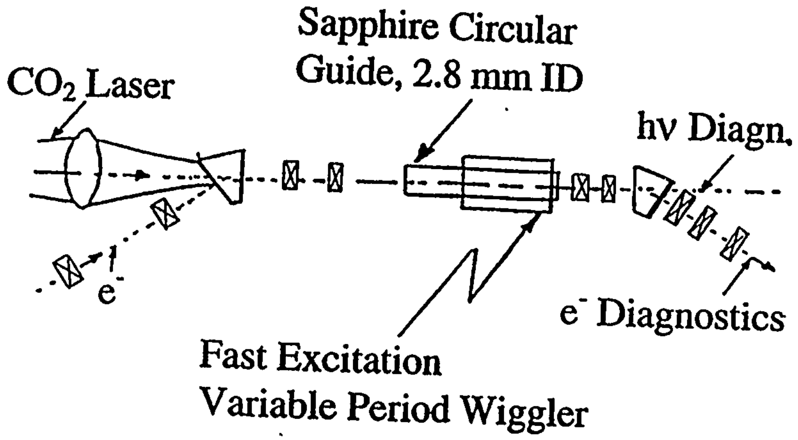

CN8-123-95

CN8-122-95

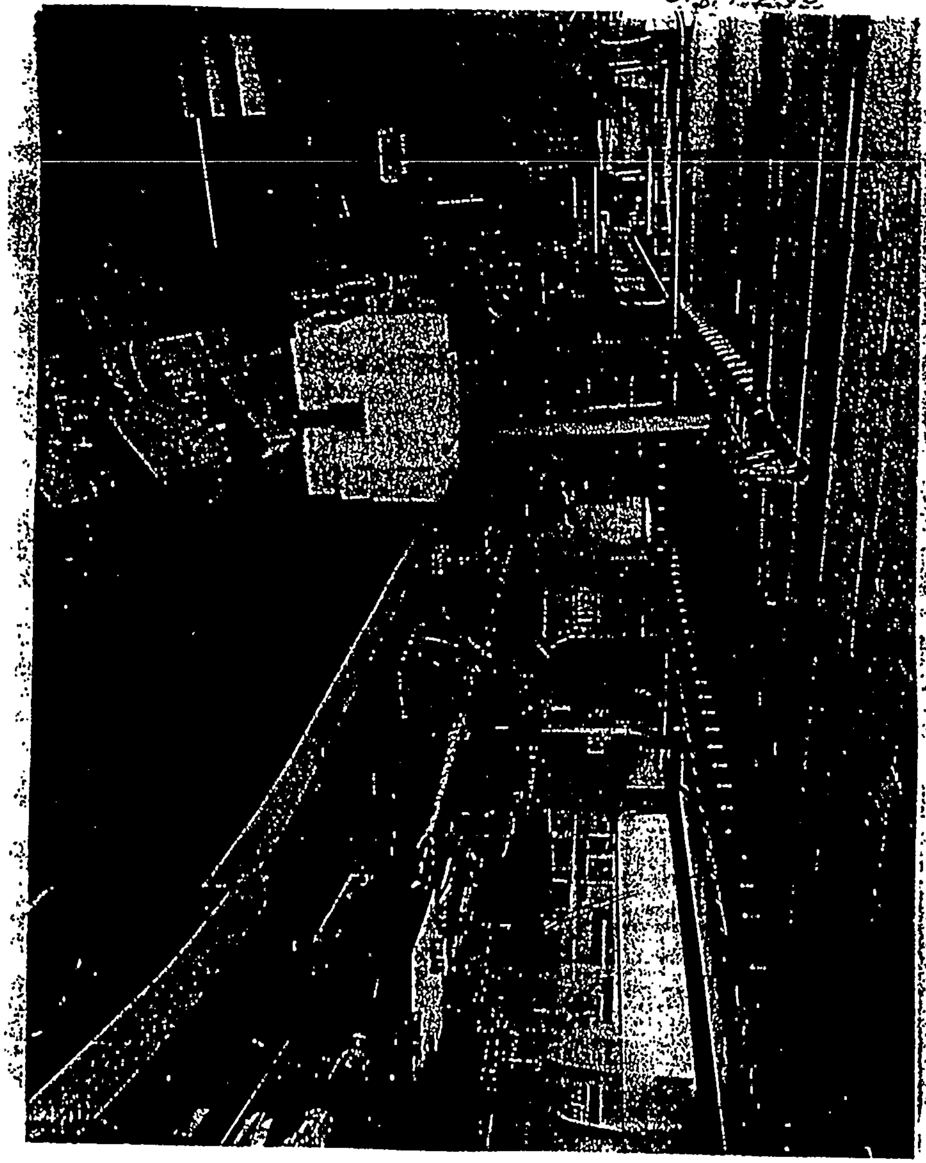

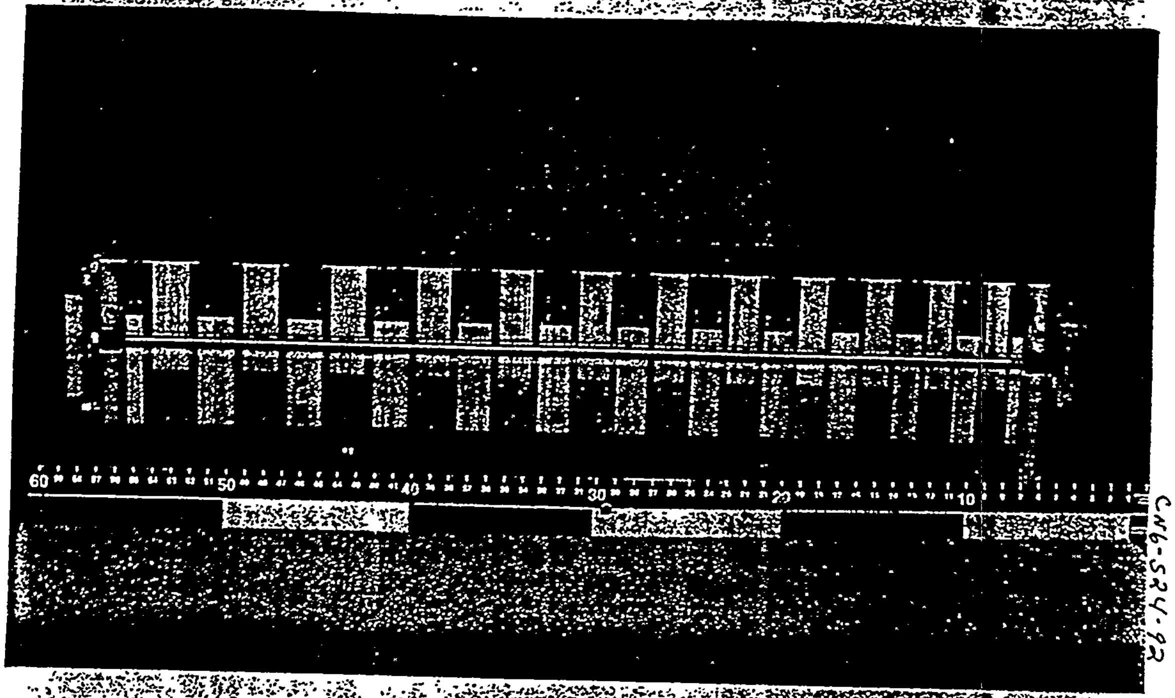

CN6-524-92

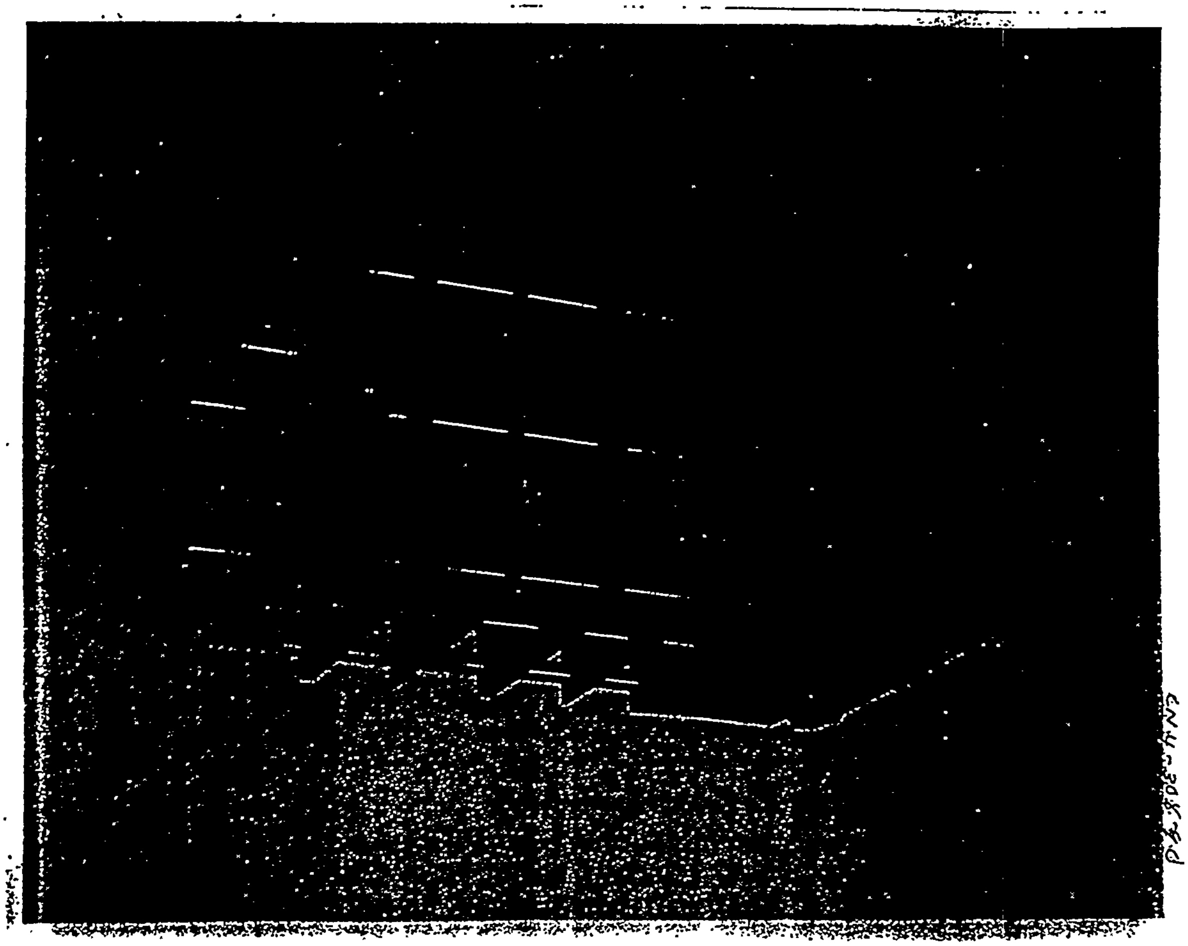

CN4-304-92

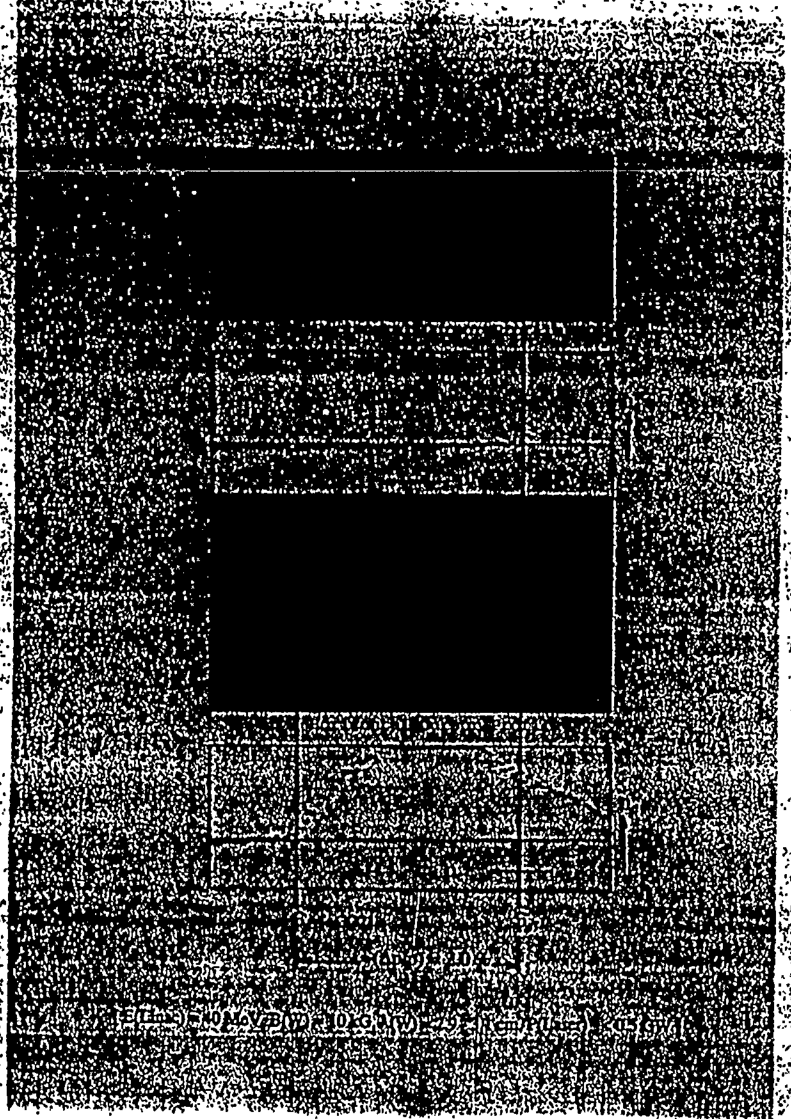

CN4-2-96

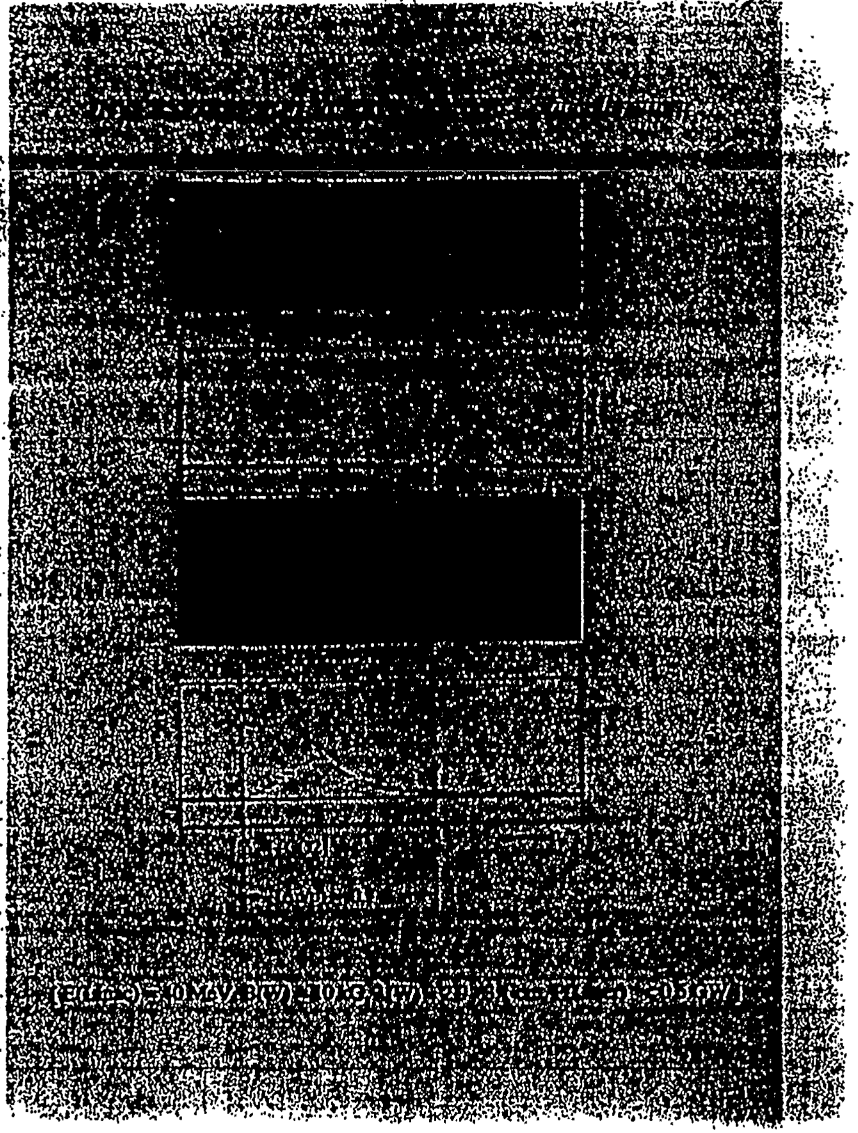

CN4-1-46

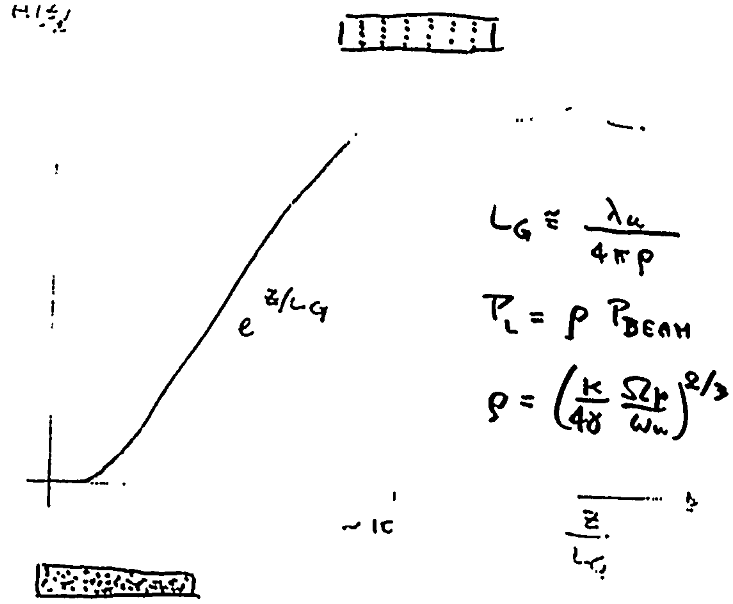

$$L_G \approx \frac{\lambda_u}{4\pi\rho}$$

$$P_L = \rho\, P_{BEAM}$$

$$\rho = \left(\frac{K}{4\gamma}\frac{\Omega_p}{\omega_u}\right)^{2/3}$$

THE INSTABILITY LEADS TO AN ORDERED STATE

"1-D ELECTRON CRYSTAL"

IF
1. $\underline{\sigma_E < \rho}$ (1985)
2. $\varepsilon \lesssim \lambda/4\pi$ (1985)
3. $\beta_u \sim L_G$ (1988)

IFEL e Acceleration

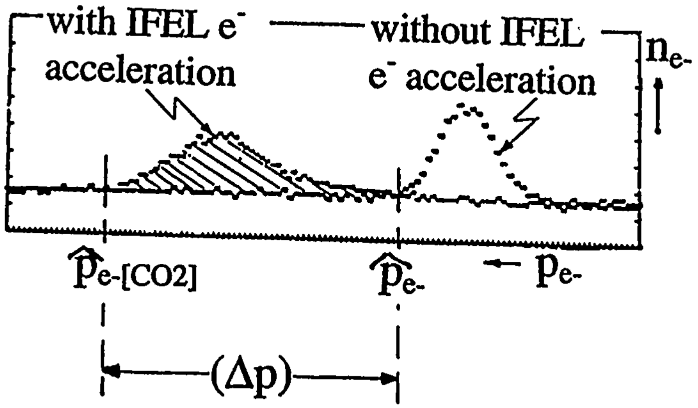

E_{linac}=40 MeV, B_w=10kG,
λ_w=2.9-3.1 cm, W_{laser}=1.GW

An Injector-prebuncher for a Plasma Electron Accelerator

M. Lampel, C. Pellegrini, R. Zhang, UCLA, Dept of Physics, C. Joshi, UCLA, Dept of EE,
Los Angeles, CA 90095, and W. M. Fawley, LBL, Berkeley, CA 94720

ABSTRACT

Optimum operation of a plasma beat-wave or wakefield accelerator requires an injected beam consisting of a train of electron bunches separated by the plasma wavelength, with each bunch in the train having a length much shorter than the plasma wavelength, and the capability of controlling the relative phase of the electron bunches and plasma wave. The typical plasma wavelength is about 0.1 mm, requiring a bunch length of about 10 to 20 μm, which is difficult to achieve with conventional RF based injectors. In this paper we describe an electron accelerator-buncher system based on a photoinjector and an FEL, which can satisfy the plasma accelerator requirements.

INTRODUCTION

An injector of up to 25 MeV beam energy is proposed to supply the Plasma Beat Wave Accelerator (PBWA) [1] with a high quality (ϵ = 05 π mm-mrad at full energy) electron beam of sufficient intensity (~ 1 nC per pulse) to allow capture and acceleration by the PBWA of a significant number of electrons to the GeV energy range. The injector will be based on proven technology from the Saturnus laboratory [2], with upgrades of both the BNL RF gun [3], and the Plane Wave Transformer (PWT) accelerator [4]. The system will provide 1 nC average micropulse charge focused to a 100 μm spot diameter at the injection point. A FIR FEL is proposed as an optical pro-buncher. Phase locked pre-bunching of the electron pulse into 10 - 20μm long bunchlets will allow control of the relative phase of the electron bunchlet and the plasma wave. Such control will aid in minimizing PBWA electron beam final energy spread and emittance. The optical pre-buncher/ final focus system may need to be an achromatic and isochronous system to second or perhaps third order to maintain the bunchlets shape after exiting the optical resonator.

PBWA REQUIREMENTS

A PBWA operates by mixing two lines from a drive laser in a plasma whose parameters are chosen so that the beat between the laser lines matches the plasma frequency. We assume a multi-terawatt 1 μm laser system as the drive laser system for the PBWA. The PBWA requirements dictate the design of the injector so that efficient matching can occur. Table 1 shows the top level parameters upon which the design is based.

TABLE I

Parameter	Design Value
Emittance (unnormalised, rms.)	0.5 π mm-mrad
Energy spread (rms.)	2%
Injector beam energy	>2 MeV
Average charge in bunch (bunchlet)	1 nC (10^4 e)
Bunchlet length	30 - 60 fs
Bunchlet diameter (2σ)	<200 μm
Phase Control absolute relative	 +\- 1 ps <30 fs

Injection phase control of the bunchlets facilitates optimization of the PBWA for acceleration, reducing the energy spread and emittance of the PBWA accelerated beam. Absolute timing is relaxed because the electron pulse can be much longer than the laser pulse. However relative timing of the plasma beat waves with the electron bunchlets becomes necessary. A nonlinear optics control method of phase locking bunchlet formation to the beat wave produced by the lasers is necessary. Several possibilities exist to achieve this and detailed studies will be done to identify the most likely candidates so that the issue will be resolved before the optical bunching experiment is begun. We note that the options include: 1) Use of a beatwave-plasma interaction to produce 100 μm phase locked radiation to seed an FEL amplifier and; 2) use of nonlinear index of refraction changes in a plasma, due to a plasma beat-wave interaction, to control the optical path length, thus the relative phase, of 100 μm light.

The baseline injector system uses the technology of the Saturnus experiment. The Saturnus hardware represents all the hardware needed for the injector, except for the experiment specific final focus into the PBWA, and phase locking of the electron pulse to the PBWA laser system.

0-7803-3053-6/96/$5.00 ©1996 IEEE

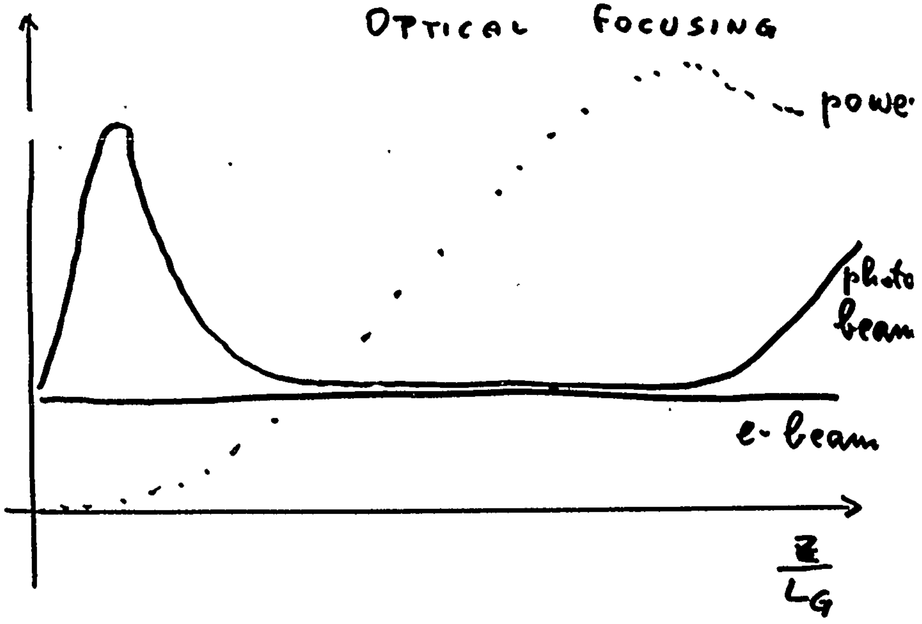

INJECTOR DESCRIPTION

A standard RF power system consisting of a modulator and klystron runs a photo-cathode RF gun (0-5 MeV) and an PWT (pulse wave transformer) accelerator section (5-25 MeV). The electron beam generated in the gun is focused by bucking solenoids so that it has proper size entering the accelerator. X-Y steering magnets correct for any small mechanical misalignments. After exiting the accelerator section the beam travels through a beamline guided and focused by dipole and quadrupole magnets. These magnets match the electron pulse into the FIRFEL for prebunching. A final transport section matches the beam into the PBWA for acceleration by the plasma wave.

The modulator and klystron provide up to 35 MW, approximately 7 MW to the electron gun and the rest available to the PWT. The design of the modulator is taken from the present modulator for the Saturnus experiment, capable of running at 5 pps. The klystron will be a SLAC XK-5 of which UCLA currently has two available for this project.

Fourth harmonic light of the PBWA laser drives the photocathode. The gun itself is the second generation of the successful Brookhaven National Laboratory rf gun. A slight modification of the length of the first cavity, to 0.6 λ, results in an increased electron beam brightness (a decrease in beam emittance) over the original "half cavity" design.

The PWT is a high gradient standing wave accelerator. Several engineering and fabrication improvements are proposed for the new injector: A simplification of the internal cooling of the structure; use of all metal sealing surfaces for greater radiation resistance and better vacuum properties; redesign of the "disks" to reduce the maximum surface gradient. This improved PWT has been fabricated and tested with low level RF power and has been installed into the Saturnus beamline. In order to reach 25 MeV two PWT structures will be used.

THE FEL AS AN OPTICAL BUNCHER

The requirements on the pre-buncher are that ~10 μm bunches spaced 100 μm apart are injected into the plasma beat wave accelerator with emittance and energy spread within the acceptance of the PBWA. An FEL naturally bunches electrons onto a fraction of the optical wave being amplified, one wavelength apart. From this is it is quite clear why an FEL can be used as the PBWA pro-buncher.

Matching operation of the pro-buncher to produce the beam desired for injection into the PBWA leads to setting the operating point of the FEL in terms of energy, undulator length, and field strength.

GINGER calculations for a master oscillator-power amplifier (MOPA) FIR FEL configuration have been done to begin examining the performance of a pro-buncher. Table II gives the GINGER parameters of the electron and optical beams studied for the oscillator and the amplifier.

Table II

Electron Beam Parameters Oscillator and Amplifier	
Electron beam energy	21 MeV
Micropulse current	150 A
Micropulse length (fwhm)	12 ps
Micropulse spacing	10 ns
Normalized emittance (edge)	10 π mm-mrad
Resonator Parameters, osc.	
Single pass gain	2.4
Power in spontaneous emission after 1 pass	15 W
Saturated power (peak)	180 MW
Resonator length	1.5 m
Round trip time	10 ns
Undulator Parameters Oscillator and Amplifier	
Undulator period	4 cm
Undulator length, osc.	1 m
Undulator length, amp.	0.8 m
On axis magnetic field	1.04 T
path length correction factor $K^2/2$	11.3

The GINGER code test case is based on a parabolic electron bunch in z of total length 16 ps. The undulator is linear with external quadrupoles providing focusing in the wiggle plane.

The oscillator is assumed to have 60% net cavity reflectance, with a net cavity detuning that is 0% of slippage.

Figure 1 displays results from GINGER showing the bunching of the electrons at the end of the amplifier undulator. The first pulse displayed, at a time 1.33 ps into the bunch, demonstrates the excellent bunching possible through the FEL mechanism. The majority of electrons are clearly bunched very sharply in phase over

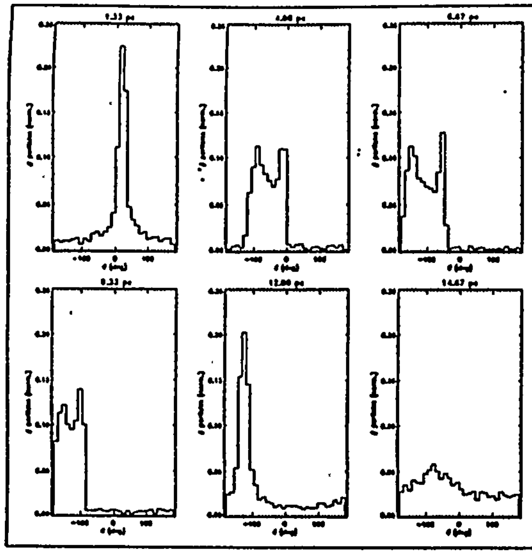

Figure 1:
Electron Beam bunching at six slices in time at the amplifier undulator exit.

~60°, corresponding to less than 20 μm. The forward part of the electron pulse is well bunched because the optical fields propagate from the rear to the front due to the slippage of the electron beam. The bunching parameter is about 0.7. To increase the number of well bunched slices, we will consider in future calculations two potentially beneficial effects: 1) tapering the undulator, and; 2) use of a waveguide in the amplifier to reduce slippage.

The amplifier needs a source of 100 μm light to start it. Two possibilities exist: The FEL oscillator could be built as the source. The MOPA configuration clearly provides a complete solution to the problem of getting 100 μm light, but is expensive and does not solve the phasing problem between the bunchlets and the PBWA beatwave. A second possibility would be to use the beatwave to produce a 100 μm seed for the FEL amplifier directly. This gives automatic phasing between the bunchlets and the wave. An initial calculation indicates that injecting the two lines from the drive laser into a plasma will produce at least 100 kW of coherent 100 μm light in a f/1 cone angle. As can be seen from Table II this power is several orders of magnitude greater than the spontaneous emission at the end of the first pass.

REFERENCES

1) Measurements of the Beatwave Dynamics in Space and Time, A. Lal, K. Wharton, D. Gordon, C.E. Clayton, M. Everett, C. Joshi, PAC95, May 1-5, Dallas, TX

2) The UCLA Compact High Brightness Accelerator, P. Davis, G. Hairapetian, M. Hogan, C. Joshi, S. Park, C. Pellegrini, J.B. Rosenzweig, G. Travish, R. Zhang

3) Multipole Field Measurements in the SLAC/BNL #3 RF Gun, D. Palmer, R. H. Miller, H. Winick, X.J. Wang, K. Batchelor, M. Woodle, I. Ben-Zvi, PAC95, May 1-5, Dallas, TX

4) Initial Operation of the Plane Wave Transformer (PWT) Linac R. Zhang, P. Davis, G. Hairapetian, M. Hogan, C. Joshi, S. Park, C. Pellegrini, J.B. Rosenzweig, G. Travish, PAC95, May 1-5, Dallas, TX

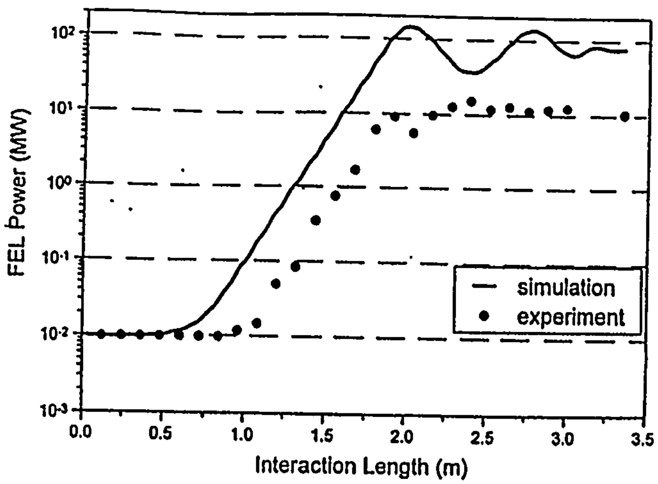

Figure 6

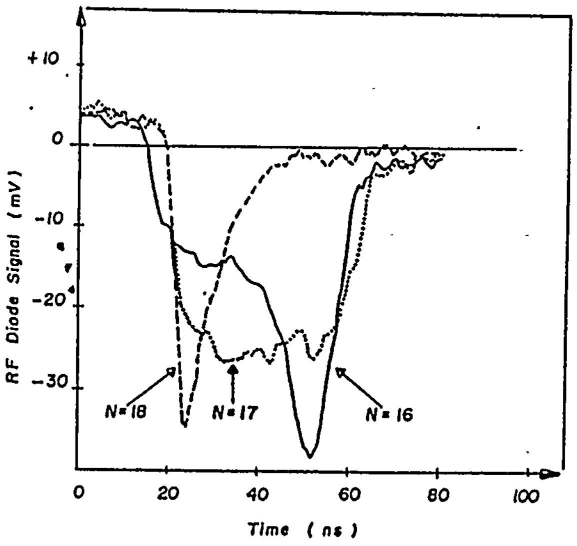

Figure 7

COMMISSARIAT A L'ENERGIE ATOMIQUE

Centre d'Etudes Scientifiques
et Techniques d'Aquitaine

Analysis of the beam bunching produced by a free electron laser

J. Gardelle, J. Labrouche, G. Marchese,
J. L. Rullier, D. Villate,
with
J. T. Donohue

submitted for publication in Physics of Plasmas,
june 1996

Preprint CESTA /5

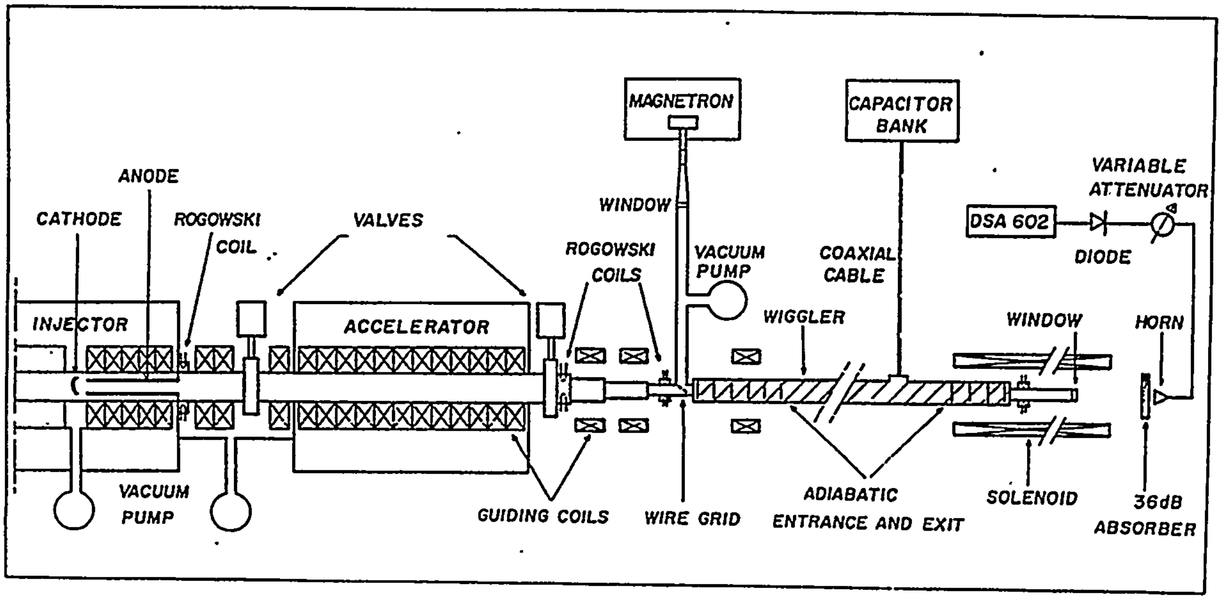

Figure 1

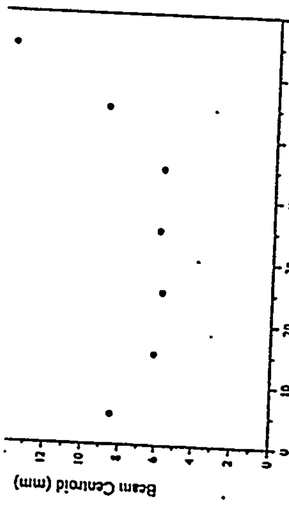

Figure 2

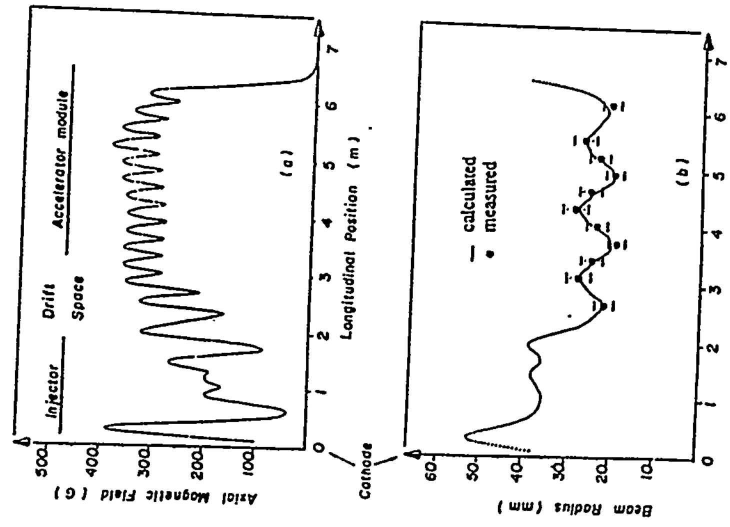

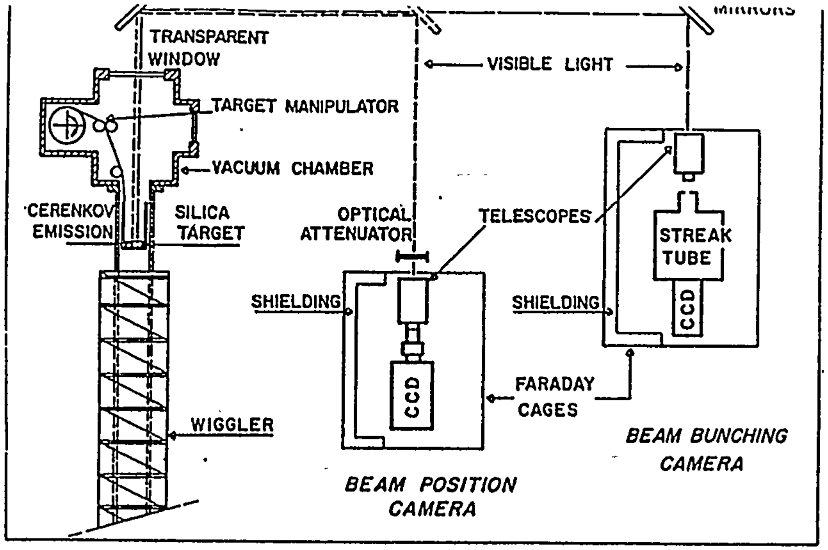

Figure 8

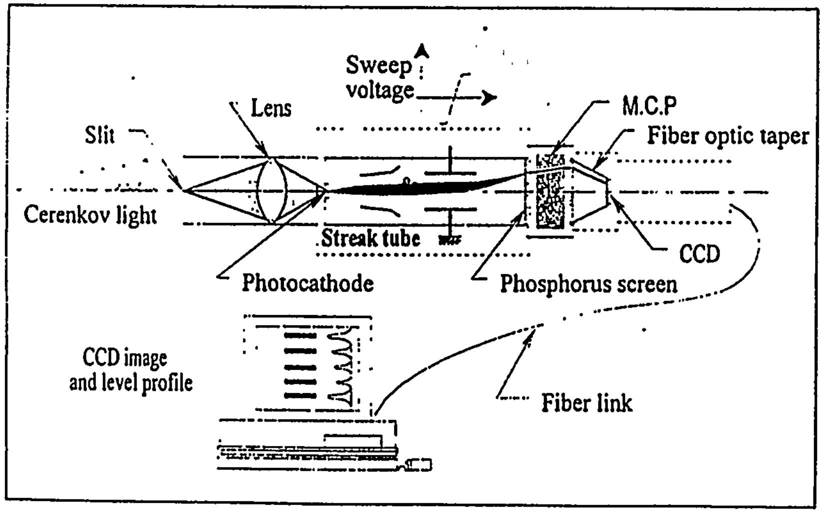

Figure 9

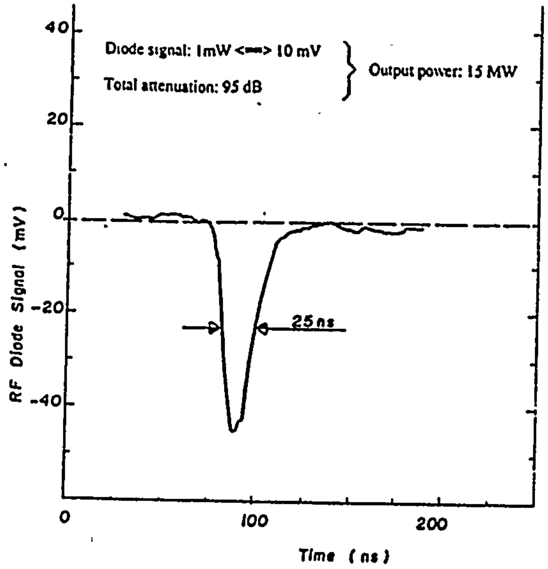

Figure 4

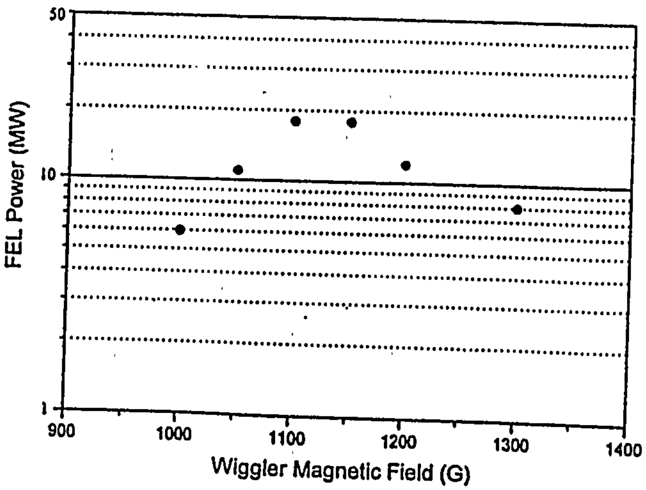

Figure 5

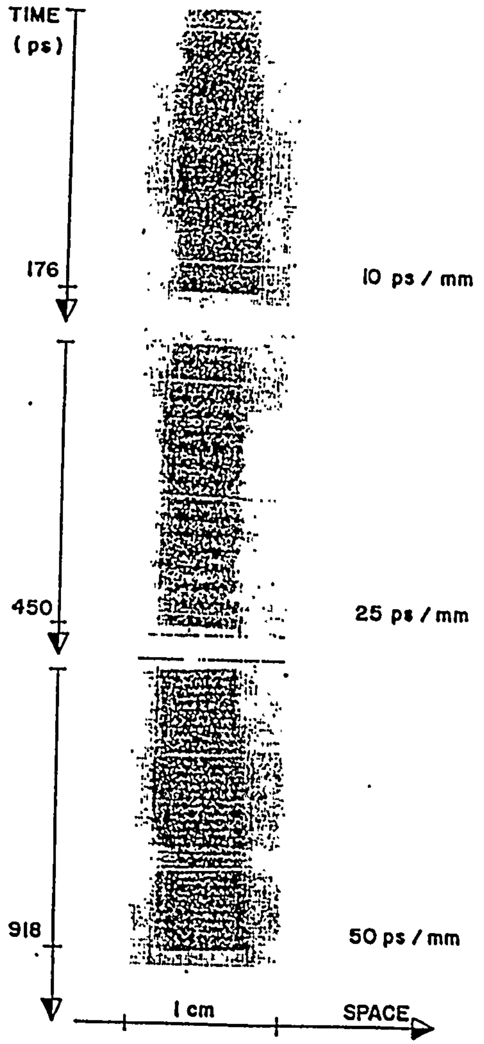

Figure 13

NEW ADVANCES IN INVERSE CERENKOV ACCELERATOR

W. Kimura, STI

NEW ADVANCES IN INVERSE ČERENKOV ACCELERATION

W. D. Kimura

19 August 1996

Work supported by U.S. Department of Energy, Grant No. DE-FG06-93ER40803

OUTLINE

- The Past
  - What is inverse Čerenkov acceleration (ICA)?
  - Past experimental results
- The Present
  - ICA with an IFEL prebuncher
  - 100 MeV ICA Demonstration Experiment
- The Future (?)
  - Inverse transition acceleration (ITA)
  - Inverse diffraction acceleration (IDA)

COLLABORATORS/CONSULTANTS

- STI Optronics, Inc.
  - Gerald Kim
  - Richard Romea
  - Loren Steinhauer
- Brookhaven National Laboratory
  - Igor Pogorelsky
  - Karl Kusche
  - Richard Fernow
- University of California, Los Angeles
  - Yabo Liu
- Consultants
  - Prof. Jorge Fontana
  - Prof. Richard Pantell
  - Prof. David Cline

STI OPTRONICS

INVERSE ČERENKOV ACCELERATION (ICA)

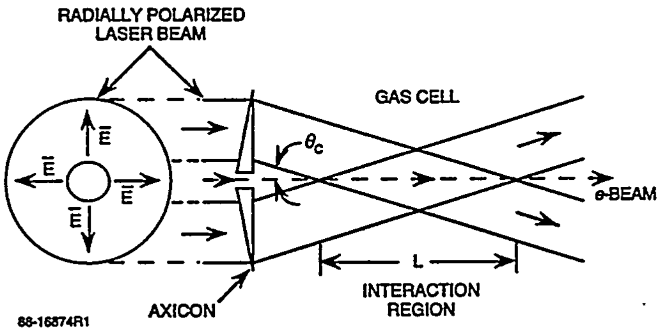

- Phase Matching Condition: $n\beta \cos \theta_c = 1$
  Where n = Index of Refraction of Gas, βc = Electron Velocity
- Maximum Energy Gain: $\Delta W \propto \sin\theta_c\sqrt{PL/\lambda}$
  Where P = Laser Peak Power, λ = Laser Wavelength
- Significant *E*-Beam Focusing Also Possible
- Experimentally Demonstrated at Stanford in 1981
  Using Gaussian Laser Beam

STI OPTRONICS

DESCRIPTION OF ICA EXPERIMENT

- Objectives:
  - Demonstrate improved ICA using radially polarized laser beam and axiom focusing developed by Fontana and Pantell
  - Compare with model predictions
- Experiment Located on Beamline #1 of the Accelerator Test Facility (ATF) at Brookhaven National Laboratory
- Major Components of ICA Experiment
  - Hydrogen gas cell where ICA interaction occurs
  - Optical system for converting linearly polarized CO_2 laser beam to radial polarization
  - Electron beamline system connected to gas cell
  - Electron energy spectrometer that uses image intensifier/ CCD camera detector system

STI OPTRONICS

SCHEMATIC PLAN VIEW OF GAS CELL

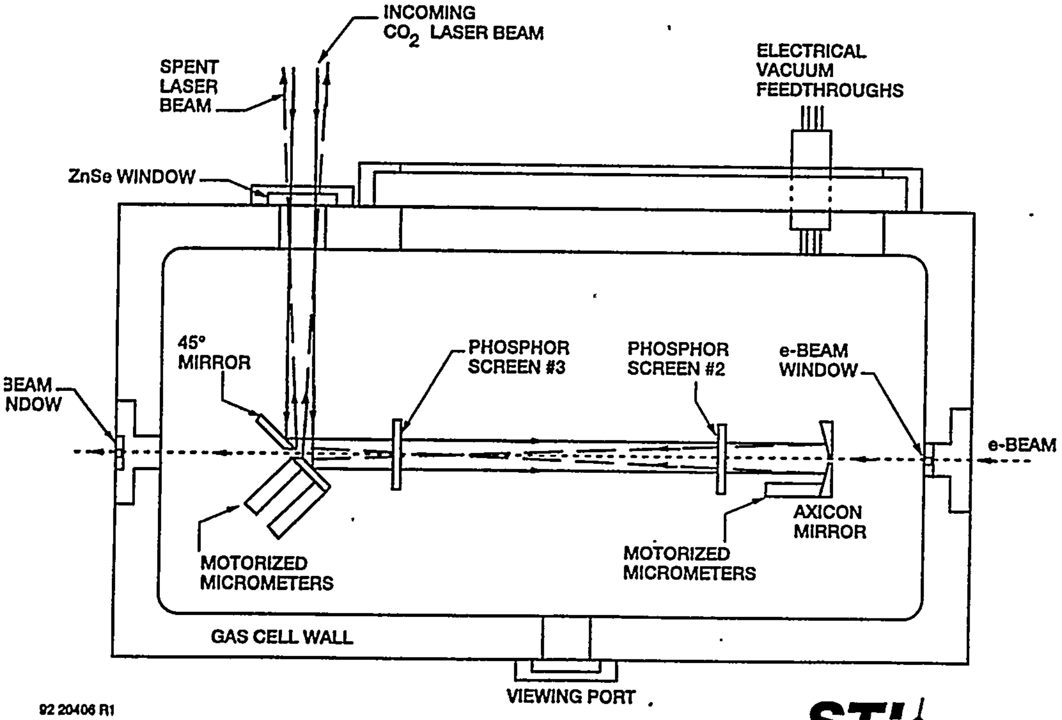

STI OPTRONICS

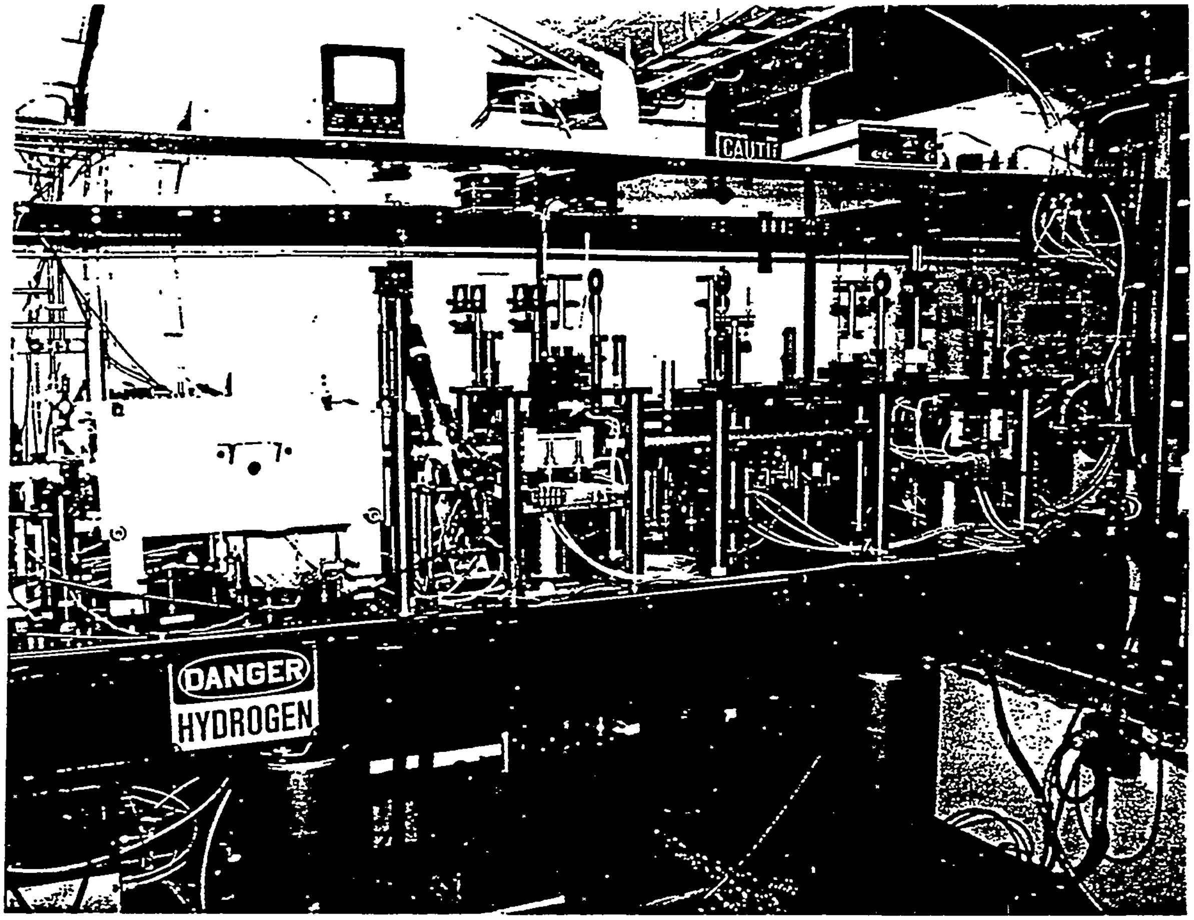
CAUTI
DANGER
HYDROGEN

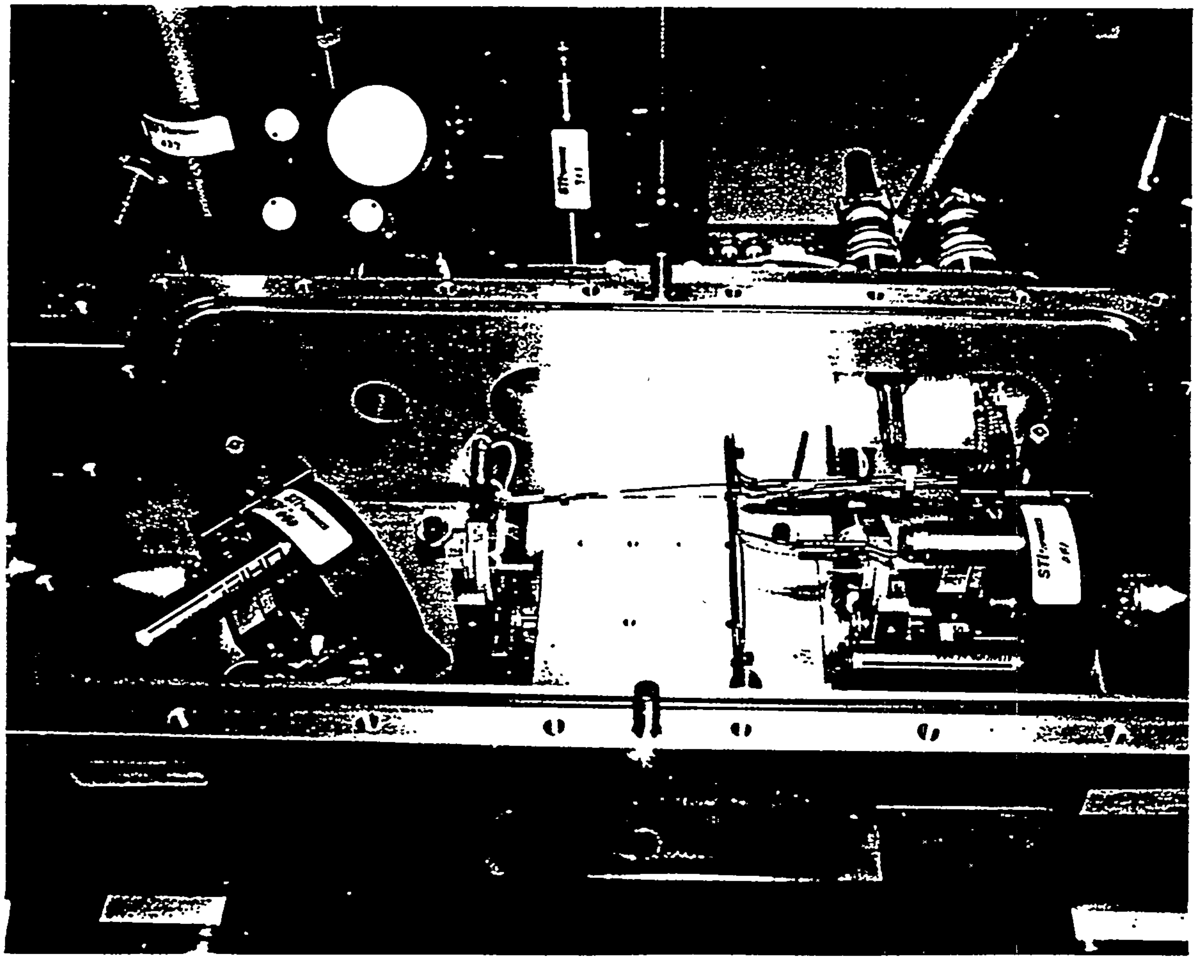
STI

SCHEMATIC OF ICA EXPERIMENT OPTICAL SYSTEM

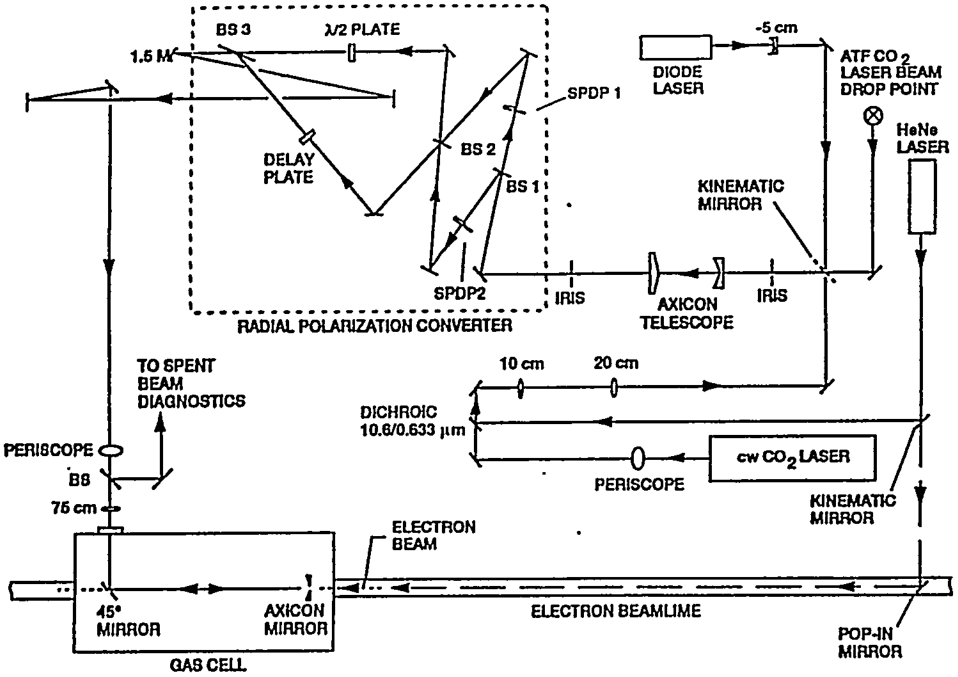

92 20407R1

STI OPTRONICS

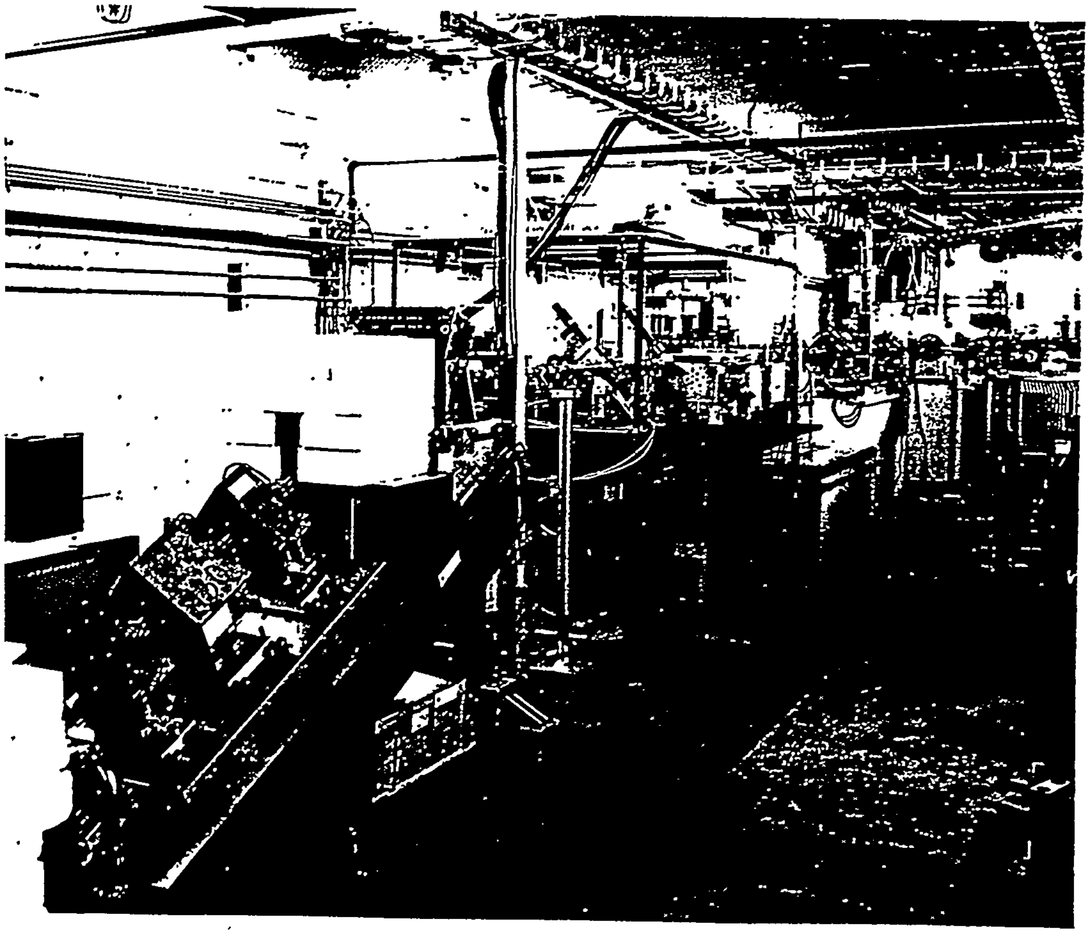

TYPICAL ICA EXPERIMENT SYSTEM PARAMETERS

Electron Beam

Source:	BNL ATF
Beam energy:	55 MeV
Intrinsic energy spread (σ):	≈ ± 0.1 MeV
Normalized emittance:	~ 3 π mm-mrad
Electron bunch length:	≈ 10 ps (FWHM)
Pulse format:	Single pulse

Laser Beam

Laser:	CO_2
Wavelength:	10.6 µm
Pulse length:	220 ps
Peak power delivered to interaction region:	<1 GW
Pulse repetition rate:	Single shot

Interaction Region (Gas Cell)

Phase matching medium:	Hydrogen gas
Čerenkov angle:	20.08 mrad ± 0.08 mrad
Length of electron/laser beam overlap:	≈ 12 cm
Length of gas traversed by electrons:	43 cm
Thickness of diamond film e-beam windows:	2.1 µm

STI OPTRONICS

EXAMPLE OF EXPERIMENTAL RESULTS

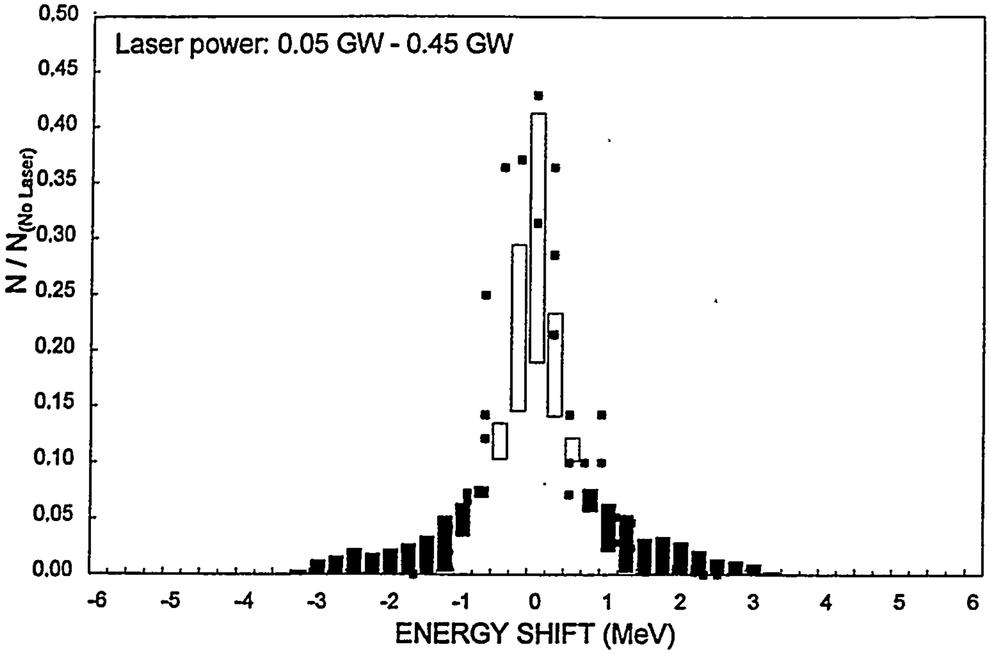

(Uncalibrated data)

STI OPTRONICS

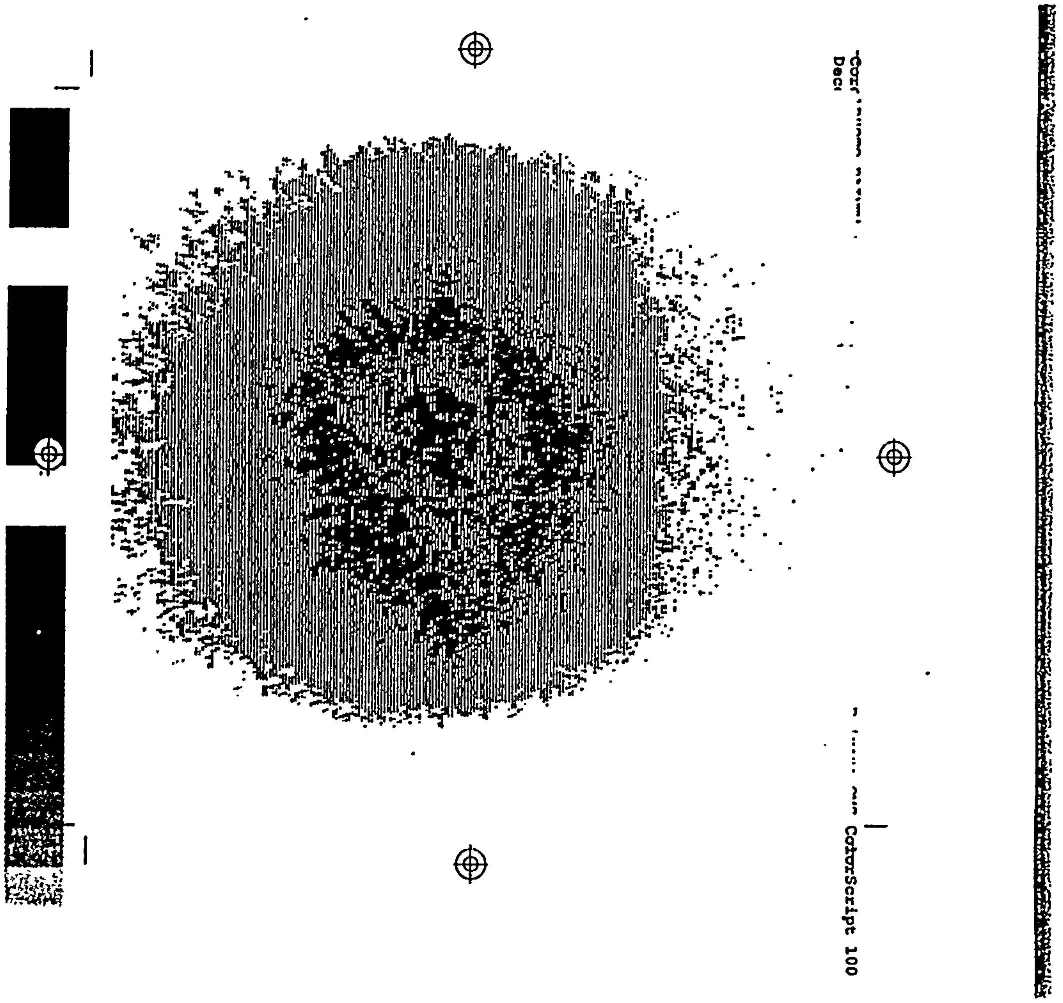

NEXT PHASE OF EXPERIMENT IS TO DEMONSTRATE 100 MeV NET ENERGY GAIN

- Goals of Experiment
  - Prebunching of electrons at optical wavelengths
    - need to bunch electrons into smaller phase space
    - important for efficient acceleration
  - Staging of acceleration sections
    - need to rephase light wave with bunched electrons
    - important for scaling to higher energy gains
  - 100 MeV net acceleration
    - energy gain depends on laser peak power
    - total number of accelerated electrons affected by many other factors (e.g., gas scattering, emittance, trapping, etc.)

LASER PULSE SHAPE MEASUREMENT

- Data Represents Width of Central *E*-Beam Energy Subspectrum

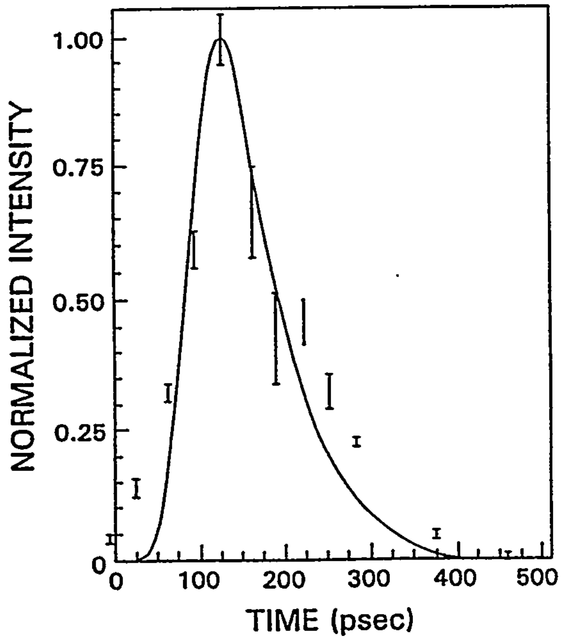

DESCRIPTION OF 100-MeV ICA DEMONSTRATION EXPERIMENT

- Use ATF *e*-Beam (65 MeV) and Upgraded CO_2 laser (250 GW-1 TW)
- Use Existing IFEL as Prebuncher
  - In collaboration with A. van Steenbergen (BNL)
  - Provides nearly ideal bunching at optical wavelengths
  - Probably will not need magnetic chicane
  - Locate upstream of existing ICA experiment
- Use Existing Gas Cell as ICA Acceleration Stage
  - Use doublet or triplet to refocus *e*-beam from IFEL into ICA cell
  - Demonstrate rephasing of laser beam with bunched electrons
  - Demonstrate acceleration of bunch (i.e., trapping)
- Lengthen Gas Cell for 100-MeV Demonstration
  - Single-stage, 27-cm long interaction length
  - Predict ~370 MeV/m acceleration gradient for ~250 GW delivered laser power

STI OPTRONICS

CONCEPTUAL LAYOUT FOR 100-MeV LASER ACCELERATOR

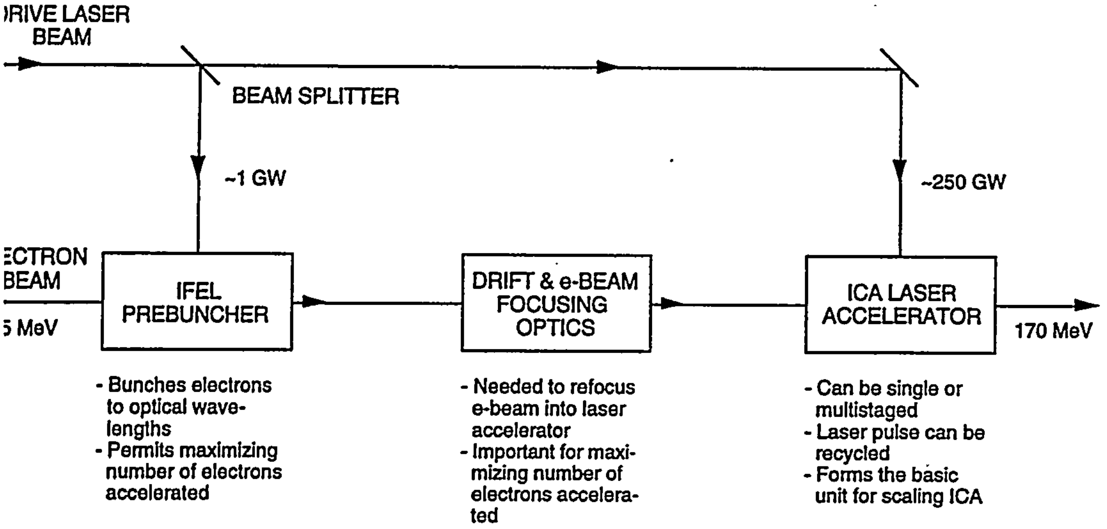

RIVE LASER BEAM

BEAM SPLITTER

~1 GW

~250 GW

ECTRON BEAM

5 MeV

IFEL PREBUNCHER

DRIFT & e-BEAM FOCUSING OPTICS

ICA LASER ACCELERATOR

170 MeV

- Bunches electrons to optical wavelengths
- Permits maximizing number of electrons accelerated

- Needed to refocus e-beam into laser accelerator
- Important for maximizing number of electrons accelerated

- Can be single or multistaged
- Laser pulse can be recycled
- Forms the basic unit for scaling ICA

STI OPTRONICS

UPDATE ON ICA/IFEL COMBINED EXPERIMENT

- Analysis and Modeling of Combined Experiment in Progress
  - Use existing IFEL and ICA codes
  - Use TRANSPORT and PARMELA to model beam transport
- Upcoming IFEL Experiment Will Include Measuring Prebunching
  - Use coherent transition radiation (CTR) diagnostic built by BNL/UCLA
  - Same diagnostic will be used during combined ICA/IFEL experiment
- Afterwards, IFEL Will be Moved to Position Upstream of Present ICA Experiment
  - First combined experiments will be done at moderate laser powers to verify rephasing and trapping of bunches
  - Later, ICA experimental hardware will be modified to handle upgraded CO_2 laser power

STI OPTRONICS

SCHEMATIC OF ICA/IFEL COMBINED EXPERIMENT

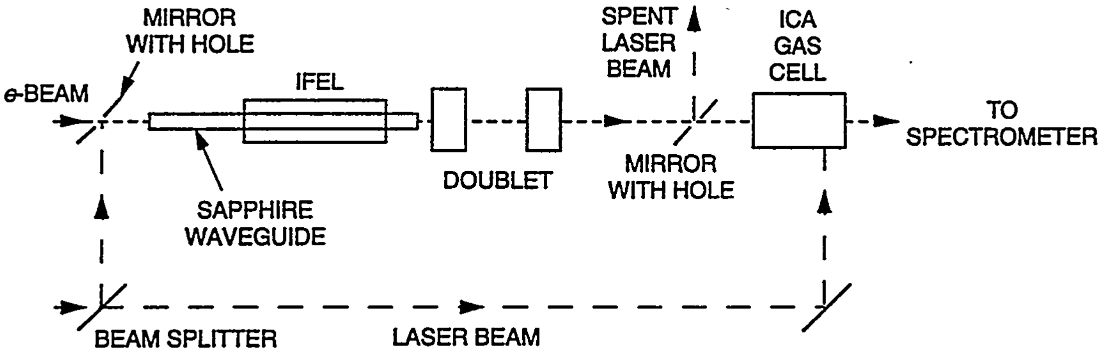

STI OPTRONICS

BASIC CONFIGURATION FOR ITA

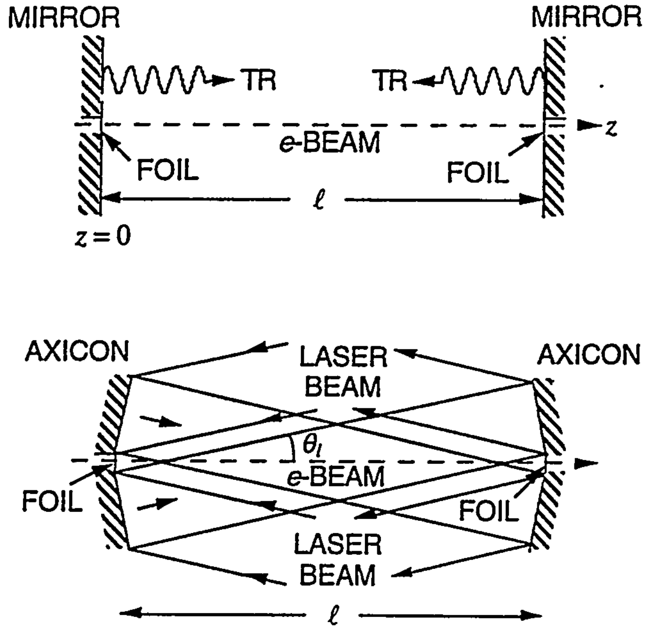

INVERSE TRANSITION ACCELERATION (ITA) AND INVERSE DIFFRACTION ACCELERATION (IDA)

- Transition Radiation (TR) is Well-Known; Diffraction Radiation (DR) is Very Similar
  - DR occurs when relativistic charged particle passes through an aperture or over an edge rather than through a foil like TR
  - Angular and spectral characteristics of DR similar to TR, becomes identical to TR when the aperture size goes to zero
- Just Like ICA and IFEL, the Inverse Process Should be Possible
  - Idea first suggested by J. R. Fontana
  - Additional helpful comments from R. H. Pantell, K. T. McDonald, and R. B. Fiorito
- Key Concept is Formation Length L_f for TR or DR
  - L_f is nominal distance for appreciable coherent superposition of TR fields from polarizations induced in medium
  - L_f is also distance within which fields from electrons significantly interact with surface via virtual photons

"FORMATION LENGTH" FOR TRANSITION RADIATON: L_f

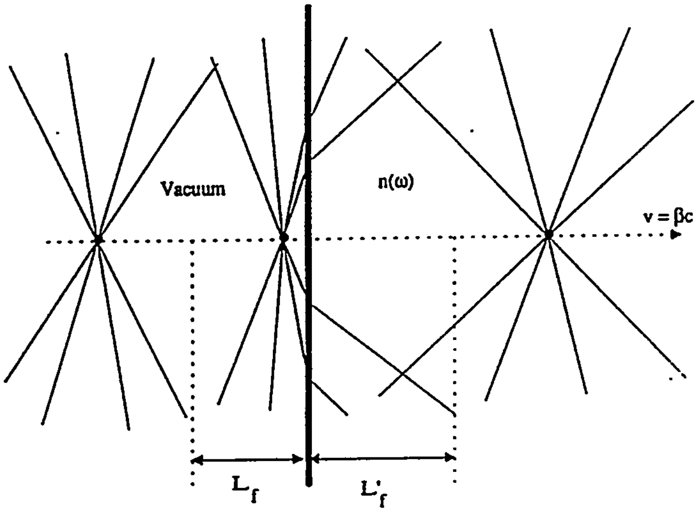

Field Reorganization

- Relativistic Particle Induces a Polarization in Medium
- L_f is a Consequence of Requirement for Coherence of Radiated Intensity

---

ANALYSIS OF INVERSE TRANSITION ACCELERATION (ITA)

- Earlier Classical Analysis [J. Appl. Phys. 72, 3237 (1992)]
  - Used ICA axicon-focusing geometry without gas
  - Shorten interaction length to limit phase slippage between electrons and light wave, define distance as L_π
- Performed Classical TR Analysis (Submitted to Appl. Phys. Lett.)
  - Showed that TR formation distance $L_f = L_\pi/\pi$
  - Showed that angular dependence affected by geometry
- Performed Quantum Mechanical Analysis (Submitted to J. Appl. Phys.)
  - Limiting interaction length ℓ permits satisfying momentum conservation through uncertainty principle (R. H. Pantell, 1979)
  - Showed that $\ell = L_\pi$ for optimum interaction
  - Derived same angular dependence as classical analysis

NGULAR DEPENDENCE OF TRANSITION RADIATION

- For $\gamma = 1000$, $k\ell = 20$

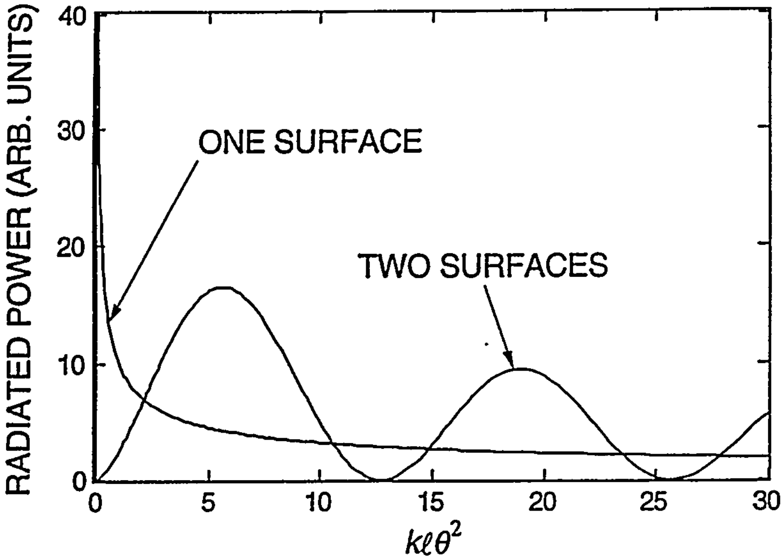

STI OPTRONICS

CLASSICAL ARGUMENT FOR LIMITED INTERACTION LENGTH ℓ

s Related to Phase Slippage of
ectron Phase Relative to Wave:

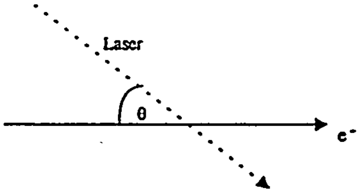

$$\psi = \omega t - \kappa z(t)$$

$z(t)$ = electron's longitudinal position

$\kappa = \frac{\omega}{c}\cos\theta$

Slip distance L_π = distance over which $\Delta\psi = \pi$

$$L_\pi = \frac{\pi}{k\left(\frac{1}{\beta} - \cos\theta\right)} \approx \frac{\lambda}{\theta^2 + 1/\gamma^2}$$

Note: $L_\pi >> \lambda$ in general

STI OPTRONICS

QUANTUM-MECHANICAL ARGUMENT FOR LIMITED INTERACTION LENGTH

Uncertainty Principle: $\Delta p L \geq \frac{\hbar}{2}$

Δp = momentum uncertainty

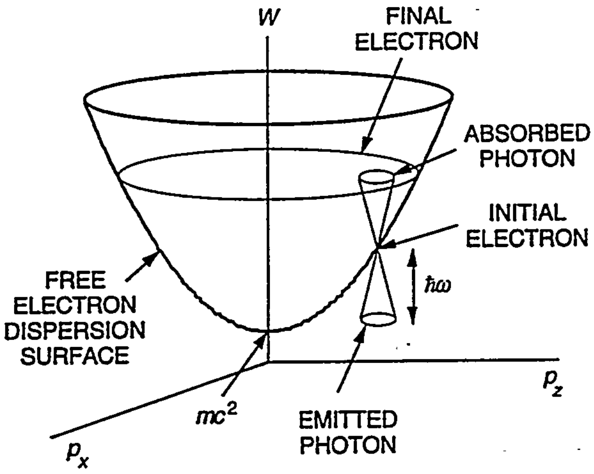

From R.H. Pantell, 1979

electron-photon pair can <u>temporarily</u> violate energy and momentum conservation

STI OPTRONICS

RADIATED TRANSITION RADIATION VERSUS $k\ell$

- For $\gamma = 1000$

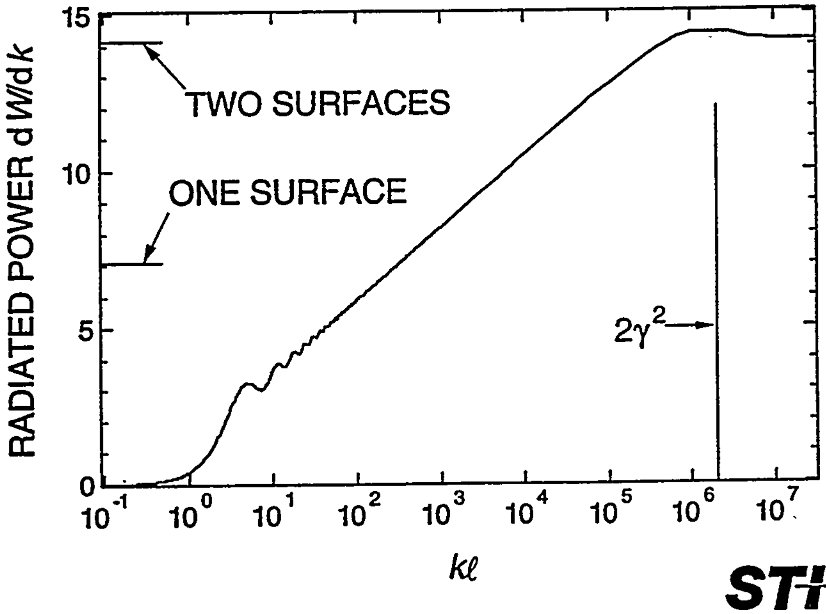

STI OPTRONICS

ADVANTAGES OF ITA/IDA AND ISSUES

Advantages:

- Medium-free process
- No synchrotron losses
- High acceleration gradient possible
  - assume limited by optical damage intensity $I_{\max}$, then
    $\langle dW / dz\rangle(\mathrm{eV/m}) = 7.8 \times 10^3 \theta e \sqrt{I_{\max}(\mathrm{W/cm^2})}$
  - for $I_{\max} = 5 \times 10^{11}\,\mathrm{W/cm^2}$, $\lambda = 10.6\ \mu\mathrm{m}$, $\theta = 100$ mrad,
    $\langle dW / dz\rangle \sim 0.6\ \mathrm{GeV/m}$

Issues:

- Optical damage limits; however, may be able to solve by moving axicon away from foils/apertures
- P. Sprangle, *et al.*, identified two other limitations
  - *e*-beam self-field damaging aperture
  - reflected self-field losses (i.e., spontaneous TR or DR losses)
  - we are presently examining the implications of these limitations
- Wakefield and space-charge effects, and their affect on emittance

STI OPTRONICS

ALYSIS OF INVERSE DIFFRACTION ACCELERATION (IDA)

Sending Electrons Through Aperture Rather Than Foil Changes Process to IDA

- In general, as aperture size increases the amount of DR decreases relative to TR
- Efficiency of inverse process decreases proportionally
- Amount of decrease for single-boundary DR case goes as

$$[J_0(kr_a \sin \theta)]^2$$

assuming $\gamma \to \infty$, where J_0 is Bessel function of 1st kind order zero, r_a is aperture radius

Example: If $\lambda = 10.6\ \mu\mathrm{m}$, $\theta = 10$ mrad, and $r_a = 0.17$ mm, then DR is reduced roughly 20% compared to TR

Similar properties expected for double-boundary DR case

STI OPTRONICS

ALTERNATIVE ITA/IDA FOCUSING GEOMETRY

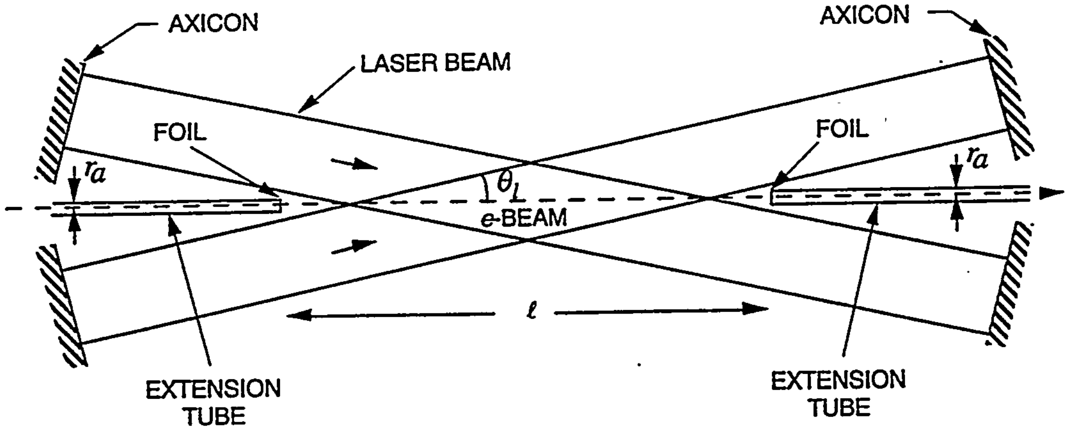

CONCLUSION

- Inverse Čerenkov Experiment Entering New Phase
  - Features IFEL prebuncher
  - Near-term goal is to demonstrate optical bunching, staging, and trapping
  - Long-term goal is to demonstrate 100 MeV net energy gain
- Inverse Transition Acceleration or Inverse Diffraction Acceleration May be Attractive New Scheme
  - Further analysis still needed
  - Relatively simple proof-of-principle experiment may be possible

PLASMA BEAT WAVE ACCELERATOR (PBWA) AND OVERVIEW OF PLASMA ACCELERATION

T. Katsouleas, USC

Overview of Plasma Acceleration

and plasma beat wave accelerator

T. Katsouleas
University of Southern California

Collaborators:
T.C. Chiou, L. Hsu, S. Lee (USC)
W.B. Mori, K.C. Tzeng, C. Joshi,
C. Clayton, D. Gordon, C. Pellegrini,
K. Marsh, J. Dawson (UCLA)
J. Wurtele (UCB), G. Shvets(Princeton)
C. Decker (LLNL)

Challenges

High Energy Colliders

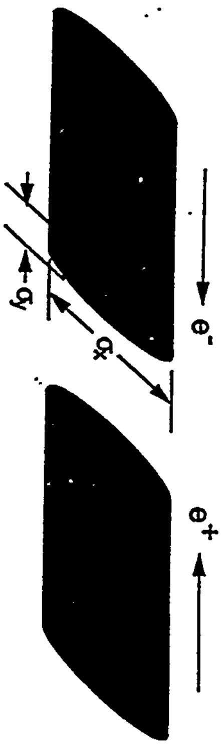

physics → >1 TeV in <10 km ← \$

⇒ **Gradient >100 MeV/m**

physics → $\mathcal{L} = \frac{fN^2}{4\pi\sigma_x\sigma_y} > 10^{33}\,\text{cm}^{-2}\text{s}^{-1}\left(\frac{U}{1\ \text{TeV}}\right)^2$

e.g. $N=10^{10}$, $\sigma_x\sigma_y=10^{-4}\ \mu\text{m}^2$, $f=10^3$,

Wall Plug Power = $\frac{4\ \text{MW}}{\eta}$

$\eta >$ few % ← \$

physics → Small σ_y ⇒ Beam quality

$\varepsilon_N < 0.1$ mm-mrad ← \$

Three basic laser-plasma accelerator schemes: proposed by Tajima and Dawson in 1979

Laser Plasma Group

- A single short-pulse (LWFA)

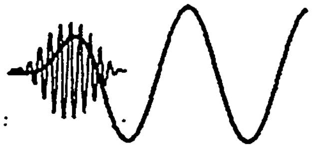

France
Texas
Japan

- Two-frequencies, i.e., a train of pulses (PBWA)

(Could vary spacing and duration of pulses)
: Umstadter et al.

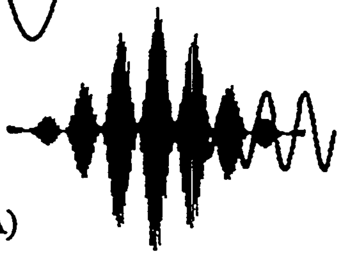

UCLA
France
Japan

- Raman forward scattering instability (SMLWFA)

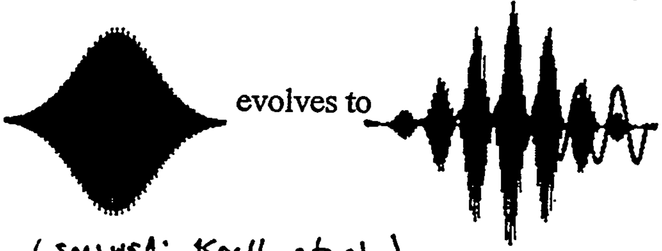

(SMLWFA: Krall et al.
Andreev et al.)
No wavebreaking

several recent experiments
LLNL *
RAL *
Japan
U of M
NRL

ACCELERATION--

Why Plasmas?

* CONVENTIONAL ACCELERATOR $E \sim 20 MeV/m$ ⇒ 10's of km machines

* PLASMA WAVES => LARGE $E_{\parallel}$

$$E \sim \sqrt{n_o}\ V/cm$$

$$\Rightarrow E \sim 10-100\ GeV/m \quad \text{for} \quad n_o \sim 10^{16}-10^{18}$$

* $V_{\phi} \sim C$

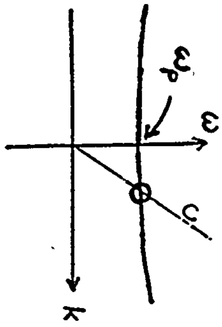

* PLASMA CONFINES POWER SOURCE

laser & beam self-focusing

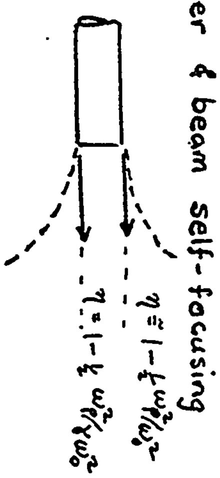

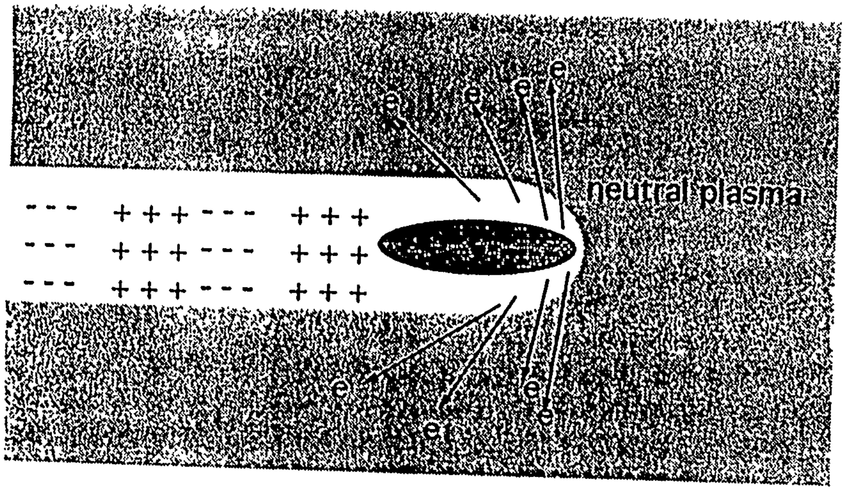

To excite plasma waves:

$\Delta\tau_{FWHM} < 2\pi/\omega_p$ (for a Gaussian electron bunch)

Given a bunch length of: $\Delta\tau_{FWHM} = 4$ ps

Requires a plasma of : $n \gtrsim 10^{14}$ cm^{-3}

Theoretical Models

Linear, 2-D

$$\frac{\partial^2 n_1}{\partial t^2} + \omega_p^2 n_1 = \underbrace{\pm\omega_p^2 n_b}_{PWFA} + \underbrace{\frac{n_0}{m}\nabla\cdot\vec{F}_p}_{LWFA} \qquad \vec{F}_p = \frac{-e^2}{2m^2\omega^2}\nabla E_0^2$$

LWFA ($n_b=0$)

$$n_1 \sim \nabla\cdot E \Rightarrow (\partial_t^2+\omega_p^2)E(r) = \frac{\omega_p^2}{e}F_p\ (r)$$

$\Rightarrow$ 1) $E(r)$ follows $I^{LASER}(r)$

2) $|E| \propto \partial_z I$, NOT I $\Rightarrow$

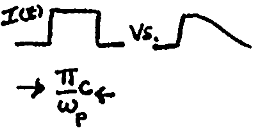

PWFA ($F_p = 0$)

$n_1(r)$ follows $n_b(r)$

$$(\nabla^2 - \tfrac{1}{c^2}\partial_t^2)\vec{E} = \frac{4\pi}{c^2}\partial_t\vec{J} + \nabla(\vec{\nabla}\cdot\vec{E})$$

$$\Rightarrow E_z(r) \propto \int d\xi' d^2r' d\theta' \cos k_p(\xi-\xi')\, K_0(k_p|\vec{r}-\vec{r}'|)\, \underline{n_b(r',\xi')}$$

1) $E_z(r)$ smears out over k_p^{-1} for $n_b(r)$ narrow

where $k_p^{-1} = c/\omega_p$

& $\xi = z - ct$

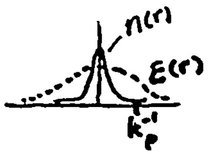

2) Steeply rising [illegible]

SIMPLEST SCALING LAWS

linear theory, wide waves

$$eE = \varepsilon\sqrt{n_0}\ \text{eV/cm}$$

LWFA: $\varepsilon = \frac{1}{4}\left(\frac{V_{os}}{c}\right)^2$, $\omega_p\tau_{pulse} \approx \pi$

$\varepsilon \approx \frac{1}{2}\left(\frac{V_{os}}{c}\right)$ $V_{os}/c >> 1$

PBWA: $\varepsilon = \frac{1}{4}\int_0^{\tau_{pulse}}\left(\frac{V_{os}}{c}\right)^2\omega_p dt$

WFA (particle) $\varepsilon = \frac{n_b}{n_0}$ 1 pulse, $\tau_{cutoff} \leq \omega_p^{-1}$

ΔY_{Lp} = 12c

PBWA: Evolution of Laser Intensity and Accelerating Field

Laser Plasma Group

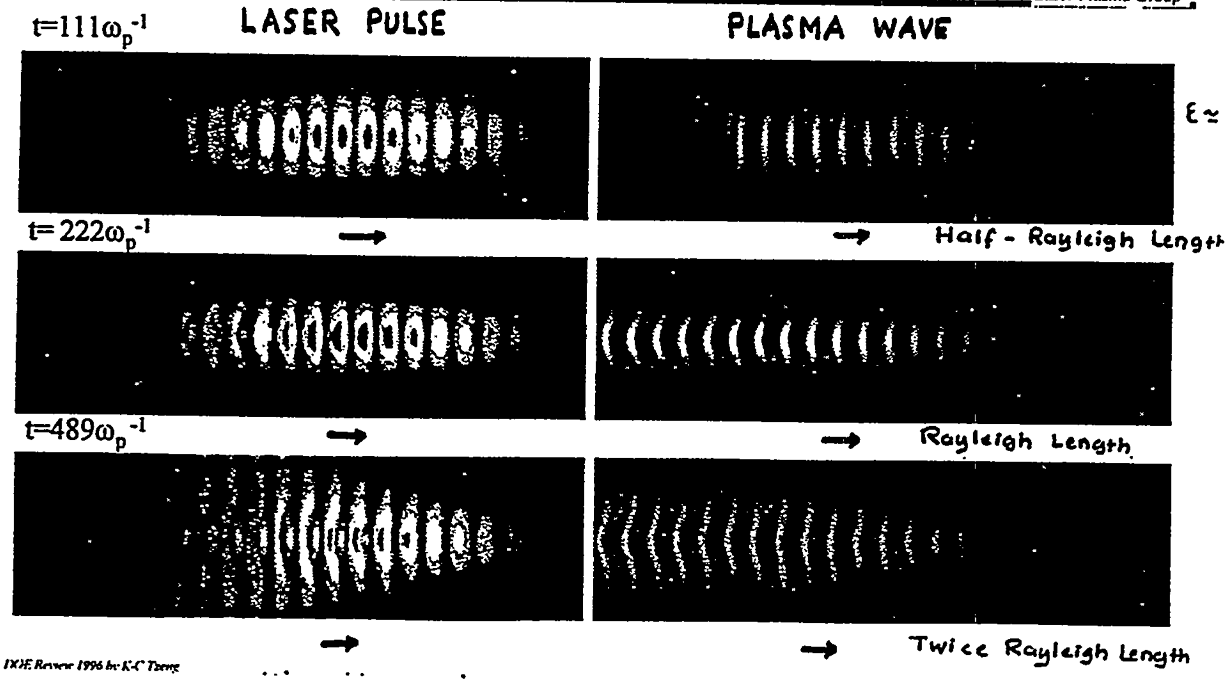

DOE Review 1996 by K-C Tzeng

LASER SELF-FOCUSING IN BEAT WAVES

mechanisms

1-D

plasma wave $\Rightarrow \frac{\delta n}{\gamma} \Rightarrow$ laser group velocity variation

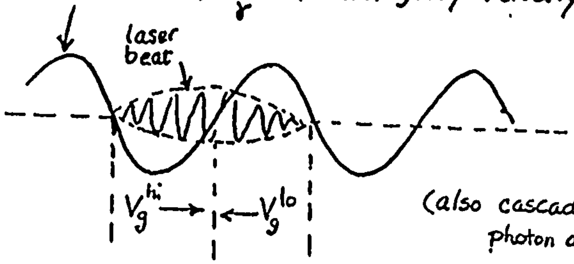

(also cascading, photon acceleration)

2-D

(Gibbon & Bell)

$V_\phi \cong c\left(1+\frac{1}{2}\frac{\omega_p^2}{\omega^2}\right) \Rightarrow$

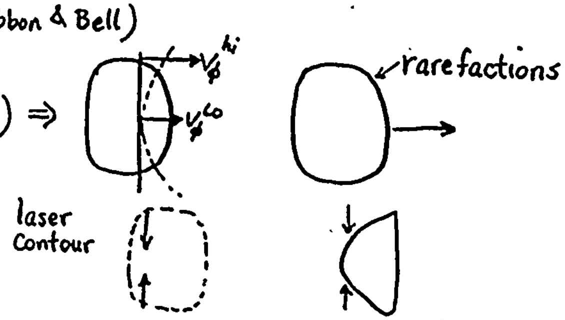

Threshold : $\delta n/n > \frac{1}{4}\left(\frac{100\mu}{\sigma}\right)^2\left(\frac{10^{17}}{n_0}\right) = \frac{1}{4}$ for GeV ex.

Length scale : $\sqrt{2}\left(\frac{\sigma}{100\mu}\right)\frac{1}{\sqrt{\varepsilon}}\sqrt{\frac{10^{17}}{n_0}}\,\frac{1\mu}{\lambda}$ cm $= 2$ cm for GeV Design

Detailed view of experimental setup

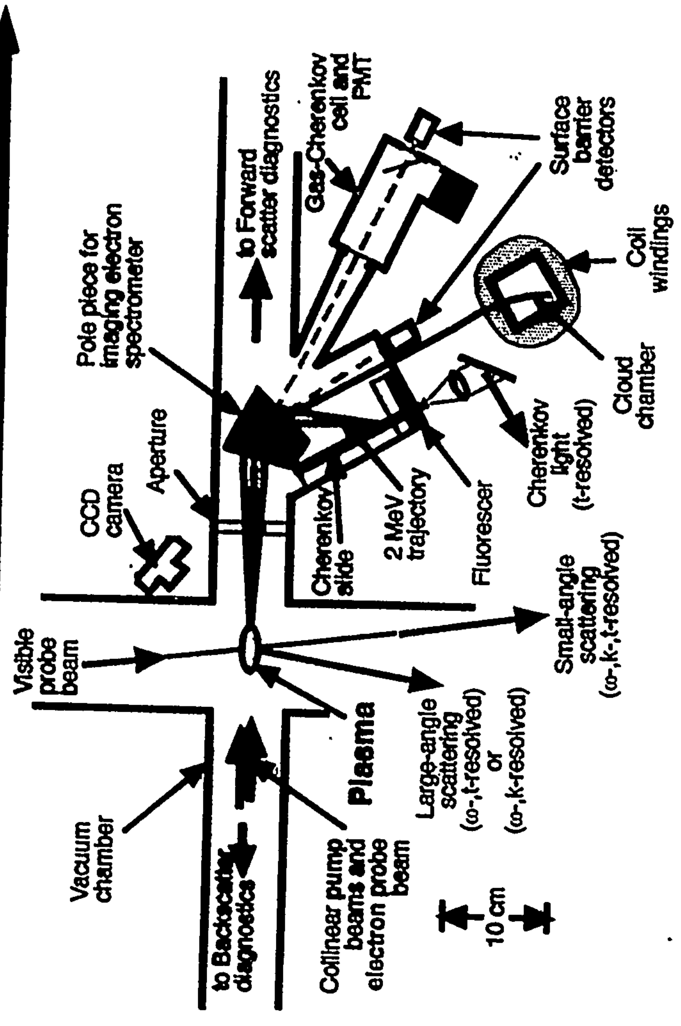

2nd Generation Plasma Accelerators

Goals: **Address issues of beam quality and significant energy gain**

- **energy:** 100 MeV
- **energy spread:** $\Delta\gamma/\gamma < 5\%$
- **emittance:** $\varepsilon_n < 10\,\pi$ mm-mrad
- **number of particles:** $N > 10^8$

Simulations show...

Energy Spread: **w/o pre-bunching:** $\Delta\gamma/\gamma < 25\%$

with pre-bunching: $\Delta\gamma/\gamma < 5\%$ for $\Delta Z < .06\,\lambda_p$

$$\Rightarrow \tau_{bunch} < 60 \text{ fsec}$$

Emittance Preservation:

$$\varepsilon = \frac{\sigma^2}{w}\left[\frac{\gamma m c \omega_p}{2eE_o \sin\phi}\right]^{-1/2} \Rightarrow \sigma_{inj} < 60\,\mu$$

Cumulative electron energy spectrum with Mars laser

Laser Plasma Group

- Data acquired over many laser shots
- Spectrum falls rapidly on both sides of injection energy
- Electrons observed out to 30 MeV

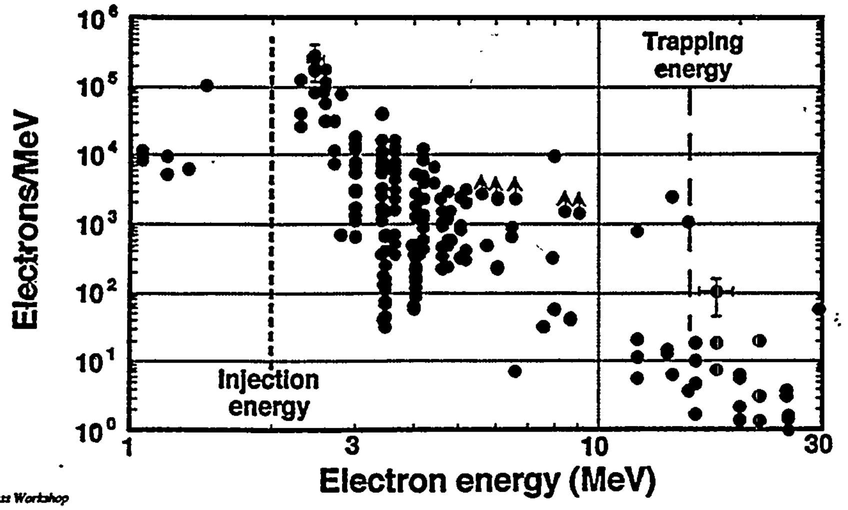

1996 Snowmass Workshop

Histogram Summary

100 MeV params, 15MeV injection

$\varepsilon_O = 3\,\pi$ mm mrad (Z_o=1.2cm, w_o=185μm)

$\varepsilon_N = 7\,\pi$ mm mrad

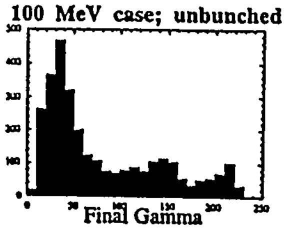

$\varepsilon_N = 10\,\pi$ mm mrad

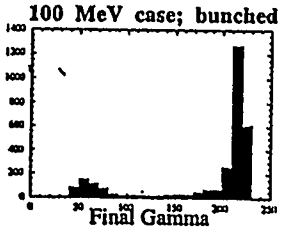

1 GeV parameters, 10MeV injection

$\varepsilon_O = 10\,\pi$ mm mrad (Zo=3.1cm, w_o=100μm)

$\varepsilon_N = 28\,\pi$ mm mrad

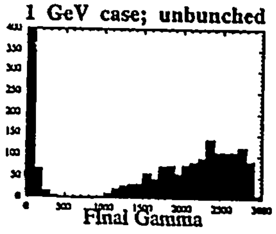

$\varepsilon_N = 15\,\pi$ mm mrad

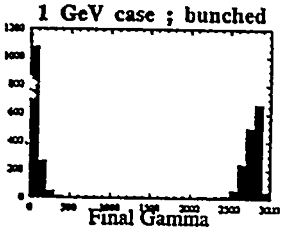

Goals of the new UCLA experiment

- Inject a large # of particles
  Accelerate $\Theta(10^8)$
- 100 MeV – via laser upgrade (rise time, L_R)
- Preliminary staging / beam quality
  experiments (pre-buncher)

One GeV in a single stage

UCLA Laser Plasma Group

Laser wavelengths	1.05 and 1.06 μm
Plasma density	10^{17} cm^{-3}
Plasma source	Multiphoton ionization
Laser pulse length	4 ps (2 ps)
Laser power	14 TW (22TW)
Laser spot size (2σ)	200 μm
Raleigh range ($2Z_o$)	6.2 cm
Plasma homogeneity	few %
Peak plasma wave amplitude	$E/E_{max} \approx 0.5$
Peak accelerating gradient	160 MeV/cm
Final energy	1 GeV

$\frac{V_0}{c} = .23$

Requirements of Accelerators (continue) :

Limits to Energy Gain :

(1) Dephasing :

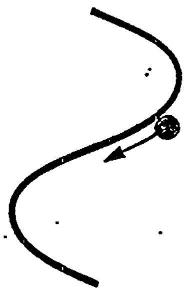

$$E_{max} \sim 1GeV \cdot \frac{10^{18}}{n_0} \cdot \left(\frac{1\mu m}{\lambda_0}\right)^2 \cdot \frac{\delta n}{n_0}$$

(2) Diffraction :

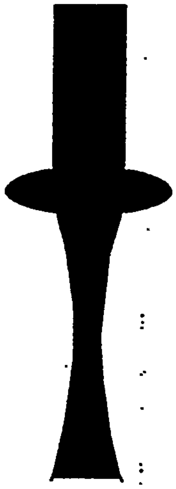

$$E_{max} \sim 1GeV \cdot \sqrt{\frac{n_0}{10^{18}}} \cdot \left(\frac{\sigma}{30\mu m}\right)^2 \cdot \frac{1\mu m}{\lambda_0} \cdot \frac{\delta n}{n_0}$$

Example : UCLA experiment

$n_0 \approx 10^{16}$, $\frac{\delta n}{n_0} \approx 0.3$, $\lambda_0 \approx 10\mu m$, $\sigma \approx 50\mu m$

Dephasing limit ⇒ 300MeV

Diffraction limit ⇒ 30MeV

Diffraction may be overcome in a channel

(Durfee & Milchberg '93)

(Sprangle, et al.)
(Katsouleas, et al.)

Laser propagated 23 Rayleigh lengths in plasma:

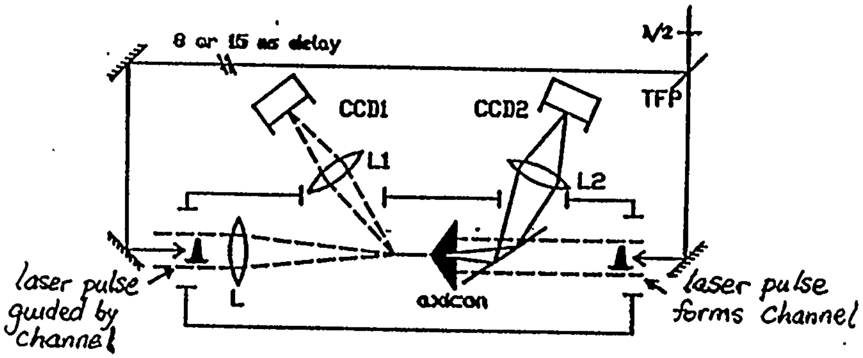

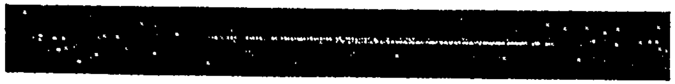

axicon alone

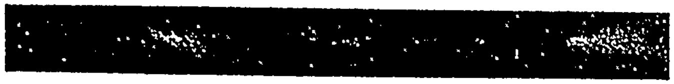

guided beam

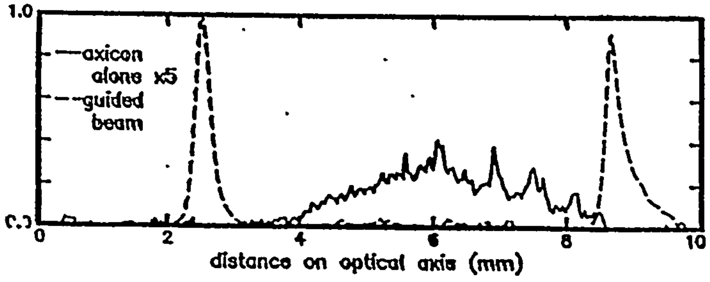

Why is $\Delta\gamma$ > Dephasing Limit ?

Linear Theory

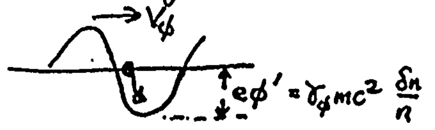

$$\Delta\gamma' = \frac{e\phi'}{mc^2} = \gamma_\phi \frac{\delta n}{n}$$

$$\Delta\gamma \approx 2\gamma_\phi \Delta\gamma' = 2\epsilon\gamma_\phi^2$$

$$\gamma_\phi^2 = \frac{\omega_0^2}{\omega_p^2} = 70 \quad \epsilon \approx \frac{1}{2} \quad \Delta\gamma \approx 70$$

(35 MeV)

Errors:

1. $\Delta\gamma' \sim 2\frac{\phi'}{mc^2}$ TOP TO BOTTOM $\times 2$

   BEAM'S SELF-CURRENT ⇒ LARGE ENOUGH FOCUSING TO OVERCOME PLASMA WAVE DE-FOCUS FROM TOP TO MI

2. Non-linear group velocity of laser

$$\gamma_\phi^2 = \frac{\omega_0^2}{\omega_p^2} \times \frac{\gamma_{osc}+1}{2} = \frac{\omega_0^2}{\omega_p^2} \times 1.6$$

3. $\frac{e\phi}{mc^2} > \epsilon$

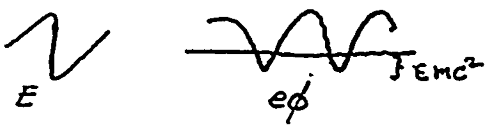

Hollow Plasma Channel :

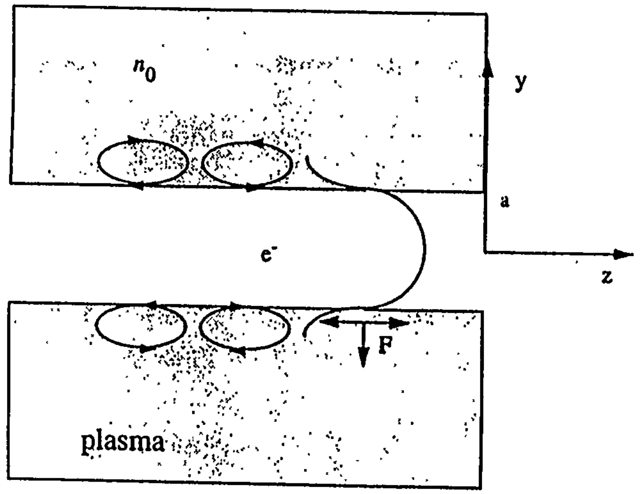

(1) Hollow channel confines laser like an optical fiber.

(2) Wakefield is excited at channel edge. (A surface plasma wave)

(3) Fringe fields reach to the center of the channel and can accelerate particles.

(4) Accelerating field - uniform across the channel
Radial force - small
⇒ Good beam quality

Comparison of Laser Wakefield in Homogeneous and Hollow channel plasma

Laser :

wavelength :	$1.0\mu m$	Energy :	7.5 J
pulse length (FWHM) :	0.25 ps	spot size :	$41\mu m$
Rayleigh length :	$0.5cm$		

Wakefield :

	Homogeneous plasma	Hollow channel plasma
density (n_0) :	$5\times10^{16}cm^{-3}$	$6.7\times10^{16}cm^{-3}$
channel radius :	—	$20.5\mu m$ ($k_pa = 1$)
Wake amplitude ($eE_z/m\omega_pc$) :	0.34	0.17
Gradient (eE_{Max}) :	$7.3GeV/m$	$4.3GeV/m$
Acceleration length :	$0.5cm$	$1m$
Energy Gain :	$37MeV$	$4.3GeV$

Channel Formation :

(A) Acoustic wave :

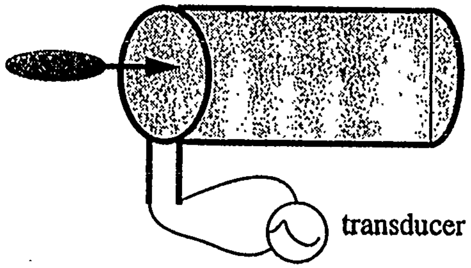

(B) Foam target :

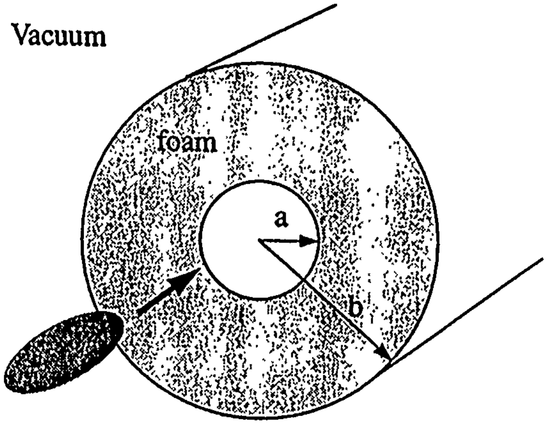

Channel Formation (continued) :

(C) Laser blow out :

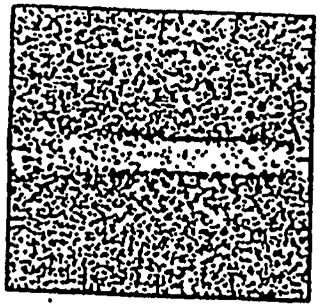

(D) Blocked Gas Jet

Side view :

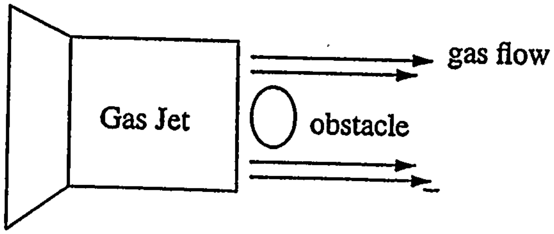

Top view :

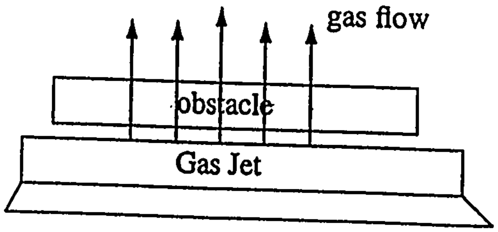

III. WAKEFIELD ACCELERATORS

ANL Dielectric Wakefield Experiment

(Gai, et al, PRL 61, 2756, '88)

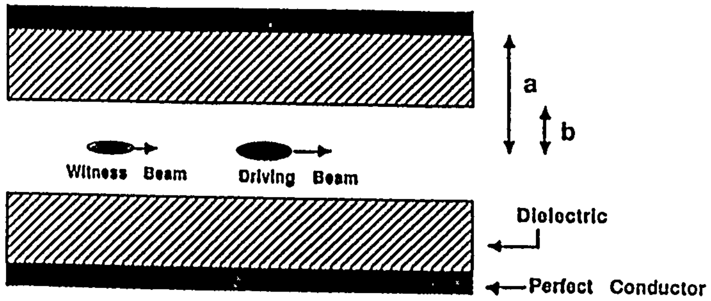

parameters
    beam: Q=2nC length=25ps radius~3mm

    dielectric: length=50cm a=1.3cm b=0.6cm ε~6

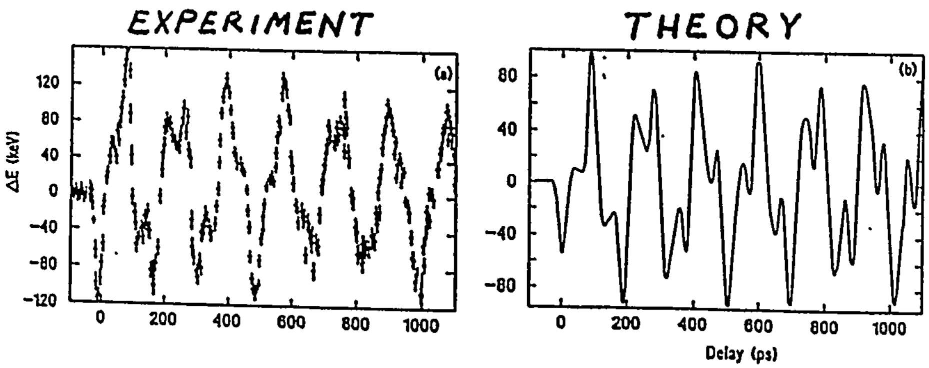

Measured Gradient = .3-.5 MeV/m

Plasma Wakefields at ANL

parameters
    hollow cathode discharge plasma: $n=10^{13}\ cm^{-3}$
        length=30cm
    beam: $n=5 \times 10^{11} cm^{-3}$

Experiment
(Rosenzweig, et al '89)

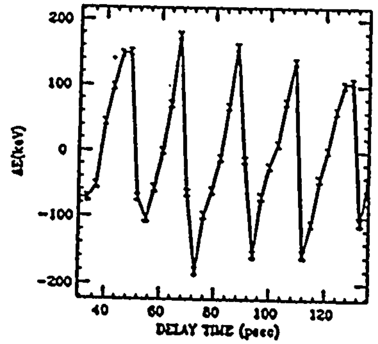

2-D PIC Simulation
(UCLA group, '89)

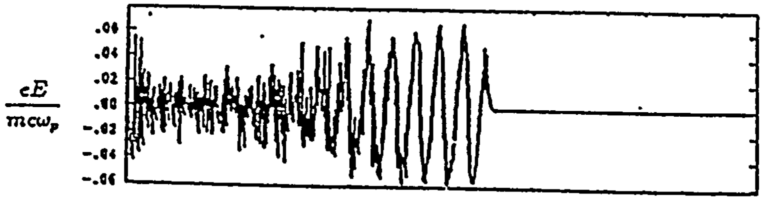

Measured Gradient ~ 5MeV/m

Improved designs are being explored

ANL
UCLA
Novosibirsk
U.Tokyo

1. Ramped drive beam current => Large transformer ratio (R = $\delta\gamma_{trailer}/\gamma_{driver}$):

(Bane, et al., '85)

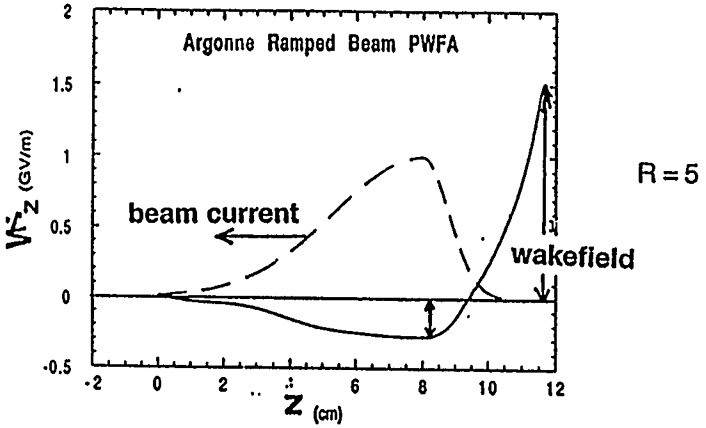

2. Dense drive beams ($n_{beam} > n_{plasma}$)
=> Good wake structure for beam quality:

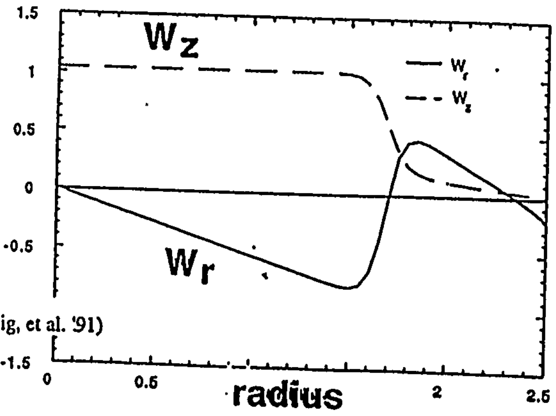

(Rosenzweig, et al. '91)

Wakes in the Blowout Regime

Rosenzweig et al ('91)

what is blowout?

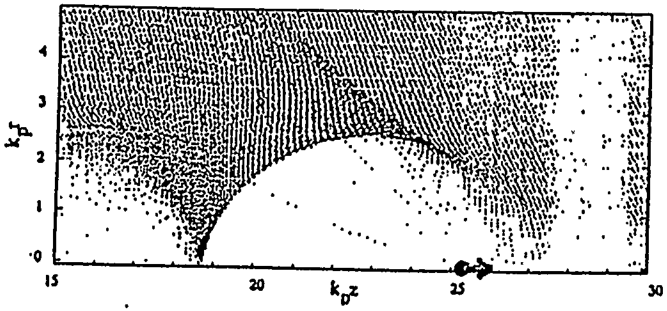

All plasma electrons are expelled from a channel

When plasma is driven by a superintense

laser: $V_{osc}/c > 1$

particle beam: $n_b > n_o$

why is it important?

largest gradients $E > \sqrt{n_o}$ V/cm

linear focusing

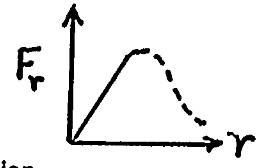

uniform acceleration

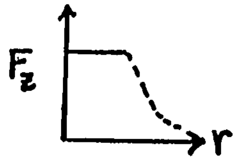

Key step in assessing plasmas for TeV colliders is a 1 GeV plasma accelerator test

Proposal: A 1 GeV Plasma Acceleration
test at SLAC-FFTB

Blowout Occurs Similarly For Preformed And Tunnel Ionized Plasmas

X-Y Phase Space $\sigma > c/\omega_p$

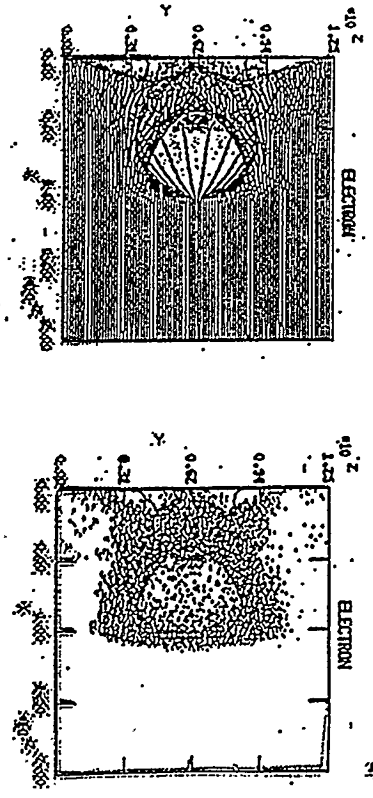

Contour Plots of Accelerating Field
peak field given by 1-D scaling

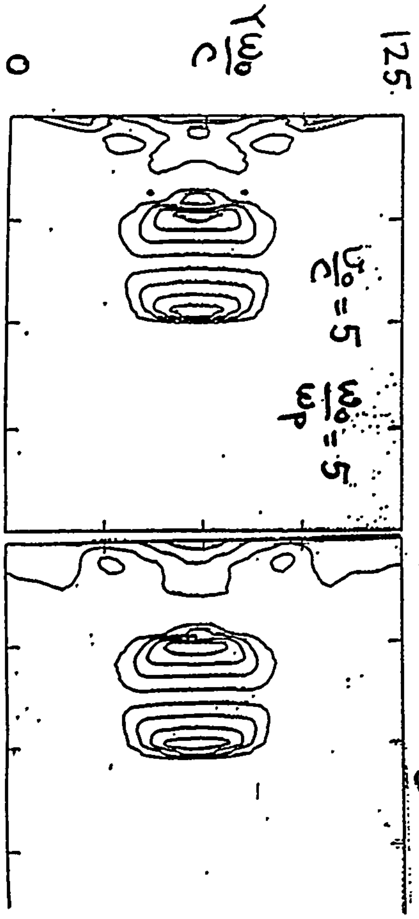

SLC Wakefield in a Plasma

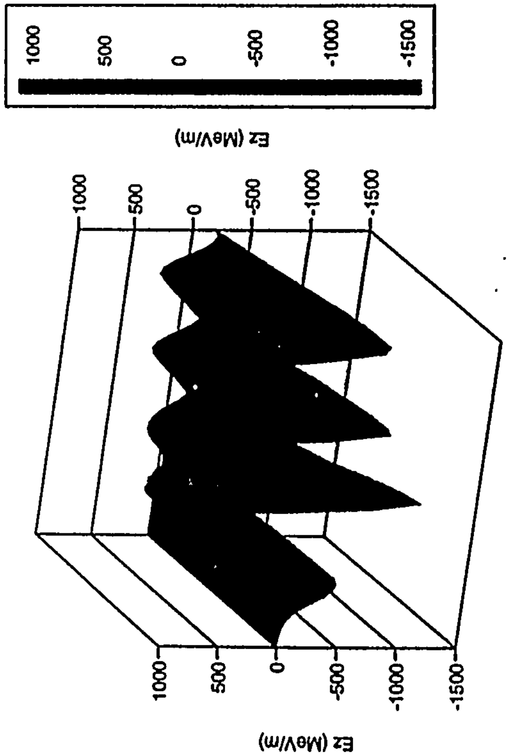

Beam: N=4e10, σz=0.47mm, σr=100μm, (γ=1e5)
Plasma: no=2.5e14, (nb/no =3.7, λp=2.1mm)

Why a 1 GeV Plasma Experiment at SLAC?

SLC 50 GeV Driver is IDEAL!

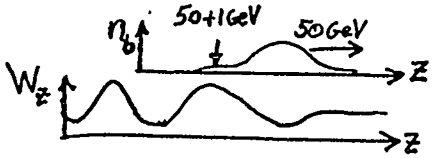

$\sigma_z = 0.47mm$ @ 6.4nCoul

$W_z \sim GeV/m$

High $\gamma \Rightarrow$

$\left.\begin{array}{l}\text{no instability}\\ \text{no pump depletion}\\ \text{no distortion}\\ \text{no diffraction}\\ \text{no phase slippage}\end{array}\right\}$ CLEAN TEST

Beam vs. Laser

- efficiency
- long "Rayleigh" length $\beta \equiv \frac{\sigma^2}{\varepsilon} >> L_R \equiv \frac{\pi\sigma^2}{\lambda}$
- physics issues - electron hose - can test by raising n_o
- technology issues - pulse shaping

Test Blowout Regime $(n_b > n_o)$

Extend from mm to m scales

Collect Richter Bet!

Applications of Plasma Accelerators

★ Plasma Wigglers

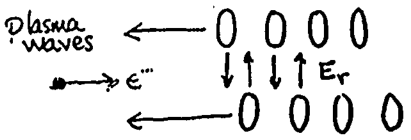

$E_r \Rightarrow a_w \sim .1-1 \quad (B_{eff} = 30T)$

$\lambda_w \sim 100\mu$

★ Ultra-fast chemistry

plasma accel. pulse structure :

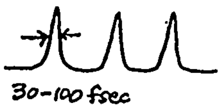

pump/probe w/ e⁻ or X-rays

★ Hi Power IR Sources (GWatt @ THz)

PBWA + DC B-Field ⇒ propagating Cerenkov wake

$$\frac{E_{e.m.}}{E_{e.s.}} \approx \frac{\omega_c}{\omega_p}$$

★ Novel Photon Accelerators (light sources)

"Designer light"

★ In Situ Applications – e.g., metal fatigue

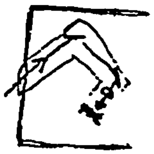

★ Lower Cost M

LOW COST HADRON CIRCULAR COLLIDERS

per... Tieman ...!!

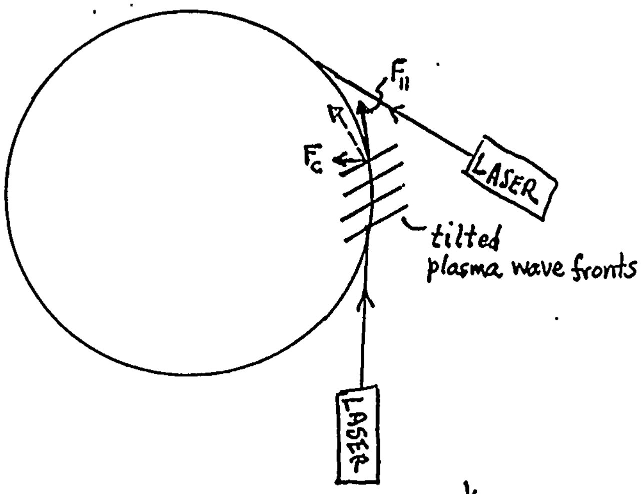

1. Tilt fronts w/ optical mixing:

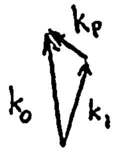

2. F_c component – $eE_c \sim 10 GeV/m \equiv 30 Tesla$

   ⇒ magnetless

3. $r = \frac{V_\perp}{\omega_{c\,eff}} \approx \underline{1 km} \times \frac{U}{5 TeV} \times \frac{10 GeV/m}{eE_c}$

   ⇒ Compact

4. Facilitates laser staging

Comparison of Laser Instabilities

initial pulse

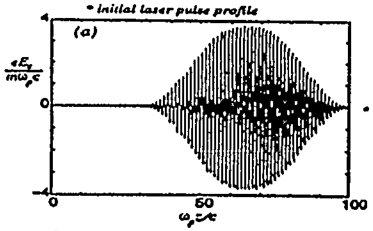

• Initial laser pulse profile

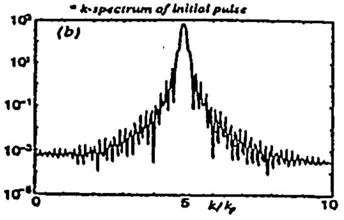

• k-spectrum of initial pulse

Homogeneous plasma

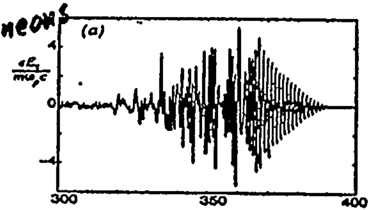

• Pulse profile in 1-D homogeneous plasma at t=300

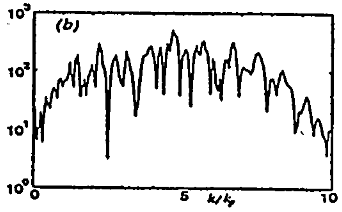

• k-spectrum of the pulse in 1-D homo. plasma at t=300

parabolic channel

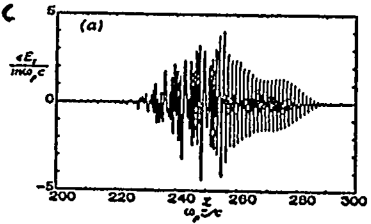

• Pulse profile in parabolic channel plasma at t=200

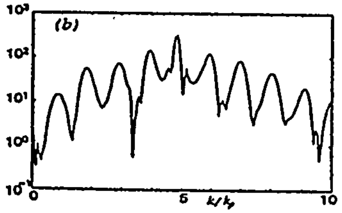

• k-spectrum of the pulse in parabolic channel plasma at t=200

Hollow channel

$K_pa=1$

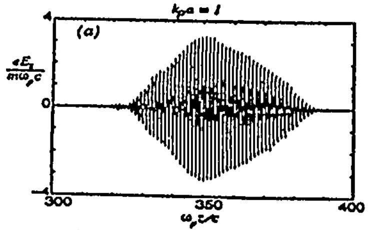

• Pulse profile in hollow channel plasma at t=300

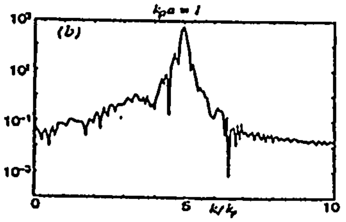

• k-spectrum of the pulse in hollow channel plasma at t=300

PLASMA WAKEFIELD ACCELERATOR (PWFA) & SYSTEM DESIGNS

A. Skrinsky, Novosibirsk

PLASMA WAKE FIELD ACCELERATION

A.Skrinsky
INP, Novosibirsk

August 1996

To shrink the scale (and cost) of HEP facilities, we need advances in acceleration physics and in technologies.

Speaking over-simplistic, this way includes higher magnetic fields for cyclic accelerators and higher accelerating gradients for linear accelerators.

I intend to discuss the second line - and a single particular approach - only.

Additionally to VLEPP project, we have discussed at that time the possibility to use the huge energy, stored at existing and - especially - planned proton beams of super-accelerators. This option was called the "proton klystron", and the way was shown to excite by such beams 1 cm wave length range linear accelerating structures up to the limit of accelerating gradients.

Since that time, in our Lab and in many other labs this level was proved practical for GHz (cm wave) range, short pulse, normal conducting accelerator structures - just have enough RF power and use proper technology for structures!

The ways to extreme gradients.

Suggestions and attempts to higher gradients were made by many people through decades and for many times.

For us, at Novosibirsk, the main drive in the direction, since 1960s, was *Linear Collider* hope for hundreds of GeV electron-positron collisions.

When we first presented publicly (1978) the VLEPP project, which incorporates 100 MeV/m accelerating gradient for normal conducting short pulse linacs, this "high gradients problem" was considered by the majority as a main one in linear collider business (even obstacle!).

100 MeV/m is close to the ultimate limit for metallic accelerating structures: electric field at the surface is additionally few times higher, and it starts to produce “cold currents”, and occasional discharges degrade the surface instead of improving it (training process fails).

Hence, to reach much higher gradients we need to shift from the solid materials shaping of electromagnetic fields to plasma based structures.

(At really high electric fields, the exposed surface in any case converts into something close to plasma.)

inside plasma, plasma electrons and electro-magnetic fields oscillate coherently and the limit for maximal electric field looks differently. More or less universal limit (if we intend to use efficient “resonant excitation”) can be evaluated such a way:

electric field energy density should be less than (rest frame) energy density of plasma electrons.

In equations:

$$\frac{E_{ultim}^2}{8\pi}=n_e m\, c^2 \ ,$$

hence

$$E_{ultim}=\sqrt{4\pi\cdot n_e m c^2}=\sqrt{\frac{4\pi\cdot e^2}{r_e}\cdot n_e}$$

Later on, we shall feel additionally the “naturality” of this limit.

To reach very high electric fields (in vacuum or in plasma) - as a stand-alone goal - is not a problem at all. For example, while passing a laser focus - hence, at the micron distances - particles are accelerated at GeV/cm rate.

But it is not an "accelerator", which is:
a device to accelerate particles at macroscopic distances up to "unlimited" energy!

To organize high accelerating (longitudinal, parallel to beam particles velocity!) electric field in plasma devices of very different type, number of approaches were proposed (through decades!) and are under consideration now. Among them:

- smokotron;
- laser beam excitation;
- two laser beams beat-wave acceleration;
- plasma wake field acceleration (PWFA).

For the first three approaches I myself, very personally, do not see any way to reach high gradients and perfect phasing at long distances for arranging a "high energy accelerator".

The last one - PWFA - up to now was based, in considerations and experiments, on driver electron beams of modest energy - the most natural transition from electron beams of klystrons, exciting usual linacs, or "two-beam accelerator"

But, as we shall see later, it is not the way to extreme gradients: we need to use as <u>high energy - *"rigid"* - beams</u>, as economically possible.

This is the way:
to overcome plasma and beam-plasma (local) instabilities
and
<u>to replace efficiently the accuracy of solid surfaces</u>, which shape fields in usual linacs.

And a very important component of the whole approach is to arrange a proper focusing channel to keep the beams "very carefully" aligned.

* Plasma (hydrogen!) should be arranged in advance - driver beam ionization is too weak.

And ionization should be close to 100%.

* In good approximation, we can take in to account plasma electrons mobility only - ions (protons) can be considered as of infinite mass.

The electron temperature can be considered negligibly low.

* For the very beginning, driver and accelerating beams can be considered “absolutely rigid”.

plasma oscillations.

The phase velocity along the axis is determined by velocity of driver beam - in all our considerations it will be the light velocity “c” (all the beams are ultra-relativistic).

Local resonant frequency of plasma oscillations is the “electron plasma frequency”:

$$\omega_e = \sqrt{\frac{4\pi e^2 n_e}{m_e}}$$

As was shown above, the limiting accelerating field in plasma - under resonant excitation - is

$$E_{ultim} = \sqrt{\frac{4\pi e^2}{r_e} \cdot n_e} \quad .$$

The real accelerating field should be, say, 3 times lower. Hence, the plasma density needed to achieve accelerating field should be not less than

$$n_e = \frac{9}{4\pi} \cdot \frac{r_e}{e^2} \cdot E_{acc}^2 \quad .$$

Hence, to achieve $1\ \mathrm{GeV/m}$ we need to use plasma density 10^{15}.

Let us evaluate number of particles in the driver bunch, which we need for to excite in plasma accelerating field needed. We assume, the driver beam radius is about the minimal radius of plasma oscillations, which is

$$\lambda/2\pi.$$

The balance of energies - the stored in "plasma tube" per 1 cm and lost by driver particles at this distance:

$$\frac{E^2}{8\pi} \cdot \pi \cdot \frac{\lambda^2}{(2\pi)^2} \cdot 2 = e\, N_{need} E \cdot \frac{1}{2} \quad .$$

Hence

$$N_{need} = \frac{1}{8\pi} \cdot \frac{E \lambda^2}{e} \quad .$$

For 1 GeV/m=30 kGs and 1 mm wave length:

$$N_{need} = 1 \cdot 10^{10}$$

(of course, the estimate assumes all the particles passing in a proper oscillation phase!).

[illegible] bunch particles among the microbunches, separated by distance λ. This train, while traveling at speed of light, should excite plasma oscillations resonantly.

Hence:

$$\lambda = \frac{2\pi \cdot c}{\omega_e} = \sqrt{\frac{\pi}{r_e n_e}} \ .$$

For plasma density

$\underline{1*10^{15}}$,

it is equal to

$\underline{\lambda = 1\text{mm}}$.

bunch train of length = 1 cm, the mean current in the train would be

$$\frac{1\cdot 10^{10}\cdot 3\cdot 10^{10}}{6\cdot 10^{18}} = 50\,A \ .$$

The necessary peak current in micro-bunches should be 10 to 15 times higher.

This estimate is correct for linear regime, when accelerating field is very much lower then the ultimate one; if it comes closer - the efficiency is going down.

The structure and properties of PWFA oscillations.

Results of computer simulation of PWFA process.
(axial symmetry!)

* Compensating plasma current & stability of driver-to-plasma interaction (still axially symmetric).

* Stability of high amplitude free plasma oscillations?

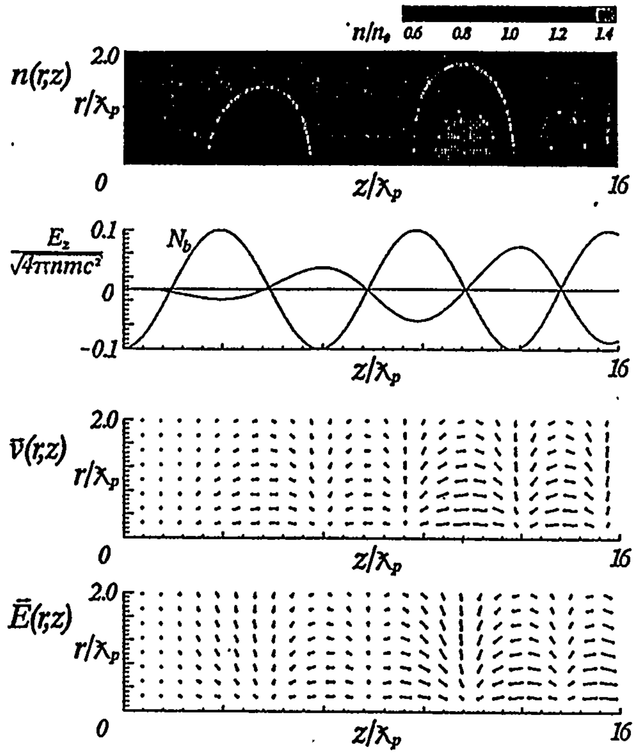

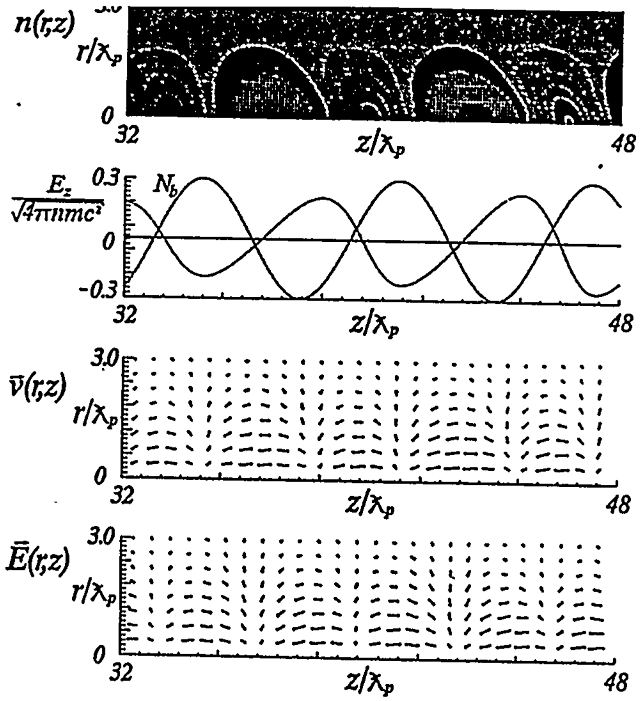

A very important problem is related to the transversal forces acting on driver and accelerated beam particles in the excited plasma channel.

These (de)focusing forces are strongly dependent on the phase of plasma oscillations; they are minimal ("almost zero") at maximums of accelerating (decelerating) fields and grow at channel radius up to fraction (around one third) of longitudinal force maximum.

And, of course, its action is higher if the beam energy is lower.

This problem makes life a lot more difficult and, in particular, pushes to higher driver beam energy.

The maximum of radial force, acting on driver or accelerating beam particles (the sum of eE_{rad} and eB_{az}) is proportional to the electric longitudinal field - accelerating or decelerating. In linear regime of plasma oscillation, this effective transversal field is about 1/3 of the longitudinal field maximum. The rise radius is about $\lambda/2\pi$ (excited plasma channel assumed to be minimal!).

So, the equation for transversal single particle motion will be:

$$\frac{d^2}{ds^2}r+\frac{2\pi}{3}\cdot\frac{gradE_{eV}\,\kappa}{E_{eV}\lambda}r=0\ ,$$

where s is the longitudinal coordinate, and κ is the fraction of transversal force maximum at the current phase.

If the coefficient is negative (defocusing), the accelerating field about 1 GeV/m leads to incurable defocusing and, hence, to the loss of particles at this phases - no matter how strong, albeit realizable, is the external focusing system.

If this coefficient is positive, effective "plasma beta-function" will be

$$\beta_{pl}=\sqrt{\frac{3}{2\pi}\cdot\frac{E_{eV}\cdot\lambda}{gradE_{eV}\cdot\kappa}}\ .$$

To direct the drive beam properly, we need appropriate external focusing - by quadrupoles (the drive beam energy is high!).

So, drive micro-bunches - #2 (and even the tail of the first one!) and the following - as well, as witness bunch, travel under combined action of the homogeneous (for given slice) focusing of plasma oscillations and alternating focusing of quadrupoles.

Hence, we need to take care on stability of incoherent transversal oscillations of all the useful particles of very different energy and at very different plasma focusing - in a time!

This incoherent problem might be analyzed more or less safely just straightforward, and we shall play with while considering "practical" application options.

following particles to the same channel as preceding ones.

less clear at the moment is coherent stability problem in its accelerator-type part.

(Partial) help to prevent coherent instability comes from the fact , that all the bunches, coherent oscillations of which are under action of coherent oscillations of preceding bunches via plasma excitation, have at "any" moment different frequencies.

It is not excluded, that to prevent coherent instability, the external focusing should be strong enough (at least, not negligibly weak), in comparison to plasma focusing.

This stability problem can be analyzed, in reasonable approximation, by considering (or simulating) the action of the oscillations of each particular slice of the beams (moving under influence of the plasma fields excited by preceding slices) on the following slices oscillations.

In first approximation, each slice response function is to be calculated in unperturbed plasma and dipole part of forces (= forces at the beams axis) should be included in oscillations equation of following slices and micro-bunches.

If these oscillations would tend to the smaller and smaller amplitudes - the process is stable.

“Transversal” micro-bunching.

To find the way to introduce a proper micro-bunch structure in the bunches of driver beam (and, also, to prepare a proper witness micro-bunch to be accelerated) is one of the crucial elements of the whole approach.

The problem looks non-trivial, because we need 0.1 mm range length of each “very high” energy micro-bunch and its positioning should take into account plasma frequency variation (non-linear regime!), hence - micro-bunches should be non-equidistant.

This positioning should prevent parts of driver micro-bunches from entering the accelerating phases, what would “eat” the plasma oscillations energy instead of to pump it in, and the plasma defocusing phases.

The phase structure of accelerating and transversal forces is quite complicated.

At the initial, linear stage, their maximums are shifted almost at $\pi/2$.

At the developed stage, which is of the main interest, this shift is going down and it is necessary to play with driver and witness bunches phasing and lengths - and even with their angular spreads! - very carefully.

Proper matching of emittances (in size and shape) in every slice of driver and witness - is the must.

to use very low emittance beams
and “transversal cutting”.

The general layout looks as following.

At some part of the (future driver) beam channel with high beta value, say, in vertical direction, we arrange local RF structure acting on the traveling bunch with the vertical force linearly depending on the position along the bunch (zero action at the bunch center).

The resulting transversal vertical momentum should be much higher than due-to-emittance internal momenta in the bunch.

Upon passing long enough free space, the different head-to-tail constituents of each bunch will be positioned differently in vertical direction.

which are transparent but the other parts of the target destroy beam components completely.

At the same place a vertically focusing lens is placed (focal length is 2 times smaller than RF section-to-target distance).

At the same distance after the target the same RF structure is located, which compensates the vertical momenta of bunch components.

Hence, at the exit of this section, each driver beam bunch will be transformed in a series of micro-bunches - properly (longitudinally) shaped and properly positioned!

Placing appropriate thin foils in the slots, we can give each micro-bunch a proper angular spread (and even proper dependence of this spread on slice position along the micro-bunch) - in correspondence to the future local plasma focusing (local beta-value).

Sequential acceleration.

It is very interesting and important to find the way to reach much higher energies than the driver energy. This energy multiplying is very similar to the usual high voltage klystron driving of linac and to the "two-beam accelerator".

The goal looks this way:
using sequence of N driver bunches of energy E_{dr}
to reach almost proportionally higher energy

$$E_{acc} ==> N^*E_{dr} .$$

The way in principle looks quite obvious. One driver (micro-bunched) bunch, via plasma excitation, transfers energy to the accelerating - "witness" - bunch up to exhaustion; then the next bunch shall replace the previous one. Then the process shall be repeated N times.

The problem is - how to arrange this process in a most efficient and cost effective way.

Pre-microbunching.

To maximize excitation efficiency of driver beam, it is worth to try to shift as much particles as possible in the useful phases of each driver bunch, using RF energy modulation - prior the final micro-bunching via sliced target.

The natural option is to use few wigs IFEL at this wave length. It can easily give energy modulation higher than energy spread in such a high quality beam. The use of following dispersive section will transform energy modulation along the bunch into density modulation of the same wave length.

But let us do not forget - we need non-equidistant micro-bunching. Hence, the transversal cutting shall follow!

we can use a single straight tunnel to host all the beams.

If we use a helix of actual curvature radius R and outer radius r, the delay dL of a train at the helix length L_0 will be:

$$dL = \frac{L_0 \cdot r}{2 \cdot R} .$$

At the length of drive energy loss, which is about

$$L_0 = \frac{E_{dr}}{gradE_{dr}} ,$$

the delay should be equal to distance between the train bunches dL_b.

The helix curvature is defined by driver energy E_{dr}, also.

Hence, the requirement for "r" will be:

$$r = 2 \cdot \frac{E_{acc}}{B_{hel}} \cdot \delta L_b \qquad \text{(CGSE)}$$

where B_{hel} is the helix magnetic field used.

As you can see straightforward, this requirement is quite moderate, at least, formally.

<u>All the tolerances are to be analyzed carefully!</u>

When such a helical delay-line is arranged along the whole linear accelerator, the driver beam, bunch by bunch, transfers the energy to the same witness micro-bunch under acceleration.

The influence of particles-plasma scattering.

Not similar to usual accelerators, at PWFA the accelerating channel is filled with plasma particles. Hence, additionally to the coherent fields, beams particles are influenced by pair collisions, also. To minimize this influence, it is worth to use "100% ionized" hydrogen plasma, which consists of protons and electrons, and we shall have in mind this option, only. There are several collision processes of possible importance.

a). Nuclear interaction of hadrons of driver/accelerating beams.

The hadron-hadron total cross-section does not exceed

$$\sigma_{hadron} \leq 1 \cdot 10^{-25} cm^{-2} .$$

Hence, the probability to loose particles in 1 km path (in our consideration - per 1 TeV) is less then

$$\sigma_{hadron} \cdot n_{pl} \cdot 1km = 10^{-25} \cdot 10^{15} \cdot 10^{5} = 10^{-5}$$

So. it is not a limitation in "any" practical conditions.

b. The bremstrahlung cross-section even for electrons and positrons is of the same order, so, it is also not important.

Hence, the single scattering processes are not a problem.

The most important process - if we do care of emittance growth - is the Coulomb multiple scattering for accelerating particles. The advance of mean square of the particle angle due to this process is

$$\delta\theta_0^2 = \frac{200}{E_{MeV}^2} \cdot \frac{x}{X_0} = 5 \cdot 10^{-24} \cdot \frac{\delta L_{acc} n_{pl}}{E_{MeV}^2} ,$$

where x/X_0 is fraction of radiation length passed. Consequently, emittance differential will be

$$\delta\varepsilon_{acc} = 5 \cdot 10^{-24} \cdot \frac{n_{pl}}{gradE} \cdot \frac{\beta_{acc}(E)}{E^2} \cdot \delta(E) ,$$

where E - the current energy in MeV; hydrogen plasma is considered of 100% ionization.

growth will be

$$\delta\varepsilon_{fin} = 5 \cdot 10^{-24} \cdot \frac{n_{pl}}{E_{fin}\,\mathrm{grad}E} \cdot \frac{\beta_{acc}(E)}{E} \cdot \delta E \,.$$

The final emittance, if influenced by in-plasma collisions only, will make up:

$$\varepsilon_{fin} = 5 \cdot 10^{-24} \frac{n_{pl}}{E_{fin}\,\mathrm{grad}E} \cdot \int_{E_{in}}^{E_{fin}} \frac{\beta_{acc}(E)}{E} \cdot dE \,.$$

This result shows the most important limitation for electron-positron collider based on ultimate gradient PWFA.

Plasma along the whole pass of beams should be prepared in advance. As was mentioned above, to minimize the plasma binary collisions influence, especially on accelerating particles for collider use, the plasma is worth to be hydrogen one, and ionization degree should be close to 100%. Let us evaluate the energy needed for such arrangement:

$$E_{source} = \pi R_{pl}^2 n_{pl} L_{acc} \eta^{-1} E_{ion} \,,$$

where

E_{ion} - ionization potential,

η - efficiency of energy transfer from ionization source,

R_{pl} - radius of plasma channel.

Example:

$$E_{source} = \pi \cdot (1mm)^2 \cdot 10^{15} \cdot 10^5 \cdot 30 \cdot 10eV \cdot 2 \cdot 10^{-19} = 200\frac{J}{Te}$$

At repetition rate "f", the power for ionization will be proportional to "f".

But the most difficult plasma related requirement seems to be the necessity to keep its density constant along the whole accelerator - in 1% range (to keep full accel-eraing gradient at the chosen witness phase).

PWFA based electron-positron collider.

Let us discuss in a very preliminary way the linear collider option, based on PWFA approach.

The general layout, I have in mind in discussion, looks a following way:

An 11 GeV electron "driver" accelerator produces trains of bunches.

Each train contains 100 of bunches, 1 cm , 10^{11} in each bunch, separated by 1 or several of the accelerator wave lengths.

Each bunch, by the using of pre-buncher and transversal cutter, is transformed in to 10 microbunches of 0.2 mm full length.

The last bunch of a train (#100) is directed in to plasma of appropriate density; all the others enter in to spiral isochronous delay-line. Traveling through plasma with properly arranged quadrupole lenses structure inside - 0.5 cm long lenses per each 10 cm, the fine-cutted bunch excites acceleration field of 1 GeV per meter.

accelerate electrons. full plasma wave length to accelerate positrons), the driver bunch is followed by “witness” (bunch under acceleration)

the 0.03 mm short bunch of the “same” energy,
containing up to $2*10^9$ particles.

Upon the last micro-bunch of driver bunch #100 - passing 10 m section - is decelerated to 1 GeV, the bunch is carefully replaced by the previous one - #99, and the microbunch under acceleration, of energy +10 GeV, is positioned the same way relative to the new bunch.

This cycle is repeated for 100 times bringing the witness to 1 TeV - upon 1 km of acceleration.

Such super-cycles are repeated at 10 kHz frequency.

The same arrangements and processing are made for a counter beam.

So, we got a 1 TeV + 1 TeV collider (electron-positron, photon-photon, electron-photon).

Using formulae on plasma scattering and plasma focusing for more or less optimized conditions, we can show, that geometrical emittance at 1 TeV of

$$10^{-13}\ \text{cm*rad}$$

is reachable

(but don’t forget of very tough tolerances!).

So, there is a hope to get 10^{34} cm^{-2}sec^{-1} with driver beams of several tens of MW mean power, at least, for photon-photon and photon electron collisions.

Novosibirsk PWFA experiment in preparation.

The test experiment is in preparation at INP to study PWFA, with hope to reach more than 0.5 GeV/m at the several tens of cm (see the figures).

Unfortunately, in spite of the most of the components are in place or prepared, we lack of financial support for, and the progress is very slow.

Maybe, somebody would get interested to enter this activity and would find - very modest - money?

Proton klystron.

With the use of intense and very low emittance beams of super-high energy proton storage rings/colliders, it looks feasible to drive PWFA linacs for to reach:
energy multiplication for ejected protons
(at least, for neutrino experiments);

to accelerate

- pre-cooled antiprotons;
- electrons, positrons;
- ionizationally pre-cooled muons;
- pions;
- and even kaons (relativistic kaons live long enough to be accelerated by energy gradients close to 1 GeV/m).

Layout of VEPP2M-PWFA complex

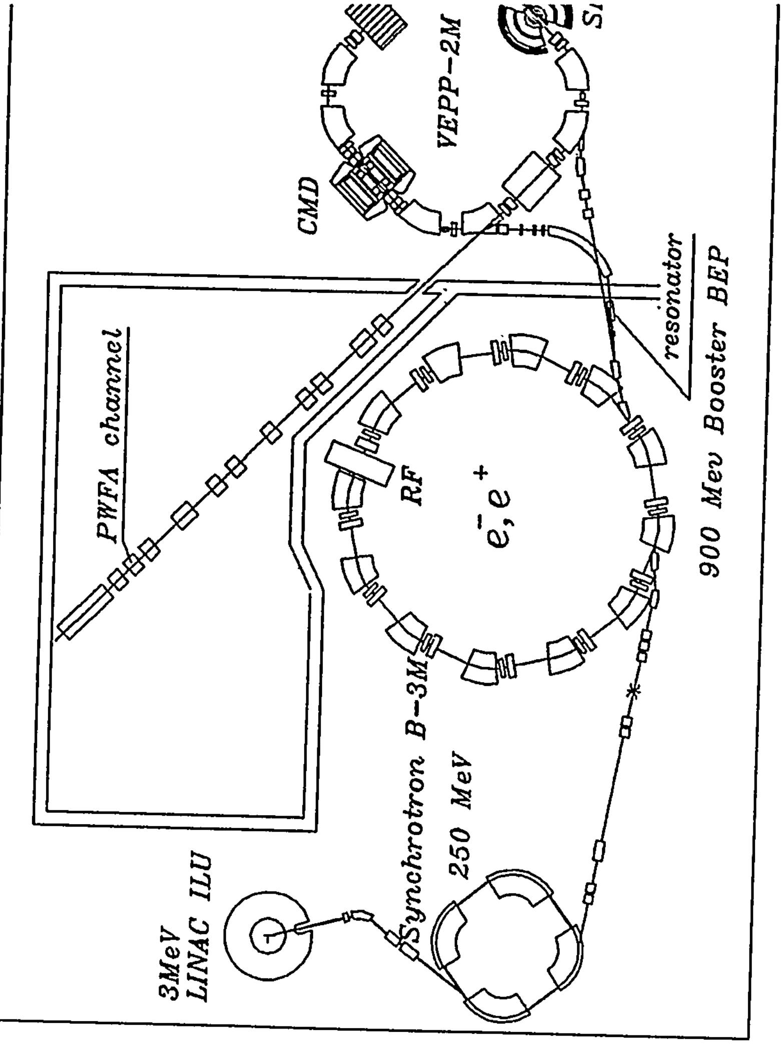

LAYOUT OF VEPP-2 EXPERIMENT

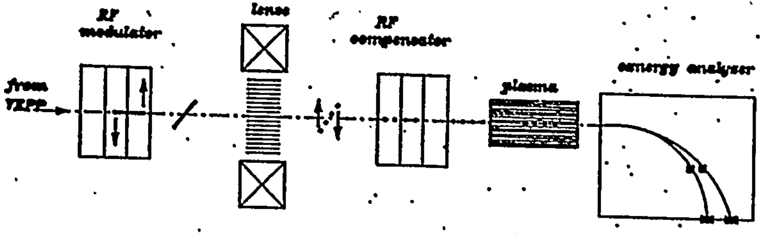

RF wavelength: .... 10 cm

RF power: .... 200 kW ($Q=10^4$)

Number of resonant cavities: .... 2 × 10

Plasma density: .... $10^{14} \div 5 \cdot 10^{16}$ cm^{-3}

Plasma length: .... up to 1 m

Total length: .... 10 m

DESIGNED BEAM PARAMETERS

Number of particles: 10^{12} $\sigma_z = 3$ cm

Particle energy: 700 MeV $\sigma_R = 0.1$ cm

<u>Open questions</u> ("non-technical"):

Stability of high amplitude free plasma oscillations.

"Drive beam - plasma" and "witness-plasma" coherent stability.

Phasing related structures and tolerances.

**Low emittance high intensity witness acceleration.
(But now, this problem seems to be solved and not
very damaging)**

PROGRESS IN LASER PLASMA EXPERIMENTS

C. Joshi, UCLA

OPEN WAVEGUIDE STRUCTURE FOR LASER ACCELERATION

R. Pantel, SLAC

The Open Waveguide Structure

R. H. Pantell

Stanford University, Stanford CA 94305

A. Structure design

An aperture array is used to establish a low-loss waveguide mode with an on-axis E_z.

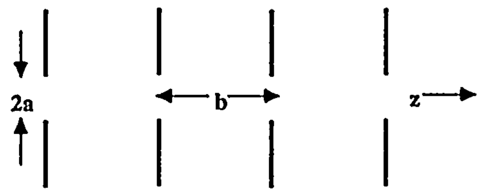

The modes are the same as those of a Fabry-Perot interferometer with planar mirrors.

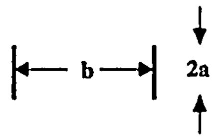

As an accelerator:

Simple structure with reasonable dimensions.

The mode has a strong component of on-axis, longitudinal field with small phase slippage per unit length.

B. Interactions to consider

1. Structure + laser : modes, material damage

2. Laser + electron beam : energy gradient, energy transfer

3. Electron beam + structure : beam loading, loss, material damage

C. Structure + laser

1. Methods for analysis:
    - a. Iteration
        - Huygen's principle
        - Kirchoff integral
    - Advantages
        - Gives transient behavior
        - Doesn't use much memory
    - b. Eigenvalue problem
    - Advantages
        - Fast solution
        - Gives complex eigenvalues

2. Mode excitation

Use lowest order Hermite-Gaussian mode with an on-axis, longitudinal field component

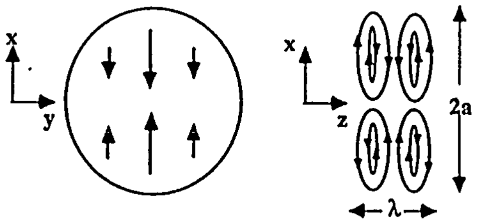

$$E(x,y) = E_0 \frac{x}{w} \exp\left[- \frac{(x^2 + y^2)^2}{w^2} \right]$$

3. Eigenfunction solution

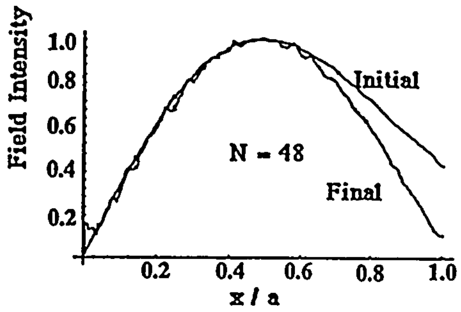

N = Fresnel Number = $\frac{a^2}{\lambda b}$

w = 0.7 a

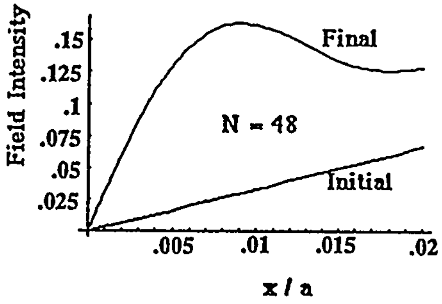

Note the increase in the gradient of the field at x = 0. Significance: 120 times the power is required in the Hermite-Gaussian mode to obtain comparable energy transfer.

4. Longitudinal field, E_Z

Obtained from $\nabla \cdot E = 0$

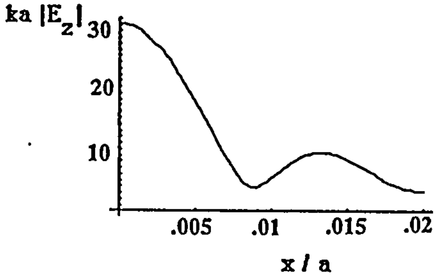

The ordinate scale is for a transverse field that is normalized to unity at its maximum value.

5. A radially polarized mode

Obtained by adding a y-polarized mode to the x-polarized mode.

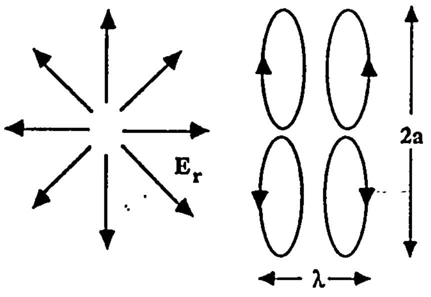

$| E_Z |$ increases by $\sqrt{2}$ relative to the linearly polarized mode for a specified power.

---

6. Structure dimensions

$$\frac{a^2}{\lambda} = 1.6 \text{ X } 10^2 \frac{P^{.5}}{|E_z|}$$

$$b = \frac{a^2}{N\lambda}$$

For $P = 25$ TW $|E_Z| = 1.5$ GV/m
$N = 48$ $\lambda = 1.0\ \mu$m

then $2a = 1.4$ mm $b = 1.2$ cm

Note: The structure dimensions are 10^3 to 10^4 times the wavelength

7. Structure modification

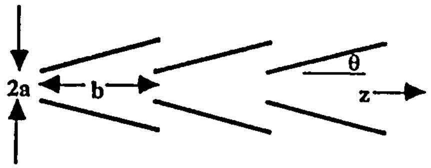

Modes are unaltered for Θ » $\Theta_d \approx 0.6\ \lambda/a$
The modification increases damage threshold and reduces loss.

For w = 0.6 a a = 0.7 mm P = 25 TW
Θ = 10 mrad, the fluence on the first aperture at r = a is 0.55 J/cm^2, and this drops to 0.1 J/cm^2 after the second aperture.
Damage threshold is 2 J/cm^2. Cone damage is important only if holes are drilled.

D. Laser + electron beam

1. Energy transfer and gradient using the eigenfunction (i.e., steady-state) solution.

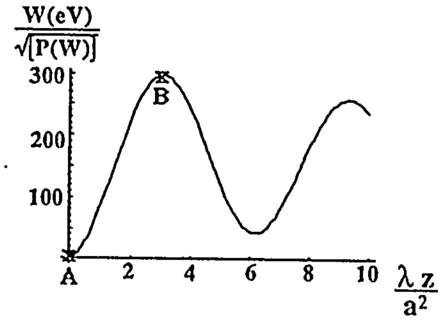

180^0 phase slippage from Point A to Point B.

It is taken that the beam energy ≥ 10 GV so that the contribution to the phase slippage from (ωt - kz) may be neglected over the relevant distance.

Terminating the structure at Point B, where the field is zero at the phase position of the electron, results in wave diffraction and very little additional energy transfer

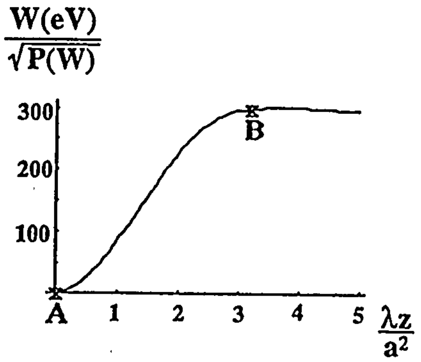

For P = 25TW,   L = 1.5m (at Point B)
and ΔW = 1.5GeV
(0.2 Gev is lost in reaching Point A)

Laser power depletion due to energy transfer to the electron beam is not included. If every RF bucket is filled, this assumption is reasonable if the number of electrons per bunch is $< 10^8$.

2. Transient solution

The steady-state is not reached in 1.5m (125 apertures). This is due to the presence of higher order modes which have not died out in this distance.

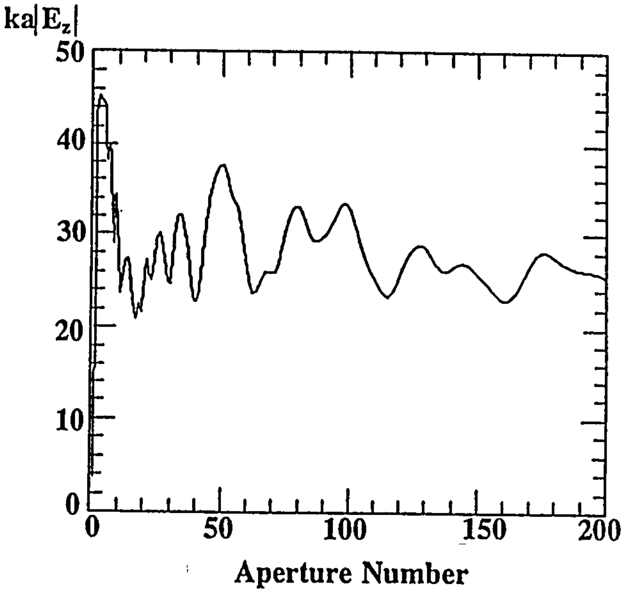

For the transient solution, with P = 25TW,
L = 1.6m and ΔW = 1.6GV

E. Electron beam + structure

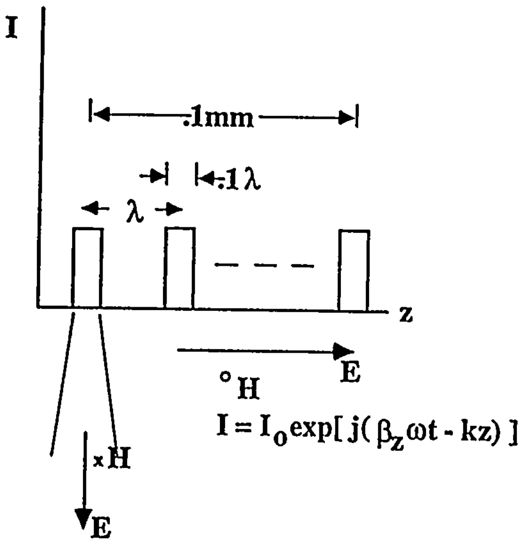

1. Radiation from the bunched beam into the waveguide mode. (Beam loading.) This limits the number of electrons per microbunch to ≈ 10^8.

2. Self-field from the microbunch. This can cause material damage and electron energy loss. Not significant at 10^8 electrons per bunch.

F. Summary

The open waveguide has the following features:

1. Simple structure with reasonable dimensions
2. Interaction is in vacuum
3. The gradient is high
4. Electron motion is linear
5. There is high energy transfer per stage
For $P = 25TW$, $\Delta W = 1.6GeV$ in 1.6m

G. Future directions

1. Combine multiple stages
2. Excite with a Fabry Perot interferometer
3. Consider finite electron beam radius:
    a. Effect on emittance
    b. Effect on energy spread
4. Consider effect of finite cone thickness

Acknowledgement

The author is grateful to John Lewellen and Dr. Joseph Feinstein for their important contributions.

LASER PLASMA PHYSICS ISSUES

E. Esarey, Naval Res. Lab.

Laser Pulse Propagation
in
Plasma-Based Accelerators

NRL

Eric Esarey
P. Sprangle, J. Krall, and A. Ting
Beam Physics Branch, Plasma Physics Division
Naval Research Laboratory, Washington, DC, 20375

Supported by DOE and ONR

Refs.
Special Issue, IEEE Trans Plasma Sci 24 (1996)

Outline

NRL

- Laser-Plasma Accelerators
- Diffraction Limitations
- Optical Guiding
    - Relativistic Optical Guiding
    - Preformed Plasma Channels
    - Plasma Channel Wakes
    - Curved Plasma Channels
- Self-Modulated LWFA
- Hose-Modulation Instability
- Experiments

Ultrahigh Power Lasers

- Laser power: P_0

$$P_0\,[\mathrm{GW}] = 21.5\,(a_0 r_L/\lambda)^2$$

r_L = laser spot size

- Laser strength parameter: a_0

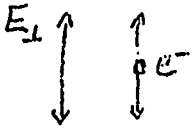

$$a_0 = eA_\perp/m_e c^2 = \gamma v_\perp/c$$

- Laser intensity: I_0

$$a_0 \simeq 10^{-9}\lambda[\mu\mathrm{m}]\left(I_0[\mathrm{W/cm^2}]\right)^{1/2}$$

- For $\lambda \simeq 1\ \mu$m

$$\boxed{I_0 \gtrsim 10^{18}\ \mathrm{W/cm^2} \Rightarrow a_0 \gtrsim 1}$$

⇒ highly relativistic quiver motion

- Compact lasers technology*

$\gtrsim 10^{18}$ W/cm^2, $\gtrsim 10$ TW, $\gtrsim 10$ J, $\lesssim 1$ ps
NRL 5 TW 2 J 0.4 ps

*Chirped Pulse Amplification, G. Mourou et al. (1985)

T^3 (Table Top Terawatt) Lasers

Laser Wakefield Accelerator (LWFA): Motivation

- Laser driven accelerators:

Transverse laser field, E_0

⇒ Axial accelerating field, E_z

- Laser field

$$E_0\,[\mathrm{TV/m}] \simeq 3\times 10^{-9} I_0^{1/2}\left[\mathrm{W/cm^2}\right].$$

- Compact lasers

$$\lambda \sim 1\ \mu\mathrm{m},\quad I_0 \sim 10^{18}\ \mathrm{W/cm^2}$$

$$\underline{\Rightarrow E_0 \gtrsim 3\ \mathrm{TV/m}}$$

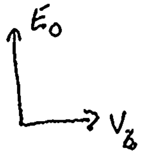

- Axial Acceleration Field (LWFA), $a_0 > 1$

$$E_z/E_0 \simeq 2\times 10^{-11}\lambda\,[\mu\mathrm{m}]\,n_0^{1/2}\,[\mathrm{cm^{-3}}]$$

- Example

$$n_0 = 10^{18}\ \mathrm{cm^{-3}},\quad \lambda = 1\ \mu\mathrm{m},\quad I_0 = 10^{18}\ \mathrm{W/cm^2}$$

$$\boxed{E_z/E_0 = 2\%,\quad E_z = 60\ \mathrm{GV/m}}$$

(Conventional Accelerators: $E_z \sim 60$ MV/m)

LASER WAKEFIELD ACCELERATOR

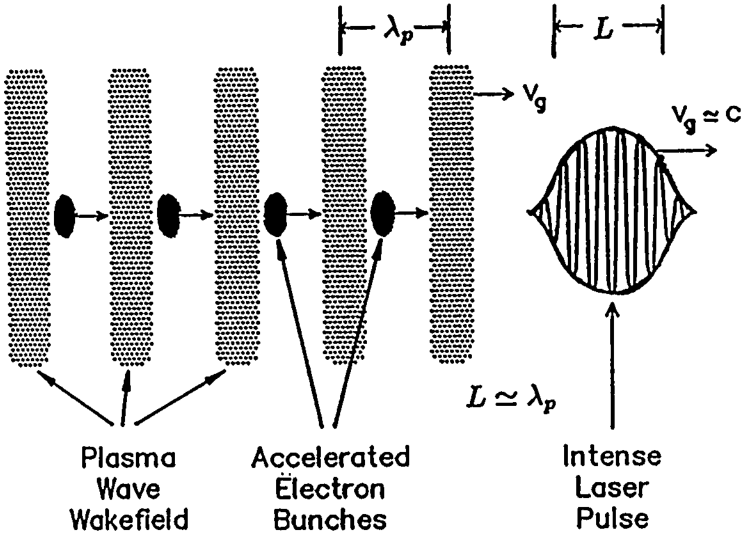

Requires: $\underline{L \simeq \lambda_p} = 2\pi c/\omega_p \sim n_p^{-1/2}$

Ponderomotive Force: $\underline{F_p \sim \nabla E^2}$

Tajima, Dawson, PRL (1979)
Sprangle, Esarey, Ting, Joyce, APL (1988)

LASER WAKEFIELD ACCELERATOR

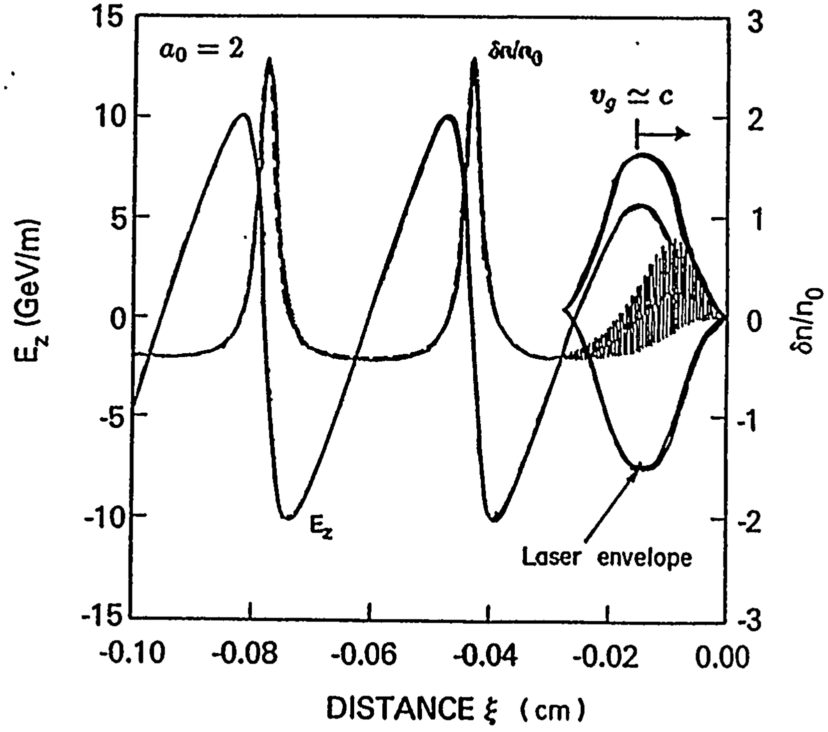

$$\xi = z - ct$$

$$L = \lambda_p \quad \Rightarrow \quad n_0 \simeq 10^{16}\ \mathrm{cm}^{-3} \quad \text{for} \quad L/c = 1\ \mathrm{ps}$$

$$E_z(V/cm) \sim n_0^{1/2}(cm^{-3}) \frac{a_0^2}{(1+a_0^2)^{1/2}}$$

Plasma-Based Accelerators

NRL

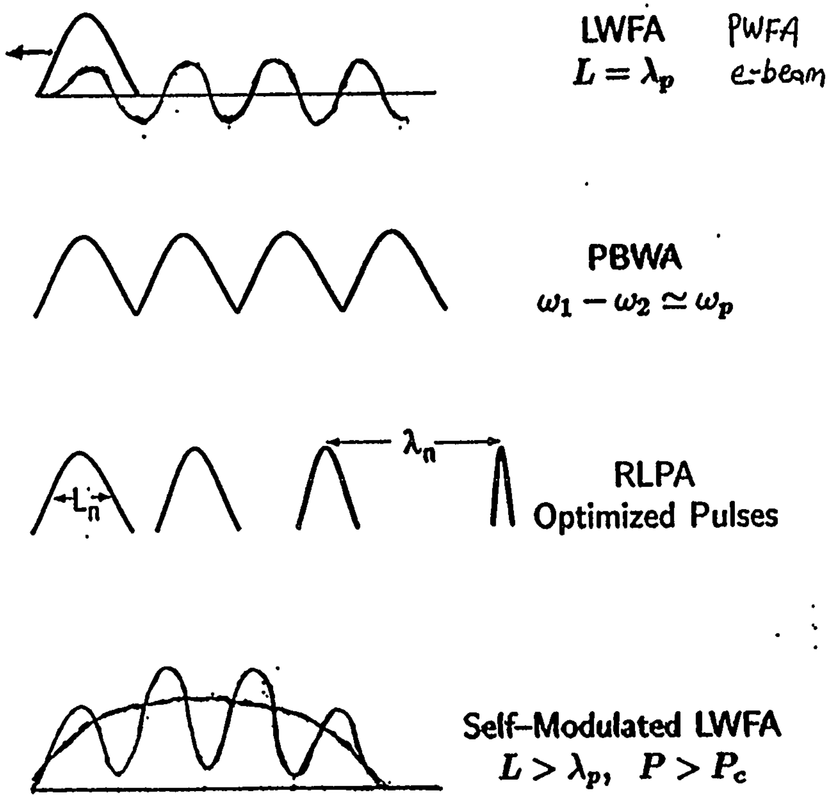

LWFA
$L = \lambda_p$

PWFA
e-beam

PBWA
$\omega_1 - \omega_2 \simeq \omega_p$

RLPA
Optimized Pulses

Self-Modulated LWFA
$L > \lambda_p, \quad P > P_c$

UCLA, NRL, Michigan, Texas
England, Japan, France, Russia

Wakefield Generation: LWFA

NRL

- Linear regime:

$$\left(\partial^2/\partial t^2 + \omega_p^2\right) E = -(mc^2/e)\omega_p^2 \nabla a^2$$

- Maximum Wakefield: $L_{laser} \simeq \lambda_p$

$a = \frac{eA}{mc^2}$

$$\boxed{E_z/E_0 \simeq a^2/(1+a^2)^{1/2}}$$

$a = \gamma v_\perp / c$

$$a^2 \simeq 0.3\lambda^2[\mu\mathrm{m}]I[10^{18}\mathrm{W/cm}^2]$$

Ex: $I = 3 \cdot 10^{18}\mathrm{W/cm}^2$, $\tau_L = 100$ fs, $n_0 = 10^{18}\mathrm{cm}^{-3}$

$$E_z \sim E_0 \sim \underline{100\ \mathrm{GV/m}}$$

- Radial profiles: $a^2(r) \rightarrow E(r)$

- Multiple pulses:

  Linear: $E_n = nE_1$

  Nonlinear: $E_n > nE_1$

∘ Single Short Pulse → Avoids Instabilities

Laser Wakefield Accelerator (LWFA)

NRL

- Theory
  - Wake–plasmon accelerator
    - Tajima, Dawson, PRL (79)
    - Mori, Masters Thesis (84)
  - Laser wakefield accelerator
    - Gorbunov, Kirsanov, JETP (87)
    - Sprangle, Esarey, Ting, Joyce, APL (88)
    - Tsytovich, DeAngelis, Bingham, CPPCF (89)
    - Katsouleas, Mori, Darrow, AIP (89)
  - Nonlinear LWFA
    - Bulanov, Kirsanov, Sakharov, JETPL (89)
    - Sprangle, Esarey, Ting, PRL (90)
    - Berezhiani, Murusidze, PLA (90)
  - 2D Nonlinear
    - Sprangle, Esarey, Krall, Joyce, PRL (92)
- Experiment
  - CPA Lasers
    - Maine, Strickland, Mourou et al., IEEE QE (88)
  - LWFA
    - Hamster et al., PRL (93): THz Radiation
    - Nakajima et al., Phys. Scr. (94): 0.7 GV/m, 7 MeV,

Laser Drivers: Pump Depletion

NRL

- Pump depletion length: L_{pd}

  [Katsouleas et al., AIP (85); Horton, Tajima, AIP (85)]

  Energy left behind in wakefield

  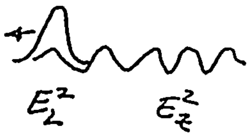

  $$E_z^2 L_{pd} \simeq E_L^2 L_{laser}$$

  LWFA: $a^2 < 1$

  $$\boxed{L_{pd} \simeq (\omega^2/\omega_p^2)\lambda_p/a^2}$$

- Electron detuning length: L_d

  $v_p = v_g$

  $$(c - v_p)L_d/c \simeq \lambda_p/2$$

  $v_g/c \approx 1 - \frac{\omega_p^2}{2\omega^2}$

  $$\boxed{L_d \simeq (\omega^2/\omega_p^2)\lambda_p}$$

- Scaling

  $$\underline{L_d < L_{pd}}, \quad a^2 < 1$$

  $$L_d, L_{pd} \sim \underline{n_0^{-3/2}}$$

  $E_z \sim n_0^{1/2}$, $\Delta W \sim \frac{1}{n_0}$

- Laser diffraction

  $$\underline{Z_R = \pi r_0^2/\lambda \ll L_d, L_{pd}}$$

Diffraction Limitations

NRL

- Acceleration distance limited by diffraction

$$L_{int} \simeq \pi Z_R, \ \ Z_R = \pi r_L^2/\lambda = \text{Rayleigh length}$$

- Single-stage energy gain: $\Delta W = eE_z L_{int}$ $(a_0 < 1)$

LWFA $$\boxed{\Delta W[\text{MeV}] = 580 \frac{\lambda}{c\tau_L} P[\text{TW}]}$$

- Example

$P = 25$ TW, $r_L = 40$ μm, $\lambda = 1$ μm, $\tau_L = 0.5$ ps

$L_{int} = 1.6$ cm, $E_z = 6$ GeV/m, $\Delta W = \underline{100 \text{ MeV}}$

$\Rightarrow$ Optical guiding is necessary

- Detuning limit (1D, $a_0 < 1$)

$$L_d \simeq \gamma_g^2 \lambda_p = (\omega^2/\omega_p^2)\lambda_p$$

LWFA $$\boxed{\Delta W[\text{GeV}] = I[\text{W/cm}^2]/n_0[\text{cm}^{-3}]}$$

- Example

$I = 10^{18}$ W/cm^2, $n_0 = 10^{16}$ cm^{-3}, $\tau_L = 1$ ps

$L_d = 25$ m, $E_z = 4$ GeV/m, $\Delta W = \underline{100 \text{ GeV}}$

Optical Guiding in Plasmas

- Index of refraction

$$\eta_R(r) = \frac{ck}{\omega} = 1 - \frac{\omega_p^2(r)}{2\omega^2} = 1 - \frac{\omega_{p0}^2}{2\omega^2}\frac{n(r)}{n_0\gamma(r)}$$

- Refractive guiding requires

$\gamma = (1+a^2)^{1/2}$

$$\partial\eta_R/\partial r < 0$$

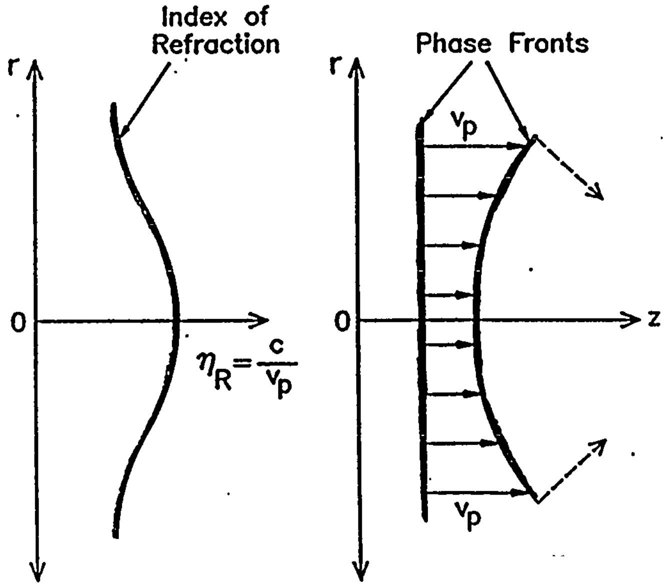

Plasma Channel Guiding

- Required depth for a parabolic channel

$$\boxed{\Delta n_0 = (\pi r_e r_L^2)^{-1}}$$

r_L = laser spot size, $r_e = 2.82 \times 10^{-13}$ cm

- Example: $r_L = 100\ \mu m \Rightarrow \Delta n_c = 10^{16}\ \mathrm{cm}^{-3}$

Plasma Density/Laser, Profile

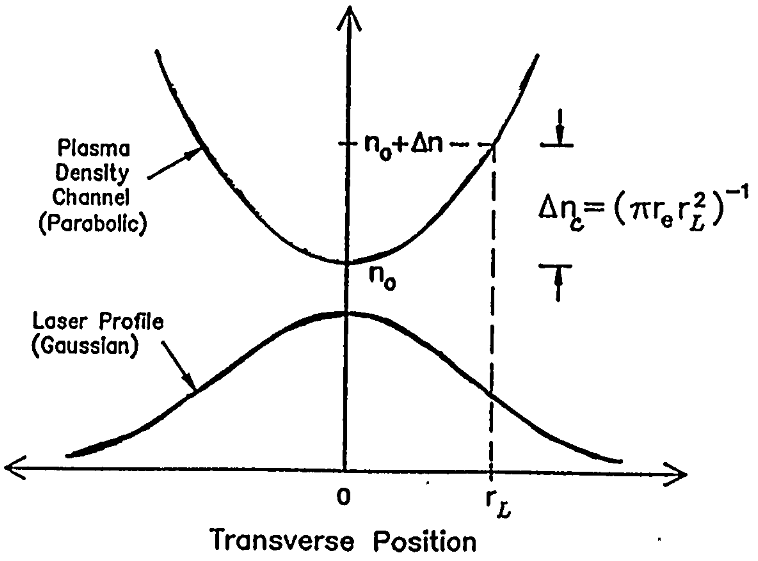

Preformed Density Channels

NRL

- Hydrodynamic expansion ionized gas/Axicon focus
  [Durfee, Milchberg, et al., PRL (93); PRE (95)] $\underline{70Z_R}$

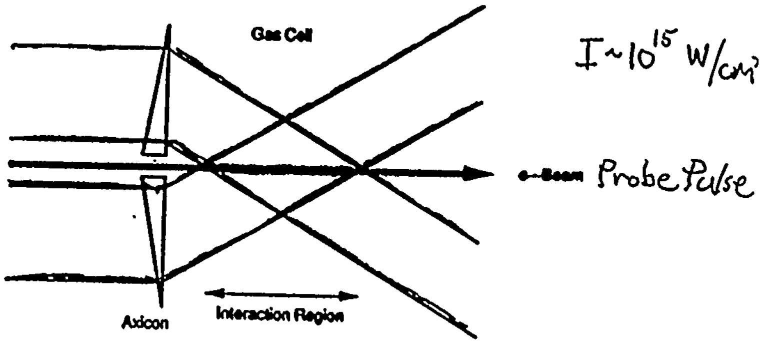

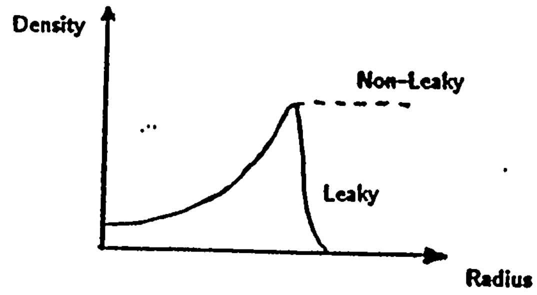

- Leaky channel stabilization [Antonsen, Mora, PRL (95)]
- Hollow channels [Chiou, Katsouleas, et al., PP (95)]
  Uniform axial field: $E_z(r) \simeq$ constant

Channel guiding - Laser intensity (a^2)

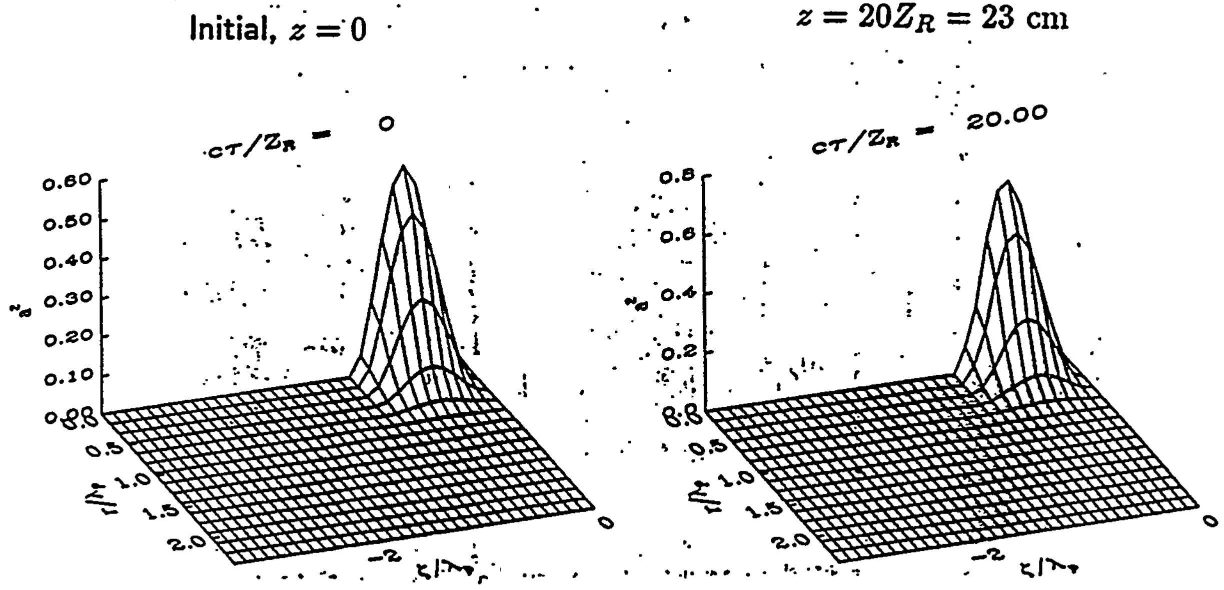

Initial, $z = 0$

$z = 20Z_R = 23$ cm

Channel-Guided LWFA: Simulations

Laser Pulse

$\lambda = 1\ \mu m$
$L = 120\ \mu m$ (400 fs)
$r_L = 60\ \mu m$
$Z_R = 1.1$ cm
$a_0 = 0.72$
$I = 7.2 \times 10^{17}$ W/cm^2
$P = 40$ TW
$W = 8$ J

Plasma

$n_0 = 7.8 \times 10^{16}$ cm^{-3}
$\lambda_p = L = 120\ \mu m$
$P \ll P_{crit} = 240$ TW

Channel

$\Delta n = 3.2 \times 10^{16}$ cm^{-3}
$\Delta n / n(r_L) = 0.4$

Channel-Guided LWFA: Acceleration

E_z on axis

$z = 20Z_R = 23$ cm

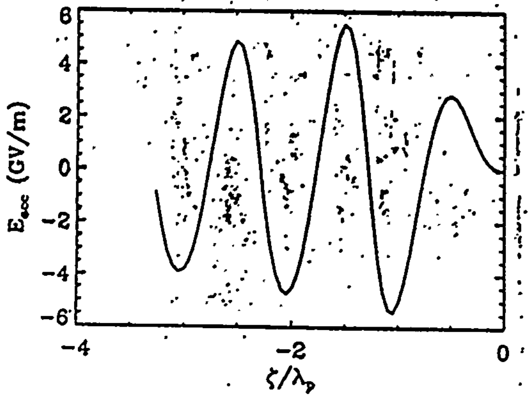

Electron energy verus time

5.25 GeV/m

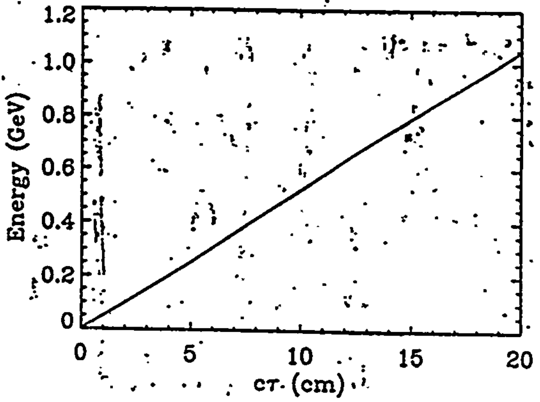

Channel guiding:

Plasma electron density

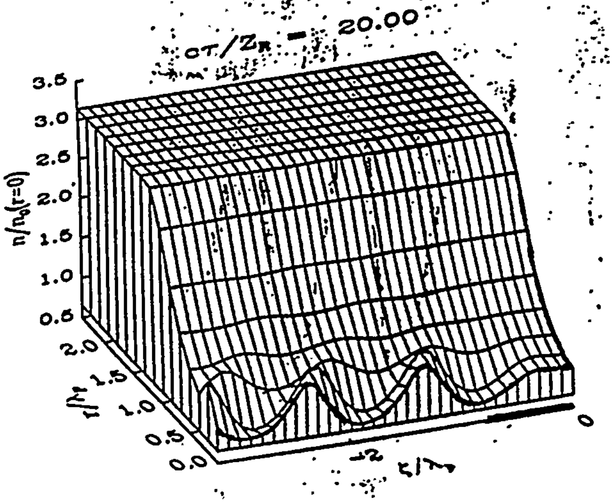

r_S versus time

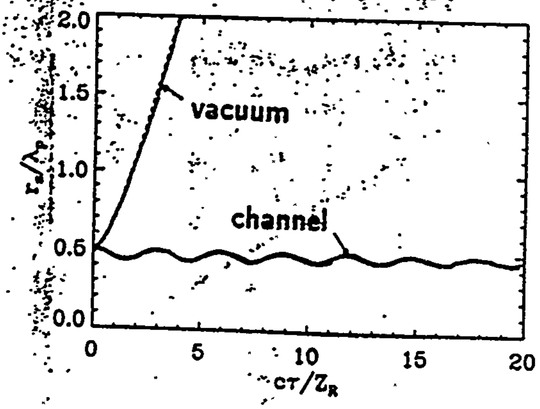

Relativistic Optical Guiding

NRL

- Standard theory [Max, Arons, Langdon, PRL (1974), Sprangle, Tang, Esarey, IEEE-PS (1987)]

$$\eta_R(r) = 1 - \frac{\omega_{p0}^2}{2\omega^2}\frac{1}{\gamma(r)}, \quad \gamma = \left(1 + a^2(r)/2\right)^{1/2}$$

- Critical laser power

$$\boxed{P \geq P_{crit}[\mathrm{GW}] \simeq 17\,(\omega/\omega_{p0})^2 \sim 1/n_0}$$

- Example

$$n_0 = 10^{18}\ \mathrm{cm}^{-3}, \ \lambda = 1\,\mu\mathrm{m} \ \Rightarrow \ P_{crit} = 20\ \mathrm{TW}$$

- Nonlinear theory [Sprangle, Esarey, Ting, PRL (1990)]

$$\eta_R(r) = 1 - \frac{\omega_{p0}^2}{2\omega^2}\frac{n(r)}{n_0\gamma(r)}$$

➡ Does not prevent short pulse diffraction, $\underline{L \lesssim \lambda_p}$

We have written a code that accelerates a distribution of non-interacting test particles in the time-resolved wakefield given by the Slow Time-Scale Model:

Test particle distribution 5.25 GeV/m

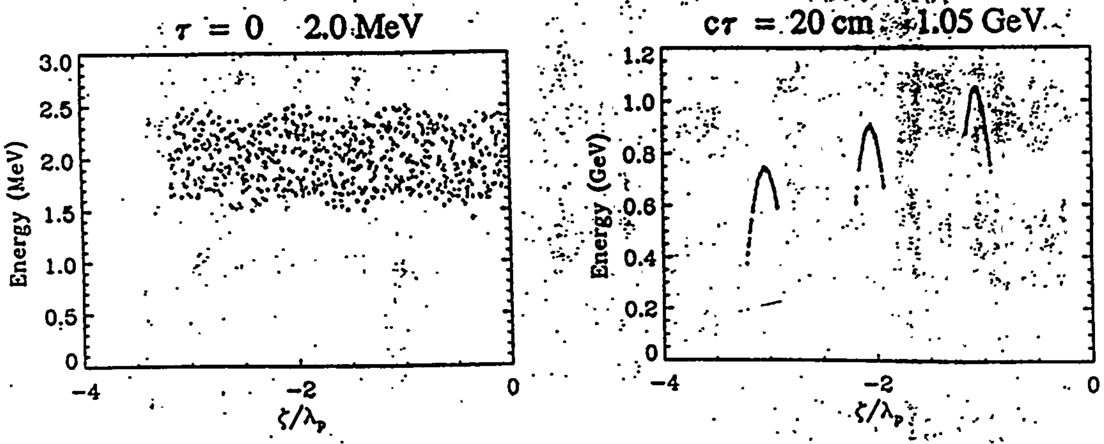

Self–Modulation of Laser Pulses

- Long pulse $L > \lambda_p$ with $P > P_{crit}$
- Wakefield self-modulates laser pulse
  [Sprangle, Esarey, Krall, Joyce, PRL (1992)]

$$\eta_R(r) = 1 - \frac{\omega_{p0}^2}{2\omega^2}\left(1 + \frac{\delta n(r)}{n_0}\cos k_p\xi\right)$$

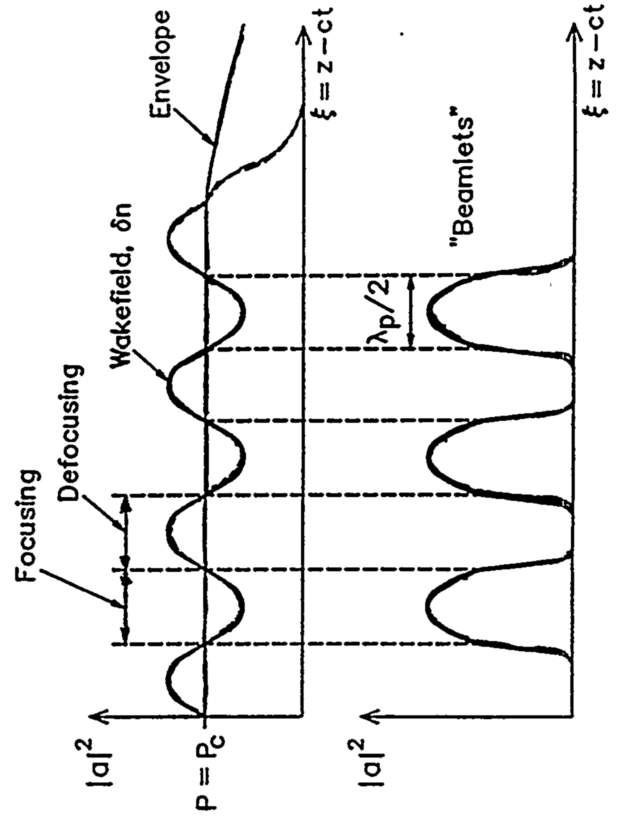

Relativistic optical guiding: long pulse,

$L = 10\lambda_p, \quad P = P_{crit}, \quad a_0 = 0.09$

$P = P_c = 17\left(\frac{\omega}{\omega_p}\right)^2$ GW

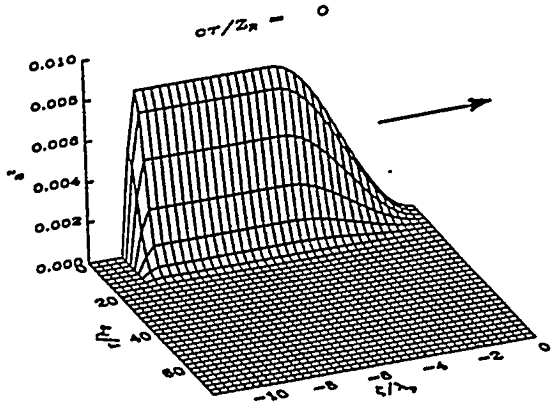

$z = 0$

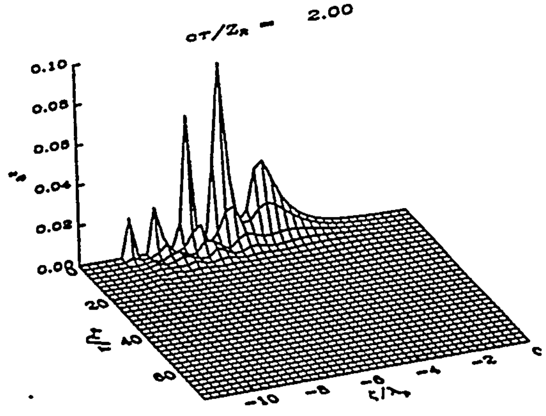

$z = 2Z_R$

Self–Modulated LWFA

NRL

- Theory
  - Self–Modulation
    - Andreev, Gorbunov, Kirsanov et al., JETPL(92)
    - Sprangle, Esarey, Krall, Joyce, PRL (92)
    - Antonsen, Mora, PRL (92)
  - Acceleration
    - Krall, Ting, Esarey, Sprangle, PRE (93)
  - Self–Modulation
    - Esarey, Krall, Sprangle, PRL (94)
    - Andreev, Kirsanov, Gorbunov, PP (95)
  - Forward Raman Scattering
    - Mori, Decker, Hinkel, Katsouleas, PRL (94)
- Experiment
  - Forward Raman Scattering
    - Joshi et al., PRL (81): 1.8 MeV
  - Self–Modulated LWFA
    - Nakajima et al., PRL (95): 30 GV/m, 18 MeV
    - Coverdale et al., PRL (95): 3 GV/m, 2 MeV
    - Rutherford: 50 GV/m; 40 MeV 100 MeV
    - Michigan
    - NRL

Self–Modulated LWFA

NRL

- Operation Regime
  - Pulse length: $L > \lambda_p \sim 1/\sqrt{n_0}$
  - Power: $P > P_{crit} \sim 1/n_0$

  For fixed L, P

  → Operate at high n_0
- Enhanced wakefields/acceleration
  - Higher densities: $E_z \sim \sqrt{n_0}$
  - Resonant excitation
  - Self–focusing: enhances $I \sim a_0^2$
  - Optical guiding: $P > P_{crit}$
- Limitations
  - Phase detuning: $\gamma_g \sim \omega/\omega_p \sim 1/\sqrt{n_0}$
  - Eventually diffracts

Krall, Ting, Esarey, Sprangle, Phys. Rev. E (1993)
Andreev, et al., JETP Lett. (1992)

Self-Modulated LWFA: Simulation Geometry

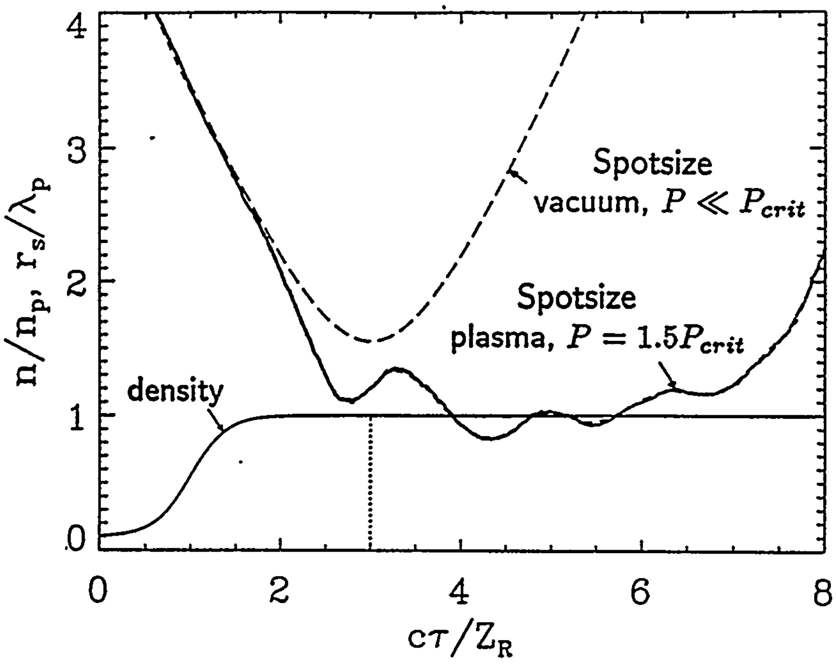

Self-Modulated LWFA: Simulations

NRL

Laser Pulse: Similar to NRL T^3 Upgrade

$\lambda = 1\ \mu m$
$L = 90\ \mu m$ (300 fs)
$r_L = 31\ \mu m$
$Z_R = 0.3$ cm
$a_0 = 0.7$
$I = 6.8 \times 10^{17}$ W/cm^2
$\underline{P = 10\ \text{TW}}$
$W = 1.5$ J

Case I: Standard LWFA

$L = \lambda_p \quad \Rightarrow \quad \underline{n_0 = 1.4 \times 10^{17}}$ cm^{-3}
$P \ll P_{crit} = 140$ TW

Case II: Self-Modulated LWFA

$P = 1.5P_{crit} \quad \Rightarrow \quad \underline{n_0 = 2.8 \times 10^{18}}$ cm^{-3}
$L > \lambda_p = 20\ \mu m$

Self–Modulated LWFA: Propagation

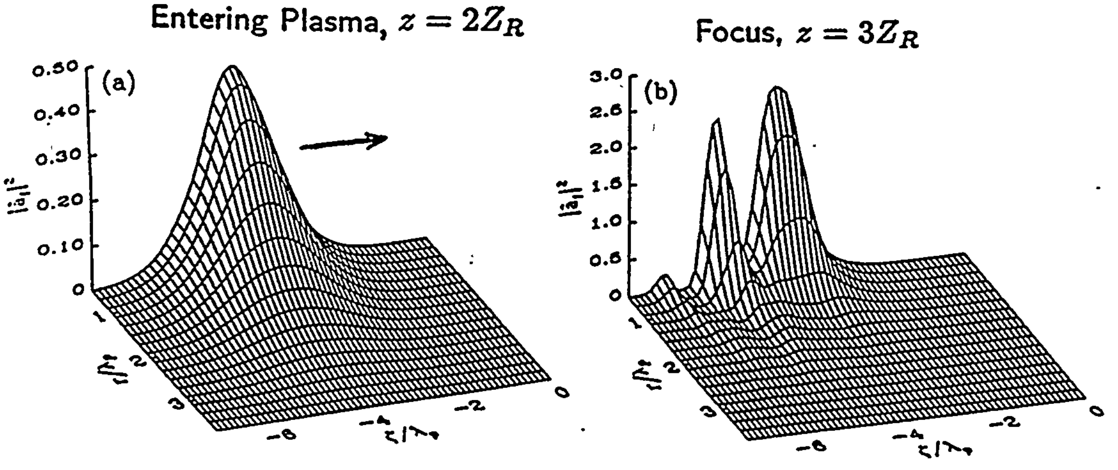

1.5 J, 150 fs, 10 TW

$P \simeq P_{crit}$, $n_e \simeq 10^{18}$ cm^{-3}

Self–Modulated LWFA: Wakefields

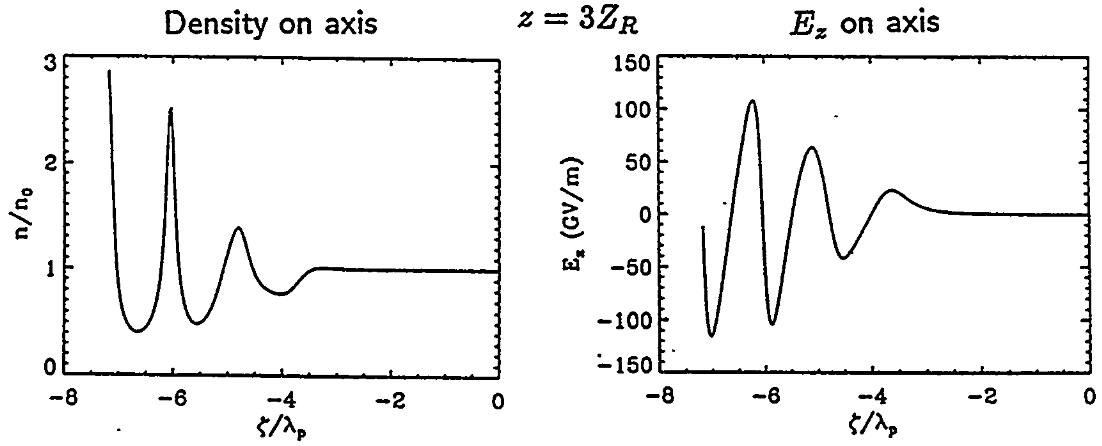

Self–Modulated LWFA: Acceleration

$E_z(r=0)$ vs. z

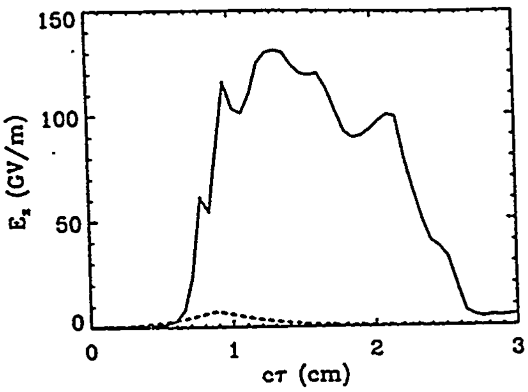

Energy vs. z

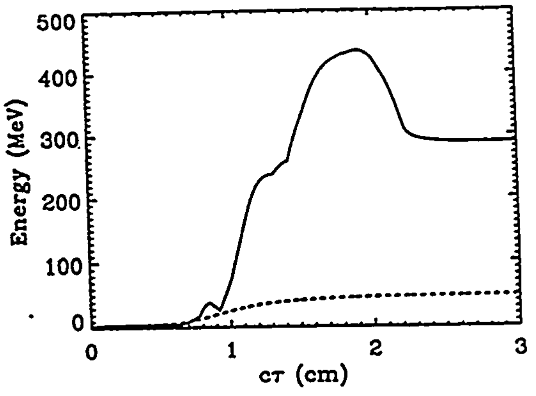

Self–Modulated LWFA:

$n_e \simeq 2\times10^{18}\,\mathrm{cm}^{-3}$, $P \simeq 1.5\,P_c$, $E_{max} = \underline{130\ \mathrm{GV/m}}$, $\Delta W_{max} = \underline{440\ \mathrm{MeV}}$

Standard LWFA:

$n_e = 10^{17}\,\mathrm{cm}^{-3}$, $P \ll P_c$, $E_{max} = 7\ \mathrm{GV/m}$, $\Delta W_{max} = 45\ \mathrm{MeV}$

$L = \lambda_p$

LWFA pump-probe experimental setup at NRL

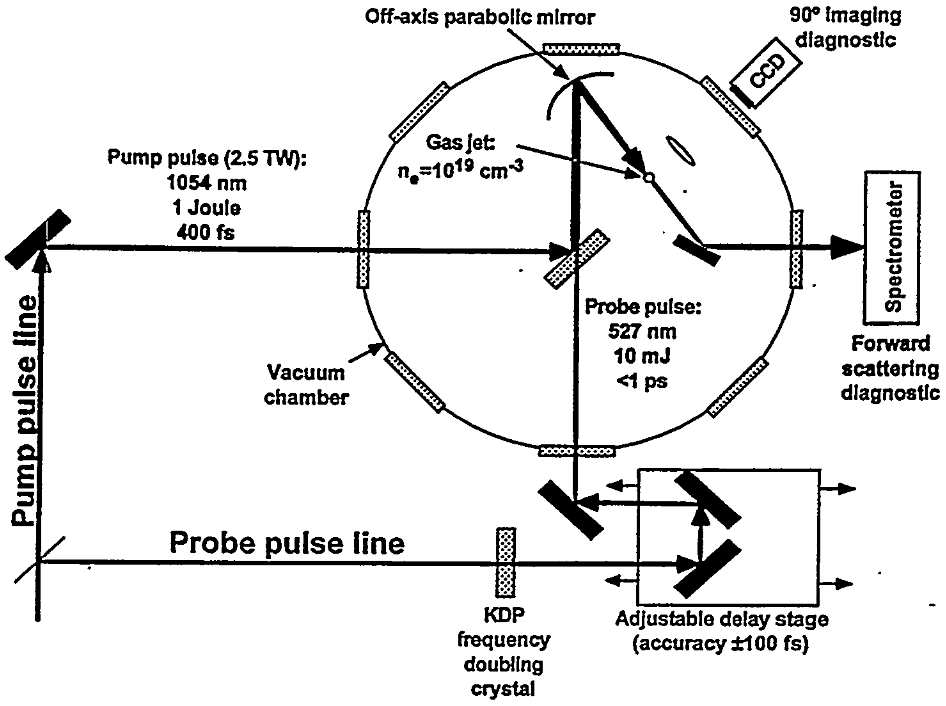

NRL

The production of highly non-linear wakefields is apparent from the forward Raman scattering spectrum

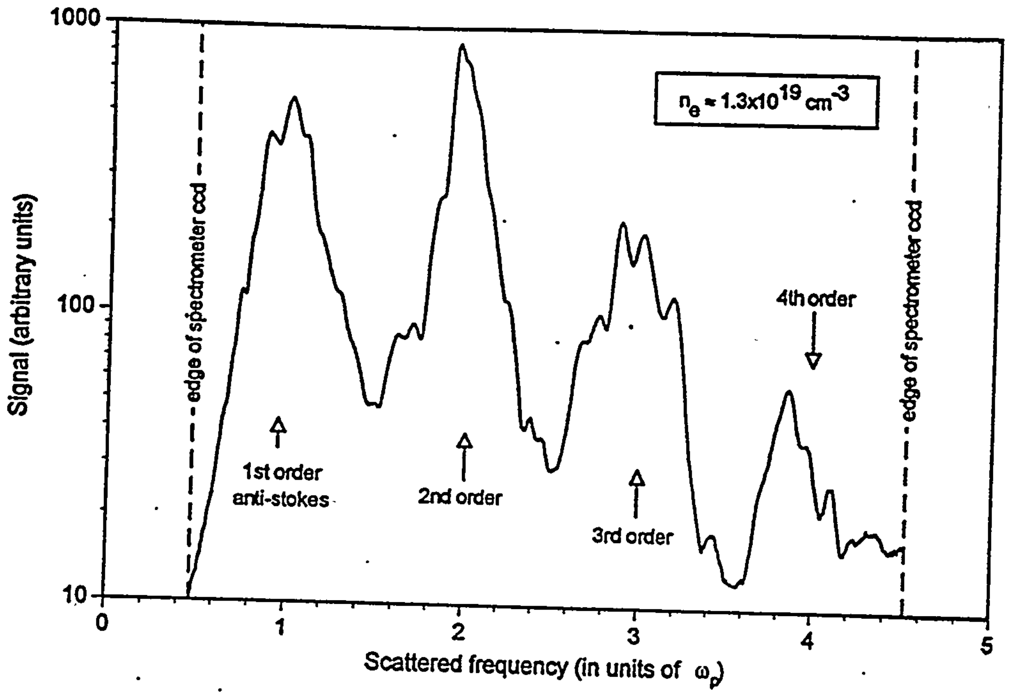

Self-modulated laser wakefield evolution in a hydrogen gas jet plasma

- Coherent Thomson scattering of the probe at ω_{probe}-ω_p(550 nm - •) shows the generation of wakefield plasma waves.
- The wakefield decays in approximately 5 ps - consistent with ion plasma motion time scales.
- Ion acoustic waves (formed from wakefield decay) scatter probe light for >50 ps (○) - consistent with plasma channel evolution time scales.

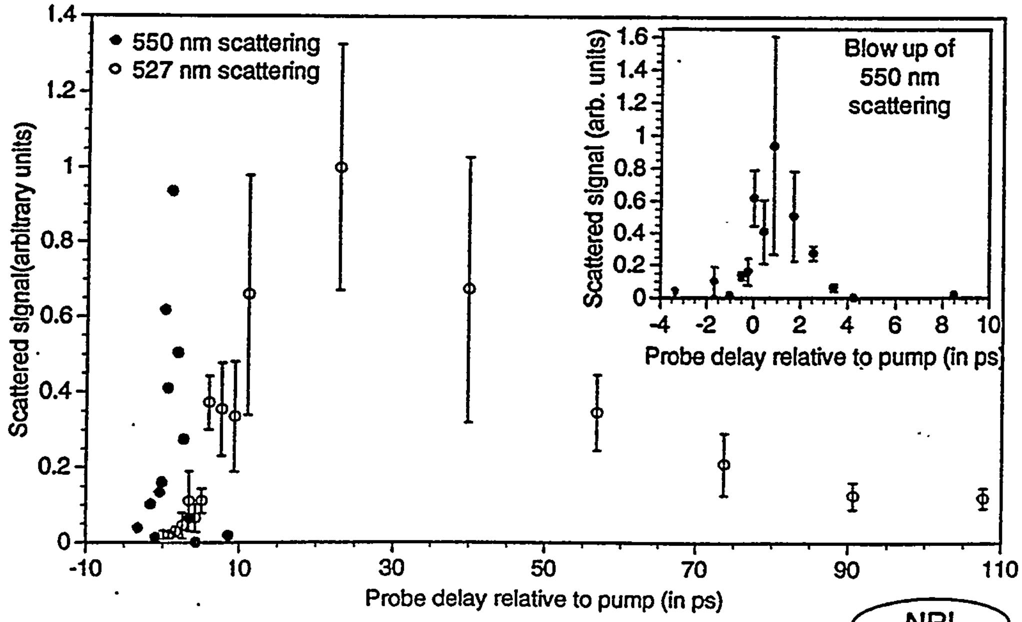

NRL

Status of the Self-Modulated LWFA experiments at the NRL

- The generation of wakefield plasma waves has been observed.
- A pump-probe technique has been used to study the temporal behavior of wakefields produced in a hydrogen (and helium) gas jet plasma.
- The wakefields are observed to decay into ion acoustic waves in approximately 5 ps.
- 90° imaging of the scattered probe light shows the probe is guided in a plasma channel for approximately 20 Rayleigh lengths.
- The plasma channel is formed by ponderomotive expulsion of electrons by the pump and subsequent expulsion of ions by space charge effects.
- Electrons accelerated from the background plasma have been observed with energies in excess of 30 MeV. The measurement of the energy spectrum is in progress.
- High energy electron production is concurrent with the observation of highly non-linear wakefields ($\Delta n/n_0 \sim 1$).

NRL

Temporal evolution of the plasma channel formed by a short intense laser pulse in an underdense plasma

- Expulsion of electrons by the pump's ponderomotive force and subsequent expulsion of ions by charge seperation forms a plasma channel in the pump's wake.
- The plasma channel is 20 Rayleigh lengths long - approximately equal to the propagation length of the self-guided pump.
- The observed evolution of the channel is consistent with hydrodynamic expansion of the plasma.

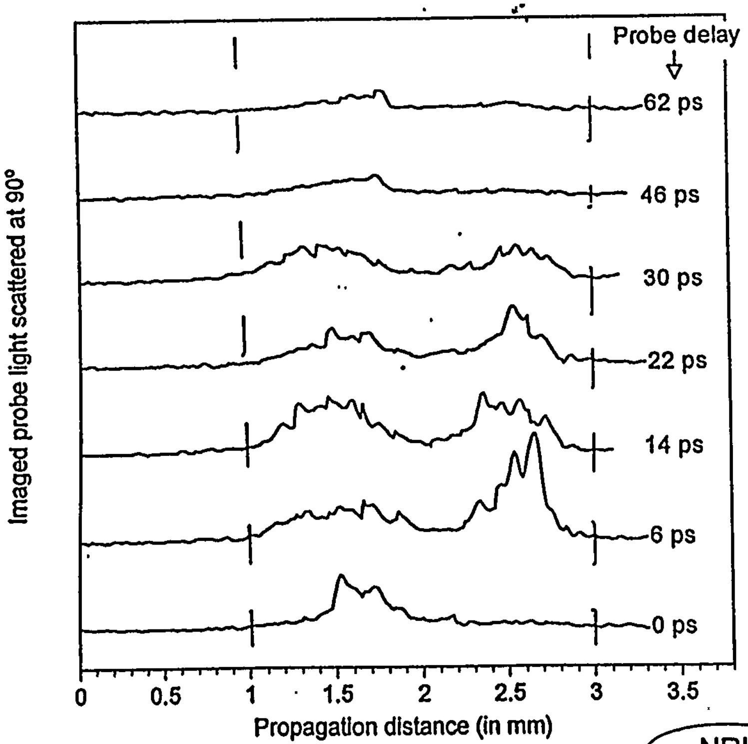

NRL

$2\,mm \simeq 20\,z_R$

Plasma Channel Wakes

NRL

[Krushelnick et al. PRL (96); Esarey et al. PRE (96)]

- Self-Modulated Regime: $L \overset{\gtrsim}{\cancel{\ll}} \lambda_p,\ P \geq P_c$

  Pump pulse ⇒ relativistic SF/electron cavitation

- Ion Motion

  Ponderomotive Force ⇒ Expels Electrons

  Space Charge Force ⇒ Expels Ions

  Electrons

$$\underbrace{e\nabla_\perp\phi}_{\text{space charge}} = \underbrace{m_e c^2 \nabla_\perp a^2/2}_{\text{ponderomotive}} + \underbrace{n_e^{-1}\nabla_\perp T_e n_e}_{\text{thermal}}$$

  Ions

$$m_i \partial v/\partial t = -Ze\nabla\phi, \quad \partial n_i/\partial t = -n_0 \nabla\cdot v$$

$$\boxed{\left(\frac{\partial^2}{\partial t^2} - C_s^2\nabla_\perp^2\right)\frac{n_i}{n_{i0}} = \frac{Zm_e}{4m_i}\nabla_\perp^2 a^2}$$

$$C_s = (ZT_e/m_i)^{1/2} = \text{ion sound speed}$$

- Guide Probe Pulse: $P \ll P_c$

Plasma Channel Wakes

NRL

[Krushelnick et al. PRL (96); Esarey et al. PRE (96)]

- Ion Motion

$$\boxed{\left(\frac{\partial^2}{\partial t^2} - C_s^2\nabla_\perp^2\right)\frac{n_i}{n_{i0}} = \frac{Zm_e}{4m_i}\nabla_\perp^2 a^2}$$

- Ex.: He, $T_e = 100$ eV

  $a_0 = 0.25,\ r_0 = 10\ \mu\text{m},\ L = 120\ \mu\text{m}$

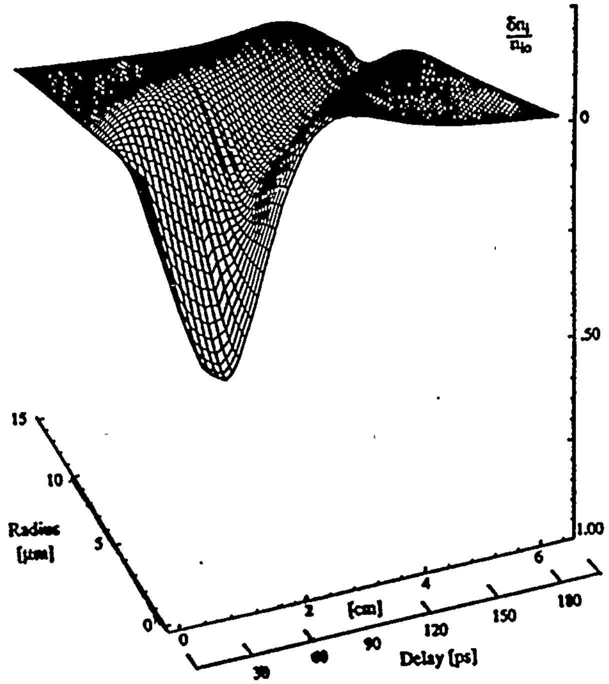

Curved Plasma Channels

[Ehrlich et al. PRL (96); Esarey et al. PRE (96)]

- Slow capillary discharge

  Radius of curvature: R_0

  Parabolic profile: $n = n_0 + \Delta n (r/r_{ch})^2$
- Intensity profile: $I \sim \exp\left[-2(x-x_c)^2/r_0^2\right]$

  Matched spot size: $r_0^4 = r_{ch}^2/\pi r_e \Delta n$

  Centroid displacement: $x_{c0} = Z_R^2/R_0$
- Guiding requires: $x_{c0} < r_{ch}$

$$\boxed{R_0 > Z_R^2/r_{ch}}$$

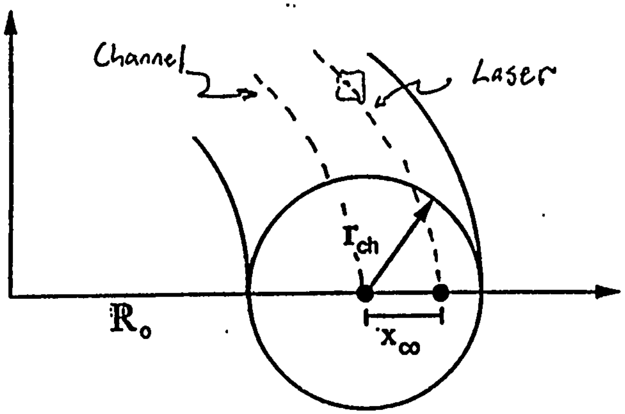

Curved Plasma Channels

[Ehrlich et al. PRL (96); Esarey et al. PRE (96)]

- Experimental parameters:

$\lambda = 0.8$ μm, $r_L = 15$ μm, 100 fs, 5 mJ, 10^{16} W/cm^2

$r_{ch} = 150$ μm, $L = 1$ cm, $n_0 = \Delta n = 5 \times 10^{18}$ cm^{-3}

- Theory:

$$R_0 > 6 \text{ cm}$$

- Experiment:

$R_0 = 4$ cm, 2% Transmision

$R_0 = 10$ cm, 85% Transmision

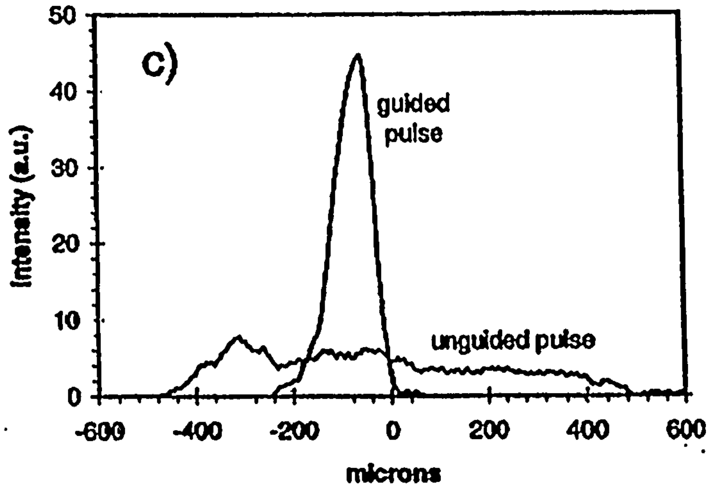

Conclusion

- Many methods to generate large wakefields

  $E \gtrsim E_0 \simeq n_0^{1/2}[\mathrm{cm}^{-3}]$ V/cm

- PWFA: $L_{fall} < \lambda_p$

  $E/E_0 \simeq n_b/n_0$

  $n_b < 10^{14}$ cm^{-3} $\Rightarrow E \lesssim 1$ GV/m

  $R = \Delta\gamma_e/\gamma_{driver} \simeq 2\pi L/\lambda_p$

  Long beams → electron hose instability

- LWFA: $L_{laser} \simeq \lambda_p$

  $E/E_0 \simeq a^2/(1+a^2)^{1/2}$

  $E \lesssim 100$ GV/m

- PBWA: $\omega_1 - \omega_2 \simeq \omega_p$

  $E/E_0 \simeq 4(a_1 a_2/3)^{1/3}$

- Multiple pulses

  Linear: $E_n = nE_1$

  Nonlinear: $E_n > nE_1$

Table II. Laser-Driven Acceleration of Electrons

	P (TW)	I (W/cm^2)	τ_L (ps)	n_p (cm^{-3})	ΔE (MeV)	E_{acc} (GV/m)
PBWA						
Japan (ILE)	0.3	10^{13}	1000	10^{17}	10	1.5
USA (UCLA)	0.2	10^{14}	300	10^{16}	28	2.8
Canada (CRL)	0.1	10^{14}	500	10^{16}	17	1.7
France (LULI)	0.2	10^{17}	90	10^{17}	1.4	0.6
LWFA						
Japan (KEK)	8	10^{17}	1.0	10^{15}	5	0.7
SM-LWFA						
Japan (KEK)	3	10^{17}	1.0	10^{19}	17	30
USA (LLNL)	5	10^{18}	0.6	10^{19}	2	-
UK (RAL)	25	10^{19}	0.8	10^{19}	100	100
USA (CUOS)	2.5	10^{19}	0.4	10^{19}	5	-
USA (NRL)	2.5	10^{19}	0.4	10^{19}	30	-

Conclusion

NRL

- Optimized pulse trains
  - Control over pulse width and spacing
  - Maintain resonant growth of wakefield
- Self–Modulated LWFA
  - $L > \lambda_p$, $P > P_c$
  - High density
  - $E \gtrsim 100$ GV/m
  - Limited by detuning
- Limits to laser drivers
  - Diffraction: $Z_R = \pi r_0^2/\lambda$
  - Detuning: $L_d \simeq (\omega^2/\omega_p^2)\lambda_p$
  - Depletion: $L_{pd} \simeq (\omega^2/\omega_p^2)\lambda_p/a^2$

$$Z_R \ll L_d < L_{pd}, \quad L_d, L_{pd} \sim n_0^{-3/2}$$

Conclusion

NRL

- Optical guiding
  - Preformed density channels
    - $\Delta n = 1/\pi r_e r_0^2$
  - Relativistic focusing
    - $P > P_c = 17(\omega/\omega_p)^2$ GW
    - Short pulses ($L < \lambda_p$) diffract
    - Long pulses ($L > \lambda_p$) self–modulate
- Instabilities ($L > \lambda_p$)
  - Raman back/side scatter
    - Loss of laser energy
    - Accelerate background electrons
  - Raman forward scatter
    - Wakefield generation
  - Self–modulation
    - Wakefield generation
  - Laser/electron hose
    - Disruption of wakefield

SELF-MODULATION OF INTENSE LASER PULSES IN HOMOGENEOUS PLASMA AND PLASMA CHANNELS

N. Andreev, Russian A.S.

Self-Modulation of Intense Laser Pulses in Homogeneous Plasma and Plasma Channels

N. Andreev *)

High Energy Density Research Center,
Joint Institute for High Temperatures
Russian Academy of Sciences

*) In collaboration with

L. Gorbunov *(P.N. Lebedev Physical Institute, RAS)*
V. Kirsanov, A. Pogosova *(HEDRC, RAS)*
A. Sakharov *(Institute of General Physics, RAS)*

August 19 - 23, 1996
ITP, UCSB, Santa Barbara

Outline

I. Introduction
  - *Physical restrictions on Laser-Driven Acceleration*
  - *Enhanced acceleration in Self-Modulated LWFA*

II. Theory of Laser Pulse Self-Modulation
  - *Main regimes of S-M*
  - *Scaling laws*
  - *Phase velocity of plasma Wake Field*

III. Selfconsistent modeling of Wake Field generation
  - *In preformed plasma channel*
  - *Flattop laser pulse*
  - *Spectral peculiarities*

IV. Summary

Physical Restrictions on Laser-Driven Acceleration

Maximum length of acceleration:

$$l_a \le L_{deph} = \frac{\lambda_p}{2(c - v_p)} c = \gamma^2 \lambda_p$$

Final energy (maximum at $l_a = L_{deph}$):

$$\varepsilon_f \cong \Delta W = eE_a l_a \cong \frac{e\Delta\varphi}{\lambda_p / 2} l_a = 2mc^2 \gamma^2 \alpha$$

Laser pulse diffraction:

$$L_{diff} = \pi Z_R = \frac{\pi^2 r_L^2}{\lambda_0}$$

In standard LWFA $E_a \sim a_0^2/2$:

$$E_{\max}[GeV/m] \cong 4.87 \times 10^4 \left(\frac{\lambda_0}{r_L}\right)^2 \frac{\kappa P[TW]}{\tau[fs]}$$

$$\varepsilon_{diff}[MeV] \cong \frac{600}{\gamma} P[TW]$$

How to Increase the Final Energy of Accelerated e^-

To enlarge the length of pulse propagation by

Optical Guiding *(to overcome diffraction)*

- in preformed plasma channel:

$$\varepsilon_{ch}[MeV] \cong 1.2 \times 10^3 \frac{P[TW]}{(k_p r_L)^2}$$ - for LWFA

- by relativistic self-focusing:

$$P \ge P_{cr} \cong 1.7 \times 10^{-2} \gamma^2 [TW]$$

$$\gamma^2 < 59 \times P[TW]$$

To enlarge the efficiency of PWF generation by laser pulse Self-Modulation

to seed the instability:

- $P \sim P_c$ ...
- *flattop pulses (with sharp leading front)*
- *induced self-modulation ($\Delta\omega \sim \omega_p$)*

Self-Modulated LWFA in plasma channel

For High Values of γ_g - Factor and Limited Pulse Power the Main Transverse Mode of Self-Modulation Can be Described in "Spot Size" Approximation

$$\left(\frac{\partial^2}{\partial\xi^2}+1\right)\left(\frac{\partial^2}{\partial\tau^2}+\Omega_0^2\right)N+4\alpha N=0,$$

where

$$\Omega_0^2=3+\frac{k_p^2L_{\perp0}^2A_0^2}{8}+\frac{k_p^2L_{\perp0}^4}{4R^2},$$

(in the channel-guiding regime $\Omega_0 = 2$),

$$\alpha=\frac{k_p^2L_{\perp0}^2A_0^2}{8}\cong4\frac{P}{P_c}.$$

There are two typical regimes of instability:

(II) $\gamma_g^2 = (\omega_0/\omega_p)^2 > (P/P_c)|\xi| > 1$

Four Waves "Nonresonant" Regime (k = 4 / L)

Instability develops in a time less than Rayleigh time. For $\tau < \alpha|\xi|/\Omega_0^3$ the solution is described by

$$N=N_0\left(6\pi\left(4\alpha\tau^2|\xi|\right)^{1/3}\right)^{-1/2}\exp\left(\frac{3\sqrt{3}}{4}\left(4\alpha\tau^2|\xi|\right)^{1/3}\right)\cos(\xi+\varphi),$$

where

$$\varphi=\frac{3}{4}\left(4\alpha\tau^2|\xi|\right)^{1/3}-\frac{\pi}{12}.$$

For $\tau > \alpha|\xi|/\Omega_0^3$ (in the channel-guiding regime) the solution goes over to the next stage (unless the nonlinear saturation earlier occurs).

There are Three Main Regimes of Laser Pulse Self-Modulation

for $k_pL_\perp < 4\gamma_g$

and $(P/P_c)\,k_pL < \gamma_g^2$ the instability is three-dimensiona

(Regions II and III)

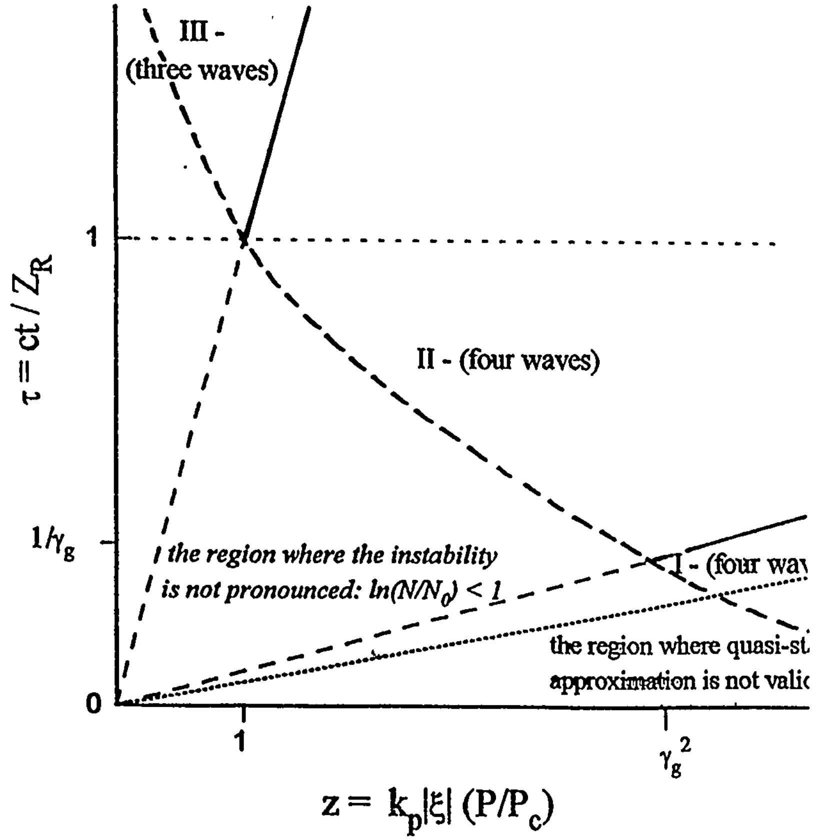

Three Waves (weak coupling) Regime of Near Forward Raman Scattering

(III) $(P/P_c)|\xi| < \Omega_0^2$

(fairly short pulse or/and low pulse power).

Instability develops in a time $\tau > \Omega_0/4\alpha|\xi| >> 1$,

i.e. over many Rayleigh lengths, that needs channel guiding.

$$N = N_0 \frac{\left(\alpha\tau|\xi|/\Omega_0\right)^{1/4}}{2\sqrt{\pi}\Omega_0\tau} \exp\left(2\left(\alpha\tau|\xi|/\Omega_0\right)^{1/2}\right)\cos(\xi+\varphi),$$

where

$$\varphi = \Omega_0\tau - \frac{\pi}{2}.$$

The phase velocity of the wake-wave:

$$V_{ph} = V_g\left(1+\frac{1}{\omega_p t_R}\frac{\partial\varphi}{\partial\tau}\right)^{-1} \approx V_g - \frac{c}{k_p z_R}\frac{\partial\varphi}{\partial\tau}.$$

For the channel-guiding regime :

$$\frac{\gamma_g^2}{\gamma_{ph}^2} = 1+4\frac{\gamma_g^2}{k_p z_R} = 1+8\frac{\gamma_g}{\left(k_p L_{\perp 0}\right)^2}.$$

It should be noted that in the case of $P << P_c$, $k_p z_R = k_0 R$.

Under conditions of numerical experiment ($k_0 R = 400$, $\gamma_g = 50$) this equation gives $\gamma_{ph} = \gamma_g/5$ *(in a good agreement with simulation results).*

Wake-Field Amplitude Is Weakly Depended On Seed Pulse Intensity

Pulse Energy E_L= 5J, τ_{pulse}= 2ps, Spot Size $L_\perp$= 30μ, R_{ch}= 60μ, n_0= 4*10^{17}om

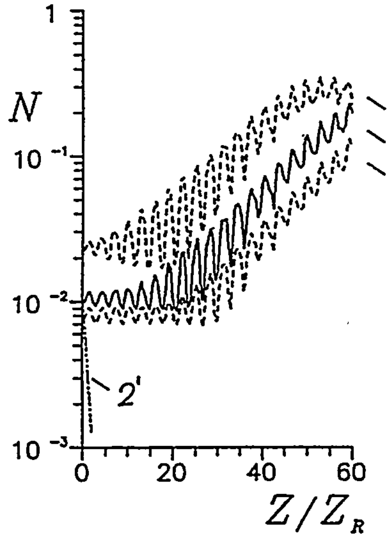

The Ratios of the Field Amplitudes of Intense and Weak, Frequency-Shifted, Pulses are:
1 - 200, 2 - 100, 3 - 30; 2' - 100, Without Channel

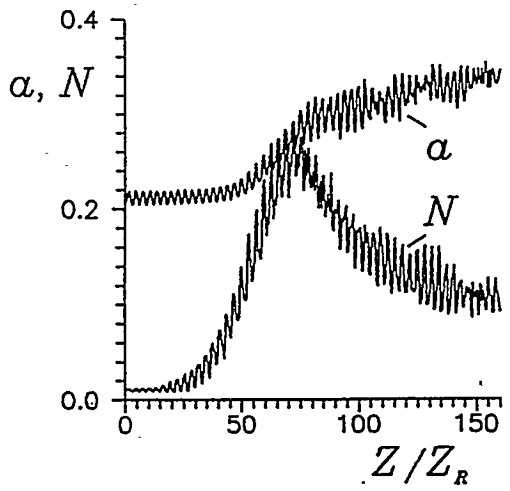

- **Pulse Generates Strong Wake Field While Covering The Distance Required For Efficient Electron Acceleratio**

$l_a = 20\, Z_R = 6$ cm

There are Three Main Regimes of Laser Pulse Self-Modulation

for $k_p L_\perp < 4\gamma_g$

and $(P/P_c)\, k_p L < \gamma_g^2$ the instability is three-dimensional

(Regions II and III)

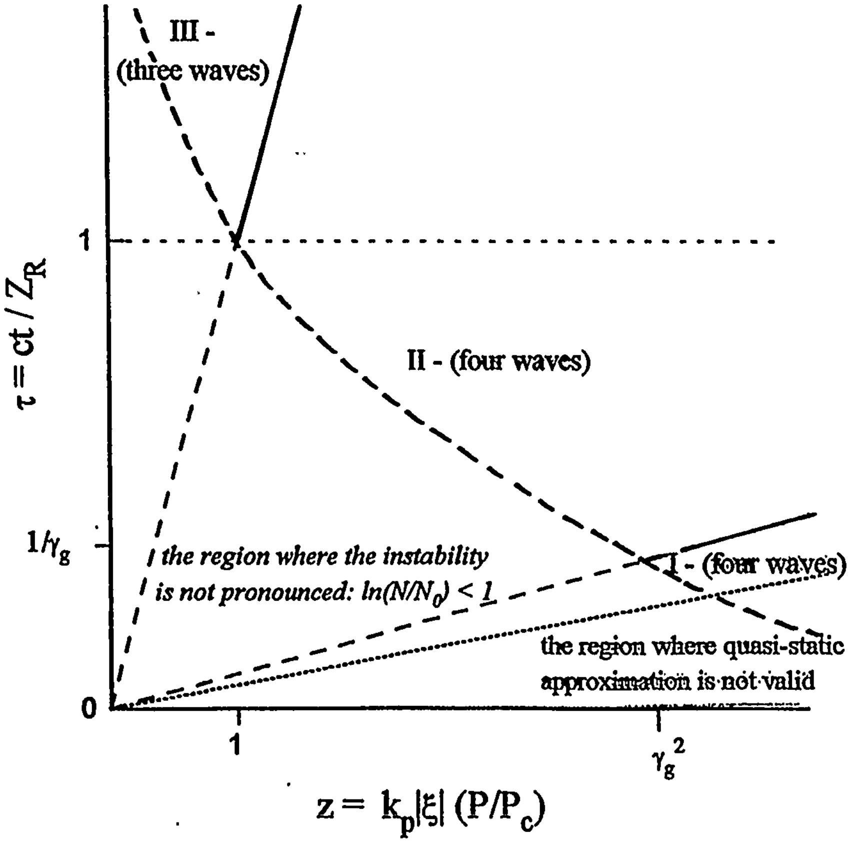

For High Values of γ_g - Factor and Limited Pulse Power the Main Transverse Mode of Self-Modulation Can be Described in "Spot Size" Approximation

$$\left(\frac{\partial^2}{\partial\xi^2}+1\right)\left(\frac{\partial^2}{\partial\tau^2}+\Omega_0^2\right)N+4\alpha N=0,$$

where

$$\Omega_0^2=3+\frac{k_p^2L_{\perp 0}^2A_0^2}{8}+\frac{k_p^2L_{\perp 0}^4}{4R^2},$$

(in the channel-guiding regime $\Omega_0 = 2$),

$$\alpha=\frac{k_p^2L_{\perp 0}^2A_0^2}{8}\cong 4\frac{P}{P_c}.$$

There are two typical regimes of instability:

(II) $\gamma_g^2 = (\omega_0/\omega_p)^2 > (P/P_c)|\xi| > 1$

Four Waves "Nonresonant" Regime ($k = 4/L$)

Instability develops in a time less than Rayleigh time. For $\tau < \alpha|\xi|/\Omega_0^3$ the solution is described by

$$N=N_0\left(6\pi\left(4\alpha\tau^2|\xi|\right)^{1/3}\right)^{-1/2}\exp\left(\frac{3\sqrt{3}}{4}\left(4\alpha\tau^2|\xi|\right)^{1/3}\right)\cos(\xi+\varphi),$$

where

$$\varphi=\frac{3}{4}\left(4\alpha\tau^2|\xi|\right)^{1/3}-\frac{\pi}{12}.$$

For $\tau > \alpha|\xi|/\Omega_0^3$ (in the channel-guiding regime) the solution goes over to the next stage (unless the nonlinear saturation earlier occurs).

Stable And Intense Wake Field Is Generated Due To Stimulated Pulse Self-Modulation In Plasma Channel

- Pulse Energy E_L= 5J, τ_{pulse}= 2ps, Spot Size $L_\perp$= 30μ, R_{ch}= 60μ, n_0= 4*10^{17}cn

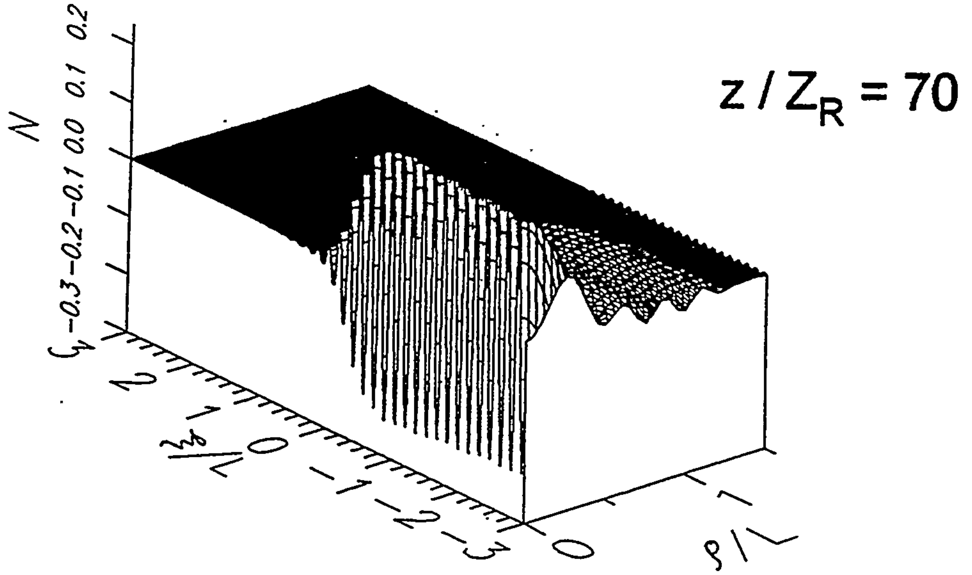

- Gain Factor γ = 50, Energy of Electrons: $\varepsilon_o \cong$ 25Mev, $\varepsilon_f \cong$ 1Gev?

Laser Pulse Spectrum

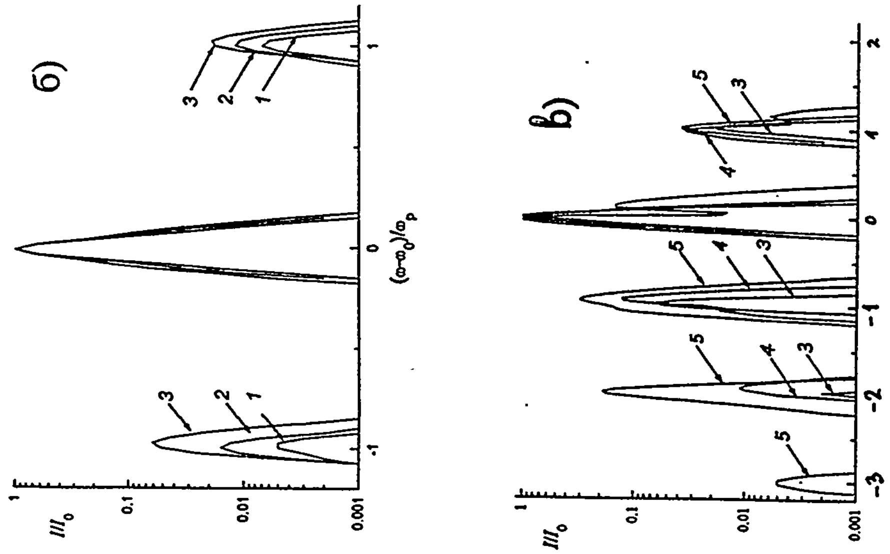

S-M of laser pulse in plasma channel

P << P_c

Analytical Linear Theory

(from spot size paraxial model)

Provides Quantitative Description of S-M Instability

$$N_0 = (\varepsilon/8)A_0^2(6\pi(4\alpha\tau^2|\xi|)^{1/3})^{-1/2}\, exp((4\alpha\tau^2|\xi|)^{1/3}) * cos(\sigma+\varphi(\tau,\xi)),$$

where $\varphi(\tau,\xi) = (3/4)(4\alpha\tau^2|\xi|)^{1/3} - \pi/12$

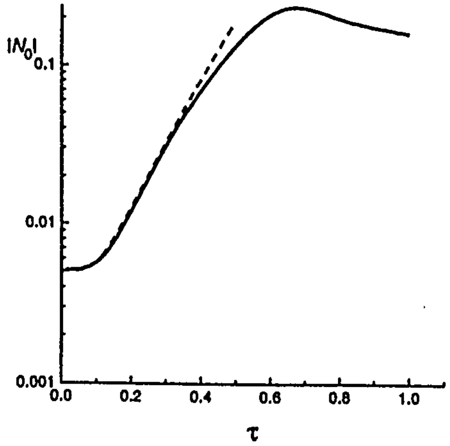

Self-Modulation of Flattop Laser Pulse

$\gamma_g^2 = 450$, $P/P_c = 0.68$, $k_p L = 54$, $r_\perp = 4.5\lambda_p$

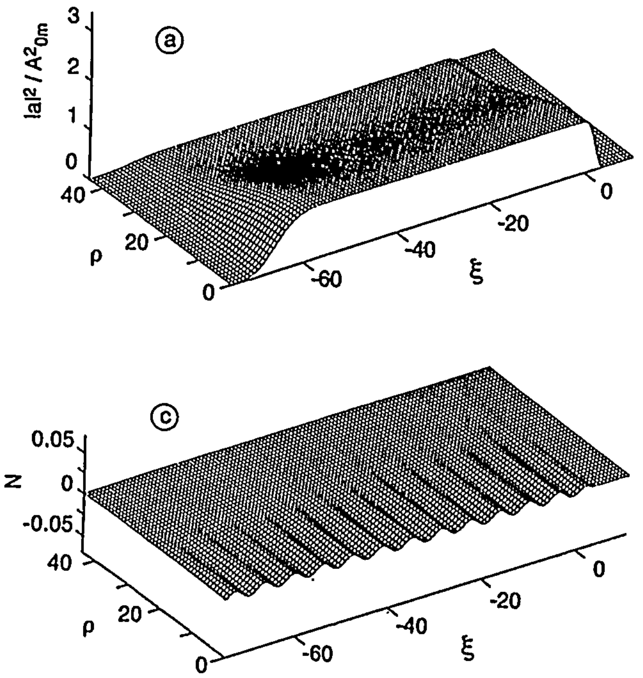

$Z = 0.$

Dynamics of 3-D Pulse Self-Modulation

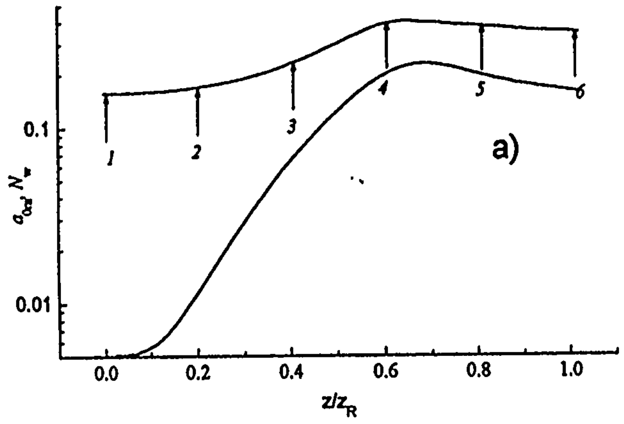

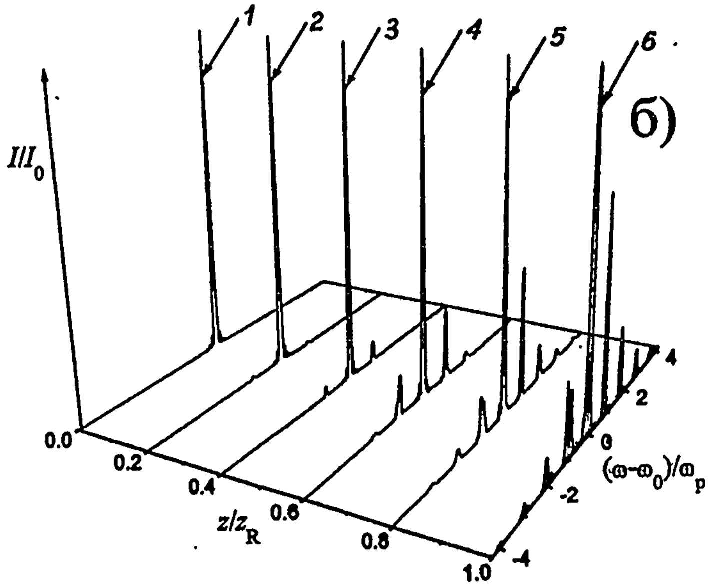

Laser Pulse Spectrum

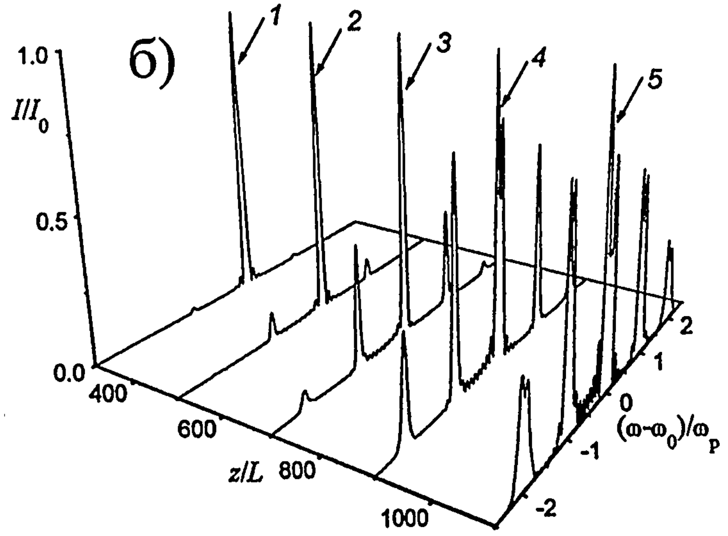

Laser Pulse Spectrum

1-D S-M Laser Pulse Instability

Direct FRS

At the Final Stage of Instability
The Phase Velocity of Excited Wake Field
Is Close to the Group Pulse Velocity

$$\gamma_{ph} / \gamma_g = (1 + F(K_w)(\alpha k_p L)^{1/2} \gamma_g{}^2 / k_p z_R)^{-1/2}$$

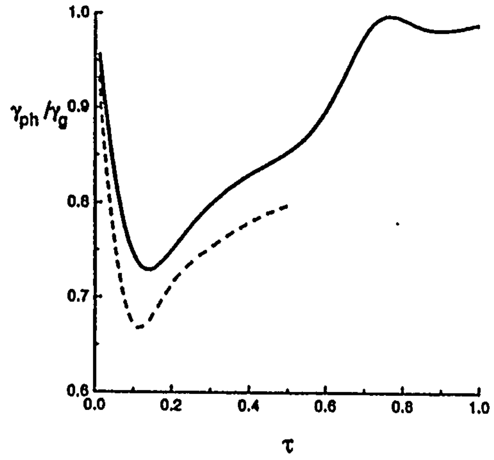

Direct-Forward Raman Scattering
(*1-D instability*)
Is Unimportant for Low Enough Pulse Power

$$(P / P_{cr})\, k_p L << \gamma_g{}^2$$

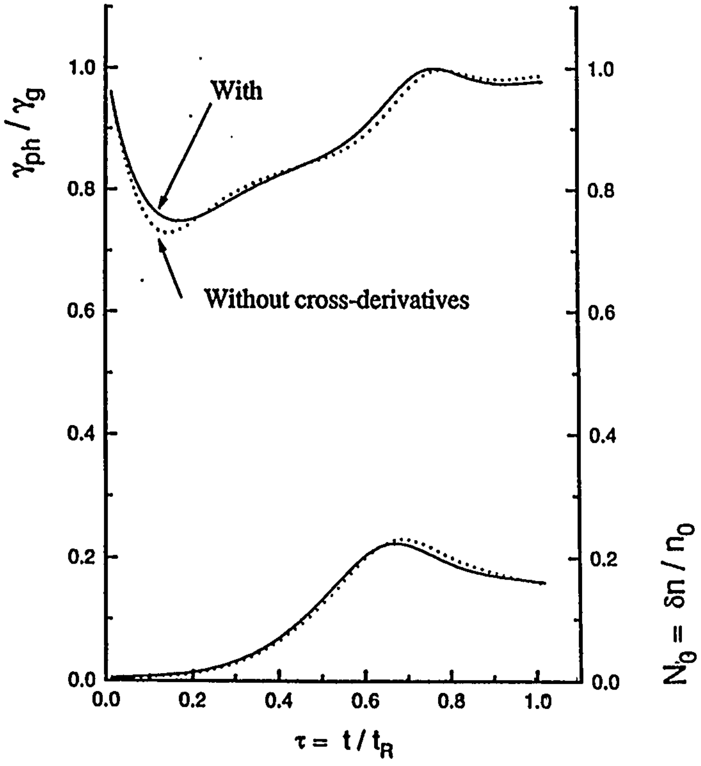

$Z = 0.6 Z_R$

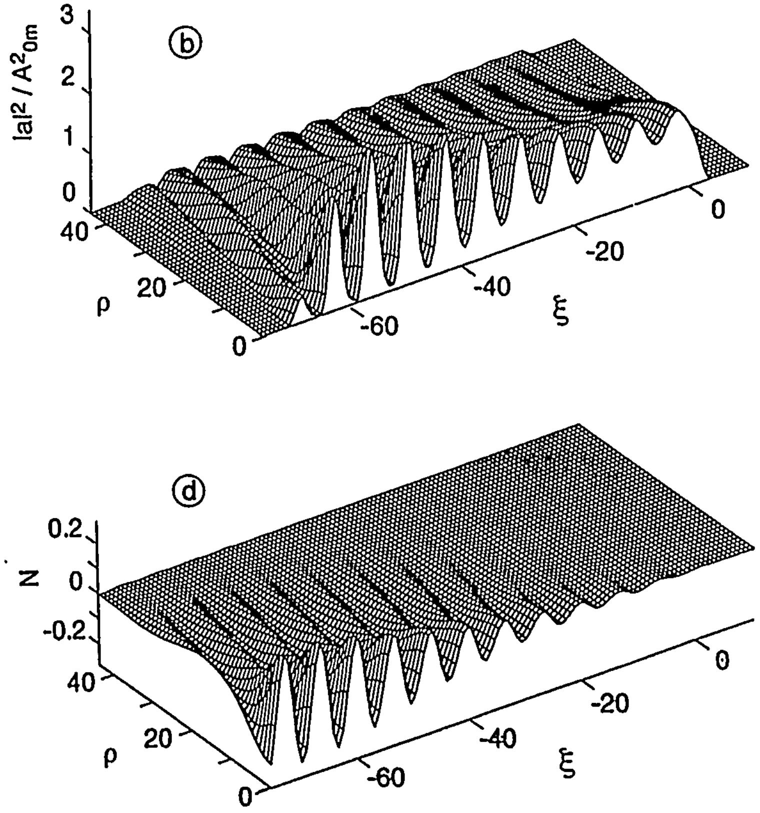

Self-Modulation of Intense Laser Pulses in Homogeneous Plasma and Plasma Channels

N.E.Andreev *)

High-Energy Density Research Center, Joint Institute for High Temperatures, Russian Academy of Sciences, Moscow, Russia

The study is made of the basic features of the self-modulational instability of high-intensity (I~ 10^{17}-10^{18} W/cm^2) laser pulses in underdense uniform plasmas and plasma channels. This instability is known to cause the longitudinal modulation of the pulse envelope with the characteristic scale equal to the plasma wavelength $\lambda_p=2\pi c/\omega_p$ (the pulse length is assumed to be much greater than λ_p) and, as a result, the onset of this instability is accompanied by the generation of ultrastrong plasma wake fields. The problem is analyzed analytically and numerically; both the linear and nonlinear stages of the instability are considered. The whole set (including three- and four-wave processes) of the possible linear 1D and 3D axisymmetrical) regimes of the self-modulation is classified, analytical solutions (including the expressions for the amplitude and the phase velocity of the excited plasma wave) are obtained, and the conditions for the realizations of these regimes and their combinations are found. Basing on the obtained results we separated two 3D regimes and three 1D regimes that can occur under realistic conditions of laser-plasma interactions. For different stages of the instability, a special attention is paid to the variations of phase velocity of the excited plasma wave, which is of a primary concern for using the excited wake field for the electron acceleration and to the peculiarities of the spectrum of the self-modulated laser pulse, which can be utilized for the diagnostics of the pulse self-modulation and wake-field generation.

Our results indicate that the maximum deviations of the phase velocity of the excited plasma wave from the group velocity of the pulse occurs at the early stage of instability. However, we have found that, in several cases, these deviations can be also large at the stage of the developed instability when the large-amplitude plasma wave is excited. For example, for the 3D regime that corresponds to $P << P_{cr}$ (where P is the pulse power and P_{cr} is the critical power for relativistic self-focusing; such a regime can occur if the pulse is guided in a preformed plasma channel), the decrease in the γ-factor corresponding to the phase velocity of the excited plasma wave can be substantial.

The obtained results are discussed with application to existing experimental data on the self-modulation of laser pulses and to using the self-modulation of laser pulses for an enhanced laser wake-field acceleration.

*) In collaboration with:
L.M. Gorbunov (*Lebedev Physical Institute of RAS*)
V.I. Kirsanov, A.A.Pogosova (*HEDRC of RAS*)
A.S. Sakharov (*Institute of General Physics, RAS*)

$Z = 0.6 Z_R$

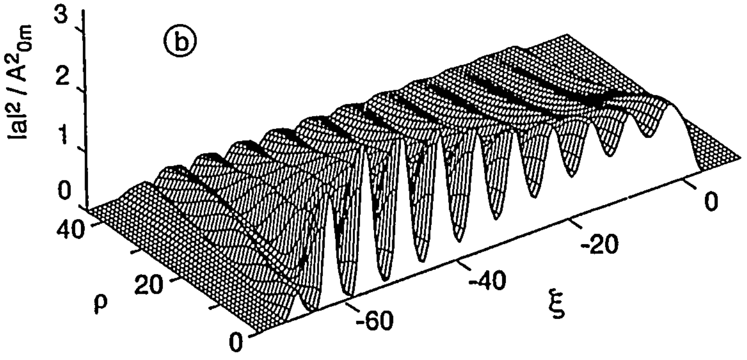

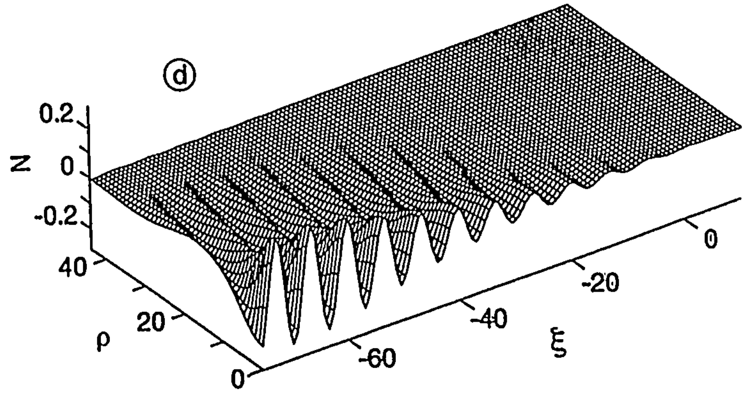

BEAM DYNAMIC ISSUES IN PLASMA WAKEFIELD ACCELERATORS

B. Breizman, UT-Austin

BEAM DYNAMIC ISSUES IN PLASMA WAKE FIELD ACCELERATORS

B.N. Breizman

The University of Texas at Austin
and
Budker Institute of Nuclear Physics

P.Z. Chebotaev, A.M. Kudryavtsev,
K.V. Lotov, and A.N. Skrinsky

Budker Institute of Nuclear Physics,
Novosibirsk, Russia

OUTLINE

- Introductory remarks
- Excitation of nonlinear plasma wave
- Self-modulation of the driving beam
- Radial equilibria of the modulated driver
- Beam particle dynamics
- Wave loading and emittance issues
- Concluding comments

Layout of VEPP2M–PWFA complex

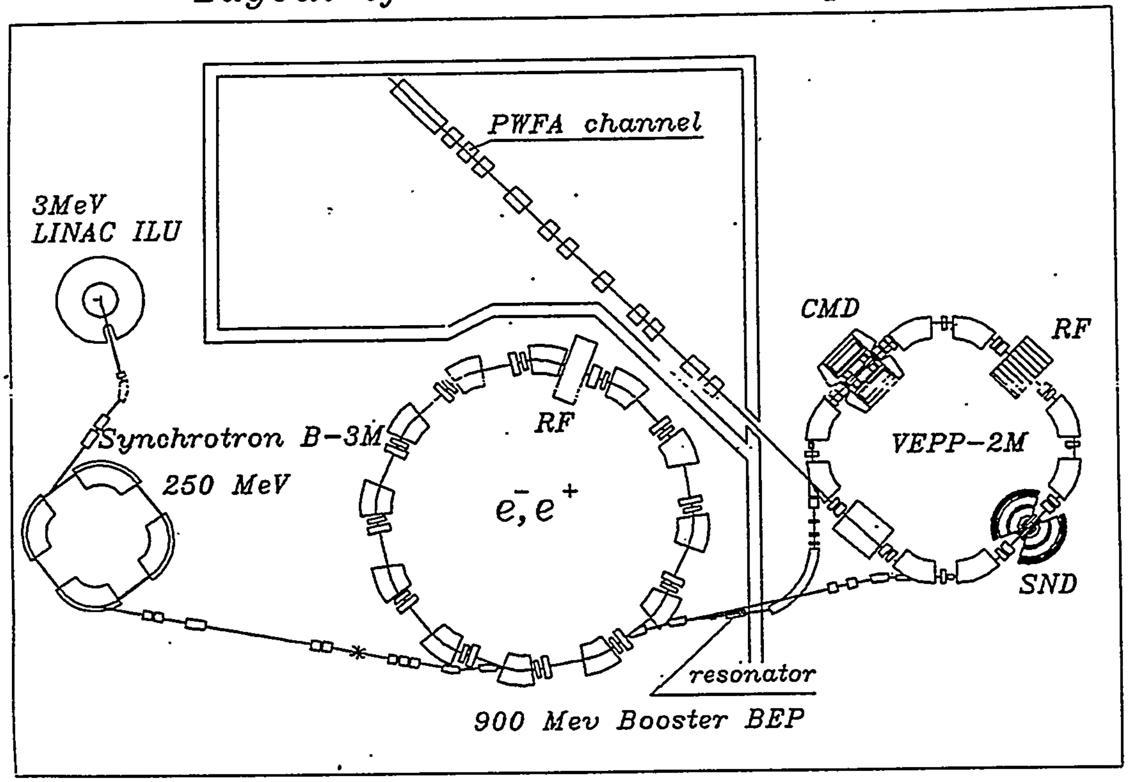

Advanced
Accelerator
Test
Facility

ARGONNE, 1988

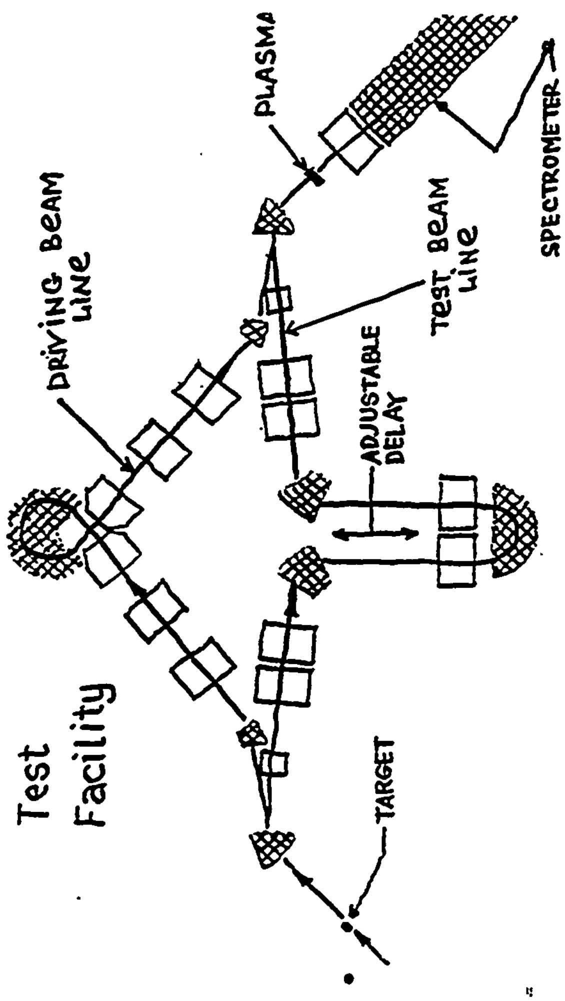

Driving beam:
21 MeV
4 nC $(2.5 \cdot 10^{10})$
$\sigma_r = 1.4$ mm
$\sigma_z = 2.1$ mm

Plasma:
$(0.4\text{-}7) \cdot 10^{13} \text{cm}^{-3}$

Accelerating gradient: 5 MeV/m

EXCITATION OF PLASMA WAVE BY ELECTRON BEAM

Linear model: $\ddot{n}+\omega_p^2 n = -\omega_p^2 n_b(z-ct)$

Nonlinear wavebreaking limit for the accelerating gradient:

$e\sqrt{4\pi n_p mc^2} = 304\sqrt{n_p(\mathrm{cm}^{-3})/10^{13}}(\mathrm{MeV/m})$

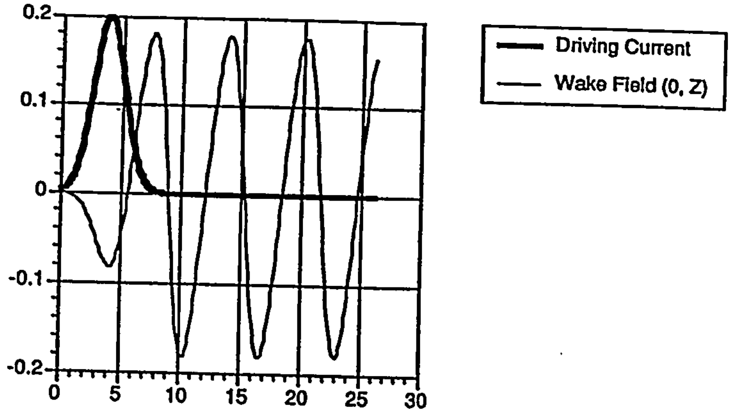

CHARACTERISTIC SCALELENGTHS

- Wavelength: $c/\omega_p = 1.68\sqrt{10^{13}/n_p(\mathrm{cm}^{-3})}(\mathrm{mm})$
- Wave excitation length: $L_b = \frac{n_p}{n_b} c/\omega_p$
- Driving beam focusing length: $L_F = \sqrt{\gamma}\, c/\omega_p$
- Driving beam deceleration length: $L_d = \gamma\, c/\omega_p$

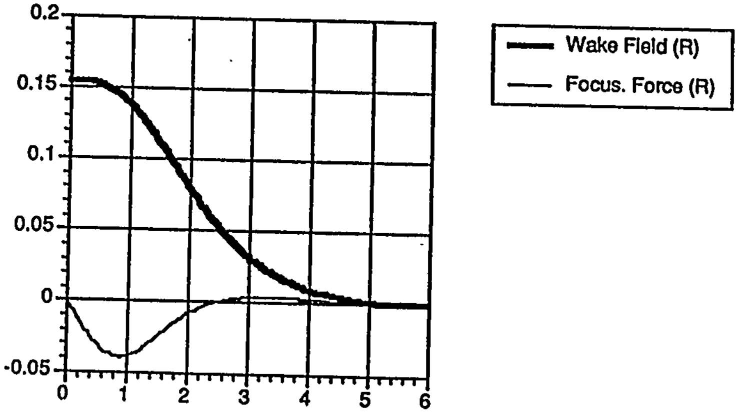

NONLINEAR NUMERICAL SIMULATIONS OF THE WAKEFIELD (NOVOCODE)

SIMPLIFICATIONS

- Fluid description of plasma electrons
- Immobile ions
- Travelling wave solution moving with the driving beam (z-ct)
- Rigid driving beam
- Axial symmetry

SIMULATION RESULTS ARE VALID UP TO THE WAVEBREAKING LIMIT

THE CODE ALLOWS FAST NONLINEAR CALCULATION OF THE FIELDS THAT AFFECT THE DRIVER

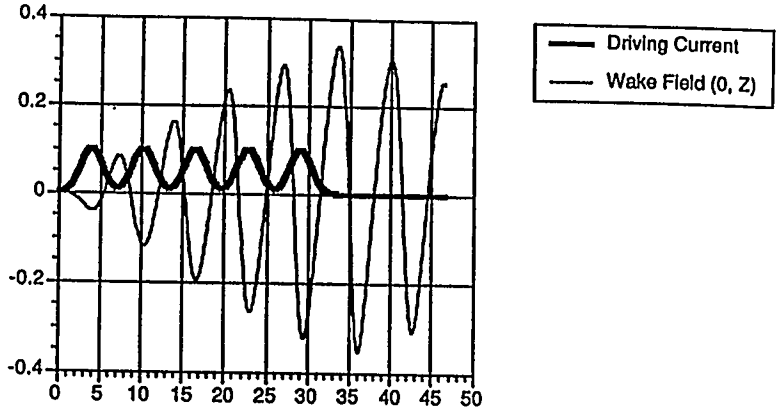

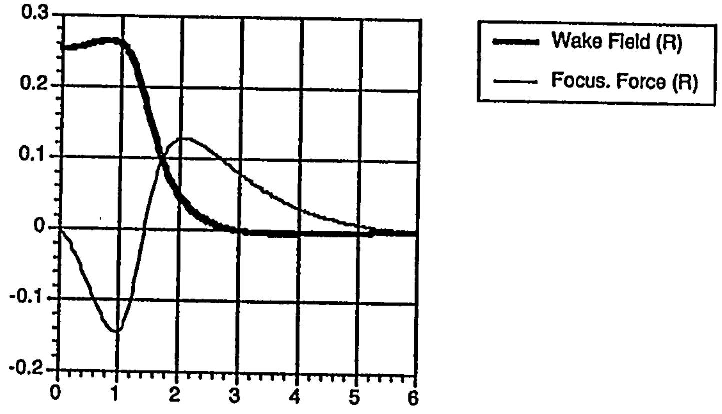

- Defocused beam electrons quickly leave the driver in their radial motion
- Focused electrons stay in the driver until they slow down

Q: Can the driver maintain its shape over a distance much longer than the focusing length?

A: Yes

Numerical tool: modified NOVOCODE

Q: Can the driver relax to an equilibrium state through self-modulation ?

A: Yes

Numerical tool: kinetic L-CODE (K. Lotov)

HOW TO “MAKE” SELF FOCUSED MODULATED DRIVING BEAM

- Choose a seed set of bunches spaced one plasma wavelength apart with a given radial profile of the beam
- Compute the fields generated by this set in the plasma
- While computing the fields, remove the beam slices that experience either defocusing or accelerating forces
- Find the distribution function of the beam particles to match the shape of the radial potential well to the given radial profile of the beam current

! Defocusing force is strong enough to expel driver particles radially in a short travel distance (~1 cm).

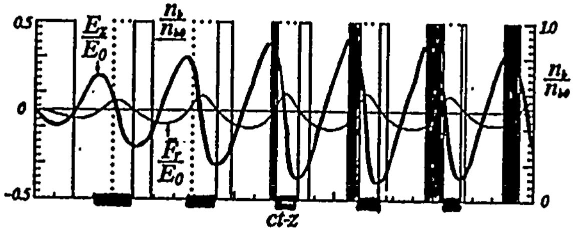

Figure 3: The driver density n_b on axis, the electric field E_z on axis, and the focusing force $\bar{F}_r$ (averaged over the bunch radius) as functions of the longitudinal coordinate $(ct-z)$. Driver parameters are: $a = c/\omega_p$, $n_{b0} = 0.1\,n_i$, modulation period $2\pi c/\omega_b = 2\pi c/\omega_p$. Shown by the dotted line is the "ejected" part of the driver.

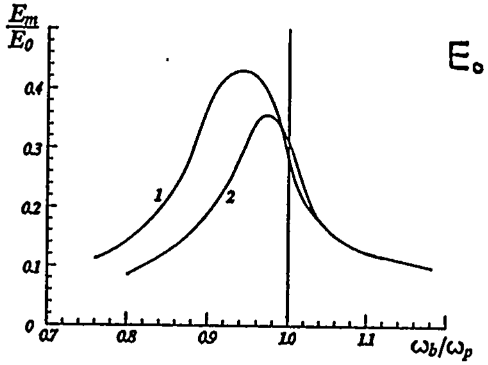

$$E_0 = \sqrt{4\pi n_0 mc^2}$$

Figure 4: The maximum accelerating field E_m versus the modulation frequency ω_b for eight equidistant electron (curve "1") and proton (curve "2") bunches with $a = c/\omega_p$ and $n_{b0} = 0.1\,n_i$ ("ejection" of defocused particles is taken into account).

High accelerating field still can be achieved.

Optimized bunch sequence:

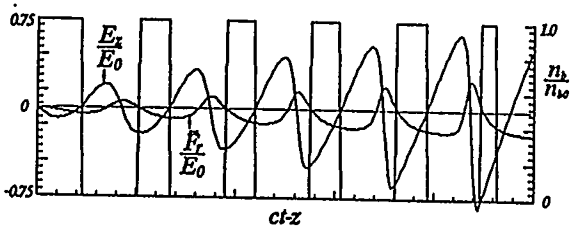

Figure 1: The driver density n_b on axis, the electric field E_z on axis, and the focusing force $\bar{F}_r$ (averaged over the bunch radius) as functions of the longitudinal coordinate $(ct - z)$. Driver parameters are: $a = c/\omega_p$, $n_{b0} = 0.1\,n_i$.

We see a driver frequency shift
caused by a longitudinal drift of the plasma wave.

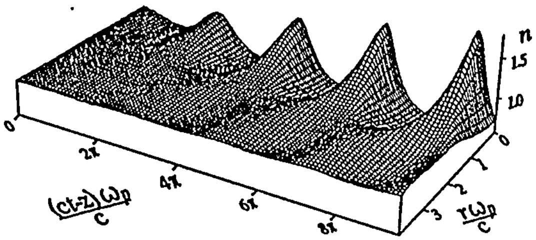

Figure 2: Plasma electron density oscillations generated by four "rigid" electron bunches with $a = c/\omega_p$, $n_{b0} = 0.15\,n_i$, and $\omega_b = \omega_{opt}$.

Why: driver current neutralization
relativistic effects

RADIAL EQUILIBRIUM OF THE DRIVER

Kinetic equation for the beam:

$$\frac{\partial f}{\partial t} + v_z\frac{\partial f}{\partial z} + v_\perp \cdot \frac{\partial f}{\partial r} + e\left(E+\frac{1}{c}v\times B\right)_z \frac{\partial f}{\partial p_z} + e\left(E+\frac{1}{c}v\times B\right)_\perp \cdot \frac{\partial f}{\partial p_\perp} = 0$$

Equilibrium "transverse" distribution $F = \int f dp_z$:

$$\frac{c}{p_0}p_\perp \cdot \frac{\partial F}{\partial r} + e\left(E+e_z\times B\right)_\perp \cdot \frac{\partial F}{\partial p_\perp} = 0 \;\Rightarrow\; F(W; M_z; z\text{-}ct)$$

$W \equiv cp_\perp^2/2p_0 - e\int_\infty^r (E_r - B_\varphi)\, dr$ -"transverse" energy;

$U \equiv - e\int_\infty^r (E_r - B_\varphi)\, dr$ - potential energy;

$M_z = \left[r\times p\right]_z$ - angular momentum.

Beam current density:

$$j_z \equiv \pi e p_0 \int_{U(r)}^{0} F(W)\, dW \;\Rightarrow\; F(U) = -\frac{1}{\pi e p_0}\left(\frac{\partial j_z}{\partial U}\right)_{z\text{-}ct}$$

- RADIAL EQUILIBRIA EXIST FOR A BROAD RANGE OF BEAM CURRENT PROFILES.

Initially $n_b = 0.05\, n_0\, e^{-(r\omega_p/2c)^2}$, $\gamma = 1000$ (electrons), $n_0 = 10^{15}\,\mathrm{cm}^{-3}$

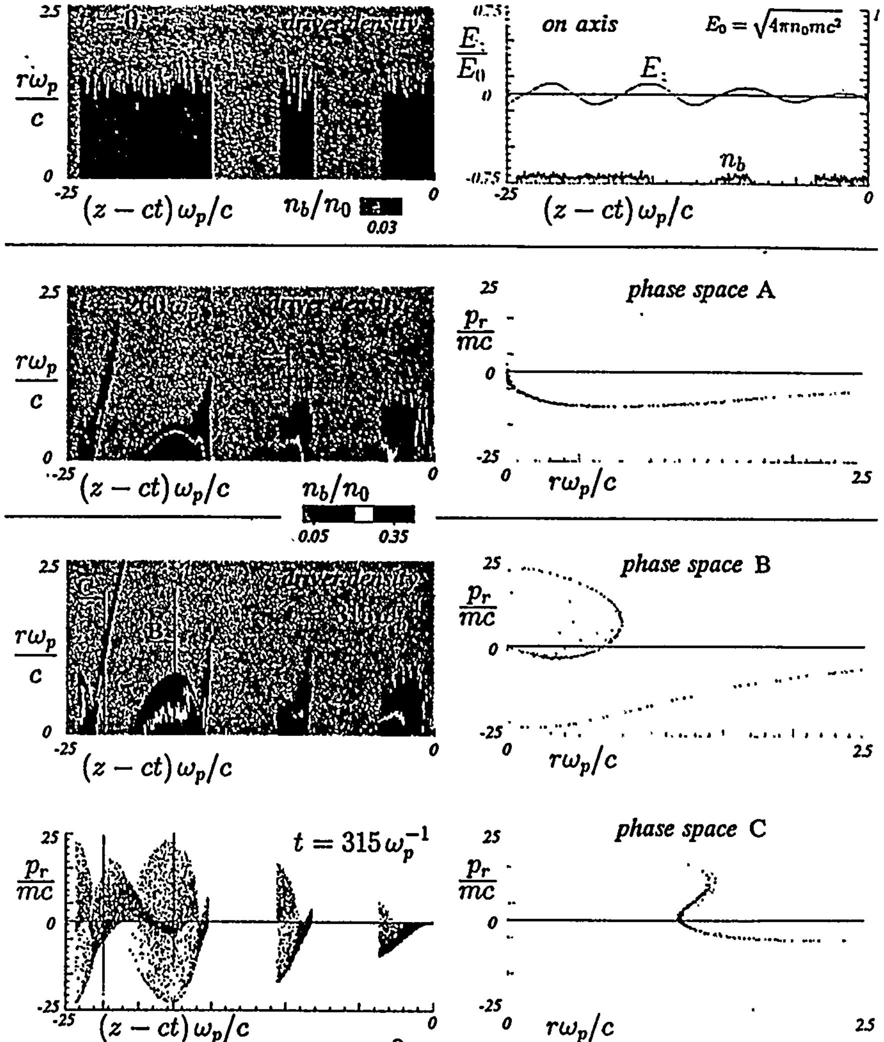

EFFICIENCY AND EMITTANCE

- Near the wavebreaking limit, large fraction of plasma electrons is expelled from the accelerating bucket.

- Radial potential well formed by the plasma ions: $U = 2\pi e^2 n_0 r^2$

- The well can accomodate up to $N = n_0(c/\omega_p)^3$ accelerated particles, with about 50% efficiency

- The accelerated beam of a radius smaller than the wavelength can utilize the wave energy from the cross section of one square wavelenght

- Large radial forces create emittance problems. Remedies:
1) reduce radial force by choosing an appropriate z-position;
2) make the beam radius much smaller than the wavelength (without deteriorating efficiency!)

- Normalized emittance: $\varepsilon = \sqrt{\gamma} r_0^2 \omega_p / c$

Establishment of equilibrium driver radius - 2

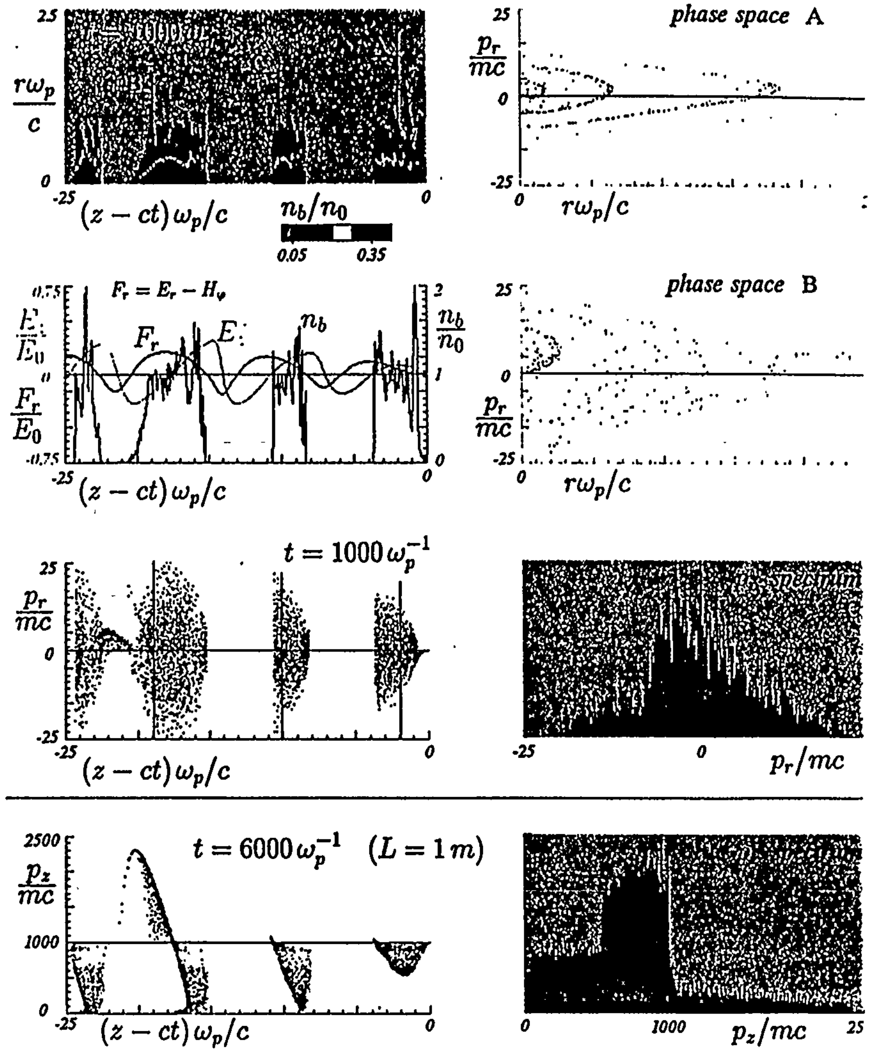

CONCLUDING COMMENTS

- Modulated electron beam can efficiently excite nonlinear plasma wave up to the wavebreaking limit

- Radial equilibrium of the modulated driver allows to substantially extend the acceleration length

- Large radial forces create emittance concerns for the accelerated beam

- Efficient hybrid codes developed to self-consistently simulate nonlinear plasma waves and their effect on both the driver and the accelerated beam

- Challenging topics:
  experiments on e-beam driven PWFA;
  azimuthal stability of the axisymmetric fields;
  possibility of using plasma as a modulator;
  staging.

BEAM DYNAMIC ISSUES IN LASER PLASMA ACCELERATORS

T. Katsouleas, USC

Beam Dynamic Issues

in laser plasma accelerators

T. Katsouleas
University of Southern California

Collaborators:
T.C. Chiou, L. Hsu, S. Lee (USC)
W.B. Mori, K.C. Tzeng, C. Joshi,
C. Clayton, D. Gordon, C. Pellegrini,
K. Marsh, J. Dawson (UCLA)
J. Wurtele (UCB), G. Shvets(Princeton)
C. Decker (LLNL)
[illegible]

Beam Loading Basics

What are N, $\delta\gamma/\gamma$, η, ε?

Plasma Wave: $E_p = -mc\omega_p/e \; n_1/n_o \cos[\omega_p(t-z/c) + \phi]$

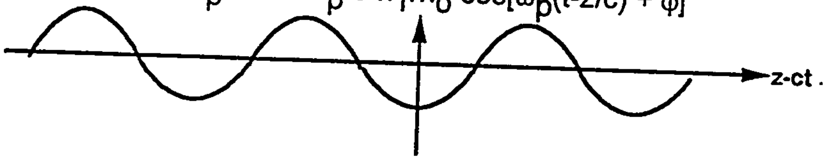

Single particle wake: $E_1 = 2\omega_p^2 K_o(k_p r) \cos[\omega_p(t-z/c)] \,\Theta(t-z/c)$

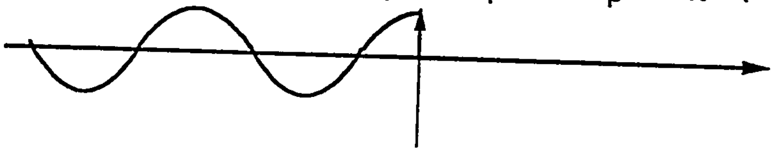

Superposition of fields: $E_p + N^{max} E_1$

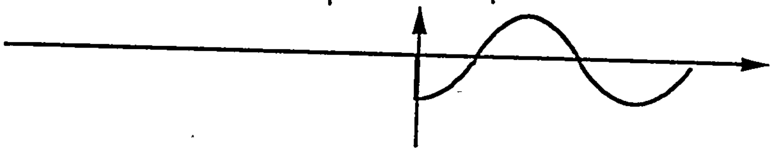

For wide waves and beams:

$$N^{max} = 5 \times 10^5 \,(n_o)^{1/2} \,A_{[cm^2]} \,n_1/n_o$$

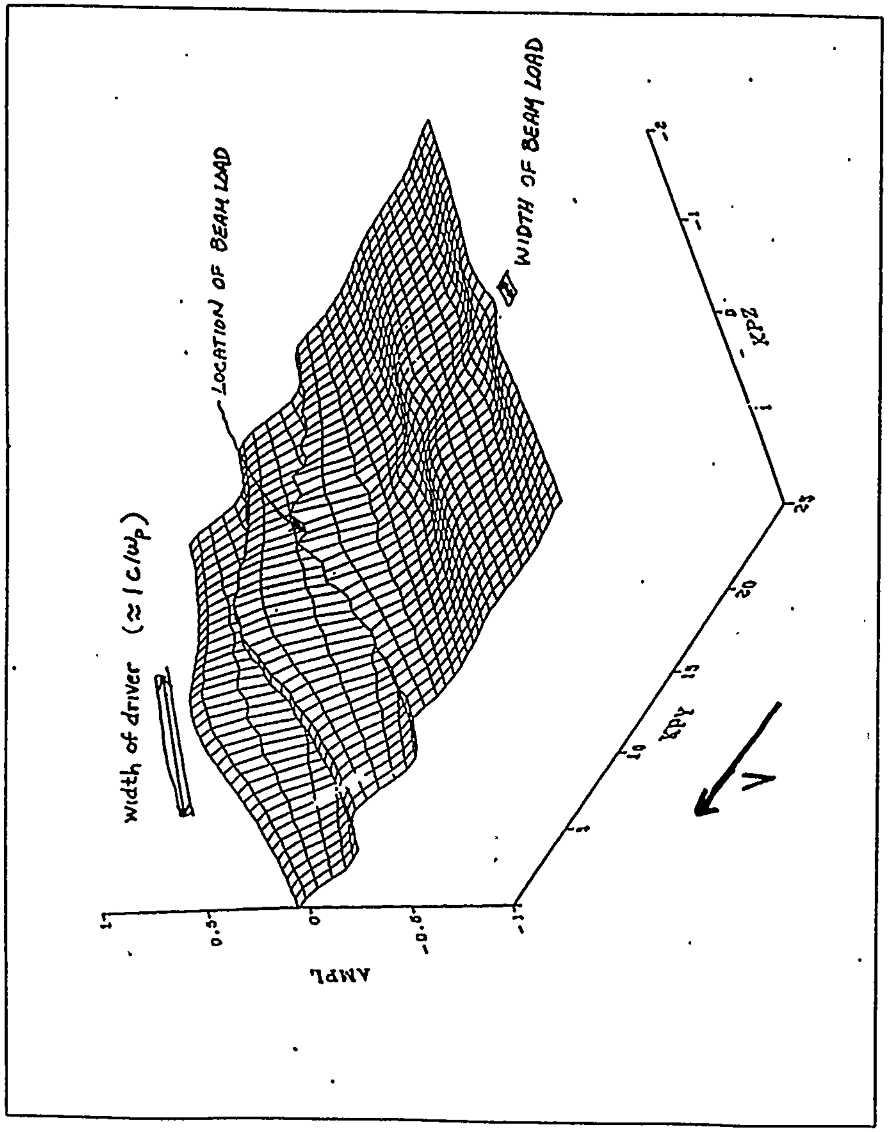

Part. Accel. 22, 81 (198

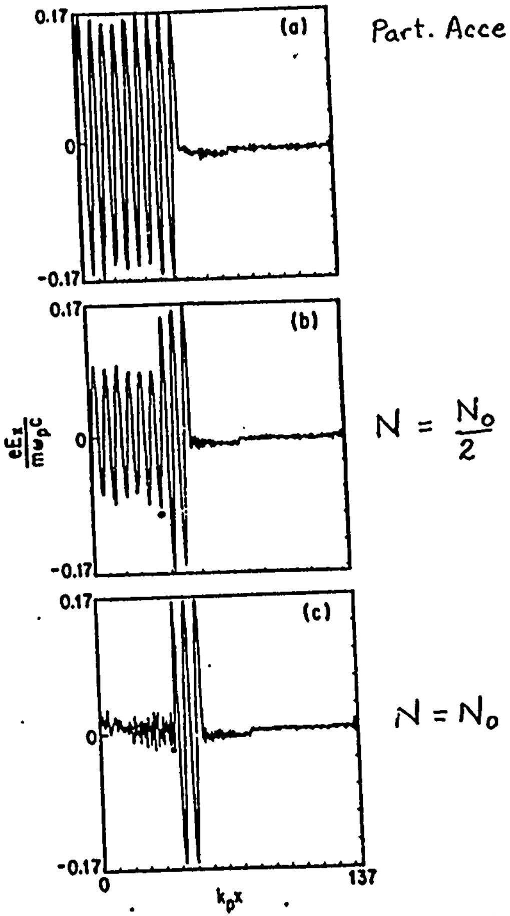

FIGURE 1 Total electric field in a 1-D simulation loaded with short bunches of (a) 0, (b) $0.5N_0$, and (c) N_0 (positively charged) electrons on the third peak of an accelerating wave. Simulation consisted of 14,000 partricles on 19024 grids; system length $= 170c/\omega_p$, particle size $= 0.11c/\omega_p \approx$ bunch width, wave amplitude $n_1 \approx 0.16n_0$ (produced by wake-field mechanism), time step $= 0.04\omega_p^{-1}$, $\omega_p t = 40$, $\gamma^{\text{beam}} = \gamma^{\text{wave}} = 60$.

Bunching Options & Tradeoffs

Correlated Energy + Chicanes, Wigglers or α-magnets

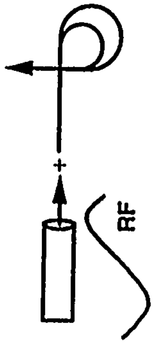

Pro: Technology Development Project

Con: Jitter/Synchronization

Fast-response Cathode + Short-pulse Laser

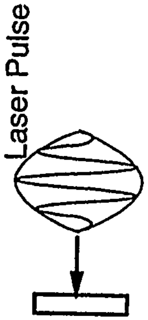

Pro: Technology Development Project

Con: Not Short Enough

Plasma Klystron

Pro: Just what you want for pulse length/synch

Con: Physics Development Project

Histogram Summary

100 MeV params, 15MeV injection

$\varepsilon_O = 3\ \pi$ mm mrad (Z_o=1.2cm, w_o=185µm)

$\varepsilon_N = 7\ \pi$ mm mrad

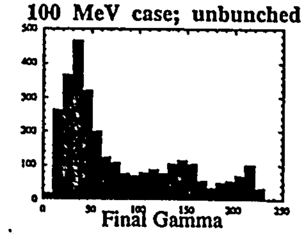

$\varepsilon_N = 10\ \pi$ mm mrad

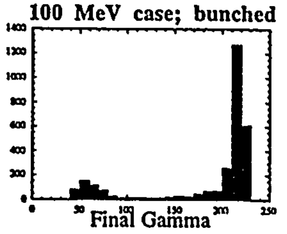

1 GeV parameters, 10MeV injection

$\varepsilon_O = 10\ \pi$ mm mrad (Zo=3.1cm, w_o=100µm)

$\varepsilon_N = 28\ \pi$ mm mrad

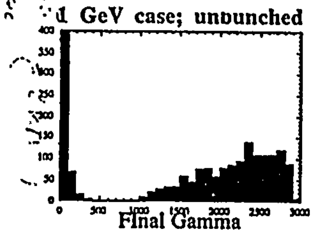

$\varepsilon_N = 15\ \pi$ mm mrad

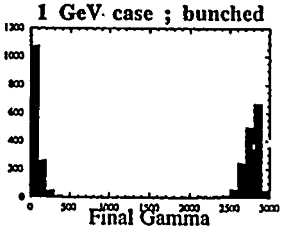

PLASMA KLYSTRON BUNCHER

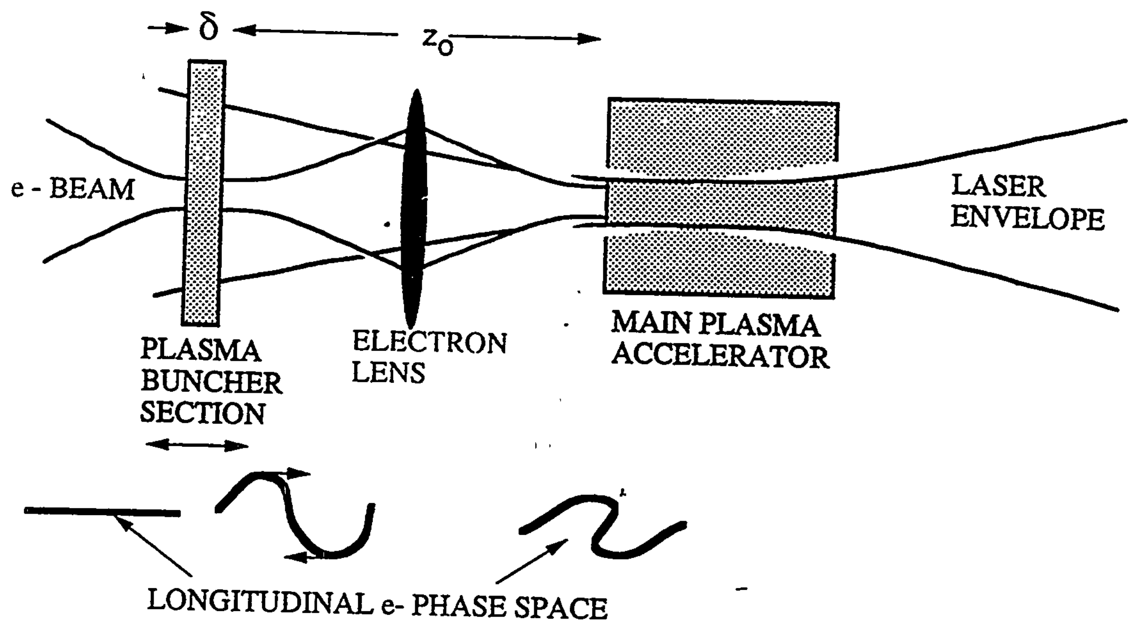

slippage: $\Delta L = (z_o/\gamma^2)(\Delta\gamma/\gamma) = \lambda_p/4$

T. Katsouleas et. al.

Test Particle Simulation of Plasma Buncher

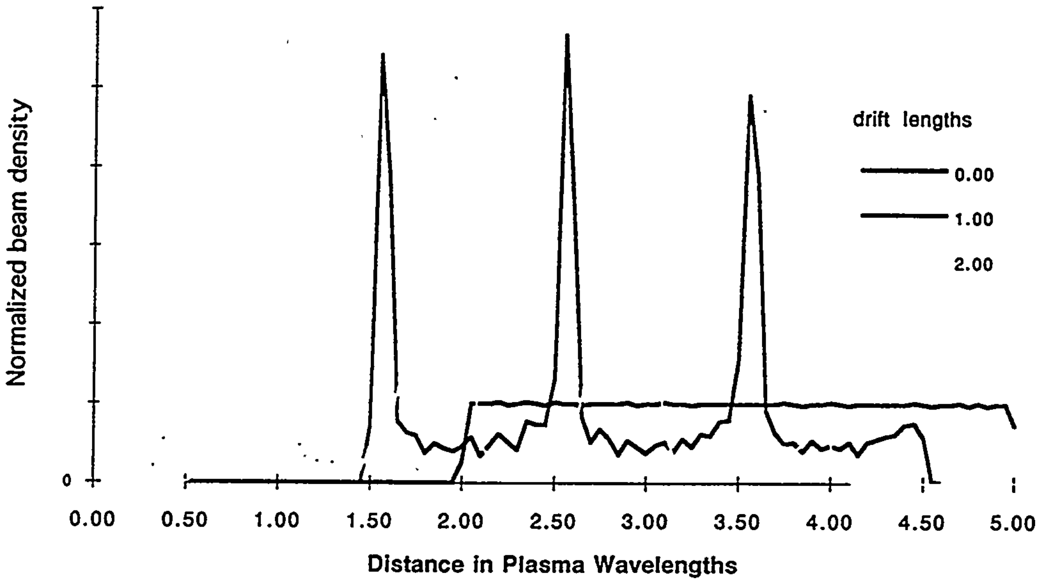

VACUUM BEAT WAVE BUNCHER

(OPTICAL KLYSTRON)

D. Gordon, et al.

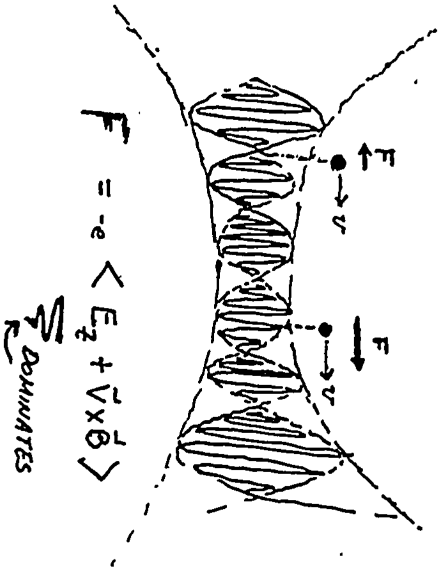

$$F = -e \langle \underbrace{E_z}_{\text{DOMINATES}} + \vec{v} \times \vec{B} \rangle$$

Similar to Esarey, et al. Phys. Rev. E ('95)

Laser Driven Electron Injection IV

D. Umstadter U. Michig

Time Evolution Of Injection Process (Transverse Injection

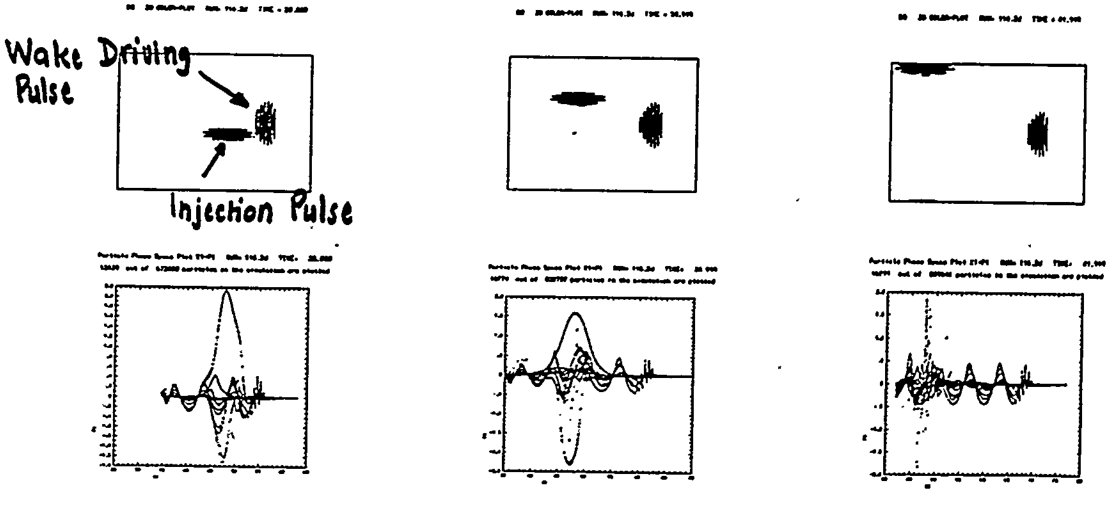

The above shows the B3 field (pointing out of the simulation plane) and the X1-P1 phase space for 2% of all particles.

UCLA - Roy Hemker

Bunching After 7 m Drift Space

250 μm Aperture at z = 25 cm (25% Transmission)

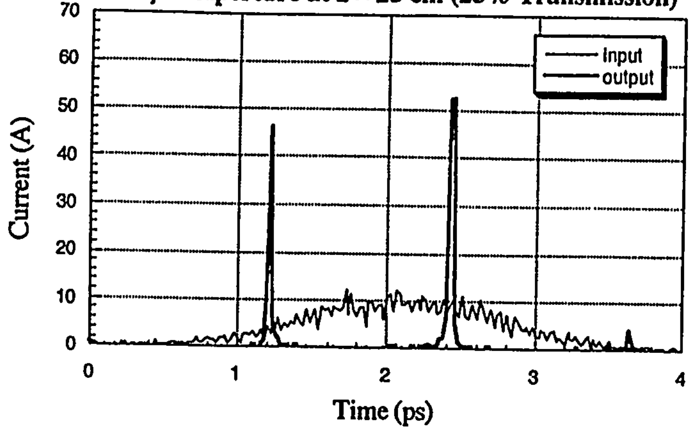

700 μm Aperture at z = 25 cm (50% Transmission)

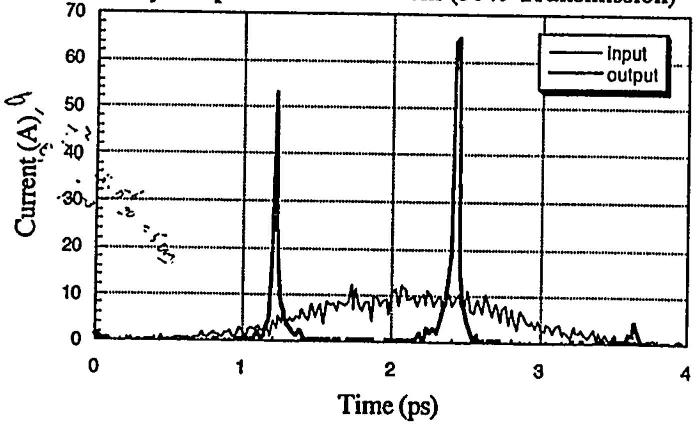

Temporal Beam Structure 20 cm Beyond Focus

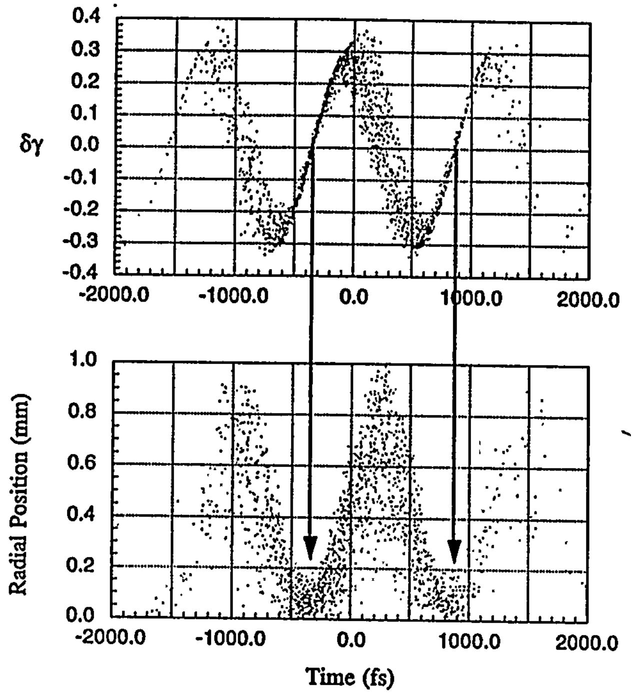

$n_p = 1.4\times10^{14}\,cm^{-3}$
$Q = 1\,nC$
$\Delta\tau = 4\,ps$

spot size = 300 μm

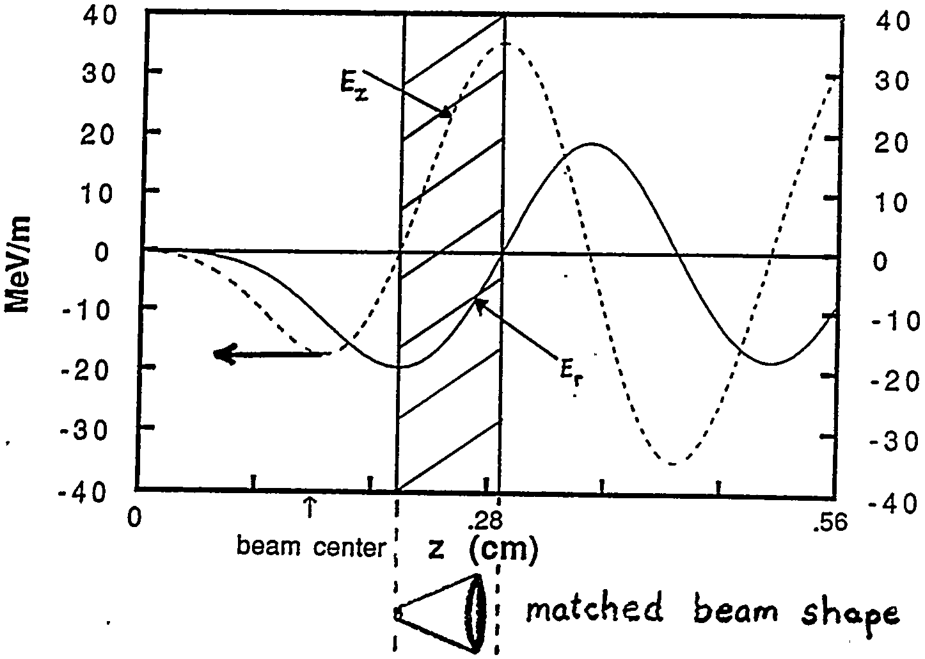

Radial Plasma Wave Fields & ε

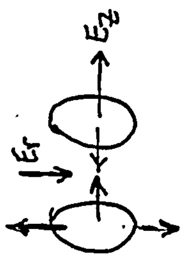

$E_z \sim E_0 \sin k_p(z-ct)\,(1-r^2/a^2)$

$\frac{\partial E_z}{\partial r} = \frac{\partial E_r}{\partial z}$ $\quad (\nabla\times E)_\theta = \frac{\partial B_\theta}{\partial t} = 0$,

linear $\left\{ E_r = E_0 \cos k_p(z-ct)\ 2r/k_p a^2 \right.$
blowout $E_r = 2\pi n_0 e r$

Focusing ⇒ betatron oscillations

$\gamma m \ddot{y} = \frac{-eE_r}{y}\, y$

Beam matching ⇒ balance of thermal press & focusing

⇒ $\beta_{beam} = \beta_{foc.ch}$

$\sigma_{eq}^2/\varepsilon = 1/k_p$

⇒ σ_{eq}

Equilibrium emittance, radius

EXAMPLE

NORMALIZED WAVE AMPLITUDE $\frac{eE}{m\omega_p c} \sim \frac{1}{2}$

$\sin\phi \sim 1/2$, $\gamma = 20$ (10 MeV injector)

SPOT SIZE $R = a\sqrt{2} \approx 100\mu$

$\varepsilon_N = 10\pi$ mm-mrad

$$\Rightarrow \quad X_{eq} = \frac{\varepsilon_N R}{2\pi\sqrt{\gamma\, E'\sin\phi}} \approx 15\,\mu m$$

for a matched beam

Test Particle Simulation Model

(R. Williams, et al. 1990)

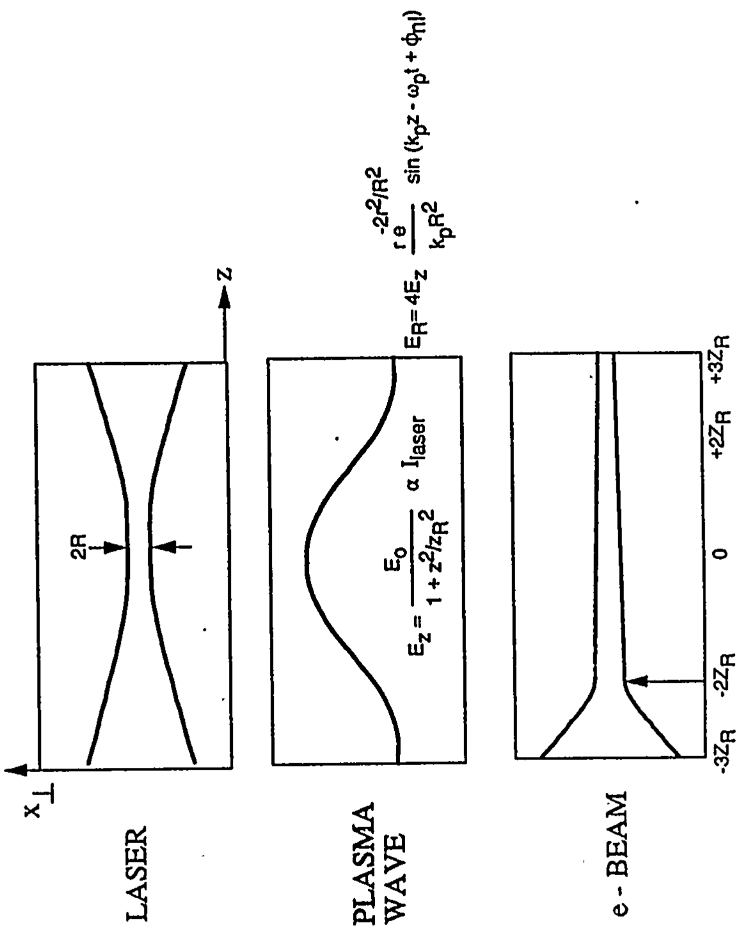

Plasma Accelerator Simulation

Real Space (r-z) of Test Particles

15,000 particles

$\varepsilon_N = 10\,\pi$ *mm-mrad*

$[<x^2><x'^2> - <xx'>^2] = 9$ *mm-mrad*

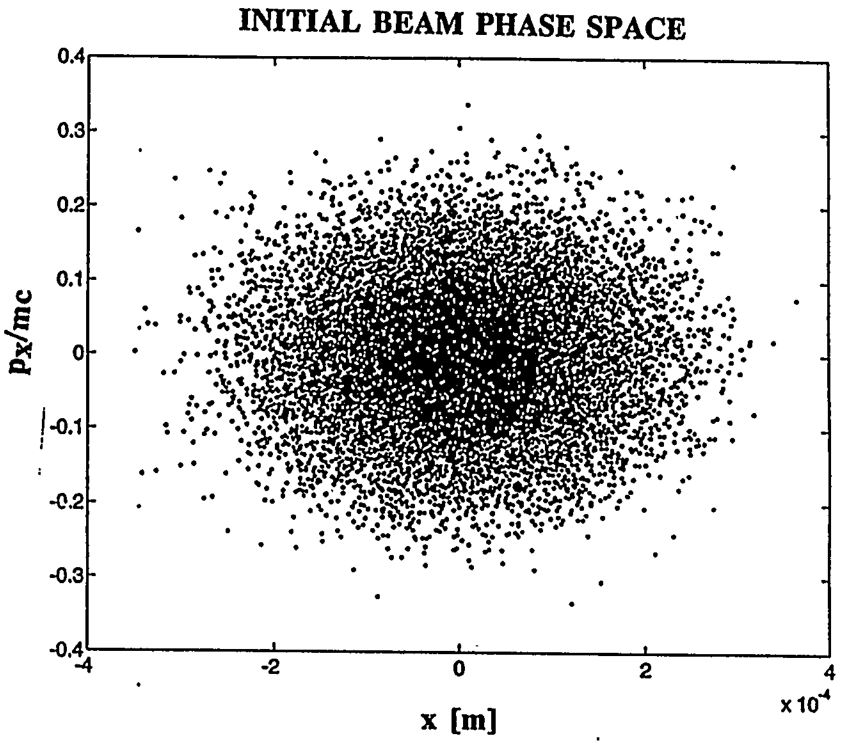

$[\langle x^2\rangle\langle x'^2\rangle - \langle xx'\rangle^2]$ = 17 mm-mrad
(avg. over particles with $\gamma > 1500$)

Synchrotron Radiation in Plasma Waves

Radial fields $\Rightarrow$

$$x_\perp = x_0 \sin k_\beta ct$$

$$P \cong \frac{2}{3}\frac{e^2}{c}\gamma^4\dot{\beta}^2 \qquad \dot{\beta} = \frac{\ddot{x}_\perp}{c} \doteq k_\beta^2 c\, x_0$$

$$= \frac{\omega_p^2}{2\gamma c} x_0$$

for ion channel focusing — n.l. blowout regime
(worst case)

$$X_0 = X_{eq} = \left(\frac{8\epsilon_N^2 c^2/\omega_p^2}{\gamma}\right)^{1/4}$$

e.g., @ 5 TeV $\gamma = 10^7$

$n_0 = 10^{16}\,\mathrm{cm}^{-3}$ $\epsilon_N = 1\pi$ mm-mrad

$\Rightarrow c/\omega_p = 50\mu$ $X_{eq} = 0.2\mu$

$P_{loss} \sim 180$ MeV/m

$P \propto \gamma^{3/2}$

P_{loss} reduced by wave shaping, hollow channels, etc.

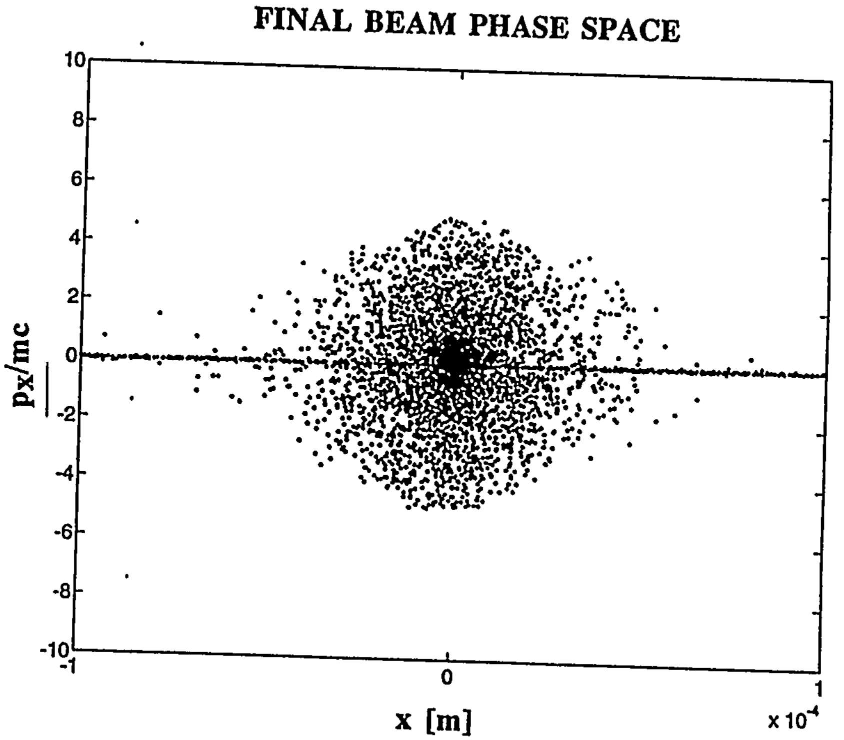

FINAL BEAM PHASE SPACE

PRODUCTION OF ULTRA SHORT LASER PULSES

C. P. J. Barty, UCSD

New Modes of Particle Acceleration Techniques and Sources
Santa Barbara, August 21, 1996

Production of Ultrashort Laser Pulses

C. P. J. Barty

Institute for Nonlinear Science
University of California, San Diego

Dr. Ting Guo	(UCSD)
Dr. Christoph Rose-Petruck	(UCSD)
Dr. Ferenc Raksi	(UCSD)
Dr. Jeff Squier	(UCSD)
Prof. Kent Wilson	(UCSD)
Dr. Barry Walker	(UCSD)
Dr. Vlad Yakovlev	(UCSD)
Dr. Jianshu Cao	(UCSD)
Dr. Michal Ben-Nun	(UCSD)
Dr. Catherine Le Blanc	(ENSTA, Paris)
Dr. Georg Korn	(Max-Born, Berlin)
Dr. Koichi Yamakawa	(JAERI, Tokyo)

Outline

- Ultrafast Perspective and Motivation
- Chirped Pulse Amplification
- Ultrafast CPA
    - Unique Concerns
    - Dispersion Control
    - Spectral Control
- Lab Tour of UCSD Systems and Applications
- Summary and Conclusions

Perspective, 100 Terawatts

100 TW = 30 x's world's electric grid capacity

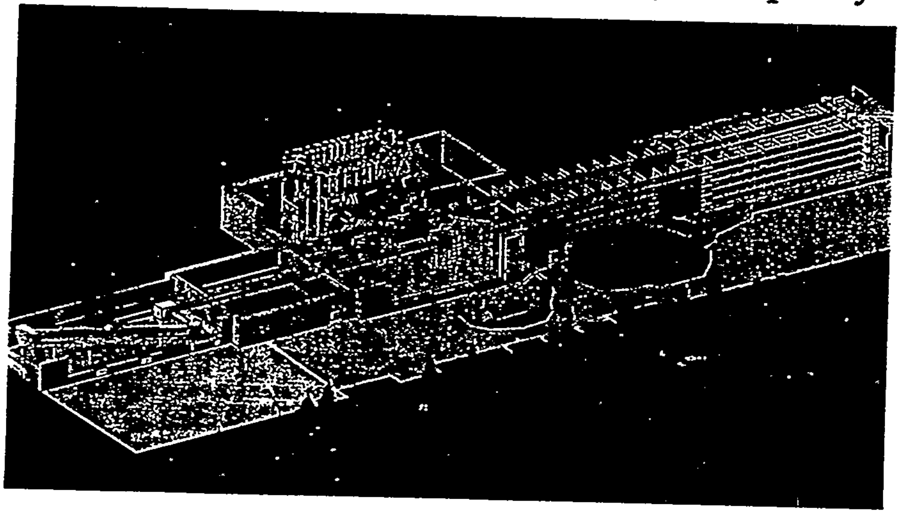

NOVA
10 beams @ 10 TW/beam = 100 TW
1 shot/ hour
1 ns pulse duration

UCSD
100 TW in single beam
36,000 shots/hour = 10 Hz
15 fs pulse duration

Perspective

15 fs ~ 5 optical cycles @ 800 nm

$c\Delta t$ = 4.5 µm

pancake of photons

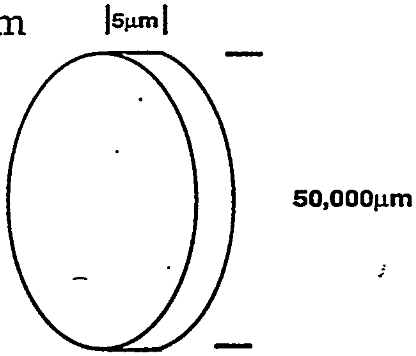

$v_{ion}\Delta t$ = 0.2 Å @ 300 K

ion and electron motion decoupled

τ_{rad} α λ^2

k-shell transitions

---

erspective

If diffraction limited and 100 TW @ 15 fs

I_{peak} = 10 Zettawatts/cm^2 = 10^{22} W/cm^2

(NOVA ~ 10^{14} W/cm^2)

E_{peak} = 3×10^{14} V/m ~ 1000 atomic units

P_{photon} = 10^{12} atmospheres

V_{focal} = 4×10^{-12} cm^3 ~ one bacterium

(NOVA ~200 cm^3)

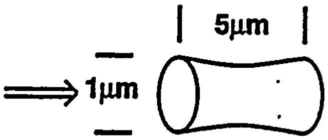

U/V = 4×10^{11} J/cm^3 = 90 tons TNT/cm^3

= 150 x10^6 K black body

= 4.2 mg/cm^3

Generic Chirped Pulse Amplification

Strickland & Mourou, Opt. Comm. 56, 219, 1985
Cook, Proc. IRE (1960), p. 310

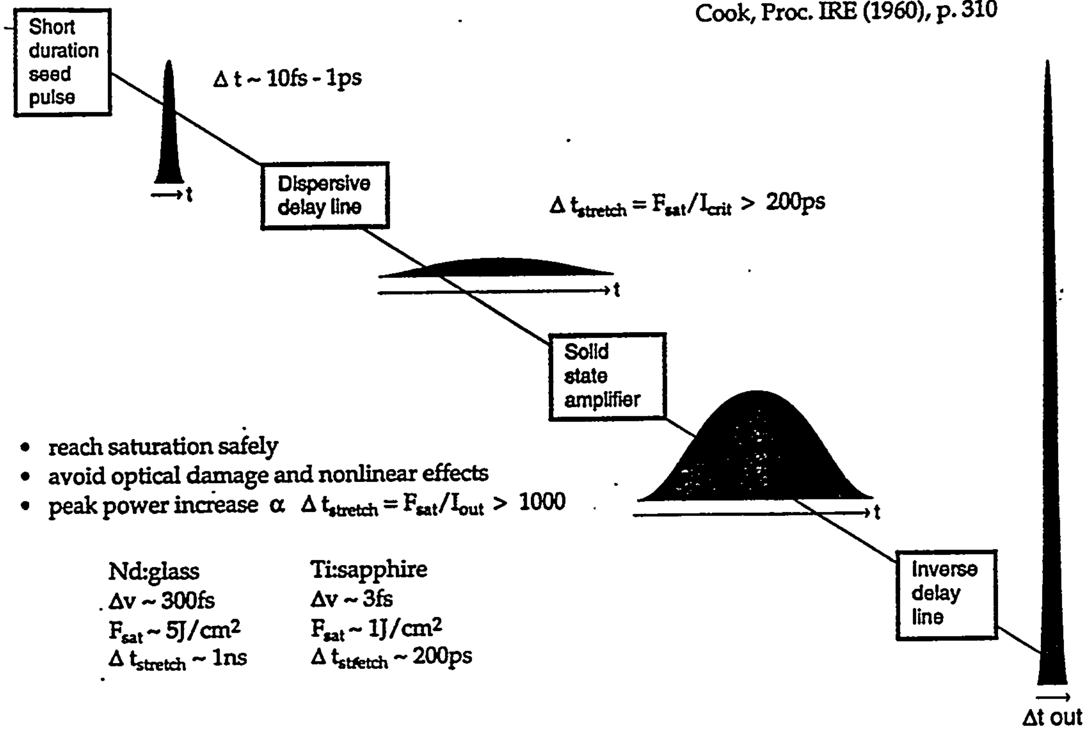

Short duration seed pulse

$\Delta t \sim$ 10fs - 1ps

Dispersive delay line

$\Delta t_{stretch} = F_{sat}/I_{crit} > 200ps$

Solid state amplifier

Inverse delay line

- reach saturation safely
- avoid optical damage and nonlinear effects
- peak power increase α $\Delta t_{stretch} = F_{sat}/I_{out} > 1000$

Nd:glass	Ti:sapphire
$\Delta v \sim 300fs$	$\Delta v \sim 3fs$
$F_{sat} \sim 5J/cm^2$	$F_{sat} \sim 1J/cm^2$
$\Delta t_{stretch} \sim 1ns$	$\Delta t_{stretch} \sim 200ps$

Energy Extraction Efficiency

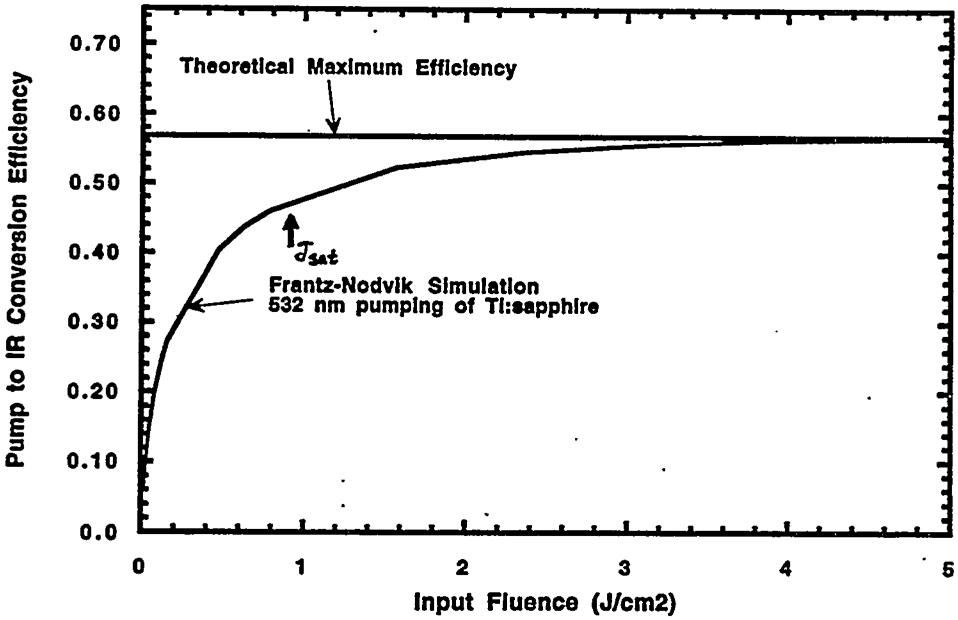

ltrashort Pulse CPA Concerns

- high order phase distortions
- gain narrowing
- refractive distortions
- bandwidth of optical components
- bandwidth and saturation fluence of gain media
- self focusing and self phase modulation by air
- damage threshold of gratings
- amplification efficiency
- beam quality
- pulse quality

volution of CPA

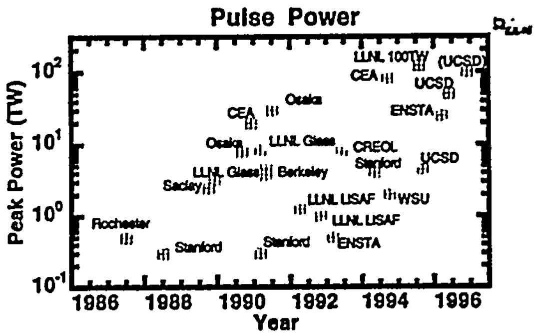

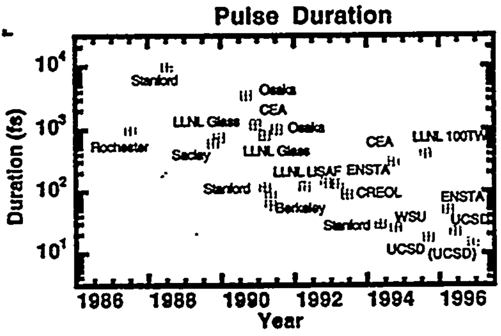

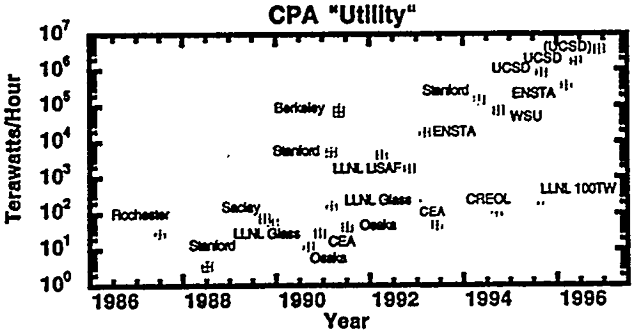

Refractive Pulse Distortions

- Curved pulse fronts
- Spatially varying group dispersion

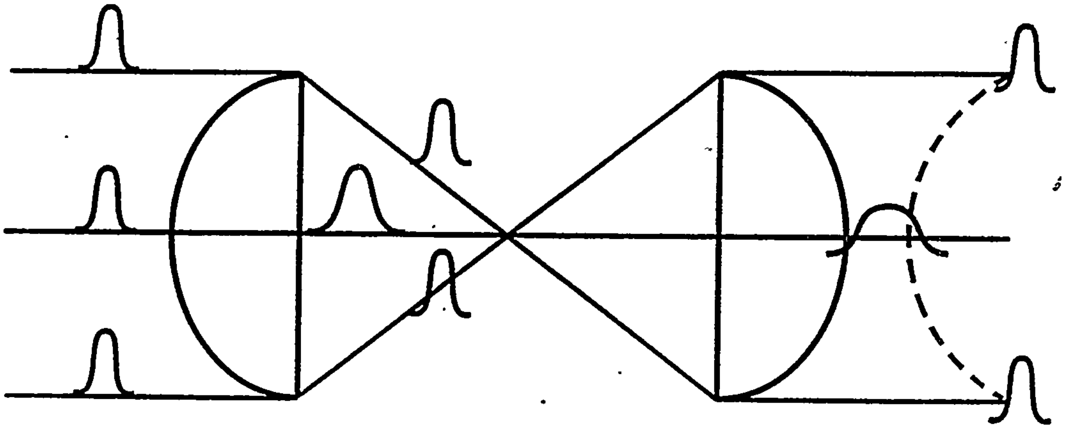

- Use reflective optics whenever possible
- Use Galilean rather than Keplerian telescopes
- Use large f-numbers, > 25
- Use achromats

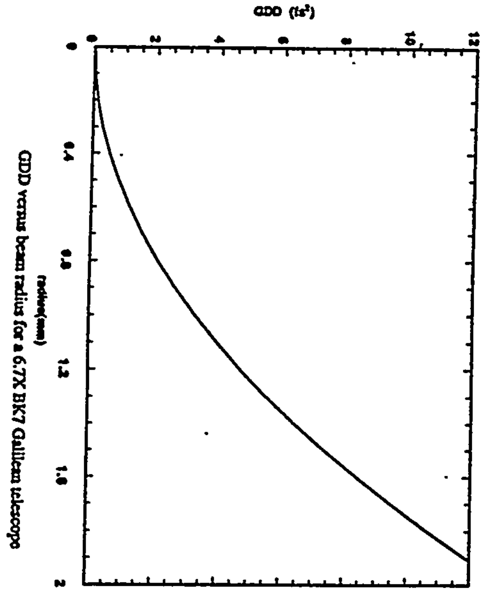

GDD versus beam radius for a 6.7X BK7 Galilean telescope

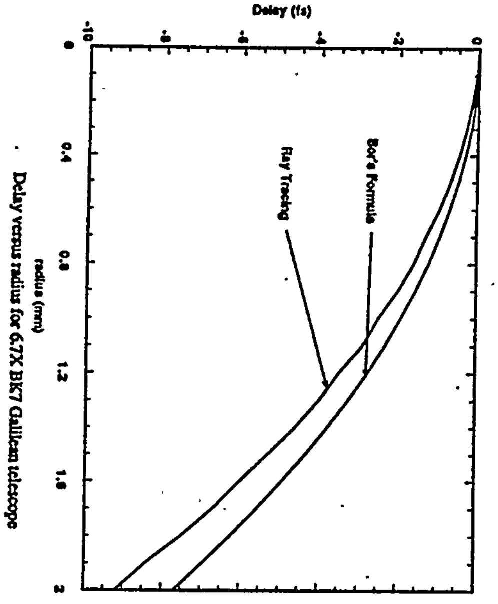

Delay versus radius for 6.7X BK7 Galilean telescope

Dispersion Control Critical

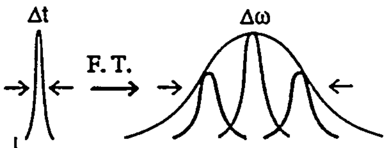

$$\omega)=\left.\frac{\partial\phi}{\partial\omega}\right|_{\omega 0}+\left.\frac{\partial^2\phi}{\partial\omega^2}\right|_{\omega 0}(\omega-\omega 0)+\frac{1}{2}\left.\frac{\partial^3\phi}{\partial\omega^3}\right|_{\omega 0}(\omega-\omega 0)^2+\frac{1}{6}\left.\frac{\partial^4\phi}{\partial\omega^4}\right|_{\omega 0}(\omega-\omega 0)^3+O\left(\Delta\omega^4\right)$$

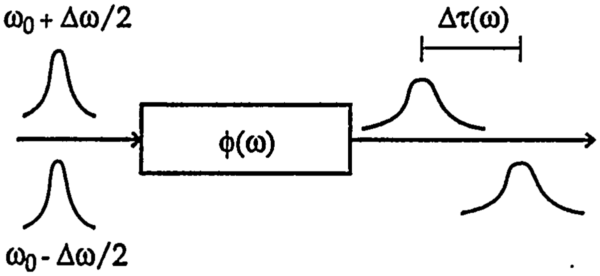

Group Delay $= \left.\frac{\partial\phi}{\partial\omega}\right|_{\omega 0}$

Group Delay Dispersion $= \left.\frac{\partial^2\phi}{\partial\omega^2}\right|_{\omega 0}$

Cubic Phase Distortion $= \left.\frac{\partial^3\phi}{\partial\omega^3}\right|_{\omega 0}$

Quartic Phase Distortion $= \left.\frac{\partial^4\phi}{\partial\omega^4}\right|_{\omega 0}$

10 fs		
	~	0.2 rad/fs
D	<	50 fs^2 (1 mm BK7)
ic	<	2000 fs^3
artic	<	30,000 fs^4

100 fs		
Δω	~	0.02 rad/fs
GDD	<	500 fs^2
Cubic	<	200,000 fs^3
Quartic	<	30,000,000 fs^4

)-fs-range CPA

- Control of Dispersion is Critical

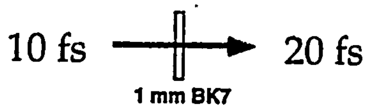

- Control of Spectral Reshaping Critical

Natural gain narrowing limit of
Ti:Sapphire ~30 fs @ 10^{12} amplification

Conventional CPA Devices

Pos. GDD Expander

$\tau_{red} < \tau_{blue}$

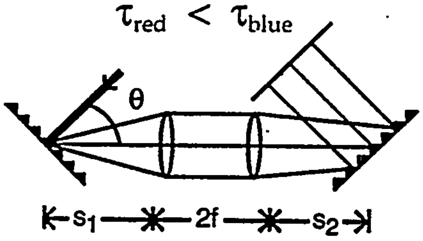

Δt = 300 ps

GDD

3,000,000 fs^2

Cubic

4,800,000 fs^3

Quartic

9,800,000 fs^4

Neg. GDD Compressor

$\tau_{red} > \tau_{blue}$

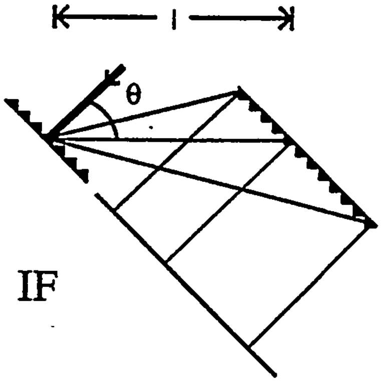

Dispersion is Matched IF and ONLY IF

- $l = 2f - s_1 - s_2$
- $\theta_{ex} = \theta_{comp}$
- lenses are paraxial
- NO material in the system

Small Mismatch = BIG ERROR

Dispersion Control

- The frequency dependent delay for any component can be described as $\tau(\lambda) = c_1\lambda + c_2\lambda^2 + c_3\lambda^3 + c_4\lambda^4 ...$
- The necessary condition for transform-limited output is $\tau_{system}(\lambda) = const$

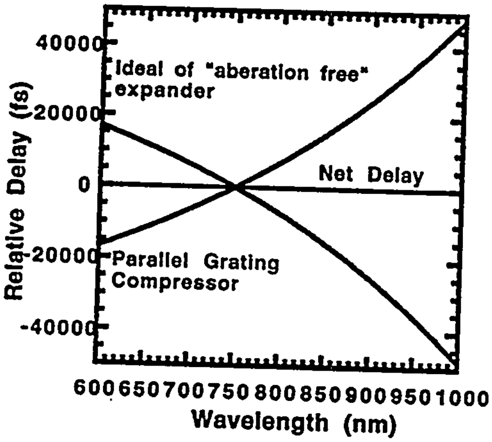

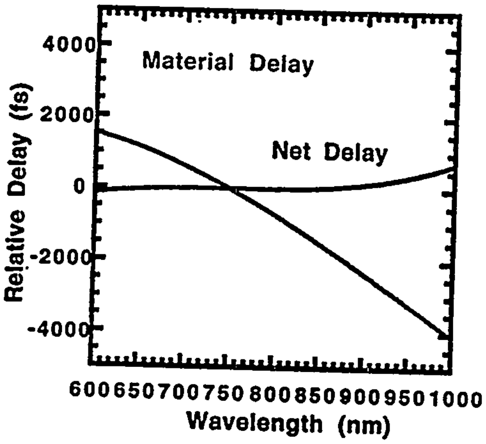

- Coefficients of an aberation free expander can be equal and opposite of a parallel compressor but not in the presence of any amplifier material

ispersion Balancing Expander

(Lemoff and Barty, Opt. Lett. 18, 1651, 1993)

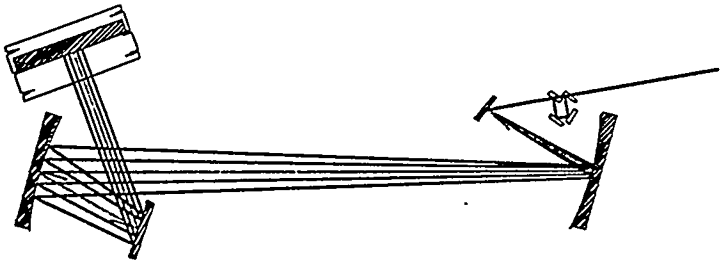

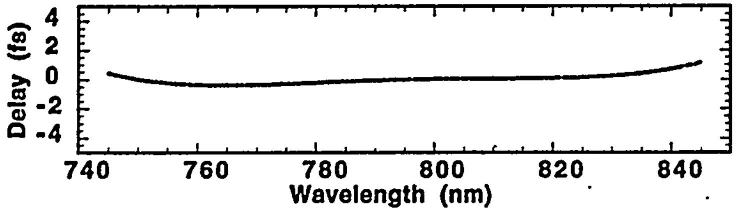

- Sperical aberrations allow control of up to quintic phase delays
- 100,000 times stretching and > 1 m of material path possible
- < 1-fs delay should allow ~12-fs amplication

pectral Reshaping during Amplification

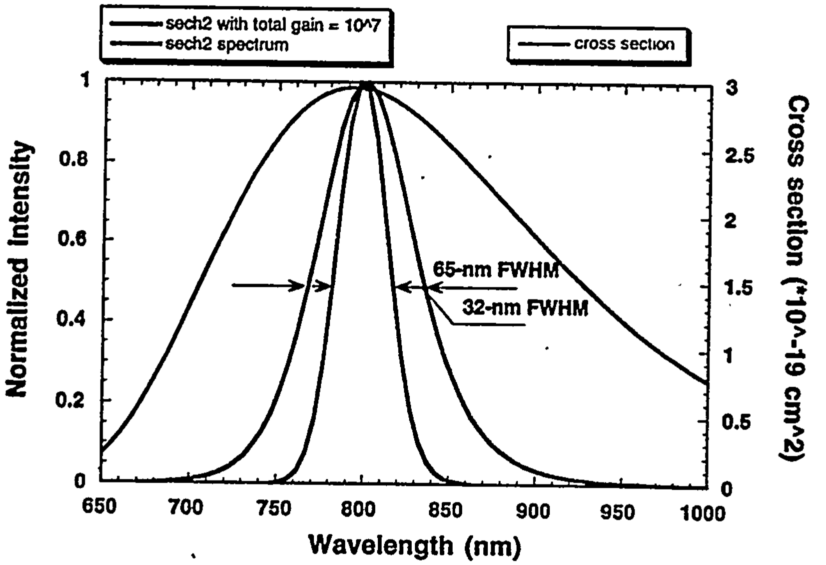

- Gain narrowing occurs as $\Delta\omega_{pulse}$ approaches $\Delta\omega_{gain}$
- A 10-fs sech^2 narrows from 65-nm to 32-nm for gain = 10^7

Regenerative Pulse Shaping (Barty et al. Opt. Lett. 21, 219, 1996)

- Most gain narrowing occurs in regen or preamp
- Relatively low gain per pass ==> only linear filter necessary
- Correct for gain narrowing on each pass
- Decreased single pass gain ==> increase round trips

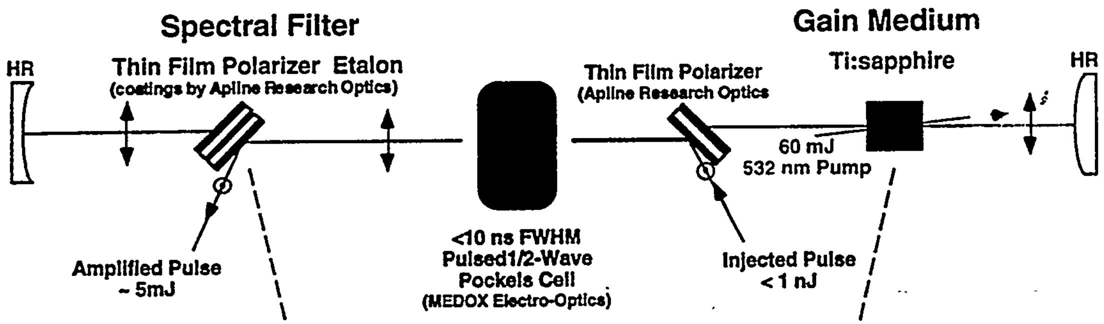

$$T(\omega) \approx \frac{c}{G(\omega)}$$

$$G(\omega) = e^{g(\omega)L}$$

$$Net\,Gain = [T(\omega)G(\omega)]^{n=\#of\ passes}$$

How to increase output bandwidth ?

$$Iout(\omega)=Iin(\omega)(1-\beta(\omega))^n G(\omega)^n$$

- $Iin(\omega)$

  Increase the input bandwidth -> 100nm spectrum
- $G(\omega)=Exp(N\sigma(\omega)L)$

  Increase the gain bandwidth -> Mixed glasses amplifiers
- $1-\beta(\omega)$

  Modulate the spectral losses ->Regenerative pulse shaping

Ideal Filter for Regenerative Pulse Shaping

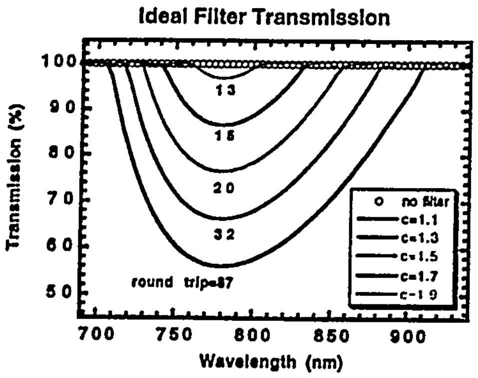

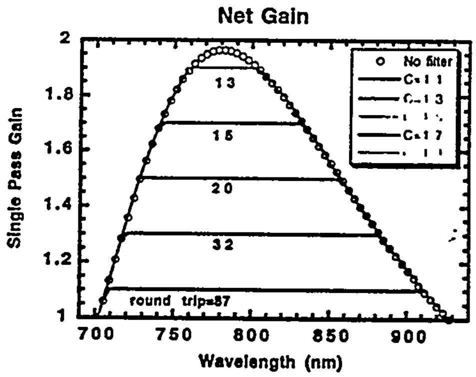

- Large modulation width desired
- Large modulation depth desired

---

tracavity Spectral Filters

Birefringent filter

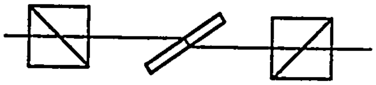

- hard to manufacture
- limited adjustability
  <40 nm FWHM

Prism sequence with spatial mask

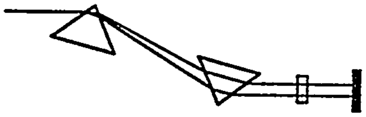

- pointing sensitive
- low resolution
  ~80 nm FWHM

Angle-tuned thin etalon

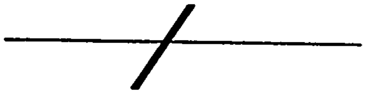

- low damage threshold
- low modulation depth
- depth and width coupled
  ~60 nm FWHM

Air-spaced etalon

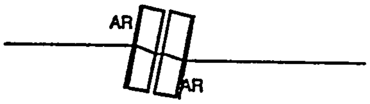

- low modulation depth
- high damage threshold
  ~60 nm FWHM

Thin Film Polarizer Etalon
(patent pending CPJ Barty et al.)

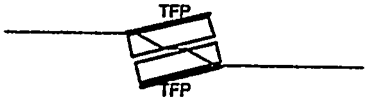

- high modulation
- low insertion loss
- high damage
- adjustable width & depth
  ~80 nm FWHM

Thin Film Polarizer Etalon (patent pending C. P. J. Barty et al)

$$T=(1-R)^2\Big/\left((1-R)^2+4R\sin^2\left(\frac{2\pi nd}{\lambda}\cos\theta\right)\right)$$

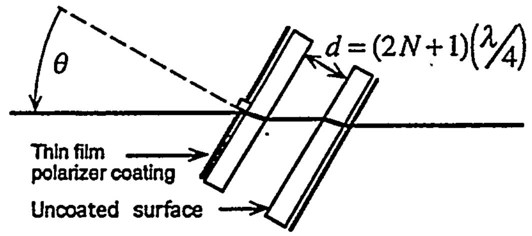

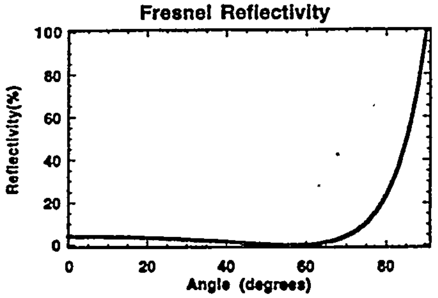

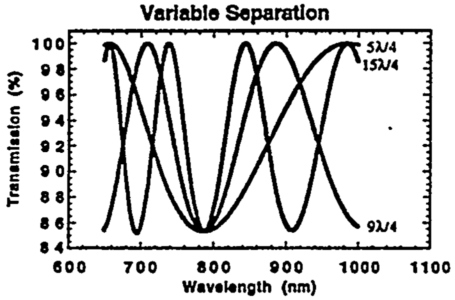

separation controls width

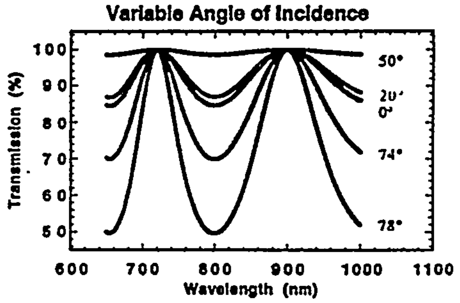

incident angle controls depth

- TFPE's provide large and adjustable modulation width and depth

---

ASE Output with TFP Etalon

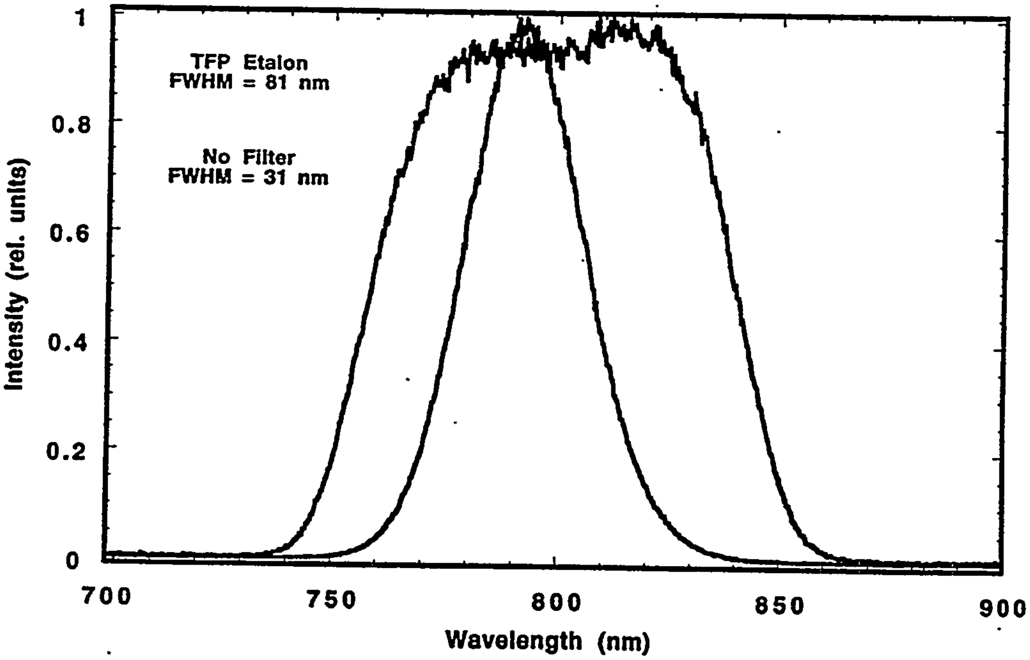

Jltrabroadband Amplification

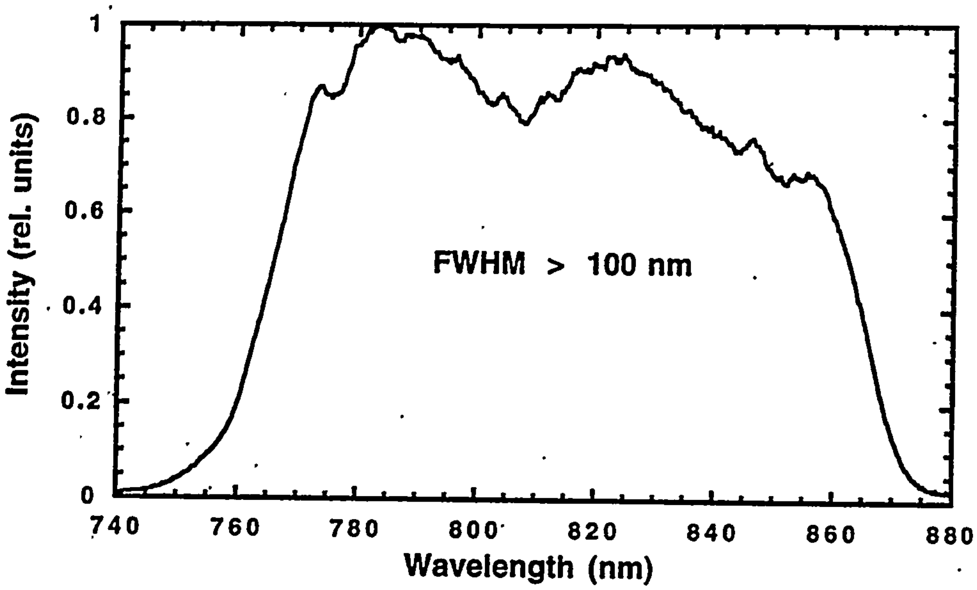

•two etalons used•

•transform limit would correspond to ~12 fs pulse•

ectronic Tunability of Amplified Pulses

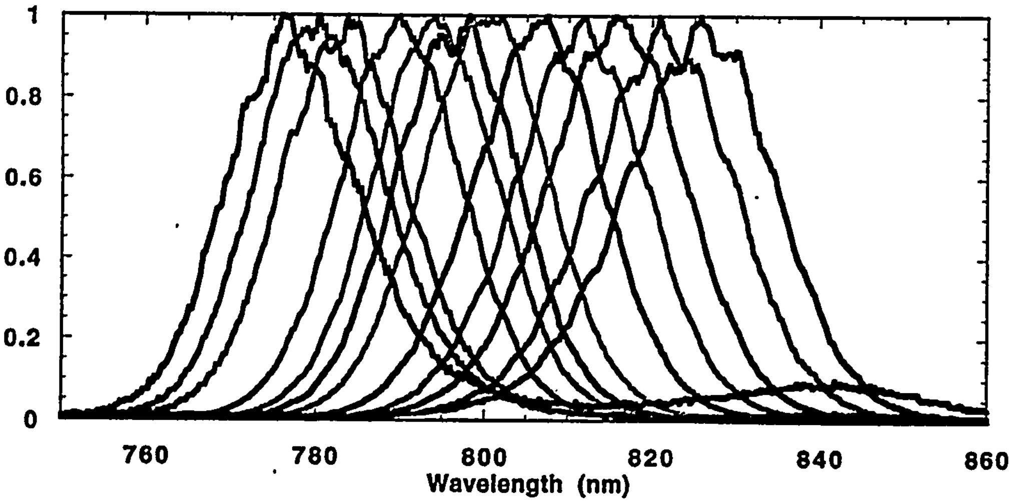

- Changing the etalon spacing tunes the output in wavelength
- Spacing change necessary is < $\lambda/2$

Two Color Amplification

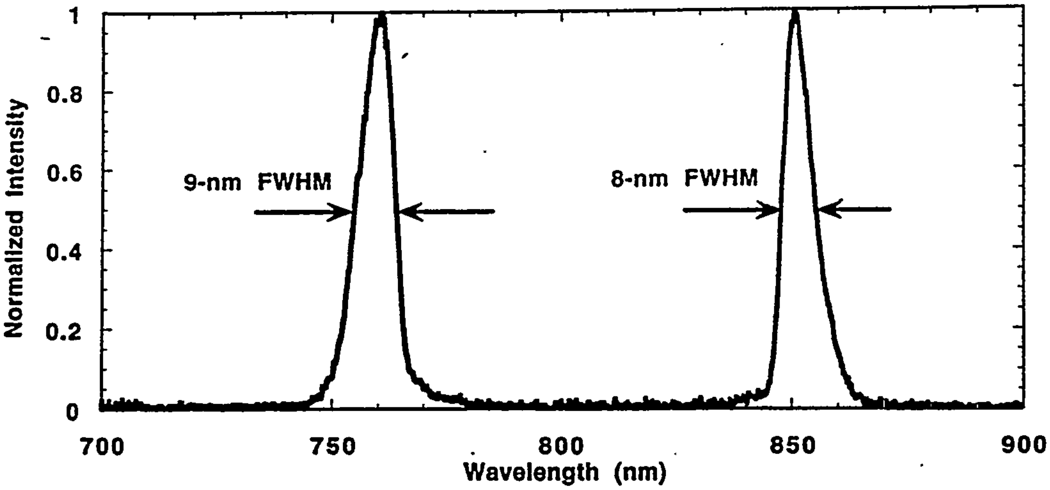

- 2 etalons were used in the regenerative amplifier
- After amplification > 20 mJ per color
- Ideal for IR generation via difference frequency mixing

or PBWA

UCSD Ultrafast Laser Systems

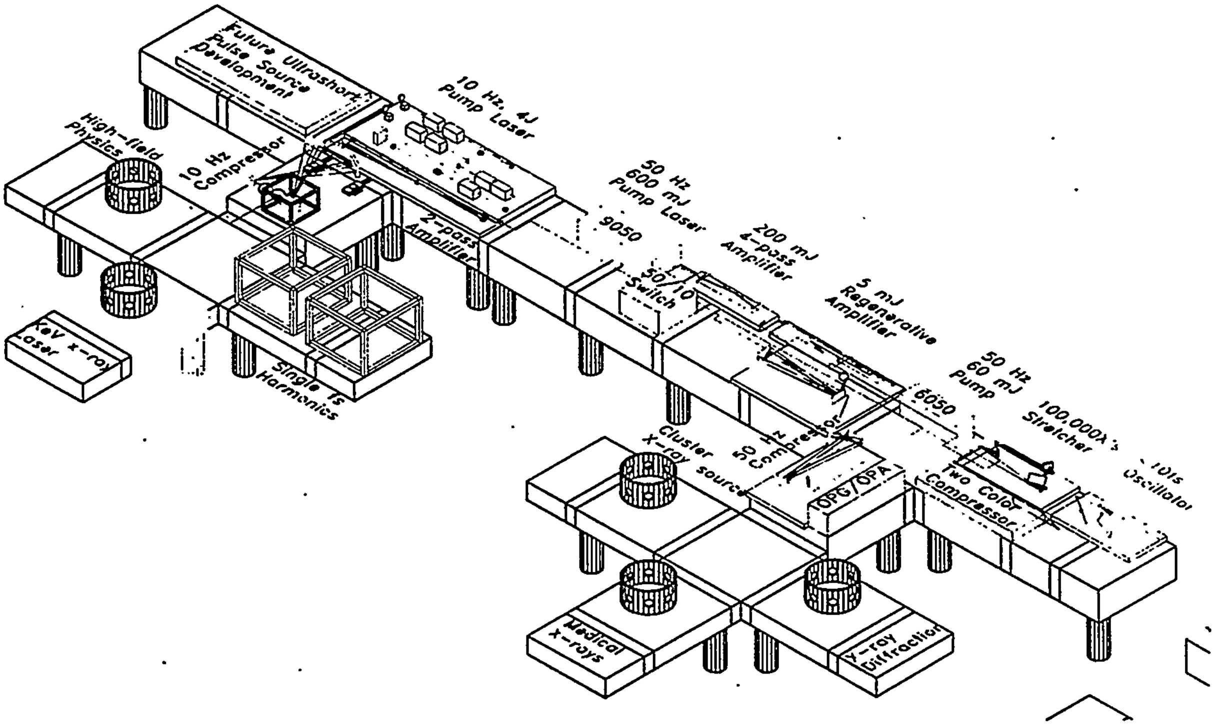

esign Goals of UCSD Systems

pump energy	extracted energy	number of passes	beam size (mm)	IR Intensity GW/cm2	IR Fluence J/cm2	amplifier rate
50 mJ	10 mJ	15	2	0.43	0.32	50 Hz
620 mJ	260 mJ	4	4.4	2.3	1.7	50 Hz
5 J	2.3 J	2	9	4.9	3.6	10 Hz

Hz system
~10 TW, ~15 fs pulses
plications: Ultrafast x-rays for studies of molecular
namics and time-gated medical imaging

Hz system
~100 TW, ~15 fs pulses
plications: High field physics, novel particle
celerators, x-ray lasers, sub-femtosecond harmonics

SD Ultrafast Systems (Barty et al. Opt Lett, 21, 668, 1996)

- Dispersion & pulse shaping allow transform-limited ultrafast amplification

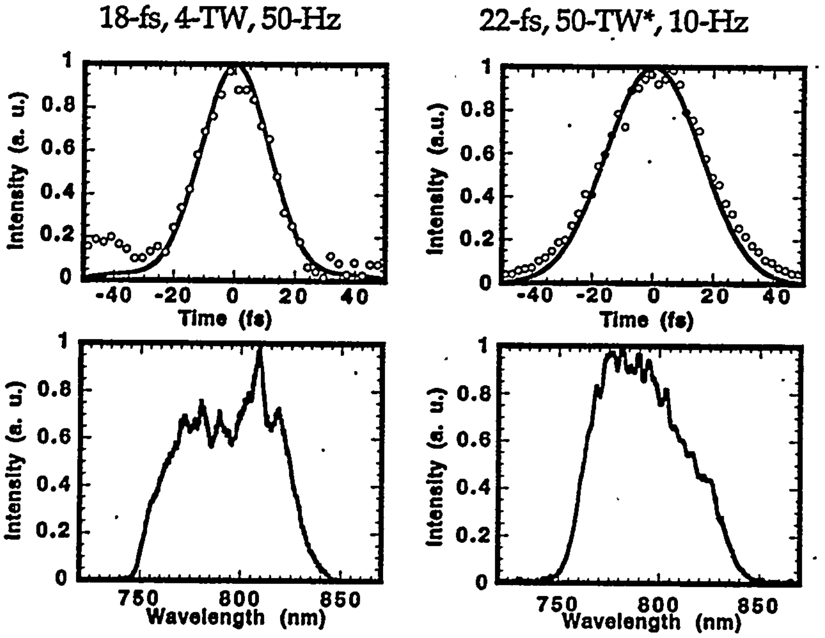

18-fs, 4-TW, 50-Hz

22-fs, 50-TW*, 10-Hz

*tests with attenuation before compression

Shorter Pulses Possible

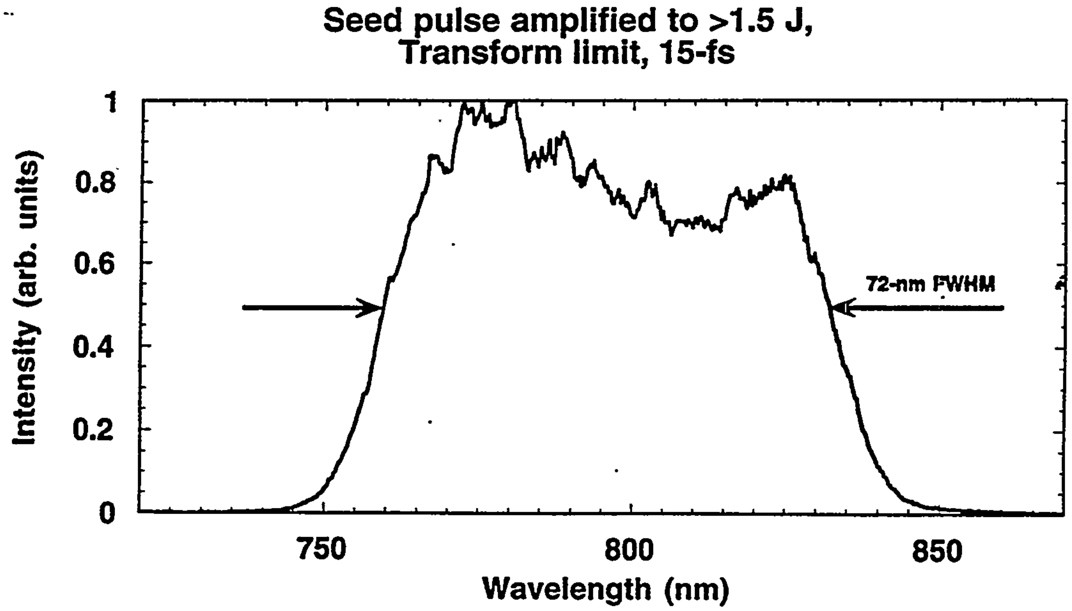

Beam Profile after Regenerative Amplifier

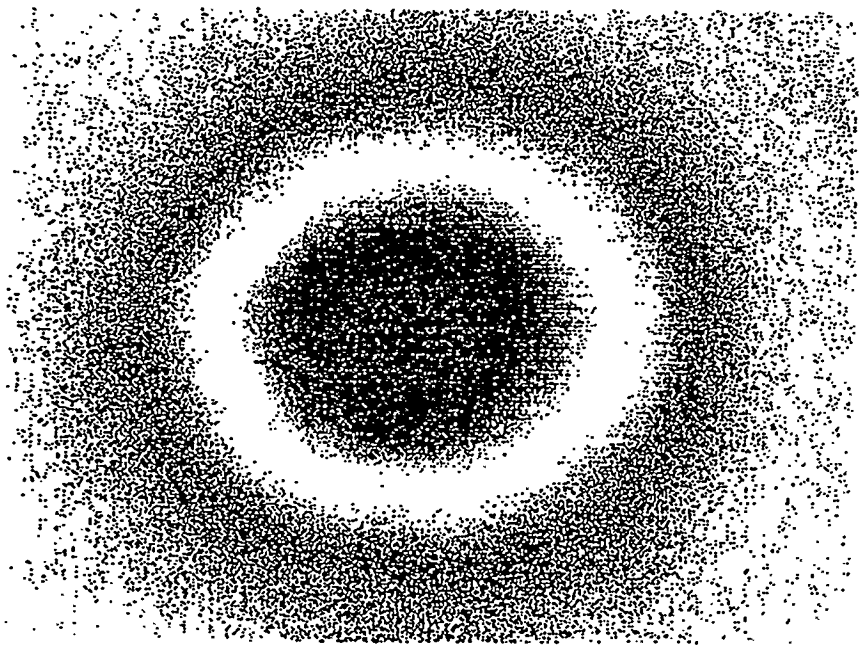

Beam Profile after 4 Pass Amplifier

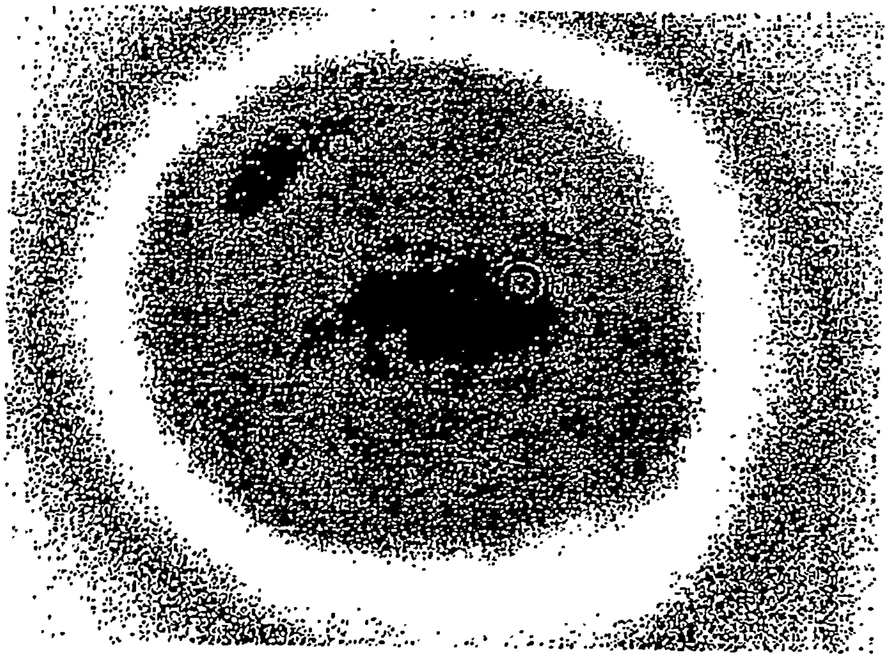

ficient High Peak Intensity Generation

Ti:sapphire vs. Diode-pumped Nd:Glass

additional losses for sapphire
- 80% for doubling before pumping
- 50% extraction from final amplifiers

benefits
- pulse duration 15 fs vs. 300 fs
- phase conjugated pump laser possible
- higher rep rate

==>> sapphire system should give 10 x's higher intensity

Summary

- Dispersion control on the femtosecond timescale
  - optimized cylindrical mirror based expander
  - 100,000 times pulse expansion
  - <1 fs pulse delay error
  - very large material paths possible
  - amplification at 80% of theoretical max demonstrated

- Gain reshaping control
  - regenerative pulse shaping
  - thin film polarizer etalon developed
  - >100 nm FWHM demonstrated
  - tunable amplification demonstrated
  - two color amplification demonstrated

- UCSD multiterawatt systems

  4 TW, 18 fs, 50 Hz (summer upgrades >100 mJ in 15 fs)
  45 TW, 22 fs, 10 Hz (summer upgrades > 1 J in 15 fs)

- Future systems based on UCSD technology

  kHz terawatt under development at UCSD (1996)
  1 Hz petawatt under development in Japan (1999)

Future Systems ??

1 Hz Petawatt Laser	Kilohertz Terawatt Laser
15 fs, 15 J	10 fs, 10 mJ
17.5 J before compression	12 mJ before compression
40 J pump energy required	27 mJ pump energy required

NOTE: Phase conjugate pump lasers with diffraction limited pump profiles already exist which are capable of producing pulses of 25 J at 6 Hz and 300 mJ at 600 Hz.

High Intensity Applications at UCSD

- Ultrafast laser produced x-rays
  - time resolved diffraction
  - time resolved absorption spectroscopy
  - high resolution, time-gated radiology
- single femtosecond high order harmonics
- ionization ignition in atomic clusters
- >10 TeV/m laser driven electron accelleration
- keV x-ray lasers
- highly relativistic laser/matter interactions
- ultradense plasma physics

Ultrashort Pulse Standing Wave Accellerator

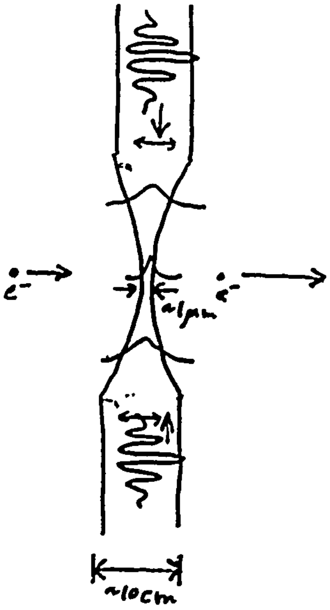

- B=0 for correct polarization
  No J×B term
- perturbation insensitive, in plane trapping
- effective field seen much shorter duration than optical pulse duration
- No plasma, & dielectric breakdown is minimized

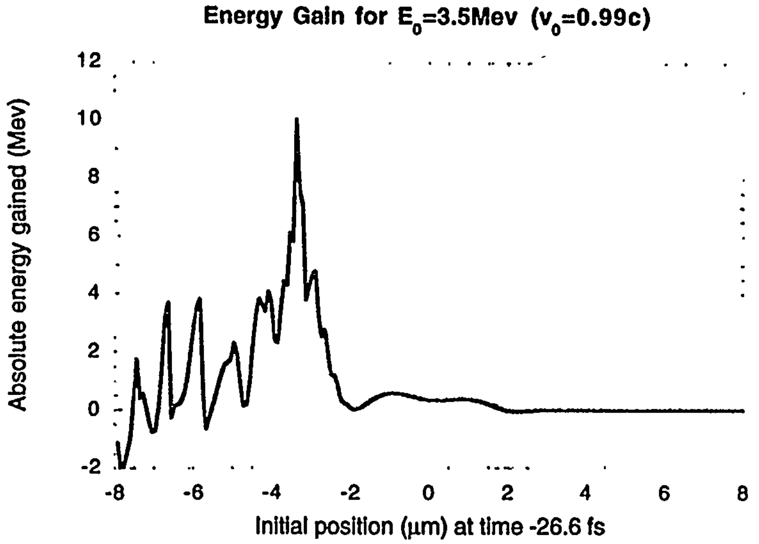
Energy Gain for E_0=3.5Mev (v_0=0.99c)
Absolute energy gained (Mev)
12
10
8
6
4
2
0
-2
-8
-6
-4
-2
0
2
4
6
8
Initial position (µm) at time -26.6 fs

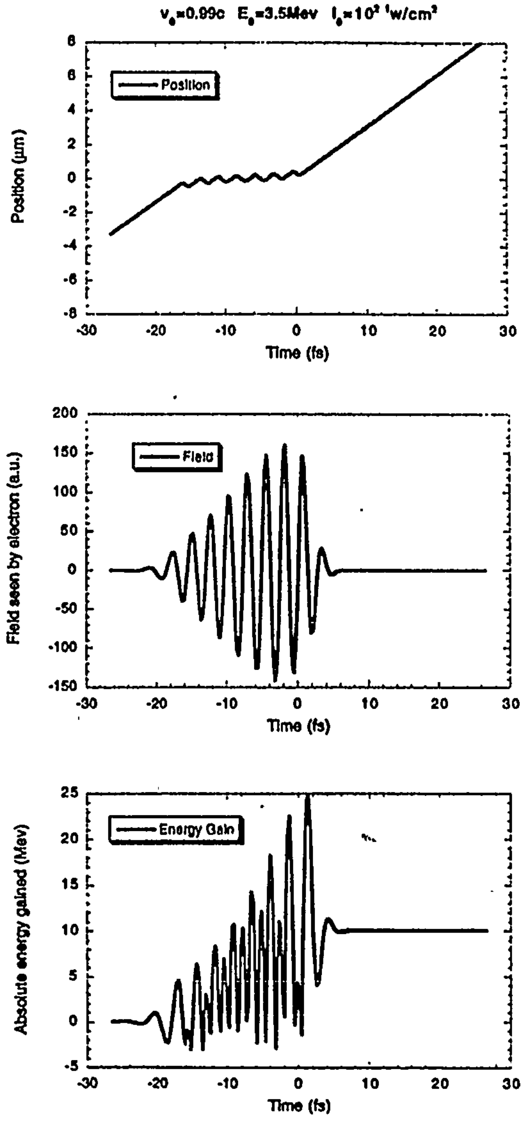
v_0=0.99c E_0=3.5Mev I_0=10^{21}w/cm^2
Position
Position (µm)
8
6
4
2
0
-2
-4
-6
-8
-30
-20
-10
0
10
20
30
Time (fs)
Field
Field seen by electron (a.u.)
200
150
100
50
0
-50
-100
-150
-30
-20
-10
0
10
20
30
Time (fs)
Energy Gain
Absolute energy gained (Mev)
25
20
15
10
5
0
-5
-30
-20
-10
0
10
20
30
Time (fs)

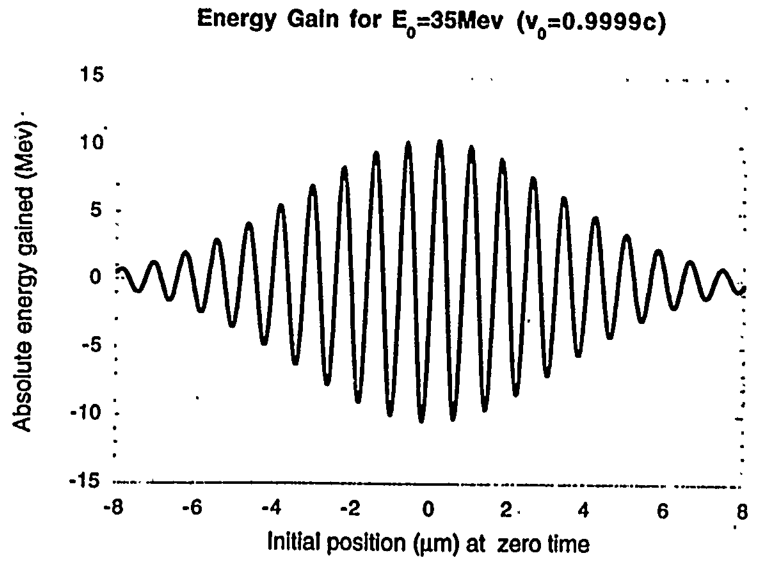

Energy Gain for E_0=35Mev (v_0=0.9999c)

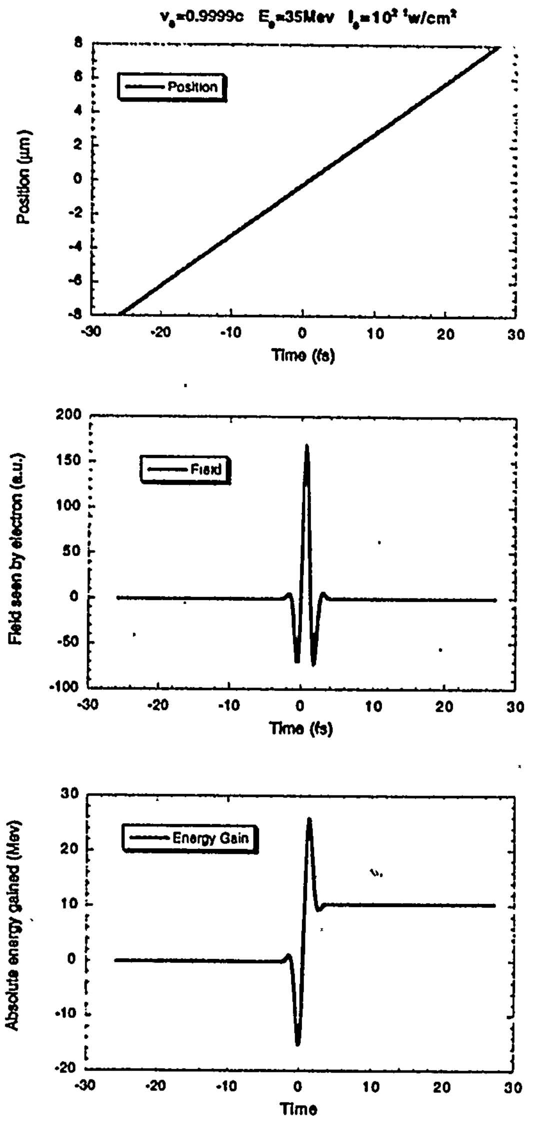

v_0=0.9999c E_0=35Mev $I_0=10^{21}$ w/cm^2

Macro stage

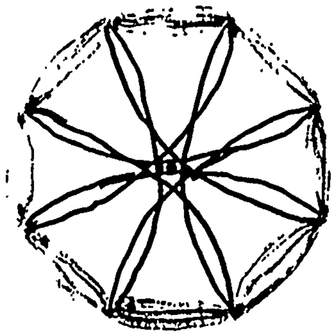

end on

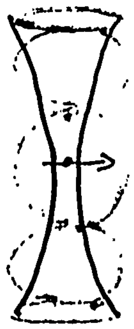

side view

example single macvostage

⇒6 focii

⇒60 MeV

⇒ 10 cm

⇓

600 MeV/m

SHORT BUNCH INJECTION, SYNCHRONIZATION, AND ACCELERATION IN LASER WAKEFIELDS

D. Umstadter, U. Michigan

CENTER FOR ULTRAFAST OPTICAL SCIENCE

Acceleration of a relativistic electron beam by a terawatt laser

D. Umstadter, J.-K. Kim, E. Dodd,
R. Wagner, S.-Y. Chen, and A. Maksimchuk

University of Michigan, Ann Arbor
http://www.eecs.umich.edu/USL-HFS

Experimental Layout of Laser Electron Accelerator

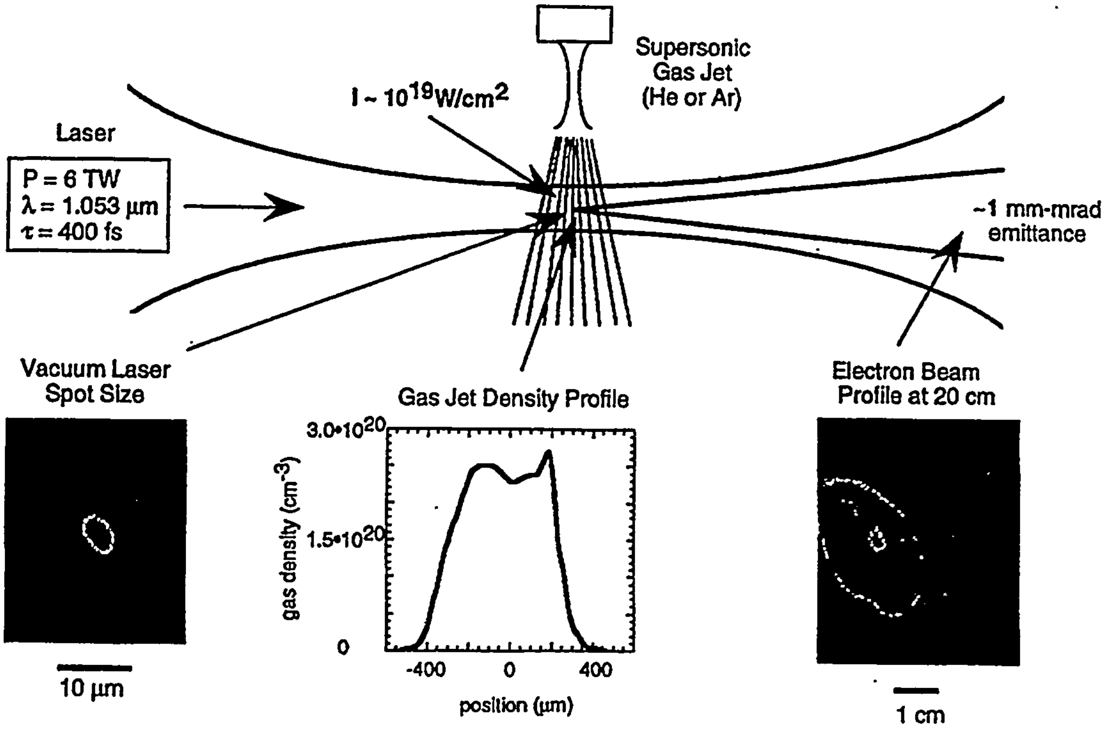

Supersonic Gas Jet (He or Ar)

I ~ 10^{19} W/cm^2

Laser

P = 6 TW
λ = 1.053 μm
τ = 400 fs

~1 mm-mrad emittance

Vacuum Laser Spot Size

Gas Jet Density Profile

Electron Beam Profile at 20 cm

Experimental Set-up to Measure Raman Forward Scattered Spectrum

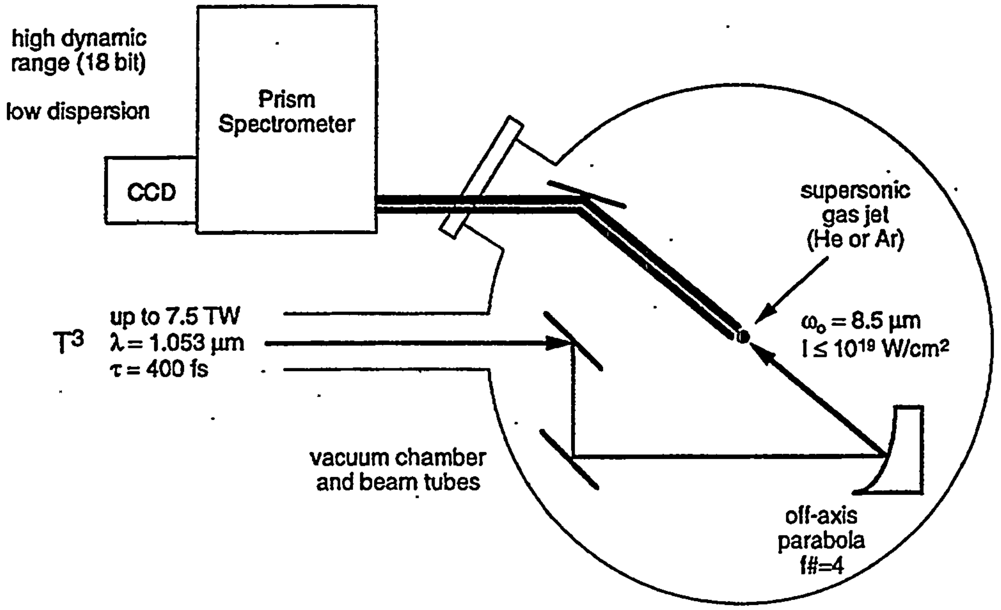

RFS Spectrum Modulates and Broadens with Laser Power

laser pulse incident on supersonic gas jet backed with 150 PSI Helium

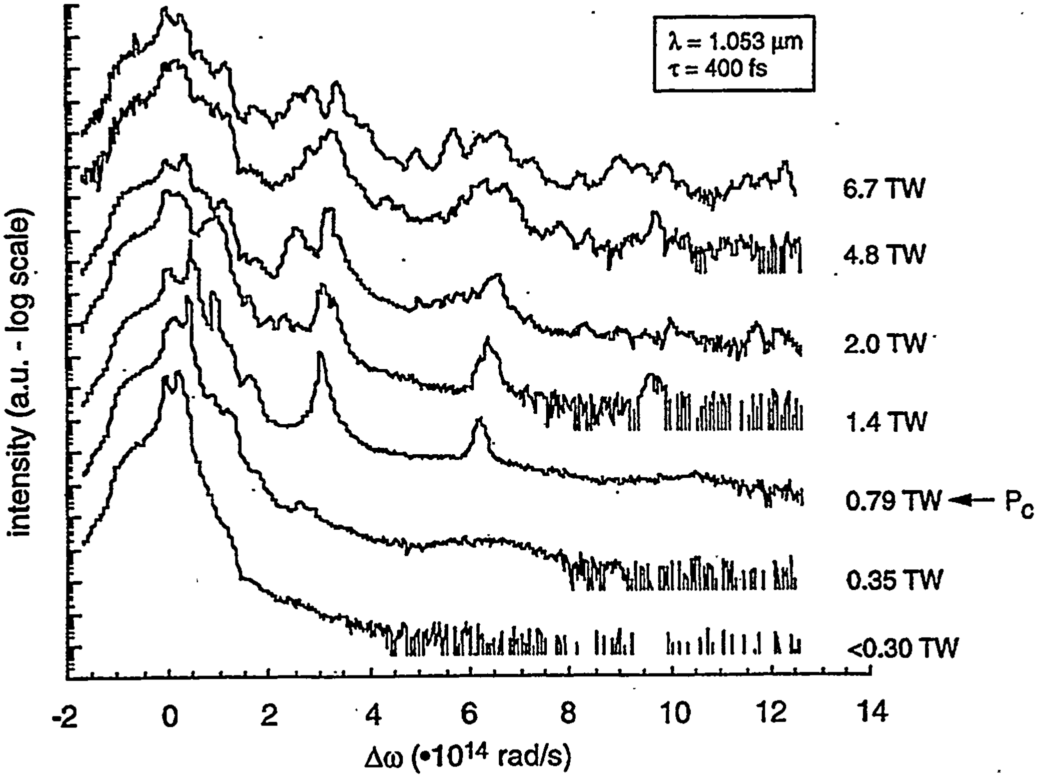

Plasma Wave Characteristics Measured in Experiments at CUOS

Physical Dimensions:

width ~ 10 µm, length 200 - 750 µm

Maximum Amplitude: $\frac{\Delta n}{n_0} \approx 0.40 \quad \rightarrow \quad \sim 2$ GeV/cm

Electron Density: $n_0 \sim 3 \cdot 10^{19}$ cm^{-3}

Temporal Duration: ~1.4 ps (FWHM)

Growth Rate: 4.0 ps^{-1} Decay Rate: 1.9 ps^{-1}

Collimated Beam of MeV Electrons Produced by Laser Plasma Accelerator

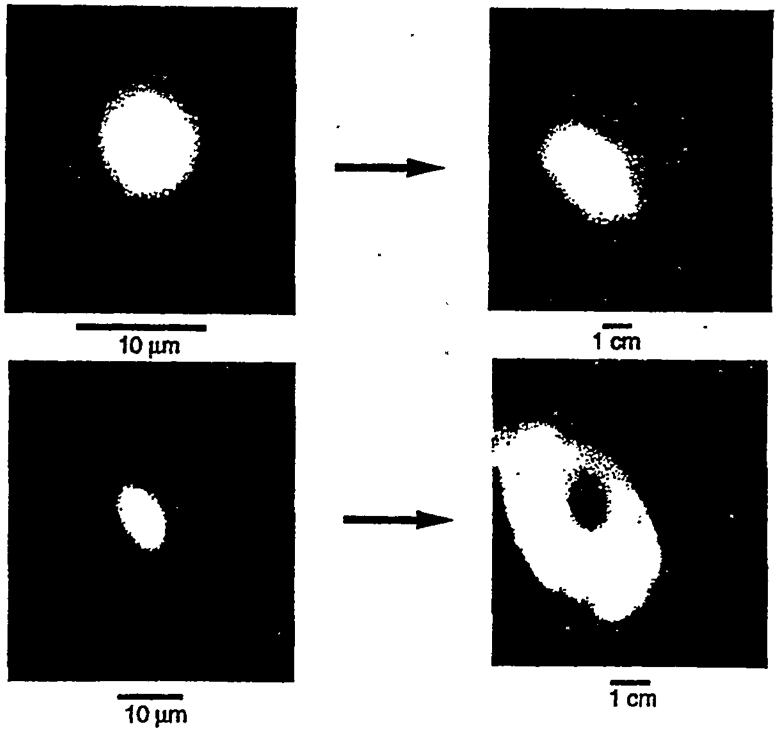

Vacuum Laser Spot

Electron Beam Profile

He gas target 5.2 TW

20 cm from plasma

3 mm-mrad emittance

Ar gas target 2.8 TW

15 cm from plasma

1 mm-mrad emittance

MeV Electron Production Has Sharp Thresholds

maximum number detected ~ 10^{10} which corresponds to ~ 1 nC

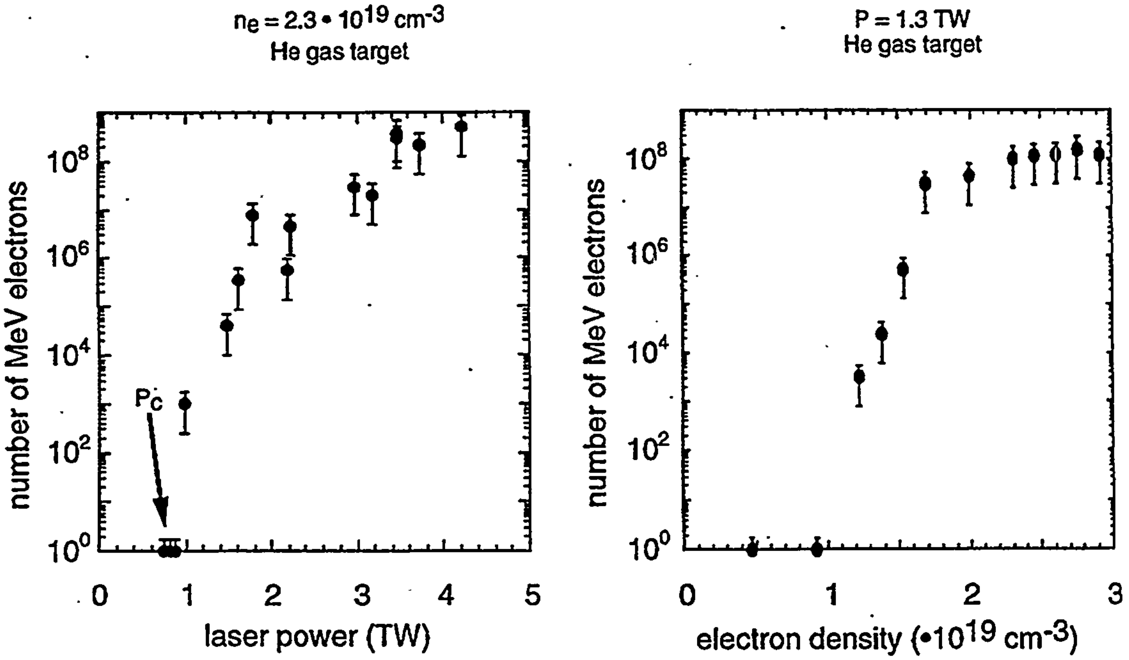

$n_e = 2.3 \cdot 10^{19}\ cm^{-3}$
He gas target

P = 1.3 TW
He gas target

MeV Electron Spectroscopy Shows Exponential Decay

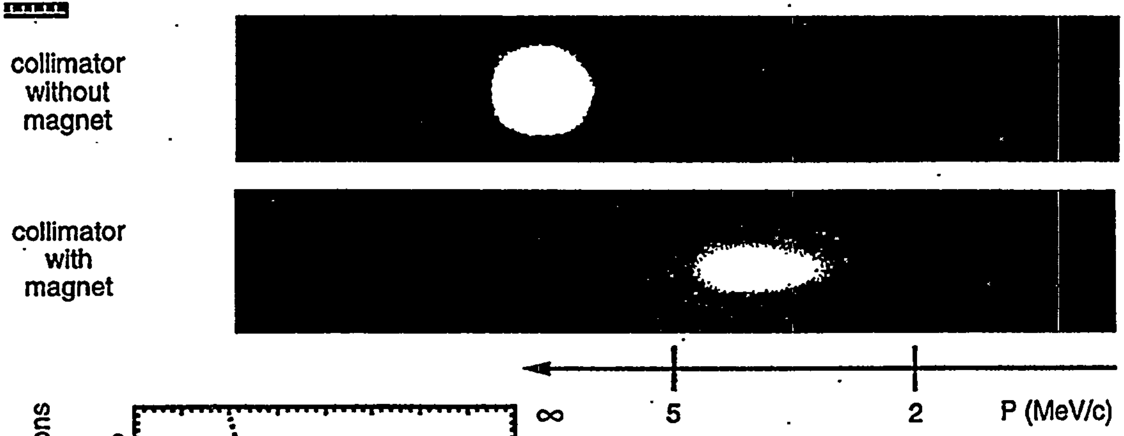

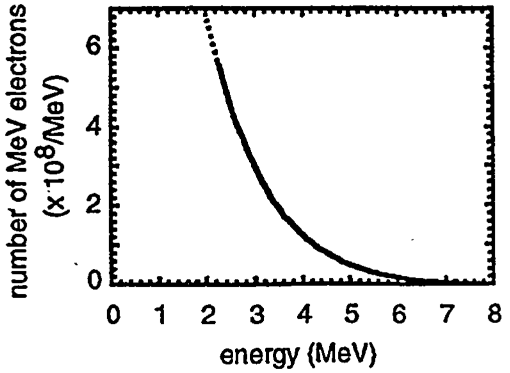

- *Energy > .6 MeV*
- *Exponential Decay*

Electron Beam Characteristics Measured in Experiments at CUOS

Maximum Number of Relativistic Electrons: $2 \cdot 10^{10}$ (3 nC)

Emittance/Divergence:

low power - 0.75 π-mm-mrad, 9° (HWHM)

high power - 0.38 π-mm-mrad, 4.5° (HWHM)

Energy Spectrum: exponential decay to > 8 MeV following

without self-channeling - $\exp(-\gamma)$
with self-channeling - $\exp(-0.67\gamma)$

Bunch Duration ≤ 1.4 ps

Threshold at 1 TW (1.5 P_c)

The Three Types of Laser-Plasma Accelerators Differ in the Temporal Characteristics of their Driver Pulses

LWFA

$$\boxed{L = c/\nu_p = c\,(\gamma m/n_e)^{1/2}}$$

PBWA

RLPA

The Optimal Sine Pulse Widths Decrease with Increasing Plasma Wave Amplitude

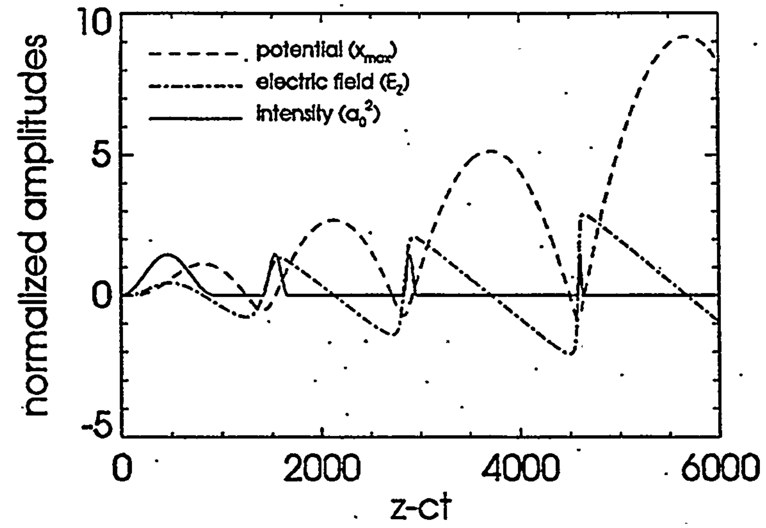

Lilac: How Does It Work?

- ***Pump pulse drives a wake field plasma wave.***
- ***The ponderomotive force of a second laser acts on electrons.***
- ***Electrons receive a drift velocity parallel to the wake field.***
- ***Electrons with a large drift velocity can be trapped in the wake.***
- ***The trapped electrons now form a beam in the plasma to be accelerated.***
- ***Remove necessity for an external source of electrons.***

Laser Injected Linear ACcelerator: one pulse drives a wakefield and another injects electrons

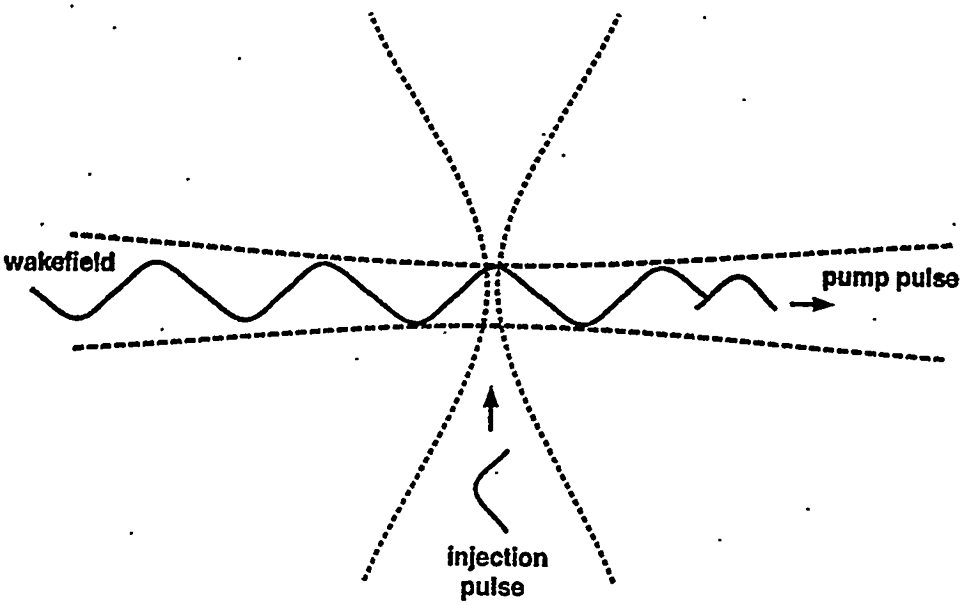

Laser Injected Linear ACcelerator: collinear case

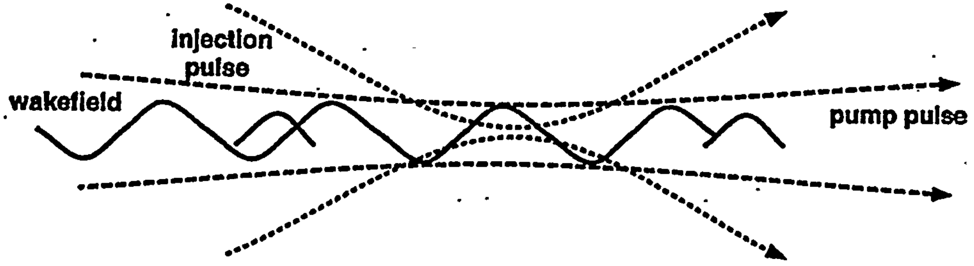

Recent Publications on Wakefields

- D. Umstadter, S.-Y. Chen, A. Maksimchuk, G. Mourou, and R. Wagner, "Nonlinear Optics in Relativistic Plasmas and Laser Wakefield Acceleration of Electrons," Science 273, 472 (1996).
- D. Umstadter, J. K. Kim, and E. Dodd, "Laser Injection of Ultrashort Electron Pulses into Wakefield Plasma Waves," Phys. Rev. Lett. 76, 2073 (1996).
- D. Umstadter, J. Kim, E. Esarey, E. Dodd and T. Neubert, "Resonant Laser-Driven Plasma Waves for Electron Acceleration," Phys. Rev. E 51, 3484 (1995).
- D. Umstadter, E. Esarey, and J. Kim, "Nonlinear Plasma Waves Resonantly Driven by Optimized Laser Pulse Trains," Phys. Rev. Lett. 72, 1224 (1994).

BEAM COOLING TECHNIQUES

A. Skrinsky, Novosibirsk

BEAM COOLING METHODS: RECENT DEVELOPMENT

A.Skrinsky

Budker INP, Novosibirsk

August 1996

---

we must use something non-Hamiltonian, for this case, - some dissipative forces.

The forces acting in (on) ensemble of particles are non-dissipative, if the projection of these forces on the individual particle velocity does not depend on this velocity (being, possibly, dependent on its coordinate at the moment of action).

If this is not the case - Liouville theorem is not valid!

Non-dissipative forces: external electromagnetic field,
coherent beam field.

Dissipative forces: friction (viscosic and "dry");
radiative friction;
electron cooling;
fast feed-back ("stochastic") cooling;
ionization energy losses.

For the case of cooling due to "full energy losses", the increment of 6-dimension density (or decrements sum for all 3 emittances) is equal to:

$$\delta_{\Sigma 0} := \frac{2 \cdot P_{fr}}{p_{\mu} \cdot v_{\mu}} \cdot \left(1 - \frac{p_{\mu long}}{2 \cdot v_{\mu}} \cdot \frac{d}{dp_{\mu long}} v_{\mu}\right) + \frac{1}{v_{\mu}} \cdot \frac{d}{dp_{\mu long}} P_{fr}$$

(the "equilibrium particle" energy losses are considered compensated by external source).

Using dissipative forces we can cool particle beams -
e.g., to low down their rest-frame temperature,
e.g., to rise their 6-dimension phase density
(to decrease the 6-dimension beam emttance - without beam intensity losses!).

Beams Cooling Methods:

- radiation and ionization cooling - due to full energy losses;
- electron cooling - the momenta decrease directly in rest-frame;
- stochastic cooling - the acting forces depend on particle coordinate in some previous moment;

- spin radiative cooling
  - caused by magnetic moments radiation.

(coherent radiation is not effective for cooling!)

Electron cooling - just 30th anniversary!

"Magnetized", low longitudinal temperature electron beams !

Ultra cold beams, including longitudinal ordering - now achieved not only in old Novosibirsk experiments
(perfect guiding longitudinal magnetic field uni-directionality;
good gun and collector technology).

Lot of installations throughout the world uses this technique.

Electron-ion collider for extreme luminosity
(Darmstadt - Novosibirsk joint R&D)

*"Very" strong electron cooling to suppress ion beam blow-up due to beam-beam interaction - for reaching

10^{33} cm^{-2}sec^{-1} electron-nucleon luminosity.

* Ion emittance control without damping rate degradation.

* Technical solution for 15 MeV electron beam device:

- immersing in to perfect longitudinal magnetic field;
- high current source to deal easily with high stored charge.

Radiation cooling - the classical example of cooling via full energy losses (and well known!).

Long and productive past.
Crucial for electron and positron colliders success.

Still the field, fast developing "technically", -
high brilliance beams for

SRS & FEL and
linear colliders.

Would be of interest for proton-proton and proton-antiproton colliders in multi-TeV range.

* Stochastic cooling - very efficient technique for high emittance, low density beams.

Correspondingly - complementary to EC for high amplitudes and low beam densities.

To reach higher densities/intensities - try to use higher and higher frequencies.

The new, still not proved approaches:

1. Electron beam internal instability - the prospect to arrange "internal amplifier" for much higher frequencies? (Derbenev)

2. SC in optical range for e^-, e^+? (Zolotarev, Zholents, Mikhailichenko):
undulator radiation sensor - laser amplifier - acting undulator (particle energy change dependent on u-u delay time).

Main non-technical problems still not clear (for me):
"dynamic range" limitations in particle deviations (half of very short wave length delay changes the sign of the action);
if the damping is really fast - amplified quanta became big and quantum fluctuation diffusion grows.

Combined use of EC and SC - the way to suppress slow ion diffusion at high amplitudes, caused by beam-beam interaction under initial discussion

Cooling of internal degrees of freedom of molecular ion beams - for high energy chemistry?

very old approach - but still not very familiar.

The power of ionization energy losses by charged particle is:

$$P_{fr}(\beta_\mu) := 4\cdot\pi\cdot r_e^2\cdot m_e\cdot c^2\cdot N_e\cdot\frac{c}{\beta_\mu}\left[\ln\left[\frac{2\cdot m_e\cdot c^2\cdot\beta_\mu^2}{I\cdot\left[1+\frac{2}{\sqrt{1-\beta_\mu^2}}\cdot\frac{m_e}{M_\mu}+\left(\frac{m_e}{M_\mu}\right)^2\right]\cdot\left(1-\beta_\mu^2\right)}\right]-\beta_\mu^2\right]$$

Consequently, the decrements sum (in cm^{-1} of cooling matter) is:

$$\delta_{\Sigma 0}(\beta_\mu) := \frac{2\cdot P_{fr}(\beta_\mu)\cdot\sqrt{1-\beta_\mu^2}}{\left(M_\mu\cdot c^3\right)\cdot\beta_\mu^3}\cdot\left(\frac{1+\beta_\mu^2}{2}\right)+\frac{\left(1-\beta_\mu^2\right)^{\frac{3}{2}}}{\left(M_\mu\cdot c^3\cdot\beta_\mu^2\right)}\cdot\left(\frac{d}{d\beta_\mu}P_{fr}(\beta_\mu)\right)$$

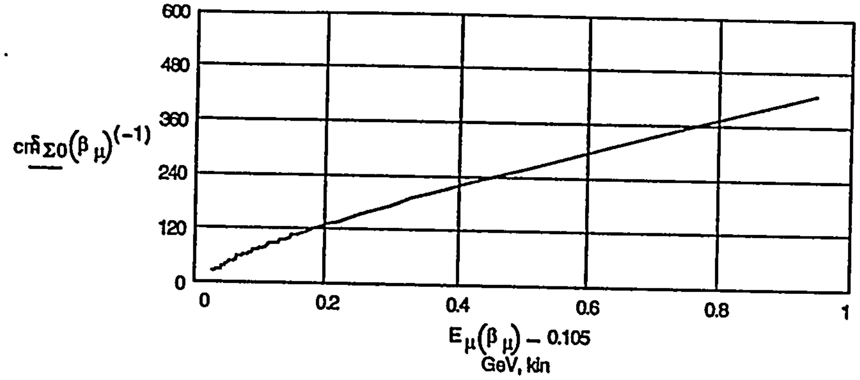

But - the multiple scattering and δ-electrons (or ionization losses fluctuations)!

The "natural" length of longitudinal cooling:

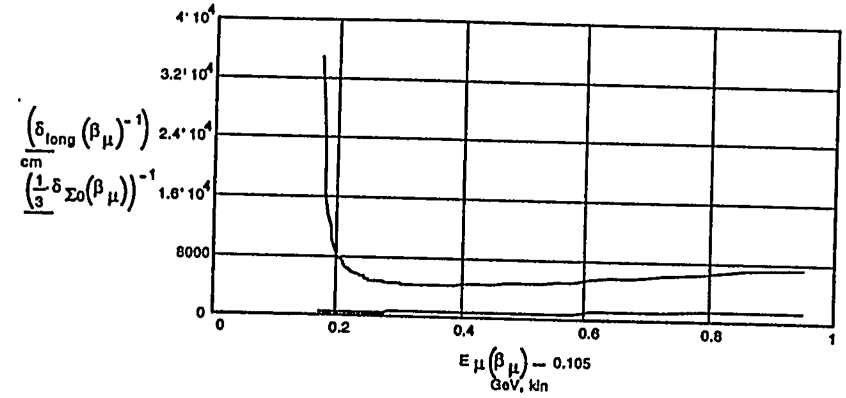

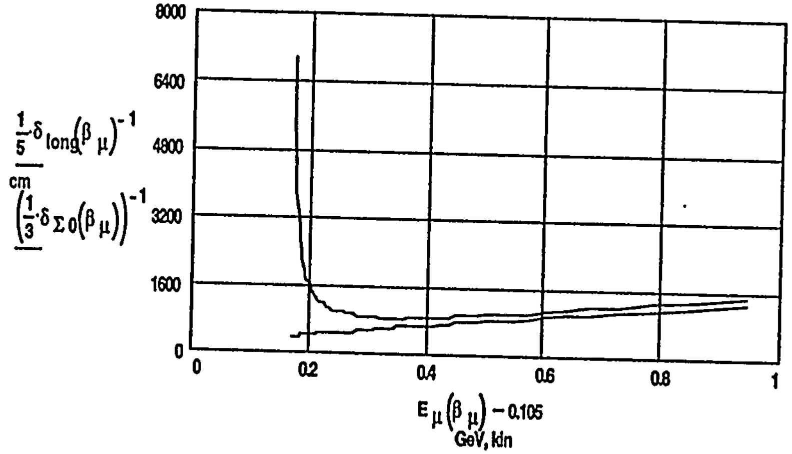

Hence, it is obligatory to redistribute the decrements sum in favor of longitudinal degree of freedom.

The balance of cooling and multiple scattering gives equilibrium angles:

$$\theta_{mean}^2 := \frac{12\cdot\pi\cdot e^4\cdot N_e\cdot Z\cdot L_c\cdot\left(1-\beta_\mu^2\right)}{M_\mu^2\cdot c^4\cdot\beta_\mu^4}\cdot\delta_{\Sigma 0}\left(\beta_\mu\right)^{(-1}$$

Consequently, it gives transversal equilibrium emittance (normalized) - dependent on beta-function in the matter:

$$\varepsilon_{neq}\left(\beta_\mu,\beta_0\right) := 4\cdot\pi\cdot r_e^2\cdot\left(\frac{m_e}{M_\mu}\right)^2\cdot N_e\cdot Z\cdot L_c\cdot\frac{\sqrt{1-\beta_\mu^2}}{\beta_\mu^3}\cdot\left(\frac{1}{3}\cdot\delta_{\Sigma 0}\left(\beta_\mu\right)\right)^{(-1)}\cdot\beta_($$

For strong focusing - b = 1 cm:

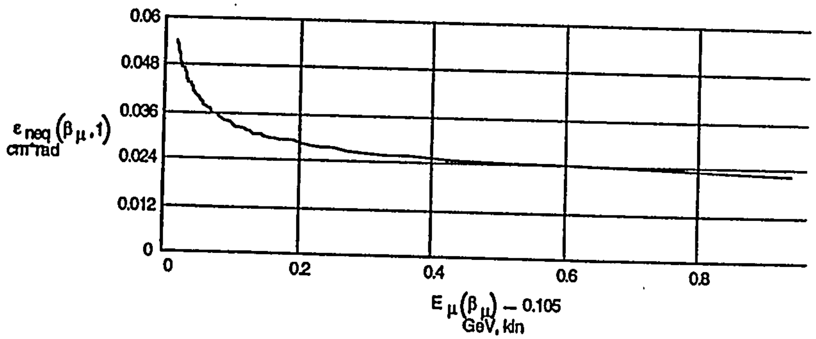

For longitudinal direction - more complexity.

$$\varepsilon_{neqlong} = \frac{\Delta p_{eq}}{p} \sigma_{eqlong} \gamma_{\mu} \cdot \beta_{\mu}$$

$$\varepsilon_{neqlong} = \left(\frac{\Delta p_{eq}}{p}\right)^2 \cdot \beta_{long} \beta_{\mu} \cdot \gamma_{\mu}$$

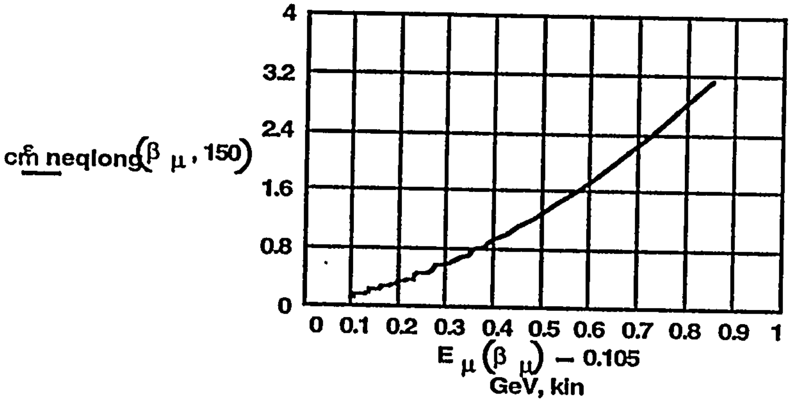

relative energy spread (due to balance struggling and cooling):

$$\Delta_E(\beta_\mu) := \sqrt{2 \cdot \pi \cdot r_e^2 \cdot \left(\frac{m_e}{M_\mu}\right)^2 \cdot N_e \cdot \left(2 - \beta_\mu^2\right) \cdot \left(\delta_{leff}(\beta_\mu)\right)^{(-1)}}$$

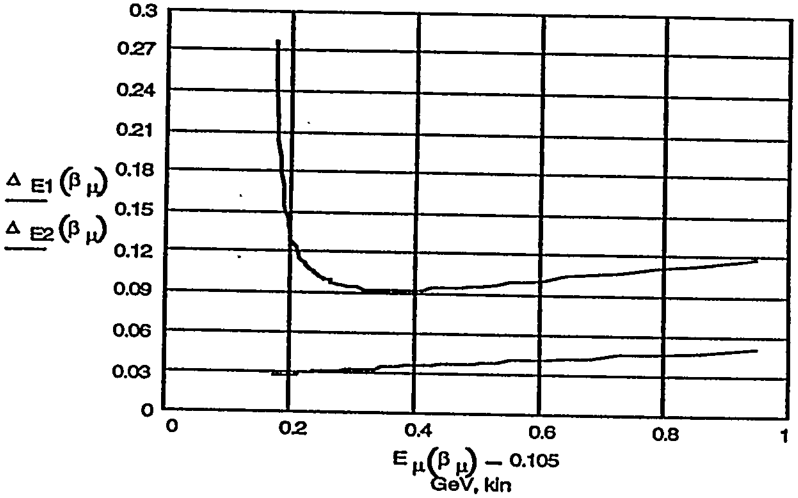

The optimal solution for transversal emittances is - to use a high current carrying (liquid) lithium thin cylinder.

Surface magnetic field - 10 Tesla.
Lithium cylinder diameter - 1 mm.

$$\beta_{li}\left(H_{max}, \beta_{\mu}, a_{li}\right) := \sqrt{\frac{10^{9} \cdot E_{\mu}\left(\beta_{\mu}\right) \cdot a_{li}}{300 \cdot H_{max}}}$$

- transversal beta-function inside Li cylinder

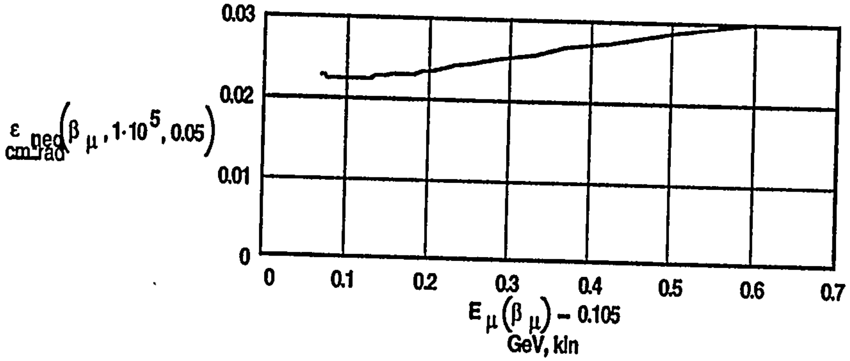

The final stage of ionization cooling is the crucially important and the most difficult part of the whole muon-muon problem.

The task is to reach minimal 6-dimension emittance of muon beam.

For this stage it means:

- to call all 3 degrees of freedom <u>simultaneously</u>;
- to distribute the decrements sum "equally" to all 3;
- to arrange the strongest transversal and longitudinal focusing.

- Solution for final stage simultaneous cooling - to transform the current carrying cylinder in to lithium-beryllium helix with “teeth like” boundary between these two metals (more of high density beryllium at larger radius of the helix - where the muon energies are higher).

D=10 cm ==>

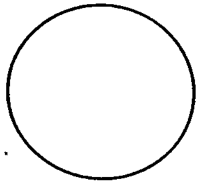

Additionally, the ionization cooling will play a key role in multi-channel pion collection approach and multiple pion-to-muon decay channels - to collect all the muons in single bunch.

Such approach is especially crucially important for producing polarized muon colliding beams.

---

* Laser cooling for non-completely stripped ions (prospect for FEL application)

- A.Sessler next talk.

LASER COOLING

A. Sessler, LBL

1. Doppler Laser Cooling

*The Doppler condition

An ion moving at a velocity of v can be resonantly excited, if the Doppler condition

$$\omega_0 = \omega_L \gamma \left(1 - \frac{v_\parallel}{c}\right)$$

is fulfilled, where $v_\parallel$ denotes the projection of v onto the direction of laser beam, $\omega_0 / 2\pi$ is the transition frequency v_0 in the rest frame of the ion, and $\omega_L / 2\pi$ is the frequency of the laser light v_L in the laboratory frame.

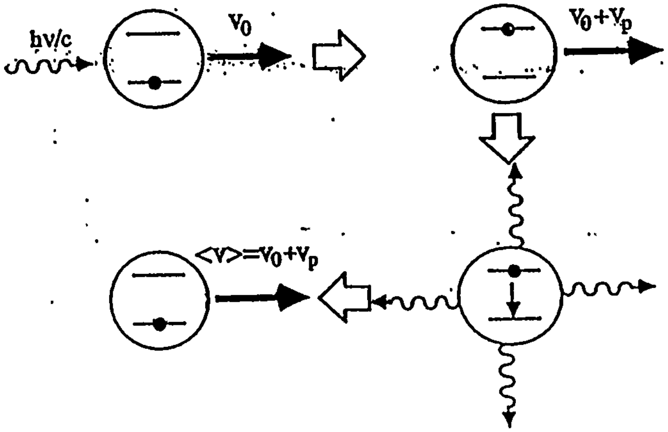

VIII. Laser Cooling

D. J. Wineland and H. Dehmelt, Bull. Am. Phys. Soc. 20, 637 (1975); T. Hanchand A, Schawlow, Opt. Comm. **13**, 68 (1975).

S. Schroder et al,Phys. Rev. Lett. **64**, 2901 (1990); J. S. Hangst, et al, Phys. Rev. Lett. **67**, 1238 (1991).

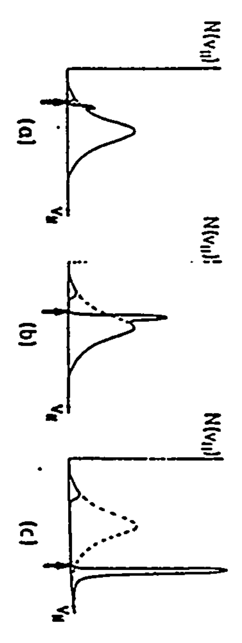

FIG. 1 (a) The spontaneous force exerted by a laser copropagating with a fast, hot ion beam is able to accelerate ions within a narrow velocity region. When scanning the laser frequency (resonant velocity is marked by an arrow), the ions are collected in a narrow velocity distribution (b), which finally results in a longitudinally cooled ion beam (c).

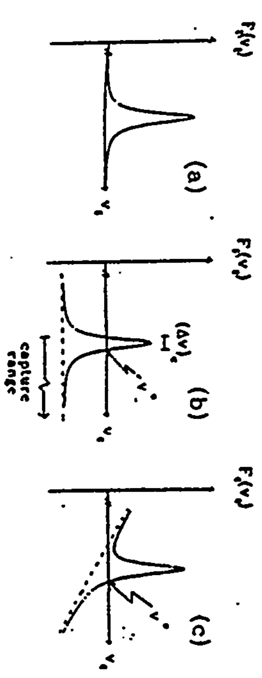

FIG. 2 (a) The spontaneous force itself has no stable point v^* (see Eq. (3)). With the help of a (b) constant or (c) linear auxiliary force $\mathbf{F}_{aux}$ (dashed lines), such a point can be generated for the combined forces (solid line).

$$F_{\|}(v^*) = 0$$

$$\frac{\partial F_{\|}}{\partial v_{\|}}(v^*) < 0$$

"Laser Cooling" of Non-Relativistic Ions

- Employ narrow band laser ($\Delta\omega <$ line width) of frequency $\omega \approx \omega_{res}$
- Momentun transfer comes mainly from the absorption process. Average momentum transfer depends strongly on ion velocity through the line shape function. Spontaneous emission gives a negligible momentum transfer.

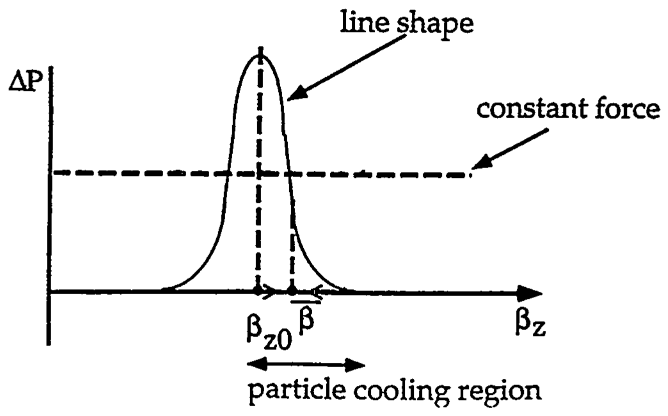

- very efficient because of steep lineshape
- works only in z-direction
- must sweep ω to collect all particles

IN ASTRID[1]

J.S. Hangst, J.S. Nielsen, O. Poulsen, J.P. Schiffer*†*, P. Shi*, and B. Wanner*‡*
Institute of Physics and Astronomy, Aarhus University
DK-8000 Aarhus C, Denmark

ABSTRACT
The ASTRID storage ring has been used to study laser cooling of low energy ion beams. We discuss the results of recent experiments involving the ion $^{24}Mg^+$. We have employed a single cooling laser and a radio frequency (RF) cavity to demonstrate the first laser cooling of a bunched beam.

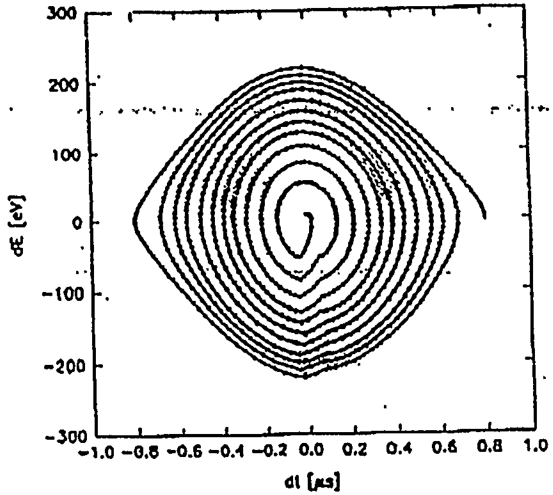

Figure 1. Longitudinal phase space plot illustrating the principle of bunched-beam laser cooling. Energy deviation and time deviation are plotted for a single particle in an RF bucket.

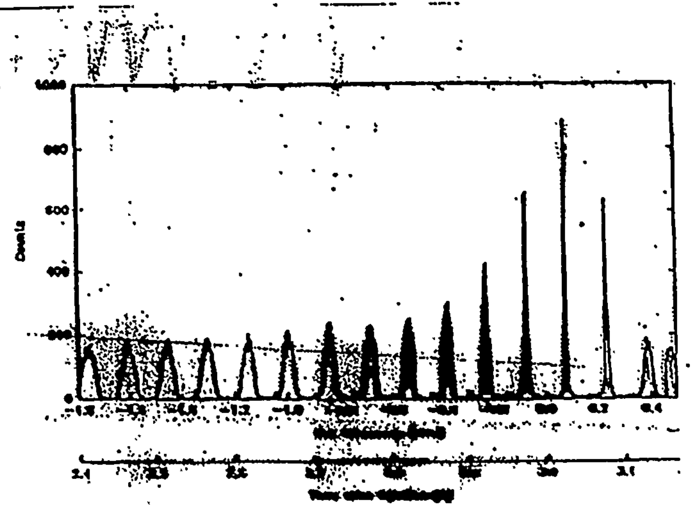

Figure 3. Time history of the ion velocity distribution during laser cooling. Each peak is an independent laser fluorescence intensity vs. velocity measurement. The numbers on the abscissa are the laser detuning at the time the measurement is made. The measurements are separated in time by 50 ms. The beam current is about 0.5 µA.

The laser has crossed the synchronous energy and has begun to accelerate particles out of the bucket.

Definition of Beam Temperatures

*Longitudinal temperature $\mathbf{T_{\parallel}}$

$$\frac{1}{2}k_B T_{\parallel} = \frac{1}{2}m(\delta v_{\parallel})^2 \ .$$

*Transverse temperature $\mathbf{T_{\perp}}$

$$k_B T_{\perp} = \frac{1}{2}m\left\langle v_x{}^2 + v_y{}^2 \right\rangle \ .$$

The above formula lead to

$$\frac{1}{2}k_B T_{\parallel} = E_0\left(\frac{\delta p}{p_0}\right)^2 \to T_{\parallel}[K] = 2.32x10^4 x\left(\frac{\delta p}{p_0}\right)^2 E_0[eV] \ ,$$

$$k_B T_{\perp} = 2E_0\frac{\varepsilon_{\perp}}{\langle\beta\rangle} \to$$

$$T_{\perp}[K] = 2.32x10^4 x\frac{\varepsilon_{\perp}[m\cdot rad]}{\langle\beta\rangle[m]}E_0[eV] \ ,$$

where $\mathbf{E_0}$ is the kinetic energy of the reference particle, $\varepsilon_{\perp}$ is the transverse beam emittance, and $<\beta>$ denotes the averaged value of the betatron function.

Note:

$$k_B = 1.3807x10^{-16}[erg/K], \ 1[eV] = 1.6022x10^{-12}[erg] \ .$$

*Doppler limit

The minimum temperature T_{min} achievable by Doppler cooling is given as

$$k_B T_{min} \approx \frac{\hbar\Gamma}{2}$$

Where k_B is the Boltzmann constant, and Γ is the spontaneous decay rate of the upper level back to the lower level; $\Gamma/2$ is the radiative linewidth of the transition.

*Maximum laser cooling force

$$F_{LC}^{max} = \left(\frac{\Delta p}{\Delta t}\right)_{max} = \frac{\hbar k_0 \Gamma}{2} \ ,$$

where k_0 is the wave number.

A more rigorous analysis yields

$$F_{LC} = \frac{\hbar k_0 \Gamma}{2}\frac{S}{1+S+\left(\frac{2\Delta(v_{\parallel})}{\Gamma}\right)}$$

where S is the ratio between laser intensity I and saturation intensity I_{sat}, i.e., $S=I/I_{sat}$, and the detuning $\Delta(v_{\parallel})$ is given by

$$\Delta(v_{\parallel}) = \omega_L\gamma\left(1-\frac{v_{\parallel}}{c}\right)-\omega_0 \ .$$

$S=0 \to F_{LC}=0$

$S=\infty$ doesn't help

$S=S_{sat} \to I$ not

Miesner, et al PRL 77(1996) 623

TSR

3×10^7 $^9Be^+$ ions

7.3 MeV

3×10^{-11} mbar ~ 25 sec lifetime

laser 300 nm (argon ion)
copropagating beams
so down-shifted to
$\lambda = 313$ nm
($\beta = 0.042$)

Cooling: electron ~~to~~ $T_h = 4000$ °K
$T_V = 500$ °K

laser $T_{\parallel}$ decreases to ~6 °K
when coupled $T_{\parallel}$ increases to ~15 °K

How effective ?

Past Achievements

(I). ASTRIDF in Denmark

For a 13 MeV $^7Li^+$ -ion beam,

$$T_{\parallel} \leq 3K \ .$$

For a 100 ke V $^7Li^+$ and $^{24}Mg^+$-ion beam,

$$T_{\parallel} \sim 1mK \ .$$

See, for example, J.S. Hangst et. al., *"Laser Cooling of a Stored Ion Beam to 1 mK"*, Phys. Rev. Lett., Vol. 67, No. 10 (1991) 1238.

(II). TSR in Germany

For a 7.3 MeV $^9Be^+$ -ion beam,

$$T_{\parallel} \leq 30mK \ .$$

In this experiment, the beam was first cooled with an electron cooling system to the temperature of

$$T_{\parallel} \sim 150K \text{ and } T_{\perp} \sim 4000K$$

Note: $T_{\parallel} \sim [mK]$ at 100 [keV] is equivalent to $\delta p / p_0 < 10^{-6}$ or $\Delta E < 0.1[eV]$. In the TSR ring, $T_{\parallel} \leq 30[mK]$ achieved by the laser cooling system corresponds to $\delta p / p_0 \leq 4x10^{-7}$. (The longitudinal temperature achieved by the TSR electron cooler corresponds to $\delta p / p_0 \sim 3x10^{-5}$.)

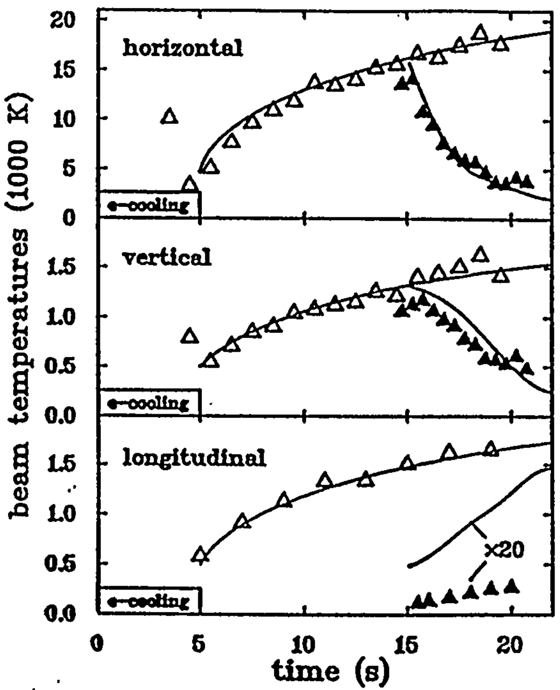

FIG. 2. Temporal evolution of the beam temperatures, observed without any further cooling after electron precooling (open symbols) and with laser cooling applied after 10 seconds (closed symbols). The solid lines show corresponding numerical results obtained from IBS theory (see text).

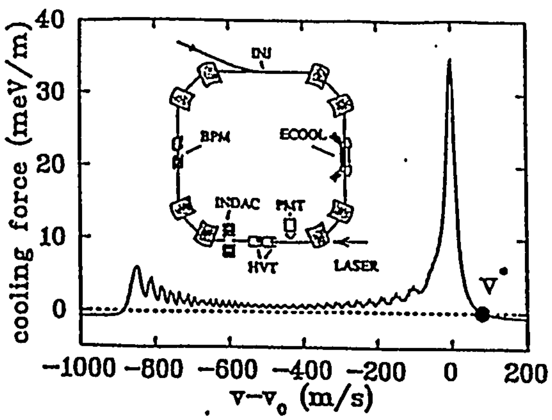

FIG. 1. Longitudinal, ring-averaged cooling force, as calculated for the experimental parameters. The resonant ion velocity v_0 is about 1.25×10^7 m/s and the ions are kept at the stable point v^*. The inset shows a schematic view of the TSR with its circumference of 55.4 m: INJ, injection; ECOOL, electron cooler; PMT, photomultiplier tube; HVT, high-voltage biased drift tubes; INDAC, induction accelerator; BPM, beam profile monitor; not shown are the twenty quadrupole magnets of the focusing structure.

VIII. Laser Cooling With Beam Coupling

H. Okamoto, A.M. Sessler, and D. Mohl, Phys. Rev. Lett. 72, 3977 (1994).

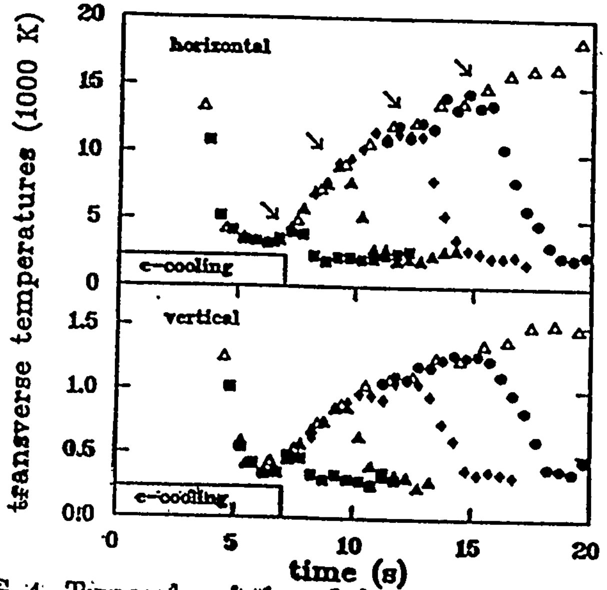

FIG. 4. Temporal evolution of the transverse beam temperatures, observed for laser cooling with various delays after electron precooling. The arrows mark the respective begin of the laser cooling process.

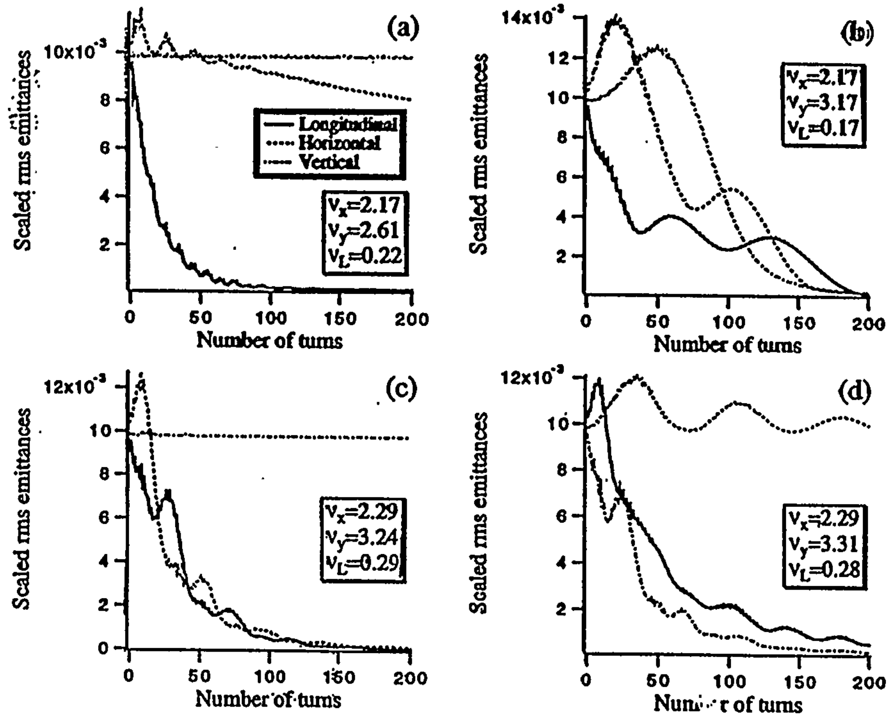

Fig. 7

Coupling RF Cavity

- The coupling cavity considered here is a pill box type excited with TM_{210} mode.
- The electro-magnetic fields

$$E_z = -V_c \sin\left(\frac{\pi x}{a}\right)\cos\left(\frac{\pi y}{2b}\right)\cos(\omega_c t + \phi_c),$$

$$\begin{cases} H_x = -\dfrac{V_c}{Z_0}\dfrac{\pi c}{2b\omega_c}\sin\left(\dfrac{\pi x}{a}\right)\cos\left(\dfrac{\pi y}{2b}\right)\sin(\omega_c t + \phi_c), \\ H_y = -\dfrac{V_c}{Z_0}\dfrac{\pi c}{a\omega_c}\cos\left(\dfrac{\pi x}{a}\right)\cos\left(\dfrac{\pi y}{2b}\right)\sin(\omega_c t + \phi_c), \end{cases}$$

where the RF frequency ω_c is given by

$$\left(\frac{\pi}{a}\right)^2 + \left(\frac{\pi}{2b}\right)^2 = \left(\frac{\omega_c}{c}\right)^2 .$$

Radiation Damping

An electron moving in a circular accelerator is, of course, accelerated and it will thus radiate. The amount of radiation is

$$p = \frac{2}{3} \frac{e^2 \beta^4 \gamma^4 c}{R^2} \quad .$$

Hence the radiated energy per turn is

$$\delta E = \frac{4}{3} \frac{\pi e^2}{R} \beta^3 \gamma^4 \quad ,$$

or, in practical units (and taking $\beta = 1$):

$$(\delta E)(\text{MeV}) = 8.85 \times 10^{-2} \, \frac{E^4(\text{GeV})}{R(\text{m})} \quad .$$

The frequency spectrum of the radiation is complicated; for low frequencies it varies as $\omega 2/3$. The radiation drops off exponentially for ω larger than a critical frequency, ω_c, where

$$\omega_c = \frac{3\gamma^3 c}{R} \quad .$$

II. Radiation Damping

Kolomenski,A. and Lebedev, A, "The Effect of Radiation on the Motion of Relativistic Electrons in Synchrotrons", CERN Symposium, 447 (1956).

Robinson, K., Phys. Rev. **111** 373 (1958); Sands, M. Phys. Rev. **97**, 470 (1955).

M. Sands, "The Physics of Electron Storage Rings, An Introduction", Stanford Linear Accelerator Center, SLAC 121 (1970).

Z. Huang, P. Chen, and R. Ruth, Phys. Rev. Lett. **74**, 1759 (1995).

Thus, on the basis of the above analysis, an electron beam in a storage ring will just damp and damp so that its transverse size becomes smaller and smaller. This is approximately true, and beams become very small indeed, but they do not become arbitrarily small. Why not? Because quantum effects need to be taken into account; i.e. that electrons radiate discrete photons and that the hard photons, which are radiated statistically, kick the electron. In fact, the size of electron beams is determined by these quantum mechanical effects. The energy spread of the beam, which also damps to zero classically, is (in a uniform field).

$$\left(\frac{\sigma_E}{E}\right)^2 = \left(\frac{55}{32\sqrt{3}}\right)\left(\frac{\hbar}{mc}\right)\frac{\gamma^2}{J_E R} ,$$

and one can see that the finiteness of σ_E is due to a quantum mechanical effect; i.e. to the non-zero nature of Phanck's constant $\hbar$. A similar formula can be given for the radial size of the beam. The vertical size is, clearly, determined by coupling to the horizontal motion.

Note that this frequency varies as γ^3 times the circulation frequency. Thus the radiation can extend up to very high frequencies.

The emission of radiation has an effect on the radiating particle. It is only for electrons that this is a significant effect, but the effect is vital in determining the property of beams in an electron storage ring. The radiation reaction can cause either damping or undamping of the electrons' oscillations (transversely and in energy) about the equilibrium orbit. If we characterize this exponential damping rate by rate constants α_x, α_y, α_E then

$$\alpha_{\begin{pmatrix} x \\ y \\ z \end{pmatrix}} = \frac{c\gamma^3 e^2 J}{3R^2 mc^2} ,$$

where the damping partition numbers satisfiy:

$$J_y = 1, J_x + J_E = 3. .$$

One can arrange by proper lattice design, as one must in a storage ring, to have damping in all three directions.

Now transform to lab

In lab $\omega^2 = \frac{k}{m\gamma}$

But $\omega' = \gamma\omega \quad \rightarrow \quad \frac{k'}{m} = \gamma^2 \frac{k}{m\gamma}$
(time dilation)

$$k' = k\gamma$$

But $\alpha = \alpha'/\gamma$ (time dilation)

$$\alpha = \frac{4}{3}\frac{e^2}{c^3}\frac{k}{m^2} = \frac{4}{3}\frac{r_0 k}{mc}$$

(The factor of 4 (vs. 2) is because I have not averaged $\sin^2\omega' t$ carefully.)

Radiation Damping Rate in a Uniform Channel

In e-frame that's all there is Huang, Chen & Ruth

$$\frac{dE_\perp}{dt'} = \frac{2}{3}\frac{e^2 a'^2}{c^3}$$

In lab $F = -kx$

In e-frame $F' = -k'x$

Motion is SHM $\omega^{2'} = k'/m$

$$a' = \frac{k'x}{m}$$

$$E_\perp = \frac{1}{2}mx^2 = \frac{1}{2}m\left[\sqrt{\frac{k'}{m}}x\right]^2$$

$$E_\perp = \frac{1}{2}k'x^2$$

$$\alpha' \equiv \frac{1}{E_\perp}\frac{dE_\perp}{dt'} = \left(\frac{1}{\frac{1}{2}k'x^2}\right)\frac{2}{3}\frac{e^2}{c^3}\frac{k'^2x^2}{m^2}$$

$$\alpha' \equiv \frac{1}{E_\perp}\frac{dE_\perp}{dt'} = \frac{4}{3}\frac{e^2}{c^3}\frac{k'}{m^2}$$

Emittance Limits

For light :

Gaussian Beam Focus

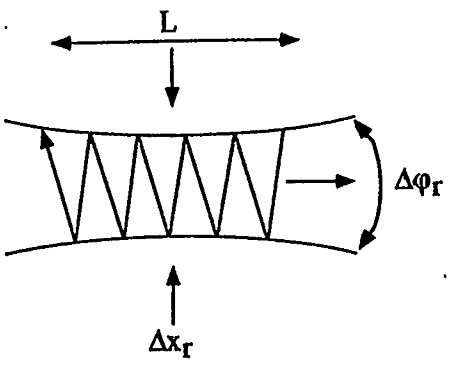

$\Delta x_r \sim \sqrt{\lambda L}$ $\qquad$ $\Delta\varphi_r \sim \sqrt{\lambda/L}$

$$\varepsilon=(\Delta x_r)(\Delta\varphi_r)\ge\lambda$$

For particles :

$$E=\frac{m\ x^2}{2}+\frac{k'\ x^2}{2}\ge\frac{\hbar\omega}{2}$$

$$\omega=\sqrt{k'/m}$$

$$x=x_0\sin\ \omega t$$

$$\left(\frac{m}{2}\dot{x}^2\right)=\frac{m\omega^2x_0^2}{4}=\left(\frac{k'x^2}{2}\right)=\frac{k'x_0^2}{4}$$

$$2\left[\frac{k'x_0^2}{4}\right]\ge\frac{\hbar}{2}\sqrt{k'/m}$$

$$x_0^2\ge\frac{\hbar}{k'}\sqrt{k'/m}$$

$$\varepsilon=\frac{\dot{x}}{\gamma c}x=\frac{\omega}{2c\gamma}x_0^2\ge\sqrt{k'/m}\,\frac{1}{2c}\frac{\hbar}{k'\gamma}\sqrt{k'/m}$$

(angle compression)

$$\varepsilon\ge\frac{\hbar}{2mc\gamma}=\frac{\lambda_c}{2\gamma}$$

$$\text{or}\quad \varepsilon_n\ge\frac{\lambda_c}{2}$$

III. Stimulated Radiation Cooling

E.G. Bessonov, "Radiative Method of Ion Cooling in Storage Rings", Lebedev Institute Report # 6 (March, 1994).

E. G. Besonov and K-J Kim, "Radiative Cooling of Ion Beams in Storage Rings by Broad Band Lasers, LBL Report and Phys. Rev. Lett. (to be published), (1995).

Uniform Channel

Damping transversely until :

$$\varepsilon_n = \frac{\lambda_c}{2}$$

where $\lambda_c = \frac{\hbar}{mc} = 3.86 \text{ x } 10^{-13}\,\mathrm{m}$ (for electrons)

for light : $\varepsilon(\mathrm{min}) = \frac{\lambda}{2}$

this limit is reached for a diffraction limited beam

Contrast a channel with a synchrotron :

$$\varepsilon_{ny}(\mathrm{min}) = \left[\frac{55}{32\sqrt{3}}\right]\frac{\lambda_c\gamma}{2\nu_y}$$

$$\varepsilon_{nx}(\mathrm{min}) = \left[\frac{55}{32\sqrt{3}}\right]\left[\frac{(1-2n)^2}{n(1-n)}\right]\lambda_c\gamma^3 \qquad 0 < n < 3/4$$

Why ? Because forced emission in a synchrotron where r_e is the classical electron radius. However, on resonance, the cross section is

$$\sigma = \frac{\lambda^2}{2\pi}$$

where λ is the wavelength of the laser (in the ion's frame). This enhancement is a well-known effect, reminding one of slow neutron scattering and, currently, used in laser cooling. However, the laser line width must be rather broad in this case, since the spread in frequencies within the ion beam is rather large, and thus most ions are not in resonance. This means that the average cross section is greatly reduced from the maximum value given above, but since the maximum is $(\lambda/4\pi r_e)^2 \approx 10^{18}$ times the Compton cross section, even with an averaging factor one still gains a great deal.

For a relativistic ion the radiation reaction is large (γ^2 times the non-relativistic case) and thus the efficacy of damping is considerable. Putting all this together one obtains (approximately) the damping rate for vertical oscillations (similar formulas can be obtained for each degree of freedom)

$$\tau = \frac{SR}{c\lambda\ell\gamma}\left(\frac{\Delta f}{f}\right)\frac{P_A}{P}$$

Stimulated Radiation Cooling

It has recently been proposed, by E.G. Bessonov that in ion beams, one can stimulate radiation damping (6). Firstly, the magnetic field (which accelerates the charged particle and causes it to radiate) is replaced by the field of a laser beam. Secondly, the laser frequency is chosen so that there is resonance with a bound electron on the ion.

Thus, realizing that ions don't radiate significantly and therefore radiation damping is negligible for them, it is proposed to employ the electrons in ions to do the radiation and transfer the resulting momentum kick to the ion as a whole. If the magnetic field (from a laser) is in resonance with an atomic spacing of levels, then the cross section can be very large; that is, an electron can readily be excited to an upper level.

For an incident laser photon, off resonance, the cross section is simply the Compton cross section:

$$\sigma = (8/3)\pi r_0^2$$

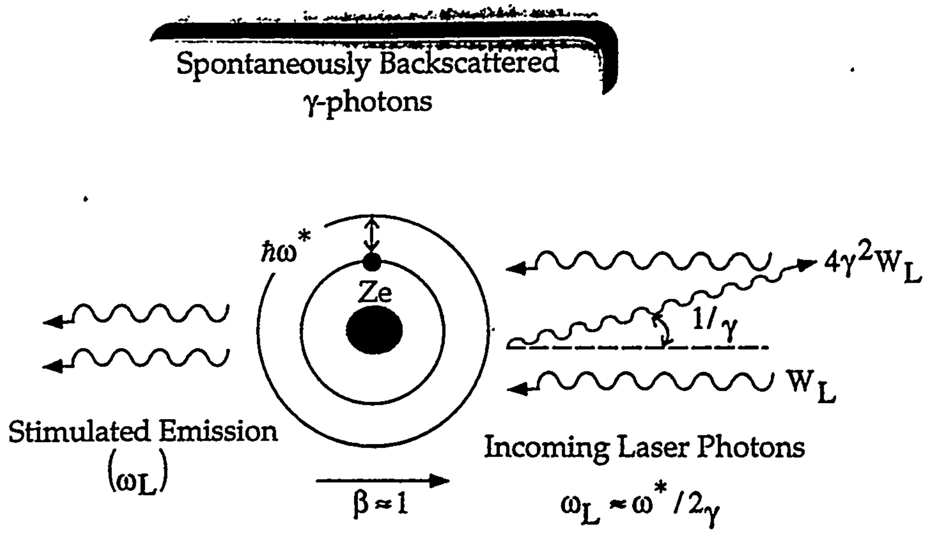

- Cross-section at exact resonance : → "Laser Cooling"

$$\sigma \approx \lambda^{*2} \approx \left(\lambda^*/r_e\right)^2 r_e^2$$

- Average cross-section with bandwidth Δω : → "Radiative Ion Cooling"

$$\sigma \approx \left(\lambda^*/r_e\right)\left(\omega_L/\Delta\omega\right)r_e^2$$

AMS

where S is the cross section of the laser beam, of frequency f and spread Δf, and power P, R is the radius of the storage ring, l is the length of the interaction region, and PA is $m_em_ic^5/e^2$. In a numerical example Bessonov finds the transverse damping time, for a hydrogen-like oxygen ion beam at 125 GeV nucleon is 26 seconds.

Notice that this scheme, in contrast with the laser cooling scheme to be described later, requires a laser of wide line width (rather than a very narrow line width) and an rf system on the storage ring capable of restoring the ion's energy a few times (for damping requires that the ion lose its energy a number of times, just as in radiation damping, but unlike laser cooling where the change in ion energy is very very small).

Example II : Hydrogen-Like O- Ion in RHIC

- $C = 3.8$ km , $\gamma = 135$, $Mc^2\gamma = 2$ TeV, $Z = 8$, $N_i = 8.3 \times 10^9$

  $t_b = 224$ ns, $\sigma_Z = 20$ cm, $\varepsilon_X = 3 \times 10^{-7}$ mrad, $\beta_X = 1$m, $\frac{\Delta\gamma}{\gamma} = 2.5 \times 10^{-3}$

$\Rightarrow$ $\hbar\omega^* = 653$ cV, $\langle \hbar\omega^S \rangle = 88$ keV, $\lambda_L = 5100 \mathring{A}$

- $\varepsilon_X > \varepsilon_L$ If $Z_R = 7.3$ m then $\sigma_{Lx} = \sigma_X$ at the waist. Choose

  $\sigma_{Lx} = \beta x / 2 = 0.5$ m to maximize overlap.

- In this case, we can choose $I = I_{sat}$: required acc. vol.p = 0.3 MV

$\Rightarrow$ Laser power : $W_L = 6.2$ mJ, $P_L = 28$ kW (feasible with laser or FEL)

- Performances :

  $\langle \dot{\eta}^S \rangle = 8.8 \times 10^{17}$ #/sec

  $\tau_X = \tau_y = 26$ sec , $\tau_\varepsilon = 52$ sec

  $\sigma_e / E = 2.5 \times 10^{-4}$, $\varepsilon_X = 4 \times 10^{-13}$ mrad

  (increased !) (decreased lots !)

Example I : Hydrogen-Like Pb Ion in LHC

- $C = 27$ km , $\gamma = 3000$, $Mc^2\gamma = 575$ TeV , $Z = 82$, $N_i = 9.4 \times 10^7$

  t_b(bunch sep.) $= 135$ ns , $\sigma_Z = 7.5$ cm , $\varepsilon_X = 3 \times 10^{-9}$ mrad

  $\beta_X = 0.5$ cm , $\Delta\gamma / \gamma = 2 \times 10^{-4}$

$\Rightarrow$ $\hbar\omega^* = 68.7$ keV , $\langle \hbar\omega^S \rangle = 0.2$ GeV , $\lambda_L = 1080 \mathring{A}$

- $\varepsilon_X < \varepsilon_L$ laser x-section is larger than ion's if $Z_R \geq 1.68$ cm

  choose : $Z_R = \sigma_{Lz} = \sigma_Z = 7.5$ cm

  - choose : $I = I_{sat} / 712 \Rightarrow$ Acc. voltage $V = 12.3$ MV(1 GeV/ion)

$\Rightarrow$ Laser power : pulse energy $W_L = 56\mu J$, $P_L = 420W$ (feasible)

- Performances :

  $\langle \dot{\eta}^S \rangle = 3.5 \times 10^{15}$ photons/sec

  $\tau_X = \tau_y = \tau_\varepsilon = 52$ sec

  $\sigma_\varepsilon / E = 7.1 \times 10^{-4}$, $\varepsilon_X = 3 \times 10^{-15}$ mrad

  (increased !) (decreased lots !)

BEAM EMITTANCE IN PWFA

G. Stupakov

CRYSTAL ACCELERATOR (PLASMA WAKE IN CONDUCTION ELECTRON AND CHANNELING)

P. Chen, SLAC

CRYSTAL CHANNELING ACCELERATION

Pisin Chen
Stanford Linear Accelerator Center
Stanford University

presented at

Symposium on "New Modes of Particle Acceleration Techniques & Sources", ITP, UCSB, Aug. 21, 1996.

I. WHY ACCELERATION IN CRYSTALS?

A. What is the ultimate acceleration gradient that man can ever in principle attain?

Other than acceleration in a quark-gluon plasma (inside neutron stars?), the highest possible acceleration gradient is in the crystal.

In plasma accelerators, acceleration gradient is

$$G \sim \sqrt{n_p}\ \text{eV/cm},$$

where n_p is the plasma density. Typically,
$n_p \sim 10^{14} - 10^{18}\,\text{cm}^{-3} \Rightarrow G \sim 10\,\text{MeV/cm} - 1\,\text{GeV/cm}$.

- Chen & Noble (1986, 1987) proposed acceleration along crystal channels by the plasma waves excited in the conduction-band electrons. Typically, $n_p \sim 10^{22}\,\text{cm}^{-3}$, $G \sim 100$ Tajima & Cavenago (1987) suggested crystal accelerati powered by X-rays. (Using channels as micro-structures).

B. However, a high gradient is not the only requirement for linear colliders.

Stability and emittance preservation requirements are very stringent.

- Intuitively, the strong focusing channels would help. But how?

- There are further constraints in the conventional approach to linear colliders set by Nature.

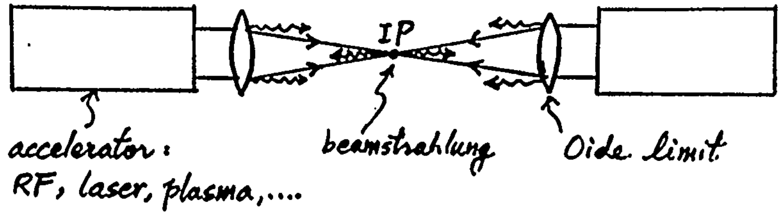

- Question : Does High Energy (accelerator-based) Physics have a long future?

  Or, can we beat these paradigms?

Answer : Acceleration and collision in crystal channels.

** This talk presents some first-order considerations toward this direction. It is evidently incomplete, and it may not even be entirely self-consistent.
<u>But I wish to motivate you that this is an exciting idea worthy of serious consideration.</u>

II. PLASMA-WAVE EXCITATION AND DECAY

A. Excitation:

A gradient $G \sim 100$ GeV/cm $\Rightarrow$ Energy density $\sim 10^8$ J/cm

- Plasma Beat-Wave Accel./Laser Wakefield (Tajima & Dawson '7

  To obtain (x-ray laser needed)

  $$\alpha_p \equiv \frac{eE_p}{m\omega_p c} \sim 10^{-2}-1 \Rightarrow \text{Laser intensity } I \gtrsim 10^{17}-10^{19} W/$$

- Laser-Acoustic-Wave Coupling (Katsouleas et al. '85)

  $\Rightarrow$ UV laser @ $I \gtrsim 10^{15}-10^{17} W/cm^2$.

- Plasma Wakefield Accel. (Chen et al. '85)

  $\Rightarrow 10^{20}-10^{22} e^-/cm^2$ for the driving beam $\Rightarrow I \gtrsim 10^{18}-10^{20} W/$

B. Decay and Damage Threshold:

Plasma Wave $\xrightarrow[\text{interband transitions}]{\text{decay}}$ Plasmon gas (in all direc

$\xrightarrow[e^- - e^- \text{ scattering}]{\text{decay } (\sim 10^{-10} sec)}$ superthermal electron gas $\left(\frac{10^8 J/cm^3}{10^{22}/cm^3} \sim 10\right.$

$\xrightarrow[\text{plasmon radiation } \& \ e^- \cdot e^- \text{ collision}]{\text{decay rate } \sim 1 MeV/cm}$ thermal electrons ($\sim$ 1mm in radius)

$\xrightarrow[\text{phonon emission}]{}$ crystal heating

- Crystal damage threshold $\sim \boxed{10^{13} W/cm^3 \text{ in a } 10^{-10} sec}$

III. ABSOLUTE DAMPING IN CHANNELING RADIATIO

Huang, Chen, and Ruth (1994),
Phys. Rev. Lett. 74, 1759 (1995)

Take a generic straight, continuous focusing system with transverse potential

$$V(x) = \frac{1}{2} K x^2 .$$

The total energy of the channeled particle (say, a e^+),

$$E = \sqrt{m^2 + p_z^2 + p_x^2} + V(x)$$

$$= \underbrace{\sqrt{m^2 + p_z^2}}_{E_z} + \underbrace{\frac{p_x^2}{2E_z} + V(x)}_{E_x} + O\left(\frac{p_x^4}{E_z^3}\right).$$

"longitudinal energy", "transverse energy"

$$\left\{\begin{matrix}\text{free relativistic}\\ \text{motion}\end{matrix}\right\} \xleftrightarrow{\text{decoupled}} \left\{\begin{matrix}\text{harmonic oscillation}\\ \text{with effective mass } E_z\end{matrix}\right\}$$

Work on relativistic crystal channeling has shown that the spin degree of freedom plays a negligible role. (Kumakhov & Komarov, 1989) Then using Klein–Gorden equation we have

$$[(-i\vec{\nabla} - \vec{A})^2 + m^2]\psi = (i\partial_t - V)^2\psi .$$

In the absence of radiation, let $\vec{A} = 0$, and look
the energy levels E and stationary state

$$\psi(x, z, t) = e^{-iEt} |n, p_z\rangle .$$

We find

$$\boxed{\begin{aligned} E &\approx E_z + E_x = \sqrt{m^2 + p_z^2} + (n + 1/2)\omega_z , \\ |n, p_z\rangle &= \left(\frac{C_n}{L}\right)^{1/2} (E_z\omega_z)^{1/4} e^{ip_z z} e^{-iE_z\omega_z x^2/2} \cdot \underset{\substack{\uparrow\\ \text{Hermite polynom}}}{H_n}(\sqrt{E_z\omega_z}\, x), \end{aligned}}$$

where $C_n = (2^n n! \sqrt{\pi})^{-1}$, L: length of channel, $\omega_z = \sqrt{K/E_z}$.

With the radiation "turned on", we find the transition ra

$$W_{fi} = 2\pi |M_{fi}|^2 \delta(E - E' - \omega_\gamma),$$

where

$$|M_{fi}|^2 \approx \frac{2\pi}{E'^2 \omega_\gamma} \sum_{j=1}^{2} \left| \langle n', p_z' | e^{-i\vec{k}_\gamma \cdot \vec{x}} (\underset{\substack{\uparrow\\ \text{photon polarization}}}{\hat{e}_j} \cdot \vec{\nabla}) | n, p_z \rangle \right|^2$$

- Conservation of longitudinal momentum:
  Integration over $z \rightarrow \delta(p_z - p_z' - k_{\gamma z})$
  $\rightarrow p_z' = p_z - \omega_\gamma \cos\theta .$
- Conservation of total energy: $\delta(E - E' - \omega_\gamma)$.

} tightly constrain the radiation reaction of the particle.

- For $\omega_\gamma \ll E$, the longitudinal energy must decrease:

$$\Delta E_z = E_z - E_z' \simeq \frac{p_z}{E_z}(p_z - p_z')$$
$$\simeq \beta(\omega_\gamma \cos\theta) < \omega_\gamma .$$

- Since the total energy is reduced by an amount ω_γ, its transverse energy $E_x = E - E_z$ must decrease by

$$\Delta E_x = \omega_\gamma(1-\beta\cos\theta) > 0 .$$

- It follows that

$$(n+1/2)\omega_z - (n'+1/2)\omega_z' = \omega_\gamma(1-\beta\cos\theta) > 0 .$$

- For a small change in E_z, $\omega_z' = \sqrt{K/(E_z-\Delta E_z)} \approx \omega_z(1+\Delta E_z/2E$
Substituting for ΔE_z, we obtain

$$(n-n')\omega_z' = (1-\beta\cos\theta)\omega_\gamma + (\omega_\gamma\beta\cos\theta)E_x/2E_z > 0 .$$

$$\therefore \quad \boxed{n > n'.} \qquad \text{QED}$$

- Transverse energy and quantum number always decrease after a photon emission, independent of emission angle.
- The external focusing environment absorbs the excess tranverse momentum, in analogy to the Mössbauer effect.

IV. GROUND STATE AND MINIMUM EMITTANCE

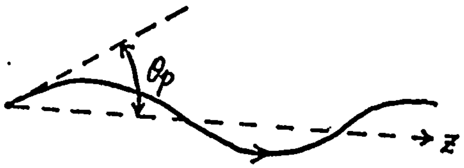

It can be shown that the action of the transverse oscillation damps according to the equation

$$\frac{1}{J_x}\left\langle\frac{dJ_x}{dt}\right\rangle = \frac{1}{E_x}\left\langle\frac{dE_x}{dt}\right\rangle + \frac{1}{2}\frac{1}{E_z}\left\langle\frac{dE_z}{dt}\right\rangle$$
$$= -\Gamma_c\Big(1+\frac{3}{8}\underbrace{\gamma^2\theta_p^2}_{\propto J_x}\Big), \qquad \Gamma_c \equiv \frac{2}{3}\frac{r_e K}{mc}.$$

We see that,

if $\gamma\theta_p \gg 1$, $\quad \frac{1}{J_x}\left\langle\frac{dJ_x}{dt}\right\rangle \cong +\frac{3}{4}\frac{1}{E}\left\langle\frac{dE}{dt}\right\rangle$;

if $\gamma\theta_p \ll 1$, $\quad \frac{1}{J_x}\left\langle\frac{dJ_x}{dt}\right\rangle \cong -\Gamma_c \gg \frac{1}{E}\left\langle\frac{dE}{dt}\right\rangle$.

The solution is

$$\boxed{\begin{aligned} J_x(t) &= J_{x0}\left[1+\frac{5}{8}(\gamma\theta_p)_0^2(1-e^{-\Gamma_c t})\right]^{-3/5}\cdot \exp\{-\Gamma_c t\}. \\ \gamma(t) &= \gamma_0\left[1+\frac{5}{8}(\gamma\theta_p)_0^2(1-e^{-\Gamma_c t})\right]^{-4/5}. \end{aligned}}$$

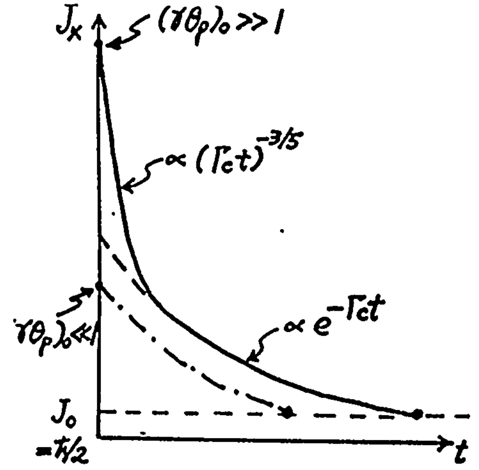

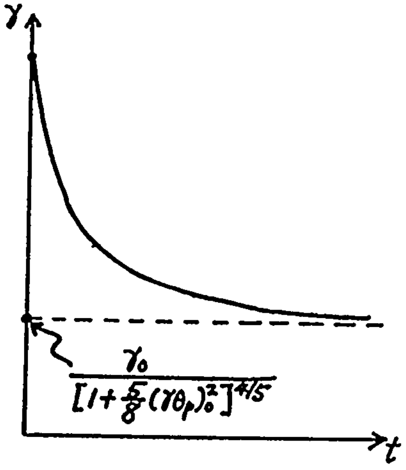

- Quantum mechanically the action of the transverse oscillatio is quantized:

$$J_x = J_n = E_x/\omega_x = (n+1/2)\hbar .$$

So J_x can only damp to its minimum value $J_0 = \hbar/2$ at the ground state. Relating this minimum action to a normalized emittance, we find

$$\boxed{\gamma\epsilon_{min} \equiv J_0/mc = \lambda\!\!\!^{-}_0/2,}$$

where $\lambda\!\!\!^{-}_c = \hbar/mc$ is the Compton wavelength.

- This is an emittance associated with the zero point energy of the ground state, and therefore is the theoretical minimum emittance one can ever attain, limited only by the uncertainty principle.

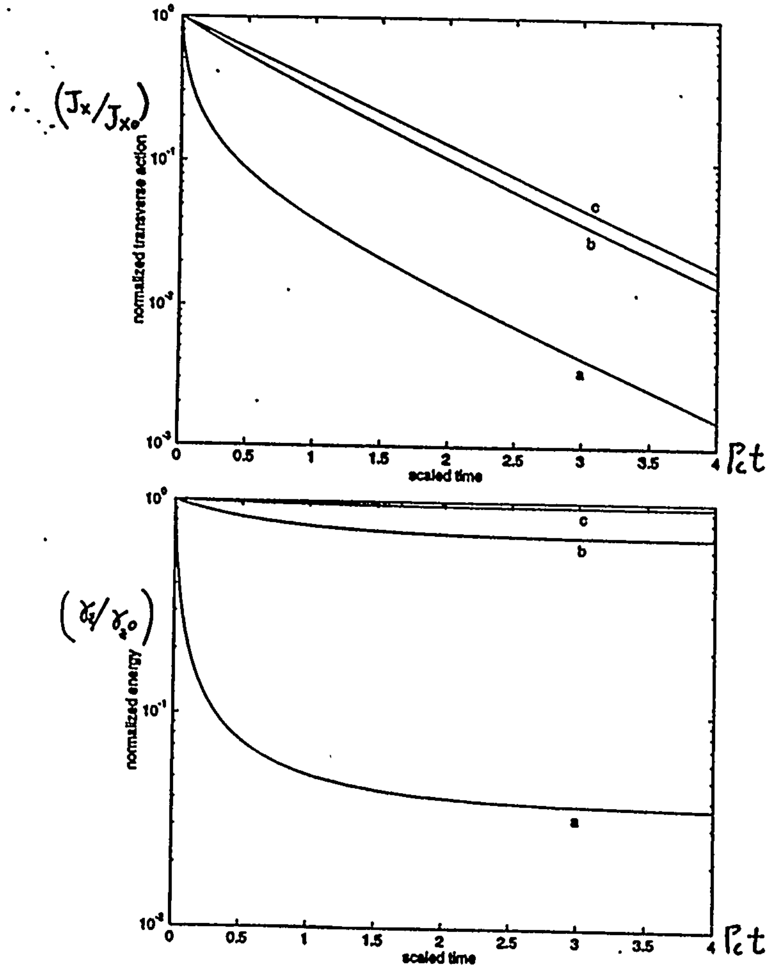

Fig. 2. (a) $\underline{\gamma_{z0}^2\theta_{p0}^2 = 100}$, (b)$\underline{\gamma_{z0}^2\theta_{p0}^2 = 1}$ and (c) $\underline{\gamma_{z0}^2\theta_{p0}^2 = 0.1}$.

- Time Needed to Reach Ground State :

Suppose the particle enters the channeling with transv energy $(n_i + 1/2)\omega_z$ satisfying the undulator condition, th it reaches the ground state in a time

$$t_g \sim \ln(n_i)/\Gamma_c \,.$$

Example :

For typical crystal channel $K \sim 10^{12} GeV/m^2 \rightarrow \Gamma_c \sim (1\, nse$

For a particle with $E_i = 100 MeV$ and is barely captured by the channel, $E_{xi} = V_{max} \sim 100 eV. \rightarrow n_i \sim 500$

$$\rightarrow t_g \sim 6 \text{ nsec.}$$

- Preservation of Longitudinal Emittance : $(= 1.8 m)$

The rate of change of longitudinal momentum is

$$\left|\frac{1}{p_z}\frac{dp_z}{dt}\right| \simeq \frac{1}{E}\left|\frac{dE}{dt}\right| \simeq \frac{\Gamma_c}{2}\gamma^2\theta_p^2 .$$

But $\gamma\theta_p \ll 1$ in our consideration. Thus

$$\left|\frac{1}{J_n}\frac{dJ_n}{dt}\right| \approx \Gamma_c \gg \left|\frac{1}{p_z}\frac{dp_z}{dt}\right| .$$

It can be shown that, when damped to the ground state,

$$\boxed{E_f = \frac{E_i}{[1+(\gamma\theta_p)_i^2/4]^2} \approx E_i \cdot [1 - \underbrace{\tfrac{1}{2}(\gamma\theta_p)_i^2}_{\ll 1}]}$$

V. RANDOM EXCITATION AND EQUILIBRIUM

- Sources of random excitation:
  - Bremsstrahlung
  - Multiple Coulomb scattering ← most severe.
  - Crystal imperfection, etc.
- Multiple Coulomb Scattering : Chen & Noble (1996) ← Lake Ta

Using Bohr's potential, one finds the local electron density

$$n_e(x) = \frac{ZNd_p}{a} e^{-d_p/a} \cdot \cosh\frac{x}{a}$$

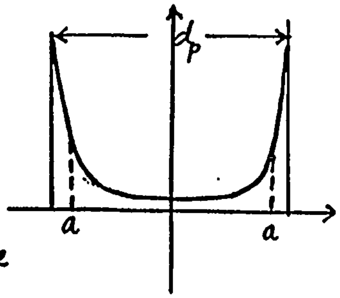

a = screening atomic radius

$$\approx .885\, a_0/\sqrt{Z^{2/3}+z^{2/3}} \,, \sim O(0.1 \text{Å})$$

For $d_p \sim a$, and $x \ll a$, we have

$$n_e(x) \sim ZN \sim \text{const.}$$

Then the focusing potential is $V(x) \approx \frac{1}{2}Kx^2$.

So multiple scattering causes

$$\frac{d\epsilon_n}{dt} \simeq \frac{c\gamma\beta_\lambda}{2}\frac{d}{dz}\langle\theta_p^2\rangle$$

$$\frac{d\langle\theta_p^2\rangle}{dz} \simeq \frac{4\pi ZN r_e^2}{\gamma^2}\underbrace{\ln\left(\frac{\lambda_D}{\lambda_c}\right)}_{\approx 10}$$ ← Debye length

$\beta_\lambda = \sqrt{\frac{E}{eK}}$ ← betatron waveleng

$$\therefore \boxed{\frac{d\epsilon_n}{dt} \simeq \frac{20\pi ZN r_e^2 c}{\gamma^{1/2}}\sqrt{\frac{mc^2}{eK}}}$$ due to excitation

Montague & Schnell (1985); Chen, Huang, Ruth (1995)

- On the other hand, channeling radiation damping gives

$$\frac{d\varepsilon_n}{dt} = \lambda_c \frac{dn}{dt} = -\lambda_c \Gamma_c n . \qquad \Gamma_c \equiv \frac{2}{3}\frac{r_e K}{mc} .$$

- Equilibrium is reached when damping = excitation.

⇒

The lowest quantum level

$$\boxed{n_{eq} \simeq \frac{1.4 \times 10^{16}}{\sqrt{K[GV/m^2]\cdot\gamma}}} .$$

For $K \sim 10^{12}\, GV/m^2$, $\gamma = \frac{5\,TeV}{0.5\,MeV} = 10^7$,

$n_{eq} \sim 200$.

- • Note that the above equation shows that for sufficiently high-energy particles, damping is more effective than excitation, so such particles can be channeled indefinitely and damped to ground state (asymptatically).
- • Somewhat counter-intuitively, the physics is in favor of the largest possible focusing strength, K, or largest possible e^- density!

VI. QUANTUM LUMINOSITY

- The damping effects that we found are not affected by acceleration, as long as the <u>adiabatic acceleration</u> condition is satisfied:

$$G \ll \omega_x E \approx \sqrt{KE} .$$

For particle energy as low as 100 MeV, we get $\omega_x E \sim 10^5\, GeV/m$.

- We can therefore envision acceleration AND colliding particles inside crystal channels in the transverse equilibrium state, <u>without the use of a final focusing system.</u>
- Luminosity Integral:

By definition,

$$\mathcal{L} = 2 f_{rep} N^2 \int dx\,dy\,ds\,dt \; n_1(x,y,z_1,t)\cdot n_2(x,y,z_2,t),$$

$$s = z_1 + t = -z_2 - t .$$

In the ground state the probability density is

$$n(x,y,z) = n_L(z)\cdot|\psi_0(x)|^2\cdot|\psi_0(y)|^2,$$

$$\psi_{x_0}(x) = \frac{1}{\pi^{1/4}\sqrt{x_0}}\, e^{-x^2/2x_0^2}, \qquad x_0 = \sqrt{\frac{\hbar}{m\omega_x}} = \left(\frac{\lambda_c}{\gamma}\sqrt{\frac{E}{K}}\right)^{1/2} .$$

At n^{th} level. $\langle x_n \rangle \propto \sqrt{E_n} \sim \sqrt{n}$. $\therefore \langle x_n \rangle \sim \sqrt{n}\, x_0$.

- Let there be n_c channels in a cluster that have captured N_c particles in each channel.
  Since there is no depth of focus problem, all N_c partic within each channel will pass through the N_c particles from the opposite side.

- Carrying out the integration we find

$$\mathcal{L} = f_{rep} \cdot n_c \cdot \mathcal{L}_c = f_{rep} \cdot n_c \cdot \frac{N_c^2}{2\pi x_0 y_0 \cdot n_{eq}}$$
$$= \frac{f_{rep} \cdot n_c \cdot N_c^2}{2\pi \hbar c \cdot n_{eq}} \sqrt{KE} .$$

- Example: 5 TeV + 5 TeV crystal collider. $N = 10^{11}$, $n_{eq} \simeq 10$
  $E_0 = 1\,\mathrm{GeV}$, $\epsilon_{n0} = 1 \times 10^{-8}$ m·rad, $f_{rep} = 180\,\mathrm{Hz}$
  Typical crystal channeling critical angle θ_c is
$$\theta_c = \sqrt{\frac{2V_c}{E}} \qquad V_c \sim 100\,\mathrm{eV}.$$
  To match the injection optics, we choose the β-function to be
$$\beta = \frac{\epsilon_n/\gamma}{\theta_c^2} = \frac{mc^2\epsilon_n}{2V_c} \sim 25\mu m.$$
$$\rightarrow \sigma_r = \sqrt{\beta\epsilon_n/\gamma} \sim 100\,\mathring{A} . \rightarrow N = n_c \cdot N_c \cong 10^4 \cdot 10^7$$
  With $K \sim 10^{12}\,\mathrm{GeV/m^2}$, we find $\mathcal{L} \sim 1 \times 10^{37}\,\mathrm{cm^{-2} \cdot sec^{-1}}$.

**Note: The beam power is as small as $P_b = 2 \times 15$ MW.

**But: What drives the accelerator? Side-injected UV laser coupled to an acoustic wave @ ~50M

VII. FIRST STEP TOWARDS THE ULTIMATE COLLI

- If one invokes the LWFA approach to drive the crystal accelerator, one would need a X-ray laser/FEL @ $\lambda \sim O($
  This technology is presently not available.

- As a first step effort, one can scale-up the channel size and experiment with mezzoscopic (artificial) crystal chann
- This is then a miniature Hollow Plasma Channel Accelera (Katsouleas, Wurtele, et al. 1994).
- First experiment in progress: Chen, Ogata, et al. (Lake Tahoe

— Using the T^3 laser ($\lambda \sim 800\,nm$) @ Takai, Japan. (SLAC-KEK-Fermilab-NEC)

↑ crystal cha fabricatic

— Crystal channels @ $d_p \sim 1\mu m$ (By NEC)

— Test wakefield excitation, laser channel-guiding, crystal damage, traped electron acceleration, etc.

fabricated according to this process. We fabricated this Pt hole array using the mother porous alumina formed under the most appropriate condition at the present stage for ordering, that is, long-period anodizing for 160 hours at 0°C. From Fig. 2A, which shows the typical defect-free area of the Pt hole array, we confirm that nanoholes with

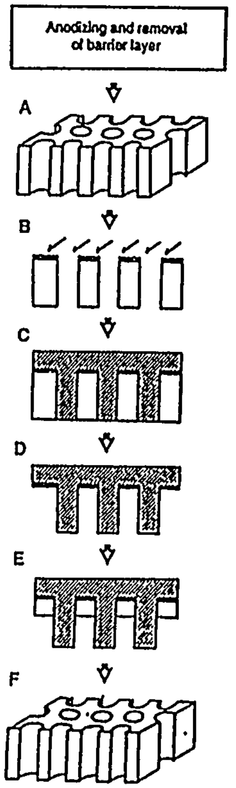

Fig. 1. Schematic diagram of the process for the fabrication of the metal nanohole array: (A) porous alumina with through holes (mother structure), (B) metal deposition with vacuum evaporation, (C) injection and polymerization of methyl methacrylate, (D) poly(methyl methacrylate) negative type, (E) electroless metal deposition, and (F) metal hole array.

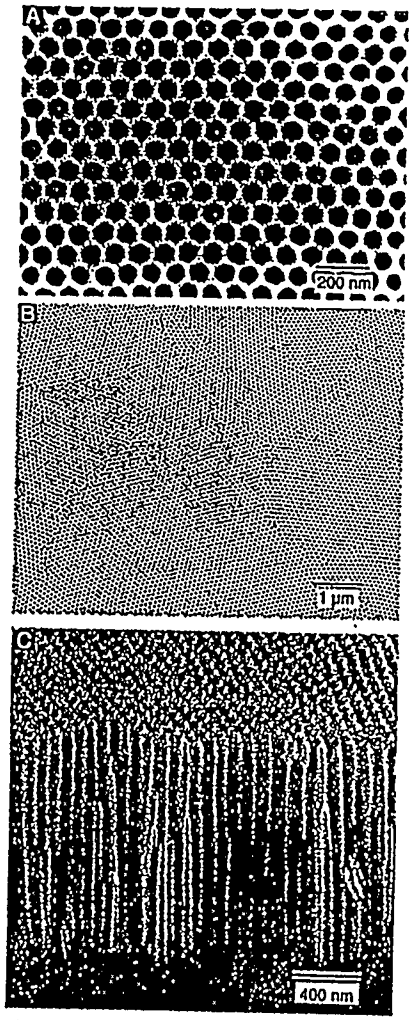

Fig. 2. SEM photographs of the Pt nanohole array: (A) view of the surface (higher magnification), (B) view of the surface (lower magnification), and (C) cross-sectional view. The anodic alumina used as a mother structure was formed at 0°C over a period of 160 hours. The duration of dipping treatment in phosphoric acid was 90 min.

Masuda et al., SCIENCE • VOL. 268 • 9 JUNE 1995

Table 2. Some properties of crystals.

crystal	$n_0(\text{cm}^{-3})$	$\bar{\lambda}_p = 1/k$	ψ_p @ 50 GeV	ψ_p @ 50 MeV
Ge	3×10^{13}	0.97 mm		
Si	8×10^{14}	0.19 mm	(110) 39 μrad	0.92 mrad
Bi	3×10^{17}	9.7 μm		
Graphite	3×10^{16}	3.1 μm		
Ni			(110) 47 μrad	1.5 mrad
Cu	8.5×10^{22}	18 nm		
Al	1.7×10^{23}	13 nm		
W			(100) 49 μrad	1.5 mrad

Plasma densities in crystals are "tunable"!

MICROWAVE INVERSE CERENKOV AND FEL ACCELERATORS: “TABLETOP” SYSTEMS FOR APPLICATIONS AT 10 -20 MEV.

T. Marshall, Columbia

MICROWAVE INVERSE FEL AND CERENKOV ACCELERATORS

T.C. Marshall, Columbia University

* These two accelerators are under construction at Omega-P, Inc., located at Yale University; support is provided by DOE SBIR's.

* Both accelerators:
- -use MW power from a 2.85GHz klystron;
- -use psec 6MeV electron bunches from an rf gun;
- -should achieve final energy ~ 15-20MeV in 1.5m.

* The MIFELA is a fast-wave, smooth-bore device, using a wiggler, and makes a spiralling electron beam.

* The MICA is a slow-wave, smooth bore device, using a hollow cylinder of alumina ($\varepsilon = 9.5$), and makes a linear electron beam. It might be less expensive to fabricate than an rf linac module.

Acknowledgment: J.H. Hirshfield and M.A. LaPointe at Omega-P/Yale; and Tingbin Zhang at Columbia

---

MICROWAVE INVERSE ČERENKOV ACCELERATOR

Introduction and Background

- Three important works related with MICA:
  - The stimulated Cerenkov effect for coherent radiation.

    J.E. Walsh, T.C. Marshall & S.P. Schlesinger, *Physics of Fluids 20, 709(1977)*
  - The inverse Cerenkov effect for electron acceleration.

    J.R. Fontana & R.H. Pantell, *J. App. Phys. 54, 4285(1983)*
  - Inverse Cerenkov Accelerator(ICA)--
    a recent experimental demonstration at BNL using co_2 laser and 50 MeV e-beam

    W.D. Kimura, et al, *Phys. Rev. Lett. 74, 546(1995)*

- MICA Project:
  - Application to compact 20 MeV accelerator using SLAC klystron.
  - Smooth-bore structure.
  - Full trapping & mono-energetic bunch.
  - Low emittance.
  - Dielectric breakdown can be overcomed by using Ez ≤ 100KV/cm.

MICA

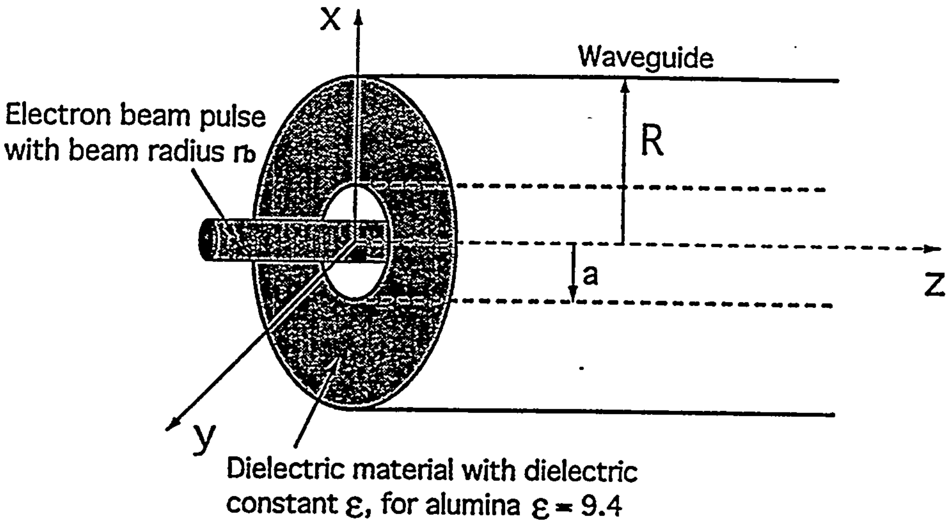

Fig. 2. In the dielectric-lined waveguide, the phase velocity of waveguide mode will be slowed to the axial speed of electrons.

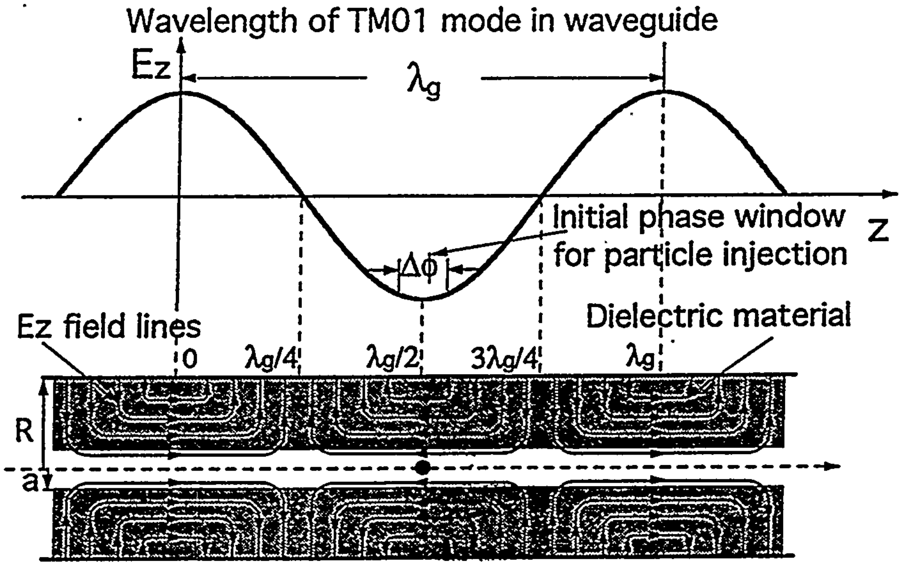

Dielectric-loaded Waveguide

Table II. Simulation parameters of MICA

Electron beam parameters		
Initial electron energy	$\gamma_0 = 13$	
Maximum initial transverse velocity	$\beta_\perp = 2.60 \times 10^{-3}$	
Initial axial velocity (6MeV)	$\beta_z = 0.9970$	
Beam radius	$r_b = 0.05$	(cm)
10A, 5 psec	$r_b/R = 0.032$	
Waveguide parameters		
Waveguide radius	$R = 1.59$	(cm)
Radius of vacuum hole	$a = 0.48$	(cm)
	$a/R = 0.30$	
Dielectric constant(alumina)	$\varepsilon = 9.4$	
Waveguide length	$z = 150$	(cm)
Waveguide mode	TM_{01}	
Radiofrequency wave		
Field power	$P = 15$	(MW)
Maximum field strength	$E_{zmax} = 6.29$	(MV/m)
Frequency	$f_0 = 2.856$	(GHz)
Normalized phase velocity	$V_{ph/c} = 0.9943$	
Free space wavelength	$\lambda_0 = 10.50$	(cm)
Waveguide wavelength	$\lambda_g = 10.46$	(cm)

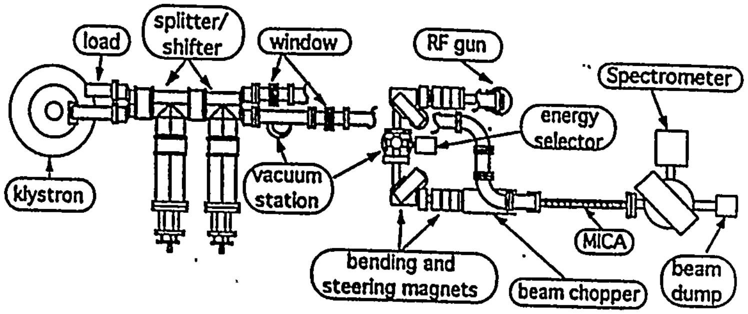

(a)

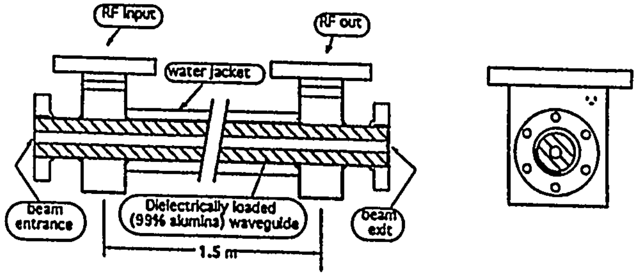

(b)

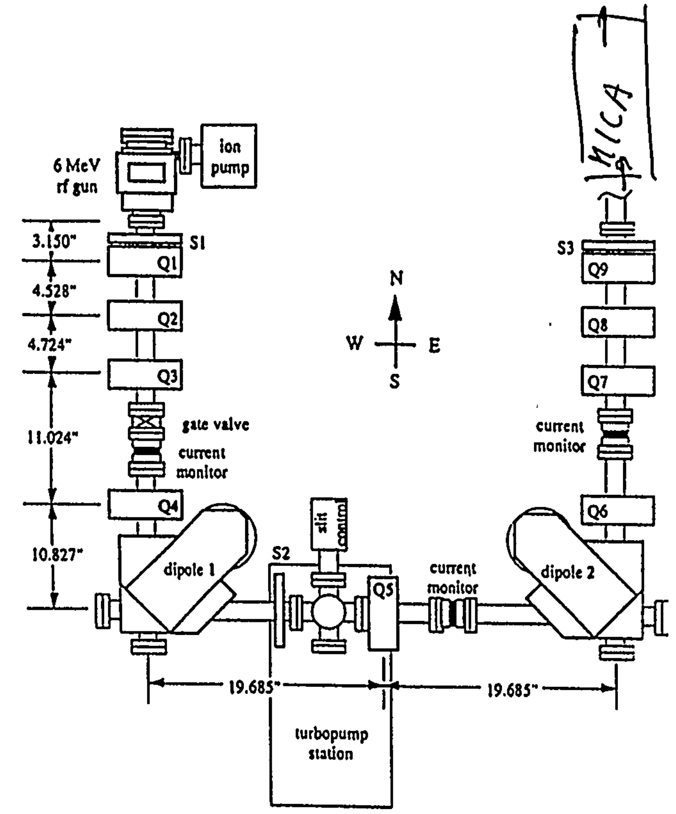

Fig. 5. Layout of the Omega-P/Yale 6 MeV beamline. It is planned to install the millimeter-wave receiving horn in the gap of dipole #2.

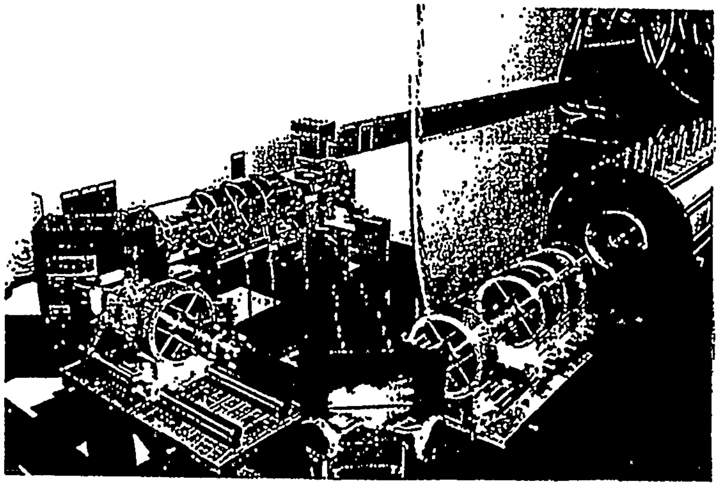

Fig. 6. Photograph of the Omega-P/Yale 6 MeV beamline taken during installation. Dipole #2 is shown in the foreground.

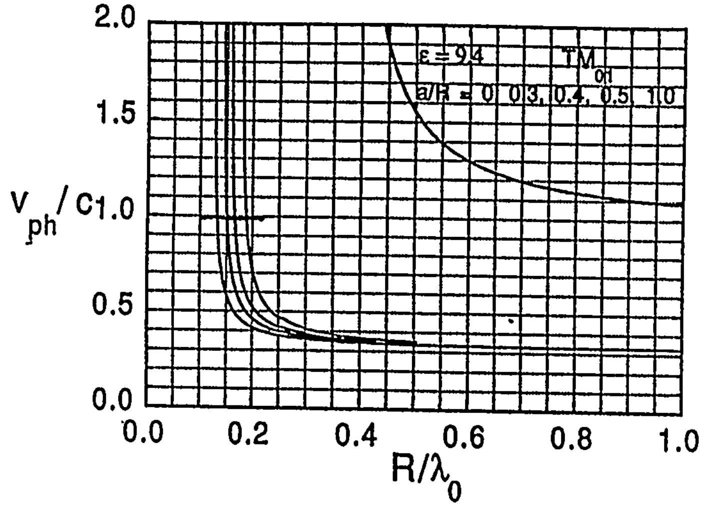

Theoretical Model (I)

A single-particle 3-D dynamic simulation

- Eigenvalue equation

$$\frac{I_1(k_{1i}a)}{I_0(k_{1i}a)} = \varepsilon \frac{k_{1i}}{k_2} \frac{J_1(k_2a)\,N_0(k_2R) - J_0(k_2R)\,N_1(k_2a)}{J_0(k_2a)\,N_0(k_2R) - J_0(k_2R)\,N_0(k_2a)}$$

- Electromagnetic field distributions for TM01 mode:

when $0 \le r \le a$,

$$E_{z1}(r,z,t) = E_0\, I_0(k_{1i}r)\cos(\omega t - k_z z)$$

$$E_{r1}(r,z,t) = -E_0 \frac{k_z}{k_{1i}} I_1(k_{1i}r)\sin(\omega t - k_z z)$$

$$B_{\theta 1}(r,z,t) = -E_0 \frac{k_0}{k_{1i}} I_1(k_{1i}r)\sin(\omega t - k_z z)$$

when $a \le r \le R$,

$$E_{z2}(r,z,t) = E_0 g_i\,[J_0(k_2r)\,N_0(k_2R) - J_0(k_2R)\,N_0(k_2r)]\cos(\omega t - k_z z)$$

$$E_{r2}(r,z,t) = -E_0 g_i \frac{k_z}{k_2}[J_1(k_2r)\,N_0(k_2R) - J_0(k_2R)\,N_1(k_2r)]\sin(\omega t - k_z z)$$

$$B_{\theta 2}(r,z,t) = -E_0 g_i \frac{\varepsilon k_0}{k_2}[J_1(k_2r)\,N_0(k_2R) - J_0(k_2R)\,N_1(k_2r)]\sin(\omega t - k_z z)$$

- Lorentz equation in cylindrical coordinates

$$\dot{\beta}_r - \mu\beta_\theta = -\frac{e}{mc^2\gamma}[(1-\beta_r^2)E_r - \beta_r\beta_z E_z - \beta_z B_\theta]$$

$$\dot{\beta}_\theta + \mu\beta_r = -\frac{e}{mc^2\gamma}[-\beta_\theta\beta_r E_r - \beta_\theta\beta_z E_z]$$

$$\dot{\beta}_z = -\frac{e}{mc^2\gamma}[-\beta_z\beta_r E_r + (1-\beta_z^2)E_z - \beta_r B_\theta]$$

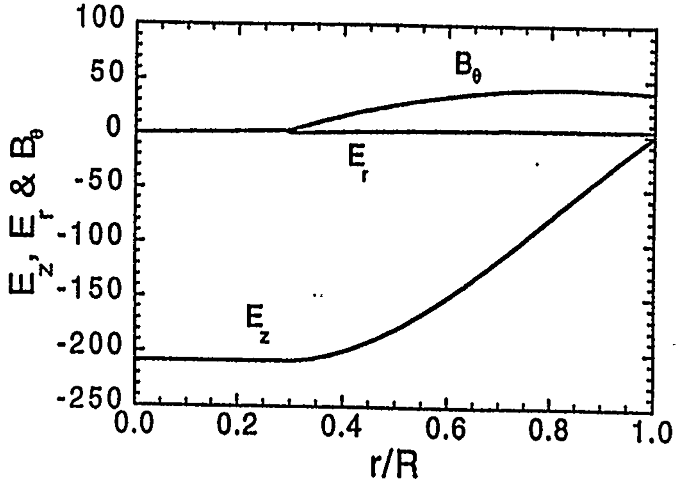

E_z, E_r & B_θ
100
50
0
-50
-100
-150
-200
-250
0.0
0.2
0.4
0.6
0.8
1.0
r/R
B_θ
E_r
E_z

Fig. 4

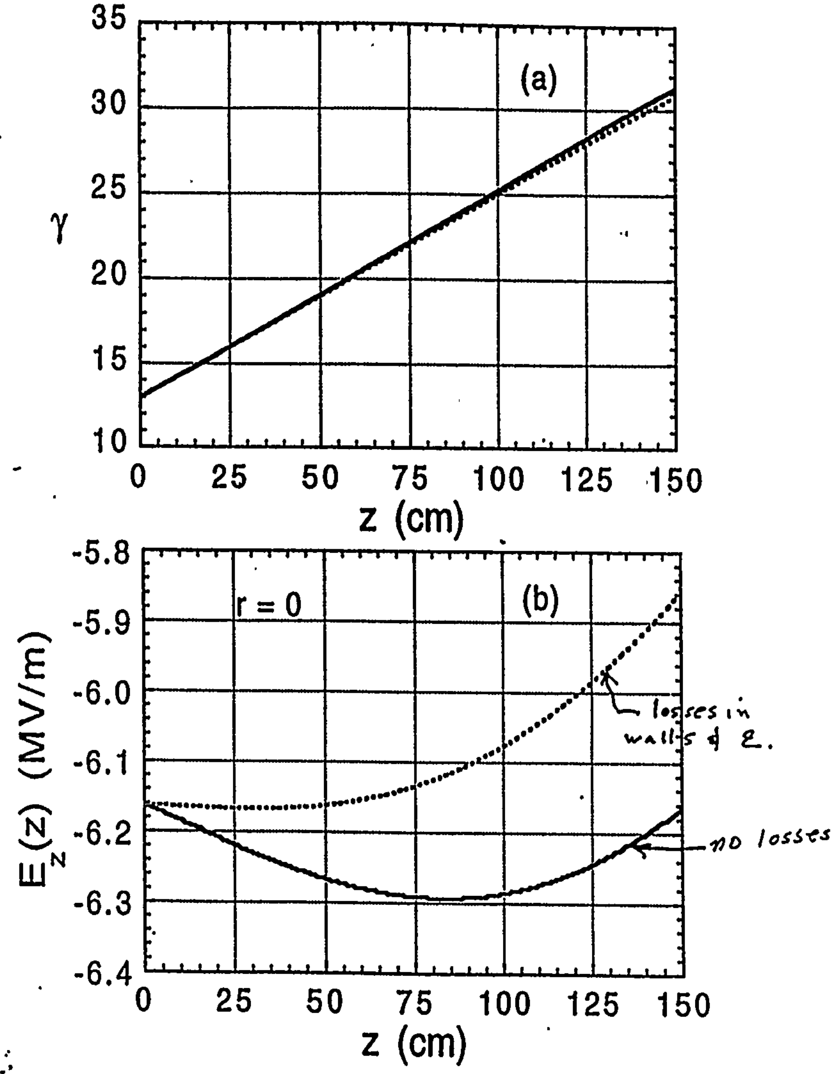

(a)
γ
35
30
25
20
15
10
0
25
50
75
100
125
150
z (cm)
(b)
r = 0
$E_z(z)$ (MV/m)
-5.8
-5.9
-6.0
-6.1
-6.2
-6.3
-6.4
0
25
50
75
100
125
150
z (cm)
losses in walls of Z.
no losses

Fig. 3

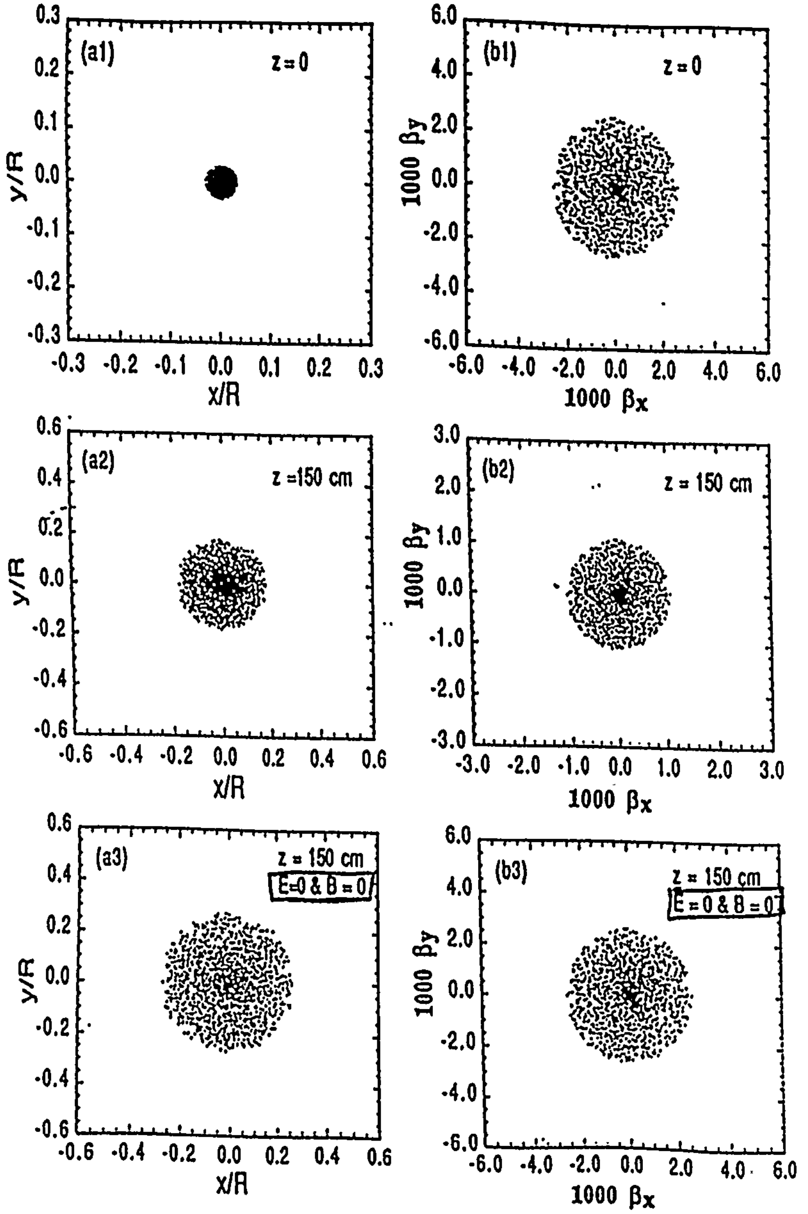

Fig5

Table III. PARMELA results about beam emittance and energy spread at the entrance and exit of the waveguide.

z (cm)	a_0 (mm)	E_{beam} (MeV)	$4\sigma_\phi$ (deg.)	$4\sigma_E$ (keV)	ε_{nxrms} (πmm mrad)	ε_{nyrms} (πmm mrad)	ε_{nzrms} (πdeg-keV)
0	0.5	6.0	5.78	68.9	3.05	2.90	24.9
150	3.0	15.6	5.83	80.2	3.05	2.91	25.8

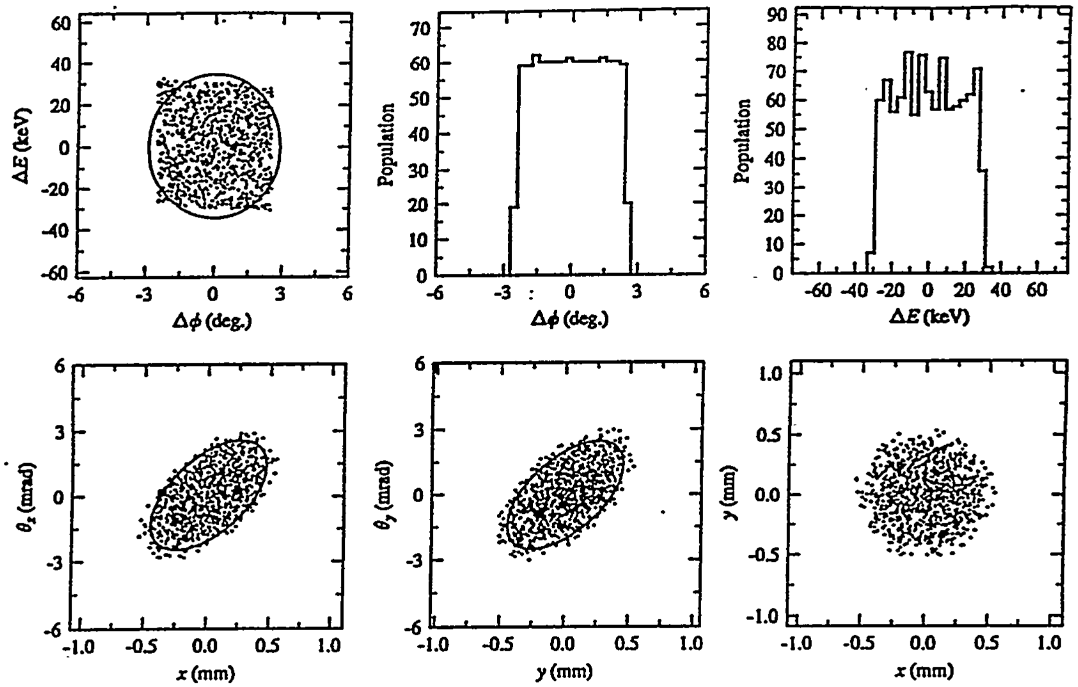
ΔE (keV)
Δφ (deg.)
Population
Δφ (deg.)
Population
ΔE (keV)
θ_x (mrad)
x (mm)
θ_y (mrad)
y (mm)
y (mm)
x (mm)

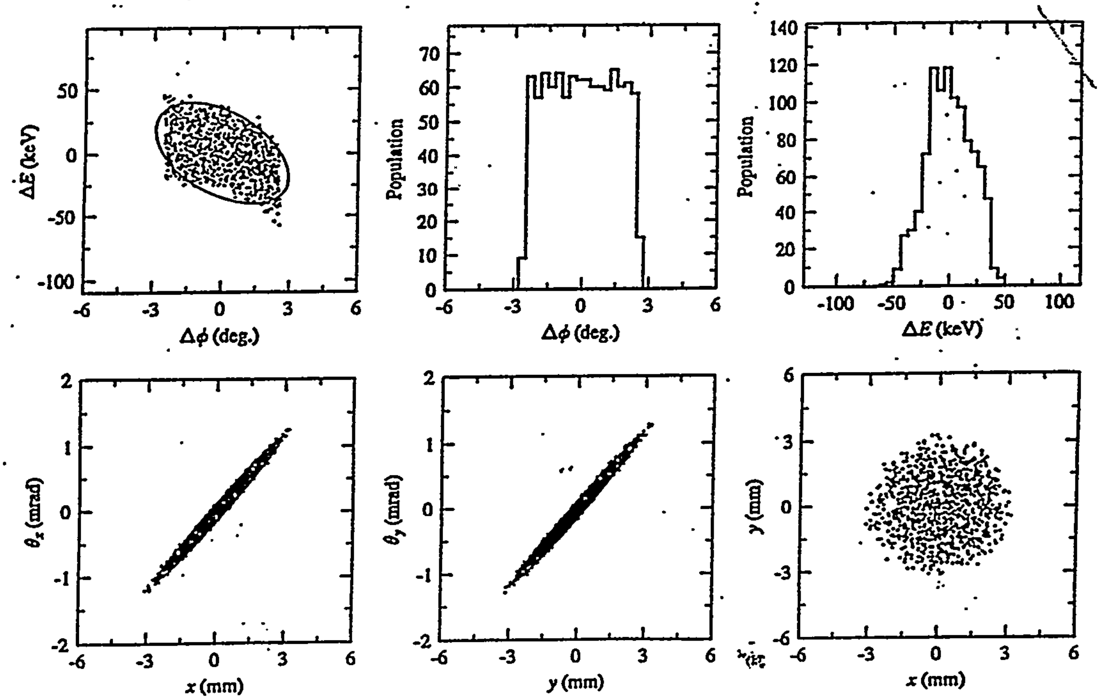
ΔE (keV)
Δφ (deg.)
Population
Δφ (deg.)
Population
ΔE (keV)
θ_x (mrad)
x (mm)
θ_y (mrad)
y (mm)
y (mm)
x (mm)

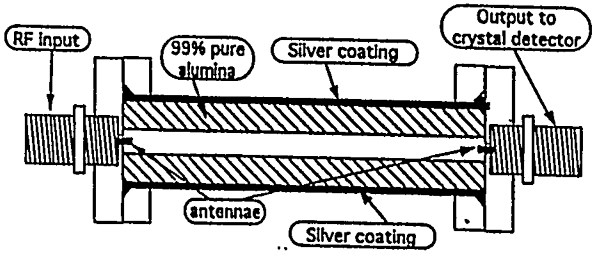

Apparatus to measure ε
and mode spectrum

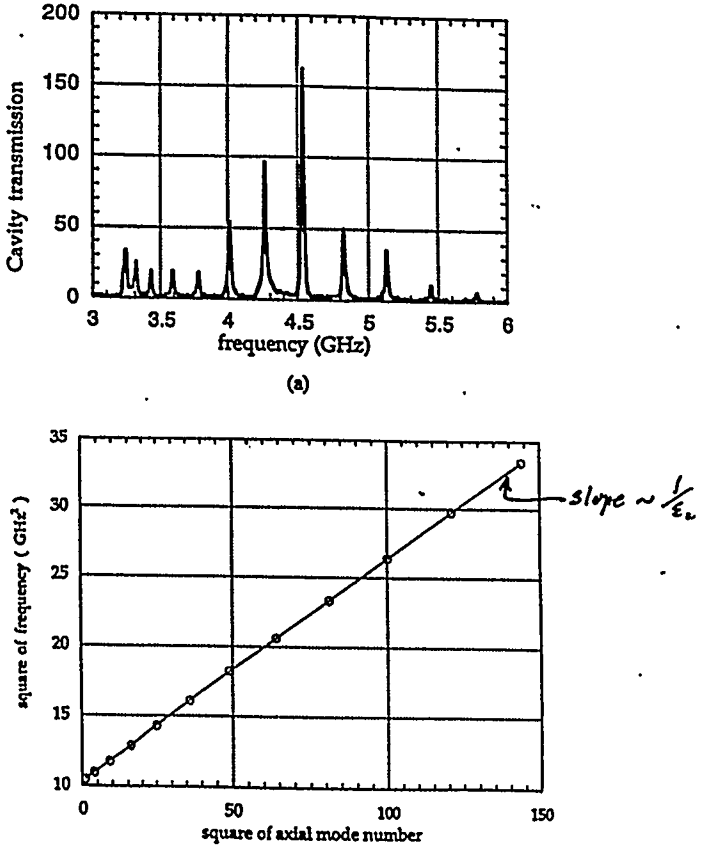

(a)

(b)

$$\omega_{onp} = \frac{c}{\sqrt{\varepsilon}}\left[K_{\perp,n}^2 + \left(\frac{p\pi}{d}\right)^2\right]^{1/2}$$

- no other modes found that did not fit onto line.

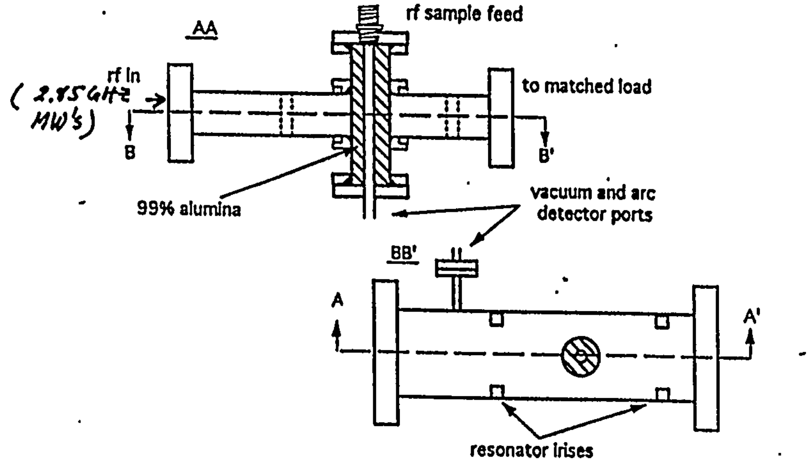

- Successful test @ 8.4 MV/m with no breakdown

Fig. 1 MICROWAVE INVERSE FEL ACCELERATOR

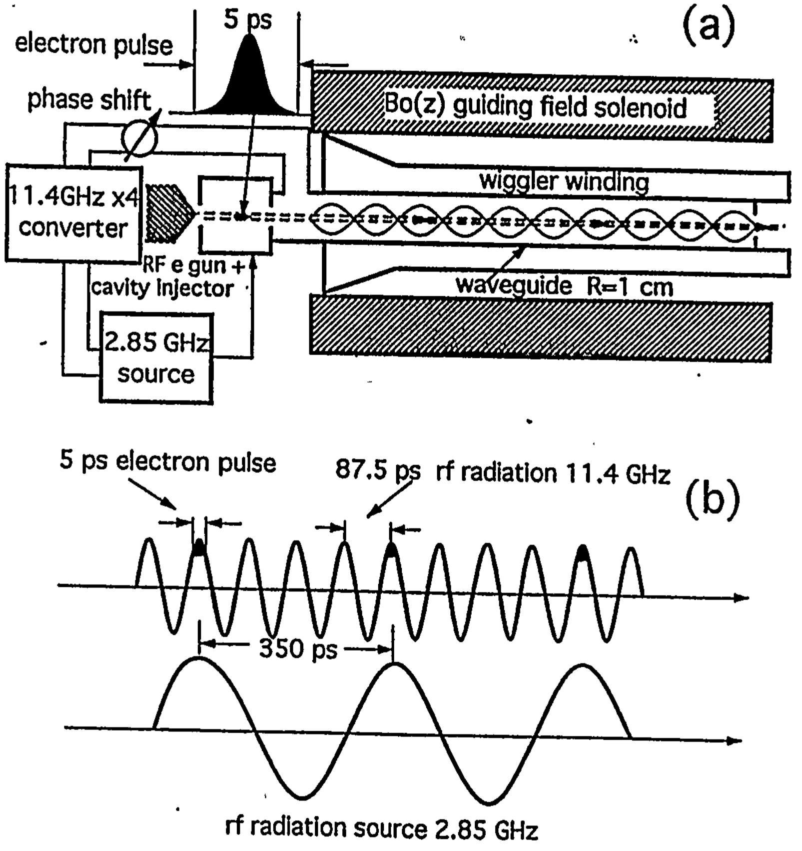

1D FEL EQUATIONS

- $$\frac{d\gamma_j}{dz} = -\frac{a_w a_s \frac{\omega_s}{c}}{\gamma_j}\sin(\psi_j)\left[1-\frac{\mu^2-2a_w a_s\cos\psi_j}{\gamma_j^2}\right]^{-1/2}$$

- $$\frac{d\psi_j}{dz} = k_w + k_s - \frac{\omega_s}{c}\left[1-\frac{\mu^2-2a_w a_s\cos\psi_j}{\gamma_j^2}\right]^{-1/2} + \frac{\partial\phi}{\partial z}$$

$$\mu^2 = 1 + a_w^2 + a_s^2$$

- $$\left[\nabla_\perp^2 + 2ik_s\frac{\partial}{\partial z} - \delta k_s^2\right]u(r,z) = -\frac{\omega_p^2}{c^2}\left\langle\frac{e^{-i(\psi-\phi)}}{\gamma}\right\rangle,$$

$$\delta k_s^2 = k_s^2 - \frac{\omega_s^2}{c^2}. \qquad u = a_s e^{i\phi}$$

STABLE ORBIT EQUATION

$$\beta_\perp = \frac{2\Omega_\perp\frac{I_1(\lambda)}{\lambda}\beta_\parallel}{\Omega_0 - \gamma k_w c\beta_\parallel \pm 2\Omega_\perp I_1(\lambda)}$$

where $\lambda = \pm\beta_\perp/\beta_\parallel, \beta_\perp$

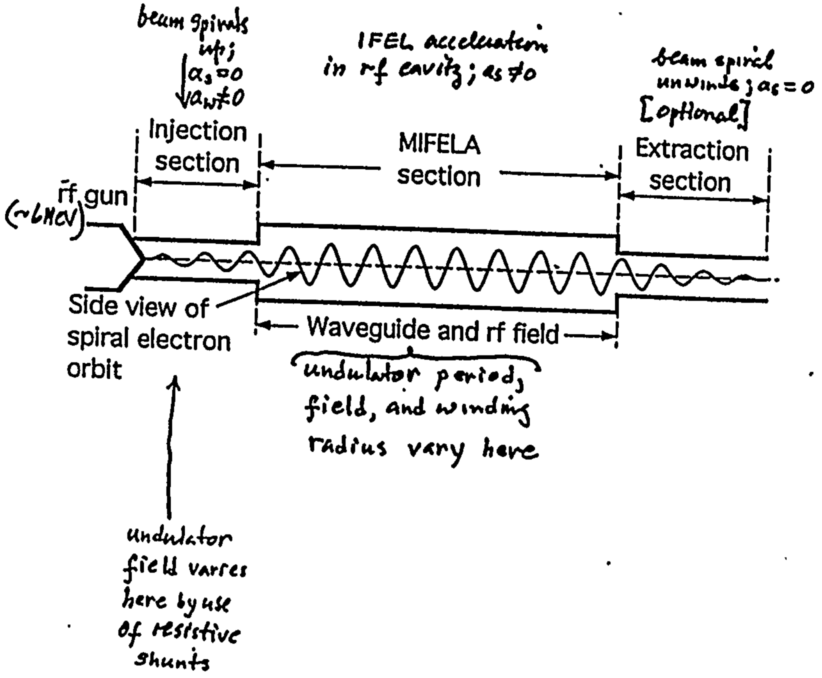

Fic 1

Table I. MIFELA Simulation Parameters

Injection Section	
Electron beam energy	$\gamma=13$
Undulator magnetic field	$B_W = 0 - 3.87$ K Gauss; linear ramp
Guiding field	$B_0 = 0 - 1.91$ K Gauss; linear ramp
Undulator period	$l_W = 10.0$ cm; constant
Injection section length	50 cm
Acceleration Section	
Electron beam energy	$\gamma = 13 - 28.5$
Electron beam current	$I_b \sim 1.0$ A
Electron beam radius	$r_b = 0.2$ cm
Undulator magnetic field	$B_W = 3.87 - 6.81$ K Gauss
Guiding field	$B_0 = 1.91 - 1.74$ K Gauss
Undulator period	$l_W = 10.0 - 12.1$ cm, linear ramp
Undulator length	150 cm
Effective undulator parameter	$a_W = 5.2 - 9.5$
Driving field wavelength	$\lambda_s = 2.63$ cm
Driving field intensity	$a_s = 0.15$ (circular polarized)
Waveguide mode	TE_{11}
Waveguide radius	$R = 1.4$ cm
Extraction Section	
Electron beam energy	$\gamma = 28.5$
Undulator magnetic field	$B_W = 6.81 - 0$ K Gauss; linear ramp
Guiding field	$B_0 = 1.74 - 0$ K Gauss; linear ramp
Undulator period	$l_W = 12.1$ cm; constant
Extraction section length	60 cm

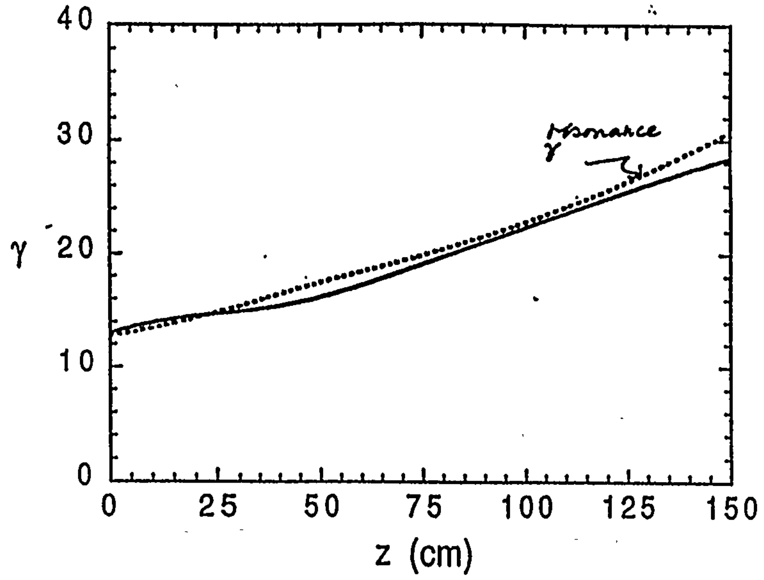

Fig 2

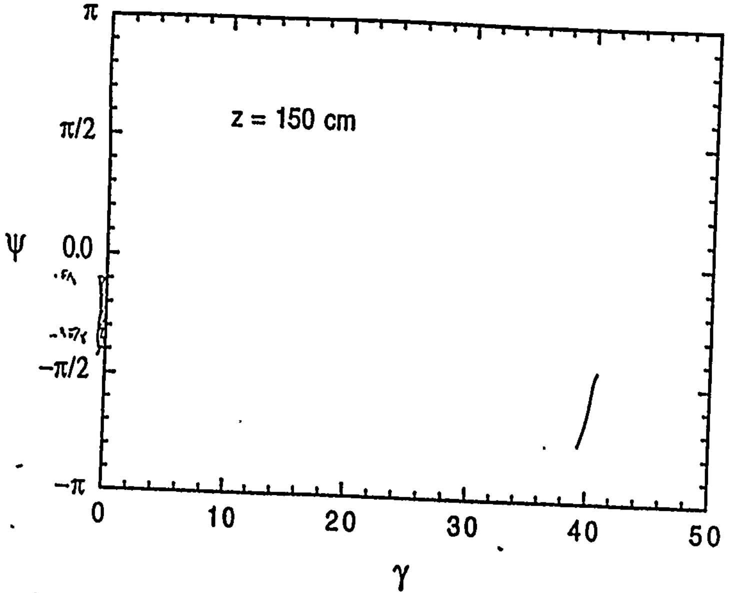

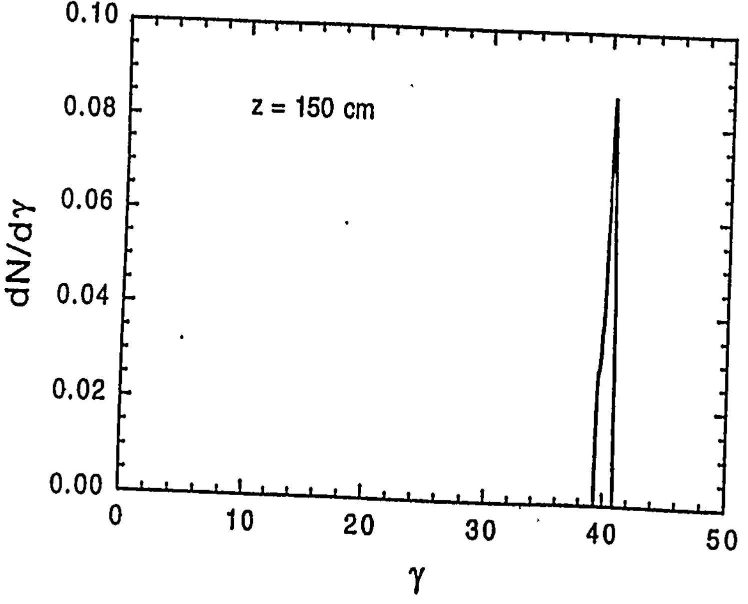

typical orbital stability plot

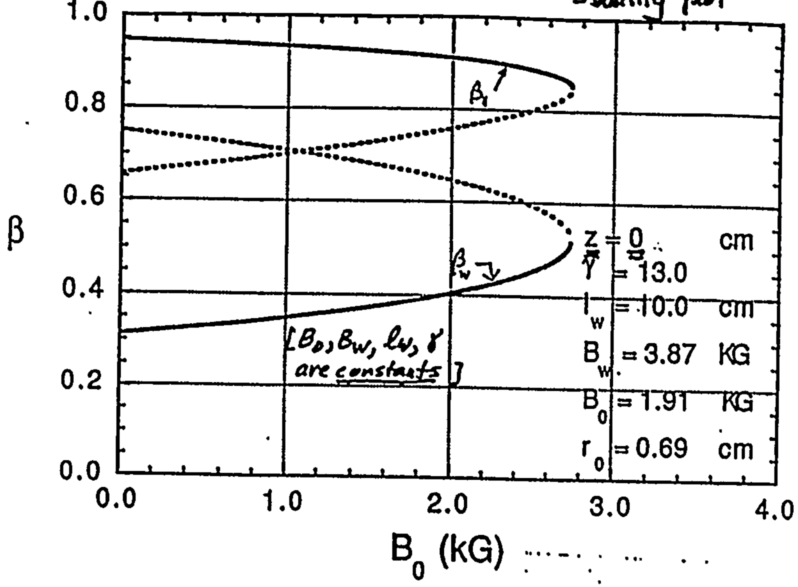

[B_0, B_w, l_w, γ are constants]

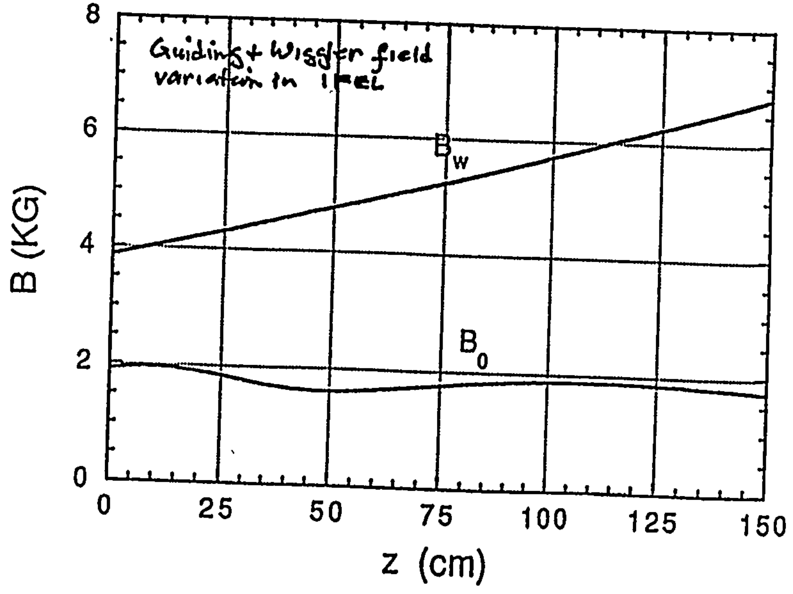

Guiding + Wiggler field variation in 1 FEL

Injection Region : $\sin^2$ taper on B_w

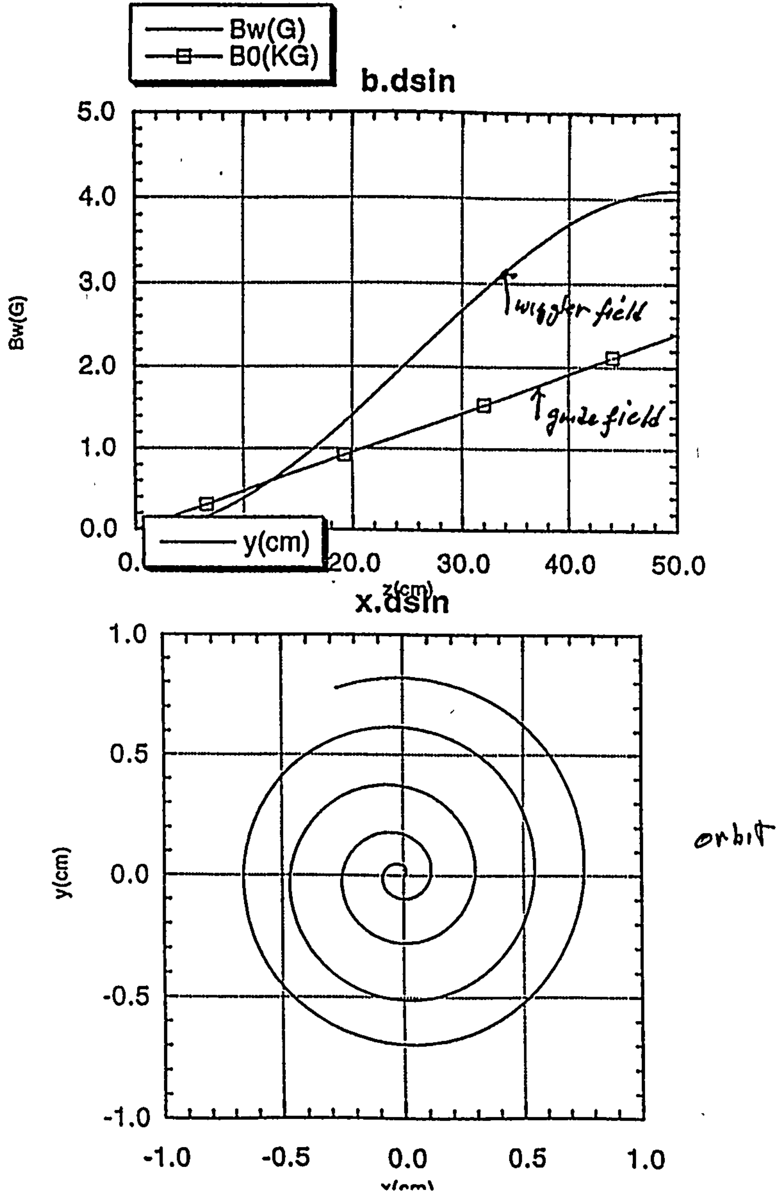

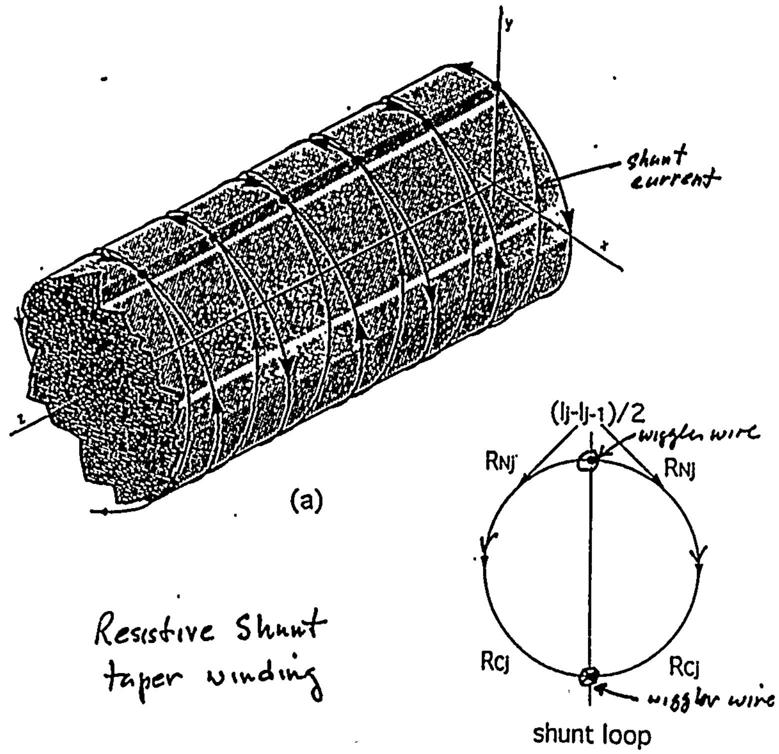

Resistive Shunt taper winding

Resistive Shunts, giving $B_w(z)$

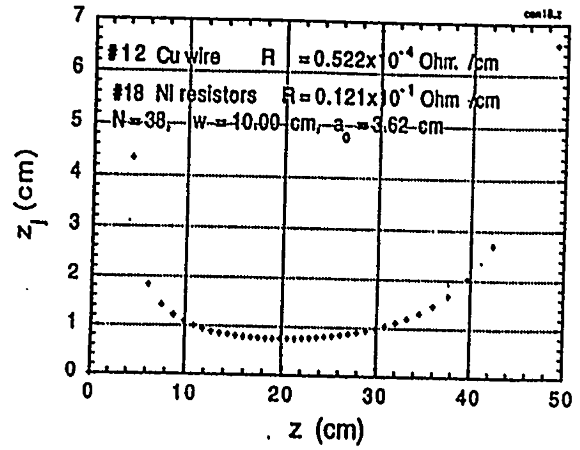

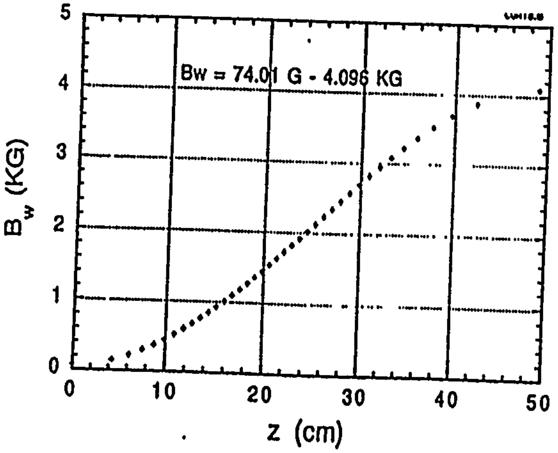

- Starting electrons from beginning, $a_w, a_s \neq 0$.
- Validated by 3D computation (R. Yoder & A. Ganguly)

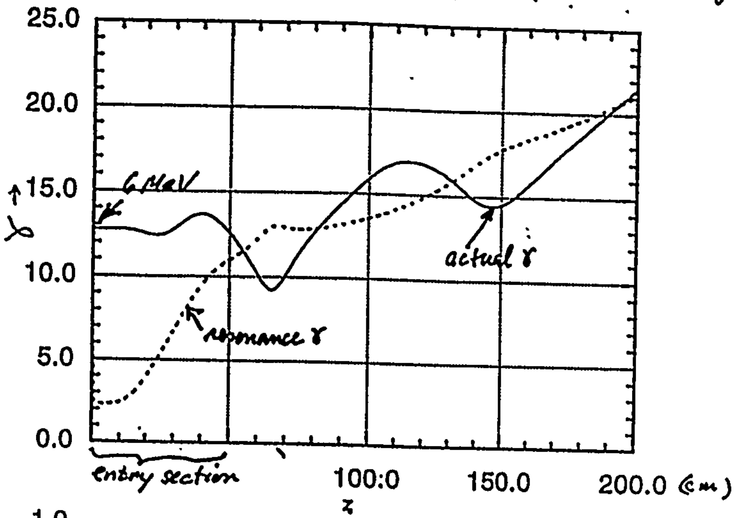

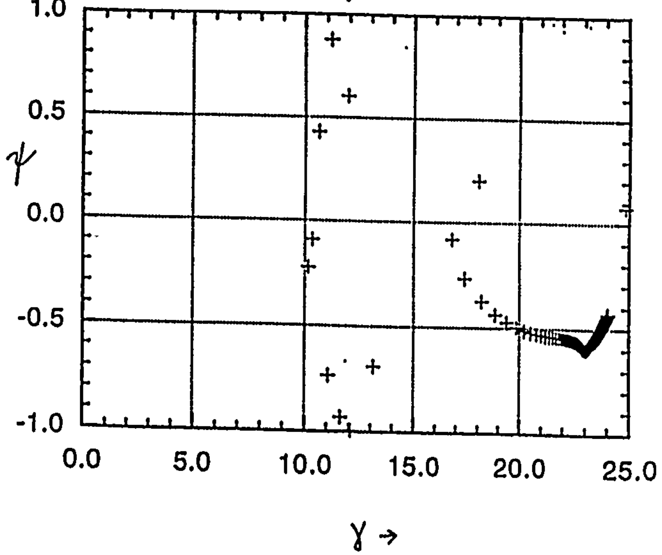

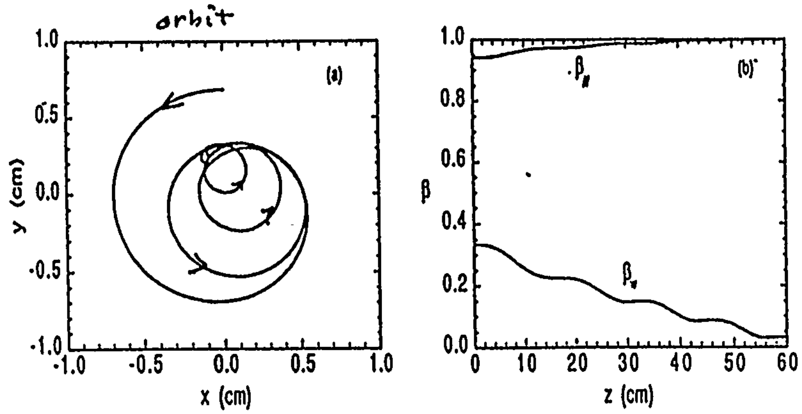

Extraction section
decrease both $B_0(z)$ + $B_w(z)$

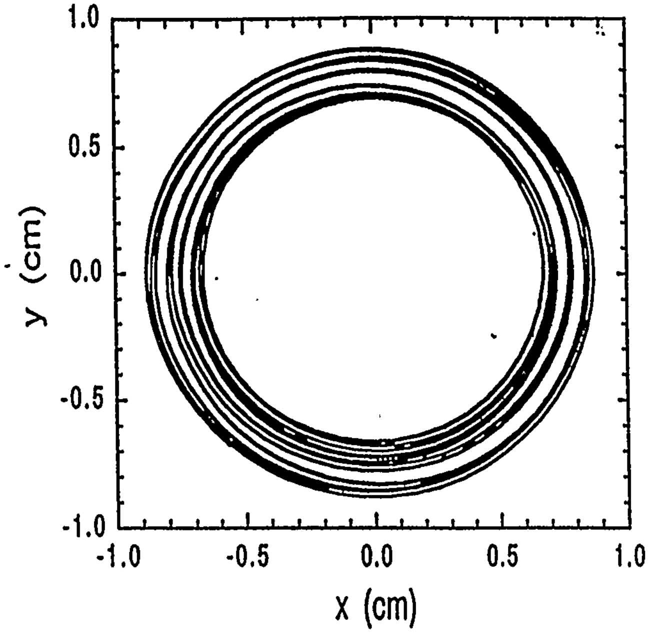

orbit cross-section
in IFEL section

Fig 5

Seventh Harmonic FEL Experiment

Columbia University

TC Marshall + Y.H. Liu

- Reported at: { Prague June '96 ["Intense Beams..."]
  Rome August '96 [FEL]

Consider a FEL undergoing a TWA interaction with several KW @ 24GHz

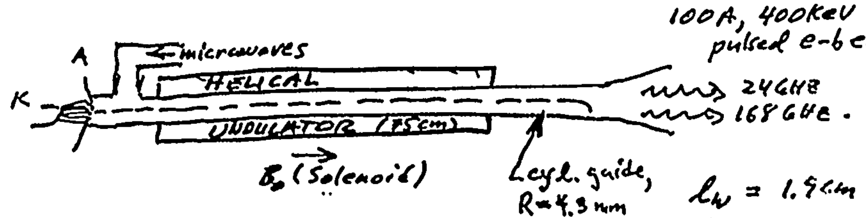

$\ell_w = 1.9$cm
$B_w = 250$G.
$B_0 = 8800$G

- Microwave Grows from 10 KW to ~ 200 KW (P_{sat} ~ 1MW)
- Substantial 168 GHz (7th Harmonic) <u>observed</u> when e-beam is moved <u>off-axis</u>.
- 168 GHz is ω, φ related to microwave signal via bunching.

$\omega = c\sqrt{k_\perp^2 + k_z^2}$
(waveguide)

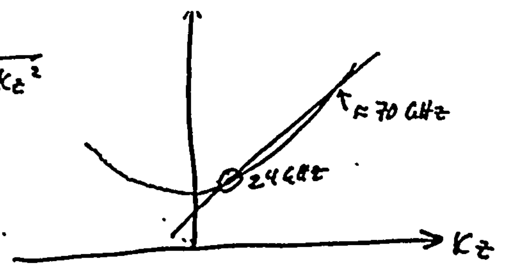

$\omega = (k_z + k_w)v_\parallel$
(beam)

- As microwave is amplified in FEL, it bunches the e-beam. (TE₁₁)
- The bunching has a broad harmonic spectrum as $P \to P_{sat}$.
- The 7th harmonic bunching currents couple well to the TE_{72} mode --

$\frac{j'_{72}}{7 j'_{11}} \approx 1$ { * wave speed of TE_{72} is ≈ same as wave speed of TE_{11} due to fortuitous relation of Bessel functions

* since $E_{TE_{72}} \to 0$ on-axis, e-beam must move to $r \neq 0$.

- Theory finds that ~30% of TE_{11} power can flow into the 7th harmonic
- Application would no doubt require a <u>mode converter</u> to make output useful.

Rome FEL " 8/96

HARMONIC MILLIMETER RADIATION FROM A MICROWAVE FEL AMPLIFIER

Y-H. Liu and T. C. Marshall

Department of Applied Physics, Columbia University, New York, NY, 10027, USA

Abstract

The objective is to generate a strong millimeter-wave FEL signal in a single pass, using a coherent microwave source (24GHz) to prebunch the electron beam for harmonically-related wave growth; the millimeter wave output is thus phase-referenced to the coherent microwave source. We use the Columbia FEL facility, operating the electron beam at 600kV, 100A; undulator period = 1.85cm and 200G (K = 0.2); electron beam diameter = 3 mm inside a 8.7 mm ID drift tube; guiding field of 8800G. Both the microwave signal (5kW input) and the harmonic millimeter signal show travelling-wave gain in the TE11 FEL waveguide modes. Obtaining power gain of ~20 for the 24GHz input wave, we have observed appreciable radiation at the second and third harmonics and a coherent relationship of the third harmonic and fundamental. Also presented are numerical solutions of the growth of the two waves using the FEL equations with slippage. Also, a strong seventh harmonic is produced, owing to the fact that the wave speeds of the TE11 (24GHZ) and TE72 (168GHz) waves are the same, and providing that the electron beam is displaced off-axis.

Introduction

If an electron beam undergoing FEL interaction is prebunched by a coherent source, then the radiation at the harmonics can be coherent with the source; the prebunching causes the harmonics to grow from an initial condition which is very much above noise input. The radiation at the harmonics will be related in phase and frequency to the source which bunches the electron beam. Recently, Piovella et al [1] have studied a waveguide FEL where the beam is prebunched by a growing wave at the low-frequency intersection, prompting growth at a harmonically-related high frequency upper intersection (or FEL mode); a similar idea was described by Sternbach [2] Thus one might generate frequency and phase stable millimeter power using a microwave source for prebunching. We have reported on an experiment which studies harmonic radiation from a FEL - configured as a travelling wave amplifier - using a magnetron source to drive the low-frequency FEL mode [3]. In this paper, we give further information regarding the experimental properties of this source as well as a numerical study of the physics. We also report the recent observation of appreciable seventh harmonic power.

Experiment

Figure 1 shows a schematic of the experimental layout, and column 2 of Table I summarizes the parameters. In this waveguide FEL, there are two unstable roots of the dispersion relation which represent growing TE11 waves at 24 and ~72GHz (third harmonic); the frequencies are given by an approximate formula, neglecting the Raman effect:

$$\omega_{1,2} = \frac{\omega_s}{1+\beta}\left[1 \pm \beta\sqrt{1-X}\,\right] \qquad (1)$$

where $\omega_s = \frac{c\beta k_w}{1-\beta}$ and $k_w = 2\pi/l_w$. X involves the cutoff frequency of the waveguide, $X = \left(\frac{1.84}{2\pi R_g}\;\frac{l_w}{\beta\gamma_{\parallel}}\right)^2$. Table I, column 1 shows corresponding parameters appropriate to this "Compton" theory. A 24GHz 5kW signal is launched along a cylindrical waveguide, enclosed by a helical undulator. A relatively small value of undulator field (~250G) is chosen so that the system behaves like a travelling-wave amplifier with a gain <50, in which case oscillation is avoided; also, a low undulator field will give stable well-behaved electron orbits in the combined undulator and guide fields. According to Table I, column 2, the apparatus is constructed so that the 24GHz wave and its third harmonic are resonant according to eq. (1).

We have found 24GHz power gain in the range of 10-20, and the spectrum of the first three harmonics (a few kW) was reported[3]. No harmonic power is obtained[3] unless there is appreciable gain for the 24GHz wave. The kW level third harmonic power output was found to be greater than the second, and both are much greater than the fourth (Figure 2). If the interaction were non-resonant, then the power of the harmonics should fall off very rapidly[4]. Figure 3 shows the result (lower trace) of mixing the 72GHz FEL third harmonic signal with the frequency tripled magnetron signal, demonstrating a fixed frequency relationship of the FEL harmonic power pulse with the lower frequency FEL wave driven by the magnetron.

We have also observed the emission of appreciable seventh harmonic power (168GHz), obtained again only when we have appreciable gain for the 24GHz FEL wave (spectrum, Figure 2). The seventh harmonic signal level is of the order of 17 kW or more, whereas the 24GHz signal is amplified to ~ 80kW level. The seventh harmonic is not a "resonant FEL interaction" and its appearance depends on two special factors. The first is that the temporal and spatial spectrum of the seventh harmonic electromagnetic wave must move at the same wave velocity as the temporal and spatial spectrum of its electron current source (the "beam wave"), the latter being set up by the seventh temporal harmonic of the bunching caused by the amplified TE11 24GHz wave. The EM wave in question that satisfies this constraint turns out to be the TE72 mode of the cylindrical waveguide[5]. The second factor is that the electron beam must be moved off-axis to overlap one of the electric field maxima of the TE72 wave-- this is done by a deliberate misalignment of our system in which the electron beam was moved about 2mm off the waveguide axis.

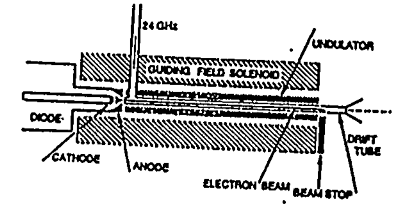

Fig. 1

Table I

	Col. 1	Col. 2
electron energy	600kV	>600kV
low frequency FEL mode	24GHz	24GHz
high frequency FEL mode	72GHz	72GHz
undulator period	2.5cm	1.85cm
aw, effective undulator parameter	0.2	0.2
guide field	0G	8800G
TE11 cutoff frequency	18.4GHz	20.7GHz
electron beam current	~100A	~100A
electron beam dia.	3mm	3mm

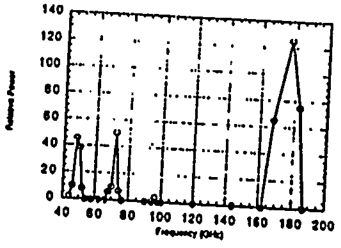

Fig. 2

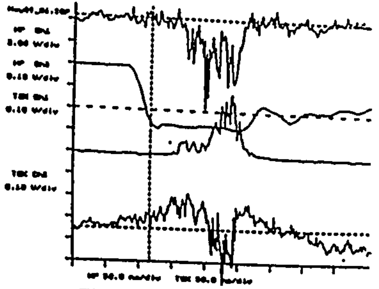

Fig. 3

Figure 1: Schematic-: a pulseline source provides a negative 150nsec pulse to a graphite diode.
Figure 2: Power spectrum scan, covering harmonics 2 - 8; beam is off-axis for 7th harmonic.
Figure 3: From below: beat signal envelope of FEL third harmonic mixed with magnetron tripled frequency; 24 GHz gain signal; diode voltage of accelerator; 72GHz detector signal

Theory

To study the coupling between the harmonically related waves, we solve numerically the set of FEL equations with slippage for the electron dynamics and two interacting waves [3]. For simplicity, we disregard the space-charge (Raman effect), which will decrease the gain and require a shorter undulator period to provide the same frequencies as this calculation. The parameters of the calculation are given in Table I, column 1. The low frequency (24GHz) TE11 FEL mode has group velocity ~ c/2, as does the seventh harmonic TE72 wave; the second and third harmonic TE11 FEL wave group velocites are higher than the electron speed (~ 0.88c).

We first define the variables x and y as

$$x = A\left[t - \frac{z}{v_{g2}}\right] \quad , \qquad y = A\left[\frac{z}{v_\parallel} - t\right]$$

where $A = \left[l_w\left(\frac{1}{v_\parallel} - \frac{1}{v_{g2}}\right)\right]^{-1}$ and v_{g1}, v_{g2} are the group velocities of ω_1 and ω_2, $v_\parallel$ is the electron axial speed, and z, t are the axis and time variables. Defining a_1 and a_2 $(a_1 = a_{s1}e^{-i\phi_1})$ as the normalized vector potentials of waves 1 and 2 which have respectively axial wavenumbers k_1 and k_2 in the waveguide, and a_w the undulator potential $\frac{eB_w l_w}{2\pi mc^2}$, where B_w is the undulator field, the electron and wave equations for the j^{th} electron are:

$$\frac{\partial \theta_{2j}}{\partial x} = l_w \bar{k}_{w2}\left(1 - \frac{\bar{\gamma}_{r2}^2}{\gamma_j^2}\right) \qquad (2)$$

$$\frac{\partial \gamma_j}{\partial x} = -l_w \frac{a_w}{\gamma_j v_{\parallel j}}\left[\omega_1 a_{s1}\sin(\alpha\theta_{2j} + \phi_{1j}) + \omega_2 a_{s2}\sin(\theta_{2j} + \phi_{2j})\right] \qquad (3)$$

$$\left\{\frac{\partial}{\partial y} + \left(\frac{\frac{1}{v_{g1}} - \frac{1}{v_{g2}}}{\frac{1}{v_\parallel} - \frac{1}{v_{g1}}}\right)\frac{\partial}{\partial x}\right\} a_1 = \frac{i}{A\left(\frac{1}{v_\parallel} - \frac{1}{v_{g1}}\right)}\frac{\omega_p^2 a_w}{2c^2 k_1}\left\langle\frac{e^{-i\alpha\theta_2}}{\gamma}\right\rangle \qquad (4)$$

$$\frac{\partial a_2}{\partial y} = i l_w \frac{\omega_p^2 a_w}{2c^2 k_2}\left\langle\frac{e^{-i\theta_2}}{\gamma}\right\rangle \quad . \qquad (5)$$

These equations also involve the following quantities: ω_p, the beam plasma frequency; α, the harmonic number; $\theta_2 = k_w z + k_2 z - \omega_2 t$; $\phi_{1,2}$, the optical phase; also:

$$\bar{k}_{w2} = k_w + k_2 - \omega_2/c \ , \quad \bar{\gamma}_{r2}^2 = k_2(1 + a_w^2)/2\bar{k}_{w2} \quad \text{and} \quad a_s = cE_s/k_s mc^2 .$$

In the simulation, the FEL works as a travelling-wave amplifier. The spatial distribution of simulation electrons has a rectangular profile, the electrons are taken to be monoenergetic, and at the undulator entrance $z = 0$ they are uniformly distributed inside the beam length with 100 simulation electrons per undulator period. For each wavelength-size strip of particles, the relative phase location of the electrons with respect to the radiation field is uniformly distributed between $-\pi$ and π. For the output format of the computational results, the electron beam pulse and the radiation pulse (each taken to be flat-topped) are plotted as a function of the variables x and y, which imply two moving "windows," the former at v_{g2} and the latter at $v_\parallel$ respectively; both are scaled in units of the undulator period. The electron motion is parallel to the x-axis while the ω_2 wave moves parallel to the y-axis; the ω_1 wave moves along the characteristic

$$x - \left(\frac{1}{v_{g1}} - \frac{1}{v_{g2}}\right)\left(\frac{1}{v_{g1}} - \frac{1}{v_\parallel}\right)^{-1} y = \text{constant}$$

The finite radial size of the electron beam is accounted for in the code using a multiplicative "filling factor" of .07 for the radiation current term on the right-hand sides of eqs. (4,5). While this can be estimated from the geometry, it is also a convenient parameter to adjust the gain of the 24GHz power so that it corresponds to our observations.

Figure 5 is an example we calculated that is relevant to this experiment. It shows the peak power growth along the undulator of the 24 and 168GHz waves starting from an initial signal of 10 ~~five~~ kW at 24GHz in the right circular "rotating" mode; the two waves travel at the same speed in this case and the computed power levels are similar to those in the experiment.

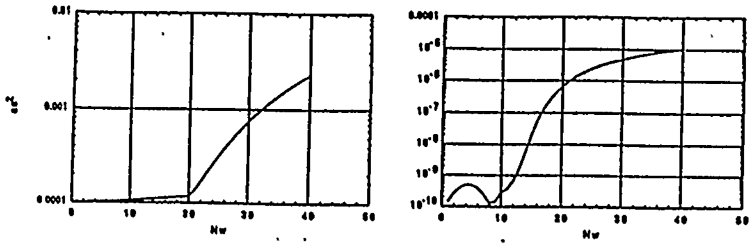

Figure 5: 24 GHz power gain (left) and 168GHz power growth from noise level.

Conclusions

We believe the harmonic power we have observed can be of use to create coherent, phase-referenced power in the millimeter spectrum for applications such as radar and accelerator physics. The third harmonic need not compete with the seventh for the free energy of the bunching, because the seventh harmonic can be suppressed by moving the beam onto the axis. On the other hand, one can suppress the lower harmonics by making the FEL interaction resonant at one microwave frequency only (by arranging that the second term in the square brackets of eq. (1) vanishes), and then move the electron beam off-axis to enhance the seventh harmonic. The latter approach may represent a very convenient way to generate appreciable 2mm wavelength power, using a FEL operating at comparatively low beam energy driven by a microwave source with kW level power output. We foresee applications of such a high power millimeter source in accelerator physics and for the purpose of plasma heating by electron cyclotron resonance.

Acknowledgement: This research was supported by the Office of Naval Research.

[1] N. Piovella et al., Phys. Rev. Lett. 72 (1994) 88
[2] E. Sternbach and H. Ghalila, Nucl. Instrum. Meth. in Phys. Res. A304 (1991), 691
[3] Y. -H. Liu and T. C. Marshall, Nucl. Instrum. Meth. in Phys. Res. (to be publ.) (1996)
[4] Y. -P. Chou and T. C. Marshall, Nucl. Instrum. Meth. in Phys. Res. A318 (1992) 528
[5] C. Wang, J.L. Hirshfield, and A.K. Ganguly: Phys. Rev. Lett. (to be publ.)

REQUIREMENTS OF BEAM EMITTANCES IN PHOTON-PHOTON COLLIDERS AND METHODS OF REALIZATION

V. Telnov, Novosibirsk

Photon Colliders, requirements to beam emittances and methods of realization

21.8.96

60% ◦ 1. Introduction

All about Photon Collider

40% ◦ 2. Laser cooling and polarization of electron (e^+) beams

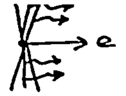

equivalent photons, E. Fermi 1924, Weizsäcker 1934, Williams, Dan 1955

$ZZ \to ZZe^+e^-$

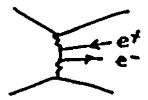

Landau, Lifshits, 1934

$\gamma\gamma \to e^+e^-$

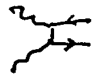

Breit, Wheeler, 1934

$\sigma \sim \alpha^2/m^2$

$\gamma\gamma \to \gamma\gamma$

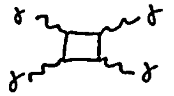

Euler 1936

$\omega \ll mc^2 \quad \sigma \backsim \omega^6$

$\hbar\omega = 2eV \Rightarrow \sigma_{\gamma\gamma\to\gamma\gamma} = 5\cdot10^{-64}\,cm^2$

$\omega \sim mc^2 \quad \sigma_{max} \sim 10^{-30} cm$

$e^+e^\pm \to e^+e^\pm\pi^0$

F. Low 1960

$\sigma \sim \Gamma_{\gamma\gamma}$ C-even resonanc

$e^+e^- \to e^+e^-\pi^+\pi^-$

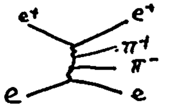

Calogero, Zemach, 1960

Experiment: $\underline{e^+e^- \to e^+e^- + e^+e^-}$ 1969, 1970 VEPP-2 Novosibirsk

$\underline{e^+e^- \to e^+e^- + \mu^+\mu^-}$ – 1974 Frascati

$e^+e^- \to e^+e^- + \eta' \hookrightarrow \rho\gamma$ – 1979 Mark-2, SPEAR

$(\Sigma p_i)_\perp \le 100 MeV$, without detection of scattered e^+e^-

Theory { Arteago-Romero, Kessler, Parizi
Brodsky, Baier-Fadin-Khoze
Balakin, Budnev, Ginzburg] $\gamma\gamma \to h$a

After 1979 - systematic study of γγ-physics
(η') Mark-2 (SPEAR)

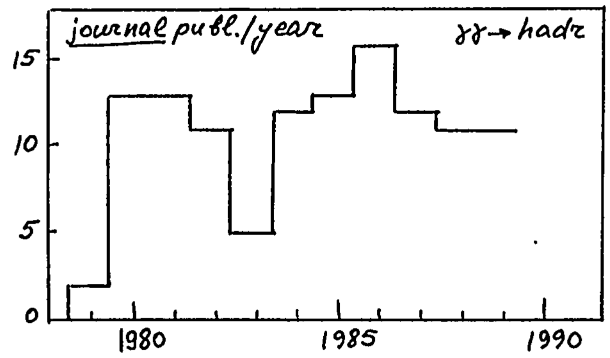

$\gamma\gamma \to X$ - new physics

- c-even resonances  $C=+(\pi^0, \eta, \eta', f_2 \dots \eta_c \dots)$
  $\sigma \propto \Gamma_{\gamma\gamma\to x} \propto \sum e_q^4$

(1γ-annihilation 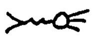 $c=-(\rho, \omega, \varphi, J/\psi, \Upsilon, Z \dots)$
(C+)
Some resonances have anamaliously small $\Gamma_{\gamma\gamma}$,
glueballs, 4-quark state? (S^*, δ, θ)

- 
jets

- 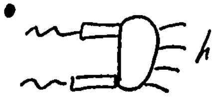 had etc
$\sigma_{\gamma\gamma} \sim 300nb$

- cross sections ($\gamma\gamma \to \pi^+\pi^-, \dots$ had)
- $q^2 \neq 0$, J=1 resonances, formfactors, structure functions, jets

Very interesting physics!

$\gamma^*\gamma^*$ at storage rings

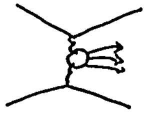

$q^2 \sim 0$

$$dn_\gamma \sim \frac{\alpha}{\pi}\frac{dy}{y}\left(1-y+\frac{y^2}{2}\right)\ln\frac{(1-y)q_m^2}{m^2y^2} \quad ; y=\frac{\omega}{E}$$

$$\underline{dn_\gamma \sim 0.035\frac{d\omega}{\omega}} \qquad \omega \ll E$$

$\therefore$ $\underline{L_{\gamma\gamma} \sim n_\gamma^2 L_{e^+e^-}}$ $\sim 10^{-2} L_{ee}$ at $\frac{W_{\gamma\gamma}}{2E_0} > 0.1$

$\underline{\sim 10^{-4} L_{ee} \text{ at } -\!/\!/\!- > 0.5}$

1. soft spectrum
2. $L_{\gamma^*\gamma^*} \ll L_{e^+e^-}$

Nevertheless, in $\gamma^*\gamma^*$ collisions a lot of interesting result

500 GeV (center of mass) ---> 2 TeV

	VLEPP	NLC	JLC(X)	CLIC	SBLC	TESLA	SLC
$L^{e^+e^-}[10^{33} cm^{-2}c^{-1}]$	15	7.1	5.2	0.7-3.4	3.75	6	$5 \cdot 10^{29}$
f [Hz]	300	180	150	2500-1200	50	5	120
# bunches/tr	1	90	85	1-10	125	1130	1
$N (10^{10})$	20	0.65	0.63	0.8	2.9	3.6	3
σ_x (nm)	2000	320	260	250	670	845	2600
σ_y (nm)	4	3.2	3	7.4	30	20	800
σ_z (mm)	0.75	0.1	0.09	0.2	0.5	0.5	1
Δt, ns in train		1.4	1.4	0.66	16	708	

$e \to \gamma$ conversion

$E_\gamma \sim E_e$, $L_{\gamma\gamma,\gamma e} \sim L_{ee}$

GKST, 1981

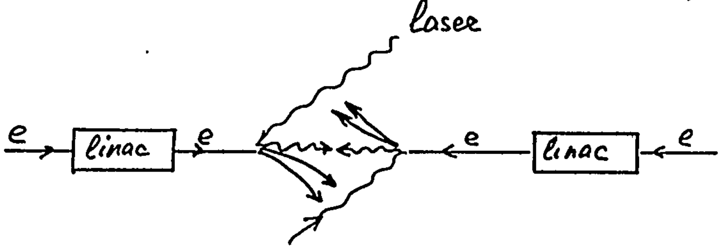

a photon Collider

(γe) 1) $\underline{\gamma e \to W\nu}$
$\sigma \sim (1-2\lambda) \cdot 5 \cdot 10^{-35} cm^2$

— factory of W

2) $\underline{\gamma e \to Z^\circ e}$

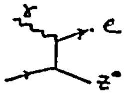

3°) $\underline{\gamma e \to e^* \to \gamma e}$

(4') $\underline{\gamma e \to \tilde{\gamma}\tilde{e} \to \tilde{\gamma}\tilde{\gamma} e}$

($M_{\tilde{e}} > E_\circ$ can be observed)

(γγ) 1) $\underline{\gamma\gamma \to hadrons}$
$\sigma > 3 \cdot 10^{-31} cm^2$!

background

2) $\underline{\gamma\gamma \to W^+W^-}$
$\sigma \sim 8 \cdot 10^{-35} cm^2$

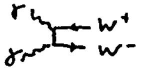

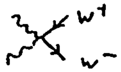

3) $\underline{\gamma\gamma \to H^+H^-}$

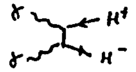

$\sigma_{\gamma\gamma \to H^+H^-} \sim 6\sigma_{e^+e^- \to H^+H^-}$
(QED only)

4) $\underline{\gamma\gamma \to L^+L^-}$

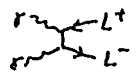

see fig. 15

5) $\underline{\gamma\gamma \to H^\circ}$

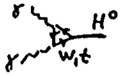

M_{H° (min. SUSY) < 120 GeV

~~6) $\gamma\gamma \to Z^\circ Z^\circ, \gamma\gamma$~~

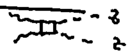

Publications on γγ, γe at linear colliders

(QSPIRES)

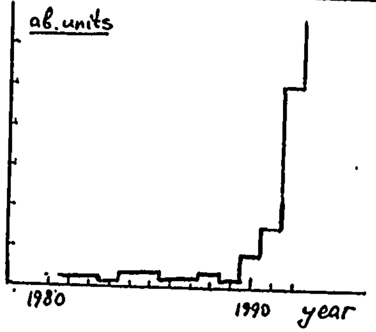

$N_{tot} > 200$ (by 1992)

40 ~~18~~ ~~16~~ (78)

Charged particle production in $\gamma\gamma$ and e^+e^--collisions

$$\sigma_{\gamma\gamma\to p^+p^-} = \frac{\pi\alpha^2}{M^2} f\left(\frac{4M^2}{W^2}\right)$$

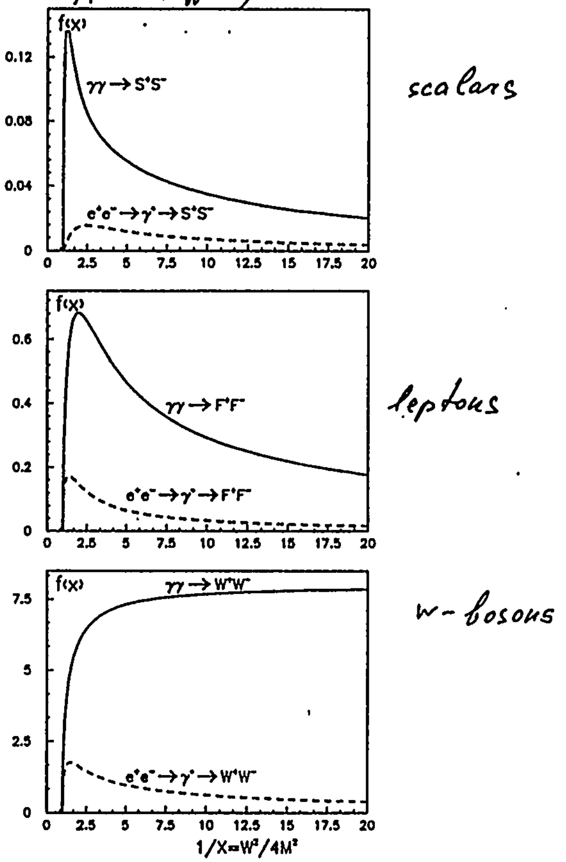

FIG.15

(7

$\gamma\gamma \to$ Higgs

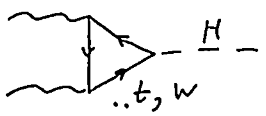

Borden
Caldwell
Boier

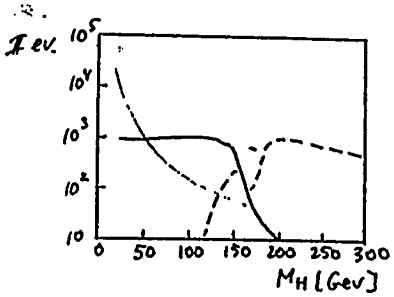

$\int L\,dt = 10\,fb^{-1}$
$(10^{33} \cdot 10^7 s)$
$\lambda_e = 0.9$
$\lambda_\gamma = -1$

—— $\gamma\gamma \to H \to b\bar{b}$
- - - $\gamma\gamma \to H \to ZZ$ $\hookrightarrow ll q\bar{q}$
$\Big\} \sim (1 + \lambda_{\gamma_1}\lambda_{\gamma_2})$

—— $\gamma\gamma \to b\bar{b}$ background
—— $\gamma\gamma \to c\bar{c}$ (5% contamination)
$\Big\} \sim (1 - \lambda_{\gamma_1}\lambda_{\gamma_2})$

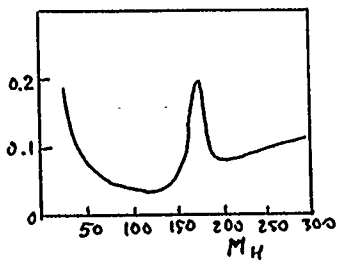

Relative Statistical error of $\Gamma_{\gamma\gamma}(H)$
$H \to b\bar{b}, Z\bar{Z}$ combined

— σ ∏ … r_0 ~

$x/X_0 \sim 0.3 \Rightarrow dn_\gamma \sim 0.3 \frac{d\omega}{\omega} \sim 10\, dn_{\gamma^*}$

$L_{\gamma\gamma} \sim 10^2 L_{\gamma^*\gamma^*}$ (in e^+e^- collision)

2 Coherent bremsstrahlung in crystals (rad. length is shorter ~ factor 10 in W)

1 and 2 disadvantages:
- a) soft spectrum
- б) background from photonuclear reactions (~10^6-10^7/collision)
- c) heat destraction

3. Beamstrahlung in e^+e^- collisions (synchrot. rad)

$n_\gamma \sim 1 \div 5\, n_e \Rightarrow L_{\gamma\gamma} \gtrsim L_{ee}$

Disadv:
- a) wide spectrum ($dn \propto 1/\omega^{2/3}$
- б) background, beam-beam coll. effects
- c) background reactions (γe…)
- d) no polarization (at $\omega \ll E_0$)
- б') large disruption angles

4 Ondulator

? $\lambda_0\ min \sim 10^{-2}$ cm ⇒ $E_\gamma \sim 100\, E_0^2$(TeV), GeV
very strong field

$E_\gamma = 6$ GeV at $E_0 = 250$ GeV
← too low

5. Backward Compton scattering

$$\underset{0.25\,TeV}{e} \longrightarrow \overset{laser\ (\omega_0 \sim 1\,eV)}{\rightsquigarrow} \gamma \quad E_\gamma \sim 0.2\ TeV \quad \theta \sim 1/\gamma$$

1. Clean γ beam
2. $\Delta E/E_\gamma \sim 10\%$ is possible
3. $L_{\gamma\gamma} > L_{e^+e^-}$ is possible due to absence of main collision effects

Resume: Compton scattering – best method of e → γ conv

$\gamma\gamma \to H \to ZZ$
$\to e^+e^- X, \mu^+\mu^- X, \nu\bar{\nu} q\bar{q}$ (one side)

Continuum background $\gamma\gamma \to ZZ$! (Jikia)

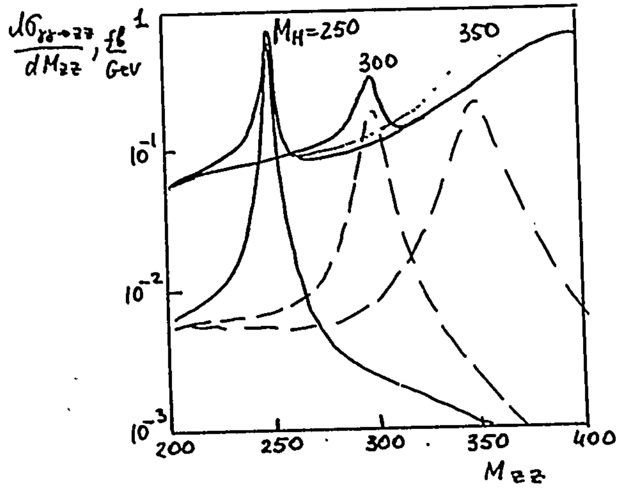

at 10 fb^{-1}

$M_H = 300$ GeV → $S = 70$, $B = 30$ $\frac{S}{\sqrt{B}} > 10$

$M_H = 350$ GeV $S = 21$ $B = 61$ $\frac{S}{\sqrt{B}} < 3$

$M_H \lesssim 350$ GeV is OK.

Resume: Physics in γγ, γe-colliders is very interesting

P

Scheme of $\gamma\gamma, \gamma e$-beams
(GKST, 1981)

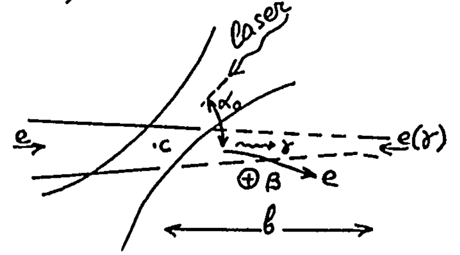

Compton scattering

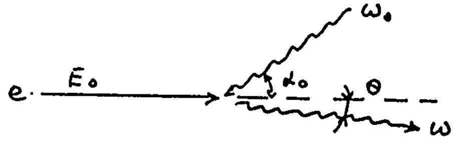

$\omega_{max} = \frac{x}{x+1} E_0$; $\quad x = \frac{4E_0\omega_0}{m^2c^4} \cos^2\frac{\alpha_0}{2}$

$(\omega_m = 4\gamma^2\omega_0 \text{ at } x \ll 1)$ $\quad \approx 15.3\left[\frac{E_0}{TeV}\right]\left[\frac{\omega_0}{eV}\right]$

For example: $E_0 = 250$ Gev
$\omega_0 = 1.17$ eV (neodium glass) $\Big\}$ $x = 4.5$, $\frac{\omega_m}{E_0} \approx 0.82$

$$\omega = \frac{\omega_m}{1+\left(\frac{\theta}{\theta_0}\right)^2}$$

where $\theta_0 = \frac{\sqrt{x+1}}{\gamma}$

Energy spectra of scattered photons

λ - helicity of electrons $(|\lambda| < 1/2)$
P_c - helicity of laser phot.

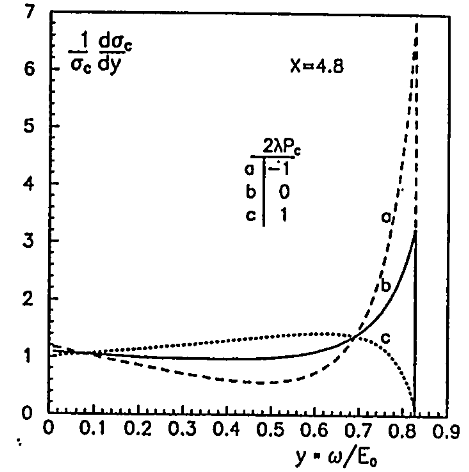

Fig.3

$\frac{d\sigma_c}{dy} \sim f_1(y) + \lambda_e P_c f_2(y)$ $\qquad y = \omega/E_0$

λ_e - longitudinal electron polarization
$|\lambda_e| < 1/2$
P_c - circular polarization of laser phot.

At $x \gg 1$ $\qquad \theta \sim \frac{1}{\gamma} \Leftrightarrow \frac{\Delta y}{y_m} \sim \frac{1}{x}$

Photon spectra for various thicknesses of laser target

numbers are thickness in coll. length

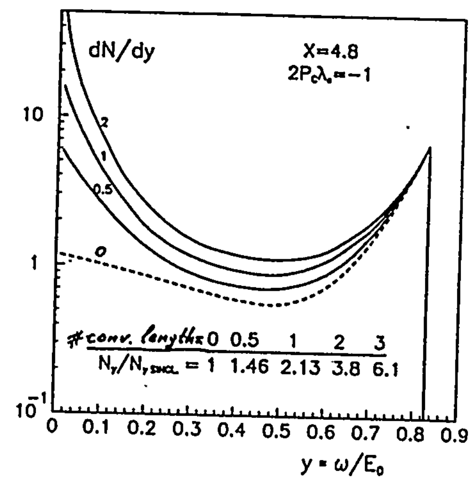

Fig.4

These spectra are normalized at $y = y_m$

$$e^{-\mu x} = e^{-\frac{x}{\lambda}}$$

Angles of Photons & electrons after Compton scatterings.

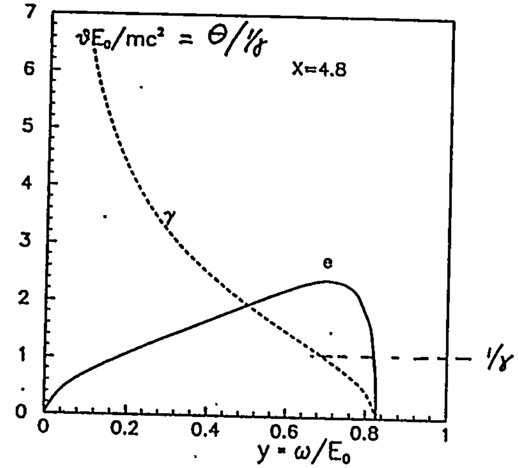

Fig.2

Optimum X

If $\omega_0 \omega > m^2c^4$, i.e $X \equiv \frac{4E_0\omega_0}{m^2c^4} > 2(1+\sqrt{2}) \approx \underline{\underline{4.8}}$

the process $\gamma_{las} + \gamma \rightarrow e^+e^-$ is possible

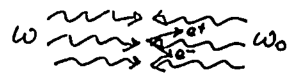

$\frac{\sigma_{\gamma\gamma \rightarrow e^+e^-}}{\sigma_c} \sim 1.5 - 2$ at $x = 8 \div 20$

as a result $\kappa \equiv N_\gamma/N_e < 0.25$

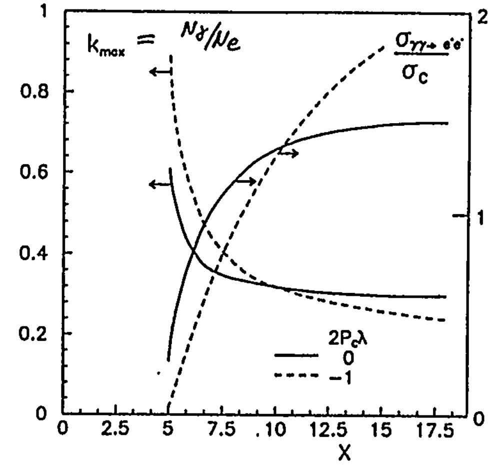

Fig.5

$X = 4.8 \Rightarrow$ $\lambda = 4.2\, E_0(TeV)$, μm

$\boxed{\omega_0 = 0.3/E_0(TeV),\ eV}$

$E_0 = 250$ GeV

$X = 4.8$ $\lambda \sim 1\,\mu m$

$X = 20$ $\lambda \sim 0.2\,\mu m$

Helicity of scattered photons vs ω/E_0 for various polarization of laser and electron beams.

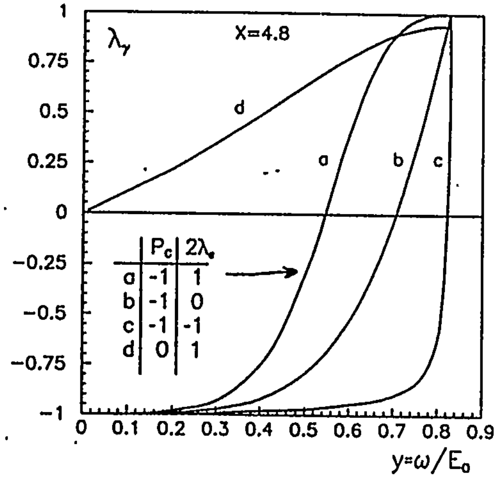

Fig.6

a) is $\overset{\text{the}}{\wedge}$ case of good monochromaticity; a) all photons in high energy peak have a high degree and like-sign polarization

Spectral luminosities L_0 and L_2 for various degree of electron polarization in the case $P_c = 1$ and $\lambda_e < 0$ (equal both beams)

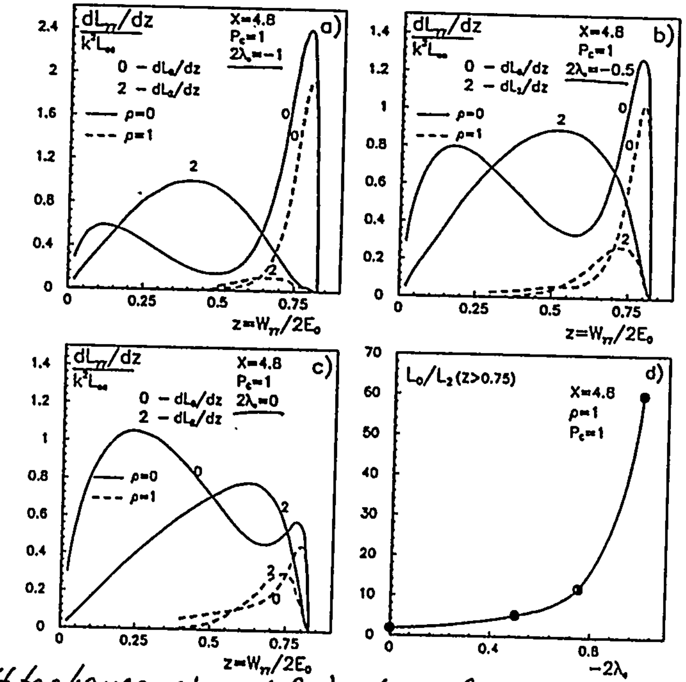

Fig.8

- If to change sign of P_c, λ_e of one beam and laser then $L_0 \to L_2$, $L_2 \to L_0$

Polarization is very important for Higgs study & search

$N_{\gamma\gamma \to H^0} \propto 1 + \lambda_{\gamma_1} \lambda_{\gamma_2} \propto L_0$ $\quad$ ($\gamma\gamma \to H \to b\bar{b}$) if $M_H \lesssim 160$ GeV

Khose at el

Jikia et al.

$N_{\gamma\gamma \to q\bar{q}} \propto 1 - \lambda_{\gamma_1} \lambda_{\gamma_2} \propto L_2$ − background

news $\underline{\gamma\gamma \to q\bar{q} g}$ even at L_0 ⇒ decrease significance of $\underline{H^0}$ (but not too much

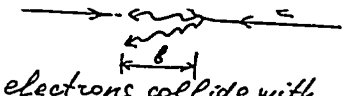

electrons collide with the most high energy photons

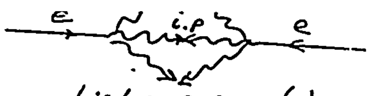

high energy of γ − smaller spot size

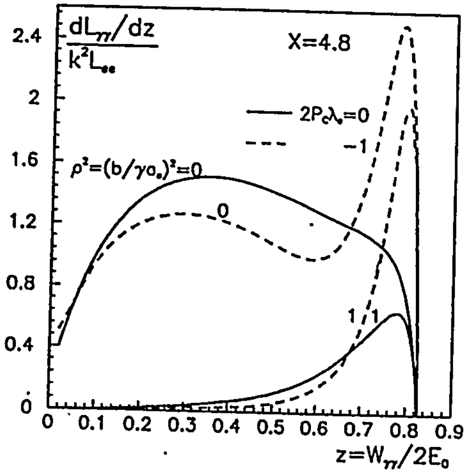

$$\rho^2 = \left(\frac{b/\gamma}{a_e}\right)^2$$

$$L_{ee} = \frac{N^2 f}{2\pi a_e^2}$$

Fig.7

Monochromaticity limit:

γe − energy spread of e-beam

γγ − ~5% (FWHM) at x = 4.8 and ρ >> 1

~1.5% ״— x = 20 ״—

<u>Note</u>: in γγ-collisions at $\rho \to \infty$ the monochromaticity FWHM → $\underline{const = f(x)}$

(some people think that ~~FWHM → 0~~ $L \propto (FWHM)^2$? ← mistake!)

Nonlinear effects

$\gamma_0 n + e \to e + \gamma$

$m^2 = m_0^2(1+\xi^2)$

$\xi \equiv \frac{eB\hbar}{m\omega_0 c} \equiv \frac{eB\lambda}{mc^2} \equiv \frac{eB\lambda_c}{\omega_0}$ B - field strength

$n\gamma_0 + \gamma \to e^+e^-$

$\xi \ll 1$ – Compton scattering

$\xi \gg 1$ synchrotron radiation

In the conversion region $\xi^2 \sim \frac{0.05\,E_0(TeV)}{\ell_\gamma[cm]}$

[illegible] $\Rightarrow$ $(\ell_\gamma \sim \ell_e) \nearrow$ For general case $\xi^2 \sim \frac{2}{\pi\alpha}\frac{\sigma_0}{\sigma_c}\frac{\lambda}{\ell_\gamma}K$

$\frac{\Delta\omega_m}{\omega_m} \sim 5\%$ at $\xi^2 \approx 0.3$ – limit

$$\Rightarrow \boxed{\begin{array}{l}\ell_\gamma \sim 0.17\,E_0(TeV),\,cm\\ A_0 \sim 4E_0\,(TeV),\,J\end{array}}$$ and $\underline{2\beta_\gamma \approx \ell_\gamma}$

$\Leftrightarrow x = 4.8,\ k \sim 1$

Joint requirements from diffraction and nonlinear effects:

$$\boxed{\begin{array}{l}P_0 = \frac{A_0}{\tau} \sim \frac{\hbar c}{\sigma_c} = 0.5\ TW\\ \ell_\gamma \approx \max(2\sigma_z^e,\ 0.15\,E_0[TeV],cm)\end{array}}$$ at $x = 4.8$

For various projects $\boxed{\begin{array}{l}A_0 \sim 1 \div 4\ J\\ \tau \sim 1 \div 5\,ps\end{array}}$

$1\,mm = 3.3\,ps$

$E = 0.25\,TeV$

NLC, JLC $A \sim 1\,J$ $\tau \sim 1\,ps$

TESLA $A \sim 3\,J$ $\tau \sim 7\,ps$

Laser

Wave length If $\omega_0\omega_m > m^2c^4$; i.e. $x \equiv \frac{4E_0\omega_0}{m^2c^4} > 2(1+\sqrt{2}) \approx 4.8$

the process $\gamma_{las.} + \gamma \to e^+e^-$ is possible.

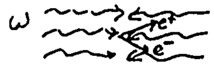

ω_0. $\frac{\sigma_{\gamma\gamma \to e^+e^-}}{\sigma_c} \sim 1.5 - 2$ at $x \sim 8 \div 20$

as a result $K \equiv \frac{N_\gamma}{N_e} < 0.25$

$x > 5$ $K_{max} \sim 25\%$

$x < 4.8$ $K_{max} \sim 100\%$

$x = 4.8$ is optimum $\Rightarrow \boxed{\begin{array}{l}\lambda = 4.2\,E_0(TeV),\,\mu m\\ \omega_0 = 0.3/E_0(TeV),\,eV\end{array}}$

Conversion coefficient, required power of the laser

$K = \frac{N_\gamma}{N_e} \approx 1 - \exp\left(-\frac{A}{A_0}\right) \sim \frac{A}{A_0}$ (at $K \ll 1$)

$A = A_0 \Rightarrow K \sim 65\%$

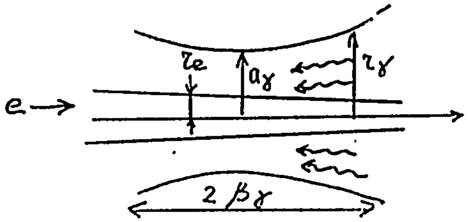

$r_\gamma = a_\gamma\sqrt{1+\frac{z^2}{\beta_\gamma^2}}$

$\beta_\gamma = \frac{2\pi a_\gamma^2}{\lambda}$ – diffraction

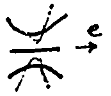

in practice $r_e \ll a_\gamma$

Optimum conditions for conversion: $\ell_\gamma \sim \ell_e$

$2\beta_\gamma \lesssim \ell_\gamma$ $(a_\gamma < \sqrt{\lambda\ell_e/4\pi})$

$$\boxed{A_0 \sim \frac{\pi\ell_e\hbar c}{2\sigma_c} \sim 15\frac{\sigma_0}{\sigma_c}\ell_e(cm),\,J}$$

where $\sigma_0 = \pi\left(\frac{e^2}{mc^2}\right)^2$

For $x = 4.8$ $\sigma_c = 0.75\sigma_0 \Rightarrow$ $\underline{A_0 \sim 25\,\ell_e(cm),\,J}$

if $\ell_\gamma \gtrsim \ell_e$ $A_0 \sim 25\,\ell_\gamma(cm),\,J$.

using grating pair

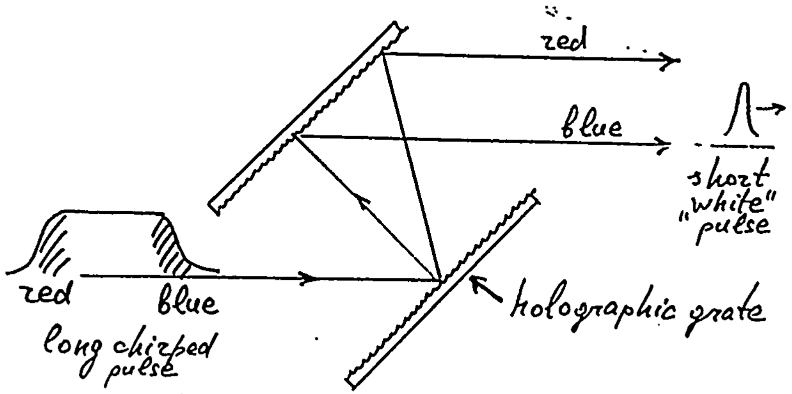

This technique is used for conventional TW laser and can be used for FEL? that solves problem of large currents.

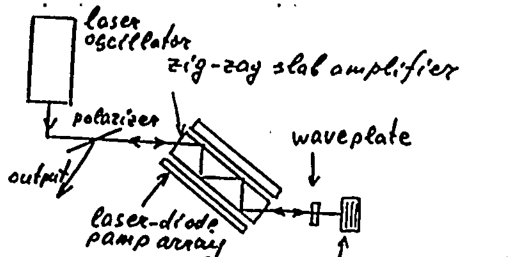

Nd:YAG 1J 400Hz
worked in 1993 (without slab motion)

C. Clayton
N. Kurnit
D. Meyerhofer

Laser for E-144 at SLAC

$P = 2TW$

$\lambda = 1, \mu m, 0.5 \mu m$

$\tau = 1 ps$ $(A \sim 1 \div 2 J)$ 1.5 - 2 diff. limit

$f = 1 Hz$

If flash lamp $\Rightarrow$ laser diode pumping

$f = 1 Hz \Rightarrow f = 10^2 Hz$

Main technologies

1. Chirped pulse stretching and compression
2. Diode pumping (gives 10% efficiency, power/cm² 100 W - 5 kW - more than necessary)
3. Zig-zag moving slab (disk) geometry of amplifier (to reduce overheating)
4. Correction of thermal distortions by phase-conjugate mirror of adaptive optic (if necessary)
5. Recombining several lasers (with slightly different frequences.
6. Accumulator cavities
7. Frequency conversion ND: 1 μm 0.5 μm 0.33 μm 0.25 μm
100% 75% 60% ~40÷50%
CO_2 10 μm → 5 μm is possible.

Resume! 10 - 20 kW lasers (1ps, 1J,) ($f \sim 10^4 - 2 \cdot 10^4$) can be built today

Free electron lasers

- variable λ
- accelerator technique

$\lambda \simeq \frac{\lambda_0}{2\gamma^2}$ λ_0 - period of ondulator.

Possible parameters

	P, TW	λ, μm	E GeV	I(kA)	λ_w(cm)	B_w G	L(m)	Ref.
10 FELX	0.3	1-4	2	2.5	15-20	10-15	~40	Saldin et al (Berkeley 94)
	0.1	4	0.15	4	6	6	5	Hiramatsu
	.	.	.	.	.	.	.	Corsini, Mich. (LC95)

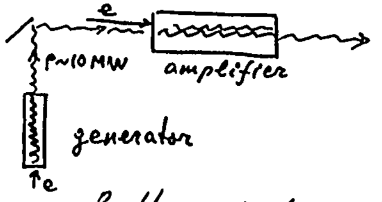

$P = 0.1 - 0.3$ TW

Both project don't use chirped pulse compression. Why?

Resume: FELs are very promising, further R&D is needed

Frequency multiplexing scheme

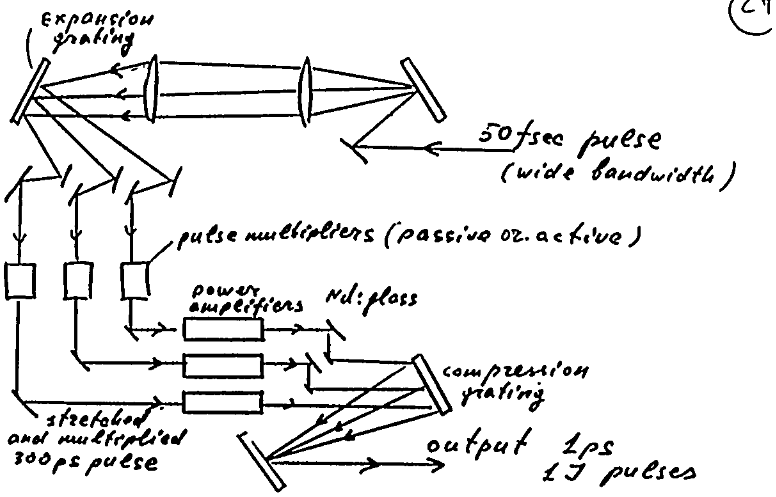

10 kW lasers → 1kW - lasers (no thermal compensation t- nique is required

32

1. With deflection of „used" electrons

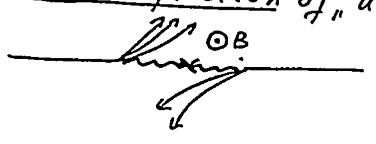

GKST 1981, 1983
Telnov NIM 1990
+Saariselka 1991

2. Without deflection

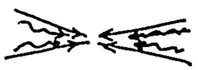

Telnov Saariselka 1991
LC93...
Balakin... Hawaii 93, LC93...

The scheme „without deflection" also provides high γγ-luminosity but

1) mixture of γγ, γe (ee smaller) – collisions (in some cases γe is small (Balakin, Sery))
2) or (and) too large disruption angles (there are examples below)
3) does not work for γe (large γγ backgr. $L_{\gamma e} < L_{ee}$)

F. Richard

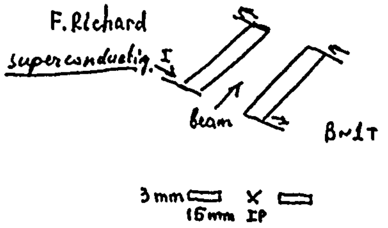

Pulsed magnet
↓ see next page
B~2T (or more)

B ~ 0.5–1T is sufficient

22

A pulse stretching, FEL amplifying, pulse compression scheme (PS/FEL/PC)

K.J.Kim, Sessler...

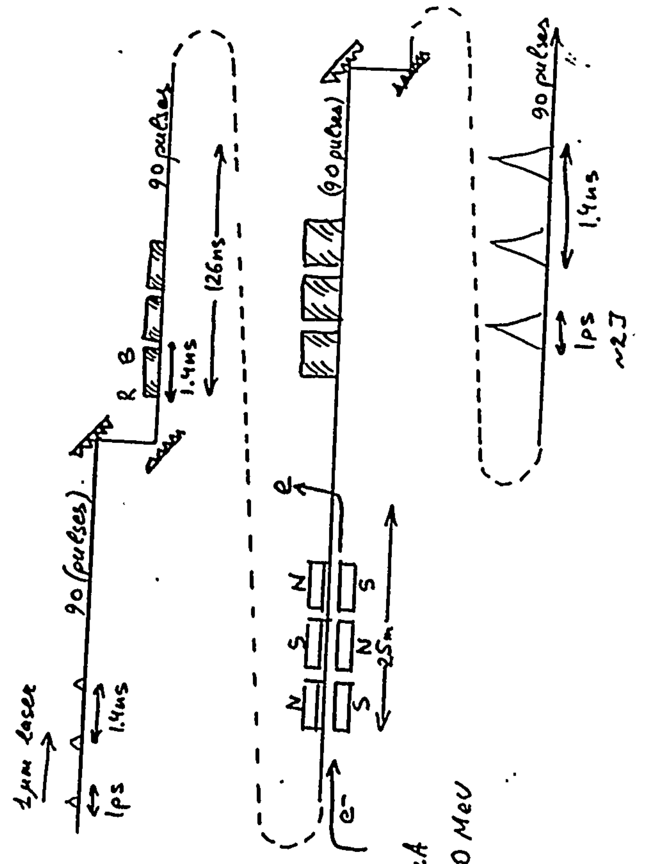

I ~ 1kA
E = 100 MeV

~~22~~ 22

Coherent pair creation in E, B field

$B = B + E$

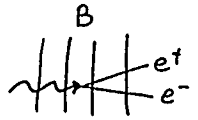

1 Erber, Rev. Mod. Phys 1966

2. Chen, Telnov PRL, 1989

In the rest system of e+e- $\underline{E' \approx B \frac{\hbar\omega}{mc^2}}$

IF $e\lambda_c E' \sim mc^2$ – spontaneous pair creation

$$\Rightarrow \varkappa \equiv \frac{\hbar\omega}{mc^2}\frac{B}{B_0} \sim 1 \qquad B_0 = \frac{m^2c^3}{e\hbar} = 4.4 \cdot 10^{13}\, Gs$$

By definition $\Upsilon \equiv \gamma \frac{B}{B_0} = \frac{2\omega_c}{3E_0} \Rightarrow \varkappa = \frac{\hbar\omega}{E_0}\Upsilon \sim \Upsilon$

Attenuation coefficient $\quad (N_\gamma = N_\gamma^0 e^{-\mu z})$

$$\mu(\varkappa) = \frac{\alpha^2 B}{r_e B_0} T(\varkappa) \qquad T(\varkappa) = \begin{cases} 0.23 \exp(-\frac{8}{3\varkappa}) & \varkappa \ll 1 \\ 0.38\, \varkappa^{-1/3} & \varkappa \gg 1 \end{cases}$$

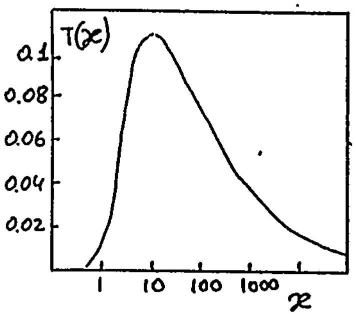

$$p \sim \mu(\Upsilon)\sigma_z \approx \frac{\alpha^2 \Upsilon \sigma_z}{r_e \gamma} T(\Upsilon)$$

$\Rightarrow \Upsilon = f(\frac{p\gamma}{\sigma_z}) \qquad p$ - probability $\gamma \to e^+e^-$

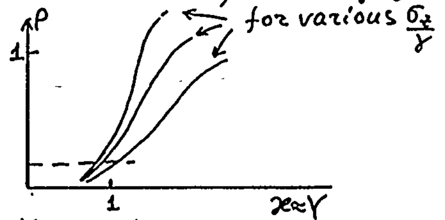

$P_{\gamma\to e^+e^-}$ is small at $\Upsilon \lesssim 0.5 \div 1$

Minimum energy in e+e- pair $\quad \mathcal{E}_{min} \sim 0.2 \frac{E_0}{\Upsilon}$

Luminosity of γγ, γe collisions.

Collision effects:

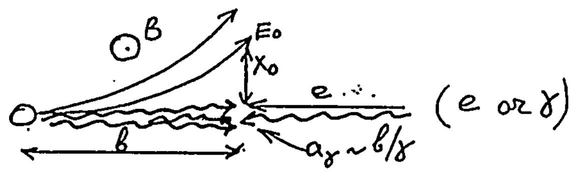

Sources of fields at i.p.

in γγ - deflected e-beam

in γe - // — // — + opposing e-beam

Collision effects

(γγ) conversion $\gamma \to e^+e^-$ in E+B field

(γe) a) beamstrahlung for electrons $(e \to e + \gamma)$,

b) $\gamma \to e^+e^-$ for photons

c) displacement of e-beam ($\Delta x > \sigma_x$ during collision)

These effect determine x_0 (and b), σ_x (for eγ)

and therefore restrict $L_{\gamma\gamma}, L_{\gamma e}$

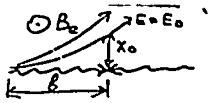

(with deflection)

$N_e \sim N_0(1-0.5k)$ create E+B field

$$\Upsilon_p = \gamma \frac{B}{B_0} = \frac{2N_0(1-0.5k) r_e^2 \gamma}{\alpha \sigma_z x_0}$$

To get deflection x_0 one needs the distance

$$b^2 = \frac{2E_0 x_0}{eB_e} = \frac{4N_0(1-0.5k) r_e^3 \gamma^2 B_0}{\alpha^2 \sigma_z B_e \Upsilon}$$

$$(a_\gamma, \min \sim \frac{b}{\gamma} \Rightarrow \boxed{L_{\gamma\gamma} \sim \frac{N^2 f k^2}{4\pi a_\gamma^2} \sim \frac{N k^2 \sigma_z B_e f}{16\pi r_e^3 B_0 (1-0.5k)} \Upsilon_p} \text{ with } \Upsilon_p \sim 1$$

For $k = 0.65$ $(A = A_0)$, $B_e = 30\,\mathrm{kG}$

$$\boxed{L_{\gamma\gamma} \sim 2\left(\frac{N_0}{10^{10}}\right) \sigma_z(\mathrm{cm}) f(\mathrm{Hz}) \Upsilon_p \cdot 10^{32}\,\mathrm{cm}^{-2}\mathrm{s}^{-1}}$$

Values of Υ_p for $P_{e^+e^-} = 0.05$

E_0, TeV / σ_z (cm)	0.25	1.0
0.01	1.3	1.7
0.1	0.6	0.9

$\Rightarrow \Upsilon_p \sim 1$

Ultimate $L_{\gamma\gamma}$ for various projects if $\varepsilon_{x,y} \to 0$

$E_0 = 250$ GeV, $k = 0.65$ $\downarrow$ $B_e = 30\,\mathrm{kG}$

	$N/10^{10}$	σ_z(cm)	$L_{\gamma\gamma}, 10^{34}$	$L_{\gamma\gamma}$/coll (10^{28})	a_γ(nm)	b(cm)	x_0(nm)	f, kHz
NLC	0.65	0.01	3	1.9	10	0.5	40	16
DLC	2	0.05	12	14	9	0.5	40	8.5
VLEPP	20	0.075	6	200	25	1.3	300	0.3
TESLA	5.2	0.1	50	60	12	0.6	60	8

beams are round

$(L_{\gamma\gamma})$max almost does not depend on the energy

Without deflection $\quad b \sim 2\sigma_z$

$$L_{\gamma\gamma} \sim \frac{N^2 k^2 f}{4\pi \sigma_x \sigma_y} \sim \frac{N k^2 \alpha \sigma_z \Upsilon_p f}{4\pi r_e^2 \gamma \sigma_y}$$

$\Upsilon_p \sim 0.6 - 17$ $(P_{e^+e^-} < 5\%)$ for various projects.

Assuming $k = 0.65$, $\sigma_y = 10\,\mathrm{nm}$ ($>$ than for e^+e^-)

$L_{\gamma\gamma}, 10^{34}$ $\quad 2E_0 = 500$ GeV

NLC	DLC	VLEPP	TESLA	LC(200) (Balakin)
1.5	7.5	3.5	30	~100

Required

$$\sigma_x \sim 2 \cdot 10^{-7} \left(\frac{N}{10^{10}}\right) \frac{E_0(\mathrm{TeV})}{\sigma_z(\mathrm{cm})}, \mathrm{cm} \quad (\text{from } \Upsilon_p \sim 1)$$

For example $N = 10^{10}$, $\sigma_z = 0.01$, $2E = 0.5$ TeV

$\Rightarrow \sigma_x = 50\,\mathrm{nm}$

Disruption angles

$$\theta_d \sim \left(\frac{4\pi r_e N}{\sigma_z \gamma_{min}}\right)^{1/2}$$

For $E_e = 0.02 E_0$ $\quad \theta_d \sim 3\left(\frac{N/10^{10}}{\sigma_z(\mathrm{mm}) E_0(\mathrm{TeV})}\right)^{1/2}$ mrad

For NLC, TESLA, DLC at $2E = 500$ GeV $\quad \theta_d \sim 15$ mrad

For $E_0 = 100$ GeV, $N = 4 \cdot 10^{11}$, $\sigma_z = 0.075$ cm (Balakin parameters)

$\theta_d \sim 70$ mrad

From the background point of view

($\sigma_{\gamma\gamma+had} \sim 400\cdot10^{-33}$)

$L_1 = L_{\gamma\gamma}/coll$ should be not too large

At $L_1 = 2.5\cdot10^{30} cm^{-2}s^{-1}$

will be 1 event/collision - that is tolerable

(these particle have mostly small $p_\perp$

At $f\sim10^4$ $L_1\sim2\cdot10^{30} \Rightarrow L_{\gamma\gamma}\sim2\cdot10^{34}$ – OK for TeV colliders

Resume: beam collision effect ($\gamma\to e^+e^-$) does not impose serious restriction on $\gamma\gamma$-luminosity

---

γe-collisions

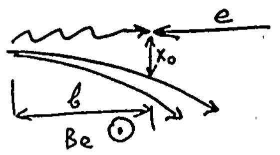

Gross section

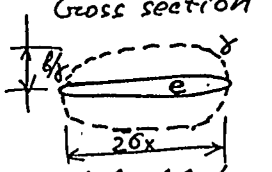

1. Electron beam must be flat
(to provide $\Upsilon < 1$ - low $\gamma\to e^+e^-$ probability)
this determines σ_x $\boxed{\sigma_x \approx \frac{N r_e^2 \gamma}{\alpha \sigma_z}}$

2. Vertical size of γ- beam $\sigma_y \sim b/\gamma$,
where b should be large enough to provide small beamstrahlung losses and beam displacement during collision $\Delta x < \sigma_x$

Note:

The field at conversion region should be small enough, to avoid grows of photon spot size

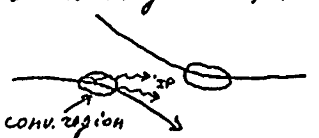

1) in the scheme without deflection magnets
$b \geq 4\div5\,\sigma_z$ (for goussian shape)

2) with magnets

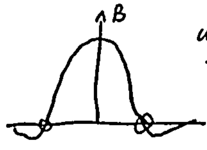

desirable shape of magn. field

Deflection by plasma (D. Cline et al)

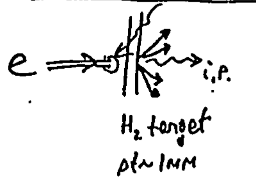

Problems!

a/ gas at conversion region will defocus electrons before conversion to photons

b/ ... distortion of laser light by plasma

$L_{\gamma e, max}$, $10^{34}\,cm^{-2}s^{-1}$

$2E_0$, TeV	NLC	DLC	VLEPP	TESLA
0.5	0.6	0.9	0.3	2.0
2	0.3	1	0.2	3.0

Beams for γe are flat

$$\sigma_x \sim \frac{N r_e^2 \gamma}{\alpha \sigma_z \psi_\sigma} \xRightarrow{\psi_\sigma \sim 0.5} 4\cdot 10^{-7}\left(\frac{N}{10^{10}}\right)\frac{E(TeV)}{\sigma_z(cm)}, \text{cm}$$

$$\left.\begin{matrix} N = 5\cdot 10^{10} \\ \sigma_z = 0.05 \\ \beta = 0.25 \end{matrix} \quad \text{or} \quad \begin{matrix} N = 10^{10} \\ \sigma_z = 0.01 \\ \beta = 0.25 \end{matrix}\right\} \Rightarrow \sigma_x \sim 10^{-5}\,\text{cm}$$

$E_0 = 1$ TeV $\qquad \sigma_x \sim 4\cdot 10^{-5}$ cm

OK.

Vertical size is large than in e^+e^- and is not a problem

low energy colliders ($E \lesssim 0.5$ TeV)

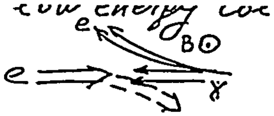

$$L_{\gamma e} \sim \frac{N^2 k}{S} \qquad S \sim 4\pi\sigma_x\, b/\gamma$$

Joint consideration of three collision effects leads to the following $L_{\gamma e}$ for various projec

$k = 0.65\,(A = A_0)$, $P(\gamma \to e^+e^-) = 5\%$, $\Delta E/E = 5\%$

$2E_0$, TeV	NLC	DLC	VLEPP	TESLA
0.5	0.6	0.9	0.3	2.0
2	0.3	1	0.2	3.0

← $L_{\gamma e}, 10^{34}$

beams are flat

$L_{\gamma e}$ is enough for $2E = 500$ GeV, but will be problems for $2E \geq 1$ TeV

Approximate formulae for $L_{\gamma e}$: $L_{\gamma e} = \min(L_1, L_2$,

$$\boxed{\begin{matrix} L_1 \sim 2\sqrt{\dfrac{N}{10^{10}}}\,\dfrac{f(Hz)\sigma_z(cm)}{\sqrt{E_0(TeV)}}\cdot 10^{31} \\ L_2 \sim 1.3\left(\dfrac{N}{10^{10}}\right)E^{1/2}(TeV) f(Hz)\cdot 10^{30} \end{matrix}}$$

(due to pair creati and beamstrahlu

due to pair creati and beam displac

Beam displacement is essential at

$$\sqrt{\frac{N}{10^{10}}}\,\frac{E[TeV]}{\sigma_z(cm)} < 15 \qquad (L_2 < L_1)$$

It is valid for

$$E < E_{max} \propto \frac{\sigma_z}{N^{1/3}}$$

	2 Emax, TeV
TESLA	1.8
SBLC	1.1
VLEPP	0.9
CLIC	0.7
NLC	0.4
JLC	0.3

(rough estimate)

$$L_{\gamma\gamma}(z>0.65) \sim 0.35 \frac{k^2 N^2 f}{4\pi (b/\gamma)^2} \sim 0.7 \cdot 10^{36} \left(\frac{N}{10^{10}}\right)^2 \frac{E^2(TeV)}{b^2(mm)} f(kHz)$$

$k^2 = 0.6$ $(A = 1.5 A_0)$, a numerical factor 0.35 follow from the simulation with $\sigma_x = \sigma_y = b/2\gamma$

$$b_{min} \sim max(3\sigma_z, \underbrace{3E[TeV], mm}_{\text{conv. length due to non linear effects}})$$

Example: TESLA $b = 3\sigma_z = 3\,mm$

$2E > 500$ GeV $\rightarrow \underline{L > 10^{36}}$ $(z > 0.65)$

NLC $b \propto E$ $L_{max} \sim \underline{5 \cdot 10^{35}}$ ( )

The main. problem how to obtain electron beams with very low emittance in both directions

How to work with such luminosity?

$L_1 \sim 10^{32} \rightarrow > 50$ events/cross $\gamma\gamma \rightarrow$ hadr.

a) at LHC the same, use large angles

b) use „super" monochromatization (L_{tot} decrease by a factor 10, but became more monochromatic)

News on collision effect in $\gamma\gamma$-collision. „Super" luminosity

V. Telnov
Proc. of Photon 95

In $\gamma\gamma$-collisions there is only one collision effect, restricting $L_{\gamma\gamma}$ – it is coherent pair production in the field of opposite „used" beam.

The threshold $\Upsilon \sim 1$.

To avoid it two methods are known:

1) 

magnatic deflection

2) flat electron beam and no deflection

$$\Upsilon < 1 \Rightarrow x_0, \sigma_x < \frac{N r_e^2 \gamma}{\alpha \sigma_z} \sim 20 \left(\frac{N}{10^{10}}\right) \frac{E_0(TeV)}{\sigma_z(mm)} \ nm.$$

$E = 250$ GeV $\sigma_x, x_0 \geq 25\,\mu m$ for NLC, TESLA

New observation

At sufficiently low energy electron beams repulse and e-m field on the axis is too low $(\Upsilon < 1)$ for coh. pair production, even in the case of infinetely narrow electron beams without any deflection by external magnetic field.

c) flat beams $\sigma_y = 0.5 \cdot 10$ with hori

d) flat beams, small b, no deflection

e) as d) but with small vertical deflection

f) flat beams, very large N($4 \cdot 10^{11}$), 2E=200, no deflection

$N = 5 \cdot 10^{10}$, $\sigma_z = 1mm$

$2E_0 = 500$ GeV

γγ-collisions (exception: f) 2E=200GeV)

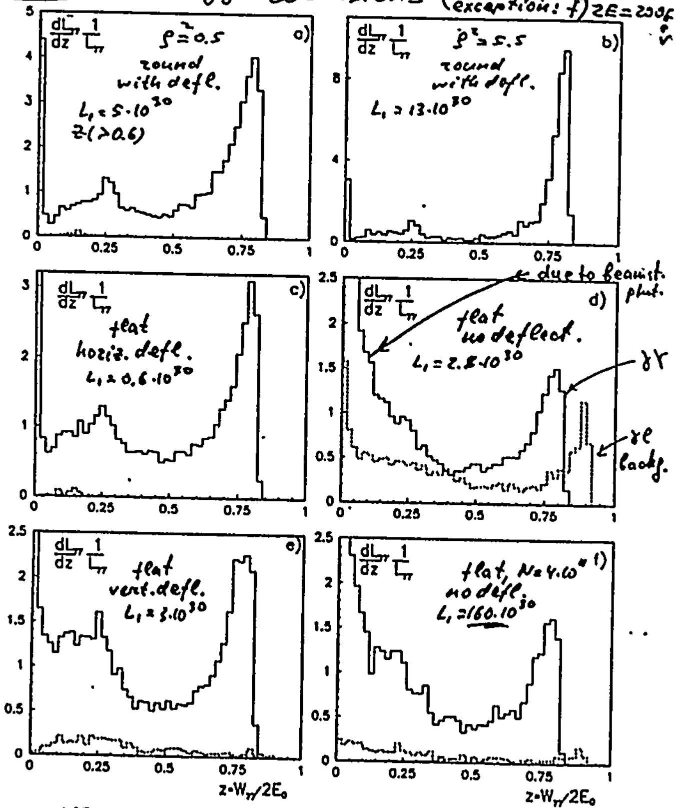

Fig.12

—— γγ

------ γe (background)

Simulation of γe-collisions

with horizontal deflection by the field $B_0 = 30$ kG

$N = 5 \cdot 10^{10}$
$\sigma_z = 1mm$
$b = 3cm.$
$\sigma_x = 50nm$
$\sigma_y = 12nm$

$N = 10^{10}$
$\sigma_z = 0.1mm$
$b = 2cm$
$\sigma_x = 100nm$
$\sigma_y = .8.nm$

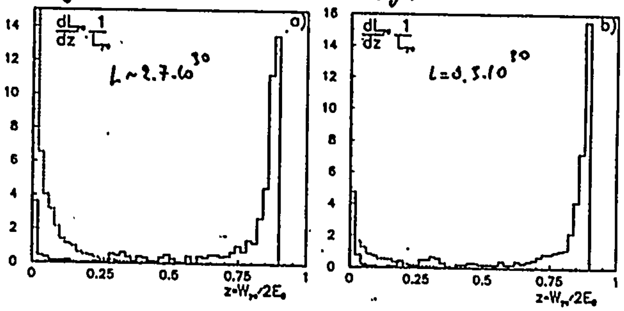

Fig.13

—— γe

------ γγ-background

esume on $L_{\gamma\gamma}$ ($2E = 500$ GeV)

$L_{\gamma\gamma}(z>0.65)$

1) With „present" damping ring for e^+e^- and $A = A_0$ (1 conv. length) $\sim 10^{33}$

2) $A = 1.5 A_0$ $\sim 1.7\cdot 10^{33}$

3) $A = 1.5 A_0$, reduced emittances (realistically $s/s_0 \sim 0.5$) $\sim \underline{3.5\cdot 10^{33}}$ $\sim 0.5 L_{e^+e^-}$

$\underline{\int L dt \sim 30 fb^{-1}}_{t \sim 10^7 cek}$ with $\frac{dL_{\gamma\gamma}}{dz}\frac{z_{max}}{L_{\gamma\gamma}} \sim 7$

$N_{\gamma\gamma\to WW} = 2.5\cdot 10^6$

$N_{\gamma\gamma\to H(300)} \sim 10^3$

$N_{\gamma\gamma\to ZZ} \sim 4.5\cdot 10^3$

Further increase of $L_{\gamma\gamma}$

1. Optimization of damping ring
2. without damping ring, Photoguns in special scheme can provide $L_{geom} \sim 5\cdot 10^{34}\left(\frac{E}{250}\right)$

$$\Rightarrow L_{\gamma\gamma}(z>0.65) \sim 5\cdot 10^{33}\left(\frac{E[GeV]}{250}\right) cm^{-2}s^{-1}$$

• • •

$L_{\gamma e}(z>0.8) \sim 0.3\, L_{geom} \approx 3\cdot 10^{33}$ (at „present" e^+e^--damp. rings)

Luminosity

Collision effects in $\gamma\gamma$ collisions (coherent $\gamma \to e^+e^-$ in the field of opposing „used" electron beam restrict $\gamma\gamma$ - luminosity at the level

$$L_{\gamma\gamma} \gg 10^{34} \div 10^{35}$$

(at N, ν, σ_z of designed linear colliders)
but electron beam sizes are not sufficiently small to allow these ultimate luminosities

Reality

$L_{\gamma\gamma}(z>0.65) \sim 0.2\, L_{\gamma\gamma}(tot)$

$L_{\gamma\gamma} \sim \kappa^2 L_{ee,geom}$

$\kappa^2 \sim 0.4$ $(A = A_0)$

$\Rightarrow \underline{L_{\gamma\gamma}(z>0.65) \sim 0.1 L_{ee}}$

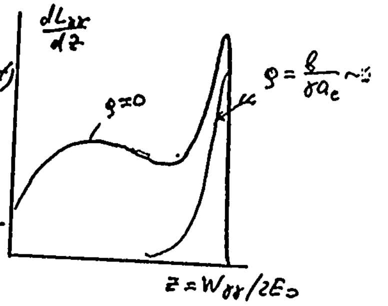

To have $L_{\gamma\gamma}(z>0.65) \sim \underline{10^{34}}$ one needs

$$L_{geom,ee} = \frac{N^2 \nu}{4\pi\sigma_x\sigma_y} \sim \underline{10^{35}}$$

With present beam emittances and modified focusing systems

	$L_{\gamma\gamma}(z>0.65), 10^{33}$	σ_x/σ_y (nm)	[illegible]
TESLA	0.9	-400/45	(← [illegible]
SBLC	0.4	-350/29	[illegible]
JLC	1	-45/10	
NLC	1.1	-70/7	
CLIC	0.85 ($\nu = 12 kHz$)	-400/8	
VLEPP	2	-500/10	

In wiggler

$\varepsilon_n = 3.3 \cdot 10^{-14} B^3(\text{kGs}) \beta_x(\text{cm}) \lambda^2(\text{cm})$

$B_0 = 15\,\text{kGs}$, $\beta = 150\,\text{cm}$, $\lambda = 10\,\text{cm}$

$\Rightarrow \varepsilon_n = 1.6\,10^{-6}\,\text{cm.rad}$ very good.

Intrabeam scattering

Theory is complicated. I used approximation

$$\varepsilon_x = \frac{1}{2}\sqrt{c\,\frac{I}{\sigma_{p/p}\gamma^3 g_{ox}}\left\langle\frac{H^{1/2}}{\sqrt{\beta_y}}\right\rangle} \quad \text{at } \xi = \frac{\varepsilon_y}{\varepsilon_x} = 0.01$$

g_{ox} – damp. rate of ring.

Damping – wigglers ($\frac{1}{2}\,2\pi R$)

IBS — ring

$$\varepsilon_x \propto \frac{l_0^{3/4}}{E^{1.25} B_w^{1.25} \rho_0^{1/2} \beta^{1/4} (\xi)^{1/2}}$$

Numerically: $B = 15\,\text{kGs}$, $E = 2\,\text{GeV}$, $\rho = 50\,\text{m}$

$\xi = 0.01$ $\varepsilon_x = 0.4 \cdot 10^{-4}$

$\xi = 0.1$ $\varepsilon_x = 0.11 \cdot 10^{-4}$

Note: $\varepsilon_x \propto \frac{1}{\sqrt{\xi}} = \sqrt{\frac{\varepsilon_x}{\varepsilon_y}} \Rightarrow \underline{\sqrt{\varepsilon_x \varepsilon_y} = \text{const}} = S$

ε_y is already now is sufficient, so with decreasing ε_x we can increase ξ, that makes task easier.

Resume: reduction of ε_{nx} in damping rings by a factor 5 is possible.

Now $\varepsilon_n \sim 2$ Que$\cdot 10^{-4}$ cm.rad

at $2E = 500$ GeV

	TESLA	SBLC	JLC	NLC	VLEPP	CLIC
Damping	20/1	10/0.5	3/0.05	5/0.05	20/0.075	2.5/0.04
Ph.gun	16/16	9/9	2/2	2/2	60/60	2.5/2.5

! $\varepsilon_x \varepsilon_y$ too large now. For polarized even more probl.

Possible improvements

1) improv. of guns (correlat. r–E, Sessler)

2)  combining of many bunches at low emittance (as at CLIC)

3) ----( ) compression of bunch train with low emittance

Damping rings

SR damping | 1) fluct. of SR
2) intrabeam scattering.

Without IBS

equil. ε_x (in FODO)

$$\varepsilon_n \sim 90.1 \frac{l_0}{l_{b0}} \frac{E^3(\text{GeV})}{N^3} \xrightarrow{l_b \sim 1.5 l_{b0}} 140 \frac{E^3(\text{GeV})}{N^3}\,\text{cm.rad}$$

$E = 1$ GeV, $N = 150$ (magnets)

$\varepsilon_n = 4 \cdot 10^{-5}$ (now $\sim 3 \cdot 10^{-4}$)

Resume: factor 5 in ε_{nx} is possible by increasing $2\pi R$.

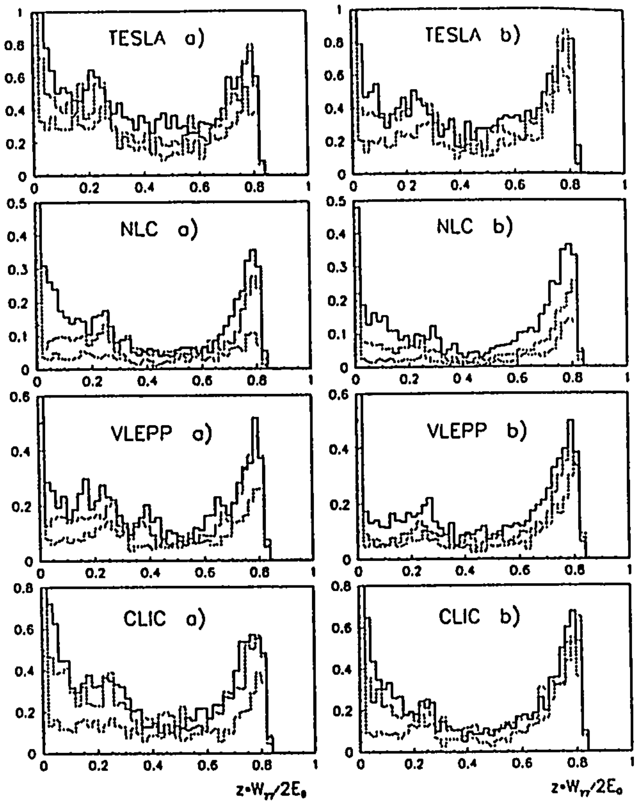

Fig. 2 $L_{\gamma\gamma}$ distributions for the scheme with magnetic deflection. Solid lines— 2E = 500 GeV, dashed — 1000 GeV, dotted — 2000 GeV. figs.a) for "nominal" emittances, b) - for horizontal emittance reduced by a factor 5. The luminosities are normalized on $L = N^2 f / 4\pi\sigma_x\sigma_y$. The histograms for JLC and SBLC are not shown. They are close to NLC and TESLA respectively (results for all projects are presented in tables).

3) Linear damping

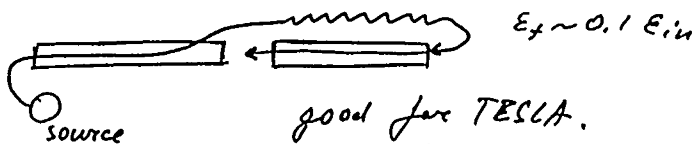

good for TESLA.

$$\varepsilon = \frac{\varepsilon_0}{1+\frac{x}{x_0}} \qquad x_0 = \frac{0.75}{\varepsilon_0 B^2}$$

In the beginning ($\varepsilon = \varepsilon_0$)

$B = 20\,kGs$, $\lambda = 10\,cm$, $\beta = 3m\sqrt{E(GeV)}$

$\Rightarrow \varepsilon_{eq.n} \sim 1.5 \cdot 10^{-4}$

B_w can vary with the energy to keep $(\varepsilon_{eq.n})_{limit} = const. \Rightarrow B^3\beta = B^3\sqrt{E} = const.$

Scheme needs careful consideration.

$B = 1T$

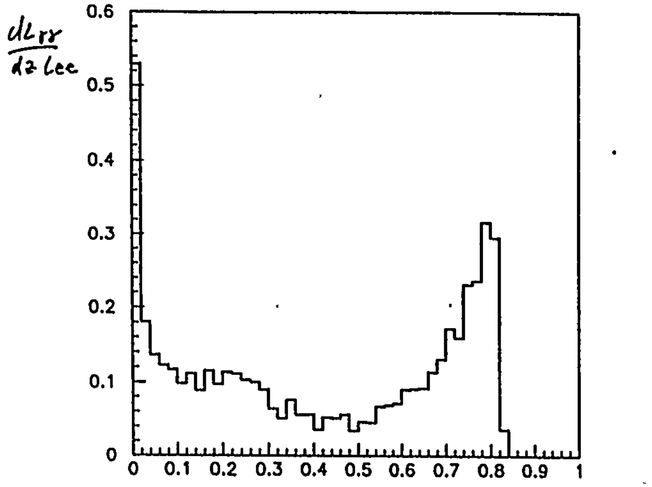

$B_x = 10\,kGs$ ✓

$\ell = 6.8\,mm$

$\beta_x = 3\,mm$

$\beta_y = 0.1\,mm$

$L_{\gamma\gamma}(z > 0.65) = 1.3 \cdot 10^{33}$

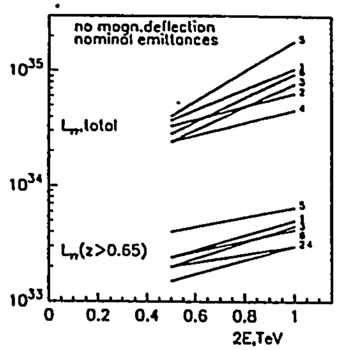

Fig.3. $L_{\gamma\gamma}$ for the scheme without deflection with "nominal" emittances. Numbers 1 — TESLA, 2—SBLC, 3—JLC, 4—NLC, 5—VLEPP, 6—CLIC.

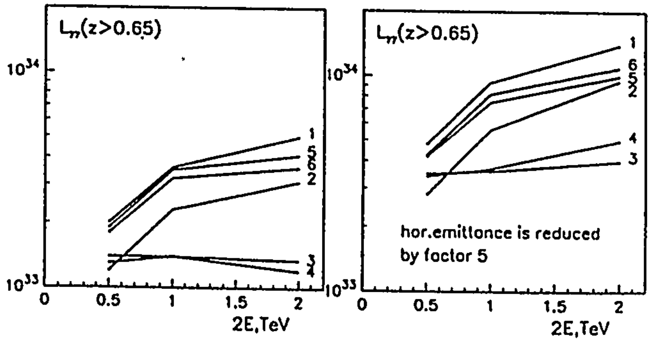

Fig.4. $L_{\gamma\gamma}$ for the scheme with magnetic deflection with "nominal" emittances (left figs.) and reduced by a factor 5 horizontal emittances (right). Numbers 1 — TESLA, 2—SBLC, 3—JLC, 4—NLC, 5—VLEPP, 6—CLIC.

Scheme of interaction region

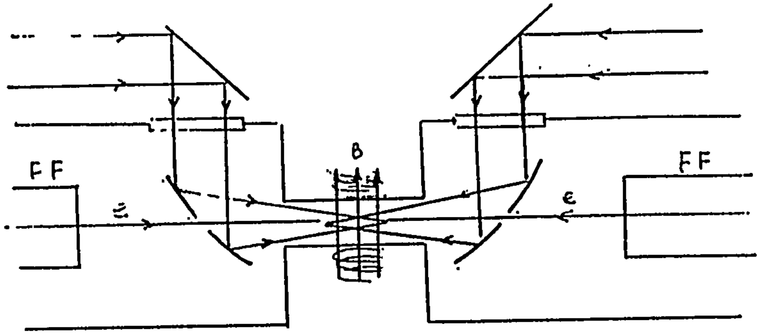

side view

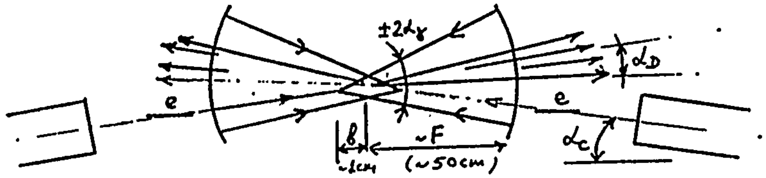

TOP view
crab-crossing →

$\alpha_\gamma \simeq \frac{a_\gamma}{b_\gamma} \simeq \sqrt{\frac{\lambda}{2\pi l_\gamma}} \approx \sqrt{\frac{\lambda}{2\pi l_e}}$; $\Rightarrow \lambda = 1\mu m$, $l_e \sim 0.1 cm$ $\alpha_\gamma \sim 2\cdot10^{-2}$ (or larger)

For example:

~disruption = ± $8\cdot10^{-3}$

~crab ~ $\alpha_D \sim 8\cdot10^{-3}$

" ~ $3\alpha_D \sim 2.5\cdot10^{-2}$

F = 50 cm, $D_{lense} \sim 5F\alpha_\gamma \sim 6cm$

J/cm² ~ $\frac{3J}{\pi(F\alpha_\gamma)^2} \sim 0.5$ J/cm² — OK
(few J/cm is max. of ...

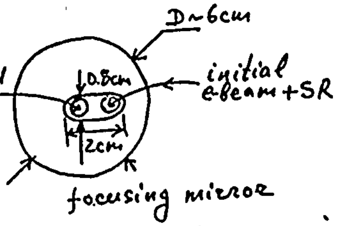

„Super" monochromatization

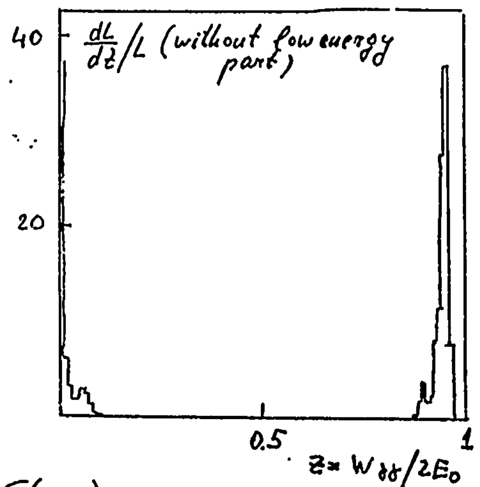

$N = 5\cdot10^{10}$, $k = 0.2$
$\sigma_x = \sigma_y = 20nm$
$\sigma_z = 1mm$
$E_0 = 200$ GeV
$X = 20$ ($\lambda = 0.2\mu m$)
$b = 2.5cm$, $B = 5 kGs$
FWHM ~ 2% ! ≡ h

$L_{z>0.9} \sim 10^{29}$: $D \sim 10^{33}$

For $t\bar{t}$-threshold study

$\frac{\sigma(W_{\gamma\gamma})}{2E_0} \sim 5\%$ for detector and ~ 1% for collider

For search for with narrow resonance (with large background,
$\int L dt \sim \frac{1}{h}$

For known resonance $t_{meas.} \sim \frac{h^2}{L}$

Flash energy!

		$X=4.8$ $A=A_0$	$X=20$, $A=0.2A_0$
A, joules	$\sigma_z = 0.01cm$	1.6	0.18 (
	$\sigma_z \sim 0.1cm$	3	2

(not proportional due to nonlinear effect).

x	0.2	0.5	1	2	4.5
E(GeV)	2.6	6.5	13	26	58

($x=4.5$ - limit due to e^+e^- pair creation)

- Laser target (below) is measured in units of Tomson collision length λ_T

  $$\sigma_c = \sigma_T(1-x) \text{ at } x \ll 1$$

- At $x \ll 1$ ↓ $$dE \sim 0.5 E x \frac{dt}{\lambda_T} \qquad x = x_0 \frac{E}{E_0}$$

  $$= 0.5 \frac{E^2 x_0}{E_0} \frac{dt}{\lambda_T} \qquad \frac{1}{E} - \frac{1}{E_0} = \frac{0.5 x_0 t}{E_0 \lambda_T}$$

  At $E \ll E_0$

- $$\frac{\varepsilon_n}{\varepsilon_{n0}} = \frac{E}{E} = \frac{\lambda_T}{0.5 x_0 t} = \frac{1}{0.5 N_{coll} x_0}$$

  $N_c = \frac{t}{\lambda_T}$ depends on laser only (at $x \ll 1$ $\sigma_c = \sigma_T$)

- $x_0 \propto E_0$, so $\frac{\varepsilon_n}{\varepsilon_{n0}} \propto \frac{1}{E_0}$

  Example: $x_0 = 0.2$, $N_c = 100 \Rightarrow \frac{\varepsilon_n}{\varepsilon_{n0}} = 0.1$, better for larger x_0.

New!!!

Laser cooling and polarization of electron(e) beams

$\tau = const$, $\theta = const$ (up to some limit) $\Rightarrow \varepsilon = const$

Normalized emittance $\varepsilon_n \equiv \varepsilon\gamma = \varepsilon_{n0} \frac{E}{E_0}$ decreases (it is important: $\sigma = \sqrt{\frac{\varepsilon_n}{\gamma}\beta}$)

Idea is not new, but problems:

1. What happends with polarization?
2. What is energy spectrum?
3. What is beam heating.?

Important param:

$$x_0 = \frac{4 E_0 \omega_0}{m^2 c^4} = 15 \left[\frac{E}{TeV}\right]\left[\frac{\omega_0}{eV}\right]$$

In one collision $\Delta E_{max} = \frac{x}{x+1} E_0$

Reduction of normalized emittance

$X = X_0$ on the figs below

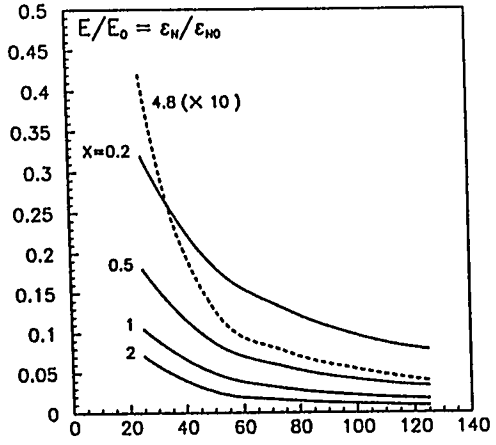

t/λ_T — ~ number of coll. (at $x \ll 1$)

λ_T - Tomson col. length

$\frac{t}{t_T} = 50$ $\frac{\varepsilon_{N0}}{\varepsilon_N}$ up to ~100

For $x \not\ll 1$ $\sigma_c = f(x)$

Below are result of simulation

for $X_0 = 0.2 - 4.5$

for different polarizations

Notations: P_c - circular laser polarization

ζ_z - longitudinal electron polariz.

After scattering

$$\zeta_z = \frac{\zeta_{z_0} f_1(y) + P_c f_2(y)}{f_3(y) + P_c \zeta_{z_0} f_4(y)}$$

$$\sigma_c = \sigma_c^0 + \zeta_z P_c f(x)$$

Electrons can get polarization if laser is polarized

Example of energy spectrum
(with the largest σ_E/E on previous fig)

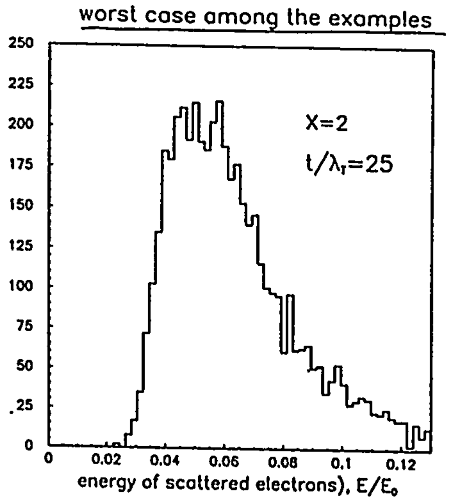
worst case among the examples

no low energy tail !

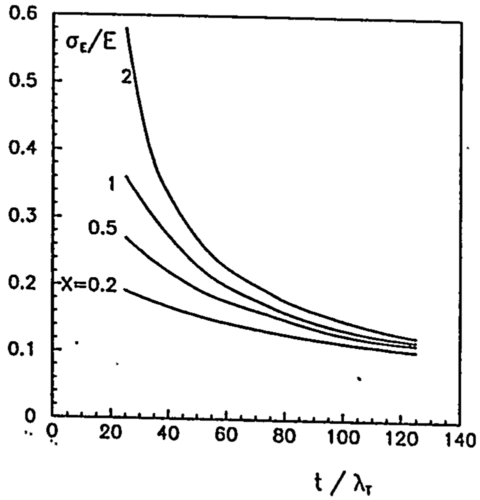

Shape have high energy tail

Does polarized electrons loss the polarization?

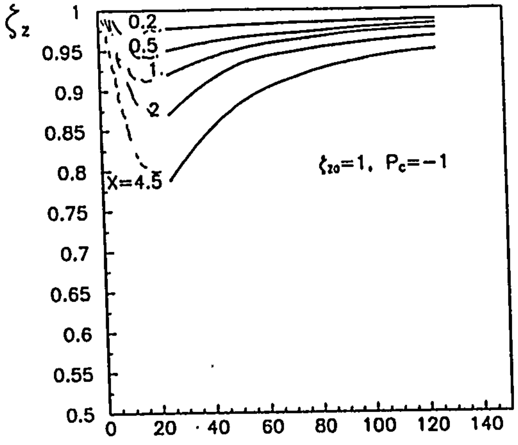

small depolarization, but it recovers if laser is polarized

Polarization of electrons (positrons) by polarized light

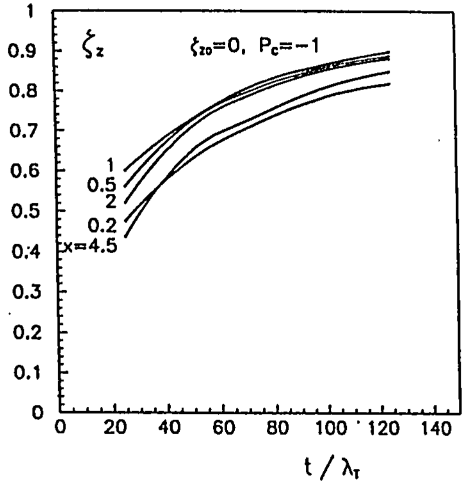

!

Positrons for linear colliders can be polarized in this way and polarized laser

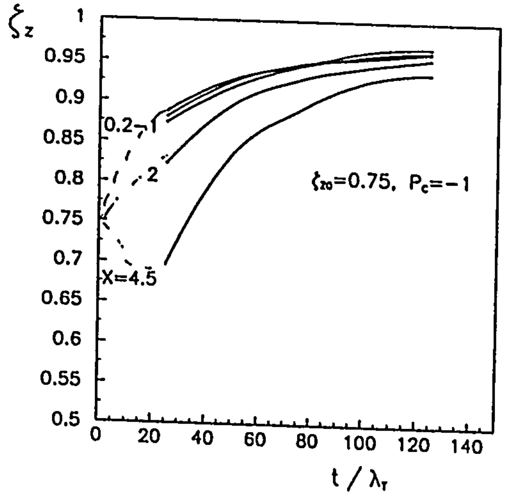

polarization improves

Un-polarized laser

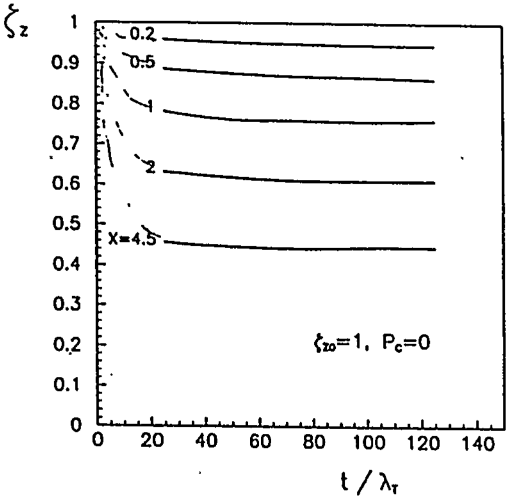

Loss of electron polarization
is small for small X,
but significant for X > 1

Fast polarization of beams in storage rings by helical ondulator

Ondulator is similar to laser with small X and will polarize beams.

From previous fig. follows that polarization time ~ damping time!

$$P = \frac{2}{3}\frac{e^4 B^2 \gamma^2}{c^3 m^2}$$

ondulator regime $\alpha = \frac{\lambda_0}{R} < \frac{1}{\gamma} \Rightarrow B < \frac{mc^2}{e\lambda_0}$

λ_0 - period of ondulator

$$Pt = \gamma mc^2 \Rightarrow \boxed{t_p \sim \frac{\lambda_0^2}{r_e \gamma c}}$$

$\left.\begin{matrix}\lambda = 5 cm\\ \gamma = 10^4\end{matrix}\right\}$ $t_p = \underline{0.3 \text{ сек}}$ $B \sim 0.3$ кГс.

Let $2\pi R = 500 m$, $L_{ond} \sim 20 m$

then the electron is in ondulator $\frac{L}{2\pi R}$ part of time, so real polarization time

$$T \sim \frac{L}{2\pi R}\frac{\lambda_0^2}{r_e \gamma c} \sim \underline{7.5 \text{ сек}} \text{ (for considered case)}$$

This is much shorter than "natural" polarization time in storage ring

Good for B, c-τ-factories

Electron polarization vs electron energy loss

(in one laser flash)
(X changes during damping)

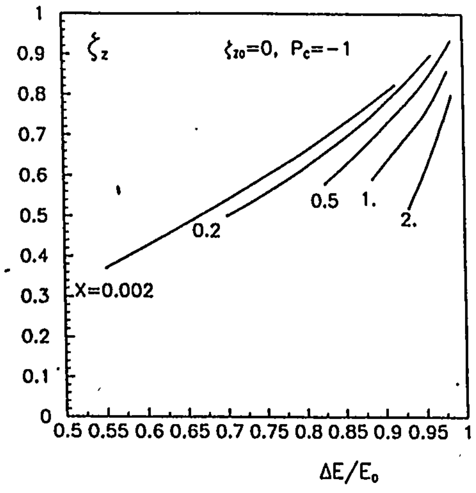

At low X there is universal curve.

$\frac{E}{E_0} = 0.1 \Rightarrow \zeta_z = 80\%$

Example, requirement to laser power

$$\left.\begin{array}{l} t/\lambda_T = 75 \\ X_0 = 0.5 \\ \lambda = 0.25\,\mu m \\ E = 6.5\ GeV \end{array}\right\} \Rightarrow \zeta_{e^+} = 82\% \qquad \varepsilon_n/\varepsilon_{n0} = 0.05$$

$$\sigma_E/E \sim 0.05\% \text{ at } E = 100\ GeV$$

Flash energy

$$\eta = \frac{eE\hbar}{m\omega_0 c} \lesssim 1$$

at $2\beta_\gamma \sim l_\gamma$. $\quad \eta^2 \sim \frac{1}{4\alpha}\frac{\lambda}{l_\gamma}\frac{t}{\lambda_T} = 1$

$$\Rightarrow l_\gamma \sim 0.065\,cm \quad (2ps)$$

Required flash energy

$$A \doteq \frac{t}{\lambda_T} \cdot \frac{\hbar c\, l_\gamma}{\sigma_T} \sim 75 \cdot 5 \cdot 0.065 = 25\,J$$

$\underline{t = 70\lambda_T}$ Similar consider. gives

$A \sim 10\,J \quad l_\gamma \sim 0.045\,cm \quad P = 7\,TW$

$\zeta_{e^+} = 72.5\% \quad \varepsilon_n/\varepsilon_{n0} = 0.09$

$\sigma_E/E \sim 0.1\%$ at $E = 100$ GeV.

If one flash is used many times (~ 50) and $\Delta A/A \sim 0.4$ ($\pm 20\%$), then increase of σ_E/E only a little ($\frac{\sigma_E}{E} = 0.1\% \to 0.015\%$ at 100 GeV.

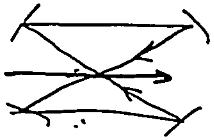

Less than 10 laser flash for NLC train (90 bunches)
1 for TESLA

$$P \sim 10\,J \cdot \frac{16 \cdot 10^3}{10} \sim 16\,kW \quad NLC$$

$$15\,J \cdot \frac{8 \cdot 10^3}{50} \sim 2.5\,kW \quad \begin{array}{c} JLC \\ TESLA \end{array}$$

OK.

Conclusion.

1. Reduction of emittance by a factor $10-100 \left(= \frac{\varepsilon_{in}}{\varepsilon_{ou}}\right)$ in one stage of cooling
2. Production of polarization (e^+!)
3. Helical ondulator in storage ring can polarize beams much faster than „natural" rad. polarization

Applications: 1 and 2 — linear colliders

3 — b, τ-$\bar{\tau}$ factories

Limit on ε_n due to angles in Compton scattering

$$\theta_{in\ beam} = \sqrt{\frac{\varepsilon_n}{\beta\gamma}} = \theta_{scat} \cdot \frac{E_{out}}{E_{in}}$$

(valid if $\eta \ll 1$) pure Compton

$$\varepsilon_{n,lim} \sim 0.5 \frac{\beta}{N_{coll}\,\gamma_0} \sim 5 \cdot 10^{-10} \text{ m r}$$

(with many cascades)

here $N_{coll} = t/\lambda_t$ in one stage ~ 50

β - beta function in cooling region (of electron beam) ~ 1mm (may be smaller)

For comparison: NLC $\varepsilon_{xn} = 2.5 \cdot 10^{-6}$ m r

$\varepsilon_{yn} = 1.5 \cdot 10^{-8}$

for $\beta = 0.01$ $\frac{\varepsilon_{lim}}{\varepsilon_{nxNLC}} \sim 10^{-5}$ $\frac{\varepsilon}{\varepsilon_{nyNLC}} \sim 10^{-3}$

- Laser cooling and polarization of electron (e+) beams

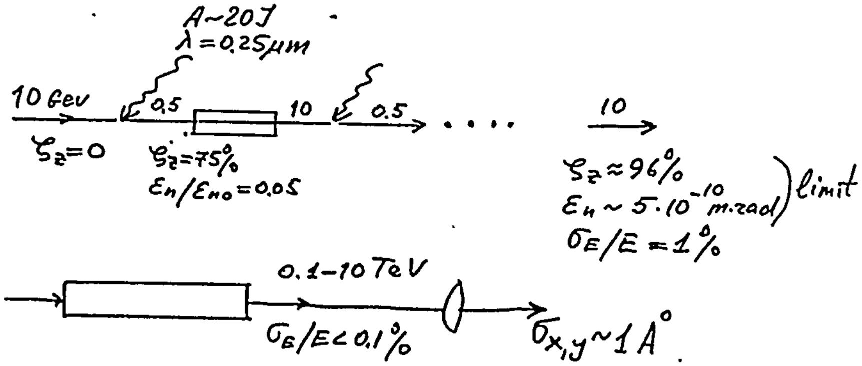

- Fast polarization of beams in storage rings by helical ondulator

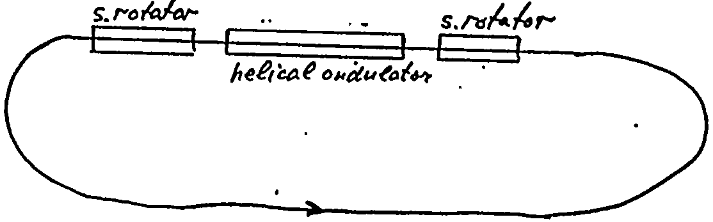

$$T_{polar} \sim \frac{L_{ond}}{C_{ring}} \frac{\lambda_0^2}{r_e \gamma c} \sim 10s$$

~ damping time of ondulator

PARAMETRIC X-RAY RADIATION AS SOURCE OF SHORT PULSES OF X-RAY BEAM

A. Shchagin,KIPT

"Parametric X-ray radiation
as Source of Short pulses
of polarized X-ray beam"

A.V. Shchagin, Z. Parsa

Institute for Theoretical Physics,
Santa Barbara, CA, August 22, 1996,

—— " ——

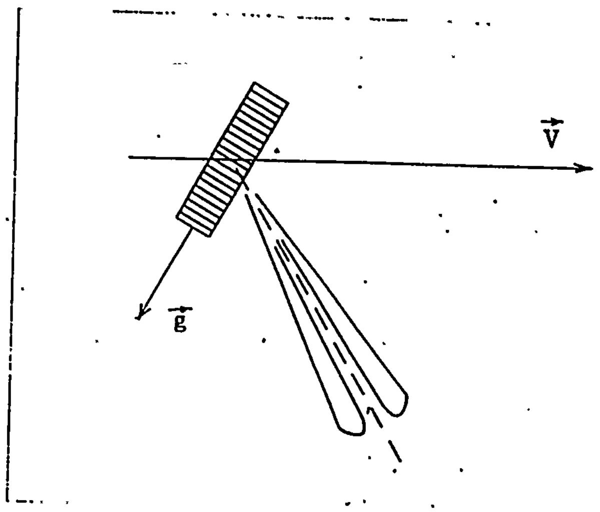

References and history of PXR

Theory

[1] Ya.B. Fainberg and N.A. Khizhnyak, Zh. Ehksp. Teor. Fiz. 32 (1957) 883.

[2] M.L. Ter-Mikaelian, High-energy electromagnetic processes in condensed media, (Wiley-Interscience, New York, 1972).

[3] V.G. Baryshevskij, Channeling, radiation and reactions in crystals at high energies (BGU publ., Minsk, 1982) [in Russian].

[4] G.M. Garibyan and C. Yang, X-ray transition radiation (Arm. SSR publ., Erevan, 1983) [in Russian].

[5] D. Dialetis, Phys. Rev. A 17 (1978) 1113.

[6] I.D. Feranchuk and A.V. Ivashin, J. Physique 46(1985)1981.

[7] H. Nitta, Phys. Lett. A 158 (1991) 270;

[8] A. Caticha, Phys. Rev. B45(1992)9541.

Experiments

[9] Yu.N. Adishchev, A.N. Didenko, V.V. Mun, G.A. Pleshkov, A.P. Potylitsin, V.K. Tomchakov, S.R.Uglov, and S.A. Vorob'ev, Nucl. Instrum. Methods Phys. Research B 21 (1987) 49. Tomsk, USSR

[10] A.V. Shchagin, V.I. Pristupa, N.A. Khizhnyak, Phys. Lett. A 148(1990)485. Kharkov, USSR

[11] R.B. Fiorito, D.W. Rule, X.K. Maruyama, K.L. DiNova, S.J. Evertson, M.J. Osborne, D. Snyder, H. Rietdyk, M.A. Piestrup, and A.H. Ho, Phys. Rew.Lett. 71(1993)704. USA

[12] S. Asano, I. Endo, M. Harada, S. Ishii, T. Kobayashi, T. Nagata, M. Muto, K. Yoshida, H. Nitta, Phys. Rev. Lett. 70 (1993) 3247. ~~Japan~~

A.V. Shchagin, N.A. Khizhnyak. Review of PXR properties. Will be published in October issue NIM B, 1996 Kharkov, Ukraine

Electron beam

Energy E_e = 50; 100; 200 MeV
Charge 1 nC/bunch
Bunch Lenght 300 fs
Beam Diameter 0.1 mm

Target

Si Singlecrystal
$\vec{g} = \langle 111 \rangle$
Thickness 60 μm

Setup

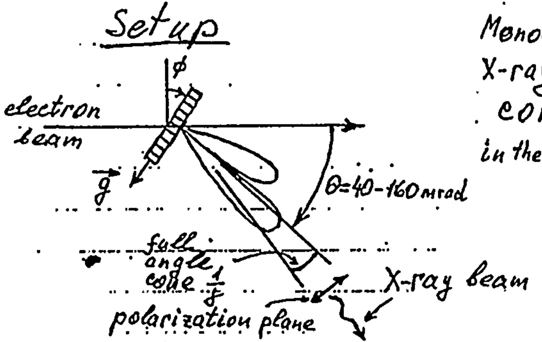

Calculations

Ter-Mickaelian's theory.
Monocromatic Polarized X-ray radiation in full cone angle $\frac{1}{\gamma}$, in the vicinity of target, $\frac{J}{S \cdot cm^2}$
X-ray beam lenght ~300 fs

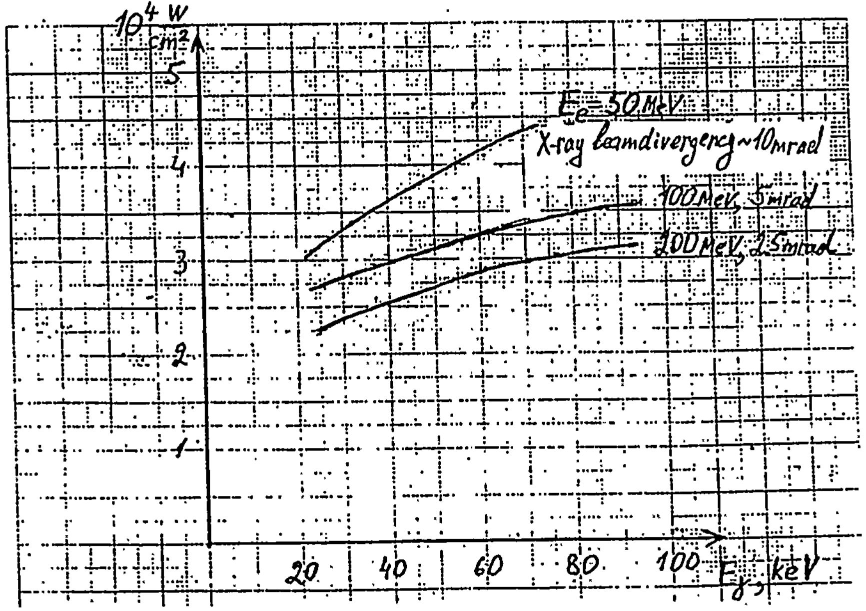

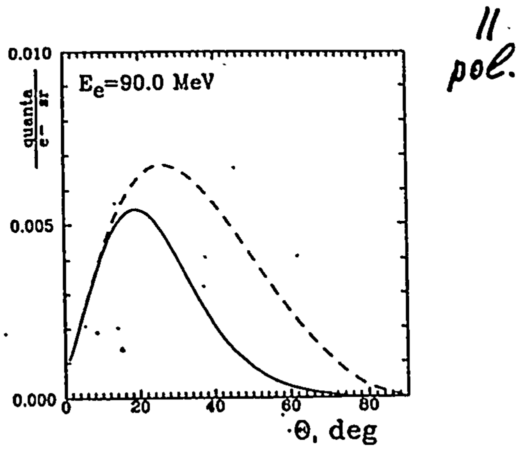
‖ pol.
0.010
0.005
0.000
quanta / e⁻ sr
E_e=90.0 MeV
0
20
40
60
80
Θ, deg

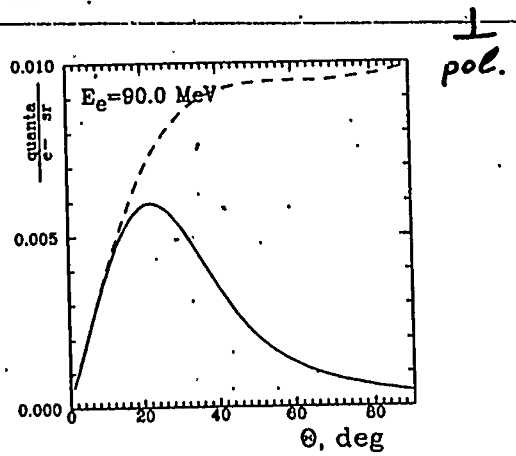
⊥ pol.
0.010
0.005
0.000
quanta / e⁻ sr
E_e=90.0 MeV
0
20
40
60
80
Θ, deg

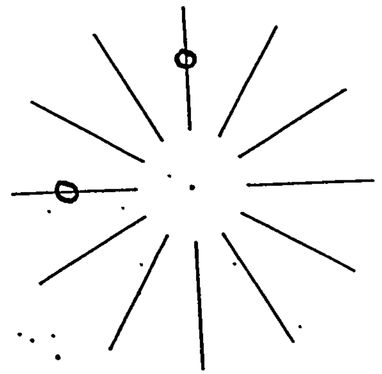

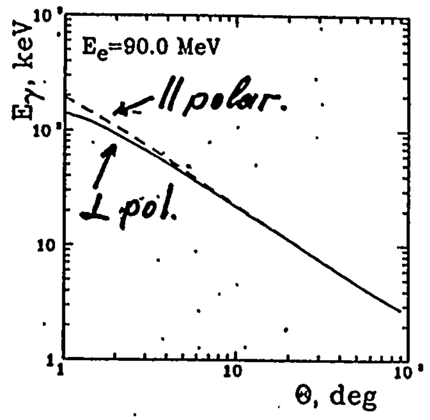
E_γ, keV
10³
10²
10
1
E_e=90.0 MeV
‖ polar.
⊥ pol.
1
10
10²
Θ, deg

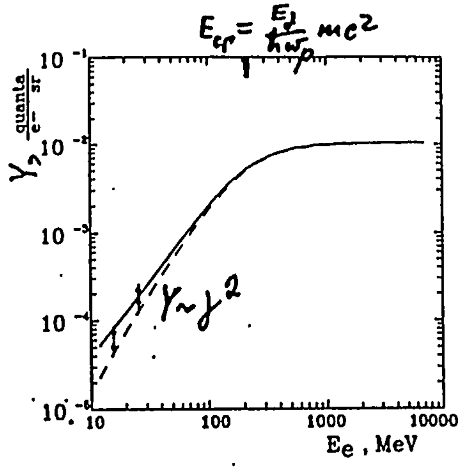

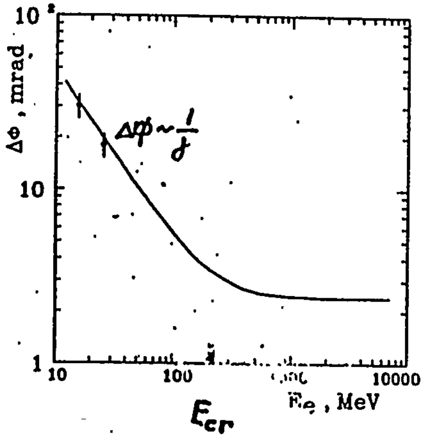

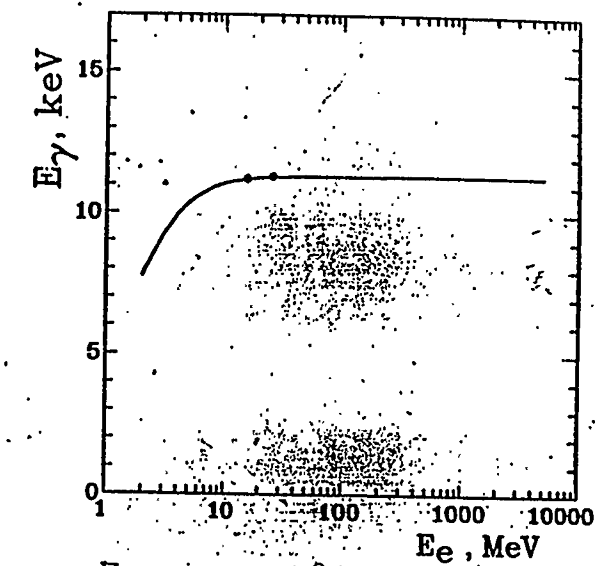

Energy of PXR peak vs function of incident electron energy.

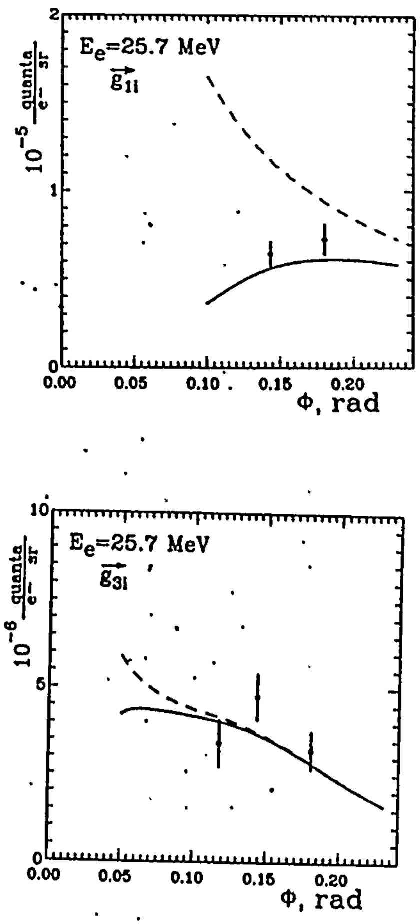

E_e=25.7 MeV
$\vec{g}_{1l}$
$10^{-5}\,\frac{\text{quanta}}{e^-\ \text{sr}}$
2
1
0
0.00
0.05
0.10
0.15
0.20
Φ, rad
E_e=25.7 MeV
$\vec{g}_{3l}$
$10^{-6}\,\frac{\text{quanta}}{e^-\ \text{sr}}$
10
5
0
0.00
0.05
0.10
0.15
0.20
Φ, rad

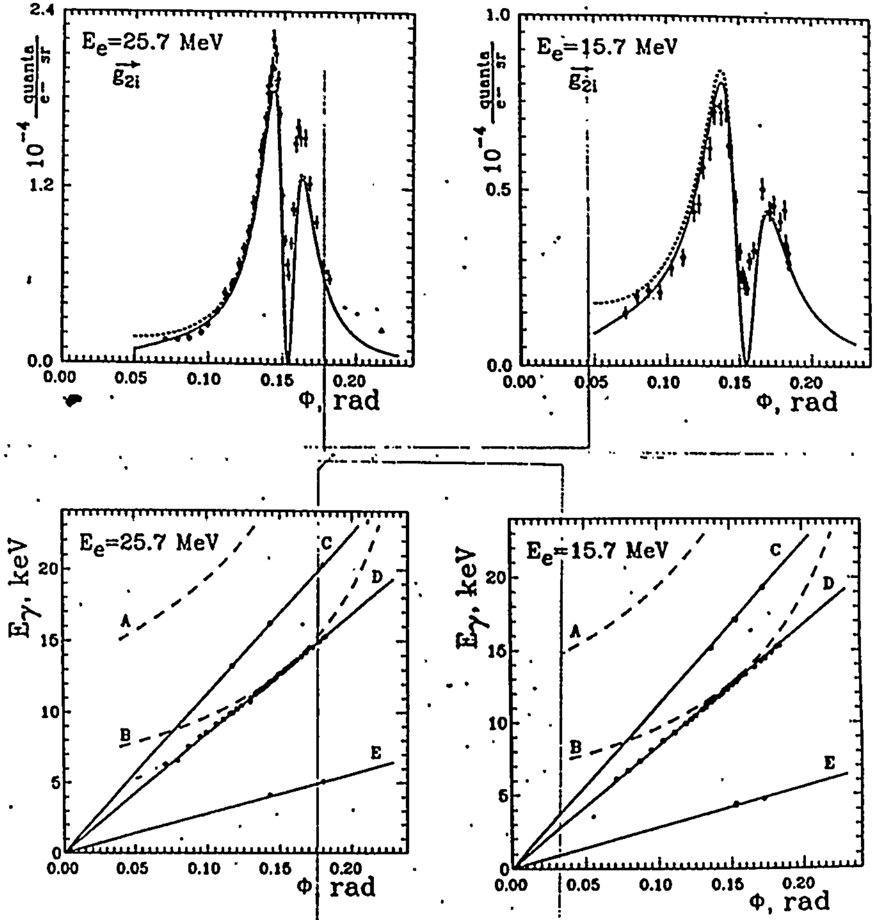

E_e=25.7 MeV
$\vec{g}_{2l}$
$10^{-4}\,\frac{\text{quanta}}{e^-\ \text{sr}}$
2.4
1.2
0.0
0.00
0.05
0.10
0.15
0.20
Φ, rad
E_e=15.7 MeV
$\vec{g}_{2l}$
$10^{-4}\,\frac{\text{quanta}}{e^-\ \text{sr}}$
1.0
0.5
0.0
0.00
0.05
0.10
0.15
0.20
Φ, rad
E_e=25.7 MeV
E_γ, keV
20
15
10
5
0
A
B
C
D
E
0.00
0.05
0.10
0.15
0.20
Φ, rad
E_e=15.7 MeV
E_γ, keV
20
15
10
5
0
A
B
C
D
E
0.00
0.05
0.10
0.15
0.20
Φ, rad

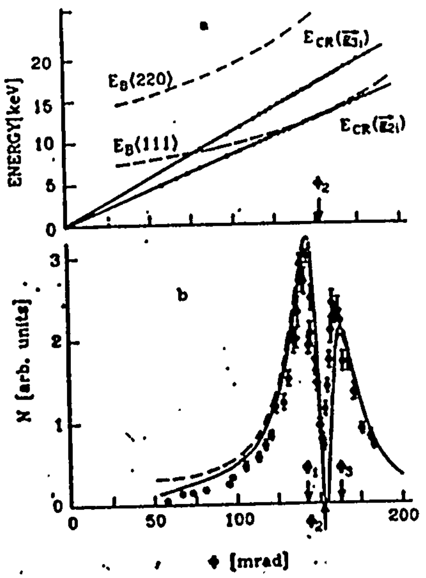

Fig. 3. (a) Peak energies in radiation spectra measured versus the crystal alignment (points). The solid lines show the coherent radiation energies calculated by formula (1) for the rows of reciprocal lattice vectors g_{2i} and g_{3i} comprising $g=\langle 111\rangle$ and $g=\langle 220\rangle$, respectively. The dashed line is the calculated Bragg energy in the direction of detection for $g=\langle 111\rangle$ and $g=\langle 220\rangle$. (b) The number of PXR quanta measured versus the crystal alignment (points with statistical errors). The dashed line is the calculation by (3) for $g=\langle 111\rangle$, the solid line shows the calculation taking into account the PXR absorption in the target.

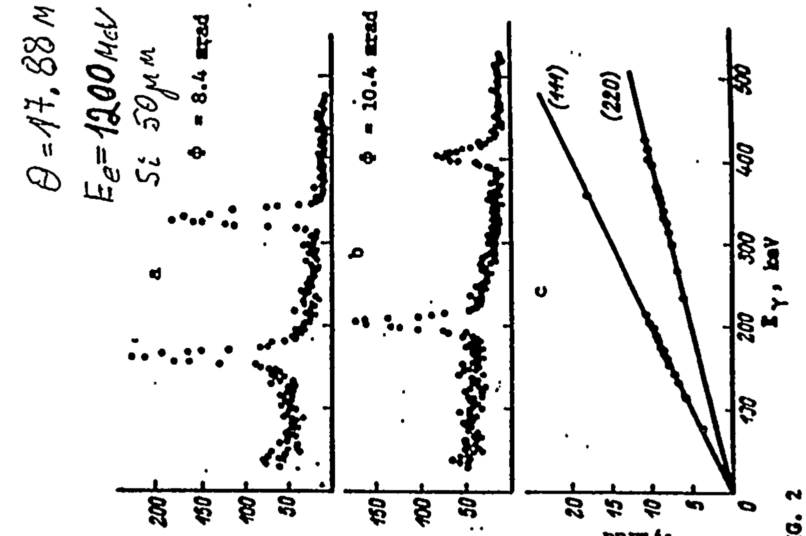

FIG. 2

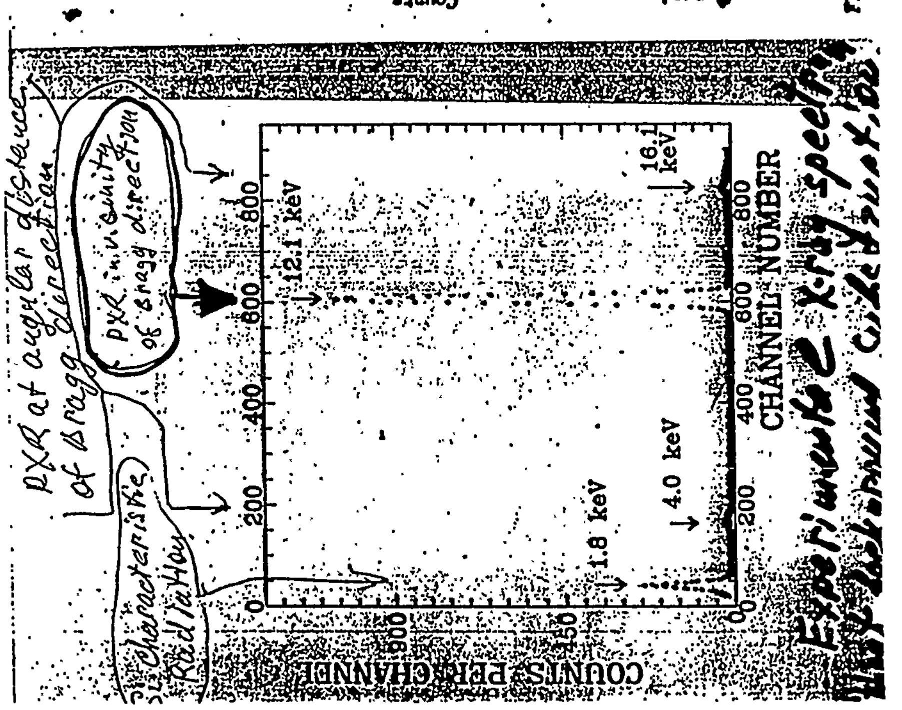

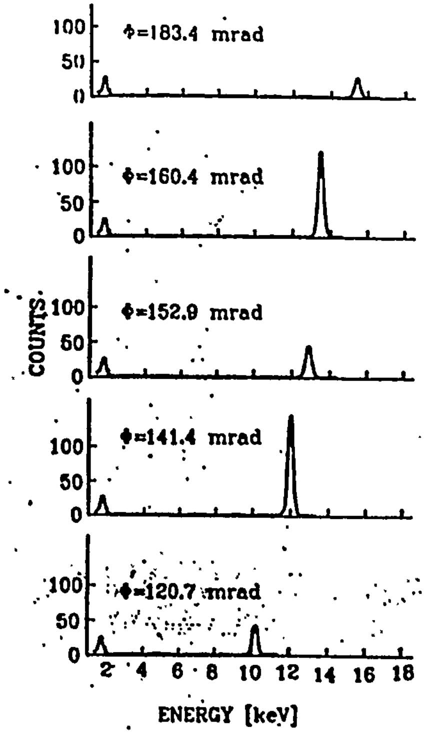

Fig. 2. Experimental X-ray spectra at different crystal alignment angles.

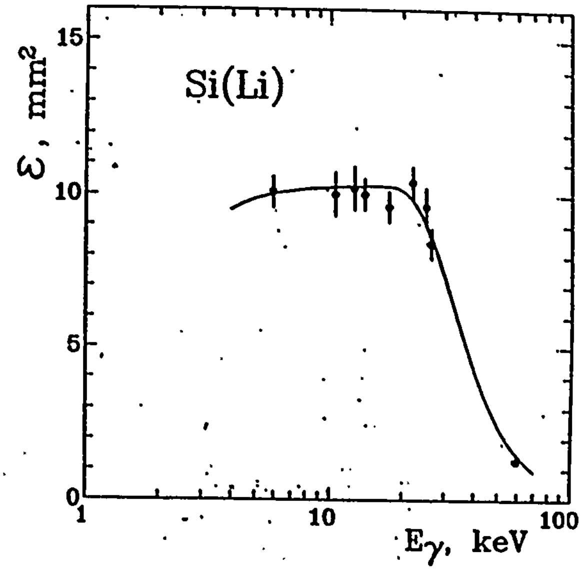

1 Experimental

The experiments were made at Kharkov Institute of Physics and Technology by using the linear electron accelerator LUE-40 at incident electron beam energies 15.7, 25.0, 25.7 MeV. The experimental setup is shown in fig.1.

As a target, we used a 17 μm thick silicon single crystal plate, whose reciprocal lattice vector $\vec{g}_{\perp} = <\bar{2}20>$ was perpendicular to the plate surface. The target was placed in the vacuum goniometer and was prealigned so that the $\vec{g}_{\parallel} = <\bar{2}20>$ should be parallel to the velocity vector $\vec{V}$ of the beam electrons, and $\vec{g}_{\perp} = <111>$ should be perpendicular to $\vec{V}$ in the detection plane at $\phi = 0$. Spectra were measured as function of the angle ϕ of target rotation an the detector direction relative to the axis perpendicular to the detection plane. Note, that at $\phi = \theta/2$ the BD for the crystallographic plane (111) is directed to the detector.

The spectra were measured by the use of the Si(Li) X-ray detector with liquid nitrogen cooling. The detector was placed 4520 mm from the target at $\theta = 305.9$ mrad to the beam axis, and was connected to the goniometer chamber by a air-free tube. In front of the 20 μm thick beryllium foil of the detector there was placed the lead diaphragm, 0.8 mm thick, with a circular aperture. The circular aperture was made with a 3.7 mm drill. The angular resolution of the detecting system with taking into account the beam spot size on the target was about 2 $mrad$. The detector's efficiency as a function of X-ray quantum energy was measured with the lead diaphragm through the use of the set of intensity-calibrated X-ray radioactive sources. The energy resolution of the spectrometer at $E_{\gamma} = 6.4\ keV$ was found to be 286 eV.

The charge of the beam that has passed through the target during the exposure time was measured by a secondary-emission monitor placed behind the target and the charge-to-code converter.

The experimental procedure have been described in [?]. The experimental layout and more detail about the technique of absolute yield measurements can be found in [?].

PXR observed experimentally in Kharkov

in X-ray spectral band $E_{x\varepsilon} \approx 5 \div 400$ keV

at incident electron energies

[illegible] MeV

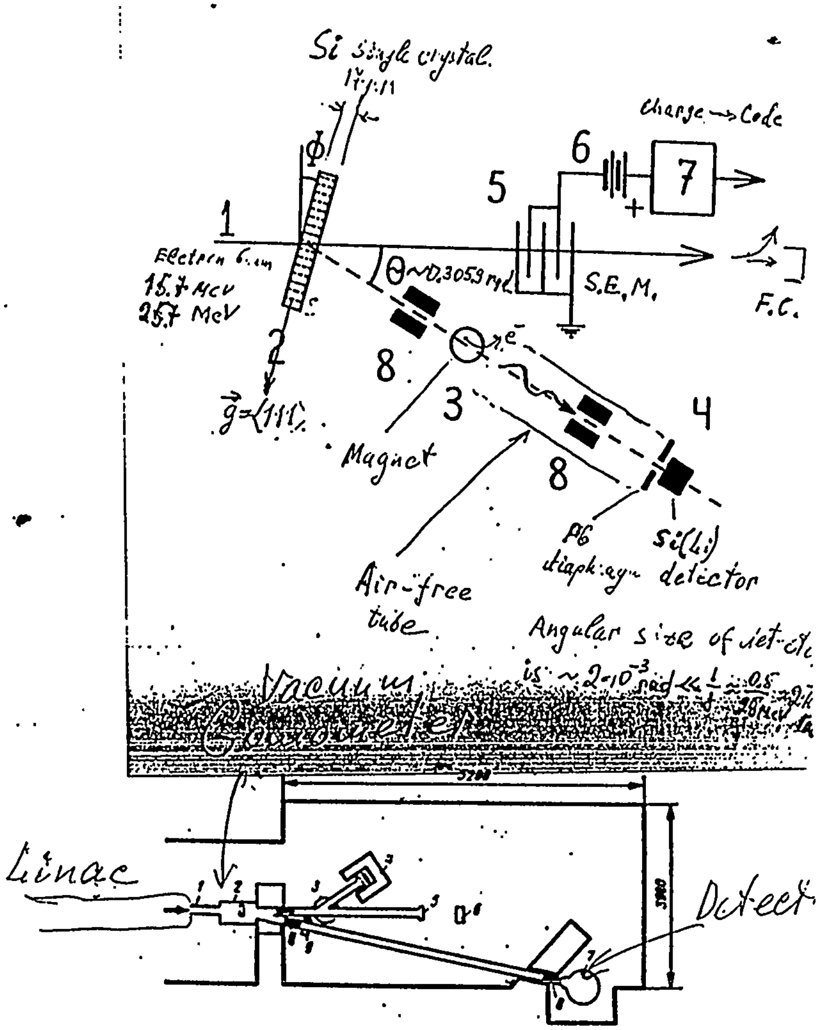

Fig. 1. Location of equipment in bunker of electron accelerator: 1) accelerator exit; 2) goniometer; 3) deflection magnet; 4) absorber; 5) Mylar foil 150 μm thick; 6) quantometer; 7) BDÉR-2-25A Si(Li) x-ray detector; 8) collimators; 9) clearing magnet.

Phys. Lett. A
148(1990)485

Energy of coherent radiation (PXR):

$$E_{CR} = \hbar\omega_{CR} = \frac{c\hbar\left|\vec{g}\cdot\vec{V}\right|}{c-\sqrt{\varepsilon_0}\vec{V}\cdot\vec{\Omega}},$$

where $\hbar$ is the Planck constant divided by 2π, ε_0 is the constant part of the medium permittivity, $\vec{g}$ is the reciprocal lattice vector, $\vec{\Omega}$ is the unit vector in the direction of the detector, c is the light velocity.

The width at half maximum of the PXR spectral peak for a detector of small angular size may be easily obtained from formula 5

$$\Delta E_{CR} \approx E_{CR}\frac{\Delta\theta}{tg(\theta/2)},$$

PXR differential yield:

$$Y_{\vec{g}} = \frac{dN}{nd\Omega} = \frac{e^2\omega L\left|\chi_{\vec{g}}(\omega)\right|^2}{2\pi\hbar c\varepsilon_0^3 V\left(\frac{c}{\sqrt{\varepsilon_0}}-\vec{V}\cdot\vec{\Omega}\right)}\cdot$$

$$\left|\frac{\left(\omega\sqrt{\varepsilon_0}/c\right)\vec{\Omega}\times\left[\left(\omega\varepsilon_0/c^2\right)\vec{V}+\vec{g}\right]}{\left[\left(\omega\sqrt{\varepsilon_0}/c\right)\vec{\Omega_\perp}-\vec{g\perp}\right]^2+\left(\frac{\omega}{V}\right)^2\left[(1/\gamma)^2+\left(\frac{V}{c}\right)^2(1-\varepsilon_0)\right]}\right|^2,$$

where dN is the number of quanta with frequency $\omega = \omega_{CR}$ (see formula 5) emitted in the solid angle $d\Omega$ as n particles with the charge e and energy E_e pass through a crystal of a thickness L; $\chi_{\vec{g}}(\omega)$ is the Fourier component of the variable part of permittivity; $\vec{\Omega_\perp}$, $\vec{g\perp}$ are the components of $\vec{\Omega}$, $\vec{g}$ perpendicular to $\vec{V}$. At $\hbar\omega_{CR} >> E_K$ the constant part of the medium permittivity is $\varepsilon_0 = 1-\left(\frac{\omega_p}{\omega}\right)^2$

The dashed (solid) line is the calculation without (with) taking into account the PXR attenuation in the target. For calculation without attenuation the factor $L = \frac{T}{\left|\vec{t}\cdot\vec{v}\right|}$ was used. With the attenuation taken into account, the factor L was used in the form

$$L = T_e\left|\frac{\vec{t}\cdot\vec{\Omega}}{\vec{t}\cdot\vec{v}}\right|\left[1-\exp\left(-\frac{T}{T_e\left|\vec{t}\cdot\vec{\Omega}\right|}\right)\right] \qquad (9)$$

where $T_e = T_e(\omega)$ is the e-fold attenuation length of radiation with frequency ω; T is the target plate thickness; $\vec{t}$ is the unit vector perpendicular to the target plane; $\vec{v} = V$

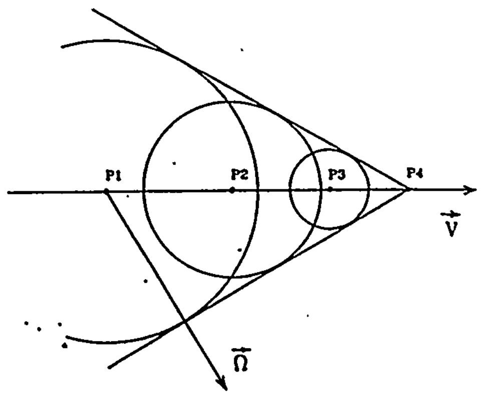

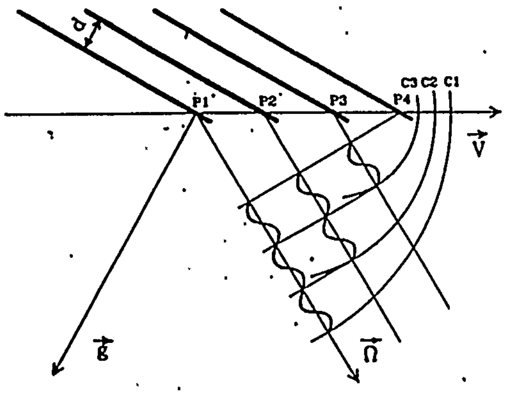

What is Parametric X-ray Radiation (PXR)?
History of investigations
Theory
Experimental
PXR properties
    - Spectral
    - Angular
    - Polarization
PXR as source of polarized pulsed
X-ray beam

GENERATION OF FEMTO-SECOND X-RAY PULSES AT SYNCHROTRON SOURCES

A. Zholents, LBNL

Generation of Femtosecond X-Ray Pulses at Synchrotron Light Sources

S. Chattopadhyay, P. Heimann, T. Henderson, K.-J. Kim, H. Padmore,
R. Schoenlein, A. Zholents, M. Zolotorev

Santa Barbara, August 19 -23, 1996
Syposium on New Modes of Particle Acceleration Techniques and Sources

There will be discussed:

Qualitative description of the primary idea

Formal description of the idea (the same as above, but with formulas)

Application to the ALS

Perspectives for further development

Qualitative description

- Duration of the synchrotron radiation pulses in storage rings is defined by the bunch length.
- Typically, the bunch length is ~30-50 ps.
- We want x-ray pulses of 50-100 fs !!!

The are two alternatives:

- Compression of the electron bunch almost in 1000 times
  - does not seem feasible
- Usage of the radiation of a fraction of the beam
  - good idea, but how to do it?

Qualitative description (cont'd)

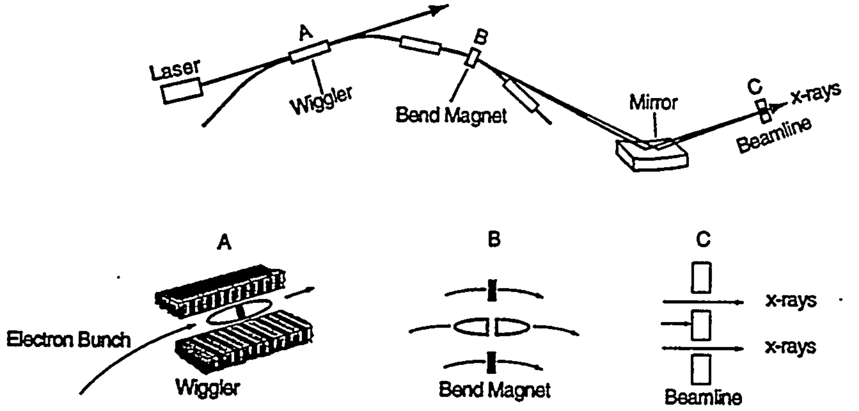

XBD 9512-05977.ILR

A schematic drawing showing the principle of the generation of the femtosecond pulses of synchrotron radiation. The electron bunch and the bunch slice are artificially magnified.

Qualitative description (cont'd)

Phase A:

- Electron bunch slice is created in the interaction of electrons with a femtosecond laser pulse co-propagating with the electron bunch in the wiggler. Due to the high electric field possible in the femtosecond laser pulse, this interaction produces energy modulation among this slice of electrons with the modulation amplitude several times larger than the r.m.s. beam energy spread.

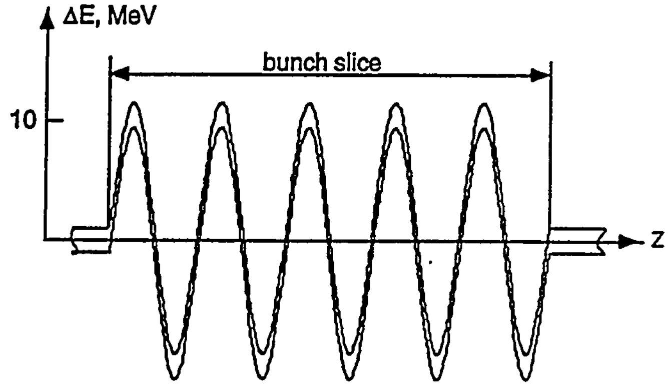

Longitudinal phase space portrait of a fraction of the electron bunch after interaction with the laser pulse

•100μJ in the 100fs laser pulse is enough to make modulation amplitude of 10MeV !!!

Qualitative description (cont'd)

Phase B:

- Electrons with large energy deviations are then transversely separated from the rest of the electron bunch at the distance several times larger than the r.m.s. transverse size of the beam. This occurs after electrons pass through the next bending magnets.

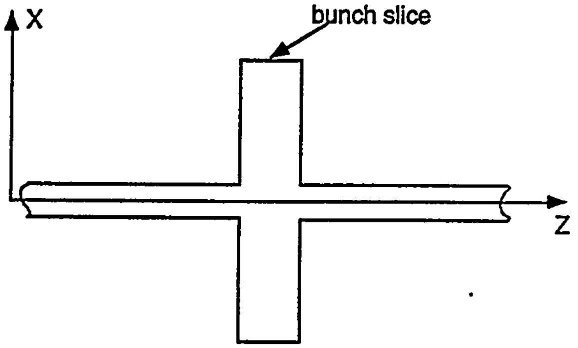

Top view on a fraction of the electron bunch

Qualitative description (cont'd)

- **Phase C:**
  - Finally, by imaging the beam to the experimental area, and by placing an aperture radially offset from the focus of the beam core, we will be able to separate out the radiation from the offset electrons .

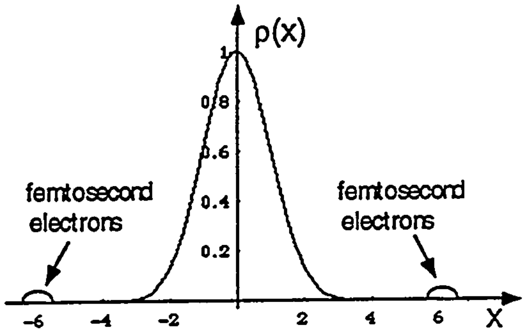

Particle density distribution in the horizontal plane at the radiation point

---

Formal description

I. Energy modulation in the wiggler.

- wiggler period satisfies the resonance condition:

$$\lambda_w=2\gamma^2\lambda_L/(1+K^2/2)$$

λ_W is the wigller period, λ_L is the laser wavelength, K is the deflection parameter

- the most efficient energy exchange between the electron and the light will take place when the far field laser radiation has the maximum overlap with the far field spontaneous radiation of electrons in the wiggler in both the transverse and longitudinal phase space.
- a superimposed field of the laser radiation $\vec{E}_L(\omega,\vec{r})$ and the spontaneous electron wiggler radiation $\vec{E}_R(\omega,\vec{r})$ is written :

$$\vec{E}_L(\omega,\vec{r})+\vec{E}_R(\omega,\vec{r})$$

Formal description (cont'd)

Total field energy:

$$A \sim \iint \left| \vec{E}_L(\omega,\vec{r}) + \vec{E}_R(\omega,\vec{r}) \right|^2 dS\, d\omega$$

can be written as a sum of the energy of the laser pulse A_L the energy of the electron radiation A_R and an exchange energy:

$$A = A_L + A_R + 2\sqrt{A_L A_R \Delta\omega_L / \Delta\omega_R}\cos(\varphi). \qquad \Delta\omega_R \geq \Delta\omega_L$$

Here $\Delta\omega_R$ is the bandwidth of the wiggler radiation and $\Delta\omega_L$ is the bandwidth of the ght pulse.

Spontaneous radiation of electrons in the wiggler is equal:

$$A_R \cong \pi\alpha\hbar\omega_L \frac{K^2/2}{1+K^2/2},$$

Thus, the amplitude of energy modulation is:

$$(\Delta E)^2 \cong 4\pi\alpha A_L \hbar\omega_L \frac{K^2/2}{1+K^2/2} \frac{\Delta\omega_L}{\Delta\omega_R}$$

---

ormal description (cont'd)

xample

$\hbar\omega_L \approx 2$ eV;

$\Delta\omega_R \approx \Delta\omega_L$ (Number of wiggler periods is ~ number of circles in the laser pulse)

$A_L = 100$ μJ

$K > 1$

$\Delta E \cong 10$ MeV (Confirmed by B. Kincaid in computer simulations)

otice, that:

typical beam energy spread in synchrotron radiation sources is 0.5 - 3 MeV

for a large K energy modulation depends from K very weakly

relatively short straight sections can be used even in high energy rings using wigglers with a large K.

Formal description (cont'd)

II. Intensity of femtosecond x-rays

- Much smaller than usual intensity of synchrotron radiation

Factor I.

- Number of electrons in the bunch is N_b.
- Number of electrons in the slice is $N_b\frac{\tau_S}{\tau_b}$.
- Factor $\eta\approx 0.2$ accounts for fraction of electrons in the right phase of the laser wave.
- Thus, number of electrons producing femtosecond pulses is $\sim\eta N_b\frac{\tau_S}{\tau_b}$. This is at least 1000 times less than N_b.

Formal description (cont'd)

Factor II.

Frequency of the femtosecond pulses is much smaller than a bunch repetition frequency.

- Limited by the available laser power P_L

  Than x-ray flux per unit of the azimuthal angle is :

$$\frac{dF(\lambda)}{d\theta}=\frac{\sqrt{3}}{2\pi}\alpha\gamma\frac{I}{n_b e}\eta\frac{\tau_S}{\tau_b}\frac{P_L}{f_0 A_L}S\left(\frac{\lambda_c}{\lambda}\right)\frac{\Delta\lambda}{\lambda}$$

- Or limited by the effect of energy modulation

$$\frac{d\sigma_e^2}{dt}+\frac{\sigma_e^2}{\tau_D}=(quant.fluct.)+(energy\ \ \mathrm{mod}ulation)=$$

$$=\frac{\sigma_{e0}^2}{\tau_D}+\frac{\Delta E^2}{2}\frac{\tau_S}{\tau_b}\frac{f_L}{n_b}$$

ormal description (cont'd)

Assuming:

$$\frac{\sigma_{e0}^2}{\tau_D}=\frac{\Delta E^2}{2}\frac{\tau_S}{\tau_b}\frac{f_L}{n_b} \qquad \left(\sigma_e=\sqrt{2}\sigma_{e0}\right)$$

We get:

$$\frac{dF(\lambda)}{d\theta}=\frac{\sqrt{3}}{2\pi}\alpha\gamma\frac{\eta I}{ef_0\tau_D}\left(\frac{\sigma_e}{\Delta E}\right)^2 S\left(\frac{\lambda_c}{\lambda}\right)\frac{\Delta\lambda}{\lambda}$$

III. Pulse duration

e minimum duration of the x-ray pulses is defined by:

- the laser pulse shape
- stretching of the electron bunch slice on the way from the wiggler to the nding magnet.

---

ormal description (cont'd)

ce stretching is related to the non-isochronisity of the beamline and can be aracterized by the differences of the pathlengths of electron trajectories:

$$\Delta\ell=\left[I_U^2\sigma_x^2+I_V^2\sigma_{x'}^2+I_D^2\sigma_e^2\right]^{1/2} \qquad \left(\Delta\ell=\int\frac{x(z)}{\rho}dz\right)$$

ere

$$I_U=\int_0^\ell\frac{U(z)}{\rho}dz,\quad I_V=\int_0^\ell\frac{V(z)}{\rho}dz,\quad I_D=\int_0^\ell\frac{D(z)}{\rho}dz,$$

three integrals I_U, I_V, I_D can vanish simultaneously only if taken over the hromat lattice . But the lattice from the interaction region to the bending magnet n not be the achromat, since a non-zero dispersion in the bend is the integral rt of the method. In a non-achromat lattice either I_U or I_V will be non-zero and associated pathlength difference can be estimated as:

$$\Delta\ell=\frac{\varepsilon_x}{\sigma_e}$$

ere ε_x is the horizontal beam emittance.

Formal description (cont'd)

- Signal to noise ratio

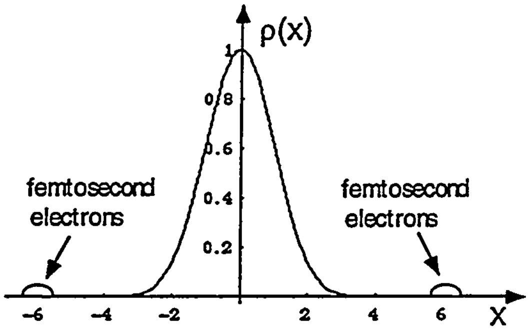

For one bunch signal-to-noise ratio is:

$$R=\frac{2\eta\tau_s}{\tau_b}\left[\phi\left(\frac{D_x\Delta E}{\sigma_x}+\frac{1}{2}\right)-\phi\left(\frac{D_x\Delta E}{\sigma_x}-\frac{1}{2}\right)\right]$$

ϕ is the error finction.

Formal description (cont'd)

- Theoretical assumption on particle density distribution in the beam

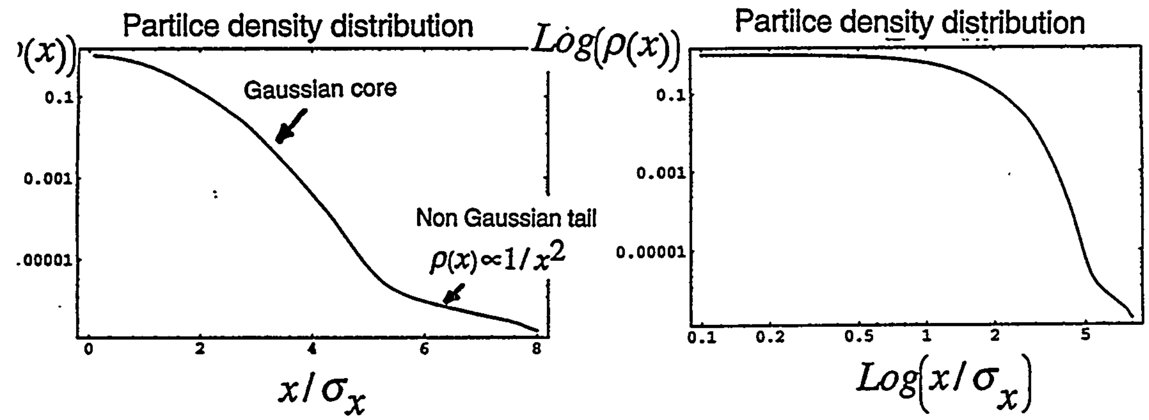

ormal description (cont'd)

Measurement at the ALS:

Beam life time versus horizontal scrapper position

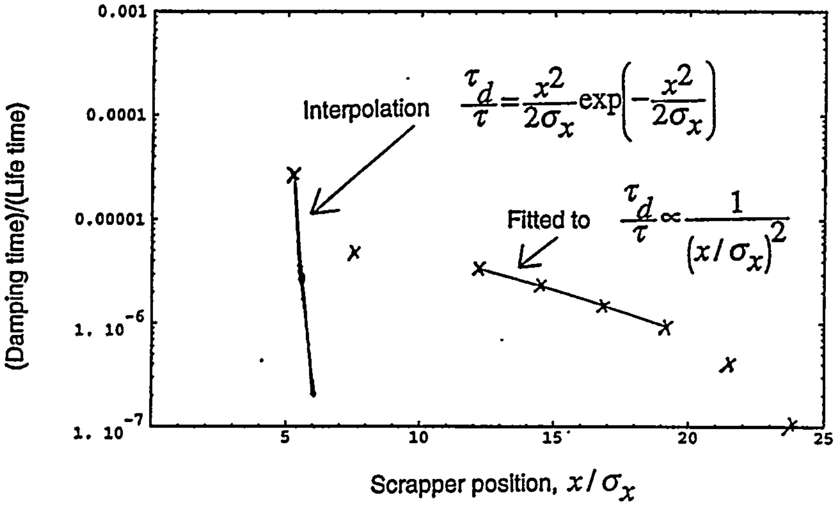

---

ormal description (cont'd)

Since $f_L << f_0$ we need an x-ray chopper in the beamline to avoid unwanted adiation and exposure of samples by the x-rays from unmodulated bunches.

Application to the ALS (cont'd)

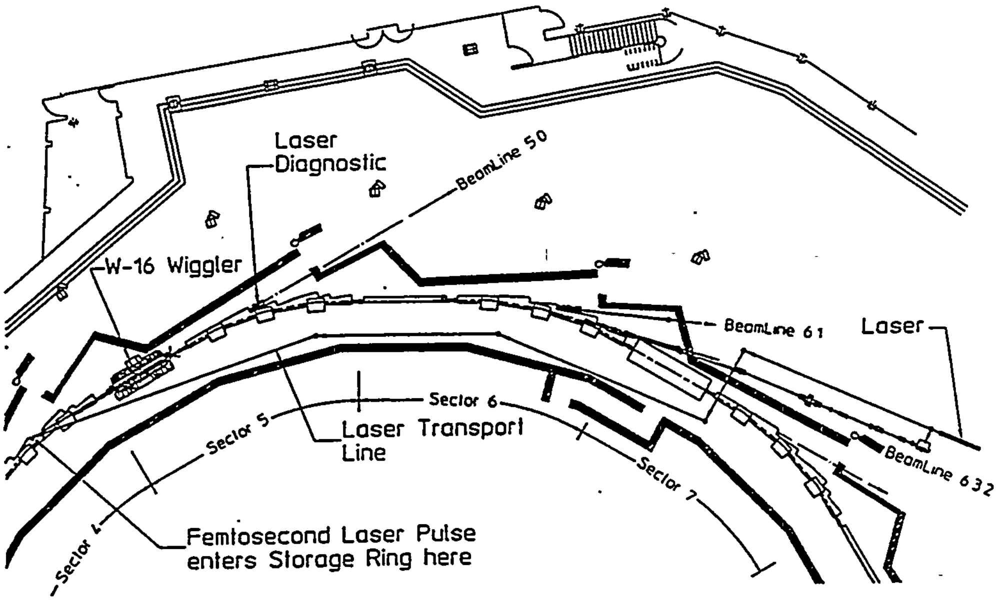

A schematic view of the ALS sectors 5, 6 and 7 showing wiggler, laser and laser beam transport lines.

Diagnostic beamline

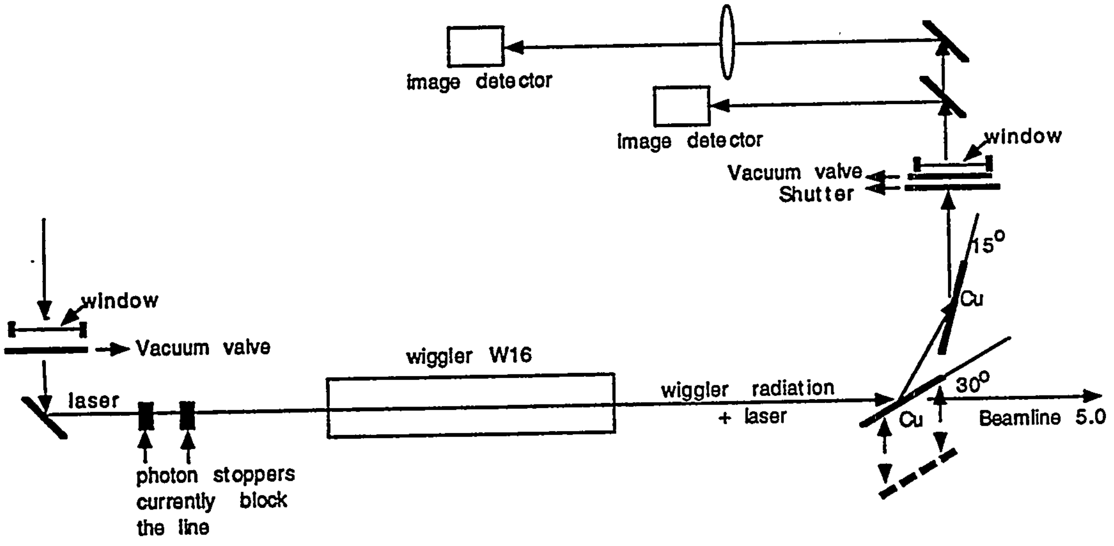

Application to the ALS (cont'd)

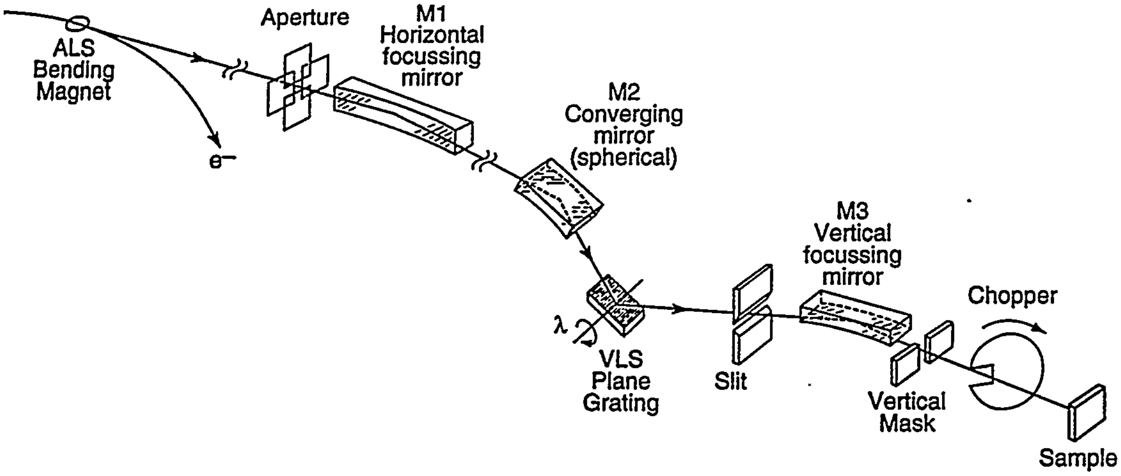

schematic of the beamline 6.3.2; bandwidth of the beamline is 12-200 Å; angular acceptance is 2.5 mrad.

---

pplication to the ALS (cont'd)

Anticipated results:

Estimated x-ray flux for 1.5W of an average power of the laser beam:

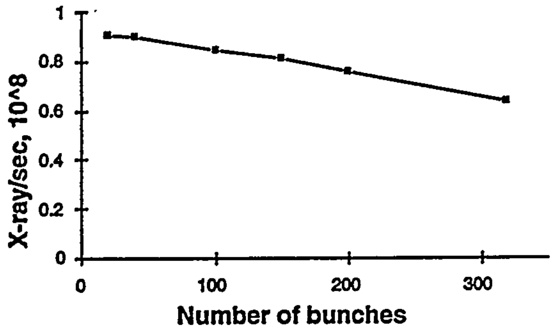

X-ray flux - number of x-ray per second - in 2.5 mrad angle and 10% bandwidth (assumed measured bunch lengthening)

Stretching of the electron beam slice is 250 fs FWHM and overall duration of x-ray pulse is ~ 300 fs FWHM

Pulse duration taken in the sector 5 can be as low as 100 fs FWHM

Signal-to-noise ratio in a single bunch is ~ 10

Perspectives for further development

- **How to get higher flux of x-rays?**

1. More powerful laser

   1.5 W —> ~ 20 W average power <—— factor 15 better

   But, beam energy spread also goes up :

   σ_e —> ~1.5 σ_e

2. LLNL is in the process of development 1kW average power with the pulse duration ~ 50 fs (???).

   Is any way to use such a laser?

A schematic view of the laser
e-beam interaction in two interaction regions

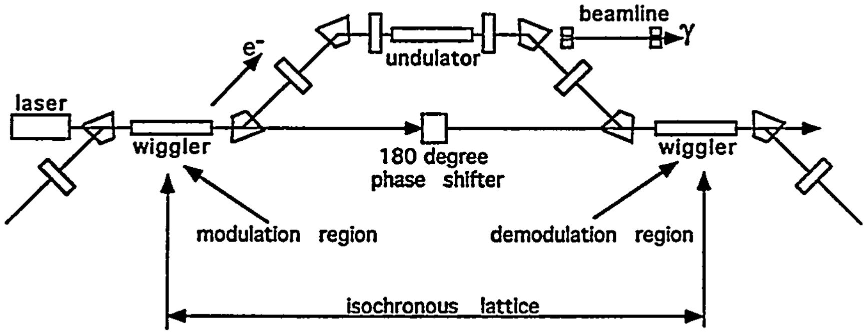

i) Utilization of the laser with 1kW average power gives improvment factor in the x-ray flux ~ 600

ii) Utilization of the undulator instead of the bending magnet gives another factor of 10

Thus, x-ray flux = 6x10^11 (x-rays/sec)

Laser e-beam interaction in two interaction regions
inside optical cavity with a pulse regeneration system

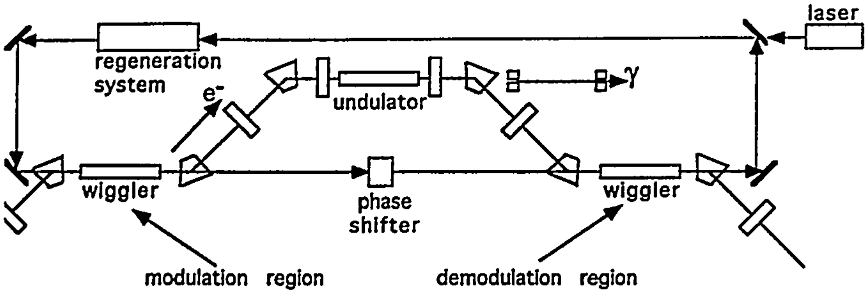

If ~ 100 circles will be possible, then factor 600 can be achieved with the laser with only 10W of average power.

X-ray flux = 10^8 x 600 x 10 = 6x10^11 (x-rays/sec)

ımmary

Modern lasers find more and more applications in accelerators

In the past - advance diagnostics:

a) polarization measurements
b) measurements of small beam sizes - "laser wire"

and:

production of high energy γ via Compton scattering

Today - shaping the beam in the phase space:

a) optical stochastic cooling
b) femtosecond pulses of synchrotron radiation

In the future - particle acceleration (?)

ADVANCED LINEAR ACCELERATOR DEVELOPMENT FOR LINAC RING COLLIDERS

D. C. Cline, UCLA

Aug 23, 96

Advanced Linac's for UCSB - ITP

Linac - Ring Colliders

David B Cline

Center for Advanced Accel

UCLA

1) Linac Ring Colliders - A Brief History

- Some examples of studies in the Past

2) Prospects for High Luminosity in a L-R Collider - Some problems with Linac Fluctuations

3) Possible application for an Asymmetric φ Factory - Some Scientific Goals

4) A High Luminosity L-R Collider Concept

   A) The Compact Superconducting Storage Ring

   B) TESLA Linac - As an Example

Summary

A High Luminosity, Asymmetric φ Factory Using a Superconducting e^+ Storage Ring and an e^- Tesla Linac Collider

by

David B. Cline,[1] Alper Garren,[1,2] Mike Green,[2] and James Rosenzweig[1]

[1]Center for Advanced Accelerators
Box 951547
University of California Los Angeles
Los Angeles, CA 90095-1547 USA

[2]Lawrence Berkeley National Laboratory
1 Cyclotron Road
Berkeley, CA 94720 USA

ABSTRACT

The search for the origin of CP violation in the $K^0/\bar{K}^0$ system and for CPT violation is best carried out using a φ factory that can also be used to tag the strangeness of the $K^0/\bar{K}^0$ system. We describe an asymmetric φ factory with these properties. We also show how a very high luminosity can be achieved using a powerful tesla e^- linac and a high current e^+ storage ring.

WORK IN PROGRESS
FOR
LAKE TAHOE MTG

Advanced Linacs — why

Not only useful for Linear Colliders at High Energy

1) Medical Accelerators / X Rays

2) Light Source etc / FEL's ...

3) Novel Flavor Factories — (this talk)

— Linac Ring Colliders should be studied in this regard —

Long ago we showed that Linac – Linac Colliders are not useful for Flavor Factories due to the "e^+ currents" in such machines —

However Linac – Ring Colliders can be useful since the e^+ are conserved in the storage ring —

CONCEPT OF A LINAC RING COLLIDER

— Early work J Rees et al —

ORIGINAL CONCEPT

—

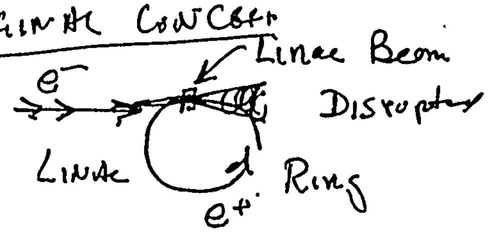

e^+ only partially disrupted

— If the e^- beam could have the same rep. rate and $f_{\text{storage ring}}$

AND

A Powerful Pinch at IP to Increase Beam - Beam Density

— HIGH LUMINOSITY MAY RESULT

Some References to
Linac Ring Colliders and
Quasi Linear Colliders

1. John Rees - SLAC 1978 -

2. Colliding a Linear Electron Beam with a Storage Ring *
P. Grosse Weissmann NIM A274, 21 (89)

3. A High Luminosity BB Factory Linear Collider using Positron Recirculation and Recovery
D Cline and C Pellegrini
NIM A 290, 297 (1990

4. Studies of High Luminosity High Disruption Beam - Beam Interaction
J.R. Boyce AIP Book 1992 -

5. On Asymmetric Collision with Large Disruption Parameter S. Hecket, G Kraft et M Free
1990 NIM A295, 286 (90)

6. Studies of a Linac Ring B Factory
B Norum UCLA ABF mtg April 93

7. The Incoherent Beam - Beam Effect in Linac Ring Colliders
C D Johnson SF Accel Conf 1991

8 On the Stability of Linac Ring Colliders
Y Baconnier CERN PS 91 -02

QUASI LINEAR COLLIDER

D. Cline
C. Pellegrini
NIM A290, 297 (1990)

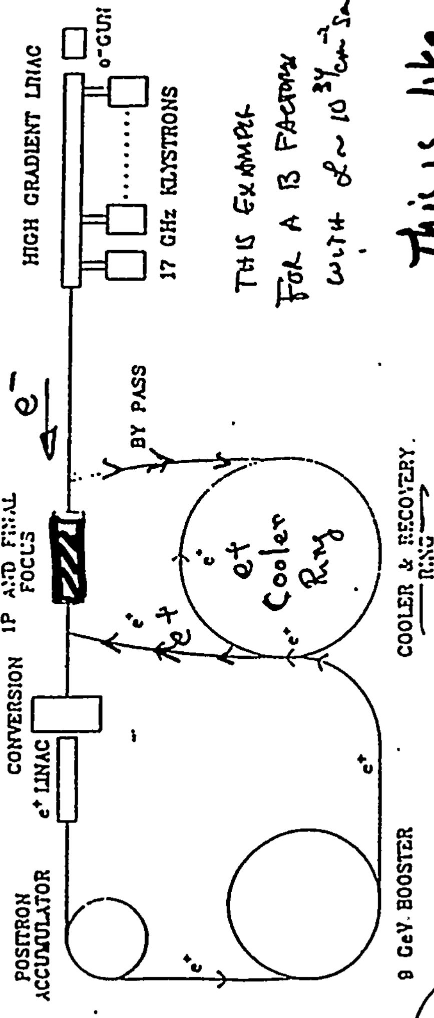

Fig. 1. The proposed scheme.

THIS EXAMPLE
FOR A B FACTORY
WITH $\mathcal{L} \sim 10^{34} cm^{-2} s^{-1}$

This is like
a Linac - Ring
Collider

A VERY
COMPLEX
SCHEME

CONCEPT - RECYCLE e^+ TO DAMP
OUT BEAM BLOW UP DUE TO
INTENSE COLLISIONS AND TO
REPLENISH e^+ SOURCE

Some Early Studies

i) Asymmetric φ Factories

Barletta
Cline
Pellegrini
(ϵ^+ – ϵ^-)
1992.

Nice
EPAC

$\mathcal{L} > 10^{33}$ cm^{-2} sec^{-1}

Quasi Linear
Collider

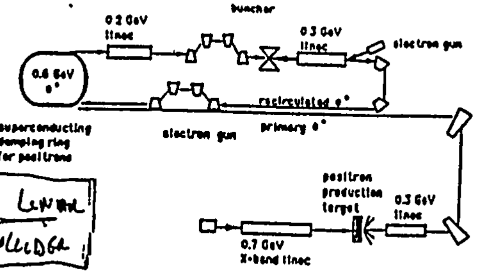

FIG.4. Schematic Asymmetric φ Factory With By-pass (as described in Table 2)

D. Cline & Al Garren

1994
London
EPAC
meeting

Ring – Ring AφF

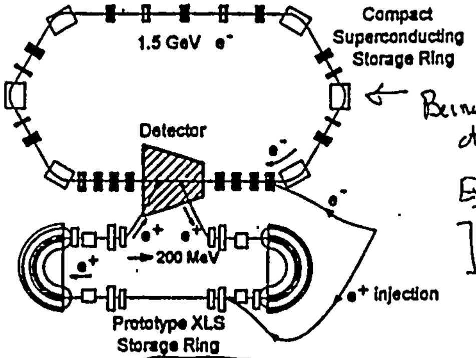

← Being Designed at UCLA

Existing Ring at BNL now

$\mathcal{L} \sim 10^{31}$ cm^{-2} sec^{-1}

Ring x Ring ~~Asymmetric φ Factory~~ Option

Table 2:

Cline, Garren (Gabella)
London EPAC mtg*
1994

		Case				
		1	2	3	4	5
Energy (GeV)	E^-	0.18	0.18	0.18	0.18	0.18
Energy (GeV)	E^+	1.5	1.5	1.5	1.5	1.5
Tuneshift	ξ	0.03	0.03	0.03	0.03	0.03
Bunch spacing (m)	S_B	10	10	10	10	10
Aspect ratio	r	0.04	0.04	0.04	1	1
Beam ratio	b	2	4	2	4	4
Current (mA)	I^+	180	360	402	360	720
Current (mA)	I^-	43	173	96	173	346
β^* values (cm)	β_y^+	2	4	4	8	1.6
	β_y^-	4	16	8	32	6.4
	β_x^+	50	100	100	8	1.6
	β_x^-	100	400	200	32	6.4
Emittances (nm)	ϵ_y^+	14.7	59	33	763	1526
	ϵ_y^-	7.3	15	16	191	382
	ϵ_x^+	367	1468	820	763	1526
	ϵ_x^-	183	367	410	191	382
Luminosity (cm^{-2}s^{-1})	$\mathcal{L}$	10^{31}	10^{31}	10^{31}	10^{31}	$\boxed{10^{32}}$

* Published in Proceedings

LINAC RING COLLIDER

Powerful Pinch!!

e^- Low Energy Lower Current

e^+, High Energy High Current

$$\mathcal{L} = f \frac{N_{e^+} N_{e^-}}{4\pi \sigma_x \sigma_y} H^{\Delta}$$

For extreme Pinch this can be 10!!

$N_{e^+} > N_{e^-}$

J. R. Boyce 2009 CEBAF

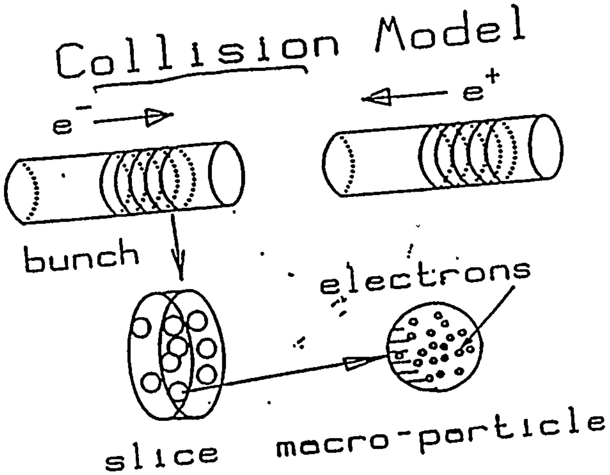

Figure 1. Colliding bunches are divided into slices, with each slice populated with a random distribution of macroparticles containing the charged particles. The overall behavior of the particles in the bunches is approximated by the behavior of the macroparticles.

WHY A LINAC-RING COLLIDER

e^- ~~Disrupted~~ Disrupted Beam Disposed

e^+ Beam Stored

THIS GIVES MORE DEGREES of FREEDOM ON THE COLLIDER

C Johnson CEBAF

$\rightarrow e^-$ $e^+ \leftarrow$

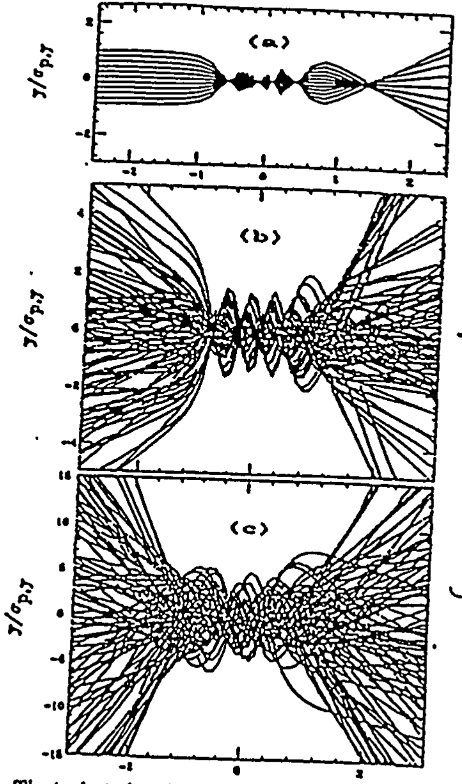

IDEAL CASE

REALISTIC CASE ?

DUE TO e^+e^- PINCH EXTREMELY HIGH DENSITY e^+e^- INTERACTION

⇒ ULTIMATE LUMINOSITY FOR BEAM X BEAM INTERACTION

Figure 2. The trajectories of individual electrons traveling from left to right through a positron bunch are plotted with respect to the center of mass of the positron bunch. The positron bunch extends from -1 to +1 along the abscissa. (a) Individaul electrons with parallel trajectories colliding with a strong positron bunch exhibit localized pinching or foci. (b) Colliding electrons with more realistic pre-collision trajectories also show the pinching effects, though not as strong. (c) Electron trajectories after bunch optics have been "matched" according to the procedure discussed in Ref. 5. The foci have been reduced significantly.

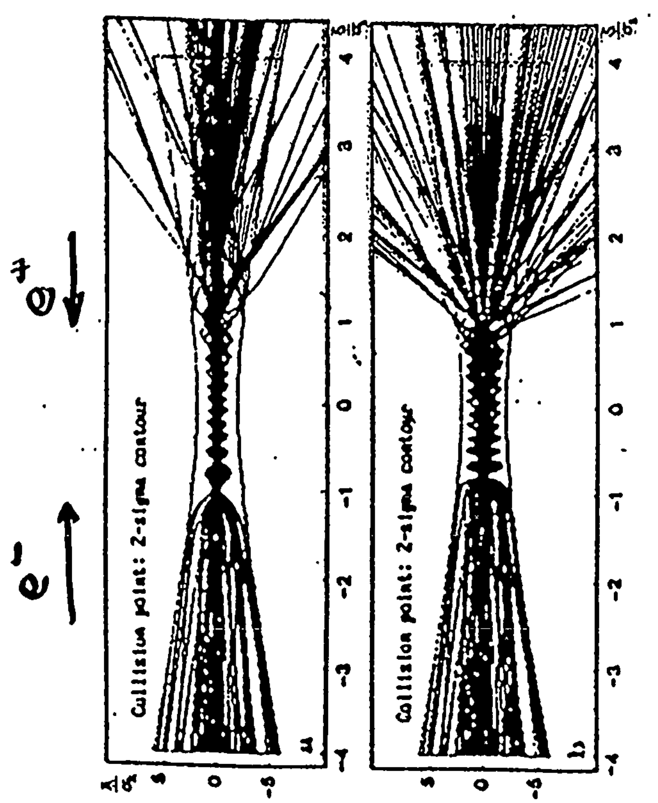

Fig. 1. Electron trajectories at the collision point viewed in the rest frame of the positron bunch with: a) Gaussian, b) parabolic longitudinal distributions.

Boyce
CEBAF

EXTREMELY
STRONG PINCH
ALWAYS
$H \gtrsim 10$

BOOST $\mathcal{L}$ BY
FACTOR OF
10

STABILITY CONDITIONS

Bocconver
CERN Report
PS91-02

1) Jitter in Linac

$$\frac{\delta I}{I} << \frac{1}{4\pi\xi_1}\sqrt{2/T_d}$$

$$\frac{\delta x}{\sigma_x} << \frac{1}{4\pi\xi_1}\sqrt{1/T_{d_x}}$$

$$\frac{\delta s}{\beta^*} << \frac{1}{4\pi\xi_1}\sqrt{\frac{1}{T_{d_E}}}$$

$T_d^{e^+} = f_{rev}\,\tau_x^{e^+}$

$T_d < 10^4$
necessary

ξ_0 - Tune Shift

2) Positron Beam "Cooling"

If $\left[1/\tau_x^{e^+}\right] \sim f^{e^-}_{rep.\,linac}$

The e^+ Bunch "cools" between Interaction

- Thus want $\tau_x^{e^+}$ to be as small as possible - Storage Ring

A SMALL PROBLEM

CEBAF?

Beam Posit

$e^- \rightarrow \leftarrow e^+$

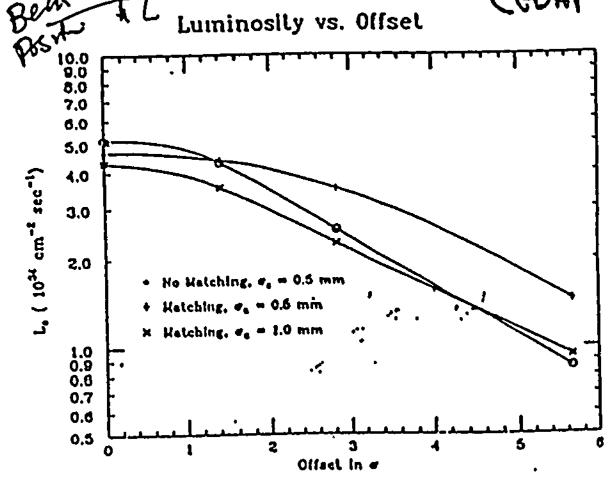

Figure 11. The luminosity of the offset collisions is plotted as a function of offset for three cases: 1) Matching is not applied to the problem; 2) Matching is applied; and 3) Matching is applied and the length of the bunches is increased from the base case of 5 mm to 1.0 mm.

Problem - ~~[illegible]~~ loss of Luminosity Due to small position errors in e^- Linac Beam - **BUT A GENTLE LOSS!**

Solution [Y. Baconnier – CERN PS 91-02]

Strong Damping e^+ Storage Ring

C Johnson

CERN

— UCLA wk 91

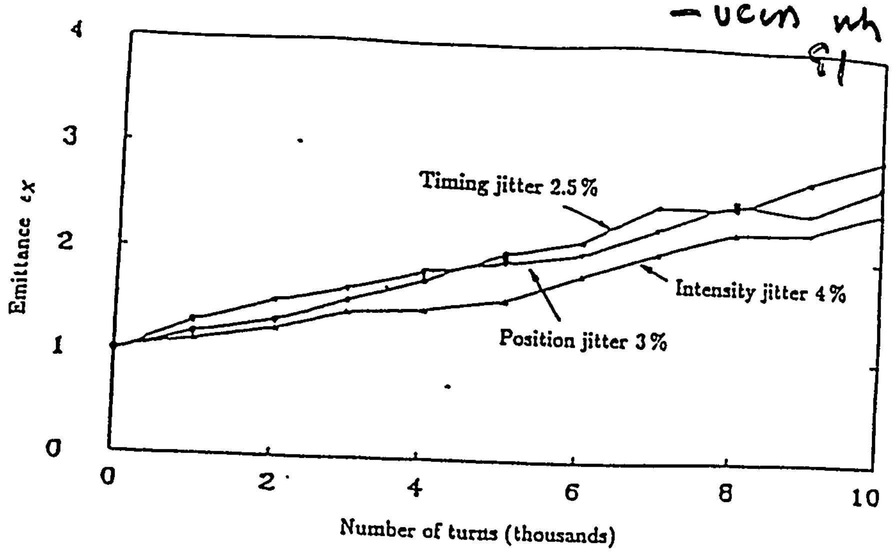

FIG. 8: Fluctuations in intensity timing and position-effect on groups of 100 positrons over 10^4 turns.

C Johnson
CERN

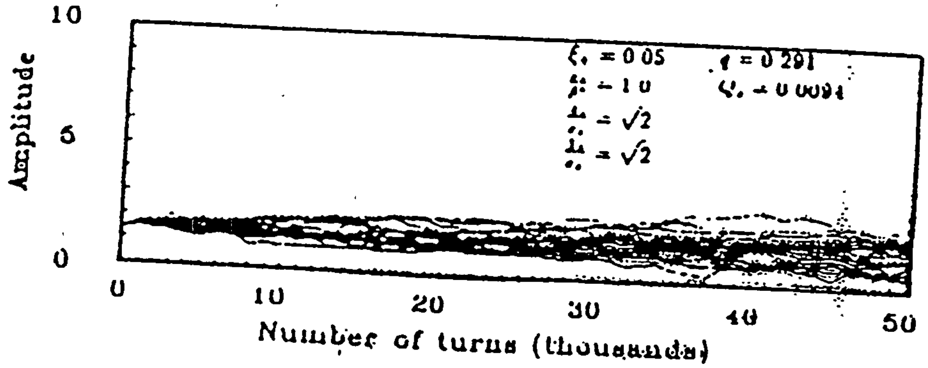

Fig. 8: Multi-turn tracking of individual positrons with simultaneous fluctuations in transverse and longitudinal position and intensity. $(\delta I/I)\text{rms} = 0.005$. $\delta x/\sigma_x = 0.01\sigma_x(\text{rms})$ random walk in X reset at $0.2\sigma_x$. $\delta s/\beta^* = 0.02\beta^*(\text{rms})$ random walk in s reset at $0.5\beta^*$.

$\delta I/I \sim 0.005$

TABLE 2

ADVANTAGES OF AN ASYMMETRIC ϕ FACTORY

UCLA mtg
1992/1993

1) K_S^0 is Boosted $\Rightarrow$ (High Resolution time)

["K_S^0 Beam"]

$\xrightarrow{e^+} \xleftarrow{e^-}$

Energy of $\pi^0\pi^0$ (π^0) increased • Easier Detection of Photon

Boost ϕ

Events folded Forward • Simpler • Smaller Detector

2) Experiments with Regenerators Possible

a) New Tests of Quantum Mechanics — P. Eberhard
b) New Tests of CPT — C. Cline

3) New Experiments Possible where K^0 or $\bar{K}^0$ is Directly Tagged to "Separate Variables" in CPT Tests

(i.e., Sanda ... include $\Delta S = -\Delta Q$ + CP + CPT ...)

[Low Energy K^0, $\bar{K}^0$ Cross Sections Large]

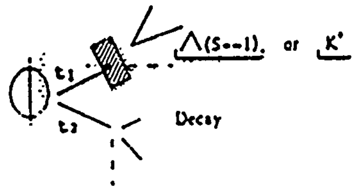

from $t_2 > t_1$ (2) Particle starts out as a a K^0 or $\bar{K}^0$

These are similar to CP LEAR but much cleaner Experiments.

Asymmetric φ Factories

① A NEW CONCEPT FOR AN ASYMMETRIC φ FACTORY TO TEST CPT… D CLINE 1992 (XXVI Int. HEP Conf. Dallas)

② ON AN ASYMMETRIC CORRELATED FLAVOR FACTORY D CLINE, A BODEK, W GABELLA, H KAGEYU KWANG – 1993 IEEE mtg – SP.

③ TESTS OF NON LOCAL INTERFERENCE … at ASYMMETRIC φ FACTORY (1993) P. Eberhard LBL-33937

④ ASYMMETRIC φ FACTORIES… P. Eberhard and S. Chattopadhyay LBNL Preprint 1993

⑤ ~~THESE~~ UCLA WORKSHOPS ON ASYMMETRIC φ FACTORY
→ 1992 (Pub. by World Scientific 1994)
→ 1993 (unpublished)

⑥ STUDY OF ASYMMETRIC φ FACTORY OPTIONS 1994 D. Cline and A Garren – London EPAC Conference Proceedings

⑦ ASYMMETRIC φ FACTORIES TO TEST CPT AND QUANTUM MECHANICS 1994 D Cline

⑧ Present status and Planned Measurements at Phi Factories J Thompson. 1994 World Scientific

⑨ A HIGH LUMINOSITY ASYMMETRIC φ FACTORY USING A SUPERCONDUCTING e^+ STORAGE RING, AND AN TESLA e^- LINAC D Cline, A Garren, M. Green, J Rosenzweig 1996 – FOR LAKE TAHOE ADVANCED ACCEL MEETING UCLA CAA

Low Luminosity Tests of
QM AT AφF

P. Eberhard
LBNL
1993
UCLA
Workshop

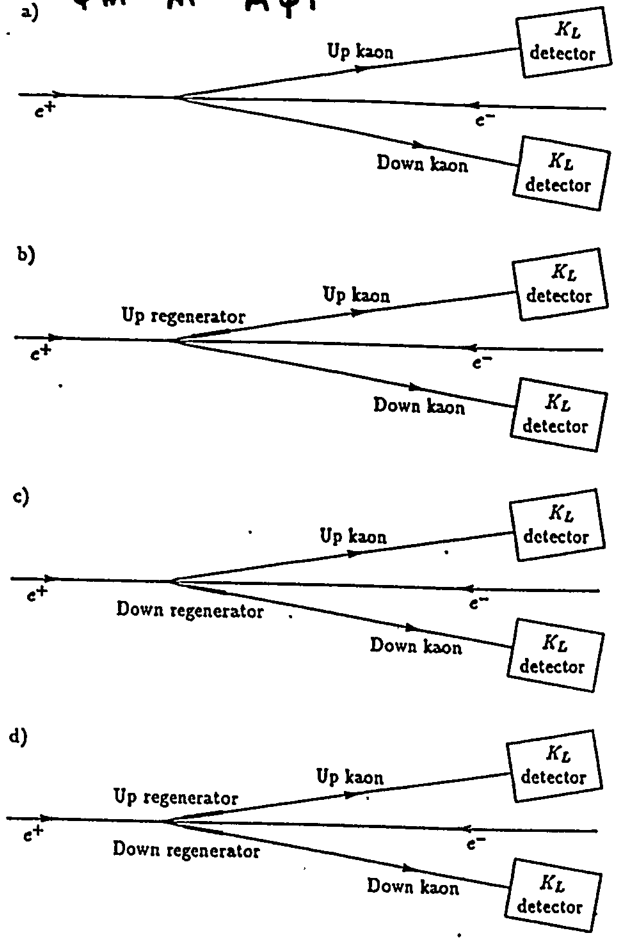

Figure 1: *Setups for the destructive interference test.*

— It would be extremely Interesting to Test QM for C̸P Amplitudes this way —

Factory e^+ energy (GeV)	2.0	3.0	9.0
e^- energy (MeV)	130	90	30
Integrated luminosity/setup (pb^{-1})	150	400	600
# of $K^0\overline{K^0}$ events : N (millions)	200	500	1000
Regenerator material	copper	copper	graphite
"Up" regenerator thickness (mm)	4	4	10
"Down" regenerator thickness (cm)	5	5	15
"Down" regenerator distance (cm)	30	42	140
$\underline{K_LK_L}$ events			
"Up" regenerator : n_{LL}^{up}	1840	1750	1600
"Down" regenerator : n_{LL}^{down}	1100	1290	910
Both regenerators : n_{LL}^{both}	3750	3820	3330

Table 2: *Orthodox predictions for the constructive interference test.*

2510

3330

Interference effect

Never Observed

THE CONCEPT OF A FLAVOR TAG AT AN ASYMMETRIC ϕ FACTORY

KIND OF A MIXTURE OF CPLEAR & ϕ FACTORY

AϕF

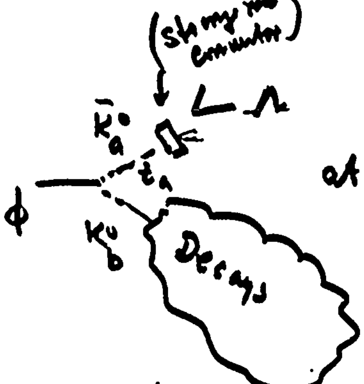

at t_a $\overline{K^0} + N \to \Lambda + K$ is Observed $(S = -1)$

At $t_b = t_a$ the b system must be a K^0 by Bose Einstein Statistics

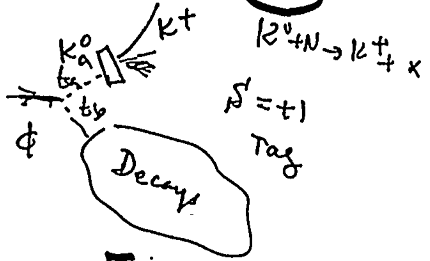

FOR A LUMINOSITY OF $\sim 10^{34}$ cm^{-2} sec^{-1}

AND $\sigma_\phi \sim 4 \mu b \Rightarrow \sim 10^{12} \phi$/year

For a 1% Tag Get

$\Rightarrow 10^{10}$ TAGGED ϕ $K^0/\overline{K^0}$

i) $\phi \gg \bar{K}^\circ_i \bar{K}^\circ_j (t_i = t_j)$; $\bar{K}^\circ_{i,j}, + p \rightarrow \Lambda + \pi^+$ For Flavor I.D. in a c
not need $\Delta S = \Delta Q$ rule for test].] STRANGENESS TAG

ii) $\phi \gg \bar{K}^\circ_i \bar{K}^\circ_j$ $K^\circ_i \rightarrow \pi^+ e^- \bar{\nu}$ $\Delta S = \Delta Q$Rule assumed $t_i = t_j$ Semi leptonic Tag
$K^\circ_j + p \rightarrow \Lambda + \pi^+$(FlavorI.D.) ST

iii) $\phi \gg \bar{K}^\circ_i \bar{K}^\circ_j$ $\pi^+ e^- \bar{\nu}_e$, $\pi^+ e^- \bar{\nu}_e$] Double Semi leptonic Tag
($\Delta S = \Delta Q$) Assumed $t_i \doteq t_j$

(Unique e^- ID using forward C counters and magnetic spectrometer.

iv) $\phi \gg K_i K_j$ (Symmetric or Asymmetric ϕ Factory)

$\hookrightarrow \pi^+ \pi^-$

$\hookrightarrow \pi^+ \pi^-$

$(t_i \doteq t_j)$

(Possible serious background from $\phi \rightarrow K_s K_s \gamma$)

THE NUMBER OF TESTS OF CPT IS LARGER
AT AN AϕF - TWO TYPES OF TAGGING
i) $\bar{K}^0/K^0 \rightarrow \Lambda$ .. K^+ Strangeness
ii) Semi Leptonic + ($\Delta S = \Delta Q$) Rule Tag

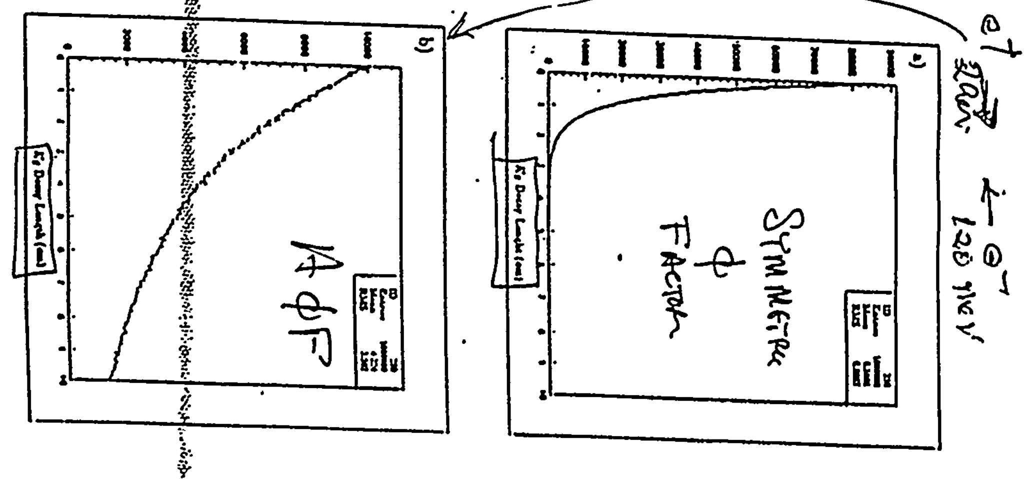

DECAY LENGTH BOOST

— Also 4π Detector

Forward Detector

The Q value for $\phi \rightarrow K\bar{K}$ is small → Lorentz Boost Sweeps $K|\bar{K}$ forward!

FIG 3: a) K_S decay length (cm) for a symmetric ϕ factory; b) K_S decay length (cm) for an asymmetric ϕ factory.

ENERGY BOOST GOOD FOR γ DETECTION

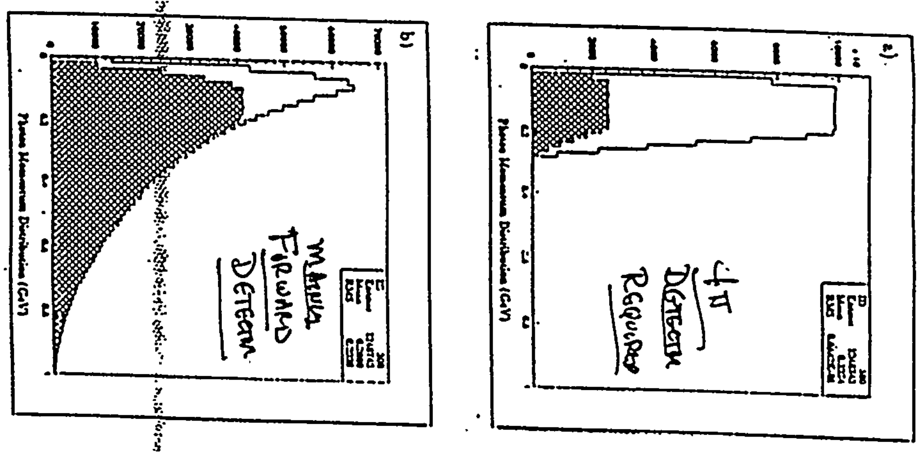

FIG. 4: a) Photon momentum distribution (GeV) for a symmetric ϕ factory; b) Photon momentum distribution (GeV) for an asymmetric ϕ factory. Superimposed in cross-hatch is the distributions for photons that are within the reference calorimeter acceptance.

TYPES OF ASYMMETRIC ϕ FACTORIES

	TYPE		ADVANTAGES		DISADVANTAGES
1)	Low energy e^+ storage ring or accumulator and high energy e^- linac	a)	Rapid damping time of e^+ means reduced instabilities	a)	Need high rep rate – High Energy e^- linac
		b)	Easy to produce low energy e^+ storage ring	b)	High energy linac expensive
2)*	Low energy e^- linac and high energy e^+ storage ring (LINAC - RING COLLIDER)	a)	Low energy super-conducting linac	a)	Expensive e^+ source
		b)	e^- trapped in e^+ bunch	b)	Rapid Damping time of e^+ ring may allow build up of instabilities – Very Important
3)	(e^-) linac or ~~(e^+) linac~~	a)	~~Requires novel e^+ source for e^+ linac~~		Not promising
4)	e^- storage ring on e^+ storage ring	a)	More difficult than a symmetric e^+e^- collider		

OUR GROUP HAS MADE CONCEPTUAL STUDIES OF NEARLY ALL TYPES

USE TWO ADVANCED TECHNOLOGIES TO GIVE $\mathcal{L} \approx 10^{34}$

(Collider and Damper

AφF

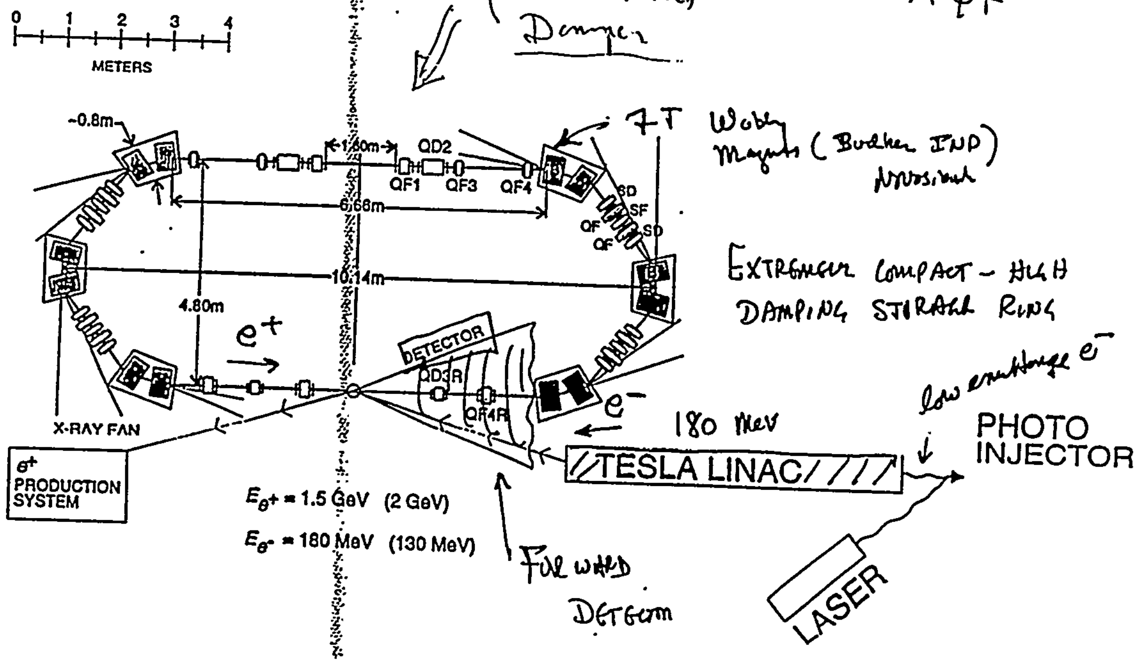

UCLA ULTRA COMPACT LIGHT SOURCE AND ASYMMETRIC ϕ FACTORY

1.5 GeV Superconducting Electron Storage Ring with Conventional Quadrupoles and Sextupoles (Circumference = 26.0 m)

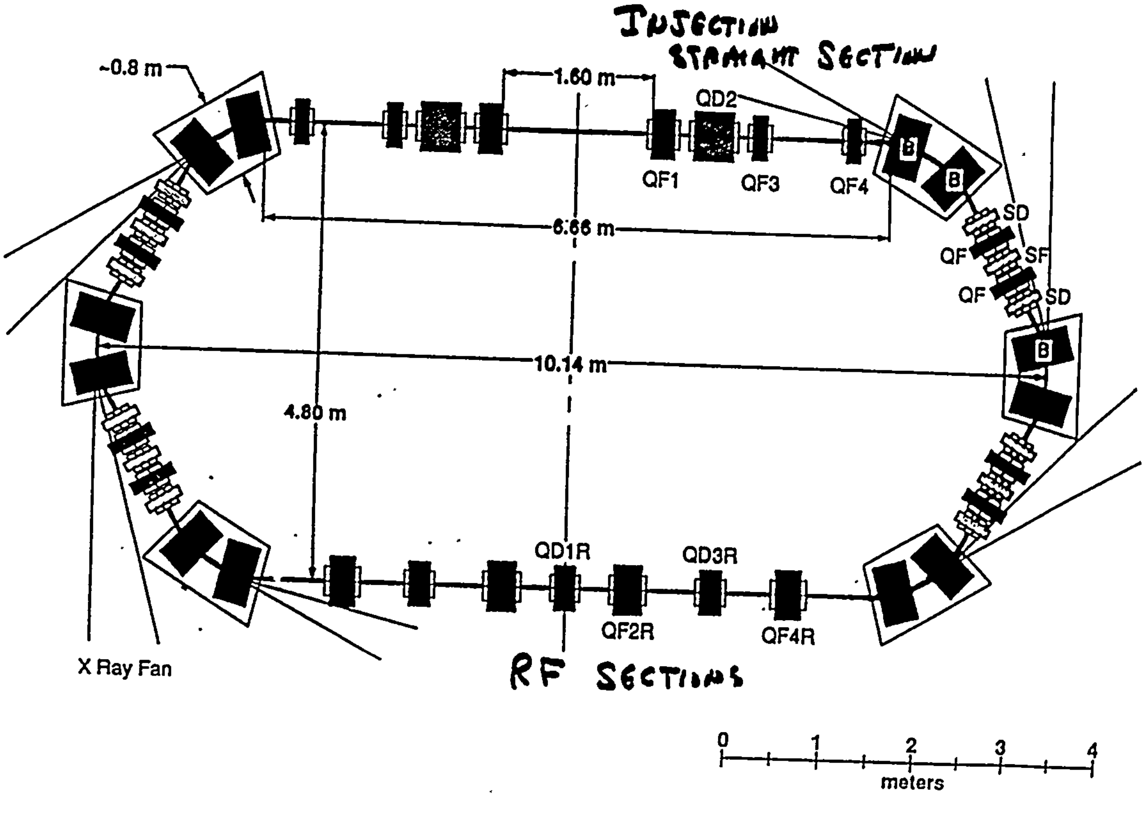

A HIGHLY DAMPED COLLIDER[redacted] RING

Table I Lattice Parameters for the [redacted] Storage Ring

Maximum Stored Beam Energy (Gev)	1.50
Projected Injection Beam Energy (Gev)	0.10
Projected Beam Current (mA)	~200
Circumference (m)	26.0
Bend Radius (m)	0.7257
Dipole Bend Angle (deg)	30.
Integrated Dipole Induction* (T m)	2.6197
Dipole Central Induction (T)	6.894
Dipole Magnetic Length along the Bend (m)	0.380
Critical Energy (keV)	10.3
Horizontal Natural Emittance* (μm)	2.34
Vertical Coupled Emittance* (μm)	1.17
Vertical Operating Emittance*(μm)	0.0234
Horizontal Tune	3.17
Vertical Tune	2.57
Horizontal Chromaticity	-2.22
Vertical Chromaticity	-5.24
Maximum Horizontal Beta Function (m)	3.09
Maximum Vertical Beta Function (m)	6.66
Maximum Dispersion (m)	1.29
Energy Loss per Turn* (MeV/turn)	0.617
RF Voltage (MV)	2.5
RF Frequency (MHz)	499.
Energy Spread (parts in 1000)	1.52
Bunch Length rms* (mm)	30.
Horizontal Damping Time* (ms)	0.412
Vertical Damping Time* (ms)	0.422
Energy Damping Time* (ms)	0.213
Quantum Lifetime (s)	2.2 10^8

* at the maximum design beam energ

Fig. 2 Orbit Functions of the Compact Storage Ring. The solid, dashed, and dot-dashed curves show βx, βy, and η

HIGH DAMPING ALLOWS THE COLLIDER BEAM TO BE RESTORED AFTER LINAC COLLISION

Full Tracking Studies have been done - dynamic Aperture calculated - 2-3D STUDIES OF MAGNET

$\tau_H \sim 400 \mu s$

$\tau_V \sim 420 \mu s$

$\tau_E \sim 213 \mu s$

A Cross-section View at the Center of the 6.9 T Compact Light Source Dipole
(The cryostat vacuum vessel and the beam tube are not shown.)

Initial Concept P. Vobly BINP Russia

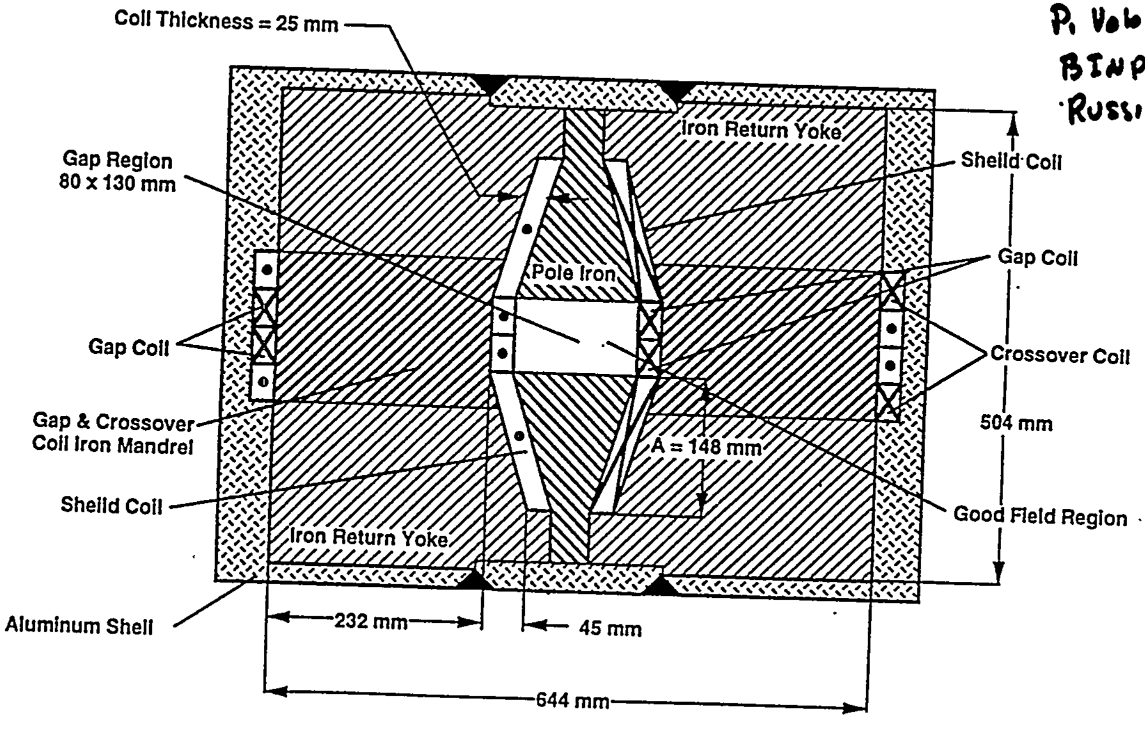

ONE FIFTH SCALE

IRON LENGTH = 376 mm

millimeters 0 100 200 SCALE

LBNL IS BUILDING A C MAGNET FOR ALS NOW!!

DYNAMIC APERATURE

AL GARREN.
LINDSAY
SCHACHINGER

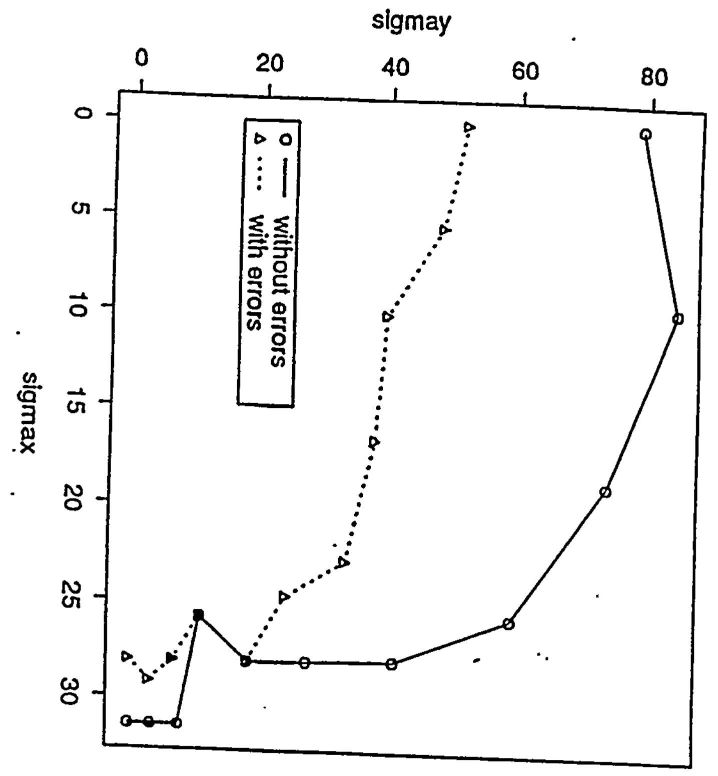

SINCE THIS IS THE MOST COMPACT
1.5 GeV STORAGE RING EVER DESIGNED
THE DYNAMIC APERATURE IS CRUCIAL

Cline
Gomm
Green
Rosenzweig
Linear
Accel.
Requirements

Table 4. Asymmetric ϕ-Factory Linac Calculations

No. of electrons	$N_e = 10^{10}$
Electron avg repetition rate	$f_e = 5 \times 10^5$
No. of positrons	$N_p = 10^{11}$
Positron period	$T_p = 87 \times 10^{-9}$
Positron avg repetition rate*	$f_p = T_p^{-1}$
Electron current	$I_e = 8 \times 10^{-4}$ $(I_e = N_e \times 1.6 \times 10^{-19} \times f_e)$
Duty cycle of electrons	$\eta = 0.044$ ($\eta = f_e/f_p$, 4 × Tesla test facility)
Accelerating gradient in Tesla linac	$E_{acc} = 1.5 \times 10^7$ ev
Electron beam energy (eV)	$E_e = 1.8 \times 10^8$
Active length of linac	$L_{acc} = 12$ m $(L_{acc} = E_e/E_{acc})$
Normalized emittance of electrons	$\epsilon_e = 2 \times 10^{-6}$
Physical electron emittance	$\epsilon = 5.678 \times 10^{-9}$ $(\epsilon = \epsilon_e/\gamma$, where $\gamma = E_e/5.11 \times 10^5)$
Positron energy (eV)	$E_p = 1.5 \times 10^9$
Luminosity (cm^{-2} s^{-1})	$\mathcal{L} = 10^{34}$

*Same as electron avg repetition rate during linac pulse.

Recent CERN Courier UCLA

17 Member

J Rosenzweig

TESLA

Article

TEST

FACILITY

The existence and particularly the experimental verification of a phase transition should be easier to see in larger nuclear systems and/or higher beam energies. The next round is the lead beam experiments which begin at CERN's SPS this year, with a longer term view at Brookhaven's RHIC collider and subsequently the LHC at CERN.

As Ingvar Otterlund pointed out in his opening address, the European Research Conference could also demonstrate the healthy age distribution in the field. Among the 110 participants, almost half of the researchers were still below 35.

From L. Csernai and K.H. Kampert

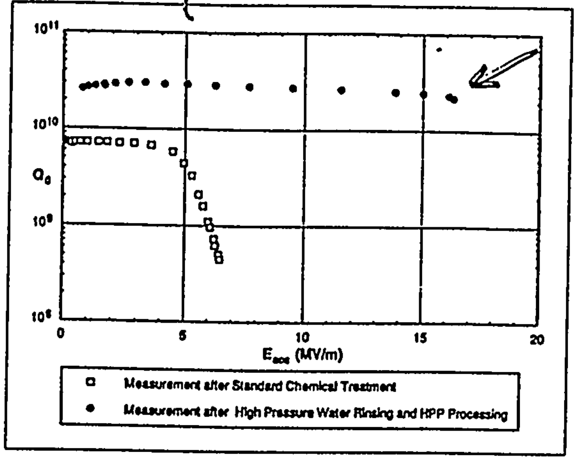

After high pressure water rinsing and high peak power (HPP) radiofrequency treatment at DESY's TESLA Test Facility, promising accelerating fields have been produced by prototype superconducting cavities for a proposed TeV Superconducting Linear Accelerator (TESLA).

Linear Colliders TESLA

The aim of the TESLA (TeV Superconducting Linear Accelerator) collaboration (at present 19 institutions from seven countries) is to establish the technology for a high energy electron-positron linear collider using superconducting radiofrequency cavities to accelerate its beams. Another basic goal is to demonstrate that such a collider can meet its performance goals in a cost effective manner.

For this the TESLA collaboration is preparing a 500 MeV superconducting linear test accelerator at the DESY Laboratory in Hamburg. This TTF (TESLA Test Facility) consists of four cryomodules, each approximately 12 m long and containing eight 9-cell solid niobium cavities operating at a frequency of 1.3 GHz.

The infrastructure to process and test these cavities has already been installed. This heroic work calls for scrupulously clean conditions to avoid contamination which would otherwise mar performance. The facility thus includes a complex of clean rooms, an ultraclean water plant and a chemical etching installation for cavity surface preparation and cavity assembly. To improve the cavity performance a firing procedure at 1500 C in an ultrahigh vacuum furnace is foreseen.

Radiofrequency power will be provided by a 4.5 MW klystron (pulse length 2ms) in connection with a modulator, built by Fermilab. This system is also used for a high peak power radiofrequency treatment (HPP) to further improve cavity performance by eliminating potential sources of field emission. For cavity testing, an existing cryogenic plant has been modified to cool the cavities to 1.8 K and measure them in vertical and horizontal test cryostats, provided by Fermilab and Saclay respectively.

Prototype cavities have been already delivered to DESY and are presently being used to commission the complete infrastructure. First measurements indicate that cavity performance can be drastically improved by advanced surface processing techniques like high pressure water rinsing developed at CERN and high peak power radiofrequency treatment developed at Cornell. Further improvements are expected from high temperature cavity annealing in the UHV furnace. The initial TTF goal is an accelerating field of 15 MV/m at a resonance (Q) value of 3 x 10⁹.

The first series cavities for the TTF arrived in September and initial beam tests of a complete TESLA cryomodule (constructed by INFN Frascati/Milan/Rome) with an injector

TESLA TTF

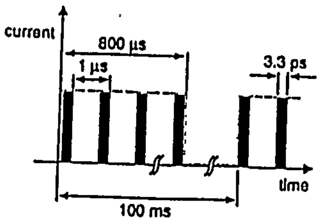

E = 500 - 800 MeV
T = 64 µA
T_{mp} = 8 mA
n_{e^-} = 5 x 10¹⁰ per bunch

Figure 1: TTF linac beam parameters.

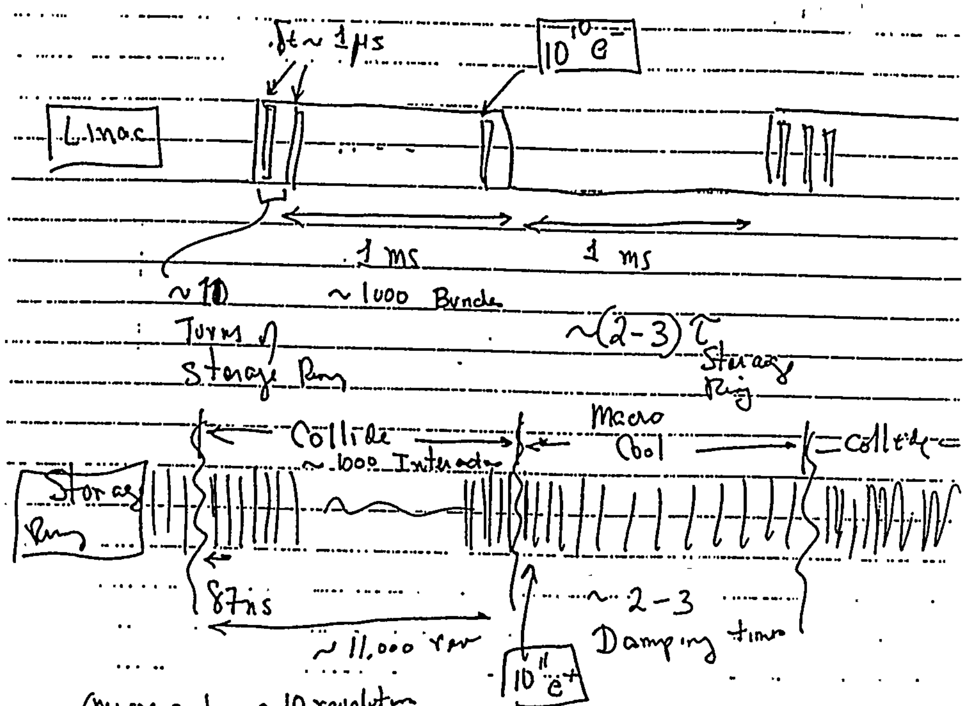

Micro cool ~10 revolution between coll.

Macro cool ~3 Damping Times after 1000 bunch crossings

Conclusions.

1) Advanced Linacs for Particle Physics

- for Linear Colliders
- for Next Generation Flavor Factories (ie Asymmetric Φ, B.. Factories)

Have different requirements on the Linacs

2) The Linac-Ring Collider is a Promising Next Step in Flavor Factories

- Strong Stability Requirements
- e^+ Cooling

$\boxed{\text{COULD GIVE } \mathcal{L} \geq 10\text{x CURRENT FLAVOR FACTORIES}}$

3) Those conditions place Constraints on the Storage Ring (strong damping) and Linac (high Rep Rate, low Emittance etc)

4) We are exploring the TESLA concept for such a collider at UCLA

SUMMARY OF SNOWMASS ACCELERATOR ISSUES

J. Wurtele, UCB

SNOWMASS96 ADVANCED ACCELERATOR WORKING GROUP

Jonathan Wurtele
UCB/LBL

Introduction
Collider design
Plasma Accelerators

Working group leaders--Swapan Chattapadyhay

Something Better Than Linear Accelerators (?)

CASCADED ACCELERATORS

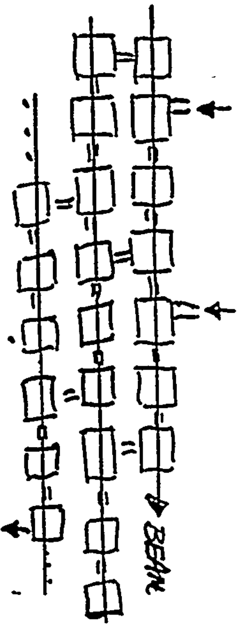

MATRIX-ACCELERATORS

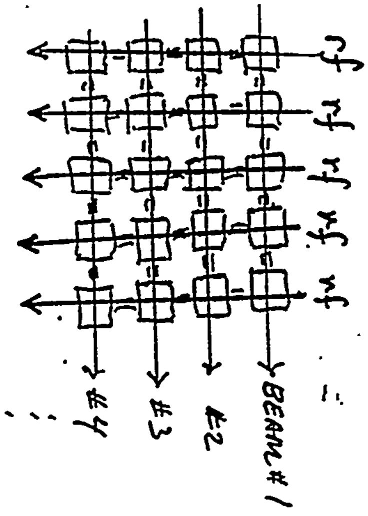

- Allows multiple bunches
- short exposure time for any one cell

Advanced Accelerator Subgroup Charge

- Discuss and evaluate concept for achieving 5 TeV with 10^{35} luminosity
  - Gradient
  - Emittance
  - Efficiency
- Identify promising R&D
  - Power sources
  - Accelerating structures and geometries
  - Instrumentation

GENERAL COMMENT

- SNOWMASS OFFERS THE OPPORTUNITY FOR THE LASER-PLASMA WORKERS TO FAMILIARIZE THEMSELVES WITH LINAC ISSUES AND FOR THE LINAC WORKERS TO BECOME FAMILIAR WITH THE ADVANCES IN EXPERIMENT AND THEORY IN PLASMA-BASED CONCEPTS

Topics

- Lasers
- THz Radiation
- RF sources
- mm wave technology
- microfabrication
- plasma-based devices
- superconductors
- Collider scaling laws
- Beam dynamics
- Laser-plasma dynamics
- New concepts

CURRENT RESEARCH

λ	POTENTIAL GRADIENT	COLLIDER LENGTH	R&D
>10 cm	100 MV/m	60 km	New superconductors
1 cm	200 MV/m	30 km	Power sources
3 mm	1 GV/m	< 10 km	Structures Power sources Fabrication
<300 µm	>10 GV/m	~ km	Channel guiding Staging Beam dynamics

COMMON THEME

HIGH Υ (>0.3)
OR
NEUTRAL BEAMS
OR
GAMMA-GAMMA

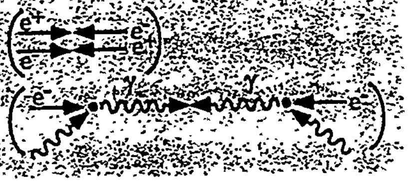

Particle Physics Implications ⟹ Hadronic + EM Backgrounds
<u>and/or</u> uncertain initial state

CLASSICAL COLLIDER PARADIGM

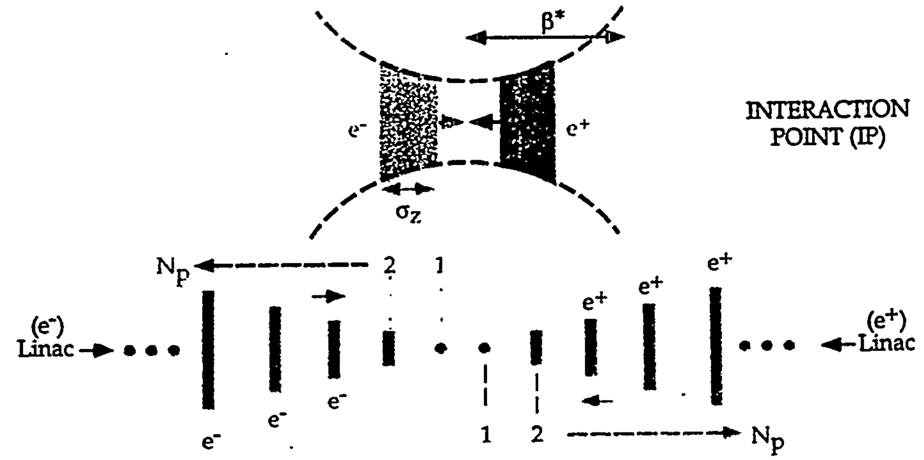

INTERACTION POINT (IP)

LUMINOSITY : $\mathcal{L} = \dfrac{f N^2}{4\pi\sigma_y^2 R}$ $(f = N_p f_{rep})$

AVERAGE POWER : $P_b = 2\gamma mc^2 N f = \eta P_W$

RADIATIVE EFFECTS OF MACROSCOPIC BEAM ELECTROMAGNETIC FIELD

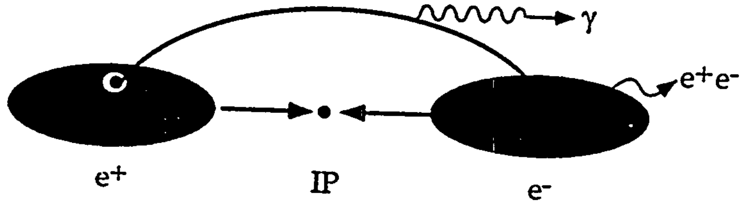

Υ = (Average photon energy) / (Beam particle energy)

δ_B = (Average beam particle energy loss) / (Beam particle energy)

BEAMSTRAHLUNG CONCERNS

If No. of particles / bunch is too large, then pairs are produced
Concern about Electromagnetic and Hadronic Backgrounds;
Large beam energy spread

- Flags for large radiative energy spreads and backgrounds:

  $\Upsilon \gg 0.3$

  $\delta_B > 0.1$

  $n_\gamma \gg 1$

- "CONVENTIONAL WISDOM" IN COLLIDER DESIGNS TO DATE:

  $\boxed{\Upsilon \leq 0.3}$

Example

Assume

$\varepsilon = 1\text{TeV}$
$L = 10^{35}/\text{cm}^2 - 5$
$\delta = 0.1$
$\eta P_W = 0.02\text{GW}$
$\sigma_z = 10\mu\text{m}$

Then

$N = 1.3\text{x}10^7$
$\sigma_y = 2.5\text{x}10^{-9}\text{cm}$
$f = 4.9\text{Mhz}$

Assume

$\lambda_{acc} = \lambda_p = 10\sigma_z$
$E_z = 10\text{GV/m}$
$\beta^* = \sigma_z$

Then

$n_p = 1.1\text{x}10^{17}/\text{cm}^3$
$\frac{\delta r}{r_p} = 10^{16}/\text{cm}^3$
$\varepsilon_N = \gamma\varepsilon = \gamma\sigma_y^2/\beta^* = 1.3\text{x}10^{-10}\text{m}$

SCALINGS

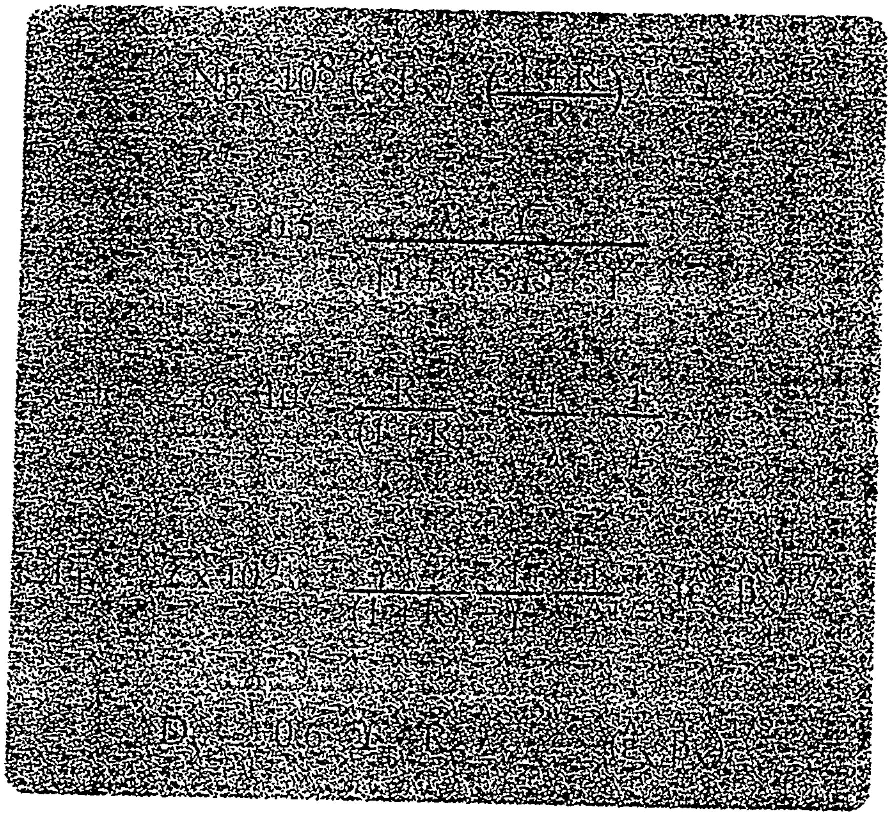

JW/ITP96
8/23/96

AT 5 TeV CENTER-OF-MASS ENERGY WITH A LUMINOSITY 10^{35} $cm^{-2}s^{-1}$, CONVENTIONAL COLLIDER DESIGN CHOICES FOR THE RADIATIVE PARAMETERS LEAD TO UNREALISTIC VALUES FOR CRITICAL COLLIDER PARAMETERS e.g. TOTAL SITE POWER WELL ABOVE A GIGAWATT, etc.

FORCED TO CONSIDER COLLIDERS WITH RADIATIVE PARAMETERS IN THE NONCONVENTIONAL REGIME:

$$\Upsilon > 0.3$$
$$\delta_B > 0.1$$

CHANGE THE PARADIGM:

UNCONVENTIONAL, BUT NOT NEW IDEAS

- GAMMA-GAMMA COLLIDERS (KIM AND XIE TALKS)
- NEUTRALIZE BEAMS AT CROSSING--*STABILITY*

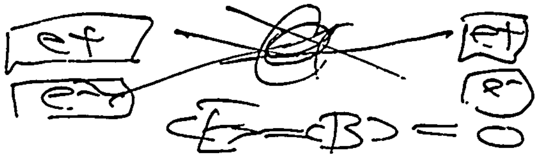

- ACCELERATE WITH HARMONICS---*LARGER SIGMA-Z*
- LOWER LUMINOSITY TO 'DISCOVERY ONLY'--*NEED UPGRADE PATH*
- PLASMA COMPENSATION--BACKGROUNDS

CHANGE OF PARADIGM (cont'd)

- Do nothing: flirt with large δ_B and Υ

$\Rightarrow$ Have to live with collisions potentially not as clean as lower energy e^+e^- colliders, but maybe it will inspire new schemes for detectors and data filtering

Exotic Collisions : Gamma-Gamma Collider

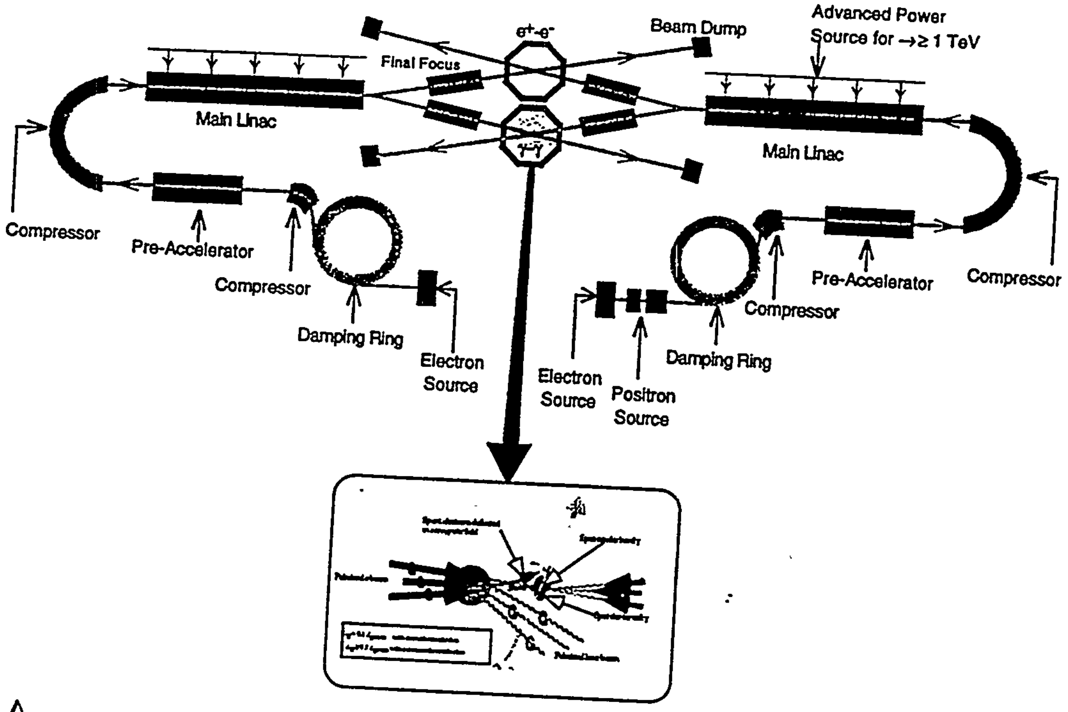

Key Issues

EFFICIENCY

~ Wall Plug ⟹ Laser
Laser ⟹ Plasma
Plasma ⟹ Beam

BEAM QUALITY

Energy Spread
Emittance

ARTIST'S IMPRESSION OF A STAGED LWFA

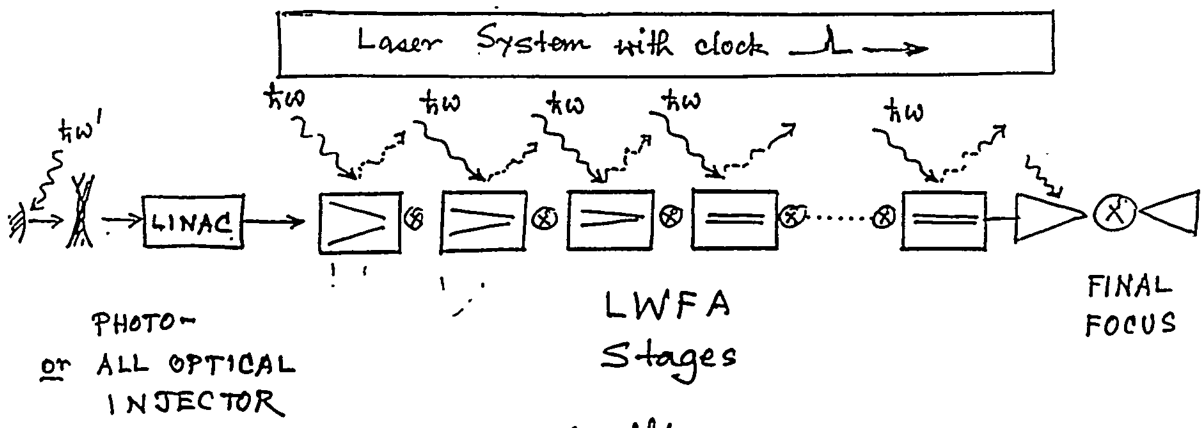

- Optical guiding
- Transverse focussing
- Various channeling and radiation cooling consideration

Laser and plasma parameters vary with distance to accomodate "staging"

Parameters for a 5 TeV LWFA

ϵ_N	10^{-7} mr	10^{-10} mr
R	1.	10^3
N	6×10^8	
δ_B	1	
γ	$\boxed{10^3}$	
D	10	
λ_{acc}	100 μm	
$\sigma_z = \beta^* =$	10 μm	
P_b	5 MW	
f	10 kHz	
$\sigma_\perp^*$	0.4 nm	

Parameters for a 5 TeV LWFA

PLASMA / LASER

$n = 10^{17}/cm^3$

$L \cong 300 Z_R \cong L_{dph.} \cong L_{dep} \sim 1m$

$\delta n \sim 0.3$

$\lambda_{WAKE} = 100 \mu m$

$\lambda = \underline{1 \mu m, 10 TW, 3 J}$

$r_{ch} = 30 \mu m \sim c/\omega_p$

$I_L = 10^{18} W/cm^2$

$E_{acc} = 10 GeV/m$

$\eta_{wake-beam} \sim 30\%$

$\eta_{WALL-LASER} \doteq 50\%$

10 GeV/stage ⇒ 500 stages

$\bar{P} = 500 \times 3J \times 2 \times 10kHz$

$= 30 MW$

Implications

Small σ_y at IP

$\Downarrow$ $\beta^* \cong \sigma_z$

Small ε

$\Downarrow$ Plasma focusing < homogeneous / channel (weaken by factor ω_p / ω_0 – hollow)

Small r_b

$\Downarrow$

$\delta n / n$ (Instabilities of laser and ebeam, Inhomogenerties, Mismatch, ...)

Beam in Plasma

$\varepsilon_N = 1.3\text{x}10^{-10}$

$$k_\beta = \frac{1}{\beta_{P1}(m)} = 7.9\text{x}10^{-2}\sqrt{\frac{E_z(GV/m)}{E(TeV)}\frac{1}{\lambda_p(m)}}$$

$\beta_{P1} = 4\text{cm}$

$\sigma_y{}^{P1} = 2.3\text{x}10^{-7}\text{cm}$

$$k_p\sigma_y \sim 1.6\text{x}10^{-2}\sqrt{\frac{\varepsilon_N(mr)}{E(TeV)E_z(GV/m)\lambda_p^3(m)}}$$

$$\boxed{E_\perp \sim k_p r E_z \Rightarrow E_\perp(\sigma_y)/E_z(0) \approx 1.2\text{x}10^{-4}}$$ @ 1TeV/beam

Problem: (Alignment of Quad ⟷ (stray field in plasma)
At 10^{-4} level codes and theory inadequate

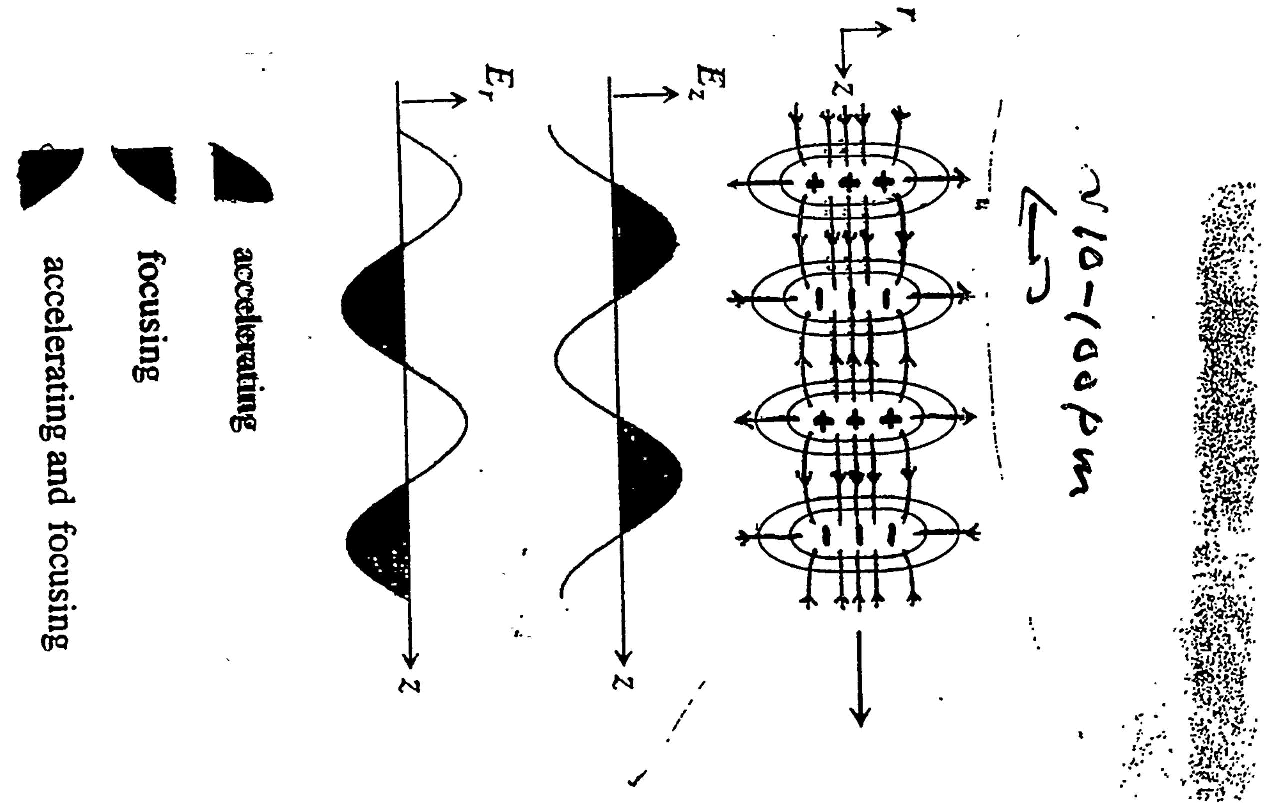

BEAM QUALITY

$\frac{\Delta\gamma}{\gamma}$ ↔ Bunch Length + $E_z(r)$

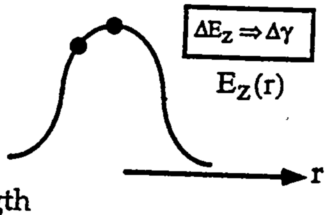

ε → Matched beam, bunch length
Linear focusing, instabilities

DESIRE :

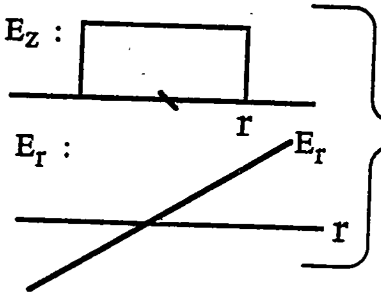

Satisfied by Wake in Hollow Channel to order w_p^2/w_0^2

PLASMA CHANNELS

- OVERCOME DIFFRACTION
- DECOUPLE TRANSVERSE GRADIENT OF LASER FIELD FROM THAT OF THE ACCELERATING WAKE
- WEAKER FOCUSING
- MANY SIMILARITIES BETWEEN LINAC STRUCTURES AND HOLLOW PLASMAS EXIST--THESE NEED TO
- BE QUANTIFIED AND BETTER UNDERSTOOD

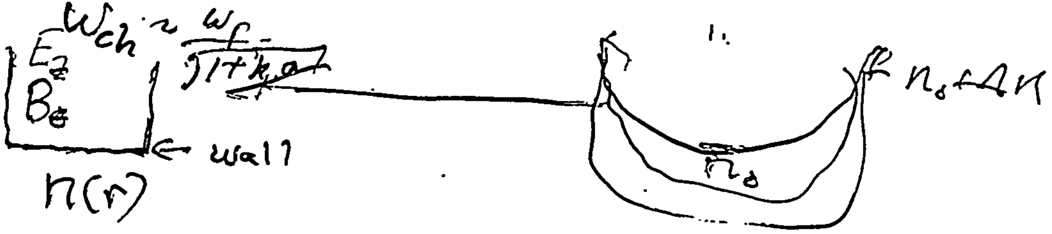

EXAMPLE

Dipole (hose) instability

Displaced Pulse

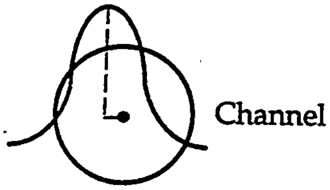

Evolution of centroid of pulse

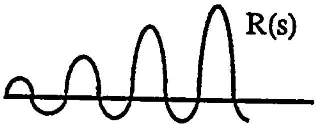

BNS in Laser-Plasma

Laser Hose ↔ E-beam bbu

E-beam : BNS Damping

$k_\beta = k_\beta(\gamma(s))$ Coherent betatron frequency sweep

Laser Plasma : $1/Z_R \leftrightarrow k_\beta$

$Z_R = Z_R(a_o(s), k_o(s))$

- Amplitude sweep $a_o(s)$ occurs naturally from relativistic guiding : $\Delta Z_R/Z_R \sim w^2 k_p^2 \, |a_0|^2/2$
- frequency chirp $k_o(s)$ applied

Criterion : $\Delta(1/Z_R) \sim \pi/L_g$

SUPRESSION

1. BNS METHOD (GS & JW)
2. DETUNED CAVITY METHOD (E.E., PS, JK)
3. LOWER Q ON HOM METHOD (TA, PM)

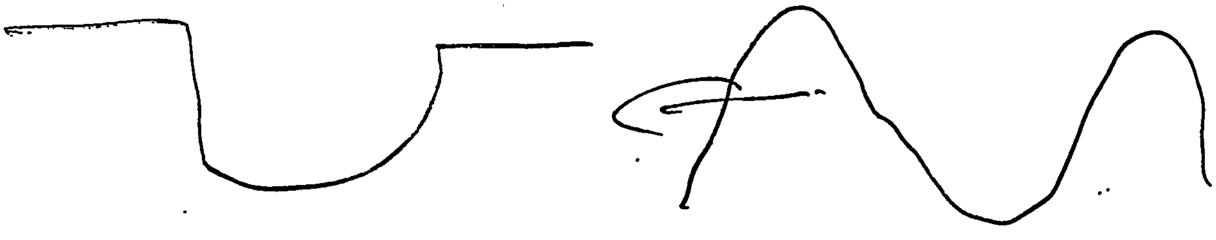

R&D for Laser Acceleration

- Pulse propagation and wake excitation at high power
- Injection and locking
- Wakefield diagnostics
- Laser development
- Acceleration of beam to 1 GeV

$\omega(S), A_O(S)$

$\omega_P(Z)$

LEAKY CHANNEL

EACH PLASMA METHOD IS ANALOGOUS TO ONE USED IN LINACS !

Main Points

1) Much is known about intense short-pulse laser propagation in plasma.

2) Instabilities can exist even for pulses of order λ_p.

3) Plasma is an active non-linear medium — its guiding properties and stability can be changed by the pulse.

4) Detailed understanding developed through experiments and theory is needed.

JW/CBP Seminar
11/17/95/LBNL

WHAT HAS CHANGED ?

- COMPACT HIGH POWER, SHORT PULSE, EFFICIENT LASERS
  DEMONSTRATED : Table Top Terawatt CPA
  solid state lasers : fast moving technology.
  Peak power sufficient. Research on rep. rate
- PHASE, AMPLITUDE AND JITTER CONTROL OF T^3 LASERS
  DEMONSTRATED : Driven by Coherent Control needed for Ultrafast Chemistry
  < 200 fs phase noise. Research on multiple pulses.
- CHANNEL GUIDING DEMONSTRATED : 10^{15} W/cm^2 ~ 70 Raleigh lengths
  Research on wake excitation and guiding at 10^{18} W/cm^2
- MICROFABRICATION (10nm) DEMONSTRATED : (LIGA)
- WAKEFIELD INSTRUMENTATION In progress at SLAC, DESY, KEK, UT Austin
- NEW IDEAS : Neutral Beam Collisions, Beam Combining, Matrixed Linacs :
  Theoretical Work in Progress

JW/ITP96
8/23/96

Conclusion

Second generation experiments and theory will need to address critical physics and technology issues, acceleration of a low energy spread, low emittance bunch with a significant number particles

- the development of diagnostics
- prebunching
- efficient coupling of laser to plasma or structure
- efficient coupling to beam

Other applications, e.g., FEL, medical, synchrotron light/x-ray sources, microslicing of beams in rings may come to fruition before TeV colliders

The realization of a laser-driven device will require innovations, (i.e., suppression of beamstrahlung and high brightness beams) as well as greater understanding and control of the laser-plasma interaction

JW/Laser Accel Wkshp,
LBNL/10/5-6/95

Thursday, August 22, 1996

Convener: D. Rule

Time	Speaker	Title
9:00 am	A. Shchagin, KIPT	Parametric X-ray radiation as Source of Short pulses of X-ray beam
9:30	A. Zholents, LBNL	Generation of Femto-Second X-Ray Pulses at Synchrotron Sources
10:05	Refreshment Break	ITP Front Patio
Convener : K. von Bibber		
10:25	D. C. Cline, UCLA	Advanced Linear Accelerator Development for Linac Ring Colliders
Snowmass 96		
11: 00	J. Wurtele, LBL	Summary of Accelerator Issues
Beam Sources - Status, Advances, and Limitations:		
11:40	K. Leung, LBL	High Current Short Pulse Ion Sources
12:20 pm	Lunch	ITP Front Patio
Convener: B. Zotter		
1:45	R. Macek, LANL	High Intensity Neutron Spallation Sources
Report on New Advances:		
2:25	W. Molzon, UCI	High Intensity Muon Source
3:05	C. Bula, Princeton Univ.	Observation of Nonlinear QED Effects in Electron-Laser Collisions
3:35	Refreshment Break	ITP Front Patio
4:00	M. Ottinger, Univ. Texas	SYN2 - A New Model for Tracking Space Charge Perturbed Snychrotron Beams
4:20	Z. Parsa, C. Pellegrini, A. Sessler, R. Siemann, J. Wurtele, V. Telnov, T .Marshall V. Gorev, R. Macek, K. Leung, D. Cline, A. Skrinsky and others. TBA	Reports* on New Advances and Round Table Discussion on Basic Issues
5:45	Beer and Chips	ITP Front Patio
6:15	Fiesta Barbeque	ITP Front Patio

HIGH CURRENT SHORT PULSE ION SOURCES

K. Leung, LBL

High Current Short Pulse Ion Source

Ka-Ngo Leung
Lawrence Berkeley National Laboratory

Conference on
New Modes of Particle Acceleration Techniques and Sources

August 19-23, 1996

Outline

- Ion-beam requirements for major accelerator facilities
- Generation of pulsed high current positive and negative ion beam
- Short pulse ion beam formation
  - ☞ for compact neutron tube application
  - ☞ for induction linacs
- Formation of high repetitive rate, very short pulse ion beam with laser driven photo-cathodes.

Pulsed-Beam Requirements

Lawrence Berkeley National Laboratory

LANSCE	H^-	17 mA	1 ms	120 Hz
SSC	H^-	30 mA	100 μs	10 Hz
DESY	H^-	20 mA	35 μs	< 1 Hz
Fermi Lab	H^-	50 mA	85 μs	15 Hz
Neutron tubes	D^+	60 μA	< 20 μs	100 Hz
NSNS (1MW)	H^-	35 mA	1 ms	60 Hz
LANSCE (upgrade)	H^-	40 mA	1 ms	120 Hz

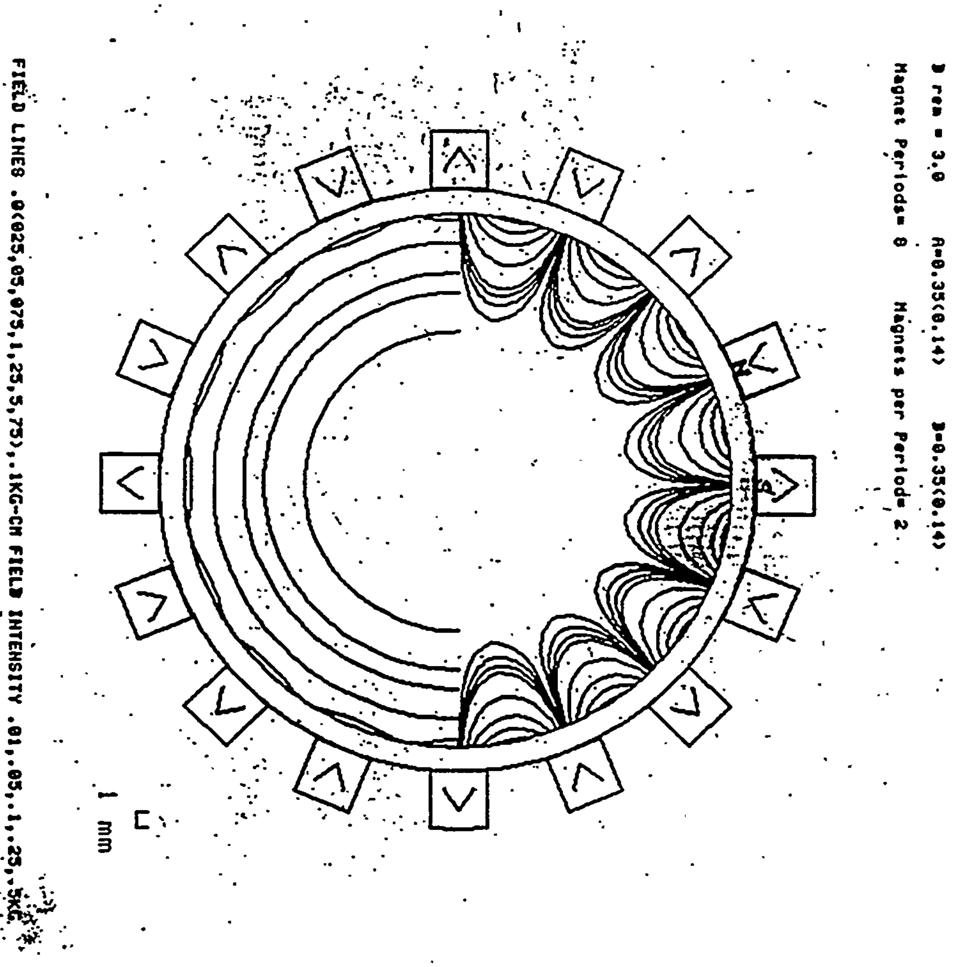

Pulsed Positive Ion Beams

Lawrence Berkeley National Laboratory

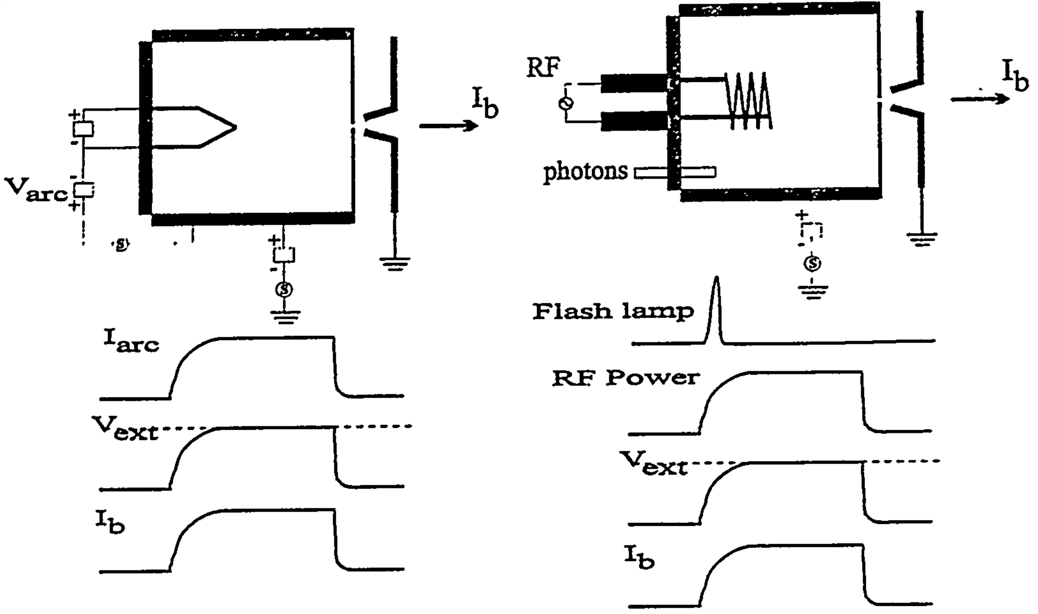

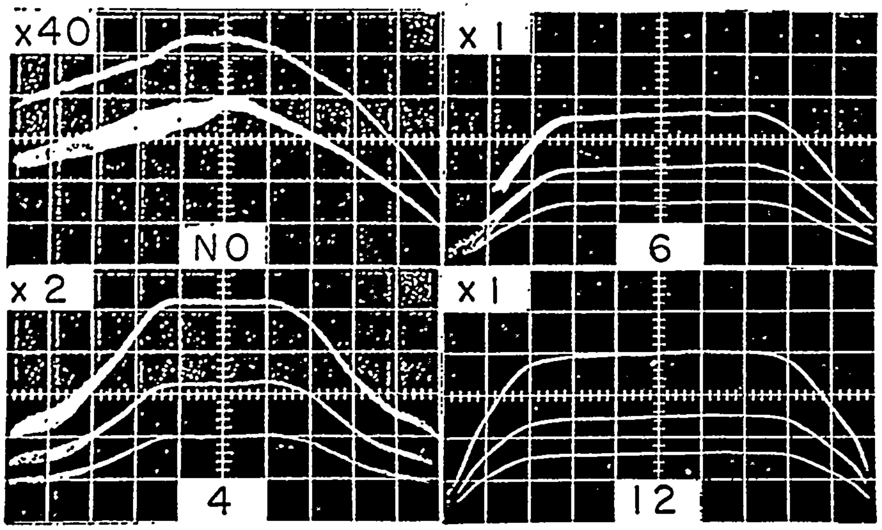

DENSITY PROFILE VS. NO. OF COLUMNS

Fig. 16 Density Profiles

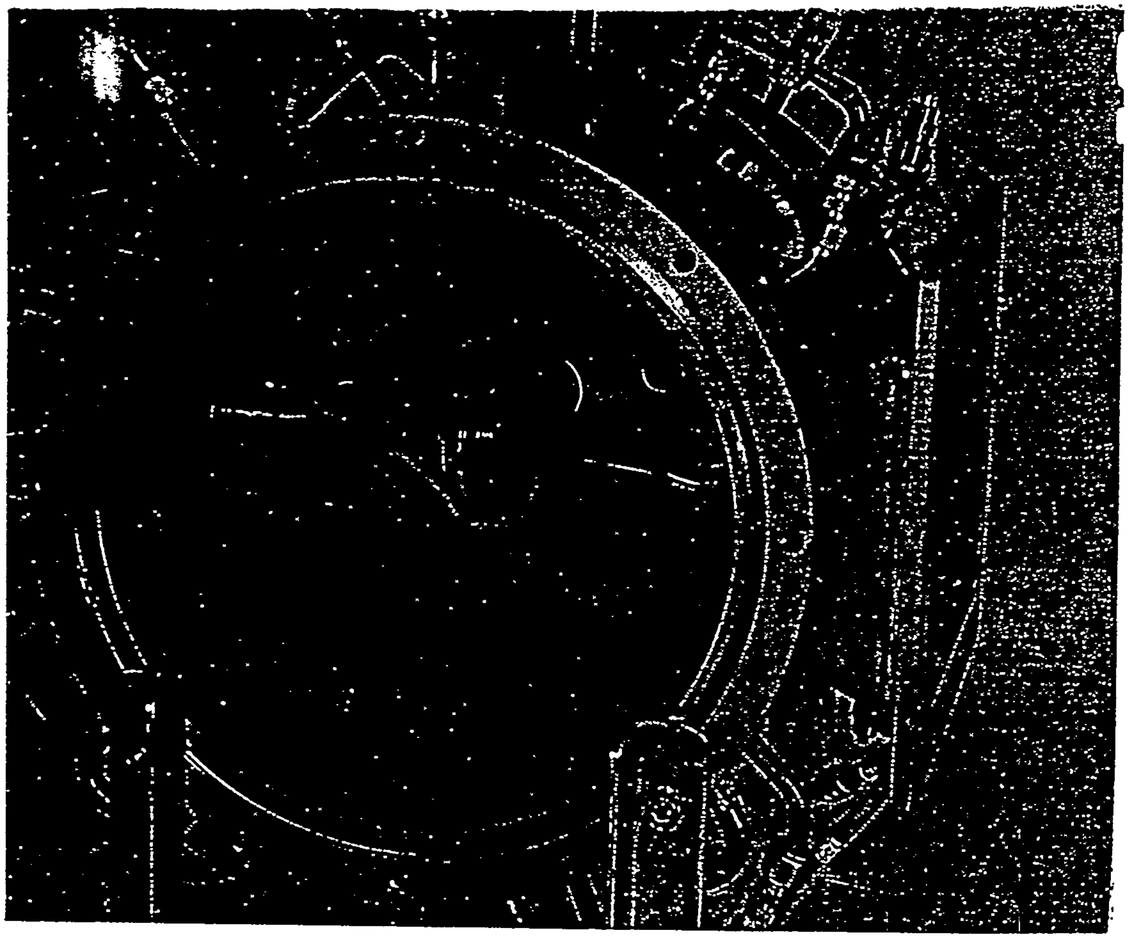

Pulsed Negative Ion Beams

Lawrence Berkeley National Laboratory

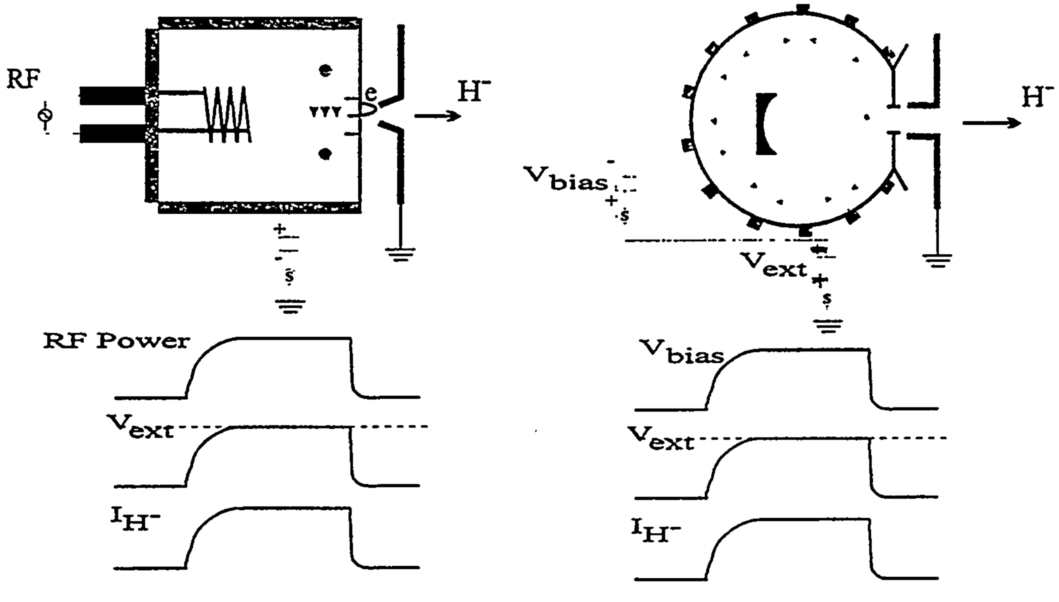

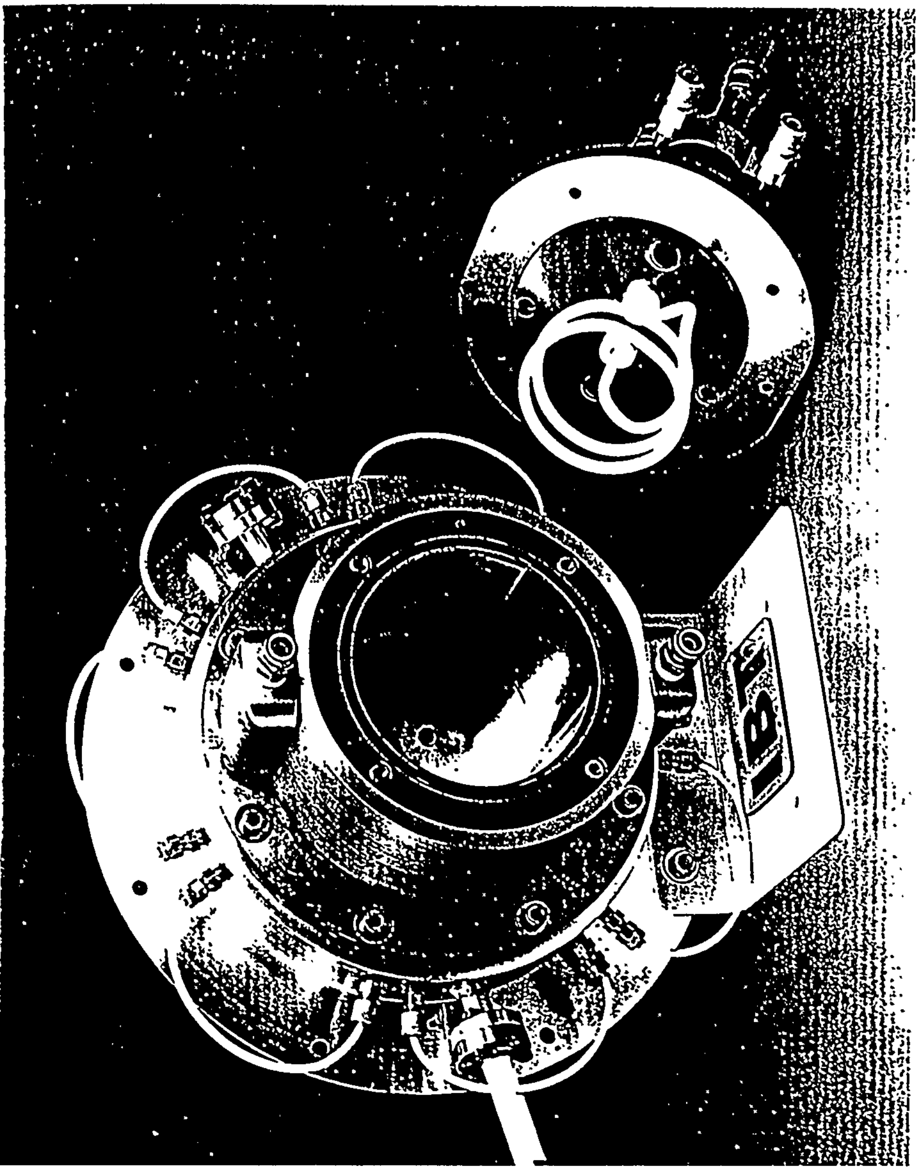

Torrance, Calif 90503 #PV119

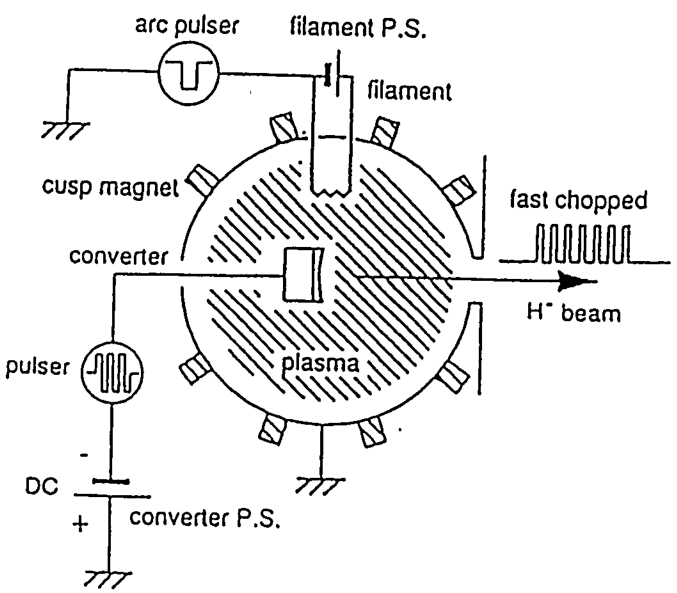

FIG. 1. A scheme of the surface-plasma H$^-$ ion source. The converter voltage is modulated with high voltage pulses triggered by the clock pulses of rf frequency from the booster synchrotron.

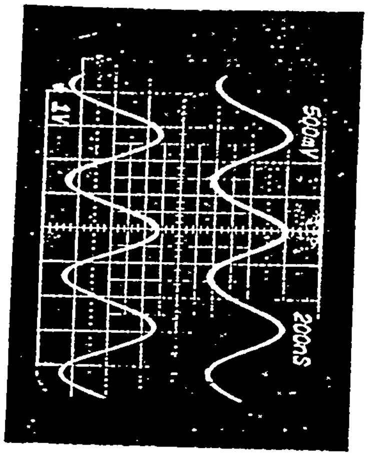

top : rf voltage

bottom : rf current

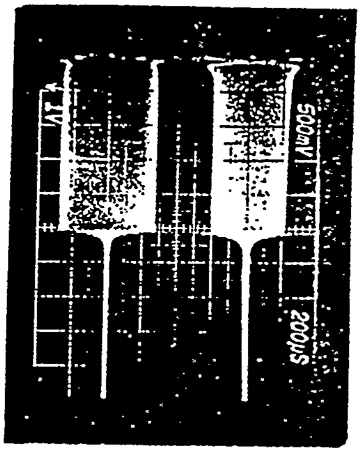

1 ms rf pulse

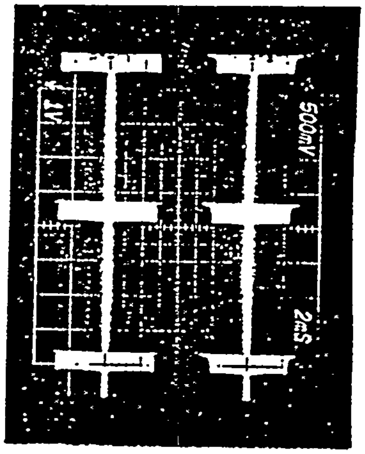

111 rf pulses/sec

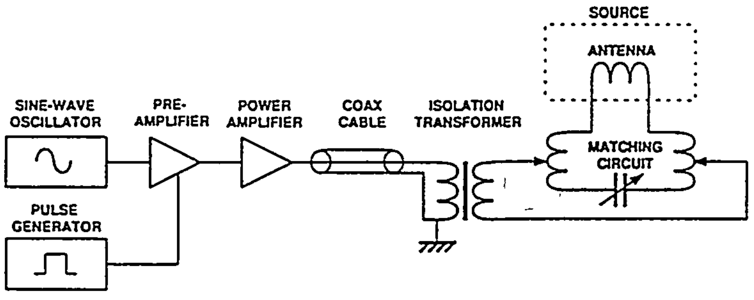

XBL 907-2408

Schematic diagram of the complete rf power system.

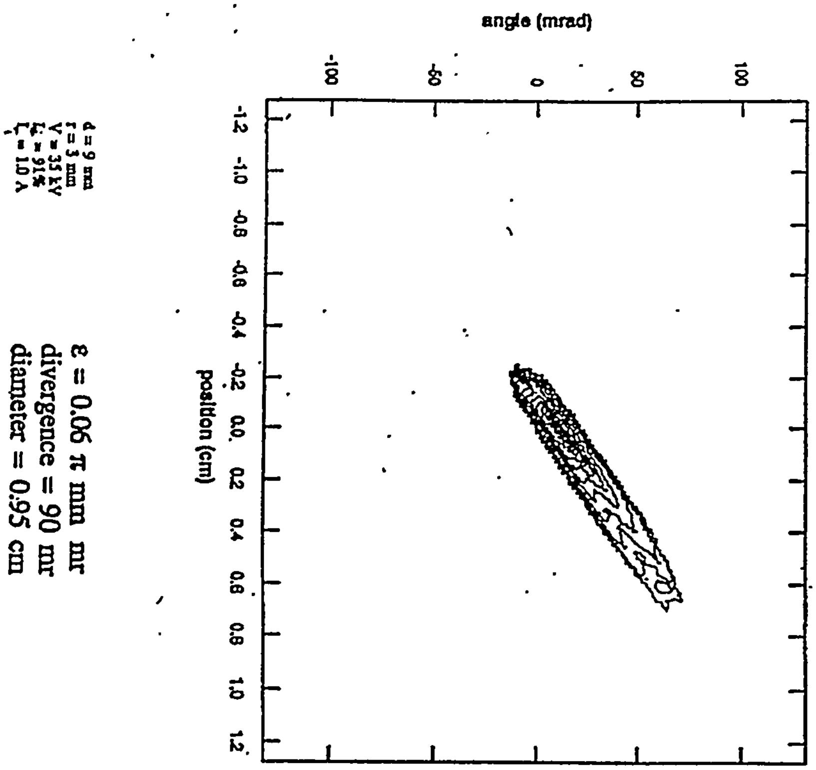
angle (mrad)
-100
-50
0
50
100
position (cm)
-1.2
-1.0
-0.8
-0.6
-0.4
-0.2
0.0
0.2
0.4
0.6
0.8
1.0
1.2
d = 9 mm
r = 3 mm
V = 35 kV
L = 91%
I = 1.0 A
ε = 0.06 π mm mr
divergence = 90 mr
diameter = 0.95 cm

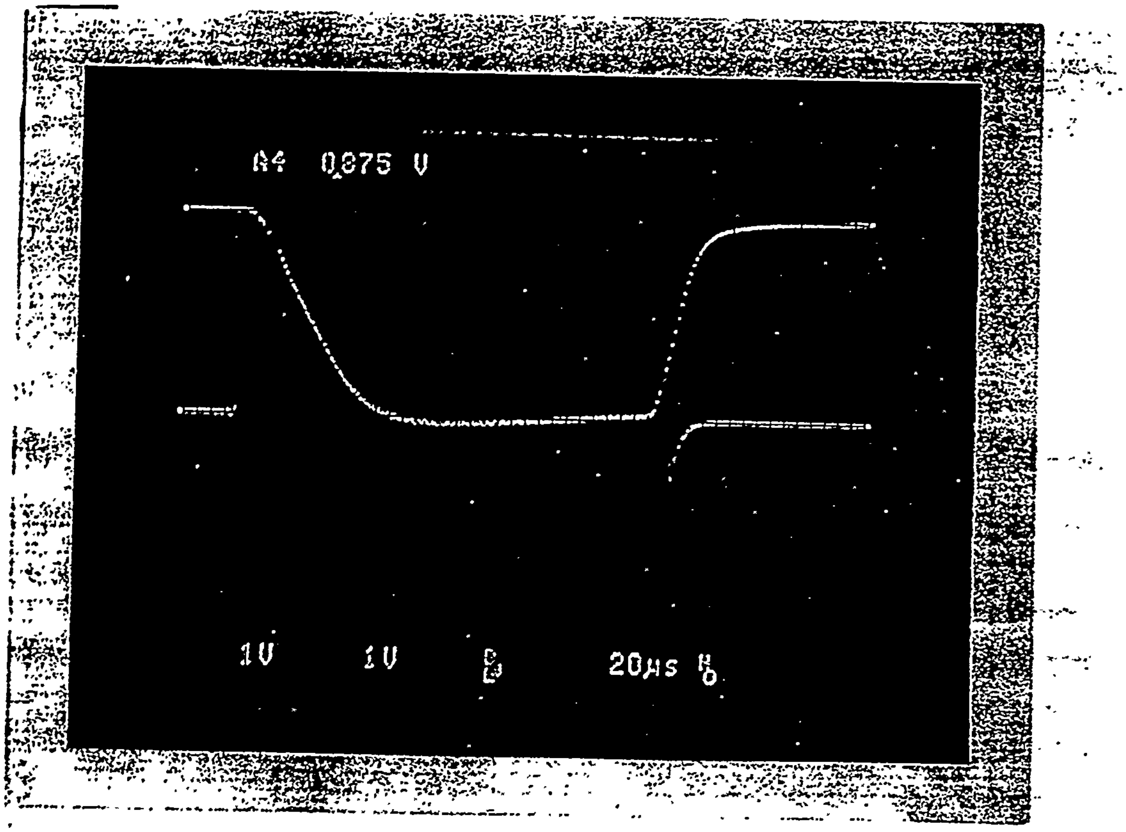
A4 0.875 V
1V
1V
20μs

Cesium Dispensing System

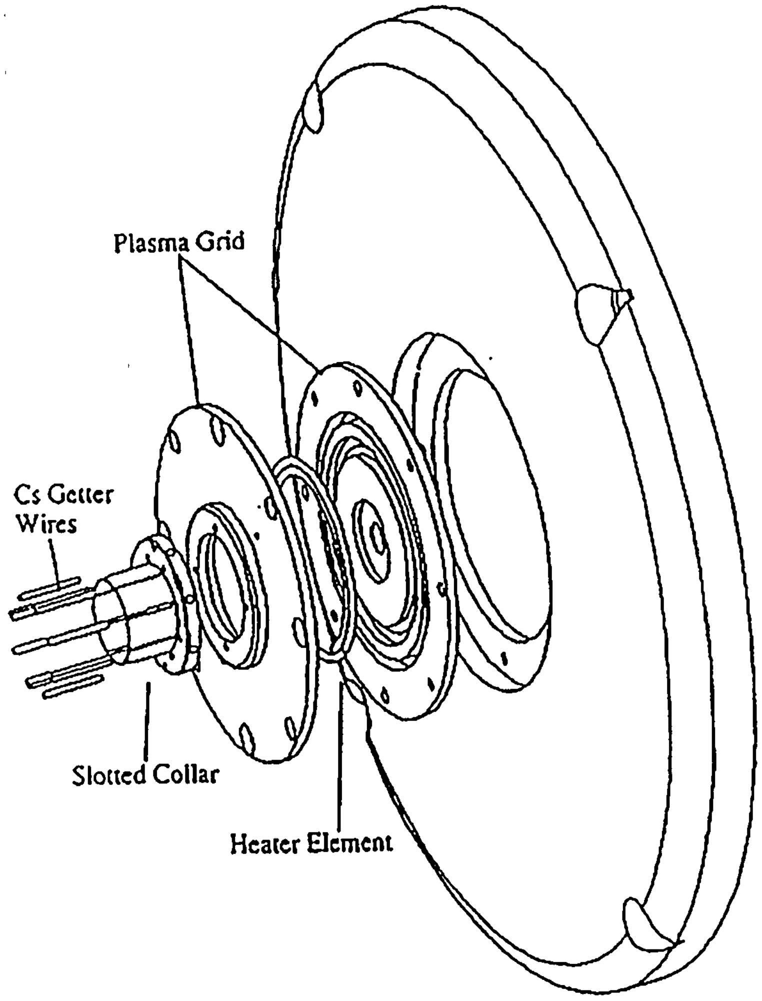

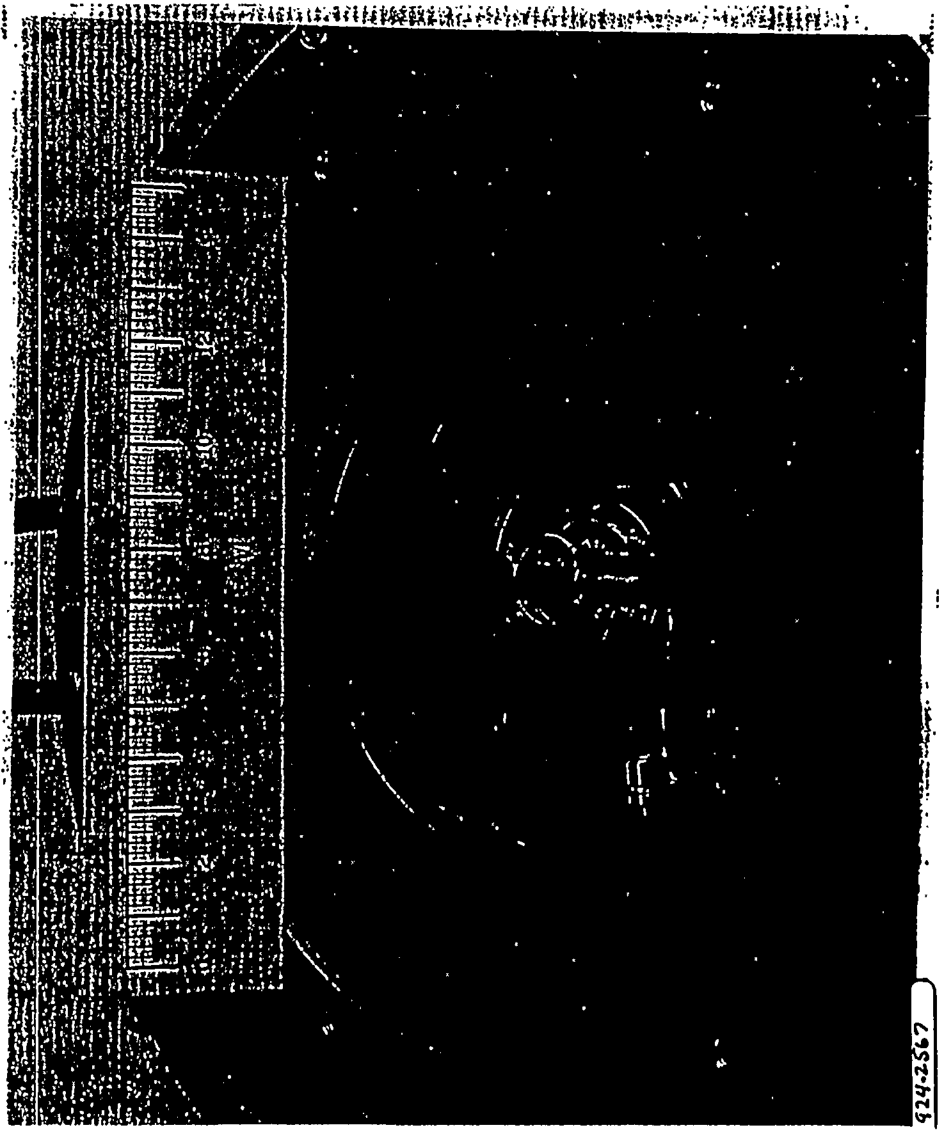

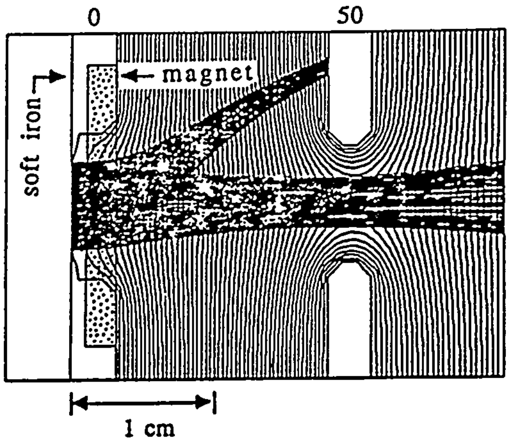

Planar Calculation Showing the Effect on the Extracted Electrons due to a Pair of Magnets Located Inside the 1st Electrodes

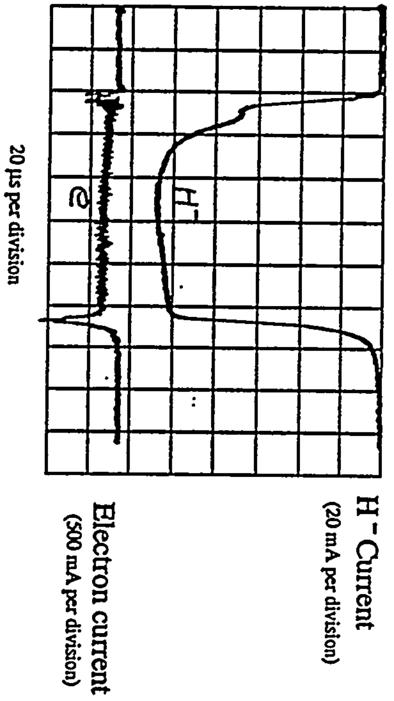

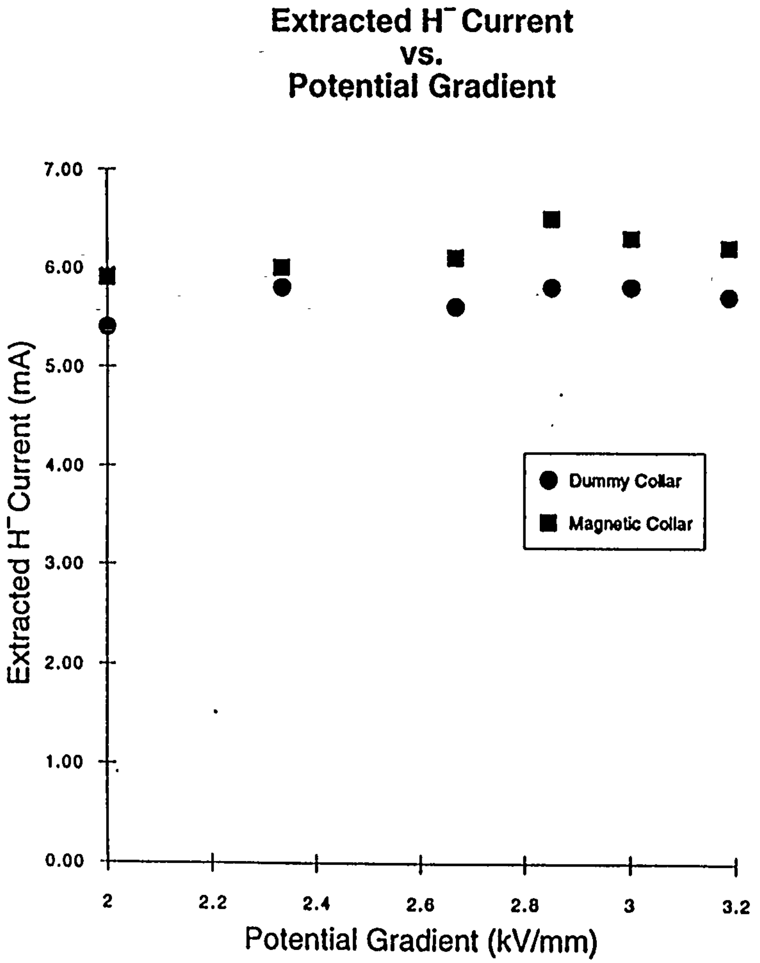

Extracted H⁻ Current vs. Potential Gradient

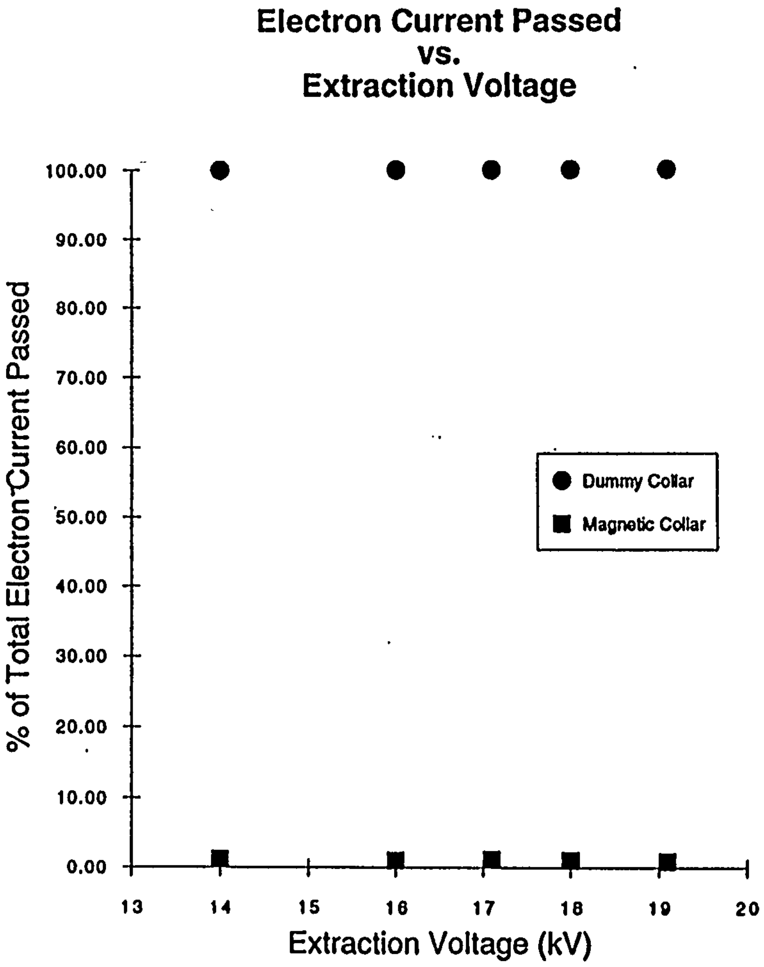

Electron Current Passed vs. Extraction Voltage

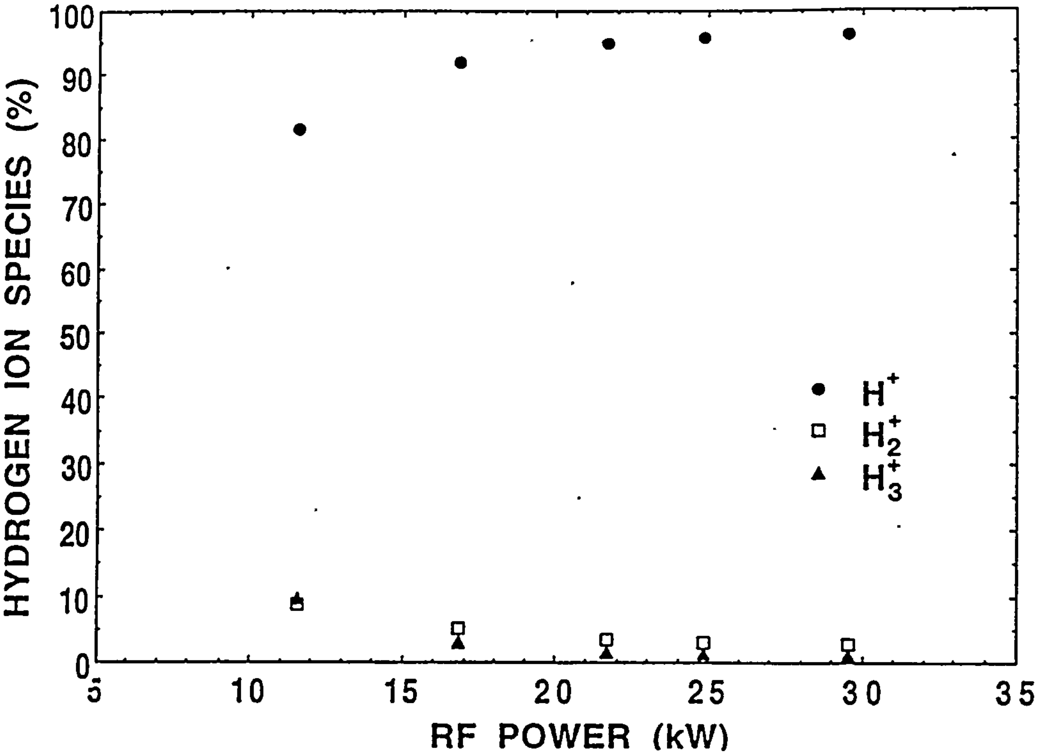
HYDROGEN ION SPECIES (%)
100
90
80
70
60
50
40
30
20
10
0
5
10
15
20
25
30
35
RF POWER (kW)
● H^+
□ H_2^+
▲ H_3^+

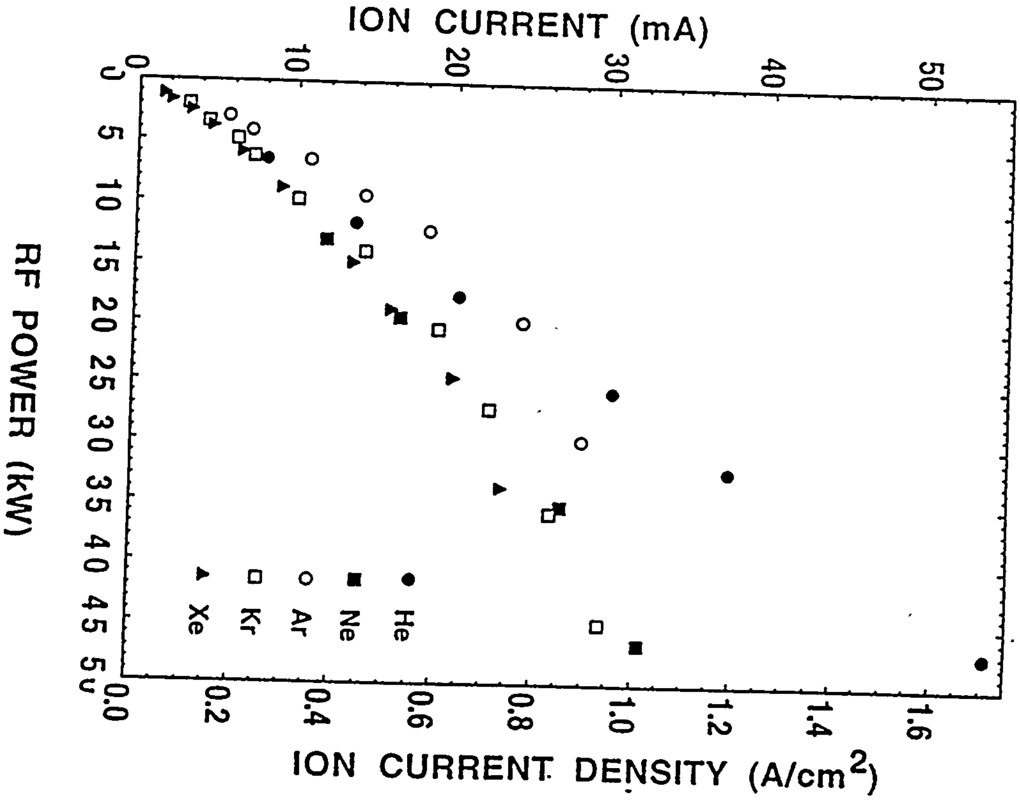
ION CURRENT (mA)
0
10
20
30
40
50
RF POWER (kW)
0
5
10
15
20
25
30
35
40
45
50
ION CURRENT DENSITY (A/cm^2)
0.0
0.2
0.4
0.6
0.8
1.0
1.2
1.4
1.6
● He
■ Ne
○ Ar
□ Kr
▲ Xe

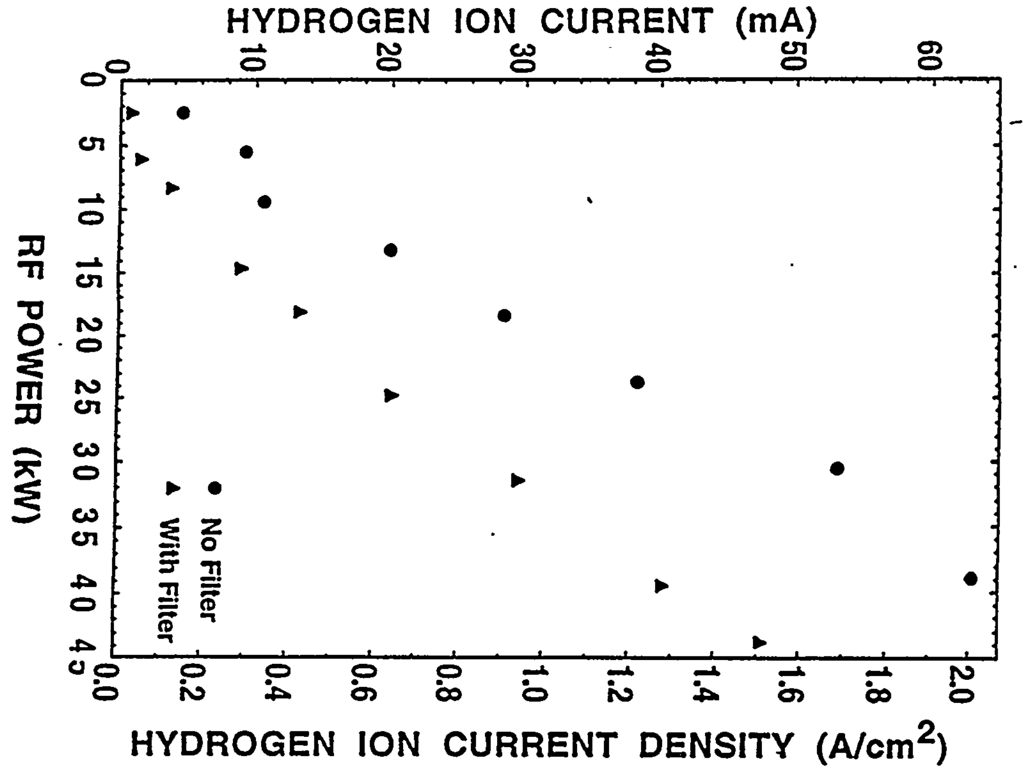

Hydrogen ion current and current density with and without magnetic filter

Torrance, CA 90503 #PV119

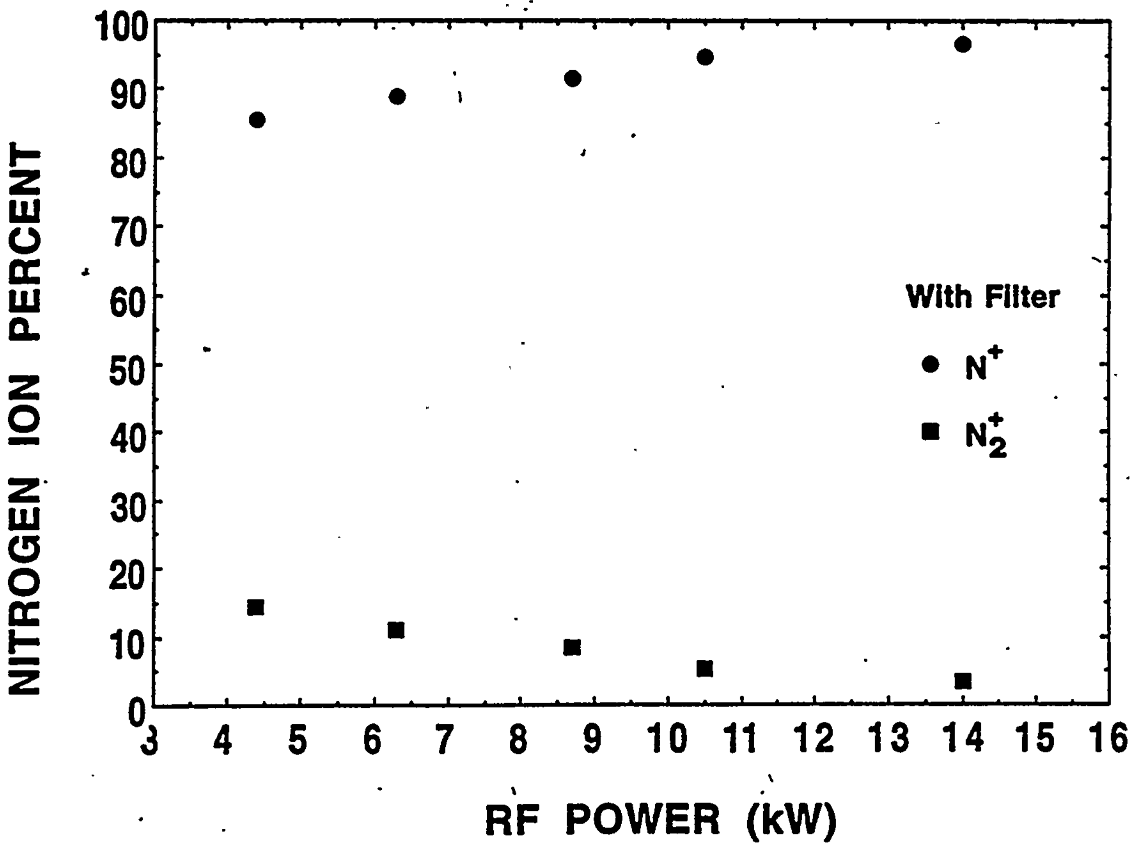

SATURATION HYDROGEN ION BEAM CURRENT EXTRACTED FROM 2 mm DIAMETER APERTURE

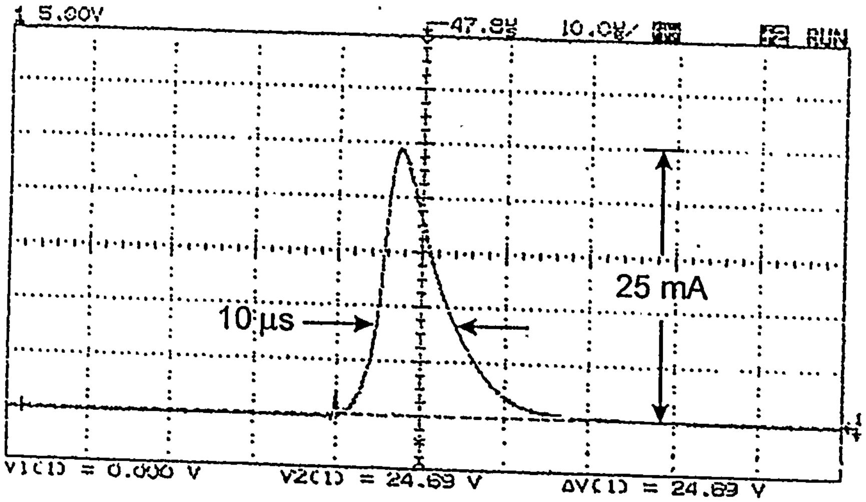

58 kW - 5.6 mTorr
[No cusp and no filter magnets]

COMPACT HIGH INTENSITY NEUTRON GENERATOR FOR BOREHOLE APPLICATIONS

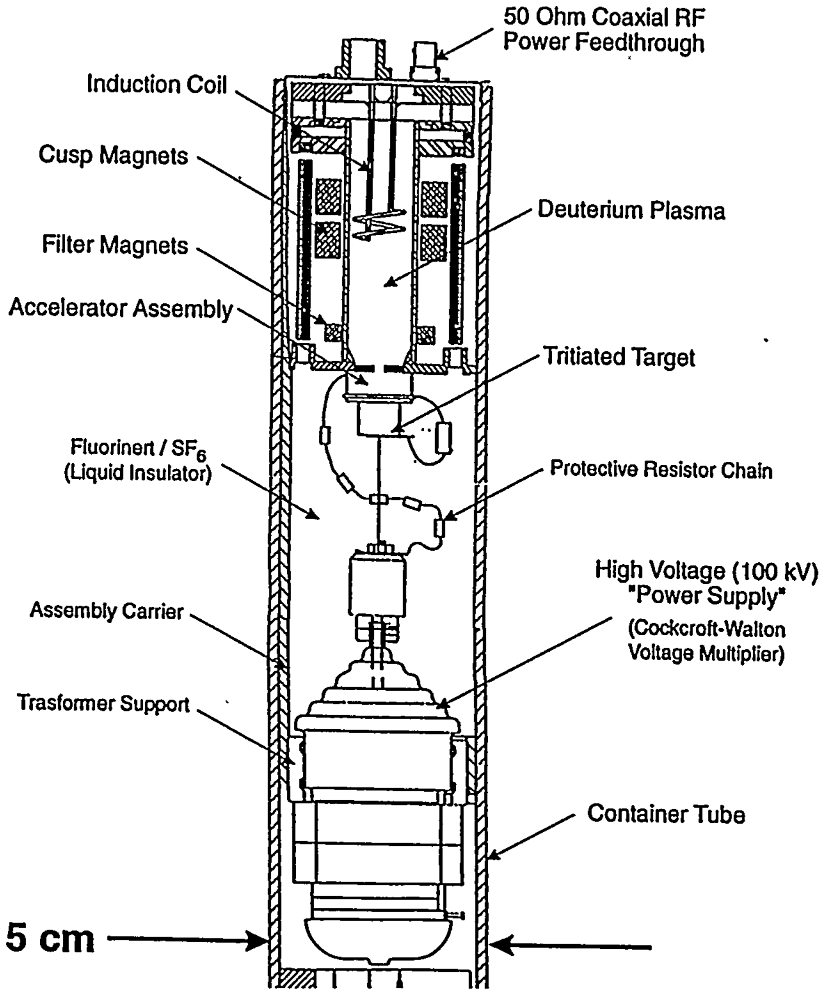

Minimum Threshold Operating Source Pressure vs. RF Power

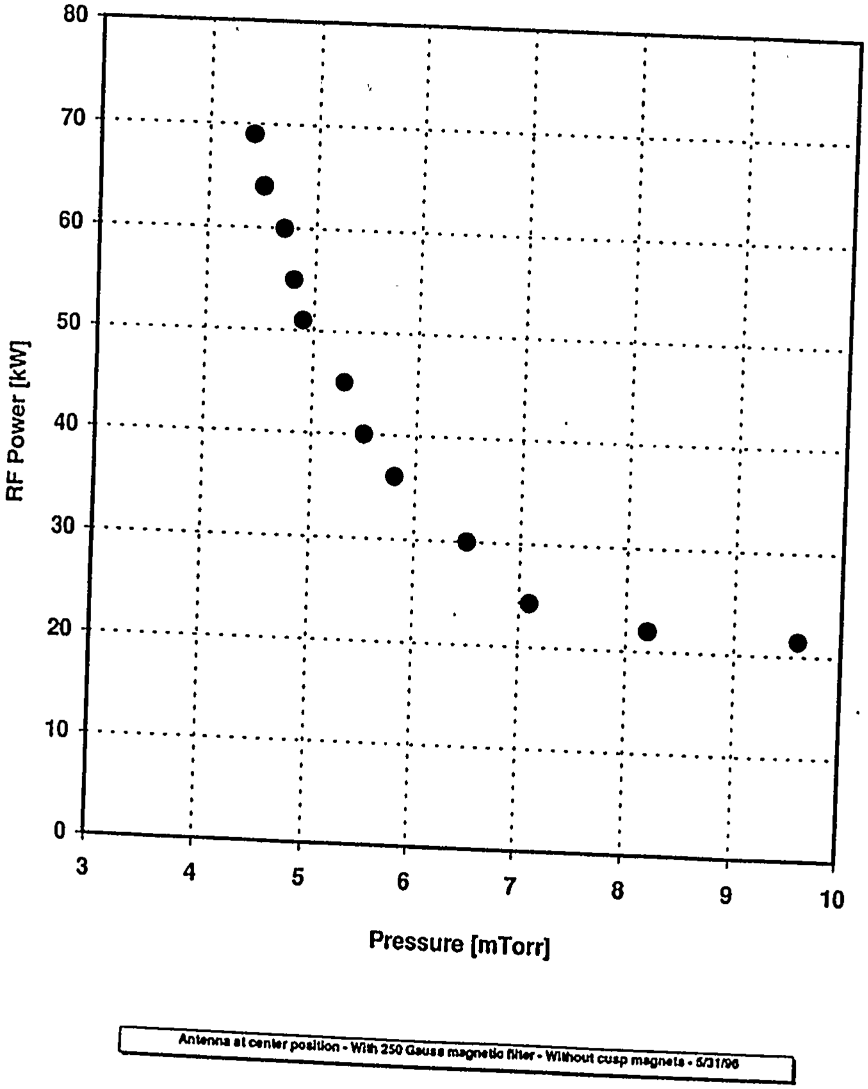

Antenna at center position - With 250 Gauss magnetic filter - Without cusp magnets - 5/31/96

Hydrogen Species Spectrum from Compact Rf-driven Ion Source

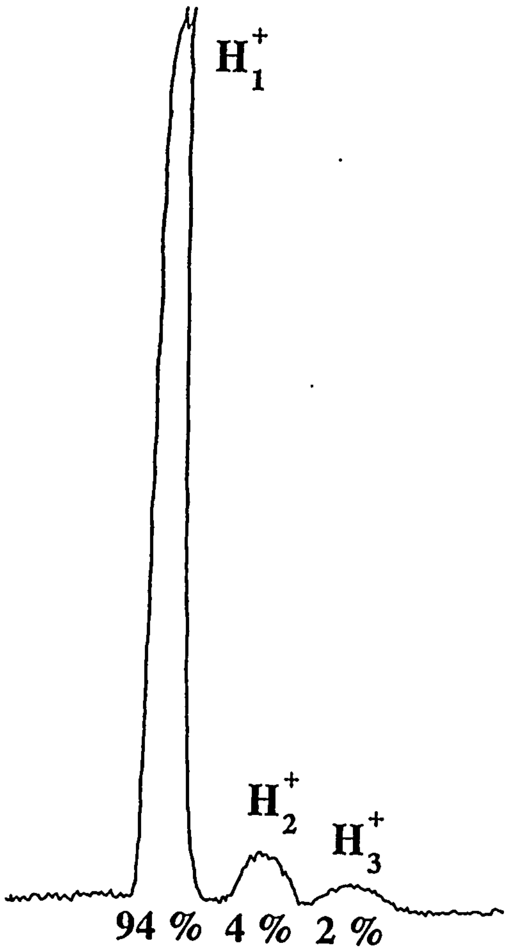

Note: An identical performance is expected for deuterium.

Hydrogen (H^+, H_2^+, H_3^+) Beam Current vs. Bias Voltage

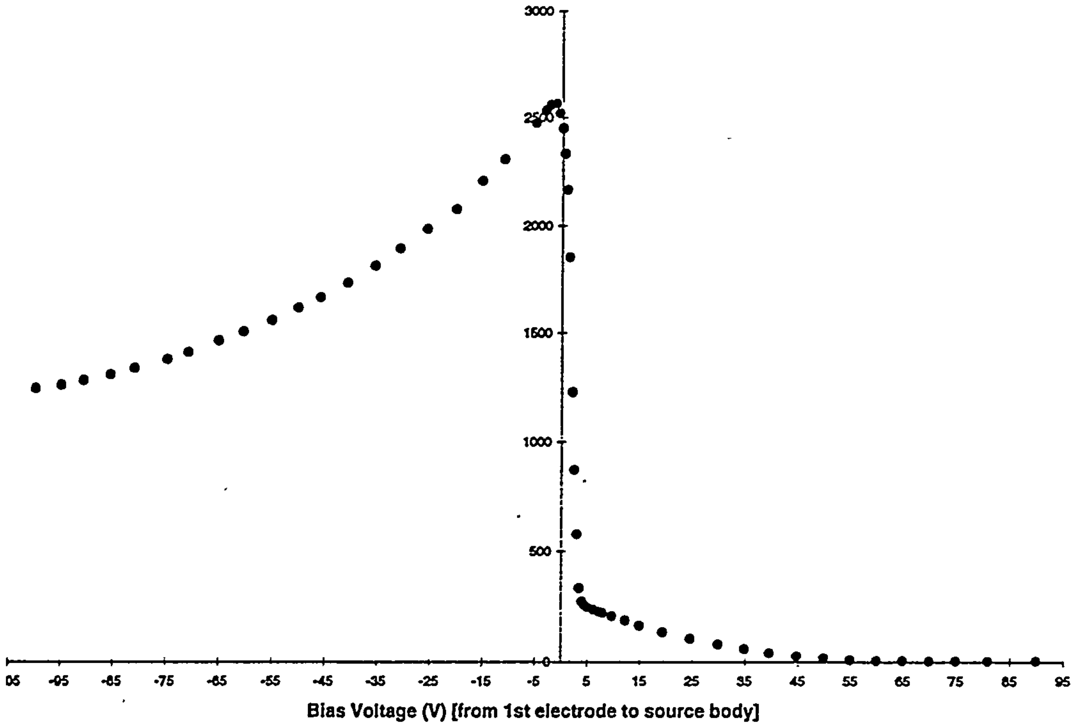

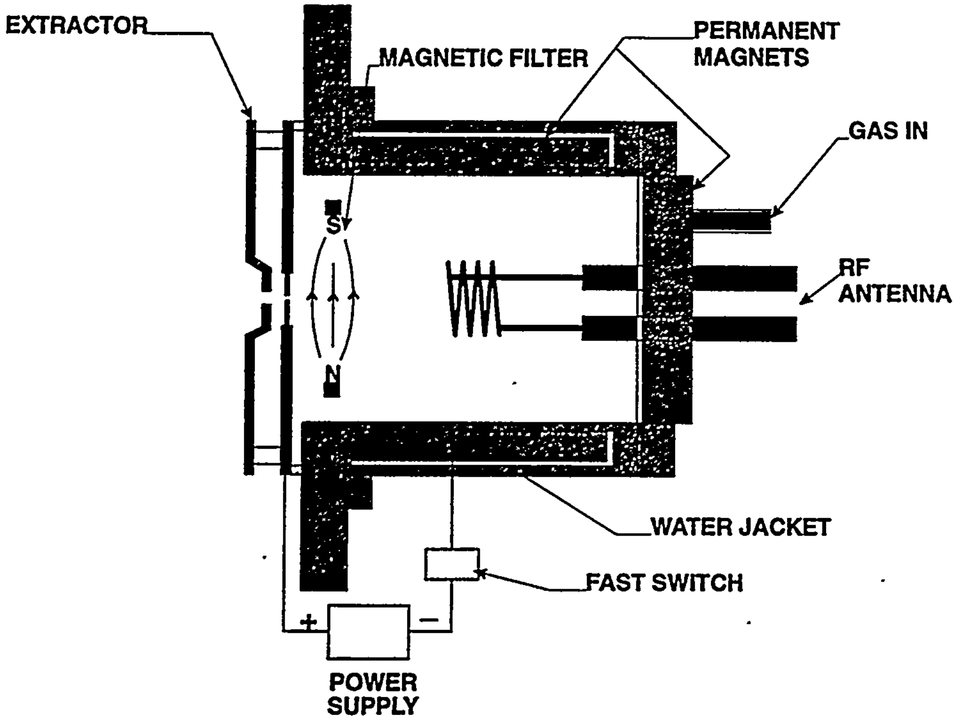

Experimental Setup for Lanthanum Hexaboride Photoemission Study

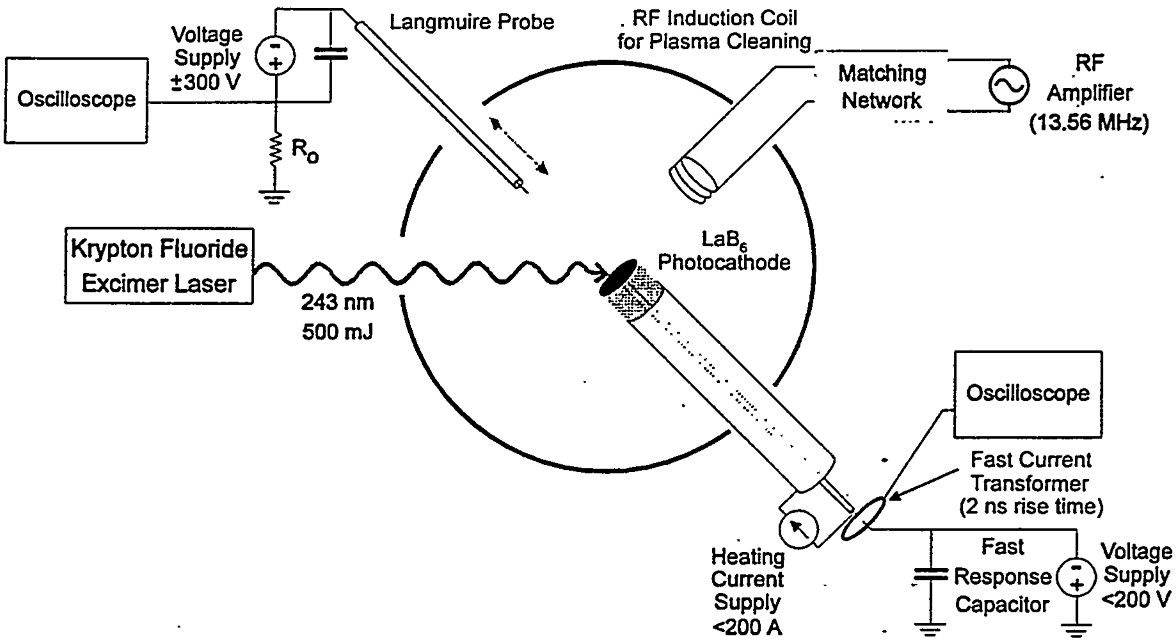

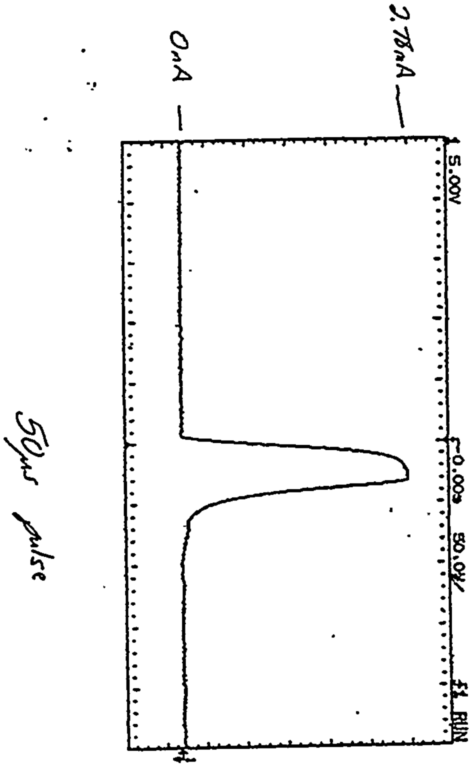

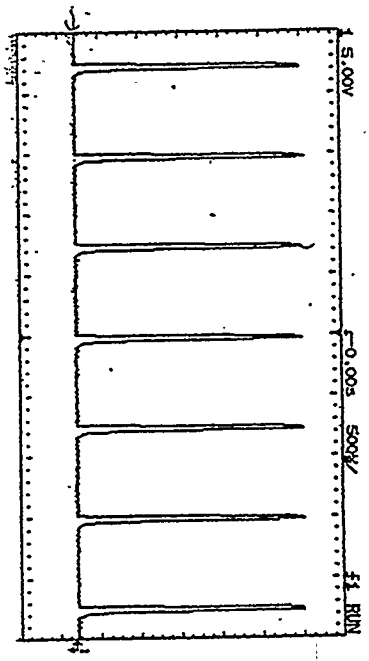

Laser Characteristics

Type: Krypton Flouride Excimer
Wavelength: 248 nm
Photon energy: 5 eV
Pulse length: 50 ns
Pulse energy: 200 - 500 mJ
Rep. Rate: 1-10 Hz

Photocathode Current vs. Voltage

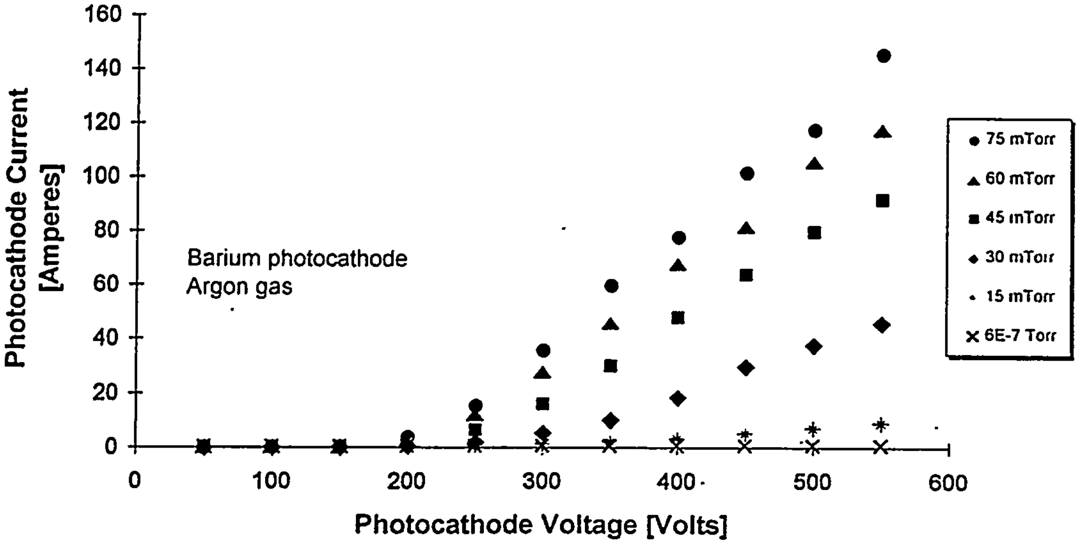

Langmuire Probe Signal

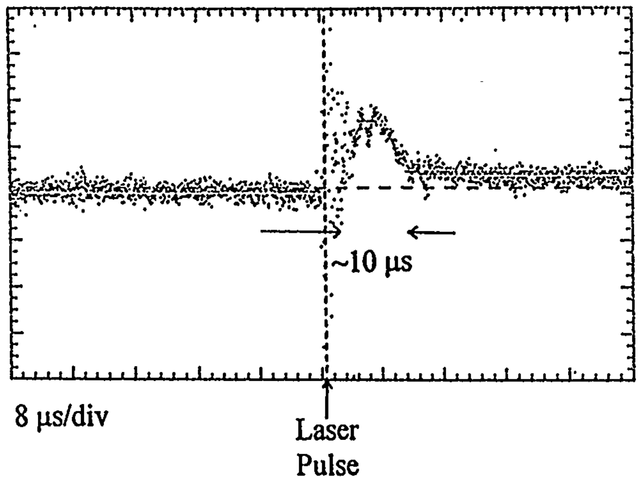

Temporal Characteristics of Laser and Electron Pulse

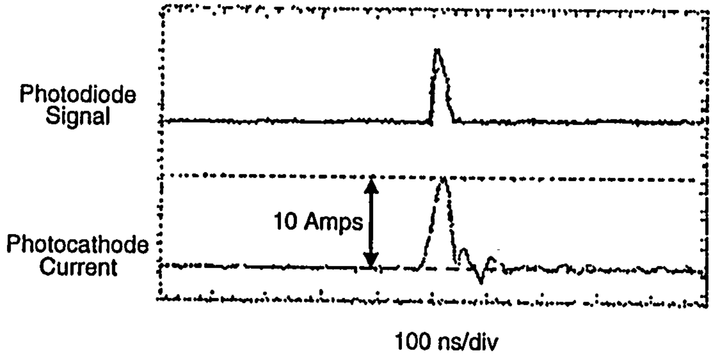

HIGH INTENSITY NEUTRON SPALLATION SOURCES

R. Macek, LANL

High Intensity Spallation Neutron Sources

(Outline for Presentation - R. Macek, 8/22/96)

- Brief survey of the field
  - CW sources
  - Long Pulse Spallation Sources (LPSS)
  - Short Pulse Spallation Sources (SPSS)
- Status, limitations & upgrade plans for existing SPSS
  - ISIS
  - MLNSC
- Comparison of RSC and Linac-Compressor Options
- Lessons for the Next Generation SPSS

Production of Neutron Beams at Spallation Sources

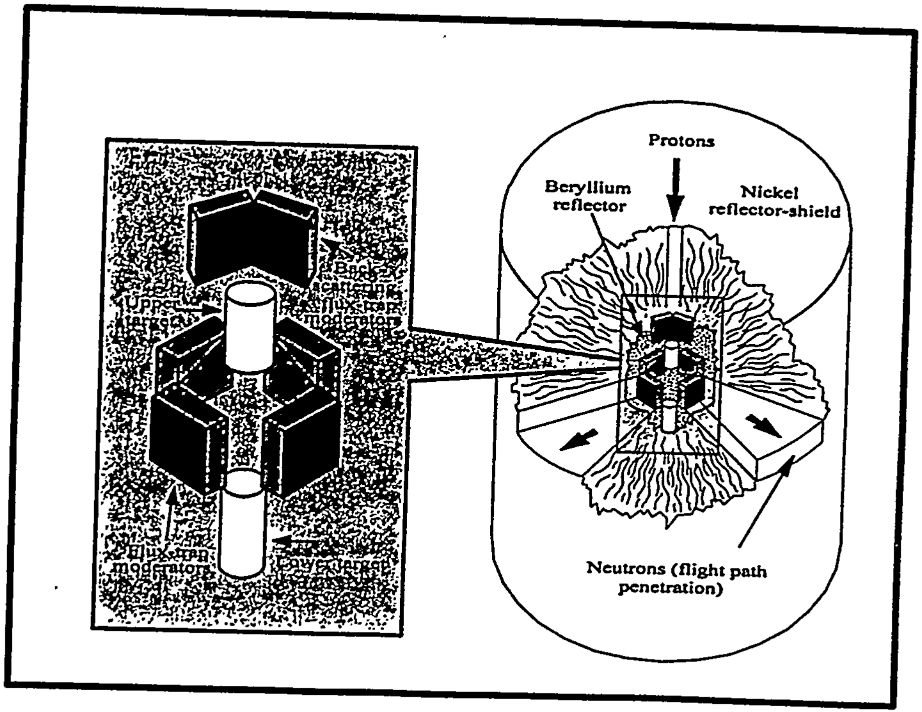

Target system

Los Alamos
Neutron Scattering Center
Experiment Hall

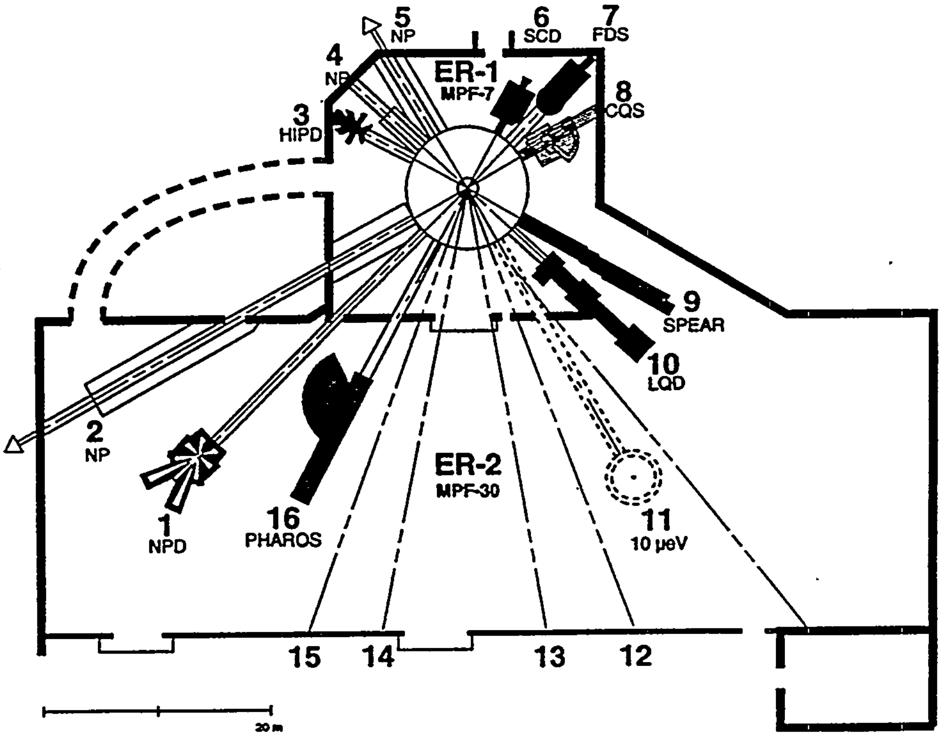

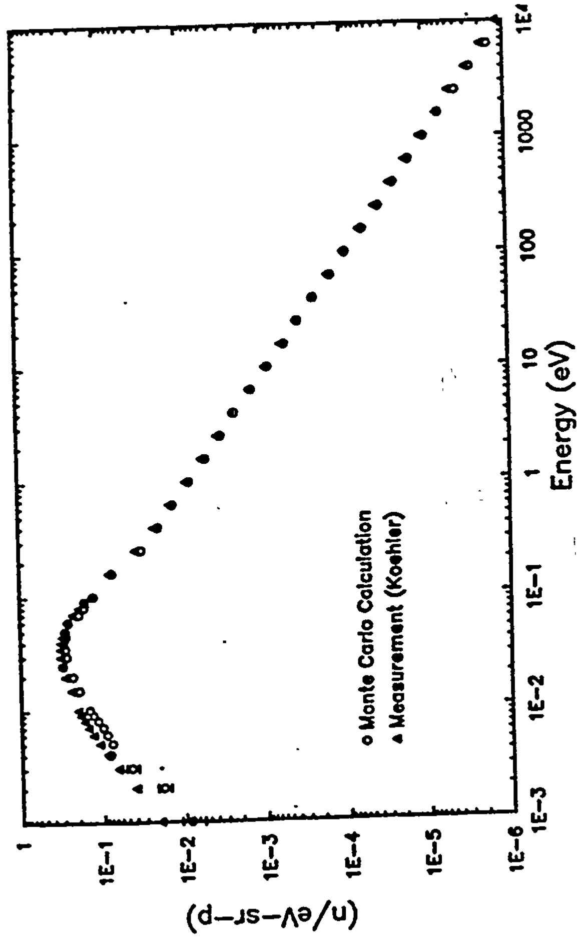

Calculated and measured neutron energy spectra from the LANSCE high-Intensity H_2O moderator.

Long Pulse Spallation Sources (LPSS)

- The SNQ proposal of the early 1980's
  - 5 MW Linac, 5 mA @ 1.1 GeV, 0.25 ms pulse duration @ 100 Hz
  - project canceled in mid 1980's
- Los Alamos LPSS proposal (1995)
  - 1 MW Linac, 1.2 mA H+ @ 800 MeV, 1 ms pulse duration @ 60 Hz
  - 0.8 MW demonstrated in 1995, 1 mA H+ @ 800 MeV, 1 ms pulse duration @ 60 Hz simultaneously with 70 μA of H- to MLNSC and operation of WNR
  - Main requirements are target and beam lines in the experimental area
  - Proposed for funding in 1999 or 2000

Continuous (CW) Sources

- 1 MW SIN-Q at PSI
  - 1.5 mA CW protons @ 590 MeV from isochronous cyclotron
  - Zircalloy rod bundle is the initial target
  - Under construction, completion in the fall of 1996
- Accelerator Production of Tritium (APT) proposal (170 MW spallation source)
  - Linac producing 100 mA CW protons @ 1.7 GeV on large target of tungsten rods
  - Target damage studies currently underway at LANSCE

ISIS

- RCS with Multiturn (~250 turns) charge exchange injection of 70 MeV H^- beam
  - Horizontal closed orbit bump in the injection straight section
  - Bump turned off at end of injection so beam clears the foil during acceleration
  - Painting in both transverse planes is needed
- Key limitations on intensity
  - Space charge tune shift of ~ -0.4 shortly after acceleration begins
  - Losses injection and during RF trapping ~ 15%
    - — Collected on absorbers
    - — ~25 rem/hr after a day's cool down
- Uranium target lifetime is a problem, Ta target has acceptable lifetime
- Upgrade potential: 300 µA
  - Dual harmonic RF to improve bunching factor

Short Pulse Spallation Sources (SPSS)

- Highest user demand, most powerful for TOF techniques
  - Pulse width < 1 µs, 20-50 ms between pulses
- ISIS & MLNSC are the most intense sources
  - ISIS sets the standard by virtue of intensity, hours per year for research, number of instruments and strength of scientific program

Facility	Type	Beam Power (kW)	E Mev	I(µA)	Rep Rate (Hz)	Pulse Width (µS)	PPP 10^13	Reliability
ISIS (RAL, UK)	RCS	160	800	200	50	0.45	2.5	80-90%
MLNSC (Los Alamos)	Linac-Compressor	56	800	70	20	0.25	2.2	75-85%
IPNS (ANL)	RCS	7	450	15	30		0.31	95%
KENS (KEK, Japan)	RCS	2.5	500	5	20		0.15	?
IN-06 (MMF Moscow) under construction	Linac-Compressor	220	700?	300?	50	0.35	4?	

PSR

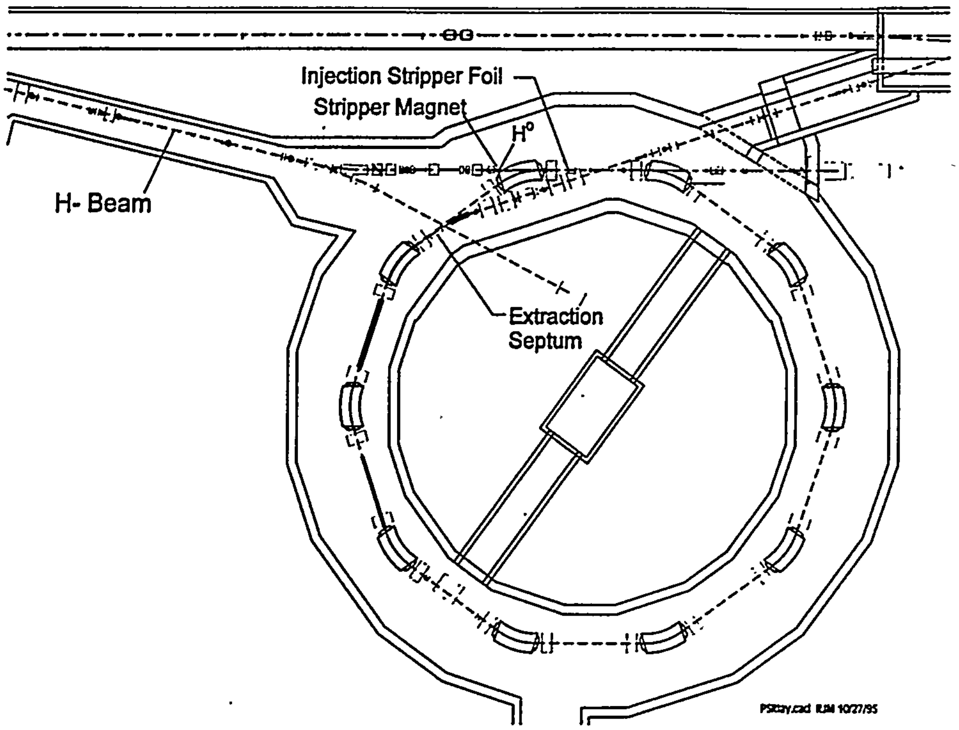

PSR/MLNSC

- **Linac-Compressor with 2-step Charge Exchange injection for ~1700 turns**
  - **H^- to H^0 via field stripping in a high field magnet followed by H^0 to conversion H^+ in a stripper foil**
- **Average current limited to ~ 75 µA @ 20 HZ by beam losses during accumulation**
  - **"First Turn" Losses (0.2 - 0.3 %)**
    - **— Excited States of H° that strip in downstream dipole**
  - **Stored Beam Losses (0.3 - 0.5 %)**
    - **— $4 - 6 \times 10^{-6}$/stored proton/turn - primarily from nuclear and large-angle Coulomb scattering in the stripper foil**
    - **— Some losses from action of RF Buncher (momentum spread)**
- **Peak current limited by a fast instability**
  - **Threshold depends on buncher voltage**
- **Peak current also limited by ion source**
- **Operational beam reliability/availability has been poor in the past**

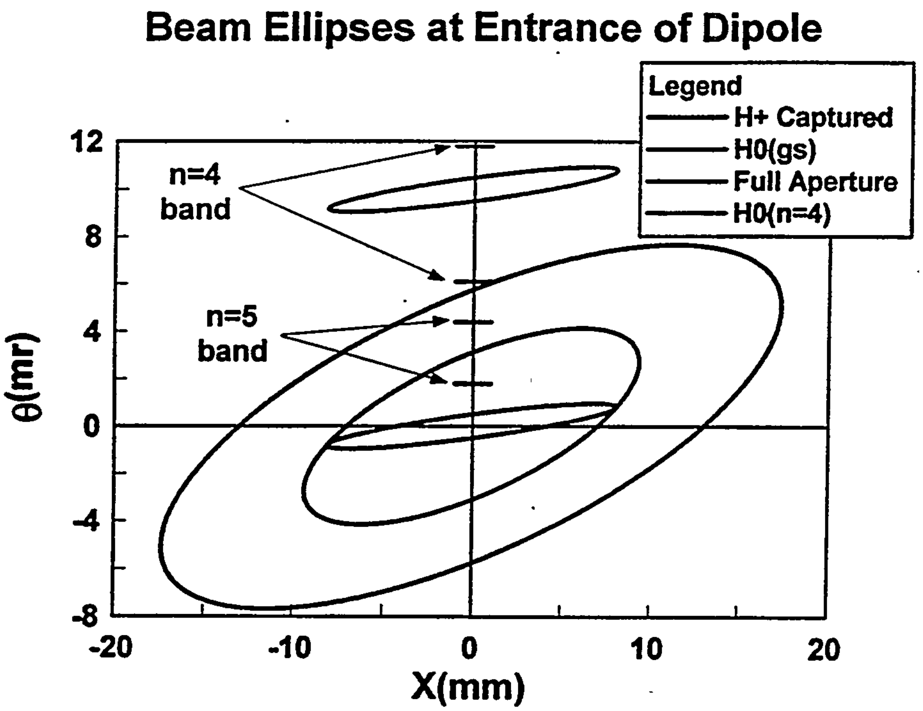
Beam Ellipses at Entrance of Dipole

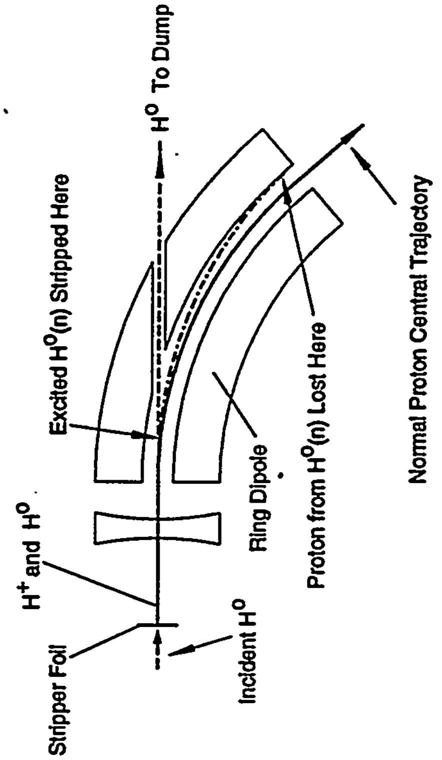

Figure 1. Schematic Layout of PSR Injection Area depicting first turn loss mechanism.

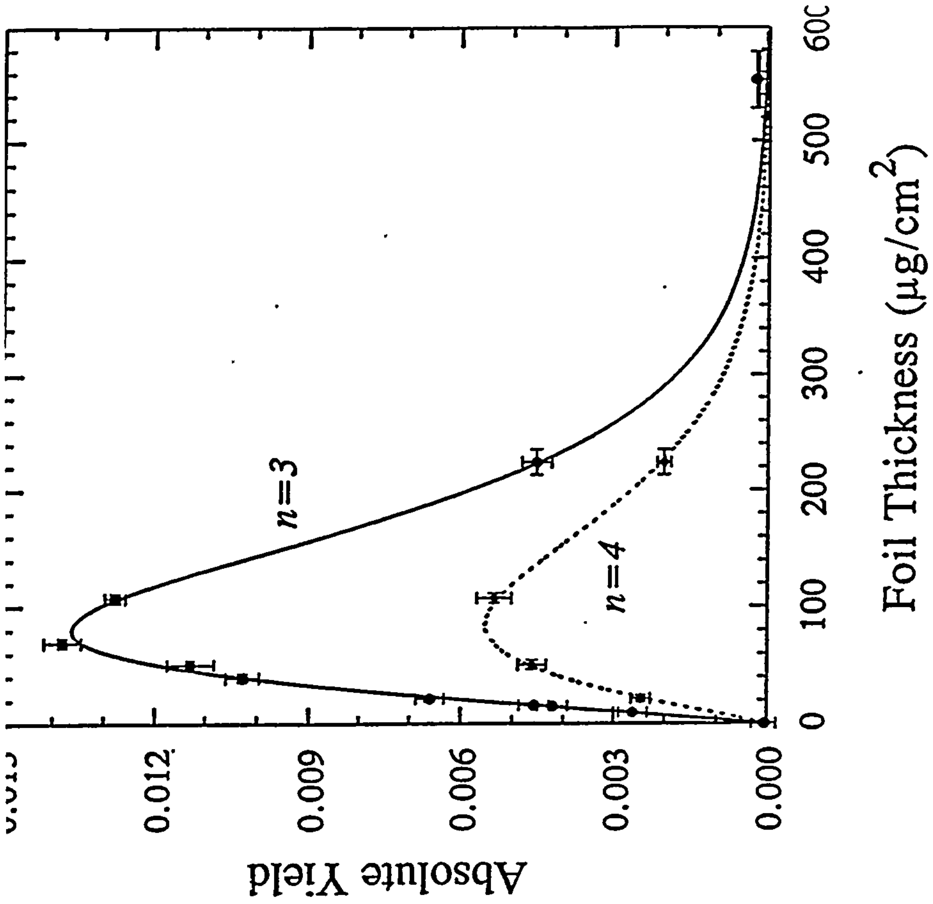

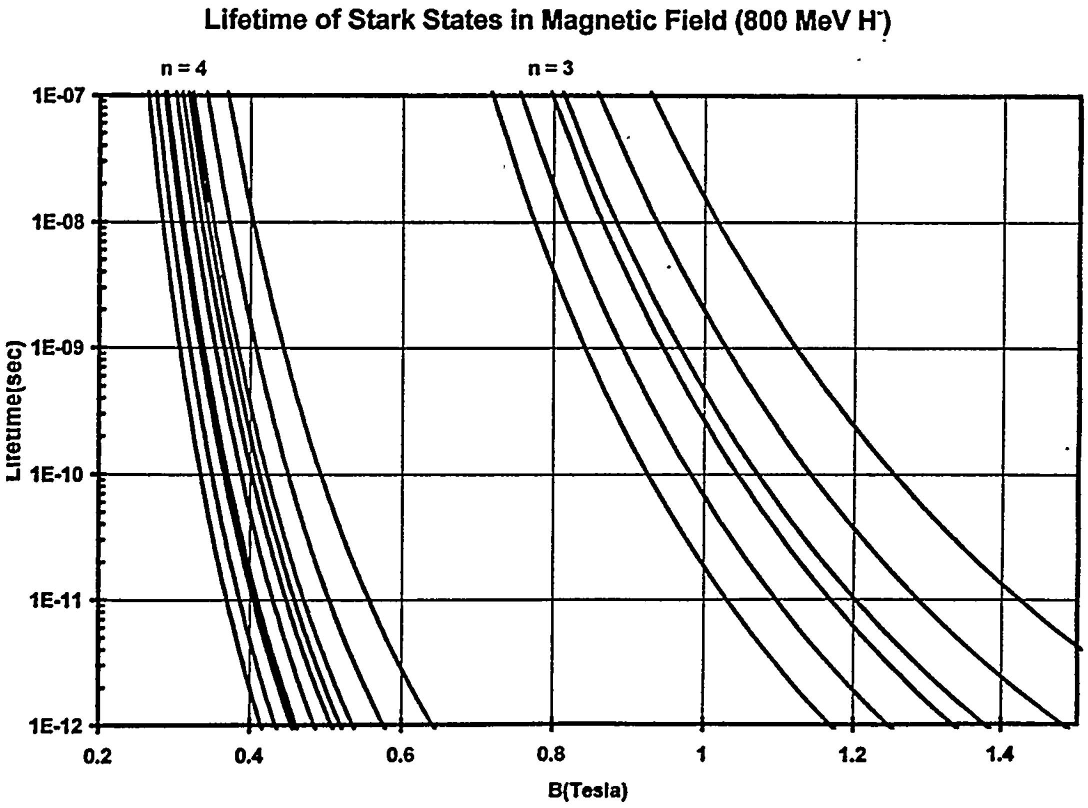
Lifetime of Stark States in Magnetic Field (800 MeV H$^-$)

Characterization of Operational Beam "Reliability"

- **Definition: Availability w.r.t. schedule**

$$\text{Availability} = \frac{\text{Uptime}}{\text{Scheduled\_Time}} = \frac{\text{Uptime}}{\text{Uptime} + \text{Downtime}} = \frac{1}{1 + \frac{\text{MTTR}}{\text{MTTF}}}$$

- **Reliability and Maintainability contribute on an equal footing**
- **Fluctuations in availability over the duration of an experiment are the main source of risk seen by the user who is given a fixed block of time**
- **Longer downtime intervals have the greatest impact on the typical SPSS user**

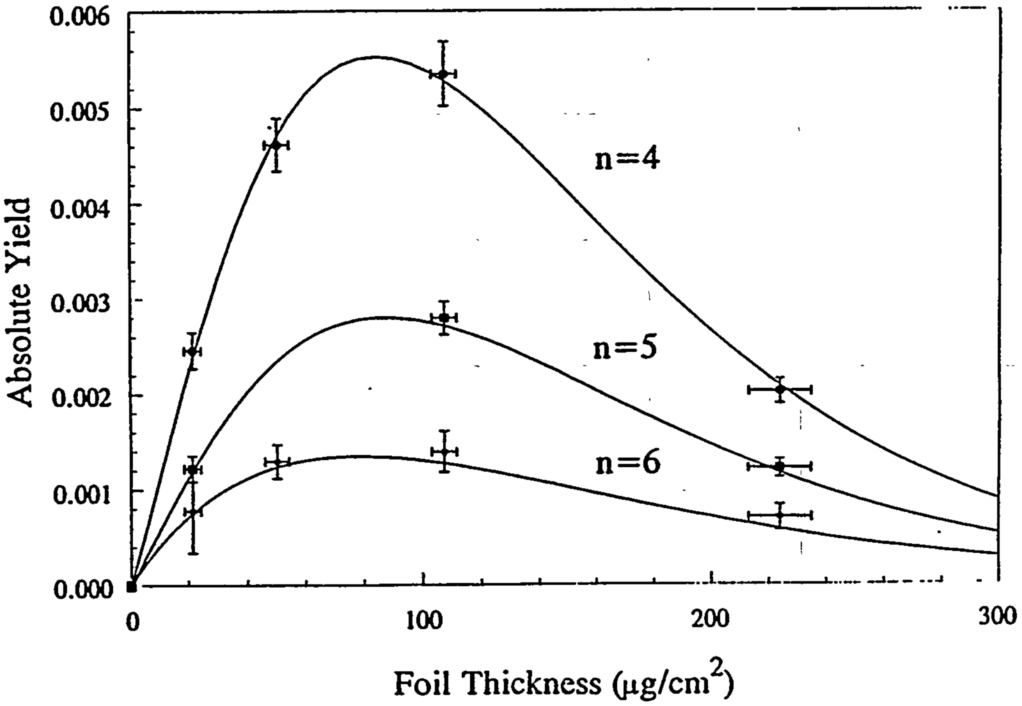

Down Time by Length of Interval

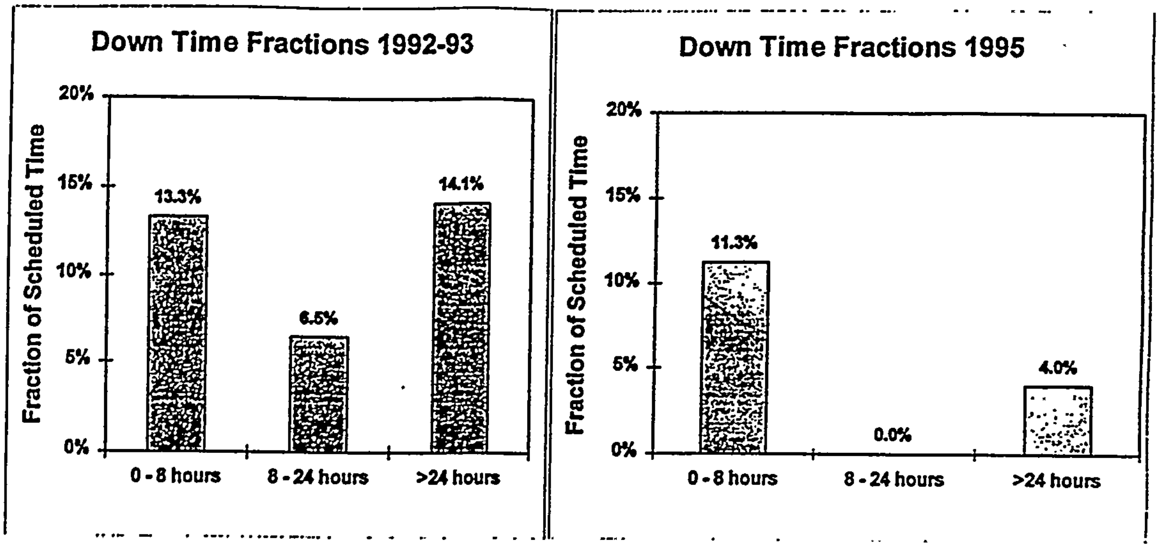

Unavailability Distributions for MLNSC

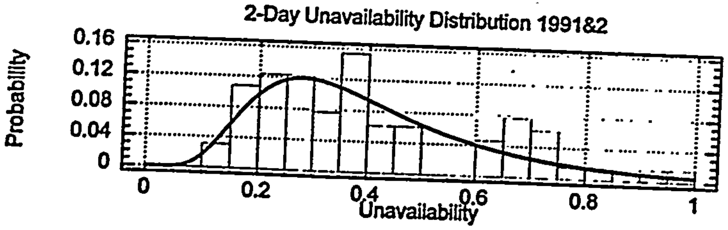

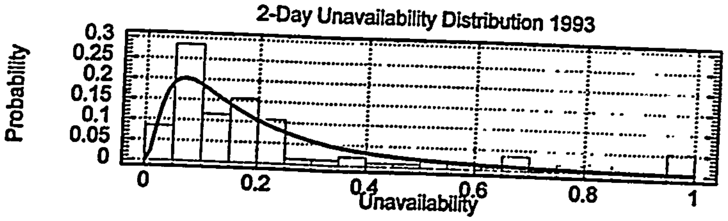

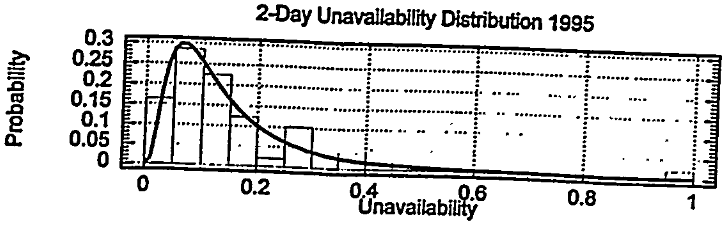

Solution: Direct H$^-$ Injection

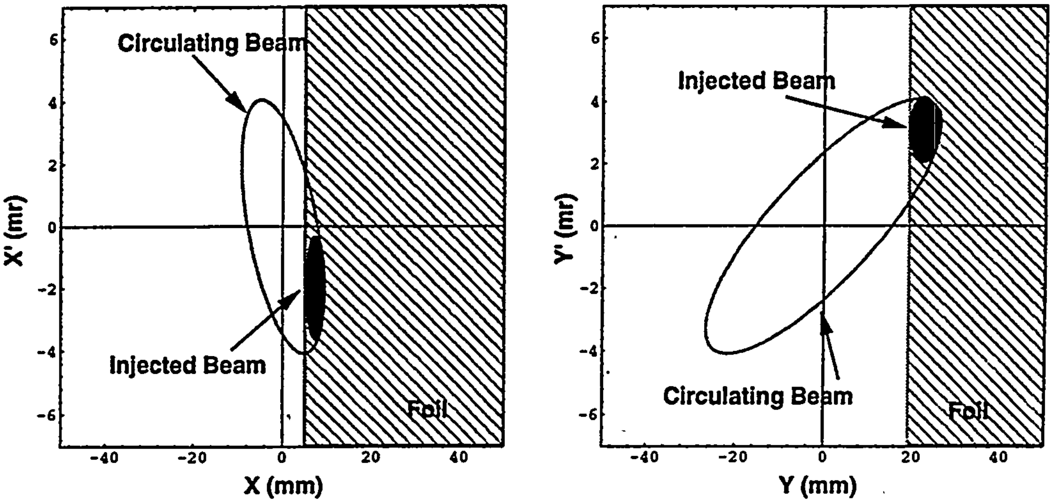

Fundamental Problem for PSR: H^0 Injection

(Underlying cause of the slow beam loss problem for PSR)

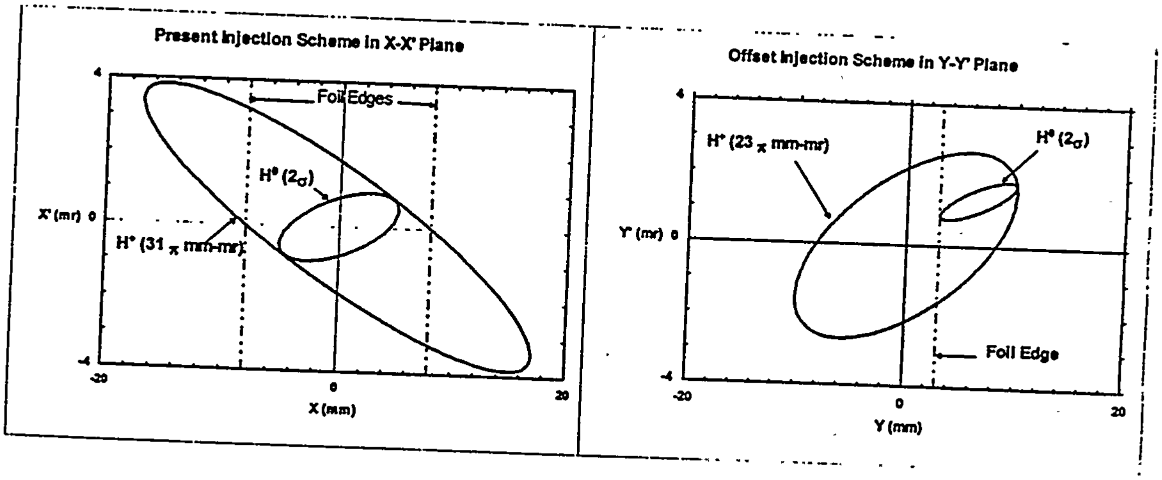

- Emittance growth of factor ~3 in bend plane of stripper magnet
- Large mismatch in the horizontal plane
- Cannot manipulate or tailor neutral beam for optimum filling ("painting") of transverse phase space to keep the stored beam off the foil as much as possible

Benefits of Direct H$^-$ Injection

- Provides optimum injection "painting" that greatly reduces the well-understood, main sources of slow beam losses
  - Factor of 10 reduction in stored-beam foil hits compared to H^0 injection
  - Factor of 4 - 5 reduction in overall loss rates after optimization of foil thickness to reduce excited states of H^0
- Other Benefits
  - Larger core & smaller tails ⇒ lower space charge density
    - Lower space charge tune shift
    - Increase threshold for collective effects including the PSR instability
  - C-magnet in ring facilitates handling 1st-turn losses

Direct H$^-$ Injection Layout

PSR Injection Line Modifications

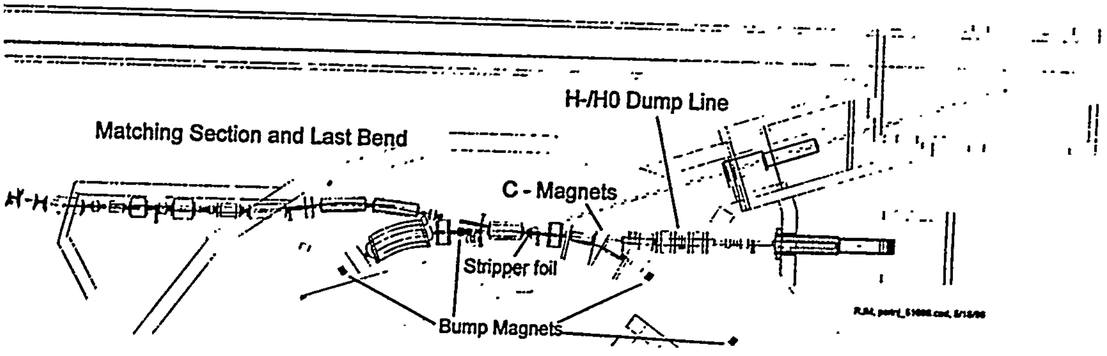

Unstable Beam in PSR

Scope trace below was taken for beam that is at the threshold for instability.
Beam is lost after being stored for ~300 µs after accumulation (450 µs of accumulation).
Note the rapid rise time (~20-30 µs) for vertical oscillations just before half the beam is lost.
The frequency spectrum of the vertical oscillations is very broad and centered around 100 MHz. All observations are consistent with e-p (2-stream) instability.

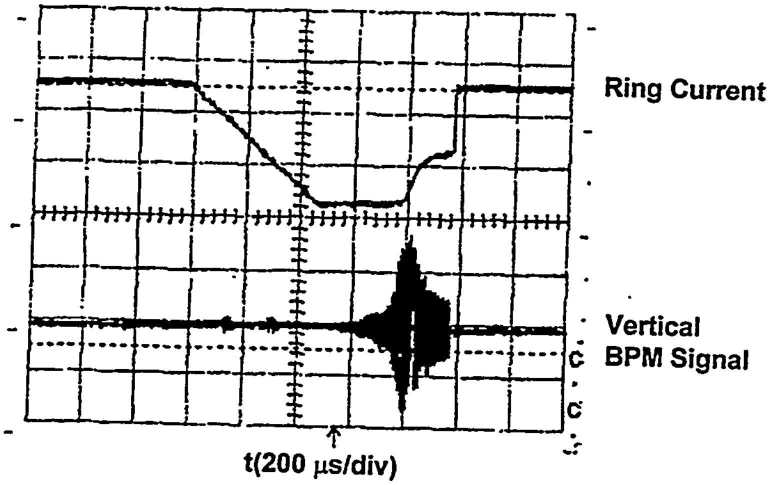

Fast PSR Instability Limits Peak Intensity

- It is a fast, transverse instability that is avoided by keeping the beam well bunched
- Threshold is a strong function of RF buncher voltage
  - Threshold of 7- 8 x 10^{12} PPP for coasting beam (buncher off)
  - Present operation is 2.2 x 10^{13} PPP with ~6 kV on buncher
  - Have accumulated up to 4 x 10^{13} PPP with 15 kV on buncher (1988)
    - — 11 kV fundamental, 4 kV 2nd harmonic
    - — maximum available from ion source with 950 µs beam gate
  - Solid demonstration of 3.4x10^{13} PPP operation at 12.5 kV (1992)
- All of the data is consistent with the theory of e-p (2-stream) instability
- Control e-p instability by suppressing electron production and/or preventing the trapping of electrons
  - Suppress various sources of electrons
  - More RF voltage on Buncher will keep inter-bunch gap free of protons and thus suppress trapping electrons in the field free or uniform field regions of the ring

PSR/MLNSC Improvement Program
Goal: 200 μA @ 30 Hz

- Direct H⁻ Injection to reduce beam losses in the ring
  - Factor of 10 reduction in foil hits, 4.5 reduction of overall beam loss rate
- Target System upgrade for better maintainability
  - 3 week replacement time instead of 10 months
- Brighter, more intense, high-duty H⁻ ion source
  - Increase intensity by 2-2.5 to ~40 mA and cut emittance in half
- RF Buncher upgrade to control PSR instability
  - Twice the voltage (to 30 kV) and add harmonics (2nd & 3rd)

Effect of Buncher Voltage

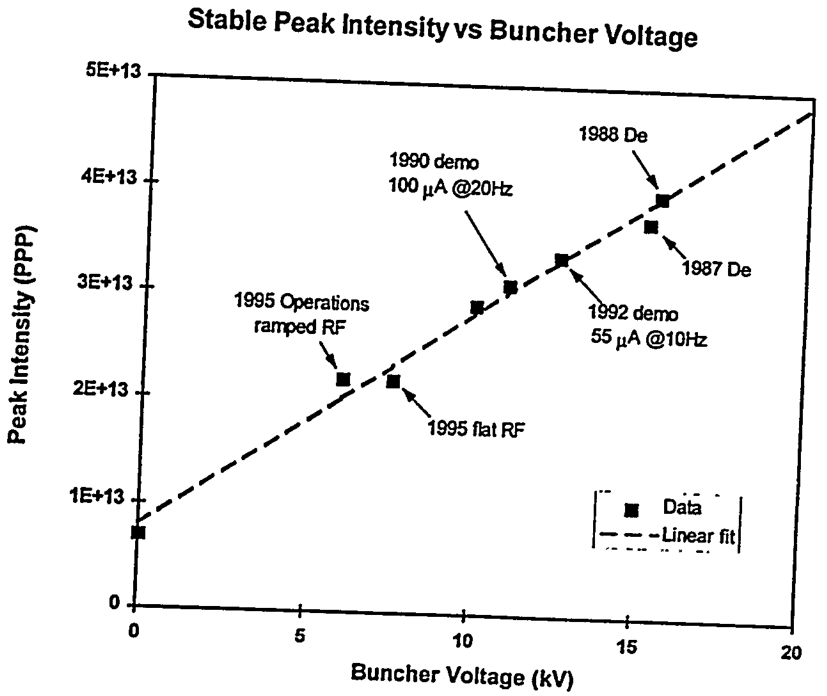

Summary Graph

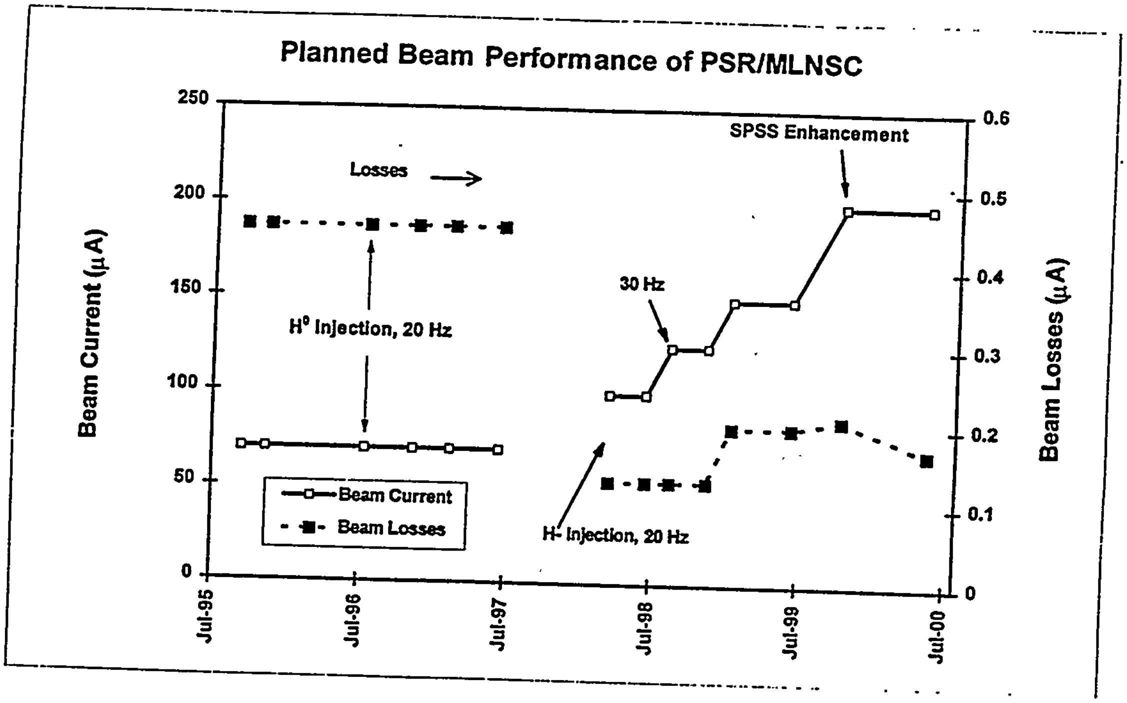

Comparison of RSC and Linac-Compressor Options

	Advantages	Disadvantages
RCS	■ Main losses are at lower energy of injection ■ Linac costs are lower ■ Mature technology, fewer unknowns ■ Higher energy, lower current for a given beam power	■ Lower space charge tune limit on maximum current for a given aperture & final energy ■ Ring complexity greater ● Rapid-cycling magnets ● More demanding ring RF ■ More time in the ring for instabilities to develop
Linac-Comp.	■ Highest space charge tune limit on maximum current for a given aperture & final energy ■ Ring less complex ● DC magnets ● No acceleration ■ Beam in the ring for a shorter time	■ All losses are at the final energy ■ Injection at the higher energy is more difficult ■ Linac costs are greater

Conclusion: Both options will go to higher intensity, choice may hinge on other uses for the facility such as LPSS or meson/kaon/neutrino beams.

Proposed Short Pulse Spallation Sources

Facility	Type	Beam Power (MW)	E GeV	I(mA)	Rep Rate (Hz)	Pulse Width (μS)	PPP 10^13
ESS	Linac-Two Compressor	5	1.33	3.8	50	1	47
NSNS (ORNL)	Linac-Compressor	1	1	1	60	~1	10
IPNS Upgrade	RCS	1	2	0.5	30	<1	10
LANSCE-NGSS	Linac-Compressor	1	0.8	1.25	60	0.6	13
JHP (KEK)	RCS	0.6-1.2	3	0.2-0.4	25-50	<1	5
Austron	RCS	0.2	1.6	0.13	25	<1	3.2

Lessons for the Next Generation Sources

- High reliability/availability is crucial with the users and must be part of the specifications up front
- Beam losses are key, they must be kept low for hands on maintenance
  - Losses from excited states of H^0 can be minimized but not totally eliminated. Optimization needs to be part of the initial design.
  - Keep the beam off the foil as much as possible.
  - Allow plenty of access room in the regions of significant losses.
- The PSR instability may still hold some surprises.
- R&D needed on intense, high brightness H^- ion sources
- Extensive R&D needed on high-power target systems

HIGH INTENSITY MUON SOURCE

W. Molzon, UCI

High Intensity Muon Sources

Symposium on High Intensity Particle Sources
Institute for Theoretical Physics
Santa Barbara

W. Molzon
University of California, Irvine
August 22, 1996

Recent History of Muon Source Development

- The MELC proposal of Djilkibaev and Lobashev
  - Proposal to search for $\mu^- N \rightarrow e^- N$ with 10^{-16} sensitivity
  - Proposed for Moscow Meson Factory
  - Contained idea for high intensity source with target in solenoid, solenoidal transport
  - Recent work on experiment at BNL using many of ideas of MELC
- AGS2000 workshop
  - Ideas for experiments in rare muon processes pursued
  - Working group led by W. Molzon
  - Working towards LOI for experiment at BNL
  - Theoretical input and encouragement from W. Marciano
- Workshop at ITP on high intensity sources and rare muon processes
  - Organized by Zohreh Parsa
  - Discussed ideas for sources, including polarized, for LFV experiments
- Muon collider work on high intensity sources
  - Workshop at Montauk in fall 1995 – proceedings
  - Have produced $\mu^+\mu^-$ **Collider: A Feasibility Study**
  - Ideas for very intense muon source using geometry of MELC

Why High-intensity Muon Sources

- Muon collider source
  - – Intensity of $10^{13} - 10^{14}\ s^{-1}$ required
  - – Muons must be captured in accelerating structure
  - – Need very short bunches at up to 30 Hz
  - – Cost set by price of muon collider – ? × $\$10^9$
- Experiments in rare muon processes
  - – $\mu^- N \rightarrow e^- N$
    - ∗ Intensity of $10^{11} s^{-1}$ needed for 10^{-16} sensitivity
    - ∗ Large macro duty cycle
    - ∗ Pulsed at 1 MHz with good *extinction*
    - ∗ Experiment uses stopped muons – hence low energy source
  - – $\mu^+ \rightarrow e^+ \gamma$
    - ∗ High polarization required to minimize backgrounds
    - ∗ Use surface muons – π decaying at rest near surface
    - ∗ Requires intensity up to $10^9 s^{-1}$

Outline of the Talk

- Physics motivation for experiments for rare muon processes
  - – Lepton flavor violation
  - – Grand unified theories and supersymmetry
- Experimental background on muon experiments
  - – Present sensitivity and limits
  - – Why the need for high intensity sources?
- Ideas for high intensity sources for experiments
  - – MELC muon beam proposal
  - – Studies of fluxes which could be achieved
- The muon collider
  - – Cartoon overview of the machine
  - – Calculations of very intense sources
  - – Technical issues with the target and collection scheme

Search for Lepton Flavor Violation

Apparantly conserved additive quantum numbers associated with each *family* of leptons

- Rigorously true in Standard Model if neutrinos are degenerate in mass

G=1	e	ν_e	u	d
G=2	μ	ν_μ	c	s
G=3	τ	ν_τ	t	b

- Not well motivated theoretically – not result of invariance with respect to gauge transformation as in electric charge conservation
- Tested experimentally in many processes
- Mass scale probed is very high –
  $\Gamma(\mu^- N \to e^- N)/\Gamma(\mu^- N \to \nu N') = 10^{-16} \Rightarrow M = 1000\, TeV/c^2$
- In essentially all extensions to Standard Model there exists LFV processes
- With advances in muon beam sources, huge improvements in sensitivity could be achieved

$\mu^- N \to e^- N$	$10^{-12} \to 10^{-16}$
$\mu^+ \to e^+\gamma$	$10^{-11} \to 10^{-14}$

Supersymmetric GUTs Motivation for LFV

- Supersymmetry is Perhaps the most realistic possibility for physics beyond the standard model
- There exist partners of all known particles – a fermion for every boson and *vice versa*
- Motivated by string theory
- Grand unified supersymmetric theories relate family structure of standard and supersymmetric sectors

$\Rightarrow$ the possibility of real predictions
$\Rightarrow$ the possibility of really seeing something

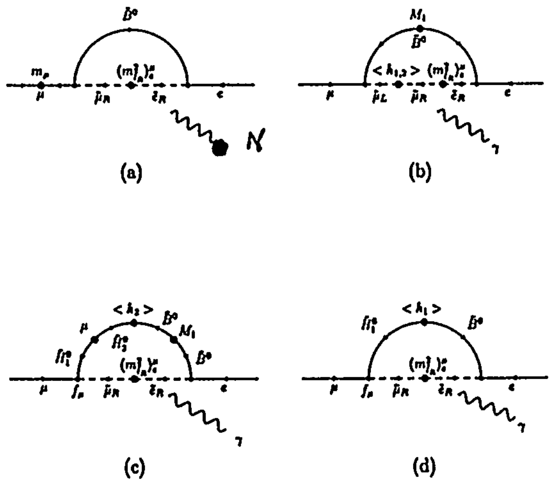

LFV Predictions From the Model of Hisano, et al.

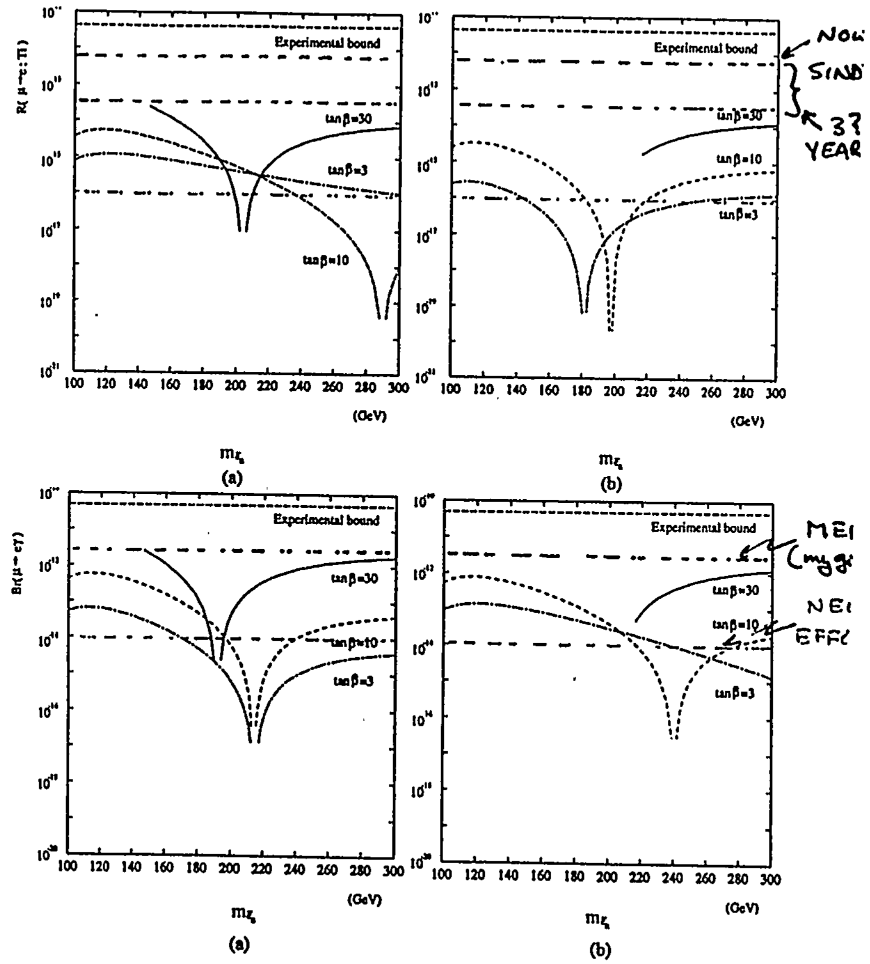

Outline of $\mu^- N \to e^- N$ Experiment

- Basic process:
  - Bring μ^- to rest in thin target
  - μ^- is captured in Coulomb orbit, cascades in
  - Can capture on the nucleus (inverse β decay)
  - Can decay in orbit
  - May convert to electron through interaction with nucleus
- Interaction is coherent over the nucleus
  - momentum transfer to nucleon is insufficient to excite nucleus
  - gain with respect to muon capture by factor of Z
- For many mechanisms, $\mu^- N \to e^- N$ is most sensitive test of LFV
- Experimental issues
  - Signature is very simple – 105 MeV electron
  - One particle final state ⇒
    no accidental coincidence background at high rates
  - Other sources of 105 MeV electrons heavily suppressed
  - Normalize to muon capture: $\mu^-(A, Z) \to \nu(A, Z - 1)$
  - Balance higher sensitivity at high Z vs.
    less experimental difficulties at low Z

Status of LFV Experiments

Best sensitivity for $\mu^- N \to e^- N$ is from SINDRUM2 at PSI

- $\Gamma(\mu^- N \to e^- N)/\Gamma(\nu N \to e^- N') < 8 \times 10^{-13}$
- Limited by "prompt" π, μ, e processes
- Presently eliminated by veto counter in beam
- Muon beam flux $10^7 s^{-1} \to 10^8 s^{-1}$

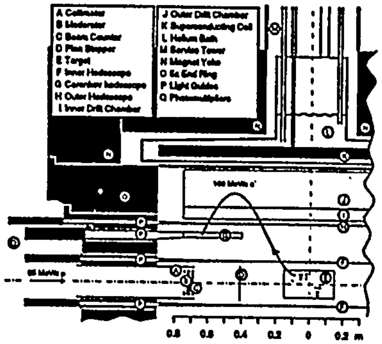

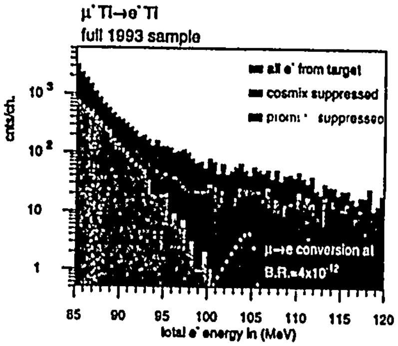

What's Needed for Improved $\mu^- N \to e^- N$ Search

- Higher intensity muon source – $10^{11} \mu s^{-1}$
- Pulsed muon beam
  - "prompt" π, μ, e processes must be eliminated
  - Can't use veto in beam
  - Background at 10^{-9} without beam veto

  $\Rightarrow$ (Beam off rate)/(Beam on rate) $< 10^{-8}$

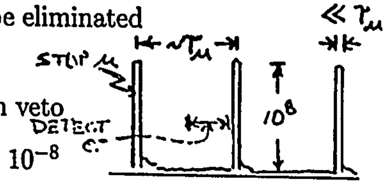

- New idea for muon source – can't increase proton flux by 10^4
  - Low energy accelerators + conventional beam
    $\Rightarrow 10^{-8} \mu/p$
  - Production target in solenoid with solenoid transport to muon stopping target
    (Lobashev MELC proposal with low energy accelerator)
    $\Rightarrow 10^{-4} \mu/p$
  - MELC proposal, except with 8-20 GeV beam
    (new initiative at BNL)
    $\Rightarrow 10^{-2} \mu/p$

Advantages of Building Muon Source at BNL

- Greatly increased muon flux per proton wrt low energy proton accelerators
- More muons per incident energy – easier job with shielding
- Muon beams also needed for muon collider
- Accelerator will be running as RHIC injector – incremental costs for running this experiment relatively small
- μ^-/μ^+ ratio near 1, so lower rates wrt low energy accelerator

---

Pulsed Proton Beams at BNL AGS

Two possibilities for achieving 1 MHz pulsed beams with $< 10^{-8}$ extinction

- Use RF structure of AGS, extract bunched
  - RF structure has 8 bunches in 2.7 μ sec revolution time
  - Beam extinction measured with one filled bunch extracted
  - Multicounter coincidence scaled at different times wrt RF structure
  - Counting rate of $< 10^{-6}$ between bunches
  - Counting rate of $< 10^{-3}$ in unfilled bunches

  } WRT FILLED BUNCH
- Use barrier bucket extraction
  - Insert two adjacent empty buckets in machine
  - Move them apart
  - Extract by moving particles into region between buckets and then to extraction
  - Tested for high frequency (100 MHz) pulsed extraction
  - Will be tested in coming year at AGS revolution frequency
- Other possibilities for improving extinction
  - Fast kicker magnets running at 1 MHz
  - RF phased with extraction to momentum disperse pulses wrt protons between pulses
  - Veto counter in beam active only during electron detection

Essential Features of MELC Muon Source at BNL

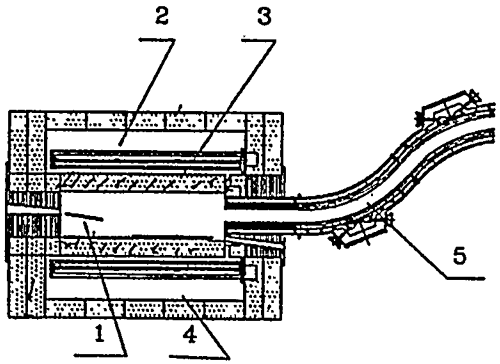

Target 8-24 GeV protons on heavy target in moderate field solenoid

- Possibly target backward to make dumping protons easy
- Pions with $p_T < 0.3Br/2$ are captured
  $r = 0.3m,\ B = 4T\ \Rightarrow\ p_T^{max}\ =\ 0.18\ GeV/c$
- Make single-ended bottle to get forward and backward pions
  - $sin^2(\theta)/B$ is constant, where $tan(\theta) = p_T/p_L$
  - pions will reflect if $B_f > B_i/sin^2(\theta_i)$
- Transport pions (and muons) in decreasing solenoidal field
  - avoid pion reflections
  - r grows only as $B^{-1/2}$
  - p_L increases, decreasing transit time

Solenoid Muon Capture System

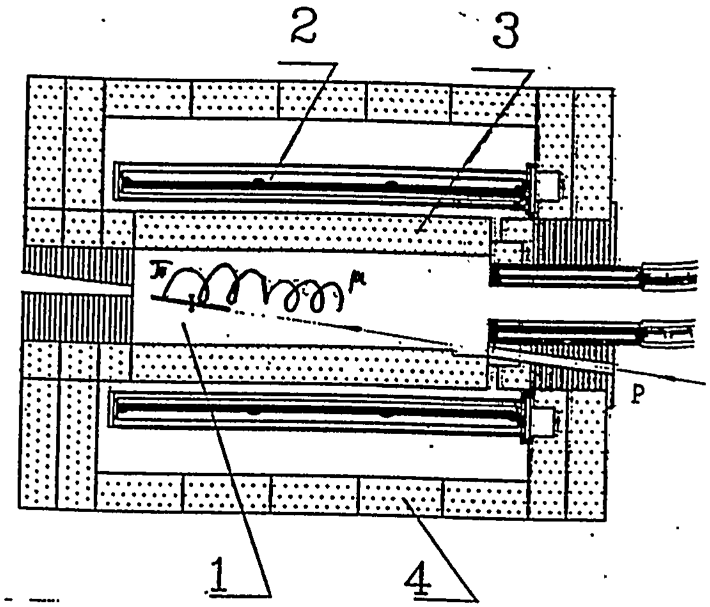

- **Proton Target (1)**
- **Superconducting Solenoid (2)**
- **Solenoid Shield (3)**
- **Iron York (4)**

Muon Yield in MELC Experiment at BNL

Muon yield is being studied with source and transport simulation with different models (Djilkibaev)

- No measurements for low energy and backward pion production
- Data recently taken (BNL E910) with TPC (interactions in gas)
- Muon yields depend on pion production model

Model	p E(GeV)	B_{ps}(T)	B_{ts}(T)	μ/p)
FLUKA	8.	2.5	2.0	0.004
SHIELD	8.	2.5	2.0	0.008
GHEISHA	8.	2.5	2.0	0.009

- Muon yield depends on production solenoid field

Model	p E(GeV)	B_{ps}(T)	B_{ts}(T)	μ/p)
SHIELD	14.	2.5	2.0	0.018
SHIELD	14.	4.0	2.0	0.030
SHIELD	14.	7.0	7.0	0.130

- Muon yield depends on proton energy

Model	p E(GeV)	B_{ps}(T)	B_{ts}(T)	μ/p)
SHIELD	14.	2.5	2.0	0.018
SHIELD	8.	2.5	2.0	0.008

- For many models and parameters μ/p exceeds 0.01

Charge Selection and Pion Absorption in Source

- Transport in curved solenoid (torroid) results in charge separation normal to bend plane
  - Drift distance of helix center given by:
    $$D \ = \ 1./(0.3B) \ \times \ s/R \ \times \ p^2/p_s$$
  - B is field in curved solenoid
  - s is distance along curved solenoid
  - R is the radius of curvature of solenoid
  - p and p_s are momentum and momentum along solenoid axis
  - $s/R = \pi/2,\ p = 0.15\ GeV/c,\ p_s = 0.12\ GeV/c,\ B = 2T$
    $\Rightarrow D = 0.49\ cm$
  - Positive (or negative) muons could be absorbed
  - High momentum muons could be preferentially degraded
- Pions and electrons return to axis of solenoid, muons in general do not
  - Absorber on axis reduces pion and electron flux

Charge Dispersion in Curved Solenoid Transport

- Solenoid bend radius 25 m
- Magnetic field in solenoid 7 T
- Path length along solenoid 20 m

MUON COLLIDER SIMULATION

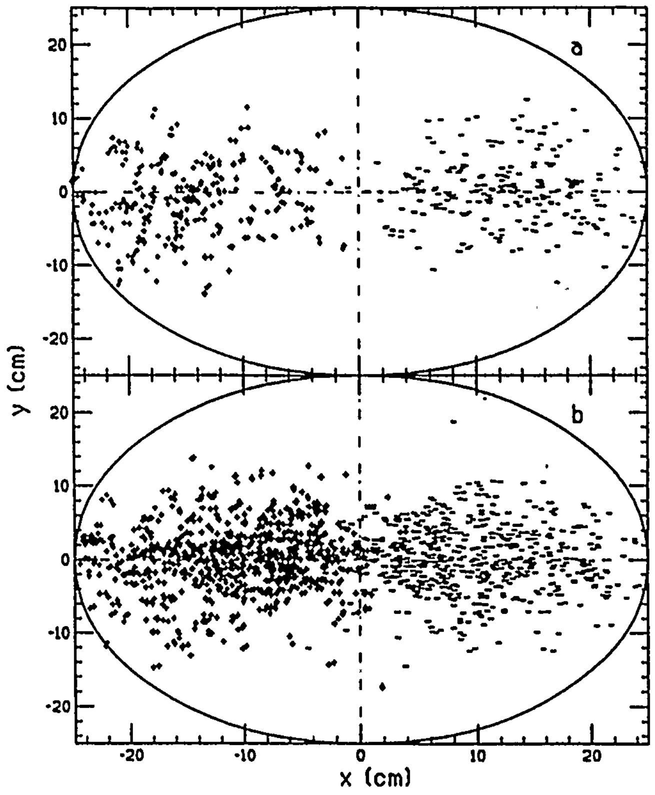

Muon Collider Overview

- $\mu^+\mu^-$ collider with CM energy 0.5-4.0 TeV
- At 4 TeV, luminosity of $10^{35}\ cm^{-2}s^{-1}$ is required to reach physics goals
- Demonstration machine could be 0.5 TeV at luminosity of $< 10^{32}\ cm^{-2}s^{-1}$
- Muon beam must be pulsed
  - Repetition rate of proton accelerator of 2.5-30 Hz
  - Very short (1-3 ns) proton pulse length
  - few × 10^{12} muons per bunch must be captured and accelerated

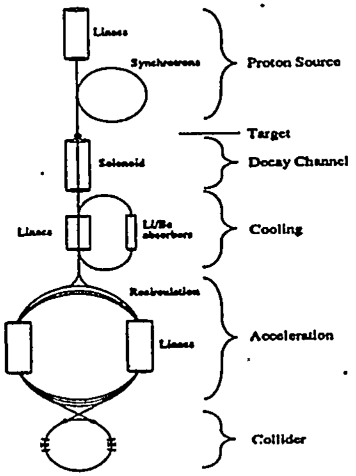

INTERLABORATORY AND UNIVERSITY COLLABORATION

Argonne National Laboratory, Argonne, IL 60439-4815, USA
Brookhaven National Laboratory, Upton, NY 11973-5000, USA
Fermi National Accelerator Laboratory, Batavia, IL 60510, USA
F. Bitter National Magnet Laboratory, MIT, Cambridge, MA 02139, USA
Lawrence Berkeley National Laboratory, Berkeley, CA 94720, USA
Stanford Linear Accelerator Center, Stanford, CA 94309, USA
Center for Advanced Accelerators, UCLA, Los Angeles, CA 90024,USA
Columbia University, New York, NY 10027, USA
Fairfield University, Fairfield, CT 06430-5195, USA
Indiana University, Bloomington, IN 47405, USA
SUNY, Stony Brook, NY 11974, USA
University of California, Berkeley, Berkeley, CA 94720-7300, USA
University of California, Davis, CA 95616, USA
University of Mississippi, Oxford, MS 38677, USA
University of Virginia, Charlottesville, VA 22901, USA
University of Wisconsin, Madison, WI 53706, USA
BINP, RU-630090 Novosibirsk, Russia
KEK, Tsukuba-shi, Ibaraki-Ken 305, Japan
DESY, Hamburg, Germany

Muon Source for Muon Collider

- Problems much harder than with source for muon experiments
  - – Requires 1-3 × 10^{13} accelerated muons per second
  - – Losses in acceleration cycle
  - – Muons must be cooled to be captured into accelerating structure
- ⇒ much more aggressive approach to muon source
  - – Same basic idea of heavy target on axis of solenoid
  - – 10^{14} protons per pulse at 2.5-15 Hz on target
  - – Reach target temperature limits
  - – Much higher field in solenoid – 20-28 T
  - – Much shorter pulse length in order to phase rotate (compress energy spread by increasing time spread)
  - – Need to operate RF cavities near production solenoid
- Same uncertainty in pion production cross sections
- Need to produce both μ^+ and μ^- – pointed out technique for charge separation in bent solenoid

Muon Collider Collection Solenoid and Target

- Very high field (20-28 T) produced by copper "insert" magnet and superconducting "outsert" magnet
- Copper magnet provides 10 T field and heat and radiation shield for 10 T superconducting magnet
- Target solenoid matched to 7 T transport solenoid
- Various options for target material considered

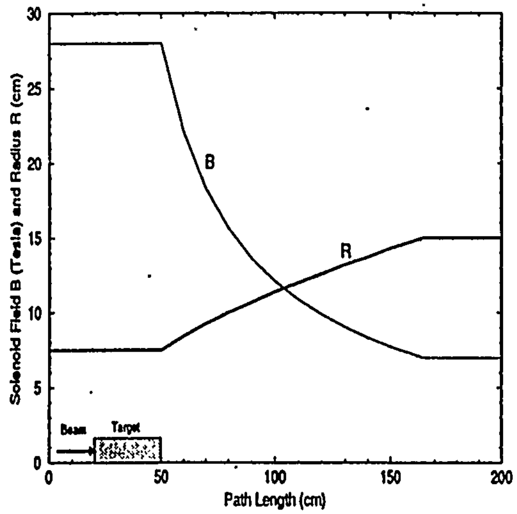

Options for Target Solenoid Construction

- Matching with RF cavities inside magnet

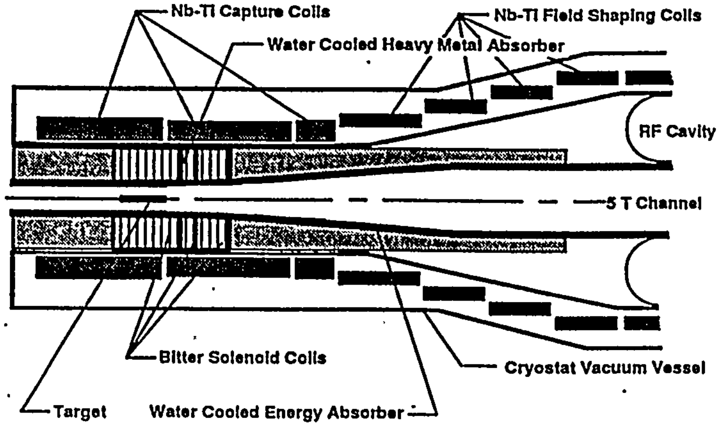

- Matching with RF cavities outside magnet

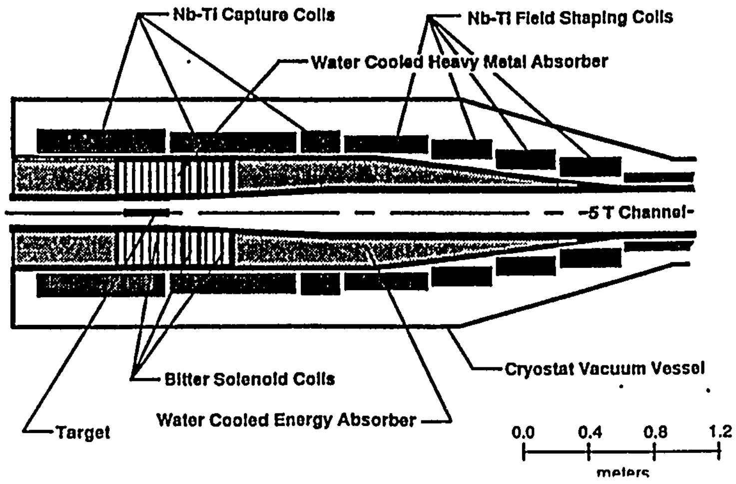

Pion Fluxes and Operating Parameters

Parameter List	8 GeV C	8 GeV Cu	8 GeV Hg	30 GeV C	30 GeV Cu	30 GeV Hg
N_p/bunch, 10^{13}	5	5	5	2.5	2.5	2.5
$N_{bunches}$	2	2	2	4	4	4
σ_t (nsec)	1	1	1	1	1	1
f_{rep} (Hz)	30	30	30	15	15	15
P_{beam} (MW)	3.8	3.8	3.8	7.2	7.2	7.2
ϵ_{Nrms}, 10^{-5} (m-rad)	4	4	4	4	4	4
ϵ_{rms}, 10^{-6} (m-rad)	4.2	4.2	4.2	1.3	1.3	1.3
β_{target} (m)	3.8	3.8	3.8	12	12	12
$\sigma(x)$ (mm)	4	4	4	4	4	4
$\sigma(x')$ (mrad)	1	1	1	0.3	0.3	0.3
B_{sol} (T)	28	28	28	28	28	28
a_{sol} (cm)	7.5	7.5	7.5	7.5	7.5	7.5
$p_{\perp max}$ (GeV/c)	0.314	0.314	0.314	0.314	0.314	0.314
A_N (m-rad)	0.17	0.17	0.17	0.17	0.17	0.17
L_{target} (cm)	57	22.5	21	57	22.5	21
r_{target} (cm)	1	1	1	1	1	1
π^+/p (MARS)	0.50	0.58	0.56	0.91	1.16	1.22
π^-/p (MARS)	0.41	0.50	0.48	0.83	1.05	1.08
π^+/p (ARC)	0.52	0.62	0.59	1.31	1.62	1.56
π^-/p (ARC)	0.37	0.51	0.52	1.15	1.62	1.53
ρ (g/cc)	2.26	8.96	13.55	2.26	8.96	13.55
C_v (J/g/K)	0.7	0.39	0.14	0.7	0.39	0.14
α, 10^{-6} (/°C)	2.9	17	-	2.9	17	-
E_Y, 10^6 (psi)	1.6	17	-	1.6	17	-
Avg. P_{target} (kW)	140	360	550	125	600	950
Max. ρ_E (J/g)	40	52	70	60	180	200
Max. ΔT (°C)	60	140	500	80	420	1400
Max. Pres. (kpsi)	0.436	116	-	0.581	348	-
Pow. Den. (kW/cc)	0.782	5.0	8.2	0.625	8.5	14.4
Heat Flux (kW/cm^2)	0.392	2.54	4.2	0.353	4.24	7.2

PROTON DRIVER

SOLENOID PROPERTIE

PION YIELD

TARGET HEATING

Pion Production Model Comparisons

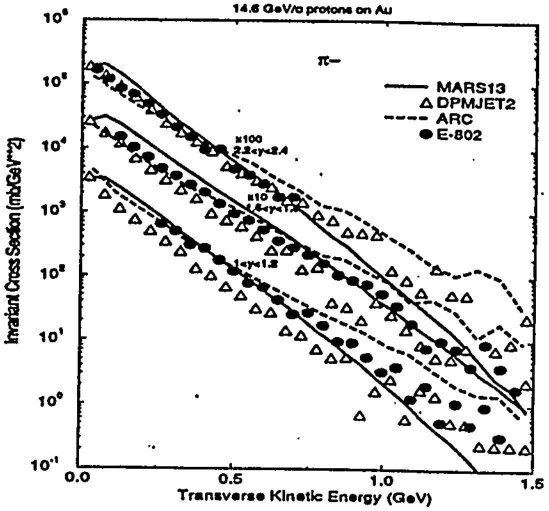

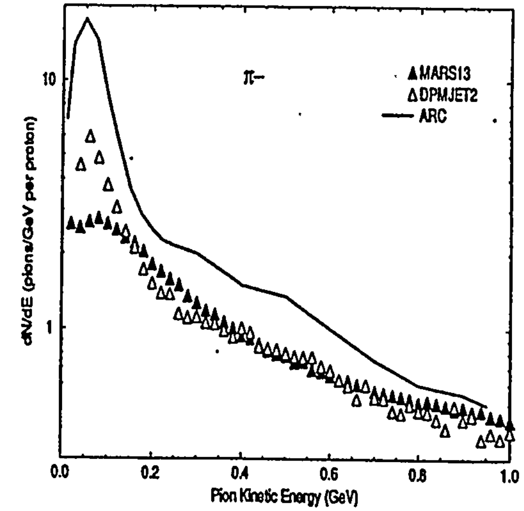

High Intensity Muon Source Summary

Required for (relatively) short term experiments and for promising new lepton collider

- Muon experiments for LFV search
  - Modest intensity on scale of muon collider
  - Uses many of same techniques
  - Early payout in physics
- Muon collider
  - Very intense source, at limit of technology
  - One of many aspects of muon collider which needs to be shown to work
  - Has potential for bringing substantial resources to developing techniques

---

- Aspects of development in common
  - Solenoid capture scheme in relatively high field
  - Dependence on pion production cross sections
  - Problems with heat and radiation shielding
- Aspects not in common
  - Muon beam time structure is very different
  - Very cool beam needed for collider is good for LFV experiments, but probably too expensive
  - Time scale for development different
  - Required intensity different, and hence details of target solenoid different

⇒ Projects are mutually beneficial, muon collider work will advance source for experiments, and experiments will provide early payout for developing technology for long timescale accelerator project

OBSERVATION OF NONLINEAR QED EFFECTS IN ELECTRON-LASER COLLISIONS

C. Bula, Princeton University

Observation of Nonlinear QED Effects in Electron-Laser Collisions

Christian Bula
Princeton University

(for the E-144 collaboration)

Symposium on New Modes of Particle Acceleration - Techniques and Sources

Santa Barbara, August 1996

The E-144 Collaboration

C. Bula, K. McDonald, and E. Prebys
Joseph Henry Laboratories
Princeton University

C. Bamber,[1] S. Boege,[1] T. Kotseroglou,[1] A. Melissinos,[1]
D. Meyerhofer,[2,3] and W. Ragg[1]
[1] *Department of Physics and Astronomy,*
[2] *Department of Mechanical Engineering,*
[3] *Laboratory for Laser Energetics*
University of Rochester

D. Burke, R. Field, G. Horton-Smith, A. Odian, and D. Walz
Stanford Linear Accelerator Center
Stanford University

S. Berridge, W. Bugg, K. Shmakov, and A. Weidermann
Department of Physics and Astronomy
University of Tennessee

Outline

- Introduction
- Experimental Setup
- Data Analysis and Results
- Summary and Outlook

Tests of QED

QED is extensively tested in the weak field regime.

- Nonlinear Optics:

  Test of QED at moderately strong fields.

  ⇒ Fields of order 10^8 V/cm are produced by focused laser beams and their interaction with atomic systems is investigated.

- E-144:

  Test of QED in fields comparable to the critical field strength of QED and in the realm where multiphoton interactions are important.

  ⇒ Study of interactions between 46 GeV electrons and photons at the focus of a Terawatt laser.
  In the rest frame of the electron, the field reaches 10^{15} - 10^{16} V/cm.

Multiphoton Interactions

- Coherent interaction of an electron with n field photons at a single space-time point.
- They become important when the parameter

$$\eta = \frac{eE_{rms}}{m\omega_o c} = \frac{e}{mc^2}\sqrt{A_\mu A^\mu} \longrightarrow 1$$

⇒ accessible in low amplitude, low frequency fields

Classical Picture

- A free electron in a circularly polarized field undergoes transverse circular motion with angular frequency ω_o and velocity $\beta_\perp = v_\perp / c$ given by

$$\eta = \gamma_\perp \beta_\perp, \qquad \text{with} \quad \gamma_\perp = (1 - \beta_\perp^2)^{-1/2}$$

⇒ weak field or non-relativistic limit: $\eta \simeq \beta_\perp$

- As η approaches unity, the classical radiation spectrum of an accelerating electron includes the nth harmonic of the wave frequency ω_o (multipole radiation).

  The emission rate of the nth order multipole is

$$Rate \propto \eta^{2n} \propto I^n$$

⇒ nonlinear for n > 1

Quantum Mechanical Picture

- The electron absorbs n wave photons and emitts a single high energy photon.

$e + n\ \omega_o \to e' + \omega$

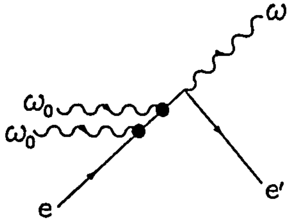

⇒ nonlinear Compton scattering

Light-By-Light Scattering

- The production of electron-positron pairs in electron laser collisions at the critical field strength can be interpreted as

  – inelastic light-by-light scattering or
  – production of matter in light-by-light collisions.

Beamstrahlung

- Field strength at laser focus is comparable to field of bunch at future e^+e^- collider.

  ⇒ $e + n\,\omega_0$ interactions with large n are similar to beamstrahlung.

- $e + n\,\omega_0 \to e'\,e^+e^-$ is close analog of important pair production background in future colliders.

The Critical Field of QED

- At the critical field, the voltage drop across a Compton wave length is equal to the electron rest mass:

$$E_{crit} = \frac{m^2c^3}{e\hbar} = 1.32 \times 10^{16}\ \mathrm{V/cm}$$

- Field strength are characterized by Schwinger parameter

$$\Upsilon = \frac{E_{rest}}{E_{crit}} = 2\gamma\, E_{lab} \frac{e\hbar}{m^2c^3}$$

- The electric field in the rest frame of a high energy electron is

$$E_{rest} = (1+\beta)\gamma\, E_{lab} \simeq 2\gamma\, E_{lab}$$

⇒ **E144:** In the rest frame of 46 GeV electrons ($\gamma = 9\text{x}10^4$), the critical field strength can be reached with a focused laser pulse of

$$E_{lab} = 7 \times 10^{10}\ \mathrm{V/cm}$$

- At the critical field, the vacuum "sparks" into e^+e^- pairs.

  ⇒ Expect copious e^+e^- pair production.

- Experiment is set up at the Final Focus Test Beam (FFTB) at SLAC.
- In a first phase, we study nonlinear Compton scattering and pair production at the electron-laser interaction point (beamstrahlung).
- Measure rates of electrons, gammas and positrons produced at the electron-laser interaction point.
- Use FFTB dump magnets as spectrometer.

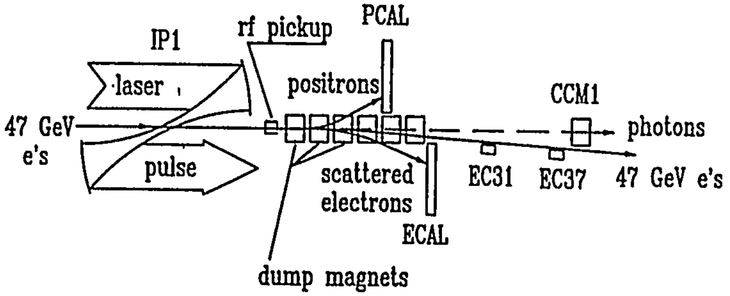

Experimental Program

Nonlinear Compton Scattering

- Measure electron spectrum beyond the linear Compton edge.
- Test nonlinear dependence of scattering rate on laser intensity for $n > 1$
- Measure spectrum of backscattered gammas and confirm shift of linear Compton edge due to increased effective electron mass in strong field, i.e. $\overline{m}^2 = m^2 (1+\eta^2)$.

Pair Production (Beamstrahung)

- Measure cross section and energy spectrum of positrons produced at the electron-laser interaction point.

Other Motivations

- Pair Production in electron-laser collisions could be excellent low emittance positron source for future colliders (no Coulomb scattering in laser target).
- Electron-laser collision technology of E-144 is precursor of e–γ and γ–γ colliders.

Laser System

- Table-top terawatt (T^3) laser.
- Phase locked to Linac RF.
- Principal: chirped pulse amplification (CPA).
  - ⇒ Stretch pulse, then amplify and compress.
- Operates at 2 wavelengths: IR (1054 nm) and green (527 nm).

- Design parameters:
  - – energy per pulse: 1 Joule for green ($\lambda = 527$ nm)
  - – pulse duration: 1.0 psec FWHM
  - – focal spot area: 15 μm^2 for green
  - – repetition rate: 1/2 Hz

- Intensities achieved (and maintained): ~ 10^{18} W/cm^2
  - ⇒ $\eta \cong 0.6$, $Y \cong 0.3$
  - ⇒ Photon density ~ $2 \times 10^{26}/\text{cm}^3$
  - ⇒ Radiation length $X_0 \sim 0.5$ mm (Pb: $X_0 = 5.6$ mm)
  - ⇒ "Photon solid"

Schematic of Terawatt Laser System

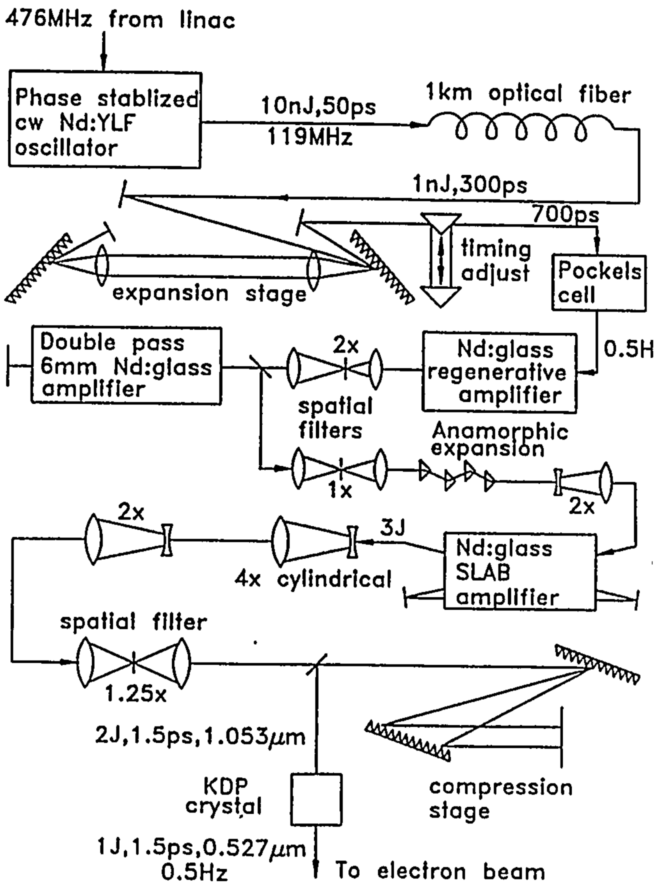

Electron Beam

- Energy: 46.6 GeV
- Charge: 5×10^9 e^- per bunch
- Bunch length: $\sigma_z \cong 870\ \mu m$ => FWHM(t) $\cong$ 7 psec
- Spot size: $\sigma_x \cong 40\ \mu m$, $\sigma_y \cong 40\ \mu m$ (typical)

Gamma Beam

- Process: Backscattered laser photons, dominated by ordinary (n=1) Compton scattering.
- Energy: 0 - 30 GeV for green laser and n=1.
- Intensity: ~ 10^7 gammas per laser shot.

⇒ High efficiency for converting e^- beam to gamma beam.

⇒ ~ 20 % of e^- passing through laser focus scatter.

Gas Cerenkov Counter CCM1

- Monitors the backscattered gamma rate (~ linear Compton rate).
- Primary measure of electron-laser overlap.
- Used to normalize the nonlinear signal.

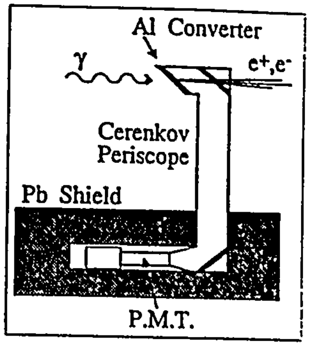

Silicon-Tungsten Calorimeters ECAL and PCAL

- 23 layers of Si and 1 X_0 of Tungsten.
- 12 (16) rows and 4 columns of 1.6 x 1.6 cm^2 pads.
- Layers for each pad are ganged into 4 longitudinal segments.
- Resolution:

$$\frac{\Delta E}{E} = \frac{0.19}{\sqrt{E}} + \frac{0.4}{E}$$

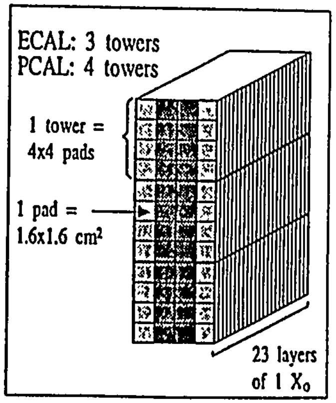

Laser Electron-Beam Overlap

- Scan laser focus across e⁻ beam in space and time.
- Monitor linear (CCM1) and nonlinear (Ecal) Compton-scatter rates.

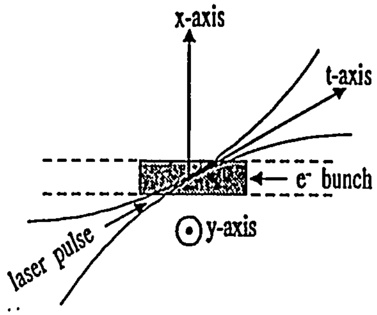

time scan

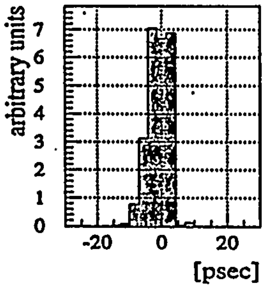

x scan

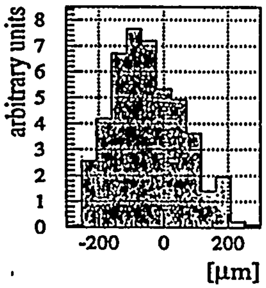

y scan

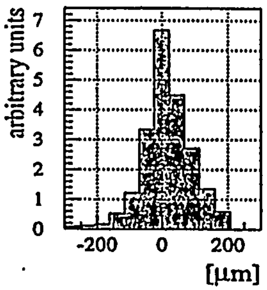

xt scan, linear rate

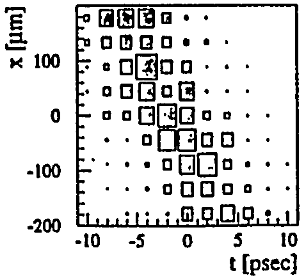

xt scan, nonlinear rate

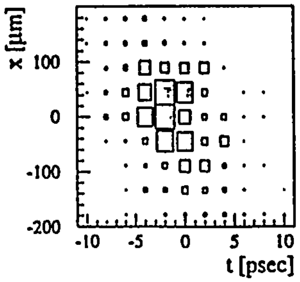

Nonlinear Compton Scattering

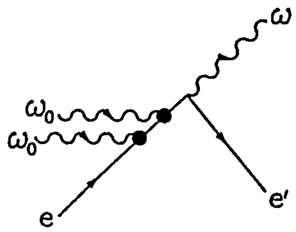

$e + n\omega_0 \to e' + \omega$

Spectra for E-144 Configuration

- IR laser ($\lambda = 1054$ nm)
- Intensity at laser focus 10^{18} W/cm² ($\eta = 0.64$)

gamma spectrum

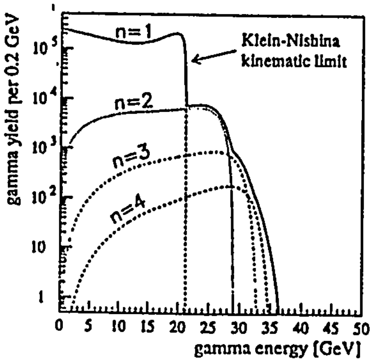

electron spectrum

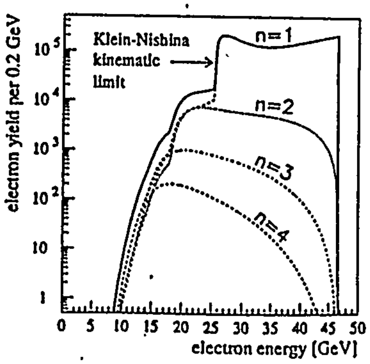

-photon Absorption vs
Incoherent "Multiple Scattering"

- Nonlinear Compton
  (coherent)

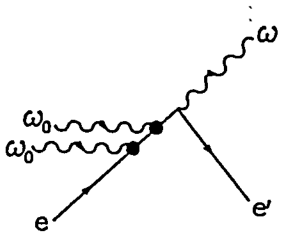

- Multiple Linear Compton
  (incoherent)

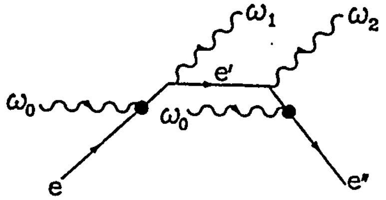

- Kinematics of the final state electrons are identical.
- Both processes are nonlinear in laser intensity.
- Spectra of final-state electrons are similar.
- Rates for E-144 configuration are comparable.

⇒ Hard to distinguish by measuring final state electrons. Gamma spectrum is free from this ambiguity.

- Cross section depends on laser intensity, which varies in spac
  and time.

  ⇒ Invariant cross section cannot be defined.

- From energy measured in ECAL row, we obtain the number of incident electrons per momentum interval:

$$\frac{dN}{dp} = \frac{E}{\langle p \rangle \Delta p}$$

- Normalize with gamma rate to form normalized yield:

$$\frac{1}{N_\gamma}\frac{dN}{dp} \simeq \frac{1}{\sigma_\mathrm{T}}\left\langle\frac{d\sigma}{dp}\right\rangle$$

  ⇒ Effects of timing jitter, errors in electron beam parameters cancel to 1. order.

- Comparison with theoretical predictions by numeric integration of $\frac{1}{\sigma_\mathrm{T}}\left\langle\frac{d\sigma}{dp}\right\rangle$ over space and time for each event.

- Simulation takes into account:
  - correct interaction geometry,
  - nonlinear and multiple Compton scattering and combinations of the two.

Green, Circularly Polarized Laser

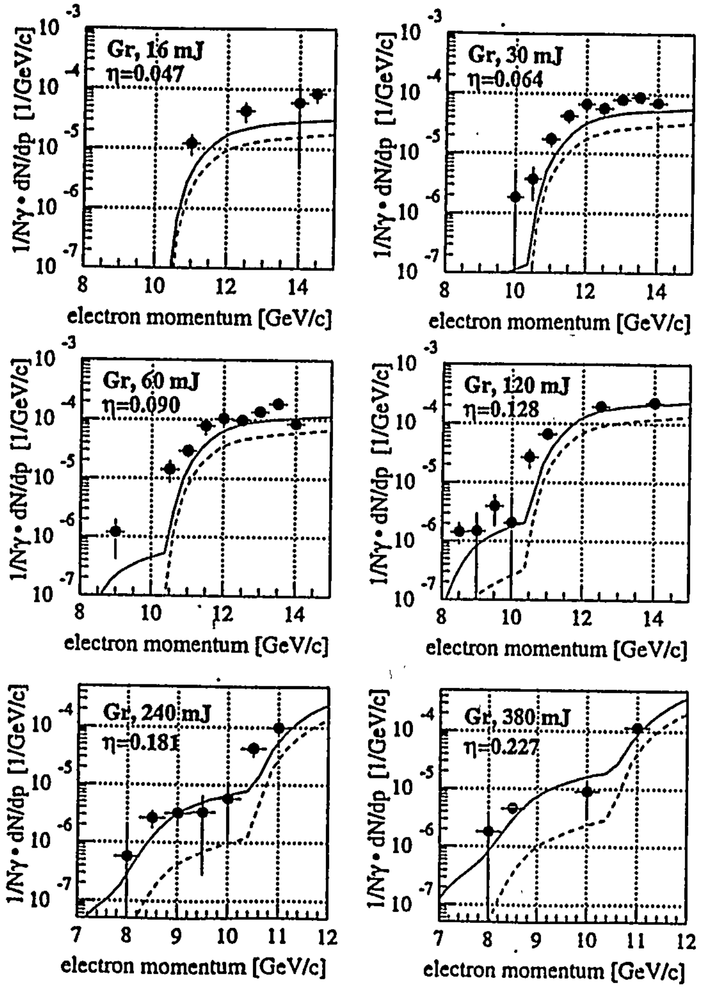

Christian Bula, Princeton University

IR, Circularly Polarized Laser

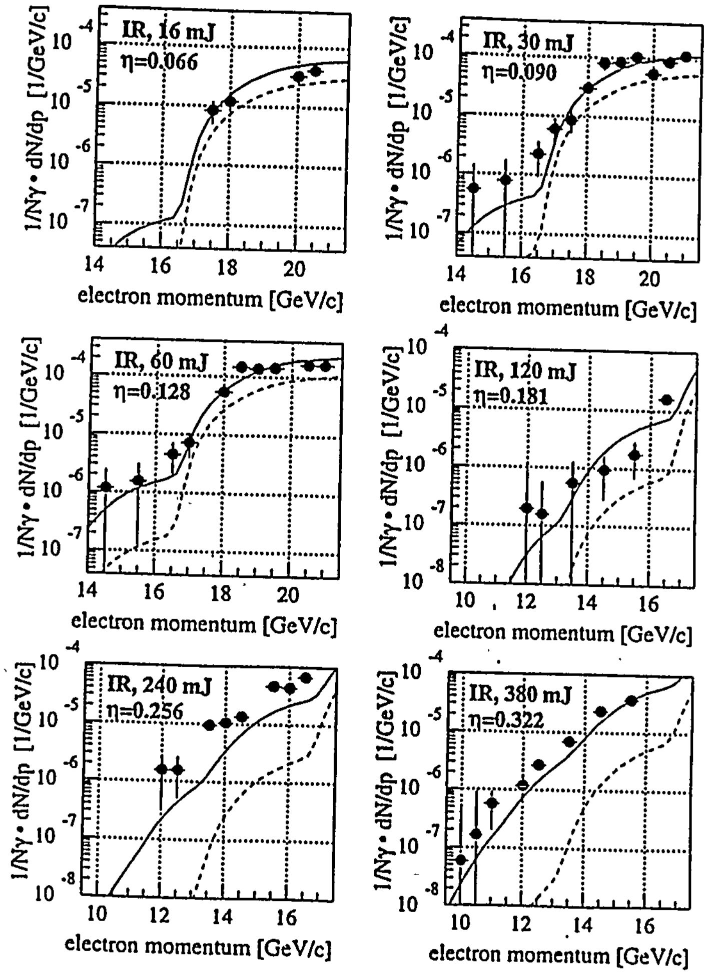

Christian Bula, Princeton University

- In 1. order approximation we expect

$$\frac{1}{N_\gamma}\frac{dN}{dp} \propto \eta^{2(n-1)} \propto I^{n-1}$$

- The shaded bands represent the simulation, including an uncertainty in laser intensity of
  - +/- 30 % for IR,
  - +50 / -30 % for green.

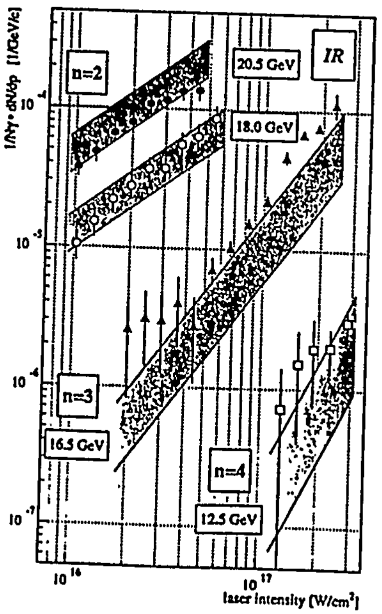

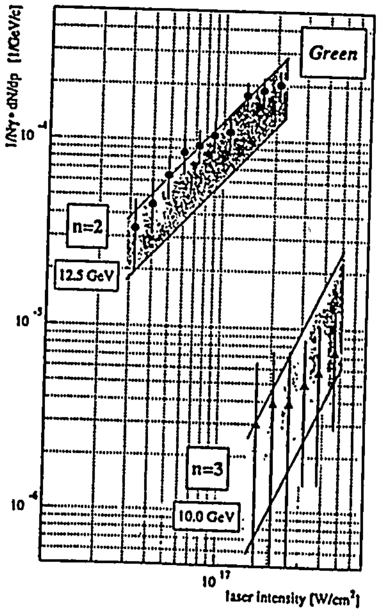

- With 46.6 GeV e⁻, pair creation is below single photon threshold.

  ⇒ Green laser is favorable, since $\gamma + n\omega_0 \rightarrow e^+e^-$ with gammas from (linear) Compton scattering needs

  $n >= 4$ for green and $n >= 8$ for IR

- Two processes contribute to pair production:

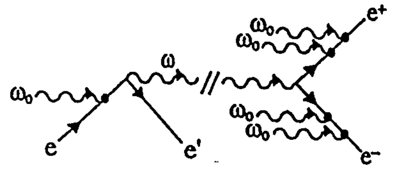

multi-photon Breit-Wheeler
2-step, real photon

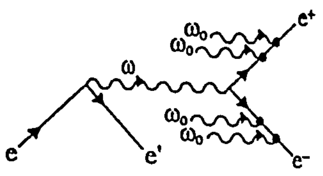

trident
1-step, virtual photon

- Calculated positron spectra for E-144 configuration:

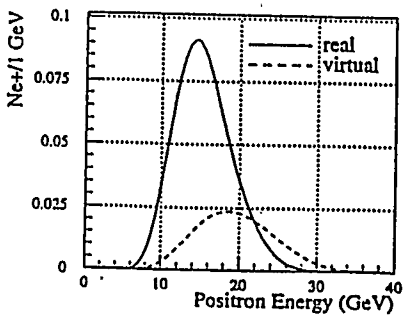

  - green laser (λ = 527 nm)
  - Y ≅ 0.4

September 94

- First positron search in electron-laser collisions.
- **Result:** 13 positrons with expected background of 4.3

December 95

- **Electron beam:** huge backgrounds due to wire mesh in beam.
  - ⇒ lots of beam tuning, unstable conditions.
  - ⇒ large spot at IP1: ~ 150 x 50 μm^2
- **Laser:** Green, 700 - 800 mJ, very stable.
- **Result:** 133 +— 22 pairs
  - ⇒ ~ 1 pair / 100 laser shots
  - ⇒ ~ 6 sigma effect

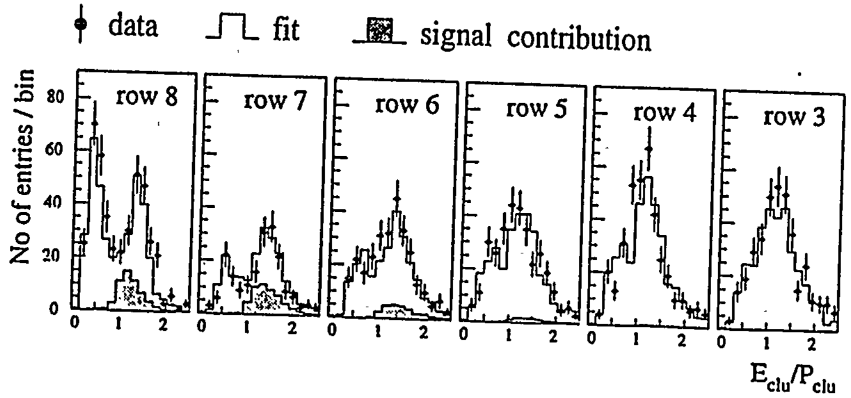

August 96

E-144

Preliminary Evidence for Positron Production in Laser-Gamma Interactions (Laser Energy ~ 650 mJ)

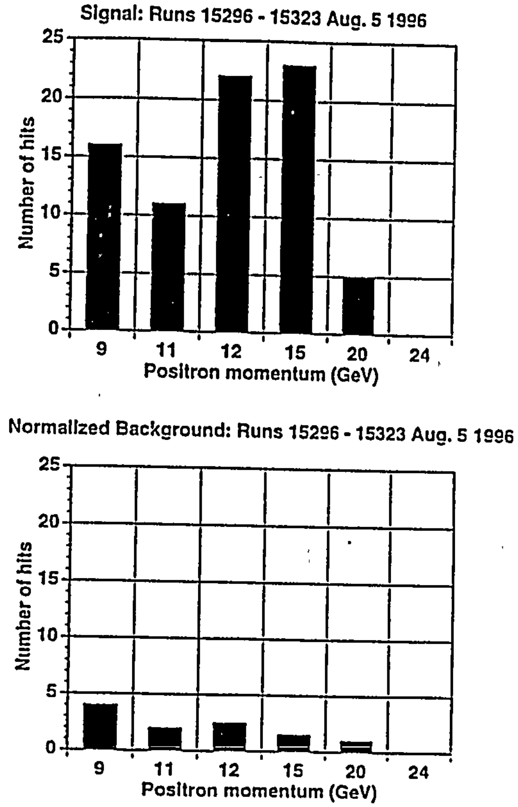
Signal: Runs 15296 - 15323 Aug. 5 1996

Normalized Background: Runs 15296 - 15323 Aug. 5 1996

- Nonlinear Compton Scattering (March 95)
  - Observed clear nonlinear signal in electron spectrum.
  - Measured electron rates in n = 2, 3 and 4 region.
  - Dependence of scattering rates on electron momentum and field intensity is in good agreement with theoretical calculations over 3 orders of magnitude.
- Positron Production
  - First indication of positron signal observed in two previous run periods (Sept 94 and Dec 95).
  - Preliminary evidence of pair production in August 96 run. Detailed analysis just started.

Outlook

- n. = 2 signal and mass shift effect in gamma spectrum (CCD spectrometer).

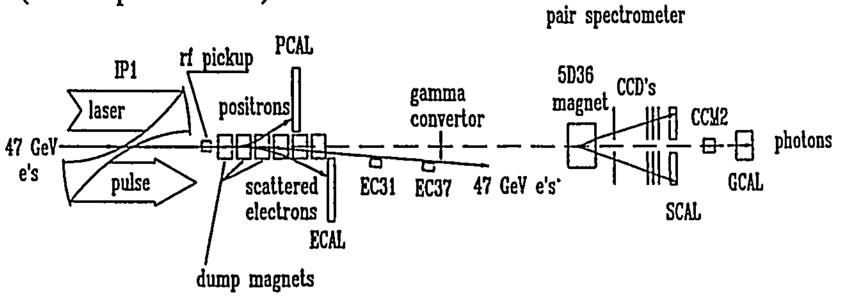

Far Future

- "Light-by-Light" scattering with real photons at IP2
  - pair production cross section
  - pair invariant mass spectrum

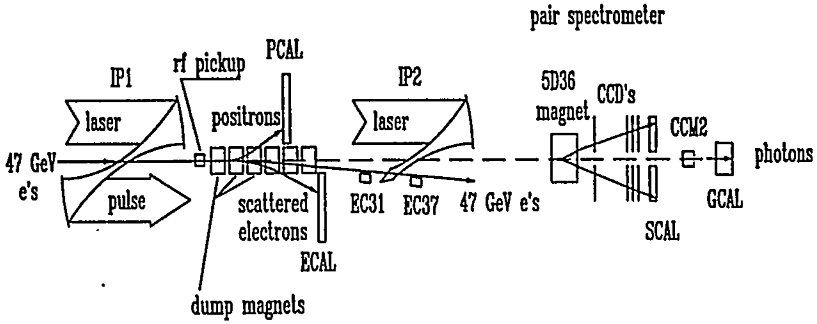

SYN2- A NEW MODEL FOR TRACKING SPACE CHARGE PERTURBED SYNCHTOTRON BEAMS

M. Ottinger, Univ. Texas

SYN2D:
PARTICLE TRACKING CODE

MICHAEL OTTINGER
UNIVERSITY OF TEXAS

AUGUST 22, 1996

OUTLINE

I. PROBLEM
II. NEW MODEL & CODE
III. DATA COMPARISON
III. RESONANCE ANALYSIS
V. CONCLUSIONS

PERTURBED BEAMS IN SIMPLE, LOW ENERGY SYNCHROTRONS.

LATTICE:

1. CIRCUMFERENCE: < 50 [illegible]
2. ELEMENTS: PRIMARILY DIPOLE & [illegible]
3. PHASE ADVANCE: [illegible]
4. RF HARMONIC: CONSTANT [illegible]

BEAM:

1. PARTICLES: PROTONS
2. EMITTANCE: < 100 π mm-mrad
3. CURRENT: [illegible]
4. ENERGY: 5 - 150 MeV
   "EMITTANCE TO [illegible]"

RUN LENGTHS:

1. [illegible]
2. [illegible]
3. [illegible]

PREVIOUS TRACKING CODES:

1. **TEAPOT** - CONVERTS MAGNETS TO THIN ELEMENTS AND TRACKS SINGLE PARTICLES THROUGH LATTICE. - NO SPACE CHARGE
(Schachinger & Talman P.A. 1987, pp35-46)

2. **SIMPSONS** - TRACKS ~1000 MACROPARTICLES AROUND THIN ELEMENT LATTICE, CALCULATING SPACE CHARGE KICK EACH TIMESTEP BY SOLVING POISSON'S EQ. ON A 10×10×10 GR
(MACHIDA SSCL-PrePrint-197)

PROBLEMS: FOR A 50 m BEAM, 1 PARTICLE

SYN2D

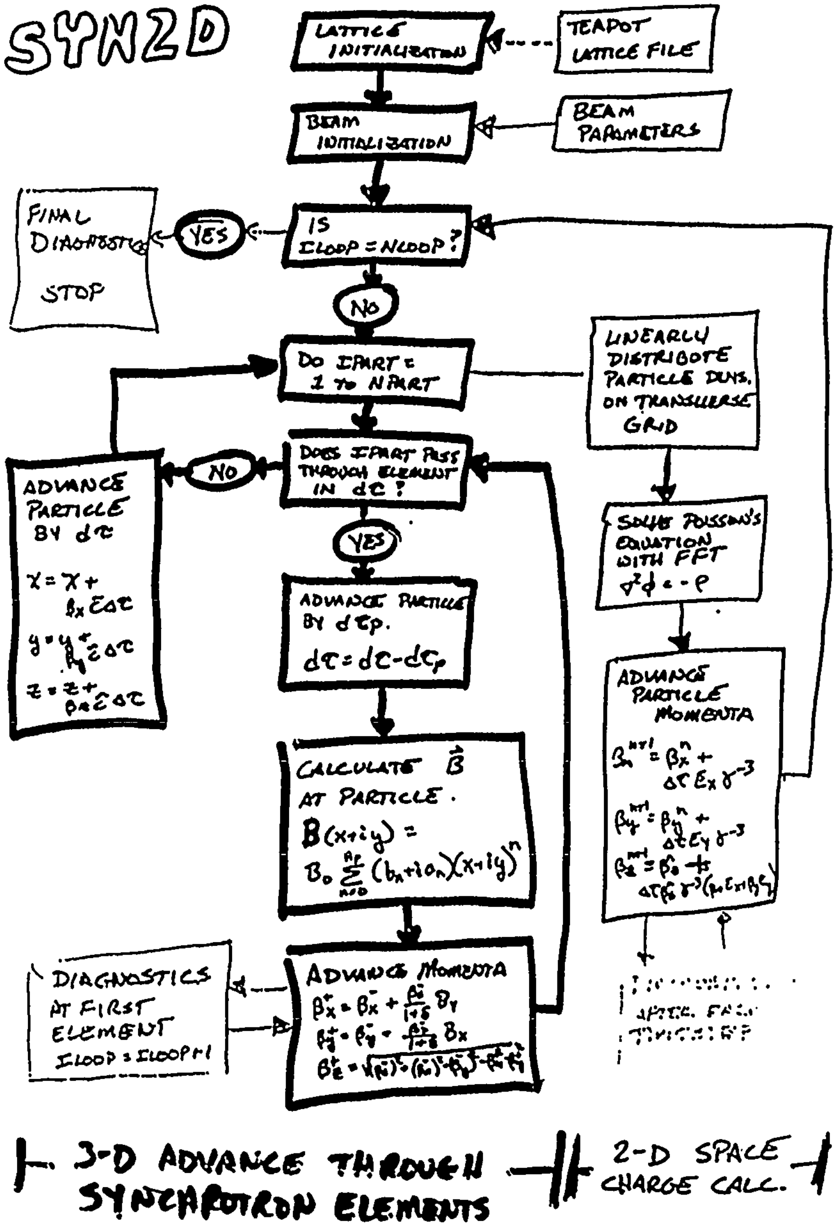

II. NEW MODEL & CODE

ASSUMPTIONS:

1. INFINITELY LONG BEAM
(VALID FOR $S >> \sigma_x, \sigma_y$)

2. STRAIGHT BEAM
(VALID FOR $r_c >> \sigma_x, \sigma_y$)

3. UNIFORM BEAM
(VALID FOR $\sigma_x(s)$ & $\sigma_y(s)$ SLOWLY VARYING)

4. LONGITUDINAL VELOCITY >> TRANSVERSE VELOCITY ($\beta_s >> \beta_x, \beta_y$)

SPACE-CHARGE ELECTRIC FIELD IS LONGITUDINALLY INDEPENDENT.

UNITLESS PARTICLE EQUATION OF MOTION:

$$\frac{d\gamma\vec{\beta}}{d\tau} = \vec{E} + \vec{\beta} \times \vec{B} \quad \text{(LORENTZ FORCE)}$$

$$= \underbrace{\vec{E}(1-\beta^2)}_{\text{TRANSVERSE}} + \underbrace{(\vec{\beta}\cdot\vec{E})\vec{\beta}}_{\text{LONGITUDINAL}}$$

WHERE $\vec{E}$ IS OBTAINED FROM 2-D SOLUTION TO GAUSS' LAW $\nabla \cdot E = \rho$

FINITE DIFFERENCED EQ OF MOTION:

$$\beta_x^{n+1} = \beta_x^n + \Delta\tau E_y \gamma^{-3}$$
$$\beta_y^{n+1} = \beta_y^n + \Delta\tau E_y \gamma^{-3}$$
$$\beta_s^{n+1} = \beta_s^n + \Delta\tau \beta_s^n \gamma^{-3} [\beta_x^n E_x + \beta_y^n E_y]$$

1. EMPIRICAL EQUATION ——

$$V_{x,y} = -\frac{1}{4\pi}\int_s \beta_{cs}^{x,y} K_{x,y}(s)\,ds$$

$$K_{x,y}(s) = \underset{Synch.}{K_{x,y}(s)} - \frac{e^2 n_0 b}{\epsilon_0 (a+b)\gamma^3 mc^2\beta^2}$$

Assuming a, b, n_0, β_{cs} vary only slightly

$$V_{x,y} = V_{x,y_0} - \frac{e^2\, S\bar{\beta}_{cs}^{x,y}\, \bar{b}\bar{n}_0}{4\pi\epsilon_0\gamma^3 mc^2\beta_s^2(\bar{a}+\bar{b})}$$

$$\boxed{\Delta V_{x,y_0} = \frac{I\,Se}{16\pi^2\epsilon_0 mc^3\beta^2\gamma^3\epsilon_{x,y}\left(1+\sqrt{\frac{\epsilon_{y,x}}{\epsilon_{x,y}}}\right)}}$$

2. SIMPSONS ●
3. SYNZD ●

TEST:
RUN CODES FOR 25 TURNS
AVERAGE TUNES
1 - VARY CURRENT
2 - VARY ENERGY
3 - VARY HORIZONTAL EMITTANCE
4 - VARY VERTICAL EMITTANCE

OPTIMAZATION OF SIMULATION PARAMETERS

1. TIMESTEP
   - BY DERIVATION $\delta\tau < 1.0$
   - OPTIMAL TIME = 0.2

2. PARTICLE NUMBER
   - [redacted]
   - POWER OF 2
   - OPTIMAL - 1024

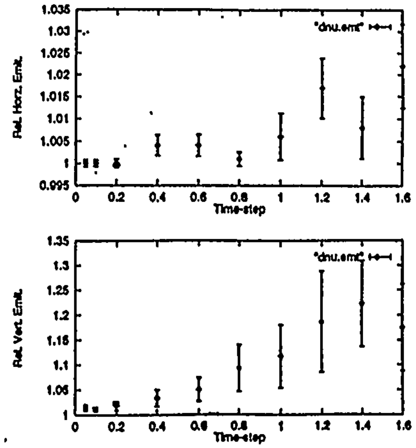

Figure 2. The top graph is the average horizontal emittance versus the time-step over a simulation run of 25 turns. The error bars show the RMS fluctuation in the emittance over all 25 steps. The bottom graph shows the average vertical [illegible]

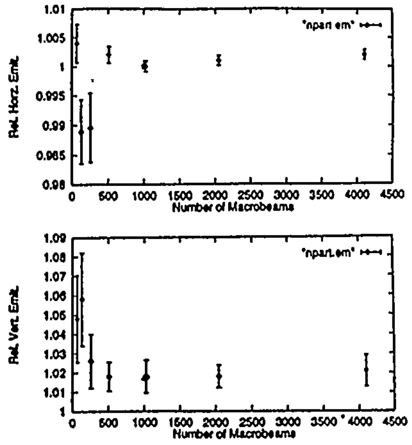

Figure 3. The top graph is the average horizontal emittance versus the number of macro-beams for a simulation run of 25 turns. The error bars show the RMS fluctuation in the emittance over all 25 steps. The bottom graph shows [illegible] vertical emittance and fluctuation during the same run. [illegible]

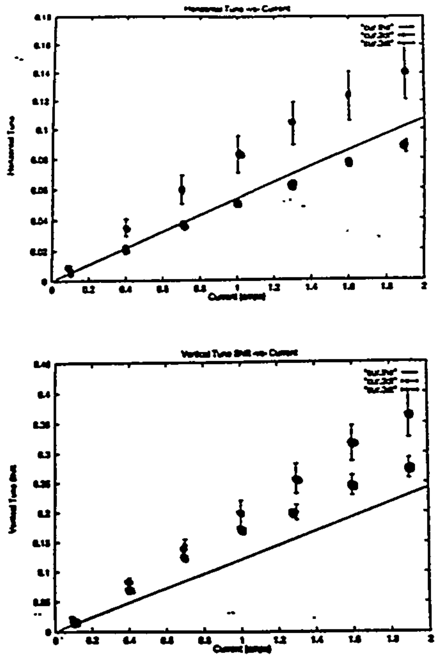

gure 8: Tune-Shifts -vs- Current. The top graph shows the average beam rizontal tune shift while the lower graph shows the average beam vertical tune-ift over a 25 turn run. The solid line is the theoretical value, the diamonds are e data from SYN2D, and the dashes are the data from SIMPSONS. The error-rs show the RMS variation in the tune-shifts. [I=0.0 - 2.0 amps, E=10MeV, $= 50\pi mm - mrad$, and $\epsilon_y = 10\pi mm - mrad$, $\nu_x = 1.75$, $\nu_y = 0.85$, $dr = .2$, $_p = 1024$]

①

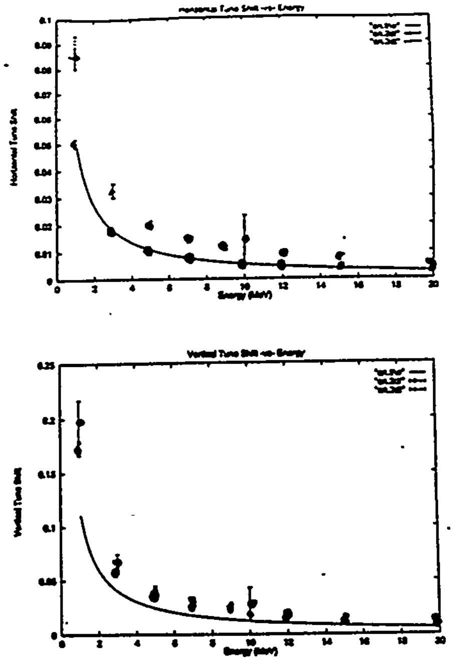

Figure 0: Tune-shift -vs- Energy. The top graph is the average beam horizontal tune-shift and the bottom graph is the average beam vertical tune-shift over a 25 turn run. The solid line is the theoretical value, the diamonds are the data from SYN2D, and the dashes are the data from SIMPSONS. The error-bars show the RMS variance in the tune-shifts. [I=0.1 amps, E=1-20MeV, $\epsilon_x = 50\pi mm - mrad$, and $\epsilon_y = 10\pi mm - mrad$, $\nu_x = 1.75$, $\nu_y = 0.83$, $dr = .2$, $N_p = 1024$]

②

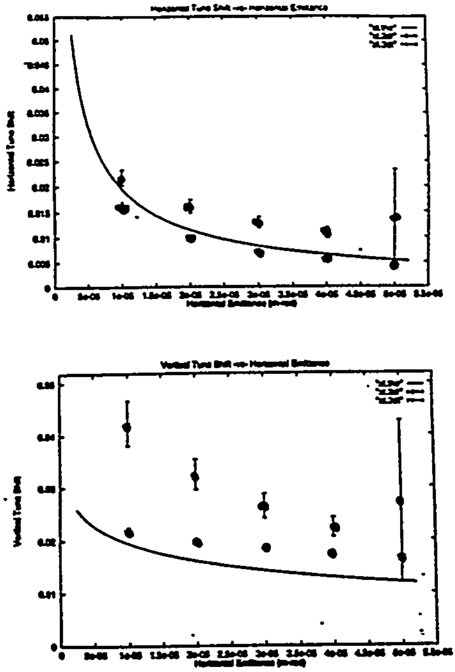

Figure 10: Tune-shift -vs- Horizontal Emittance. The top graph is the average beam horizontal tune-shift and the bottom graph is the average beam vertical tune-shift over a 25 turn run. The solid line is the theoretical value, the diamonds are the data from SYN2D, and the dashes are the data from SIMPSONS. The error-bars show the RMS variance in the tune-shifts. [I=0.1 amps, E=10MeV, $\epsilon_x = 10 - 50\pi mm - mrad$, and $\epsilon_y = 10\pi mm - mrad$, $\nu_x = 1.75$, $\nu_y = 0.85$, $dr = .2$, $N_p = 1024$]

③

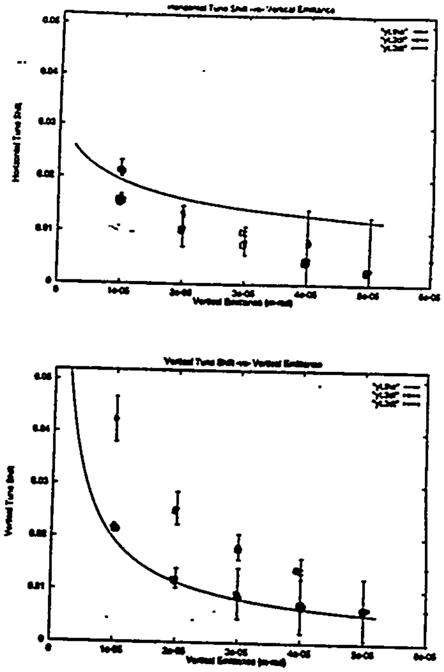

Figure 11: Tune-shift -vs- Vertical Emittance. The top graph is the average beam horizontal tune-shift and the bottom graph is the average beam vertical tune-shift over a 25 turn run. The solid line is the theoretical value, the diamonds are the data from SYN2D, and the dashes are the data from SIMPSONS. The error-bars show the RMS variance in the tune-shifts. [I=0.1 amps, E=10MeV, $\epsilon_x = 10\pi mm - mrad$, and $\epsilon_y = 10 - 30\pi mm - mrad$, $\nu_x = 1.75$, $\nu_y = 0.85$, $dr = .2$, $N_p = 1024$]

④

Horizontal Tune -vs- Current for 3 machine tunes

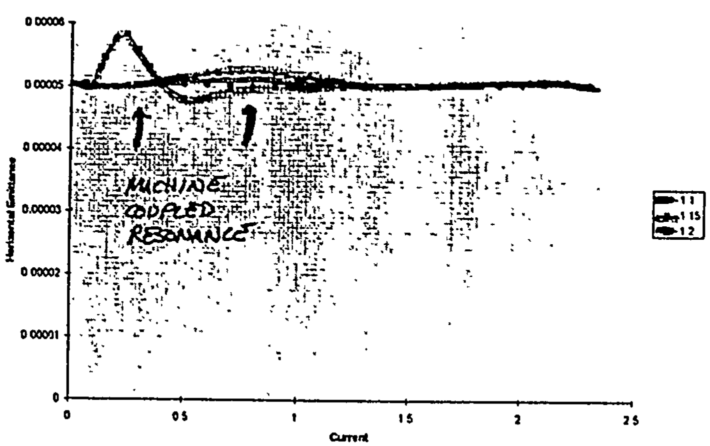

Horizontal Emittance -vs- Vertical Machine Tune for 3 currents

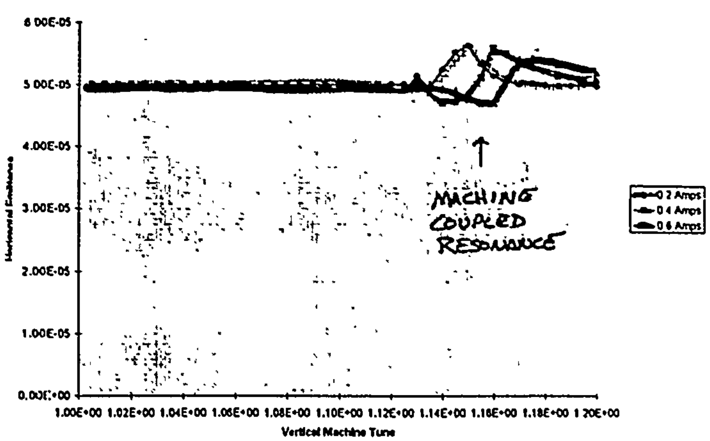

$\nu_{oy} = 1.75$

Vertical Emittance -vs- Current for 3 Machine Tunes

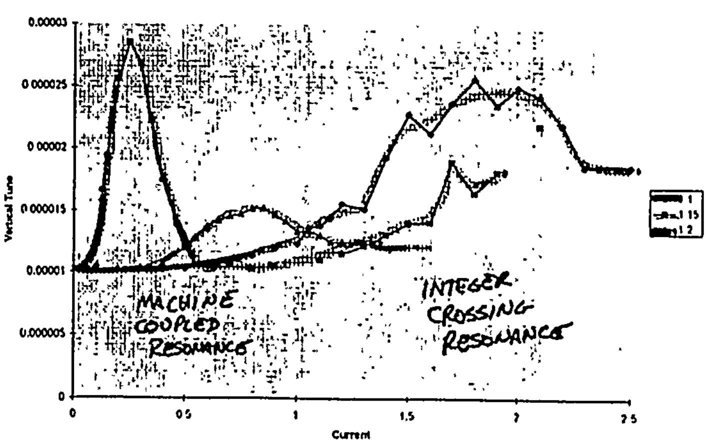

Vertical Emittance -vs- Machine Tune for 3 Currents

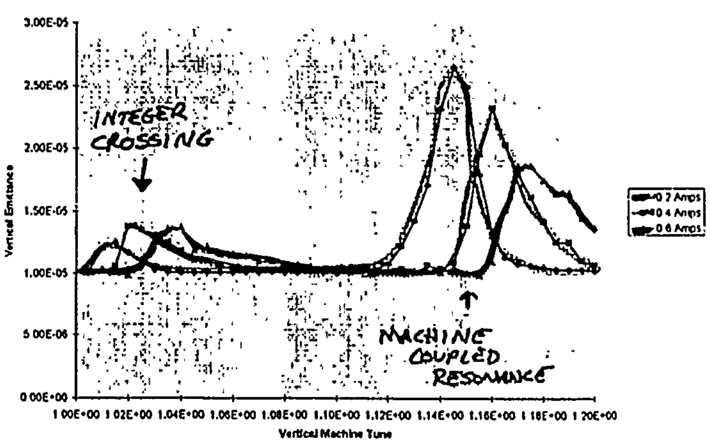

$\nu_{ox} = 1.75$

TONE SHIFT
&
SPREADING

I = 0

Current = 0.0 Amps

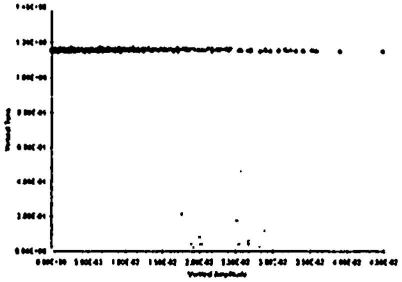

AS CURRENT INCREASES

1) AVERAGE TONE IS DEPRESSED

2) SPREAD IN PARTICLE TONE INCREASES

I = 0.1 Amps

Current = 0.1 Amps

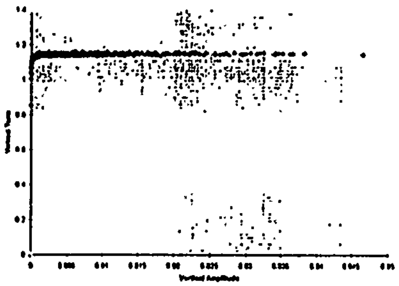

I = 1.0 Amps

Current = 1.0 Amps

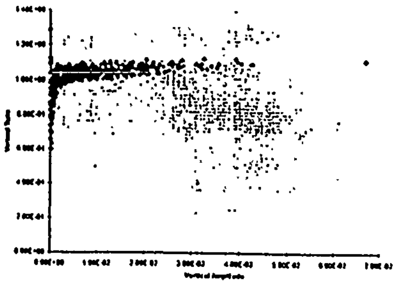

MACHINE COUPLED RESONANCE

- $4 = \nu_x + 2\nu_y$
- AMPLITUDE DEPENDENT
-

Region of Instability

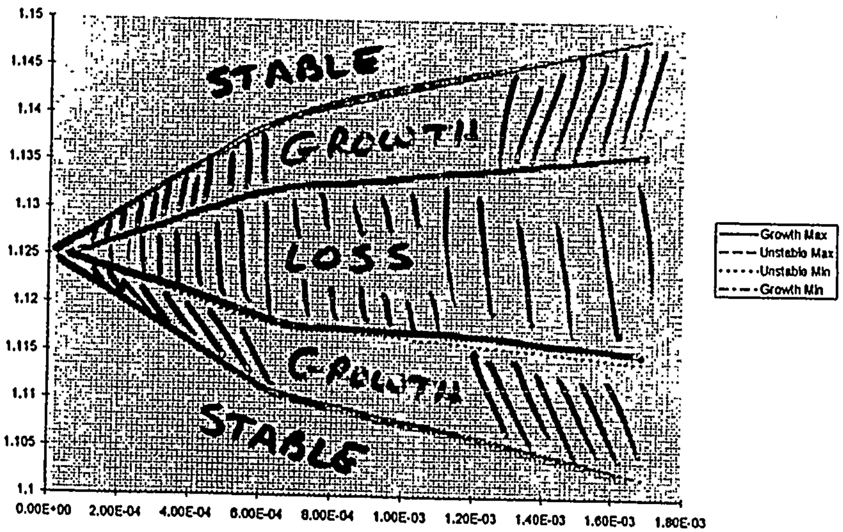

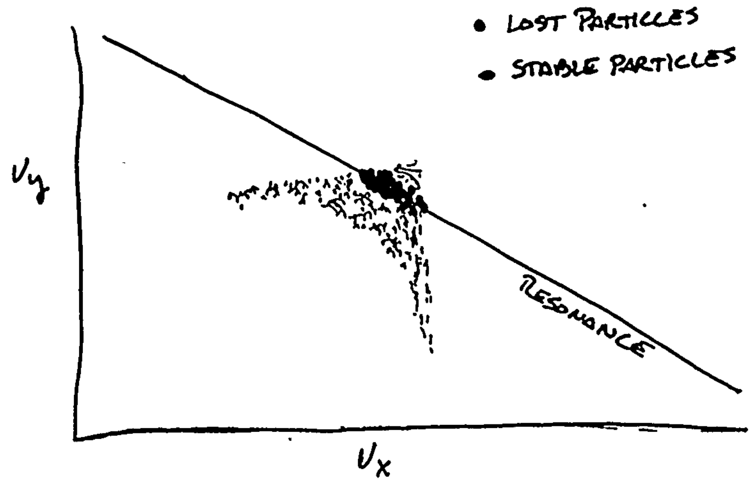

LOST PARTICLES HAVE BEAM TUNES $(\nu_{0x}-\Delta\nu_x$ & $\nu_{0y}-\Delta\nu_y)$ THAT LIE ON OR NEAR THE LINE OF RESONANCE.

OF

BEAM TUNE &
RESONANCE

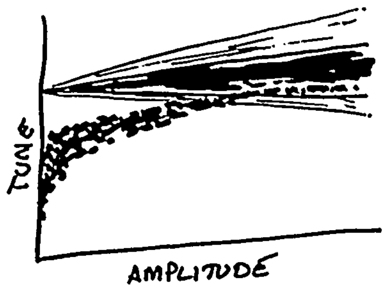

RESONANCE ABOVE
BEAM TUNE

- FEW LOST PARTICLES
- LITTLE, OR NO EMITTANCE GROWTH

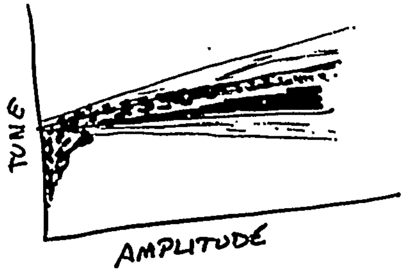

RESONANCE AT
BEAM TUNE

- MANY LOST PARTICLES
- EMITTANCE GROWTH

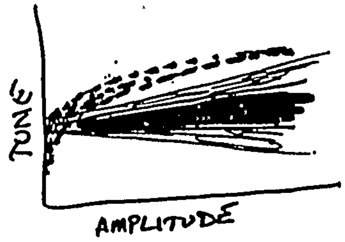

RESONANCE BELOW
BEAM TUNE

- NO LOST PARTICLES
- DIMENISHING EMITTANCE GROWTH

$\nu_x = 1.75$

$\nu_y = 1.125$

I = .4 Amps

BEAM
BELOW
RESONANCE

- FEW PARTICLES LOST
- No Emittance Growth

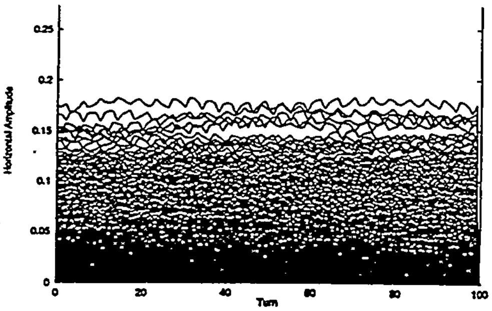

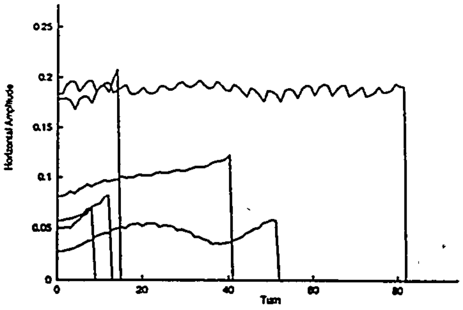

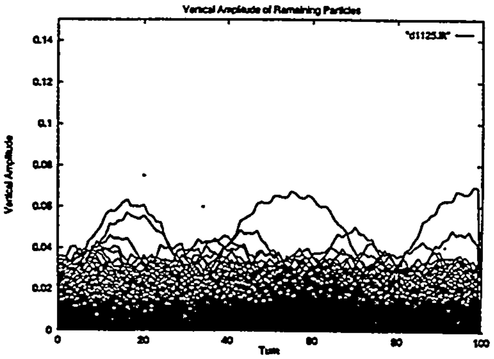
Vertical Amplitude of Remaining Particles

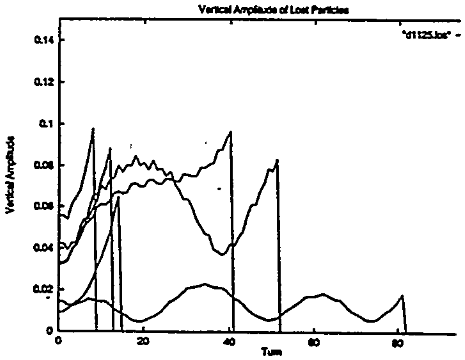
Vertical Amplitude of Lost Particles

$\nu_x =$

$\nu_y = 1.145$

I = .4 Amps

BARELY BELOW
RESONANCE

- MORE LOST PARTICLES
- NO EMITTANCE GROWTH

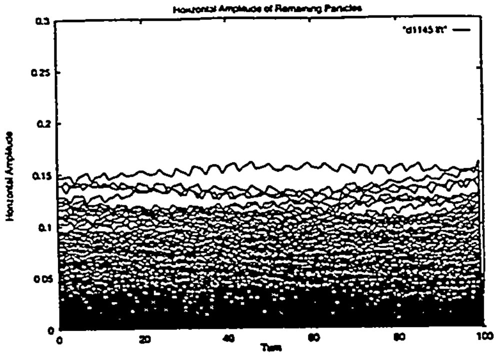
Horizontal Amplitude of Remaining Particles

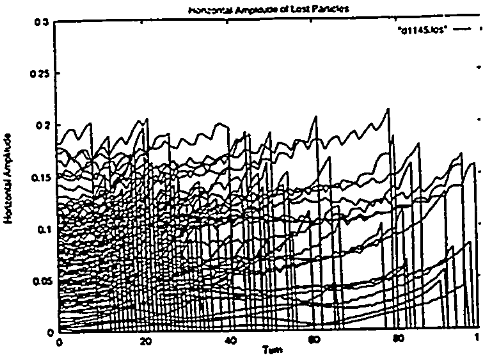
Horizontal Amplitude of Lost Particles

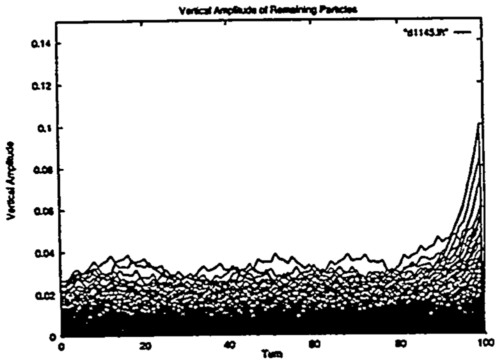
Vertical Amplitude of Remaining Particles

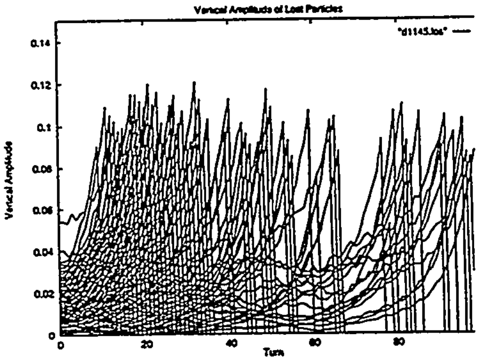
Vertical Amplitude of Lost Particles

I = .41

T RESONANCE

PARTICLE LOSS

EMITTANCE GROWTH

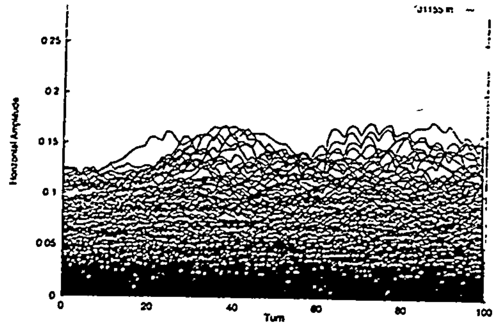

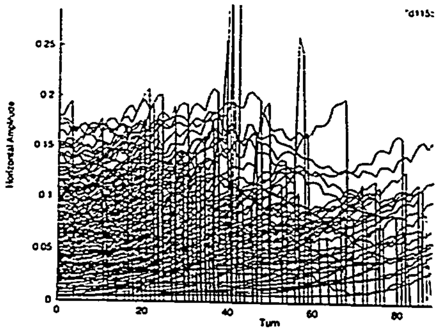

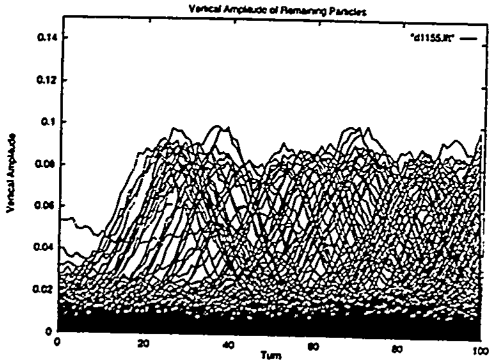

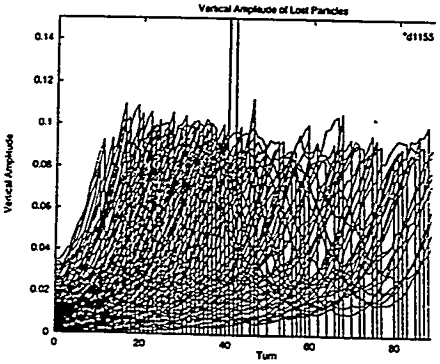

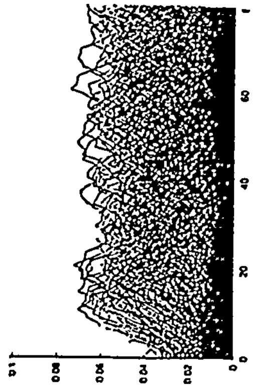

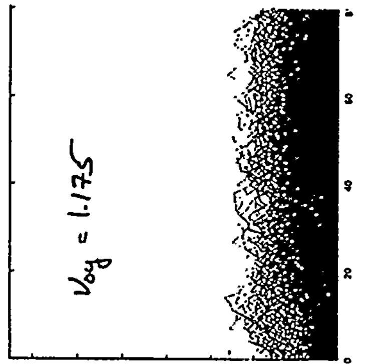

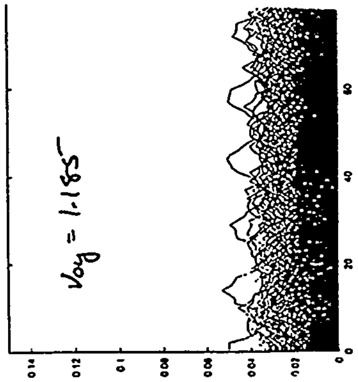

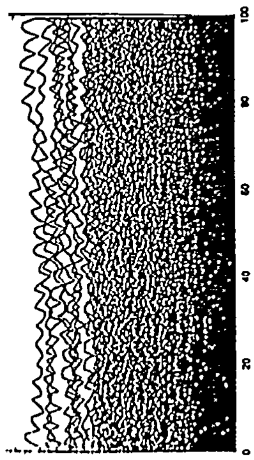

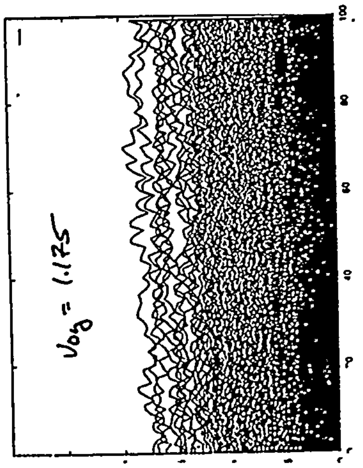

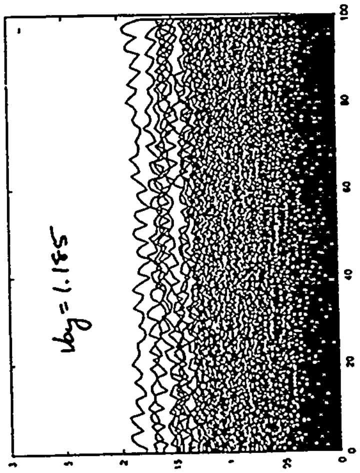

V. CONCLUSIONS

1. NEW MODEL TRACKS BEAM WITH RELIABLE DATA
2. NEW CODE IS OVER 20 TIMES FASTER THAN 3-D CODE
3. CHARACTERISTICS OF COUPLED RESONANCE SHOWN
    - OVERLAPPING OF COUPLED RESONANCE AND TUNE SPREAD
    - EXPLANATION OF PARTICLE LOSS & EMITTANCE GROWTH

FUTURE WORK

1. LONGER RUNS IN "STABLE" REGIONS
2. NEW SYNCHROTRON DESIGNS (?)
3. IMPROVE CODE RUN TIME
4. EMPLOY A δf technique to further improve run time

PHOTON ASSISTED TRANSPORT IN SEMICONDUCTOR QUANTUM STRUCTURES WITH THE UCSB FEL'S.

J. Allen, UCSB

PERTURBATIVE PARTICLE SIMULATION OF SPACE CHARGE EFFECTS FOR A K-V BEAM

W. Lee, Princeton Univ.

Perturbative

Particle Simulation of Space Charge Effects in Accelerators

W. W. Lee, Q. Qian and R. Davidson

PPPL

- Perturbative Particle Simulation Schemes
  - -- δf - scheme: linear and nonlinear
  - -- linearized trajectory scheme
- Microturbulence Simulation of Tokamak Plasmas
- Space Charge Simulation of Intense Ion Beams

Advantages of δf Scheme

- Nearly noise free
- Linear developement (together with quiet start) closely resembles Vlasov code simulation
- No numerical difficulties in the turbulent nonlinear stage
- Orders of magnitude savings in the number of particles used in comparison with total F code.

Applications

- Tokamak Physics
  - -- MHD: Internal Kink Modes
    Energetic Particle Physics (hybrid)
  - -- Kinetic: Drift Waves
    Ion Temperature Gradient Driven Modes
- Space Physics
- Accelerator Physics
  - -- Space Charge

δf particle simulation scheme

[Dimits &Lee JCP 107, 309 ('93); Parker & Lee FPB 5, 77 ('93)]

- Vlasov Equation

$$dF/dt = \partial F/\partial t + \underline{v}\cdot\partial F/\partial \underline{x} + \underline{a}\cdot\partial F/\partial \underline{v} = 0$$

- Let $F = Fo + \delta f$, then

$$d\delta f/dt = - dFo/dt$$

- Equations of motion for the j-th particle

$$d\underline{x}j/dt = \underline{v}j, \quad d\underline{v}j/dt = \underline{a}j$$

$$dwj/dt = - (1-wj)(dF_o/dt)/F_o\,|\,j$$

- Perturbed Distribution

$$\delta f = \Sigma_{j=1,N}\, wj\ \delta(\underline{x}-\underline{x}j)\ \delta(\underline{v}-\underline{v}j)$$

- Total Distribution

$$F = \Sigma_{j=1,N}\, \delta(\underline{x}-\underline{x}j)\ \delta(\underline{v}-\underline{v}j)$$

- Poisson's Equation

$$\nabla^2\,\Phi = -4\,\pi\,\Sigma_\alpha\, q_\alpha \int (F_{o\alpha} + \delta f_\alpha)\, d\underline{v}$$

- Fully Linearized scheme

[J. A. Byers, 4th Numerical Simulation Conference, 1970]

$$F_o = \Sigma_{j=1,N}\, \delta(\underline{x}-\underline{x}j0)\ \delta(\underline{v}-\underline{v}j0)$$

$$\delta f = -\Sigma_{j=1,N}\, (\underline{x}j1\cdot\partial/\partial\underline{x} + \underline{v}j1\cdot\partial/\partial\underline{v})\ \delta(\underline{x}-\underline{x}j0)\ \delta(\underline{v}-\underline{v}j0)$$

$$d\underline{x}j0/dt = \underline{v}j0, \quad d\underline{v}j0/dt = \underline{a}0(\underline{x}j0)$$

$$d\underline{x}j1/dt = \underline{v}j1, \quad d\underline{v}j1/dt = \underline{a}1(\underline{x}j0)$$

$$\delta n = - \partial/\partial\underline{x}\cdot\Sigma_{j=1,N}\ \underline{x}j1\,\delta(\underline{x}-\underline{x}j0)\ \delta(\underline{v}-\underline{v}j0)$$

$$\nabla^2\,\delta\Phi = -4\,\pi\,\Sigma_\alpha\, q_\alpha\, \delta n_\alpha$$

δf Simulation Scheme for Space Charge Effects in an Intense Ion Beam

- Governing equations

$$dF/ds \equiv \partial F/\partial s + d\underline{x}/ds \cdot \partial F/\partial \underline{x} + d\underline{x}'/ds \cdot \partial F/\partial \underline{x}' = 0$$

$$d\underline{x}/ds = \underline{x}',$$

$$d\underline{x}'/ds = \pm\kappa q\, \underline{x} - (q/\gamma^3\beta^2mc^2)\, \nabla\phi,$$

$$\nabla^2\phi = -4\pi q \int F d\underline{x}'$$

- K-V Equilibrium

$$F_O = (N/\pi 2\varepsilon_x\varepsilon_y)\, \delta(2J_x/\varepsilon_x + 2J_y/\varepsilon_y - 1)$$

$$2J_x = (x/w_x)^2 + (w_x x' - w_x' x)^2$$

$$2J_y = (y/w_y)^2 + (w_y y' - w_y' y)^2$$

- Let $F = F_O + \delta f$, [note that $d^{(0)}F_O(\underline{x}, \underline{x}', s)/ds = 0$]

$$d\delta f(\underline{x}, \underline{x}', s; \phi)/ds = - dF_O(\underline{x}, \underline{x}', s)/ds$$

- Let $w = \delta f / F \;\Rightarrow\; \delta f = \sum_{j=1,N} w_j\, \delta(\underline{x}-\underline{x}_j)\, \delta(\underline{v}-\underline{v}_j)$, we obtain

$$dw/ds = -(1-w)(dF_O/ds)/F_O$$
$$= (1-w)(q/\gamma^3\beta^2mc^2)\, \nabla\delta\phi \cdot (\partial F_O/\partial \underline{x}')/F_O$$

- Equilibrium Quantities

$$(\partial F_O/\partial x')/F_O = -[2(w_x x' - w_x' x)w_x] \,/\, [\varepsilon_x(2J_x/\varepsilon_x + 2J_y/\varepsilon_y - 1)]$$
$$= - w_x / (w_x x' - w_x' x)$$
$$(\partial F_O/\partial y')/F_O = -[2(w_y y' - w_y' y)w_y] \,/\, [\varepsilon_y(2J_x/\varepsilon_x + 2J_y/\varepsilon_y - 1)]$$
$$= - w_y / (w_y y' - w_y' y)$$

- Poisson's equation

$\nabla^2\delta\phi = -4\pi q \int \delta f\, dx'dy'$, (use $\delta\phi$ in dw/ds)

$\phi = \phi_O + \delta\phi$ (use ϕ in dx'/ds for fully nonlinear code)

- Equilibrium Electrostatic Potential

$\phi_O = - 2qN\, (x^2/a + y^2/b)\, /(a+b) + c$ (use ϕ_O in dx'/ds to linearize)

- Amplitude Equations

$$d^2w_x/ds^2 + \kappa_x w_x = 1/w_x^3$$

$$d^2w_y/ds^2 + \kappa_y w_y = 1/w_y^3$$

$$\kappa_x = \kappa_q - 2K / [a(a+b)]$$

$$\kappa_y = -\kappa_q - 2K / [b(a+b)]$$

$$K = 2q^2N / \gamma^2\beta^3mc^2$$

$$a = \varepsilon_x{}^{1/2}\, w_x$$
$$b = \varepsilon_y 1/2\, w_y$$

- Numerical Considerations

-- Number of particles ?

-- Time step: $\omega_p\, \Delta t \approx 1$,

$$\omega_p^2 = 4\pi en \left[\kappa_q + e/(\gamma^3\beta^2mc^2)\right] \text{ (?)}$$

--Grid spacing: $\Delta x \approx \lambda_D \approx \varepsilon/a\omega_p$ (?)

-- Singularity: $\delta'(x) = -\delta(x)/x \Rightarrow -(2x/\Delta^2)\delta(x)$

$$\Rightarrow f(x)\delta'(x) = -f(0)\delta'(x) - f'(x)\delta(x)$$

- Fully Linearized Scheme

$$dF/ds \equiv \partial F/\partial s + d\underline{x}/ds\cdot\partial F/\partial\underline{x} + d\underline{x}'/ds\cdot\partial F/\partial\underline{x}' = 0$$

$$F_o = \Sigma_{j=1,N}\, \delta(\underline{x}-\underline{x}j0)\, \delta(\dot{\underline{x}}-\underline{v}j0)$$

$$d\underline{x}0/ds = \underline{x}0',$$

$$d\underline{x}0'/ds = \pm\kappa_q\, \underline{x}0 - (q/\gamma^3\beta^2mc^2)\, \nabla\phi_0(\underline{x}0),$$

$$d\underline{x}1/ds = \underline{x}1',$$

$$dx_1'/ds = +\kappa_q x_1$$
$$- (q/\gamma^3\beta^2mc^2)\, [x_1\partial^2\phi_0(\underline{x}0)/\partial x^2 + \partial\delta\phi(\underline{x}0)/\partial x]$$

$$dy_1'/ds = -\kappa_q y_1$$
$$- (q/\gamma^3\beta^2mc^2)\, [y_1\partial^2\phi_0(\underline{x}0)/\partial y^2 + \partial\delta\phi(\underline{x}0)/\partial y]$$

$$\nabla^2\delta\phi = 4\pi q\, \nabla\cdot\Sigma_{j=1,N}\, \underline{x}j1\,\delta(\underline{x}-\underline{x}j0)$$

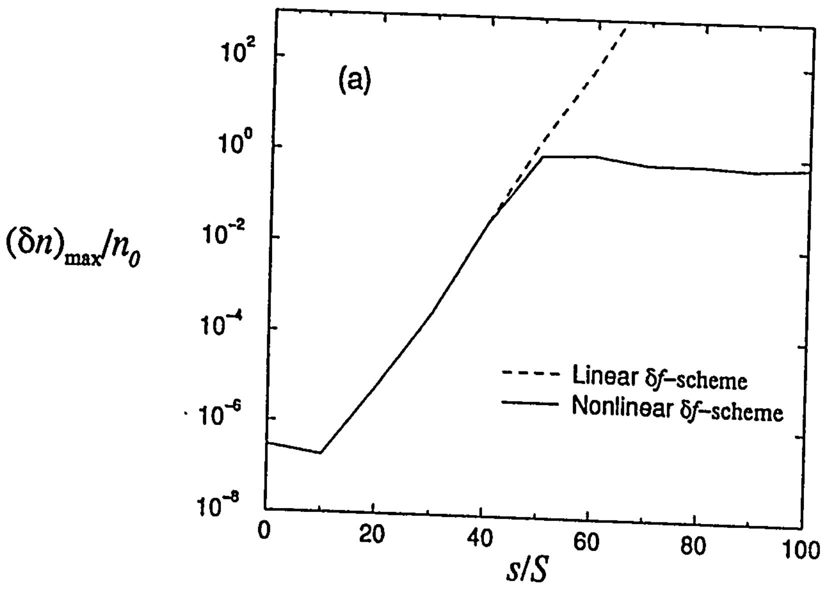

$\sigma_v = 85^0$

$\sigma = 20^0$

$KS/\varepsilon_0 = 5.77$

3.

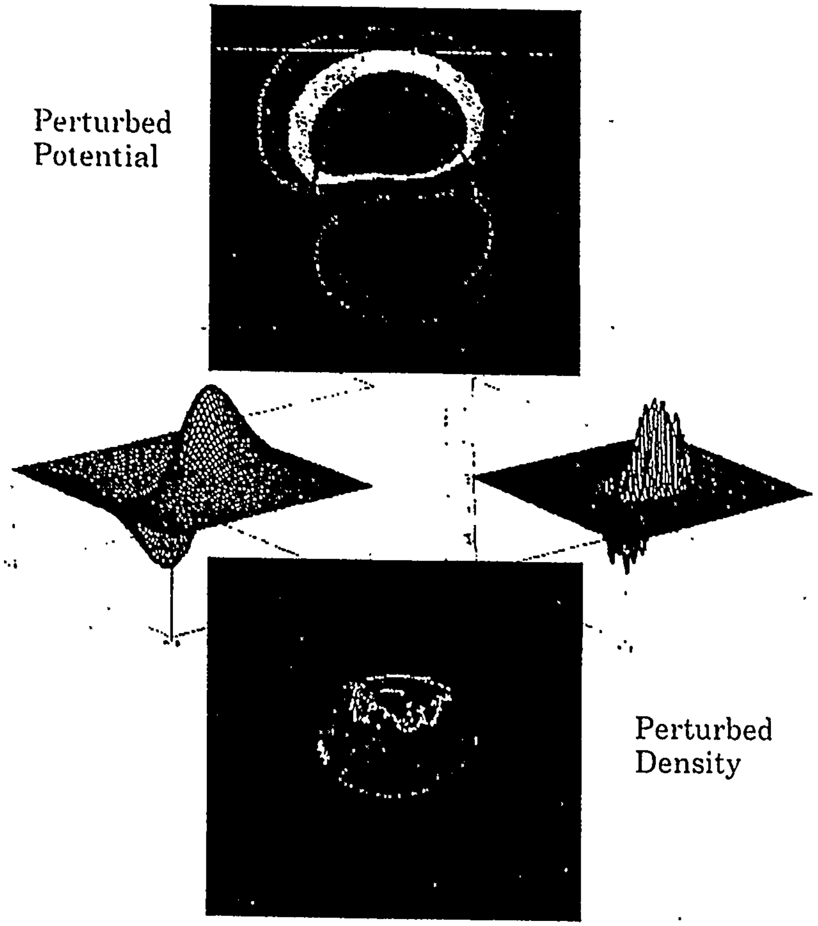

Particle Simulation of an Unstable K-V Beam in an Accelerator for Heavy Ion Fusion Research

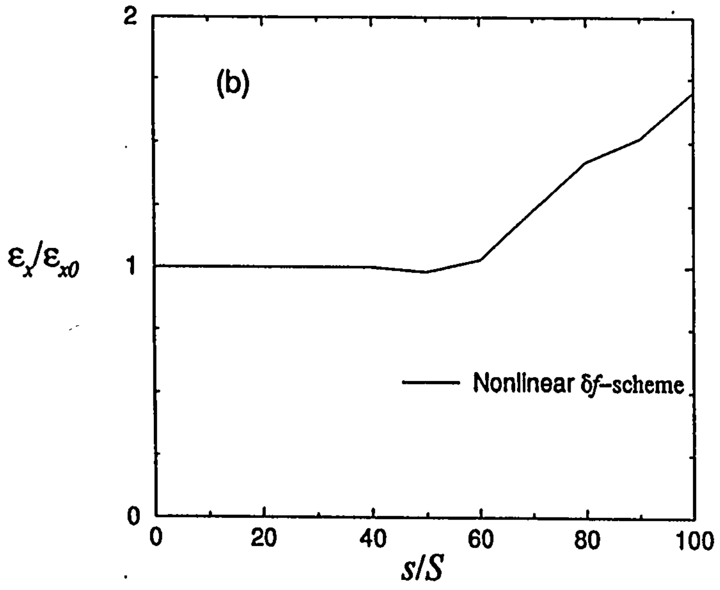

$\sigma_v = 85^\circ$

$\sigma = 20^\circ$

$KS/\varepsilon_0 = 5.77$

BEAM EFFECTS ON THE AMPLIFIED INVERSE-BREBSSTRAHLUNG ACCELERATION

M. Pato, Univ Sao Paulo

"Beam Effects on the, Amplified Inverse-Bremsstrahlung Acceleration"

M. P. Pato
Universidade de São Paulo

Nonlinear Amplification of Inverse-Bremsstrahlung Electron Acceleration

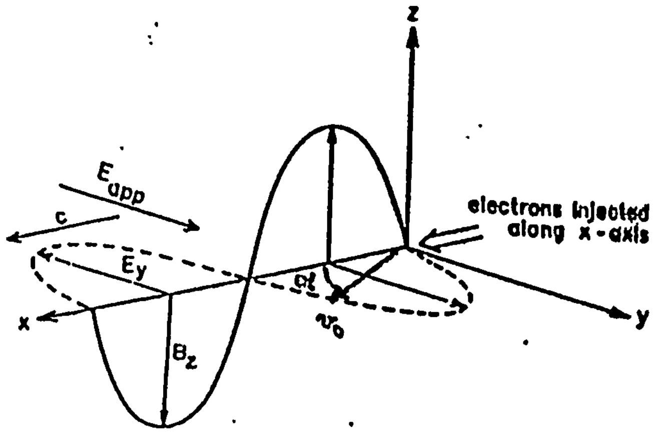

M. S. Hussein, USP
A. K. Kerman, MIT
R. Galvão, USP
A. Serbeto, UFF
A. Paes, IEAv
M. Alves, IEAv

Kawata et al., Phys. Rev. Lett. 66 (91) 2072

M. S. Hussein and M. P. Pato, Phys. Rev. Lett. 68 (92) 1136

Solution of the problem EM wave + $E_{app}^{(const)}$

$$\begin{cases} P_x c = mc^2\gamma + eE_{app}y + K_1 \\ P_y c = -\frac{e}{kc}E_{y0}\cos\varphi - eE_{app}t + K_2 \end{cases}$$

Using φ as independent variable and introducing the coordinate Q

$$Q = -\frac{k}{2cE_{app}}\left(eE_{app}y^2 + 2K_1 y\right)^2$$

$$P_y = Q'$$

$$\dot{\varphi} = kc(1-\beta_x) = -\frac{k}{mc\gamma}\left(eE_{app}y + K_1\right)$$

$$P_y = m\gamma\dot{\varphi}\frac{dy}{d\varphi}$$

Electron equation of motion:

$$\frac{dP_x}{dt} = -e\beta_y E_y$$

$$\frac{dP_y}{dt} = -e(1-\beta_x)E_y - eE_{app}$$

$$B_z = E_y = -E_0\sin\varphi \quad . \quad \varphi = k(ct-x)$$

$$\vec{\beta} = \vec{v}/c$$

Energy equation:

$$\frac{d\mathcal{E}}{dt} = -eE_y v_y$$

$$\mathcal{E} = mc^2\gamma + eE_{app}y$$

γ relativistic factor

$$E_{app} \sim (1-\beta_x)E_{laser}$$

$$mc^2\gamma = \frac{1}{2}\frac{m^2c^4 + P_y^2c^2}{\left(K_1^2 - \frac{2ce}{k}E_{app}Q\right)^{1/2}} + \frac{1}{2}\left(K_1^2 - \frac{2ce}{k}E_{app}Q\right)^{\frac{1}{2}}$$

$$x = \frac{1}{k}\left[\frac{kc}{eE_{app}}\left(-Q' - \frac{e}{kc}E_{y0}\cos\varphi + K_2\right) - \varphi\right]$$

$$y = -\frac{1}{eE_{app}}\left[\left(K_1^2 - \frac{2ce}{k}E_{app}Q\right)^{1/2} + K_1\right]$$

Equation of motion for Q:

$$Q'' = -\frac{c}{2k}eE_{app}\frac{m^2c^2 + Q'^2}{K_1^2 - \frac{2c}{k}eE_{app}Q} \mp \frac{eE_{app}}{2kc} + \frac{eE_{y0}}{kc}s$$

$$E_{app} = 0 \Rightarrow Q = -\frac{eE_{y0}}{kc}\sin\varphi + K_2\varphi \Rightarrow \langle\gamma\rangle = \text{cst}$$

Energy equation!

$$\mathcal{E}' = \frac{ceE_{y0}}{k}\frac{Q'}{\left(K_1^2 - \frac{2c}{k}eE_{app}Q\right)^{1/2}}\sin\varphi$$

Whenever $\varphi = n\pi$ $\mathcal{E}$ is maximum or minimum

$Q' = 0$ is an extra extremum

If $Q'(n\pi) = 0 \Rightarrow$ inflection poin

Non-linear behavior:

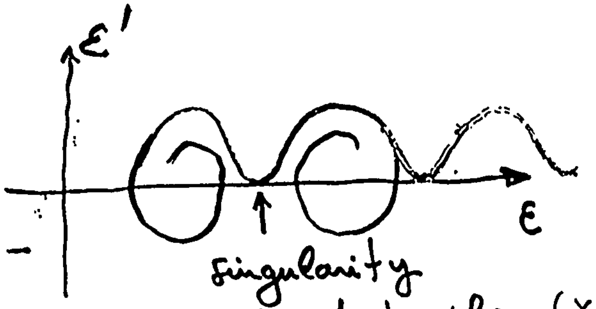

singularity
fold catastrophe (x^3)

If $-e\beta_y E_y > 0$

P_x and ε will always increase.

As $\langle (1-\beta_x) E_y \rangle = 0$, if

If Eapp oscilates the movement will be confined in the y direction.

The points where $v_y = 0$ and $E_y = 0$ are inflection points

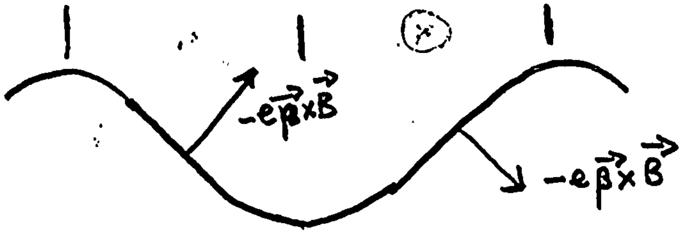

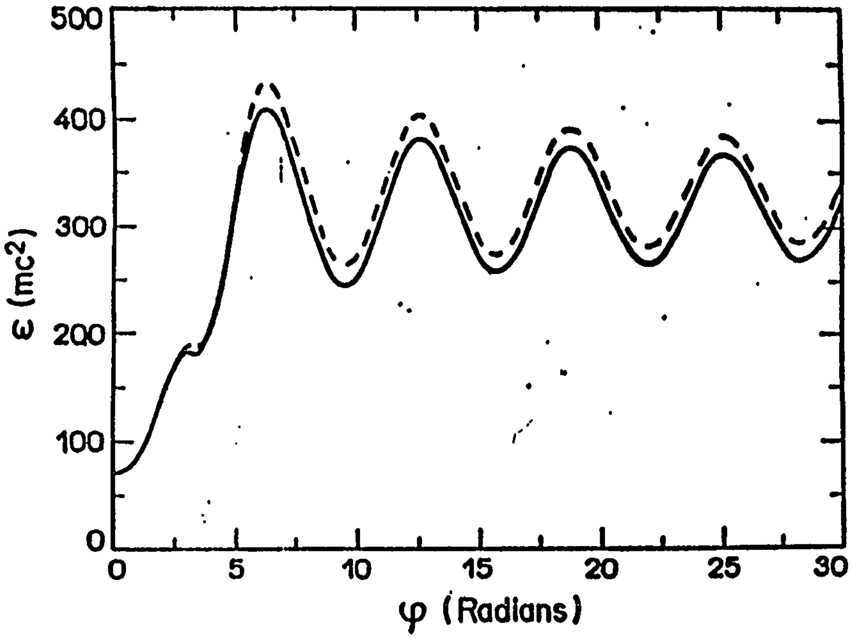

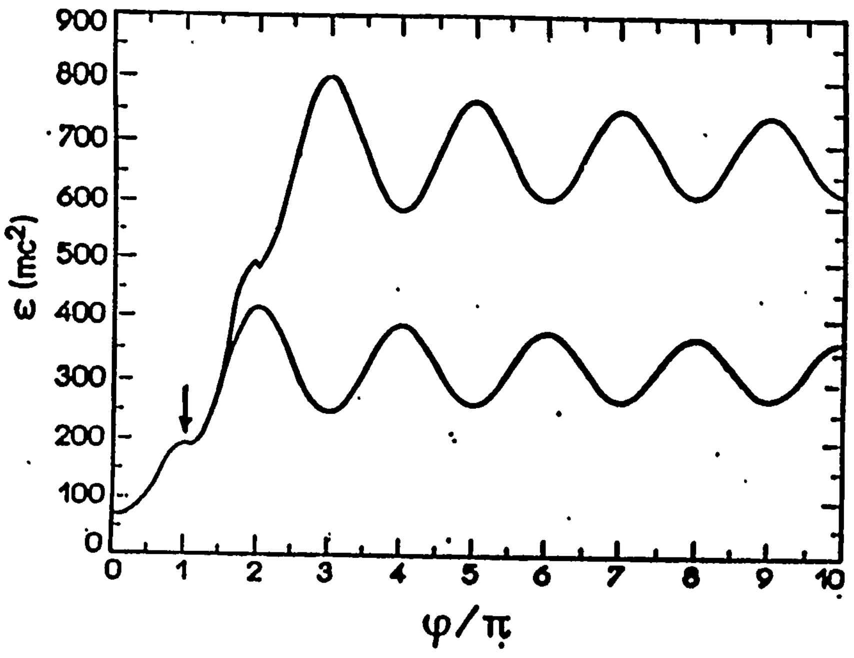
900
800
700
600
500
400
300
200
100
0
ε (mc²)
0
1
2
3
4
5
6
7
8
9
10
φ/π

Fig. 2a

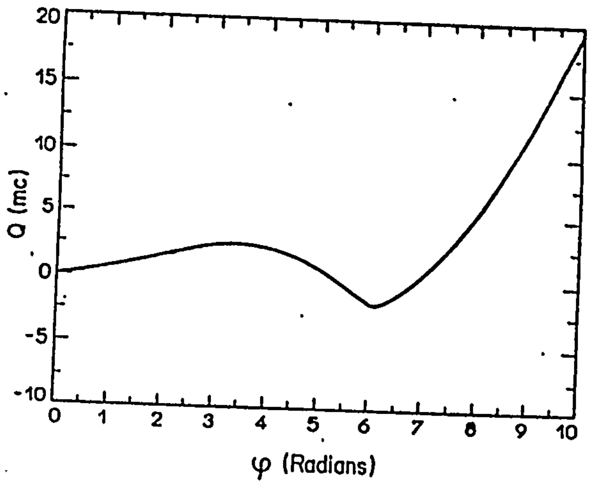
20
15
10
5
0
-5
-10
Q (mc)
0
1
2
3
4
5
6
7
8
9
10
φ (Radians)

Fig. 2b

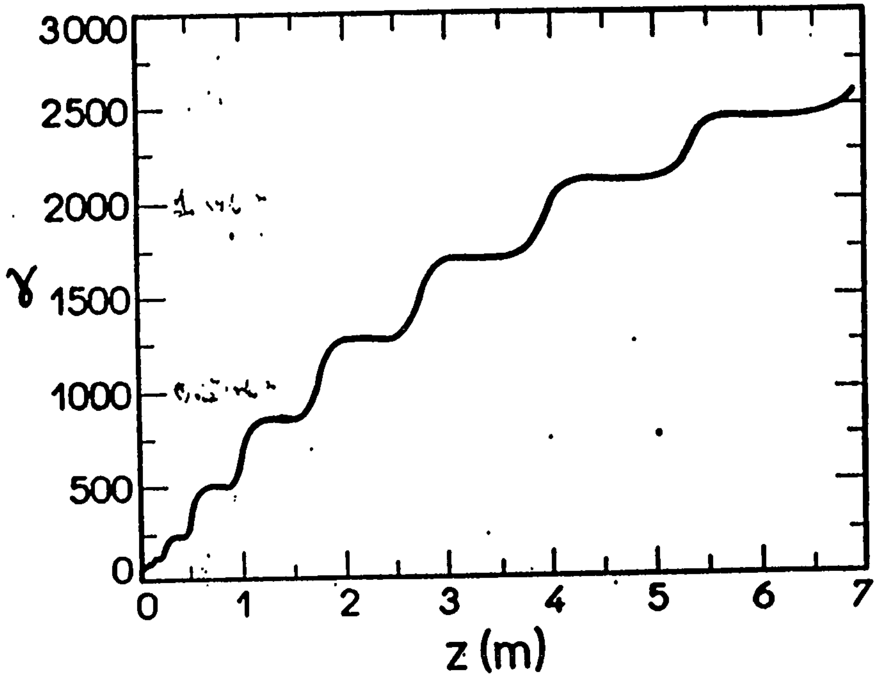

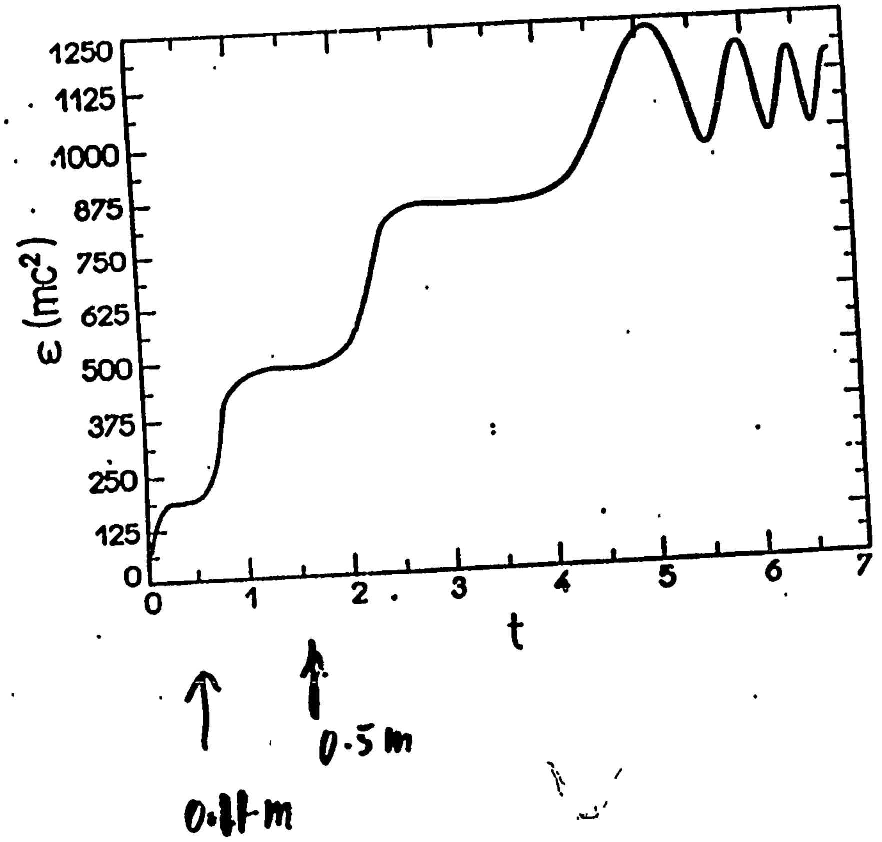

A. P. Pato, M. S. Hussein and A. K. Kerman, Nucl. Inst. Meth. Phys. Res.
A 328 (1993) 342

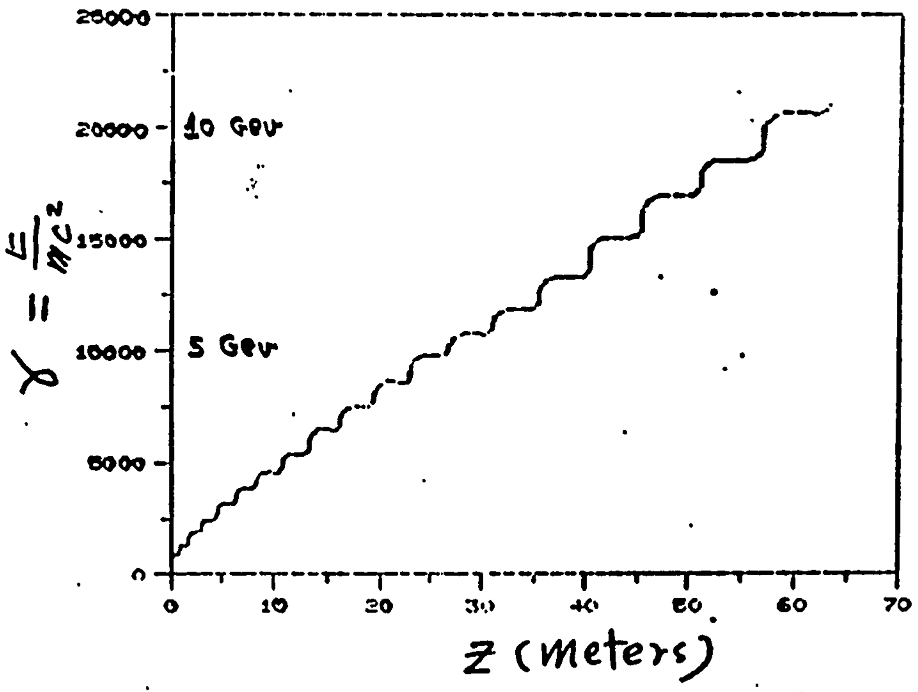

$\beta_0 = 0.9999$, $\gamma_0 = 70$

$P = 3.54 \times 10^{15}\ W/cm^2$

$\lambda = 10\ \mu m$

$E_{app} = 4.28 \times 10^{-5}\ E_L$

$\left(E_{app} \approx (1-\beta)\, E_L \right)$

$\theta_0 = 0.6°$

Space-charge effects

R.M.O. Galvão, M.S. Hussein, M.P. Pato and A. Serbeto, PRE 49, R4807 (1994)

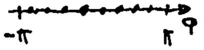

$$n(\varphi) = \frac{2\pi}{N}\bar{n}_e \sum_{j=1}^{N} \delta(\varphi - \varphi_i)$$

- resonant particle

$$\nabla^2 \phi = -\frac{n e}{\varepsilon_0}$$

$$\frac{d\mathcal{E}}{dt} = -e v_y E_y + e v_x \frac{d\phi}{dx}$$

$$\frac{d\mathcal{E}_i}{dt} = E_{y_0} \frac{\beta_i}{\gamma_i} \sin\varphi_i - 2\delta \; \mathrm{Im} \left\{ \sum_{m=1}^{\infty} \frac{\langle e^{-im\varphi_j} \rangle}{m} e^{im\varphi} \right\}$$

$$\delta = \frac{\omega_b^2}{\omega^2}\left(\frac{\omega}{c/R}\right) \quad , \; \omega_b^2 = \frac{\bar{n}_e e^2}{m \varepsilon_0} \quad , \; l = \frac{\lambda}{32}$$

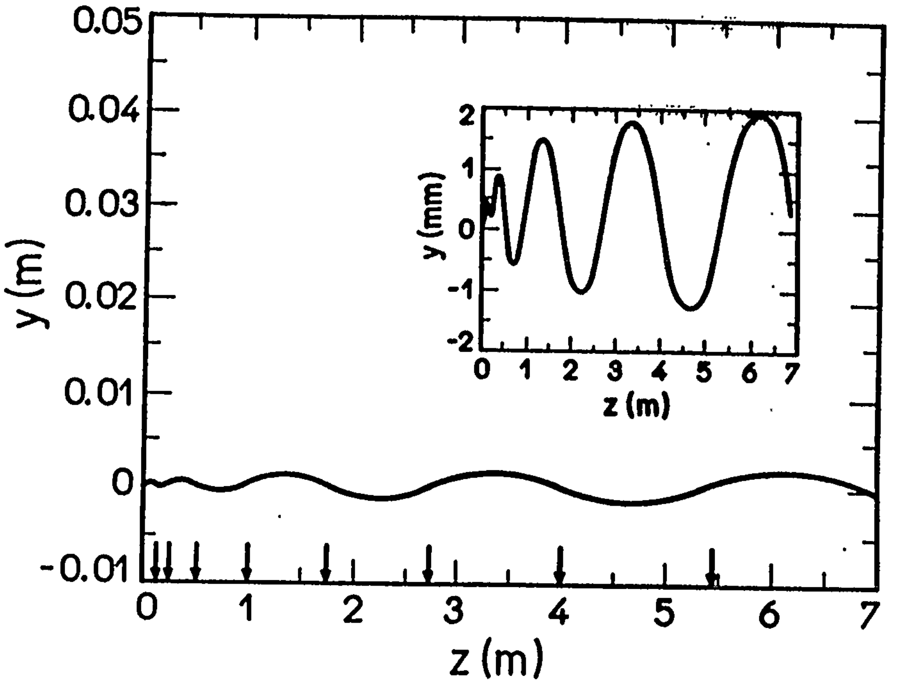

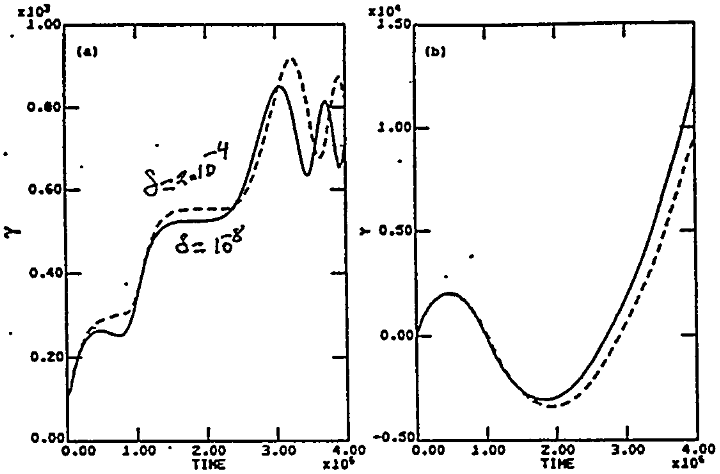

FIG. 2. Temporal profiles of $\gamma(t)$ (a) and perpendicular displacement $y(t)$ (b) of the central "tag" particles in a simulation of NAIBEA with $N = 19$ particles/wavelength. The full lines correspond to $\delta = 10^{-8}$ and the dashed lines to $\delta = 2.0 \times 10^{-4}$. Time is normalized to $\pi/16kc$.

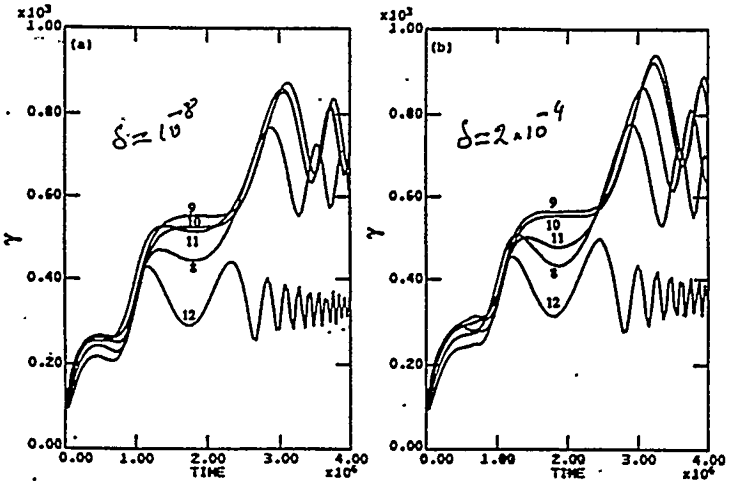

FIG. 3. Temporal profi $\gamma(t)$ for the central "tag" cle, 10, and the next two ing it, 8 and 9, and leadi 11 and 12, for $\delta = 10^{-8}$ (a $\delta = 2.0 \times 10^{-4}$ (b). Time i malized to $\pi/16kc$.

Effect of the beam density

Particle-in-cell simulation

$\bar{v}_0 = 0.95c$

$\bar{\theta}_0 = 13.83^\circ$

$E_{y_0} = 1.636\times10^{6}$ V/cm

$E_{app} = 2.23\times10^{-2} E_{y_0}$

Relativistic Maxwellian distribution

$$f(p) = \frac{Nmc^2}{2\pi kT}\frac{1}{(kT/mc^2+1)}e^{-\frac{mc^2(\gamma-1)}{kT}}$$

$T = 10, 50, 100$ and 150 keV

A.C.J. Paes et al, to be published.

6

~~$n_e = 10^6$~~

$n_e = 10^8$ cm^{-3}

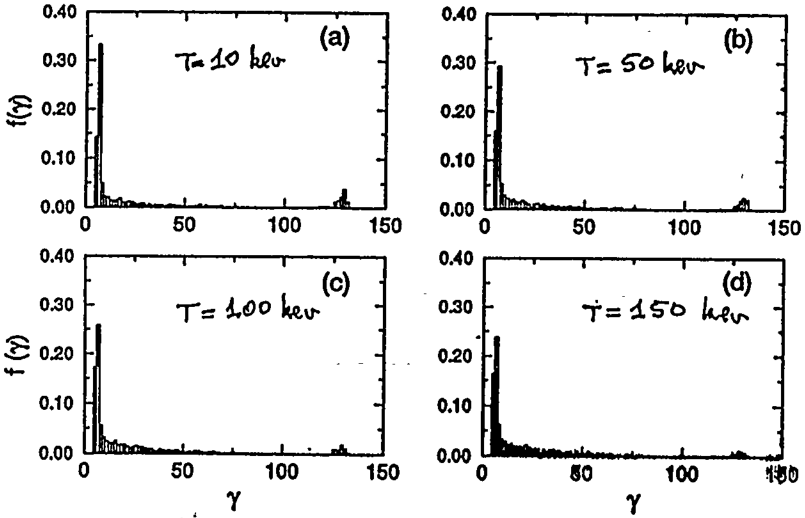

$\varphi = 8\pi$

7

$n_e = 7.96 \times 10^{12}\ cm^{-3}$

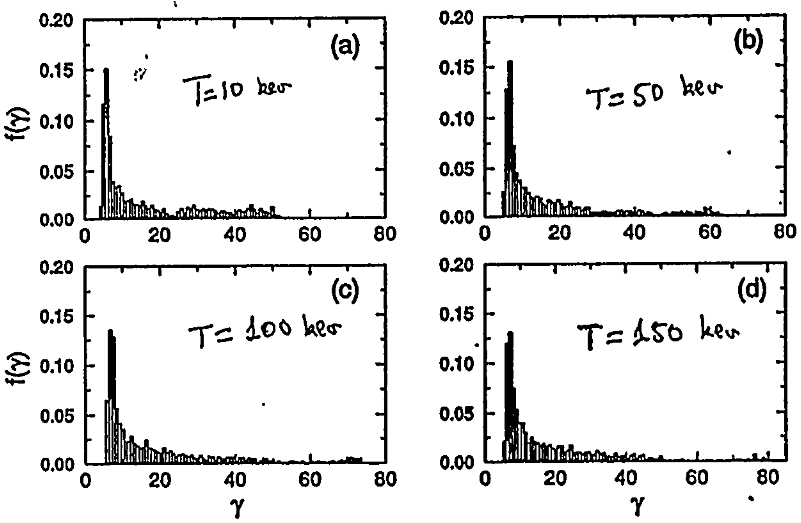

$\varphi = 8\pi$

ADVANCES WITH PSEUDOSPARK AND PRODUCTION OF HIGH BRIGHTNESS ELECTRON BEAMS: A SOURCE FOR HIGH LUMINOSITY ACCELERATORS

M. Gunderson, USC

SUMMARY AND CLOSING TALK

Z. Parsa, BNL/ITP